

**Design and Synthesis of Small-Molecule Inhibitors
of Two Cancer Targets: mTOR and MDM2/p53**

Charlotte Holly Reville

This thesis is submitted to Newcastle University
for the degree of Doctor of Philosophy

September 2011

Declaration

The work described in this thesis was carried out between October 2007 and September 2011 in the Medicinal Chemistry Laboratories, Bedson Building, Northern Institute for Cancer Research, Newcastle University, Newcastle upon Tyne, UK, NE1 7RU and in the Laboratory of Molecular Biophysics, Department of Biochemistry, University of Oxford, Oxford, UK, OX1 3QU.

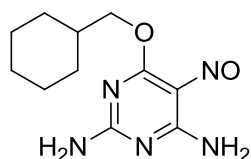
All of the research described in this thesis is original and does not incorporate any material or ideas previously published or presented by other authors except where due reference is given in the text.

No part of this thesis has been previously submitted for a degree, diploma or any qualification at any other university.

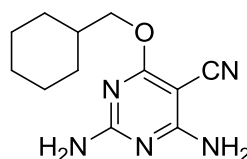
Abstract

Cancer is a disease in which cellular control over growth and differentiation has been lost. Targeted therapies for the treatment of cancer are becoming an increasing area of focus within the pharmaceutical industry and academia, due to the increasing understanding of the biology behind tumourgenesis.

There are 518 protein kinases within the human genome and they play a significant role within cellular signalling. Aberrant signalling of kinases can contribute to the development of cancer, and inhibition of kinase targets can result in either a cytostatic or cytotoxic effort. Kinases have a discrete ATP-binding domain, which presents an ideal target for small-molecule inhibitors. mTOR (mammalian target of rapamycin) is a serine/threonine protein kinase, which forms two complexes, mTORC1 and mTORC2, as part of the PI 3-K/Akt pathway, a growth/survival pathway which has aberrant signalling in a number of cancers.



NU6027
mTOR IC₅₀ = 2.6 μM
CDK₂ IC₅₀ = 2.2 μM

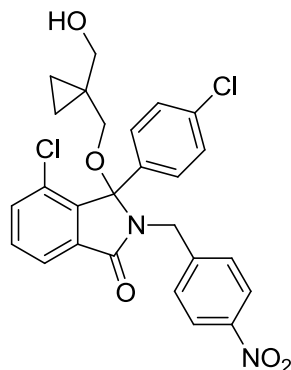


NU6227
mTOR IC₅₀ = 1.5 μM
CDK₂ IC₅₀ = 62 μM

The development of ATP-competitive inhibitors of mTOR has been based on a series of 2,6-diaminosubstituted pyrimidines, with modest activity against mTOR, as exemplified by NU6027 and NU6227 originally designed as CDK2 inhibitors. Structure-activity relationships for inhibition of mTOR have been explored. The 4-substituent was either modified to a smaller alkoxy group or completely removed, giving reduced activity. At the 5-position compounds with other substituents were then synthesised. Modifications of the 2- and 6-amino groups were also investigated. The pyrimidine heterocycle was also replaced with two pyridine regioisomers. None of the synthesised compounds showed improved mTOR inhibitory activity over NU6227 and NU6027.

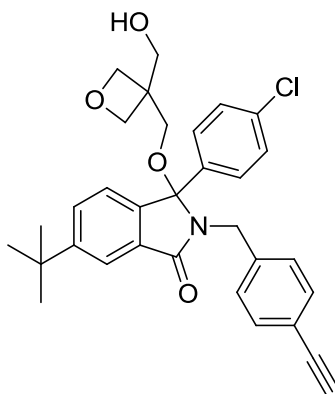
The tumour suppressor p53 is activated as a response to DNA-damage, oncogene activation and cellular stress. Once activated p53 acts as a transcription initiator, inducing the

transcription of a number of genes, including those involved in halting the cell cycle, repairing DNA-damage and initiating apoptosis. A further transcriptional target of p53 is MDM2, a negative regulator of p53. Inhibitors of the MDM2-p53 interaction have been reported including the isoindolinones e.g. NCL-00008406.



NCL-00008406
IC₅₀ = 95 nM

Structure-activity relationships (SAR) studies for the identification of replacement of the 4-nitro group showed that a 4-ethynyl substituent had a similar level of potency, along with the 4-bromo, 3-fluoro substituents. SARs around the isoindolinone A-ring identified the 6-*tert*-butyl substituent as equipotent to the parent. Synthesis of an oxetane derivative such as NCL-00018327 has demonstrated that replacing the cyclopropyl group with a 3,3-oxetane substituent either maintained or improved activity against MDM2.



NCL-00018327
IC₅₀ = 28 nM

Synthetic efforts have identified highly potent, low nanomolar, isoindolinone-based inhibitors of the MDM2-p53 protein-protein interaction. Optimal substituents for the benzyl group have been identified, avoiding the use of a nitro group which is toxic within drugs. Synthesis of an oxetane derivative has been shown to be either equi- or more potent than cyclopropyl derivatives, and this modification is predicted to improved the aqueous solubility by reducing the *clogP*. Synthesis of a *tert*-butyl analogues using an alternative synthetic route has

developed the SAR around the A-ring and resulted in an improved synthetic scheme. Purification of a range of MDM2 mutant proteins has identified a crystallisable form of MDM2 and the recently solved crystal structure of an isoindolinone bound to MDM2 should guide further improvements to potency and aid the incorporation of groups to improve physical properties.

Cancer is a disease in which control over cellular growth is deregulated. Synthetic efforts have been directed toward the development of two targeted anti-cancer agents; the kinase mTOR and the protein-protein interaction MDM2/p53. 2,6-diaminopyrimidine were identified as most inhibitors of mTOR, but demonstrated a flat SAR and no increase in potency was observed. Isoindolinones have been identified as a valuable scaffold to inhibit the protein-protein interaction and have demonstrated excellent potencies.

Contents

Declaration.....	1
Abstract	2
Contents.....	5
Acknowledgements	7
Abbreviations.....	8
1. Cancer: An Introduction	10
2. mTOR: An Anti-Cancer Target	15
2.1 Protein Kinases and Protein Kinase Inhibitors	15
2.2 Phosphatidylinositol 3-kinase Lipids (PI 3-K)	19
2.3 Phosphatidylinositol 3-kinase-like Kinases	21
2.4 Mammalian Target of Rapamycin.....	23
2.4.1 mTOR Complex 1 and 2	23
2.4.2 The Function of mTORC1 and 2 Within the PI 3-K/Akt Pathway	26
2.5 Rapamycin and ‘Rapalogs’	32
2.6 mTOR Inhibitors Targeting the Kinase Domain.....	36
3. MDM2/p53: An Anti-Cancer Target.....	52
3.1 Inhibitors of Protein-protein Interaction	52
3.2 p53, MDM2 and MDMX.....	54
3.3 p53 Cellular Function	60
3.4 Drug-like Inhibitors of the MDM2-p53 Protein-protein Interaction.....	66
3.4.1. Nutlins	67
3.4.2. Spirooxindoles	69
3.4.3. 1,4-Benzodiazepine-2,5-diones	72
3.4.4. Chromenotriazolopyrimidines.....	74
3.4.5. Imidazoindoles	77
4. The Development of ATP-competitive Inhibitors of mTOR	80
4.1 Pyrimidines as mTOR Inhibitors.....	80
4.2 Synthesis of NU6027 and NU6227	82
4.3 Modifications to the O^4 -Position of NU6227	83
4.3.1. Synthesis of O^4 -Alkyl Substituted Analogues of NU6227	83
4.3.2. 4-Unsubstituted Analogues of NU6227	86
4.4 Structure-Activity-Relationships Around the Amino Groups	87
4.4.1. Synthesis of Pyrimidine Derivatives Lacking a 2-Amino Group.....	87
4.4.2. Synthesis of 6-Hydroxylamino Pyrimidines	93
4.4 Modifications to the 5-Position.....	97
4.5 Pyridine Analogues of mTOR Inhibitory Pyrimidines.....	102
4.6 Biological Results.....	116
4.6.1. Assay details.....	116
4.7 Future Work for the Development of Pyrimidine-based mTOR Inhibitors	120
4.8 Conclusion	122

5. Isoindolinone-Based Inhibitors of the MDM2-p53 Protein-protein Interaction.....	124
5.1 Development of Isoindolinone Based Inhibitors of the MDM2 p53 Protein-protein Interaction.....	124
5.2 Isoindolinone Formation.....	135
5.3 Modifications to the <i>N</i> -benzyl Group.....	144
5.3.1 Ethynyl Replacement of the Nitro Group.....	145
5.3.2 Trifluoromethylsulfone Replacement of the Nitro Group.....	149
5.3.3. 3-Fluoro-4-Halo Benzyl Analogues.....	150
5.3.4. Benzoxadiazoles as Isosteres for the Nitro Group.....	157
5.3.5. Replacement of the 4-Nitro Group with 4-Azide.....	159
5.3.6. Biological Results for Benzyl Analogues.....	167
5.4 Analogues of the Ethynyl Group.....	171
5.4.1. Biological Results for Ethynyl Analogues.....	174
5.5 Further SAR for the Isoindolinone Ether-Groups.....	175
5.5.1. Biological Results for Isoindolinone Ether Groups.....	180
5.6 <i>tert</i> -Butyl 'A'-Ring Analogues.....	181
5.6.1. Biological Results for <i>tert</i> -Butyl Analogues.....	191
5.7 Protein Crystallography of Isoindolinone-based Inhibitors of p53/MDM2 Protein-protein Interaction.....	192
5.7.1. Crystal Structure of NCL00013774.....	203
5.8 Future Work for MDM2/p53.....	207
5.9 p53/MDM2 Assay Details.....	213
5.10 Conclusion.....	214
6. Overall Conclusion.....	216
7. Experimental.....	217
7.1 mTOR Experimental Procedures.....	219
7.2 MDM2 Experimental Procedures.....	257
General Procedure A.....	257
General procedure B.....	257
General procedure C.....	257
General procedure D.....	258
General procedure E.....	258
General procedure F.....	259
General procedure G.....	259
General procedure H.....	259
8. Bibliography.....	309
Appendix 1- Protein Crystallography.....	335
Appendix 2 Crystallography of 127.....	338

Acknowledgements

Firstly, I would like to thank my supervisors Prof. Roger Griffin, Dr Ian Hardcastle, Dr Celine Cano and Prof. Bernard Golding, for their help and guidance throughout my PhD and for giving me the opportunity to work in the lab.

I would also like to thank the bioscientists in the Paul O’Gorman building especially Prof. Herbie Newell, Lan Zhen Wang and Yan Zhao; above all Herbie for his positivity and encouragement.

I would like to thank CRUK for generous funding.

I would also like to thank Dr Mangalesh Sivaprakasam, Dr Tim Blackburn, Dr Andrey Zaytsev, Dr Benoit Carbain and Dr Kate Smith for their ‘in-lab’ guidance and assistance, and for being a pleasure to work alongside.

I would like to thank Dr Karen Haggerty and Carlo Bawn for their technical assistance and know-how and for keeping the lab running smoothly.

Dr Burcu Anil Kirmizitas, Alison Hole, Prof. Jane Endicott and Prof. Martin Noble assisted me greatly during the time in the Oxford.

Sarah Payne, Chris Coxon, Chris Matheson, Stephanie Myers , Lauren Barrett, David Turner, Ruth Taylor, Tommy Rennison, and everybody else from the Addi lab, for making my time there so enjoyable and memorable. Sarah Cully, for being a pleasure with whom to share a fume hood, and for entertaining with Christmas songs all year round.

Jonathan, thank you for your support, for proof-reading everything, for patiently explaining grammar and for dealing with all the stress.

Thanks to Mum, Dad and Emily for their support and encouragement over the last 26 years. For Grandad.

Abbreviations

ap.	Apparent
Ar	Aryl
ATM	Ataxia-telangiectasia mutated kinase
ATP	Adenosine triphosphate
ATR	Ataxia-telangiectasia and Rad3-related kinase
CAN	Cerium ammonium nitrate
CDK	Cyclin-dependent kinase
d	doublet
DCM	Dichloromethane
DDQ	3,4-dichloro-5,6-dicyanoquinone
DIPEA	Diisopropylethylamine (Hünig's base)
DMAP	4-Dimethylaminopyridine
DME	Dimethoxyethane
DNA	Deoxyribose nucleic acid
DNA-PK	DNA dependent protein kinase
ELISA	enzyme linked immunosorbent assay
Eq	Equivalent(s)
ESI	Electrospray ionisation
HATs	Histone acetyl transferases
HPLC	High-performance liquid chromatography
HRMS	High-resolution mass spectroscopy
Hz	Hertz
IC ₅₀	concentration required for inhibition of 50 % of target
IR	Infrared spectroscopy
K _d	dissociation constant
K _i	inhibition constant
KLISA	kinase linked immunosorbent assay
LCMS	Liquid chromatography mass spectroscopy
MDM2	Murine double minute protein 2
MDM4/X	Murine double minute protein 4
MS	Mass spectroscopy

mTOR	Mammalian target of Rapamycin
mTORC1	mTOR complex 1
mTORC2	mTOR complex 2
mp	Melting point
N.D	Not determined
PE	Petroleum ether (b.p 40-60 °C)
PIKK	Phosphatidylinositol 3-kinase related kinase
PMB	<i>para</i> -Methoxybenzyl
RE	Responsive elements
R _f	Retardation factor
R _t	Retention time
RNA	Ribose nucleic acid
RT	room temperature
s	singlet
SAR	Structure activity relationships
sat.	saturated
Ser	Serine
t	triplet
Thr	Threonine
TIPS	Triisopropylsilyl
TMEDA	Tetramethylethylene diamine
UV	Ultraviolet Spectroscopy

1. Cancer: An Introduction

Cancer is a disease in which cellular control over growth and replication has been lost. There are around 200 different types of cancer,¹ each characterised by significant changes within the genome. 298, 000 new cases of cancer are diagnosed each year within the UK, with around 54 % of cases being breast, lung, large bowel or prostate cancer. The 20 most common cancers by incident in 2007 are shown below (Figure 1).

Breast	45,972	(15%)
Lung	39,473	(13%)
Colorectal	38,608	(13%)
Prostate	36,101	(12%)
Non-Hodgkin lymphoma	10,917	(4%)
Malignant melanoma	10,672	(4%)
Bladder	10,091	(3%)
Kidney	8,228	(3%)
Oesophagus	7,966	(3%)
Stomach	7,784	(3%)
Pancreas	7,684	(3%)
Uterus	7,536	(3%)
Leukaemias	7,001	(2%)
Ovary	6,719	(2%)
Oral	5,410	(2%)
Brain with CNS	4,676	(2%)
Multiple myeloma	4,040	(1%)
Liver	3,407	(1%)
Cervix	2,828	(1%)
Mesothelioma	2,401	(1%)
Other	30,477	(10%)

Figure 1 The twenty commonest cancers by incident in 2007 (Taken from reference 1)

Cancer is predominantly a disease of older people, with 75% of cases reported in 2007 being in the over sixties age group, and 76% of cancer deaths being in the over sixty fives age group.¹ Traditionally cancer has been treated by surgery, with radiation therapy emerging at the end of the 19th century with the discovery of X-rays.² However, for metastasised tumours and haematological cancers a more system wide approach is needed. The development of chemotherapeutic agents began with the observation that cytotoxic agents killed rapidly proliferating cells.² The challenge lies in selectively killing cancer cells over normal cells and ensuring complete elimination of the tumour cell.² Novel anti-cancer agents are constantly being developed, assisted by the increasing understanding of the biology of tumour cells.

The tumourgenesis process can be considered a Darwinian process, in which a build up of mutations confers a growth advantage over normal cells. Mutations within the genome lead either to the activation of oncogenes or the inactivation of tumour suppressors.³ The combination of the two allows cells to continue reproducing without restraint, despite the

presence of DNA damage. Hanahan and Weinberg identified six ‘hallmarks of cancer’ which can be used to describe the behaviour of nearly all cancer cells,³ allowing the cell to overcome the regulatory pathways within the cell to prevent cancer. The six hallmarks of cancer are

- Self sufficiency to growth signals
- Insensitivity to antigrowth signals
- Evasion of apoptosis
- Limitless replicative potential
- Angiogenesis
- Tissue invasion and metastases

In a normal cell growth signals are required before progressing through the cell cycle.

However, within tumour cells the growth signals, which are transmitted *via* transmembrane receptors, are not required for growth. The tyrosine receptor kinases are overexpressed in a number of cancers, leading to cancer cells being hyper-sensitive to ambient levels of growth signals. Structural modifications to the receptors may lead to growth signal independent signalling, as well as mutations within the downstream signalling proteins. Growth signalling pathways are deregulated in a high number of cancers, allowing the continuing growth of tumours.³

Alongside the self sufficiency to growth signals, cancer cells must also be insensitive to anti-growth signals. Within a normal cell, the cell is maintained in a quiescent state by both soluble growth inhibitors and immobilised inhibitors on the surface of neighbouring cells. For tumourgenesis to occur cancer cells must evade these signals.³

These two ‘hallmarks of cancer’ allow cells to grow in an uncontrolled manner. However, for a tumour to develop, cells must also avoid death. A resistance to apoptosis is a hallmark of all tumour cells, commonly (~ 50%) this resistance is acquired *via* a mutation of p53,³ a tumour suppressor, which normally cells detects DNA-damage and can initiate programmed cell death.

A further fundamental difference between ‘normal’ cells and tumour cells is a limitless replicative ability. Normal cells cannot replicate endlessly, even in the presence of growth signals, replication can only occur for 60-70 rounds of mitosis.³ Telomeres are repeating units

of six base pairs at the ends of chromosomes. At each round of replication some of the telomeres are lost, and will eventually be completely degraded. This can result in chromosome fusion, which results in cell death. However, within nearly all tumour cells telomere maintenance is observed, in 85-90% upregulation of telomerase activity, which adds base pairs, giving an endless replicative ability.³

To support continuing growth angiogenesis must occur. To supply sufficient nutrients and oxygen, cells must lie within 100 µm of capillary blood vessels. Within normal cells angiogenesis is a tightly controlled process, but for tumours to progress, the development of these blood vessels must occur at an early to mid point in tumour formation.³

The final 'hallmark of cancer' described by Hanahan and Weinberg, is the ability to invade local tissue and metastasise to distant sites. The process of metastasis occurs within most human cancer, with tumour cells seeking a location where growth is not limited by space or a lack of nutrients. Metastasis are thought to cause 90% of cancer deaths.³

A further publication from Hanahan and Weinberg describes further characteristics which enable the development of tumours.⁴ The enabling characteristics are

- Deregulation of cellular energetics
- Genome instability and mutations
- Avoiding immune destruction
- Tumour-promoting inflammation

Deregulation of cellular energetics allows continuous growth and proliferation.⁴ Genome instability and mutations will be discussed in greater detail shortly. Avoiding immune destruction is also crucial for tumour development. Cells and tissue are continuously monitored by the immune system, which can recognise and eliminate emerging tumours. Those which survive must avoid detection by the immune system. Immunocompromised mice are more prone to carcinogen derived tumours than immunocompetent mice.⁴ The fourth enabling characteristic is tumour-promoting inflammation. Inflammation can contribute towards the development of tumours, by supplying bioactive molecules to the tumour such as growth factors, survival factors and proangiogenic factors such as extracellular matrix modifying enzymes which allows angiogenesis and metastases to occur.⁴

Luo *et al* suggest that the key to developing new treatments lies with identifying critical signalling pathways, and members of signalling pathways within tumour cells whose inhibition results in ‘system failure’.⁵ Luo *et al* have identified a further set of ‘hallmarks’ which whilst not uniquely found in cancer cells, must be tolerated for cancer cells to survive. They term these the ‘stress phenotype’.⁵

The first of the stress phenotypes is high levels of DNA-damage. Tumours have high levels of genetic instability, partially due the loss of telomeres, allowing fusion of unprotected chromosomes, partially due to mutation within the DNA repair and DNA stress response pathway, which allows the cancer cells to survive, but also allows for accumulation of DNA damage.⁵

The fusion of chromosomes can lead to translocation and amplification of genes. This in turn can lead to the second stress phenotype – proteotoxic stress, the stress caused by the misfolded proteins. Translocated genes and anuploidy can alter the stoichiometry of protein complexes within cells, leading to a build up of unfolded proteins which aggregating within cells.⁵

Further ‘stress phenotypes’ include: mitotic stress, in which the shift in chromosome distribution within cancer cells leads to rapid evolution; metabolic stress, where tumour cell get their energy from glycolysis; and oxidative stress, where higher levels of reactive oxygen species are generated by oncogenic signalling, which in turn damages DNA, leading to further transformation.⁵

These stress phenotypes contribute further to the difference between cancer cells and normal cells which can be exploited in developing selective anti-cancer chemotherapeutic agents. Luo *et al* have characterised cancer cells as having oncogenic and non-oncogene addiction.⁵ Oncogene addiction is the reliance of tumour cells on oncogenes to drive the tumourgenesis process, whereas non-oncogenic addiction is the reliance on genes which are not mutated, but are necessary for maintaining the tumour cell. The non-oncogene addiction includes genes which allow the tumour cells to cope with the cellular stress caused by the ‘stress oncogene’.⁵

There are two approaches which can be taken to exploit the difference between cancer and normal cells. The first is ‘stress sensitisation’, where vital proteins within the stress support

pathway are inhibited and the cell is sensitised to cellular stress, which should induce cell death. The second approach is stress overload in which the existing stress is intensified, to overwhelm the stress support pathways, which should also lead to cell death.⁵

2. mTOR: An Anti-Cancer Target

2.1 Protein Kinases and Protein Kinase Inhibitors

Protein kinases transfer the terminal (γ) phosphate group of adenosine triphosphate (ATP) to the hydroxyl groups of amino acid side-chains within proteins (Figure 2). This process activates proteins, usually by inducing a change in conformation. There are three classes of protein kinase: serine/threonine kinases, tyrosine kinases and dual kinases. The phosphorylation process can be reversed through the activity of phosphatases, resulting in free hydroxyl groups and orthophosphate (P_i). Without the activity of phosphatases, phosphorylation would essentially be irreversible as it is a highly favourable process, the hydrolysis of ATP to ADP has ΔG of -50.2 kCal/mol.⁶

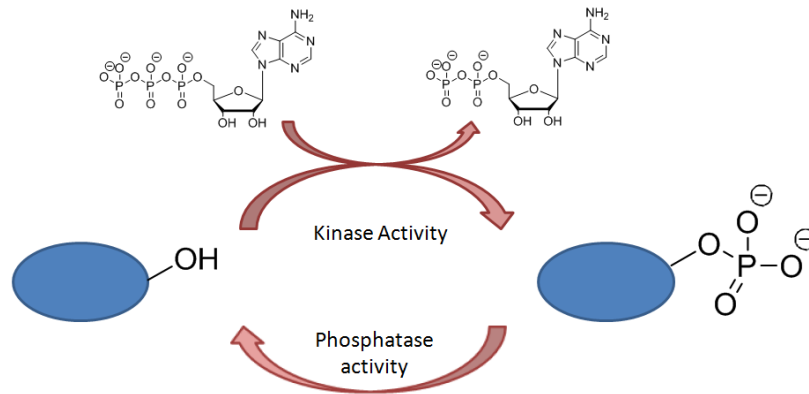
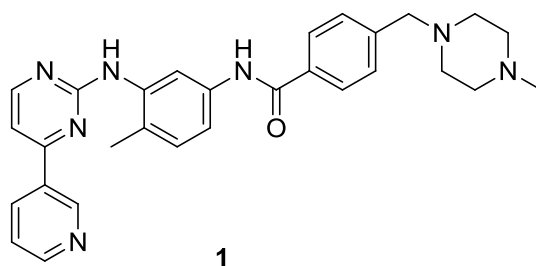


Figure 2

There are 518 protein kinases within the human genome.⁷ All 518 share a highly conserved catalytic domain, alike in both sequence and structure.⁷ The ATP-binding site lies in a deep cleft between the C- and N-terminal lobes,⁸ and consists of: a hydrophobic pocket, which binds the purine of ATP; a hinge region, which connect the C- and N- lobes; a P loop, which acts as ceiling to the pocket and the activation loop.⁸ The activation loop can undergo significant conformational changes as a result of its phosphorylation state. When phosphorylated (the 'active' form) the activation loop moves to close up a hydrophobic pocket adjacent to the ATP-binding site which is present in the unphosphorylated configuration (inactive), also known as the 'DFG out' configuration.⁸ The aspartate of the DFG binds two Mg^{2+} ions, which co-ordinate to the three phosphate groups of ATP on binding.⁹

Protein kinases play a vital role within the cell, with virtually every cellular process governed by a cascade of phosphorylation.¹⁰ Disregulation of kinase is observed in a number of diseases, including cancer, immunological, neurological, metabolic and infectious disease.¹⁰ Since the success of imatinib (**1**) (Gleevec) protein kinases have become a major focus of anti-cancer drug discovery efforts, with compounds targeting 30 different kinases reaching the level of phase I clinical trials.¹⁰



The majority of kinase inhibitors target the ATP binding site. The compounds, usually heterocycles, form one to three hydrogen bonds with the hinge region, mimicking those formed by ATP.¹⁰ Inhibitors may also bind to other regions around the adenine binding site including the hydrophobic pockets I and II, the ribose binding region and phosphate binding region.¹¹ Selectivity can be gained from these regions, but generally not from the adenine binding residues.¹¹ ATP-competitive inhibitors are also known as type I kinase inhibitors.¹¹ As this class of inhibitors target the ATP-binding site the structure should be highly conserved and not alter significantly due to mutation, as mutation may not be tolerated for ATP-binding and lead to a lack of function.⁷

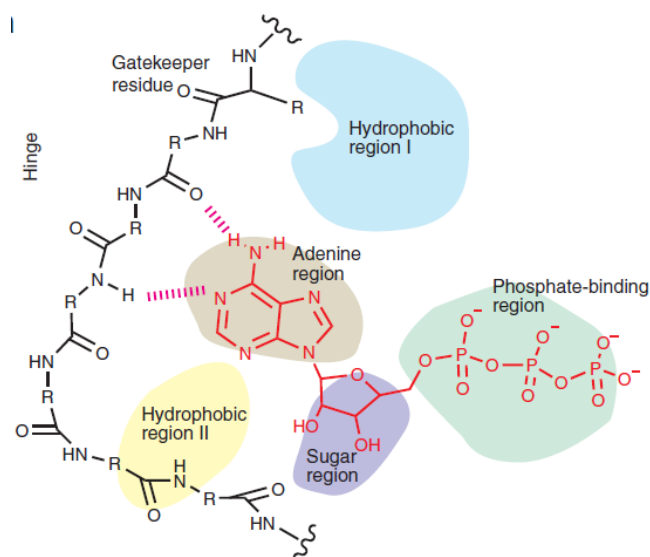


Figure 3 Representation of ATP-competitive binding site (Taken from reference 11)

Type II kinase inhibitors occupy a hydrophobic pocket adjacent to the ATP-binding site. This hydrophobic pocket is not present when the kinase is in its active form, instead it occupies a pocket formed when the activation loop is in the ‘DFG’ out configuration.¹¹ Inactive conformation inhibitors occupy the hydrophobic pocket created by the inactive configuration *via* a hydrophobic ‘tail’ but also usually have a ‘head’ group which can interact with the adenine binding site. Inhibitors which bind to the inactive conformation are sometimes known as allosteric inhibitors,¹¹ however, this term has also been applied to inhibitors such as rapamycin, which bind at a distant site and do not interact with the ATP-binding site.¹⁰

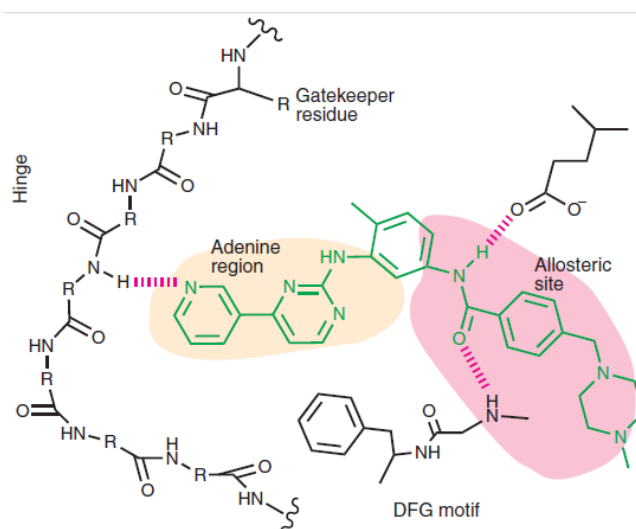


Figure 4 Representation of the allosteric binding site (Taken from reference 11)

Accessing the ‘DFG’ out conformation may allow greater selectivity for kinase inhibitors as residues exposed within the inactive conformation hydrophobic pocket are less conserved.¹¹ Inhibitors which bind to the inactive conformation may also have a greater cellular potency, as ATP has a lower affinity for inactive conformation kinases.¹¹ Imatinib (**1**) binds to the inactive conformation and locks the kinase in an inactive conformation, thus ensuring that the aspartate (from the ‘DFG’) cannot co-ordinate to the magnesium ion in the catalytic site.⁷

There are two further classes of kinase inhibitors. Class III refers to the previously discussed ‘allosteric’ inhibitors which bind at a distant site, far removed from the ATP-binding site (rather than adjacent like type II inhibitors).¹⁰ These inhibitors usually bind in a unique manner, and use an individual mechanism to inhibit kinase activity.¹⁰ By avoiding the highly conserved ATP-binding site the type III inhibitors are usually highly selective. Rapamycin, a potent and highly selective inhibitor of mTORC1, acts in this manner.

Type IV are covalent kinase inhibitors. These form an irreversible covalent bond with the active site, usually by reacting with a cysteine residue in a Micheal-type reaction.¹⁰ Type IV inhibitors usually consist of a group which bind to the ATP-binding site, thus targeting the molecule, which can then react with the nucleophilic residue.

Selectivity of a kinase inhibitor is particularly important, especially during early development of a new class of kinase inhibitor. A selective kinase inhibitor should be less toxic and will make target validation simpler,⁸ with closely related kinases most likely to share sensitivity to a particular inhibitor.¹² A single residue within the ATP-binding site can control the sensitivity of a kinase to a particular inhibitor. This residue, known as the gatekeeper residue, controls access to the hydrophobic pocket. Kinases with a larger residue at this site have a greater range of resistance to kinase inhibitors.¹² The gatekeeper residue does not affect binding of ATP as the hydrophobic pocket it controls access to is not exploited by ATP.⁷ Mutation of the gate keeper residue is a common mechanism of developing resistance to inhibitors,¹⁰ and as this area is not exploited by ATP, the kinase is still functional. Kinase inhibitors which can tolerate a variety of residues at this point can avoid this loss of efficiency.¹⁰ Zuccotto *et al* have demonstrated the influence of the gatekeeper residue on access to the hydrophobic pocket by comparing the crystal structure of CDK2 (Phe gatekeeper) and bRAF (Thr gatekeeper). The bRAF crystal structure has a larger hydrophobic pocket accessible to a small molecule, in comparison to the CDK2 inhibitor (Figure 5).¹³

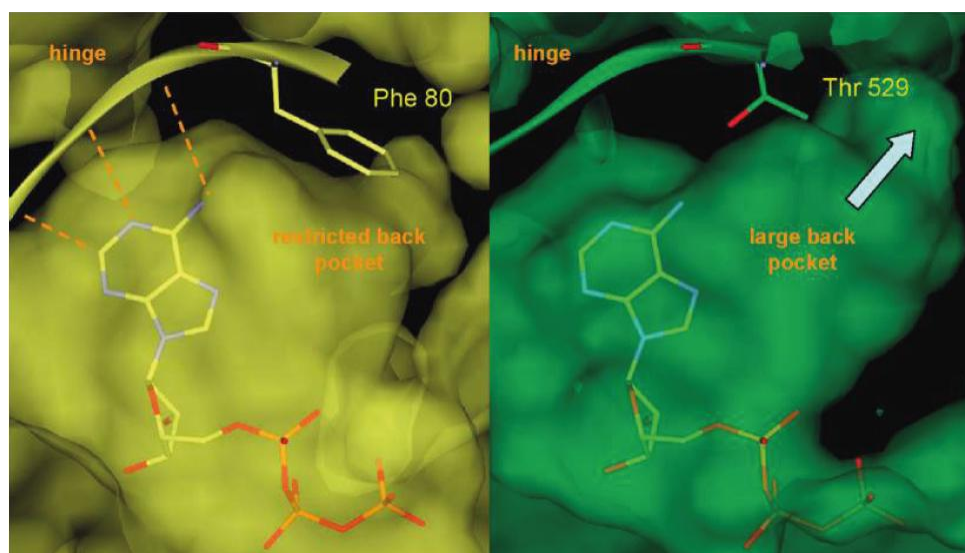


Figure 5 Comparison of the CDK2 and bRAF kinase domain, with differing gatekeeper residues (Taken from reference 13)

With the emergence of rationally-targeted agents,⁸ kinase inhibitors have been increasingly important. Alongside this, sophisticated techniques for designing of new inhibitors have been developed, aided by NMR and protein crystallography.⁸ High-throughput screening has helped identify starting points for a number of drug discovery programmes and this has now been joined by fragment-based screening to identify new starting points.

2.2 Phosphatidylinositol 3-kinase Lipids (PI 3-K)

Phosphatidylinositol lipids are comprised of an inositol ring with a phosphatidic acid group attached *via* the 1'-OH group. The inositol group can be phosphorylated by ATP at all positions around the ring apart from the 2' and 6' position by lipid kinases, with the position and combination of phosphorylation effecting function.¹⁴ Phosphatidylinositol 3-kinases (PI 3-K) phosphorylate the membrane bound inositol ring at the 3-position.¹⁴ There are multiple isoforms of PI 3-K, which can be divided into 3 distinct classes, which share a homologous core catalytic domain.¹⁴

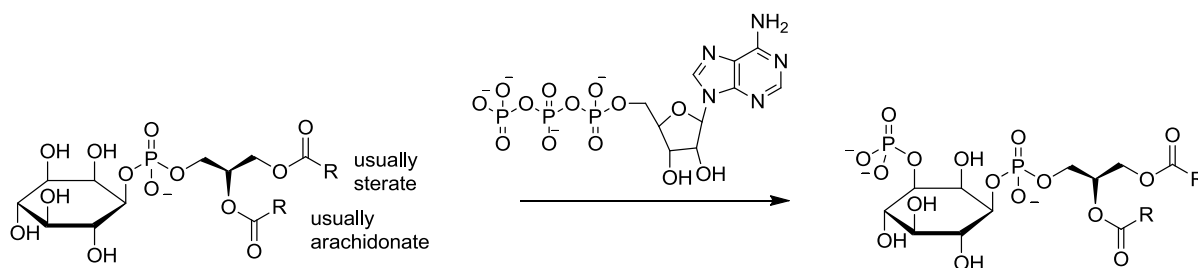


Figure 6 Phosphorylation of the inositol ring at the 3-position (Taken from reference 6)

Class I consists of a heterodimer made up of ~110 kDa catalytic subunit known as p110 and a regulatory or adaptor subunit. The preferred substrate of class I is phosphatidylinositol (4, 5) biphosphate (PtdIns (4,5) P₂) giving phosphatidylinositol (3,4,5) triphosphate (PtdIns (3,4,5) P₃).¹⁴⁻¹⁵ The activity of class I PI 3-K is reversed by the lipid phosphatase Pten (phosphatase and tensin homologue deleted on chromosome 10).¹⁶

Class I can be further divided into class I_A and class I_B. Class I_A consists of one of three isoforms of p110, either α , β or δ and an adaptor protein, one of the isoforms of p85, α , β or γ . p110 isoforms α and β are ubiquitously spread throughout cells, however p110 δ is far less common, mostly found within leukocytes. The adaptor protein p85 has two Src-homology 2 (SH2) domains which bind to phosphorylated tyrosine kinase receptors, allowing the PI 3-K to relocate from the cytoplasm to the membrane where the phosphatidylinositol lipids are

located.¹⁴⁻¹⁵ Stimulation of almost every receptor induces activation of class I_A.¹⁴ The strengths and extent of these signals differs between signals, with insulin and PDGF signalling strongly, whilst EGFR has much weaker signalling.¹⁵ Class I_A is also activated by Ras though the mechanism of this process is unclear.¹⁵⁻¹⁶

PtdIns (3,4,5) P₃ product of class I activity acts as a secondary messenger recruiting a number of proteins to the membrane.¹⁶ These proteins are recruited *via* a domain known as the pleckstrin homology (PH), a structurally conserved area of around 100 amino acids¹⁵ which bind inositol lipids with high affinity.¹⁴

Class I_B has only one isoform of p110, the γ isoform and an adaptor protein of p101 kDa, which has no sequence homology to any other known protein. Class I_B is activated by heterotrimeric G-protein coupled receptors.¹⁴

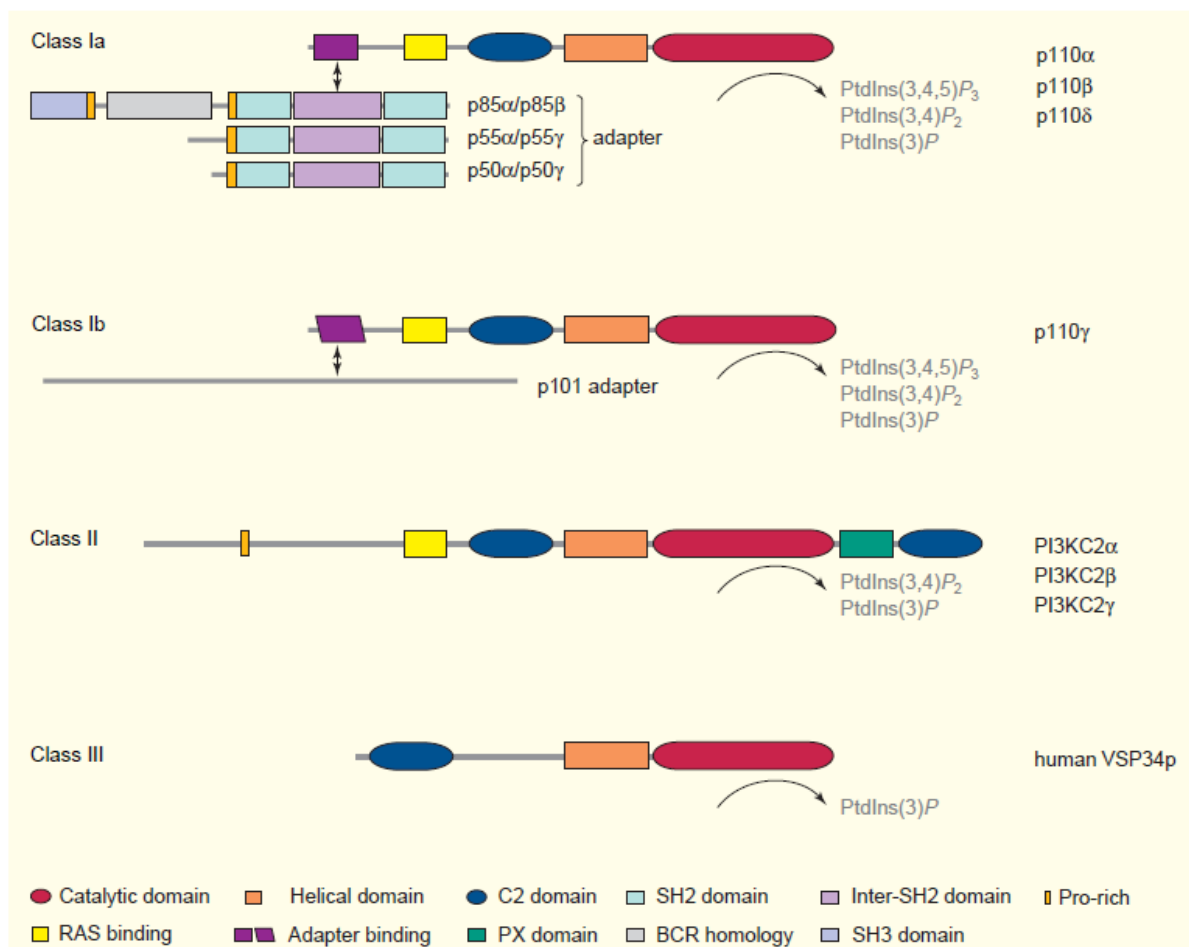


Figure 7 (Taken from reference 15)

Class II is larger than either classes I and III with a molecular mass of larger than 170 kDa, due to an extra C2 domain, which can bind to phospholipids. *In vitro* class II prefer PtdIns as substrate. Mammals have 3 class II isoforms - α , β and γ , with α and β found ubiquitously and γ primarily found in the liver.¹⁴ Class II is found at the cell membrane unlike class I which is found in the cytoplasm under resting conditions.¹⁵ The effect of class II signalling is unclear.

Class III is a homology of yeast vesicular protein sorting protein Vsp34p. *In vitro* class III only acts on PtdIns and is not stimulated by cell signalling. Class III is found in complex with p150, a Ser/Thr protein kinase – which targets class III to the membrane.¹⁴ In yeast Vsp34p has a role within protein trafficking to the vacuole and within mammals the role is thought to be similar, moving proteins to the lysosome.¹⁵

2.3 Phosphatidylinositol 3-kinase-like Kinases

The phosphatidylinositol 3-kinase-like kinases (PIKK) are a family of serine/threonine protein kinases. As the name suggests, they share significant sequence similarity (20-25%)¹⁷ to a family of lipid kinases, the phosphatidylinositol 3-kinases, rather than other serine/threonine protein kinases. PIKK family members are large, with molecular masses ranging from 280 kDa to 470 kDa.¹⁷

There are six members of the PIKK family: mammalian target of rapamycin (mTOR), DNA-dependent protein kinase catalytic subunit (DNA-PK_{cs}), ataxia-telangiectasia mutated (ATM), ataxia- and Rad 3-related (ATR), suppressor of morphogenesis in genitalia (SMG-1) and transformation/transcription domain-associated protein (TRRAP).¹⁸

The PIKK family have a range of diverse functions. mTOR controls cellular growth in a nutrient and amino acid sensitive manner. DNA-PK plays a role within non-homologous end-joining as a response to DNA double strand breaks. ATM and ATR act within the signalling pathway as a response to genome damage. ATM acts chiefly within the signalling of double strand breaks and ATR with other types of DNA-damage, such as that caused by UV light.¹⁷ SMG-1 is involved in the monitoring of RNA known as ‘nonsense mediated mRNA decay’ (NMD)¹⁹ which recognises and eliminates mRNA species which code for non-functional or harmful residues.¹⁷ TRRAP acts as a transcriptional co-activator, however, TRRAP does not behave as a kinase, instead functioning as a ‘scaffold’ recruiting histone acetyl transferases.¹⁷

The kinase domain of PIKKs (apart from TRRAP) contains the residues vital for ATP binding seen in other 'traditional' kinases, the DXXXXN and the DFG motif. This lack of the kinase motif results in TRRAP being catalytically inactive.¹⁷ Of the catalytically active PIKKs four out of five demonstrate a preference for the phosphorylation of Ser/Thr residues followed by a glutamine residue, known as S/T Q directed kinases. However, the fifth, mTOR shows no such preference for this particular motif, and as yet no mTOR motif for phosphorylation has been identified.¹⁷ It has been proposed that the difference in phosphorylation site preference lies in the role of the kinase, all catalytically active PIKK enzymes which preferentially phosphorylate the S/T Q motif function within genome monitoring and repair, whereas mTOR does not, perhaps ensuring that mTOR does not interfere with genome stability.¹⁹

The catalytic domain of the PIKKs is flanked on either side by domains known as FAT (FRAP-ATM-TRRAP) and FAT-C,¹⁸ which are always found in combination.¹⁷ The FAT domain lies on the N-terminal side of the catalytic domain and is made up of around 500 residues, however the function of the FAT domain is unclear.¹⁸ The FAT-C domain lies towards C-terminus of PIKK enzymes, it is a highly conserved region of around 30 amino acids. It has been shown to be critical for catalytic activity and mutagenesis experiments have demonstrated the importance of the conserved hydrophobic residues. It has been proposed that this region plays an important role within protein-protein interactions.¹⁸

The PIKK family also share a further structure motif known as HEAT (Huntington, Elogation factor 3, Alpha-regulatory subunit of protein phosphatase 2A and Tor1) repeats.¹⁹ The PIKK enzymes can have as many as 40-54 HEAT repeats,¹⁹ with each HEAT repeat made up of a pair of interacting anti-parallel helices linked by a flexible intraunit loop. Each helix is made up of 10-20 residues, with the intraloop made up of 5-8 residues.²⁰ Between 63-83% of the non-kinase domain of ATM, ATR and mTOR has identified as forming HEAT repeats and can form a superhelical structure.²⁰ The HEAT repeats have been identified in all PIKK family members¹⁹⁻²² and are thought to function within forming macromolecules.

Within the FAT domain on mTOR lies an area known as the FKBP12·rapamycin binding (FRB) domain.¹⁸ The FRB lies adjacent to the catalytic domain, and binds to the mTOR inhibitor rapamycin·FKBP12 complex (to be discussed in greater detail in chapter 2.5). The ~

110 residue region²³ forms four helices, a pair of HEAT repeats, one of which is unique to mTOR.²⁰

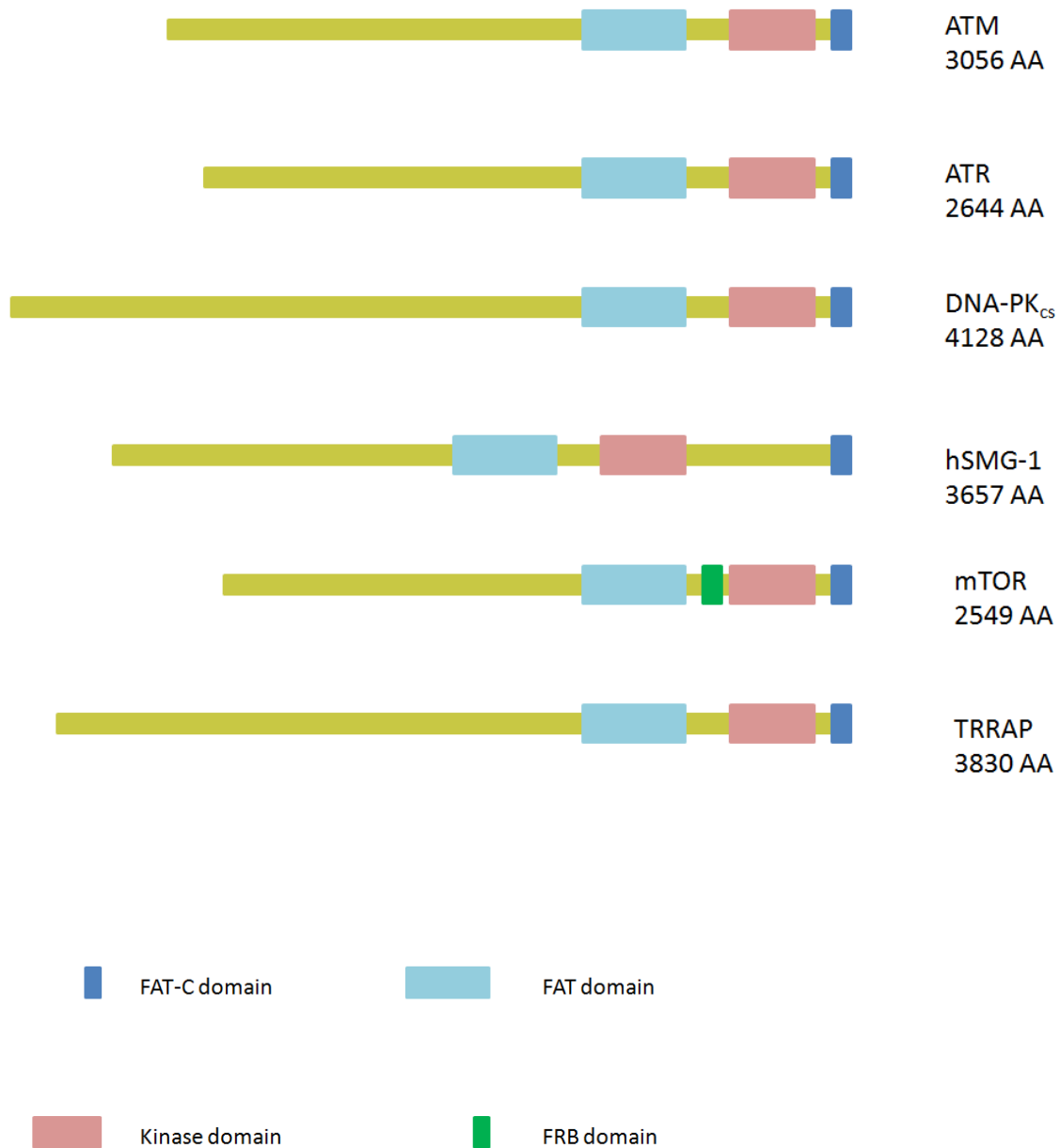


Figure 8 Structure of the PIKK with domains highlights

2.4 Mammalian Target of Rapamycin

2.4.1 mTOR Complex 1 and 2

The serine/threonine protein kinase mammalian target of rapamycin (mTOR) forms two complexes, both of which function within the PI 3-K/Akt growth/survival pathway. mTOR

complex 1, also known as mTORC1, is the rapamycin sensitive complex and co-ordinates growth signals and the availability of nutrients and cellular energy, to induce protein synthesis. It is made up of mTOR protein, raptor, mLST8, deptor and PRAS40.²⁴ Both deptor and PRAS40 (proline-rich Akt substrate of 40 kDa)²⁵ inhibit the catalytic activity of mTORC1, which is relieved on cellular signalling and will be discussed in more detail in Chapter 2.4.2,²⁴ mLST8 (lethal with sec13 protein 8) helps to activate mTORC1 by stabilising the mTOR/raptor interaction,²⁵ and although it associates with the kinase domain of mTORC1, it does not interact with substrates.²⁶ Raptor is a 150 kDa protein, with a highly conserved N-terminal domain, it has three HEAT domains and seven WD40 domains, which are important for protein-protein interactions.²⁶ Raptor acts as a scaffold, recruiting and interacting with mTORC1 substrates.²⁷ Disruption of either mTOR or raptor genes results in embryonic lethality, with death at around 5.5-6.5 days.²⁸

mTORC1 signalling is implicated in a number of cancers, due to its role within protein synthesis and its function within the PI 3-K pathway, which commonly has aberrant signalling within cancer. This includes mutant or over expressed *PIK3CA*, which is the gene coding for the PI 3-K p110 α subunit, mutation or amplification of Akt or loss of the tumour suppressor Pten.²⁹

Yip *et al* have determined the 3D structure of mTORC1 by cryoelectron microscopy.³⁰ mTORC1 was observed to form a dimer of two mTORC1 units with a cavity within the complex, the function of which is unclear. Antibody labelling identified location of PRAS40 and mLST8 binding. Incubating with rapamycin, a macrolide inhibitor of mTORC1 (see chapter 2.5) significantly reduced the levels of mTORC1, suggesting that rapamycin acts by destabilising the complex. This effect was not observed on treatment with the ATP-competitive inhibitor Torin1 (**16**).³⁰

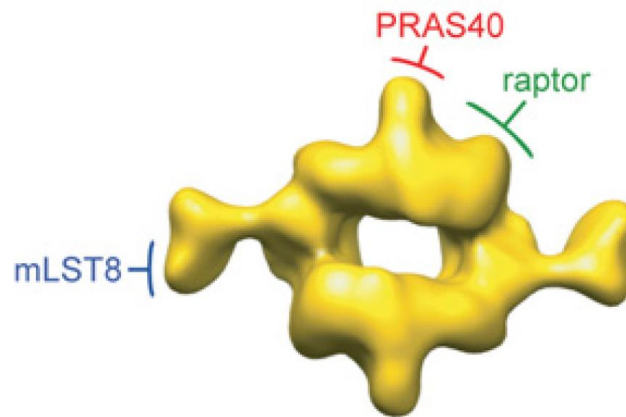


Figure 9 Cryo EM reconstruction of mTORC1 (Taken from reference 30)

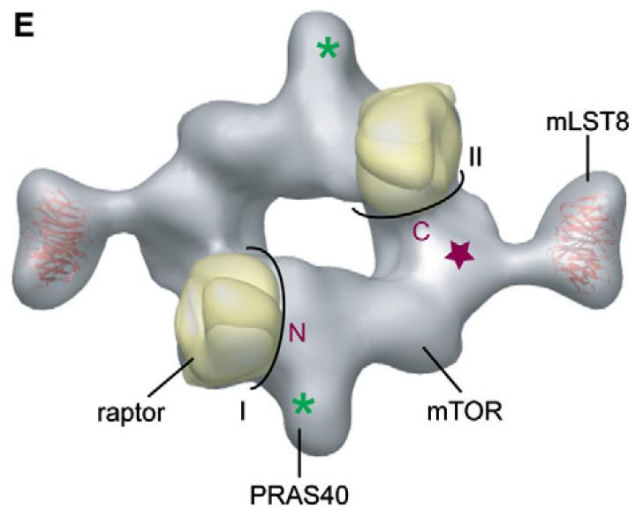


Figure 10 Cryo EM demonstrating dimer, with raptor (in gold) N and C terminus, kinase domain (purple star), binding site for PRAS40 and mLST8 and interface with raptor (black lines) (Taken from reference 30)

mTORC2 is the rapamycin and nutrient insensitive mTOR complex.²⁷ mTORC2 is made up of mTOR protein, rictor, mLST8, protor, deptor and mSIN1 (also known as mitogen-activated-protein-kinase-associated protein 1).^{24, 31} Rictor is the rapamycin insensitive companion of mTOR and protor the protein observed with rictor.²⁷ Interaction of mTOR with either raptor or rictor is mutually exclusive, complexes either contain raptor or rictor.³² Rictor knockouts result in embryonic lethality slightly later at ~ 10.5 days. Interestingly, mSIN1 knockout also results in embryonic lethality after 10.5 days, indicating that mSIN1 is only necessary for mTORC2 function but not mTORC1.²⁸ Each complex has a distinct cellular function, though both lie within the PI 3-K/Akt pathway and there are several interactions between both mTOR substrates and activators at various points within the pathway.

Guertin *et al* have observed that loss of the tumour suppressor Pten is associated with prostate cancer, and that mTORC2 activity is required in development of the tumour.³³ Pten-deficient cell-line PC-3C requires rictor to form tumours with nude mice and transforms prostate epithelial cells *in vivo*.³³ In adenocarcinoma driven by loss of Pten, loss of rictor impairs development of tumours, but has little effect on normal prostate tissue.²⁴

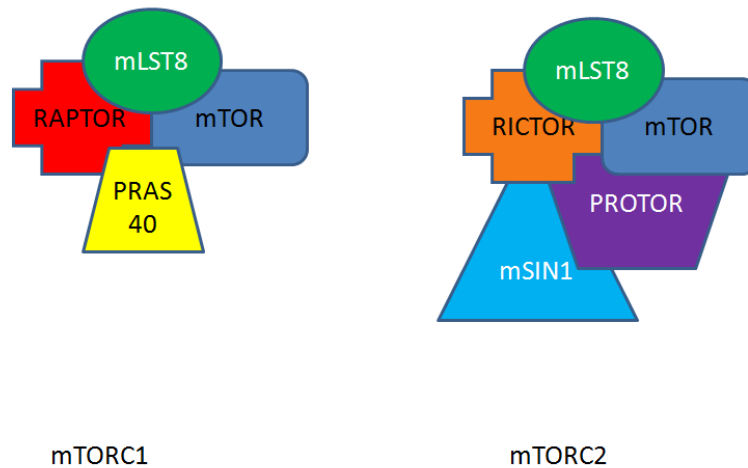


Figure 11

2.4.2 The Function of mTORC1 and 2 Within the PI 3-K/Akt Pathway

As a response to the binding of growth signals to tyrosine receptor kinases PI 3-K α is activated. PI 3-K α is comprised of a p110 α and p85 subunits and phosphorylates membrane bound PtdIns(4,5)P₂ to PtdIns(3,4,5)P₃.¹⁴ The phosphorylation of PtdIns(4,5)P₂ to PtdIns(3,4,5)P₃ can be reversed by the activity of the phosphatase and tumour suppressor Pten (phosphatase and tensin homolog deleted on chromosome ten).³⁴ PtdIns(3,4,5)P₃ is a secondary messenger and recruits a number of proteins *via* their pleckstrin homology domain, a conserved domain of approximately 100 residues, which binds PtdIns(3,4,5)P₃ with high affinity.^{14,28} Recruited proteins included Akt and PDK1. mTORC2 is also recruited *via* the pleckstrin homology domain of mSIN1.³⁵ Mutation or upregulation of the *PI3KCA* gene coding for p110 α or loss of Pten either through mutation or deletion can result in an aberrant signalling of the PI 3-K/Akt pathway. *PI3KCA* mutation is common and is observed within a number of cancers including ovarian, colorectal, breast, gastric, brain and cervical whilst Pten inactivation is observed in glioblastomas, endometrial, and prostate cancers, amongst

others.²⁹ Mutations or amplifications of Akt have also been observed in cancers, including breast, ovarian, glioblastoma and pancreatic.²⁹

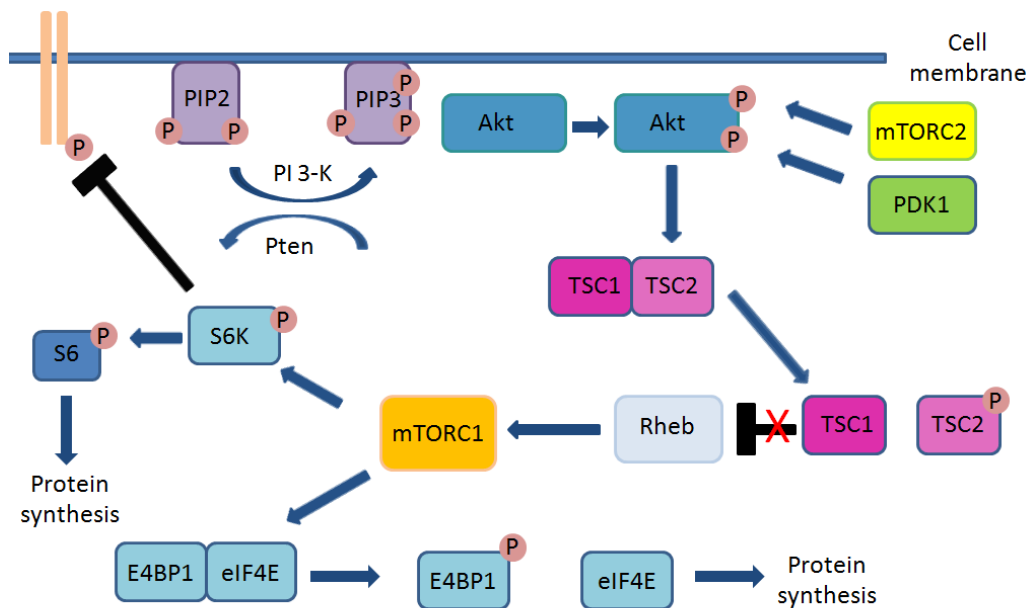


Figure 12 A simplified PI 3-K/Akt pathway

The exact mode of mTORC2 activation is unclear. mTORC2 can be stimulated on exposure to serum, in particular serum containing insulin and insulin-like growth factor 1, suggesting that mTORC2 is activated by the PI 3-K pathway.³⁶ Both mTORC2 and rictor are phosphorylated multiple times. Rictor phosphorylation at Thr1135 has been demonstrated to be sensitive to both rapamycin treatment, growth factors and levels of amino acids, which indicates that Thr1135 is phosphorylated downstream of mTORC1. An *in vitro* kinase assay indicated that rictor Thr1135 was phosphorylated by S6K, which is one of the target proteins of mTORC1.³⁷ The TSC1/2 complex, which has previously been thought to act purely as an upstream suppressor of mTORC1 activity (discussed below) has been proposed to act as a positive regulatory of mTORC2 activity. Inactivated TSC1/2 reduces mTORC2 activity, but inactivated Rheb, which is a target of TSC1/2 activity has no effect.³⁷ However the full mechanism of mTORC2 activation has yet to be deduced.

In addition to mTORC2 playing a part within actin polymerisation and cell spreading *via* PKC α and Rho,³⁸ its crucial role within the PI 3-K pathway is phosphorylation of Akt at Ser473.²⁵ This site lies within the C-terminus and is vital for full activation of Akt.²⁷ Akt is

also phosphorylated by PDK1 at Thr308, but phosphorylation at Ser473 is sufficient to ensure that some kinase targets of Akt can be phosphorylated, including the TSC1/2 complex. Full phosphorylation of Akt is required before other targets such as FOXO1/3 can be phosphorylated.²⁷ Akt controls the cell-cycle by regulating the FOXO protein, cyclin D1, p27 and GSK3. Akt also regulates MDM2, caspase-9, IKK α and Bad, controlling apoptosis. Akt phosphorylation of MDM2 induces translocation of MDM2 into the nucleus where it can inhibit the anti-apoptotic activity of p53.²⁴ mTORC2 has also been proposed to phosphorylate SK61, a target protein of mTORC1, which belongs to the same family as Akt.³⁸

Phosphorylation and activation of Akt can either control cell survival or in aberrant signalling potentially drive tumourgenesis by increasing cell growth, proliferation and migration, as well as the shift to glycolytic metabolism.²⁸ Akt phosphorylates TSC2 of the TSC1/2 heterodimeric complex at Ser939 and Thr1462.²⁶ TSC1 (also known as hamartin) is a 130 kDa protein and TSC2 (also known as tuberlin) a 200 kDa protein, which without Akt signalling form a stable heterodimer.^{26,38} When forming a stable heterodimer the TSC complex acts as a GTPase activating protein (GAP). TSC1/2 activates Rheb (Ras homolog enriched in brain) to convert bound GTP to the inactive GDP bound form.²⁵ On phosphorylation by Akt the heterodimer dissociates, inactivating the GAP activity of TSC1/2.²⁵ The Ras/MAPK pathway can also phosphorylate TSC1/2 complex through the kinase activity of Rsk.²⁵

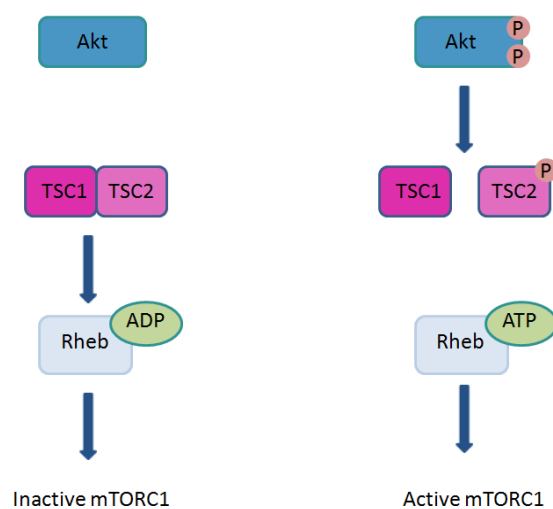


Figure 13

As protein synthesis is both an energy-rich and nutrient-rich pathway protein synthesis must be halted in times of nutrient and/or energy starvation. The energy-sensing AMP-dependent protein kinase (AMPK), which is activated by phosphorylation at Thr172 and Thr1227 by LKB1, phosphorylates TSC2 at Ser1345 and Ser1227, which activates the TSC1/2 complex.^{25,35} AMPK is activated as a response to a change in AMP:ATP ratio.²⁵ LKB1 also phosphorylates raptor at Ser792 and Ser722, promoting 14-3-3 protein binding and inactivating mTORC1.²⁵ The tumour suppressor p53 also acts *via* AMPK. On sensing DNA-damage p53 upregulates the transcription of AMPK, preventing continued cell growth in the face on DNA-damage.³⁵ AMPK can also phosphorylate p53 at Ser15,²⁴ stabilising p53 allowing increased levels of transcription of p53 cellular targets and halting the cell cycle whilst the cell is in energy-starvation conditions.

Hypoxia is also proposed to influence the PI 3-K/Akt pathway through the TSC1/2 complex. On phosphorylation, TSC2 is proposed to binds 14-3-3 proteins. As a response to hypoxia HIF (hypoxia inducible factor) is stabilised, inducing the expression of a number of genes, including those associated with angiogenesis, and Redd1 and 2. Redd1 can compete with TSC2 for binding with 14-3-3 proteins, relieving the inhibition of the TSC1/2 complex.²⁵ TSC1/2 can then act as a GAP, resulting in mTORC1 remaining inactive.

Destabilisation of the TSC1/2 complex results in loss of GAP-activity ensuing that Rheb existing as its active GTP-bound form. Rheb interacts with mTORC1, through a poorly understood mechanism, activating mTOR.²³ As Rheb is selective for mTORC1, it is thought that the protein may interact with raptor, rather than the mTOR protein itself.²⁸ Bai *et al* proposes that Rheb activation of mTORC1 is due to its interaction with FKBP38.³⁹ FKBP38 is related to FKBP12, a protein which, when bound to rapamycin, can inhibit mTORC1 (see Chapter 2.5). FKBP38 binds to the FRB domain of mTOR (but only mTOR in mTORC1) and inhibits the kinase activity of mTORC1. Bai *et al* propose that GTP-bound Rheb interacts with FKBP38, which disrupts FKBP38 binding with mTORC1, relieving its inhibitory activity.³⁹

Cellular nutrient levels have also been demonstrated to influence mTORC1 signalling. The strongest link between mTOR and nutrients is the Rag family of small GTPases.³⁵ The Rag family forms a heterodimer composed of either Rag A or B and Rag C or D. In the inactive state either Rag A or B is bound to GDP and RAG C or D is bound to GTP. However, in the

presence of amino acids the nucleotide binding switches through an unknown mechanism, to the active form.^{24, 35} The RAG heterodimer can then interact with raptor and induces the translocation of mTORC1 to the surface of endosomes and lysosomes, where it can interact with Rheb.³⁵ Interestingly, it has been shown that withdrawal of Leu has similar effect to starvation of a range of amino acids. The amino acid levels may be detected by a mechanism reliant on leucine levels.²⁵

PRAS40 is an inhibitory member of the mTORC1 complex that has been proposed to bind to the kinase domain of mTOR, preventing kinase activity.²⁸ On Akt activation PRAS40 is phosphorylated by Akt at Thr246, targeting PRAS40 to 14-3-3 binding, which relieves the inhibitory activity of PRAS40 on mTORC1 by sequestering PRAS40.^{25, 28} However, this may not be the full picture for PRAS40, as it also has a TOF sequence (discussed in more detail below), which suggests that it could be a substrate of mTORC1.²⁸

After activation mTORC1 can phosphorylate a number of target proteins involved in protein synthesis. mTORC1 targets are thought to have a TOF (target of TOR) motif, which consists of five amino acids – a phenylalanine, followed by two hydrophobic amino acid, then two acidic residues. This TOF motif is thought to be important for target protein to interact with raptor.²⁵

The two best described targets of mTORC1 kinase activity are the p70 S6 kinase 1 (S6K1) and eukaryotic initiation factor 4E-binding protein 1 (4E BP1).²⁵ Phosphorylation of 4E BP1 causes it to dissociate from eukaryotic initiation factor 4E (eIF4E). Without phosphorylation 4E BP1 is bound to eIF4E, inhibiting the translational initiation activity eIF4E.²⁶ eIF4E binds and recognises the cap, which contains a 7-methyl guanosine moiety,⁴⁰ at the 5' end of mRNA and mediates transcription of the mRNA.²⁵⁻²⁶ 4E BP1 is phosphorylated at numerous sites including Thr37, Thr46, Ser65, Thr70, Ser83, Ser101 and Ser112.²⁶ Of these four are linked to mTOR kinase activity: Thr37, Thr46, Ser65 and Thr70, with Ser65 and Thr70 lying close to the eIF4E binding site.³²

After repression of eIF4E is relieved it can form the initiation complex with proteins including eIF4G, allowing translation of mRNA with highly structured 5'-UTRs (untranslated regions).³⁸ The complex also contains eIF4F (which binds to the mRNA 5'

cap), eIF4A (an ATP-dependent helicase which unwinds mRNA secondary structure) and eIF4B which enhances eIF4A activity.^{33, 35, 41}

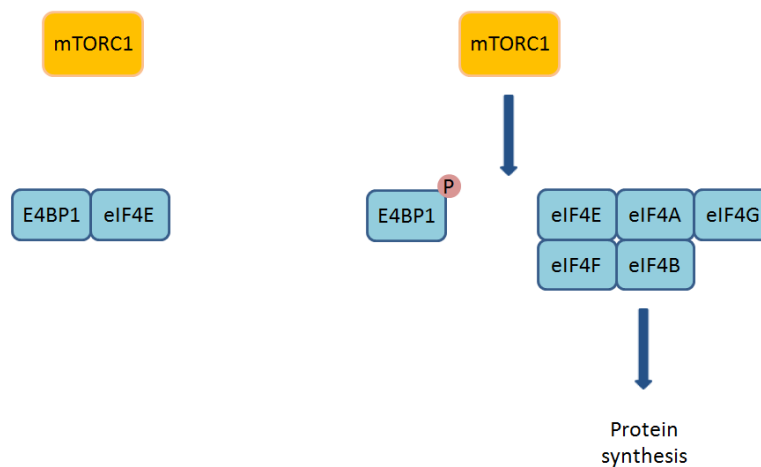


Figure 14

Phosphorylation of S6K1 at Thr389 in the linker region of S6K1 and Ser371 activates S6K1 as a kinase.²⁵⁻²⁶ S6K1 phosphorylates S6, the function of which is unclear. S6 was thought to increase transcription of mRNA with a TOP (tract of pyrimidine) mRNA, which is common within RNA coding for ribosomes and other regulators within the protein translation process.²⁶ However, later evidence did not support this theory.³⁸ Ribosome biogenesis is controlled through the activity of S6K1, which induces the translational activity of RNA polymerase I, resulted in transcription of ribosome proteins.³⁵ S6K phosphorylates a member of the initiation complex (mentioned above) eIF4B, as well as PDCD4 (phosphorylation-dependent degradation of programmed cell death 4) which blocks association of eIF4A to the complex.³³ S6K can also phosphorylate a number of other targets, including mTORC2. S6K1 is also involved in a negative feedback loop, once activated it can phosphorylate and degrade IRS-1 at Ser302, suppressing its activity, including the activation of PI 3-K.^{25, 28}

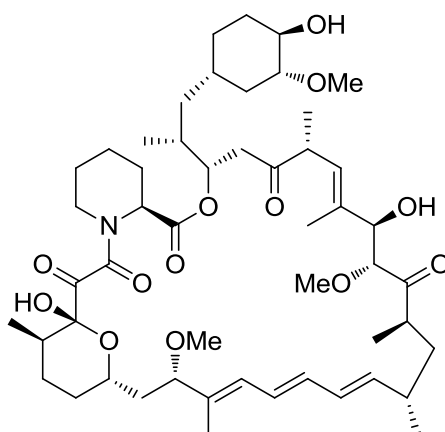
mTORC1 is also linked to autophagy, the process in which cells degrade damaged, redundant or dangerous proteins, providing substrates during low nutrient availability.³⁵ mTORC1 regulates autophagy, inhibiting it at nutrient-rich conditions.²⁵ In yeast, Atg1 plays a vital role in the inducement of autophagy. When forming a complex with Atg13 and Atg17, Atg1 functions as a kinase inducing autophagy. TORC1 phosphorylates Atg13, destabilising the complex and inhibiting Atg1.⁴² In humans, the homolog of Alg1 is Ulk1 and 2, and Ulk1 is

known to function in autophagy. mTORC1 interacts with Ulk1/Atg13/FIP200 (homolog of Atg17) complex and phosphorylate Ulk1 and Atg13.⁴²

The PI 3-K/Akt pathway has wide-reaching consequences for cellular growth and survival. Aberrant signalling within this pathway has been associated with a wide-range of cancers. As mTOR (both within mTORC1 and 2) is rarely mutated it presents an attractive medicinal chemistry target within cancer. The macrolide rapamycin was the first inhibitor of mTORC1, but also contributed to the discovery of mTOR (hence the name target of rapamycin) and is discussed in chapter 2.5, however, the development of ATP-competitive inhibitors of mTOR, which inhibit both complexes, has becoming an area of wide-ranging focus.

2.5 Rapamycin and ‘Rapalogs’

Rapamycin (**2**) is a macrolide produced by the bacteria *Streptomyces hygroscopicus*.³⁴ Discovered during the 1970's in a soil sample from Easter Island (Rapa Nui)³⁴ rapamycin was originally developed by Ayerst as an anti-fungal against *Candida albicans*, *Cryptococcus neoforms* and *Aspergillus fumigates*,⁴³ however, development was stopped on the discovery of potent immunosuppressive activity.³⁴ The deducing of the mechanism of action of rapamycin led to an increase in interest leading to the approval of rapamycin in 1997 as an anti-rejection agent.³⁴ Rapamycin is commonly used in combination with cyclosporine to prevent renal graft rejection.⁴³ However, studies at the NCI also observed anti-tumour activity within both *in vivo* and *in vitro* studies.



2

Figure 15

Rapamycin activity is derived from its activity as a potent (low and sub-nanomolar)⁴⁴ and highly selective allosteric inhibitor of mTORC1. Rapamycin interacts with the immunophilin FK506-binding protein (FKBP12).⁴³ The rapamycin·FKBP12 complex then interacts with mTORC1 *via* the FKBP12 rapamycin binding (FRB) domain, inhibiting the catalytic activity of mTORC1. The FRB domain is a 11 kDa region is adjacent to the PIKK domain, and the formation of the tertiary complex forms a ‘sandwich’ like structure.³⁴ The mechanism by which rapamycin inhibits mTORC1 catalytic activity is unclear, the rapamycin·FKBP12 complex has been proposed to act as a physical obstruction between the mTOR catalytic domain and its substrates. The formation of this complex also appears to destabilise the interaction between mTOR and raptor, despite raptor binding further than 1000 residues away from the FRB domain.³⁸ The resulting loss of the mTOR raptor complex may contribute to the loss of mTOR catalytic activity as the mTOR/raptor complex is required for catalytic activity.

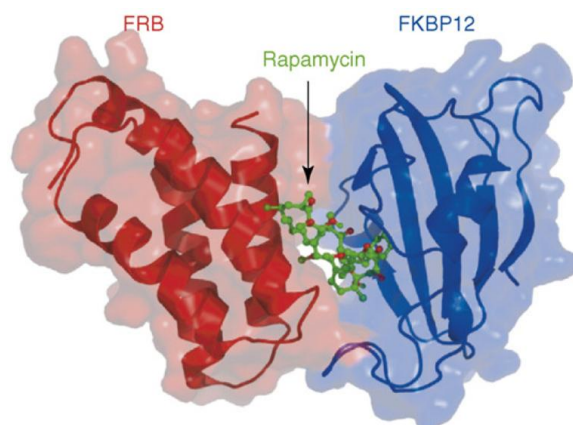


Figure 16 Structure of mTOR FRB, rapamycin and FKBP12 tertiary complex (Taken from reference 34)

Rapamycin is a highly selective molecule, inhibiting only one of the two mTOR complexes. It has been proposed that rictor or a further component of the mTORC2 complex can prevent binding of rapamycin·FKBP12, either by physically blocking the FRB domain or by allosterically altering the FRB binding site on rictor binding.³⁸ However, long term treatment with rapamycin decreases levels of mTORC2, which in approximately 20% of cell lines is sufficient to reduce Akt phosphorylation.³¹ It has been proposed that this is due to the inactivation of mTORC1 by rapamycin, which the cell then compensates for by forming more mTORC1, leaving insufficient mTOR protein available to form mTORC2.²³ Guerin *et al* also

proposed that rapamycin·FKBP12 can bind to recently synthesised mTOR protein, preventing the formation of mTORC2.³³

Rapamycin is a white solid that is soluble in organic solvent; however it is insoluble in aqueous solutions.⁴³ Rapamycin can only be given *via* oral administration; it has rapid absorption with peak concentration reached at 2 h. However, bioavailability of rapamycin is low (only around 15 %) and can vary greatly between patients.⁴⁵ Intestinal CYP450 3A enzymes and P-glycoproteins can influence absorption of rapamycin.⁴⁵

To improve the pharmacokinetic properties of rapamycin a series of semi-synthetic derivatives have been developed. All are very structurally similar to rapamycin, with modifications only at the C40 position, an area not involved in either binding to FKBP12 and mTOR.⁴⁵ Four ‘rapalogs’ have so far been developed – Temsirolimus (**3**) (or CCI-779 from Wyeth),^{34, 44} Everolimus (**4**) (RAD001 from Novartis),^{34, 44} Deforolimus (**5**) (or Ridaforolimus) (AP23573 from Ariad)^{34, 44} and Zotarolimus (**6**) (ABT-578 from Abbott).⁴⁶ All ‘rapalogs’ act *via* the same mode of action as rapamycin.⁴⁵

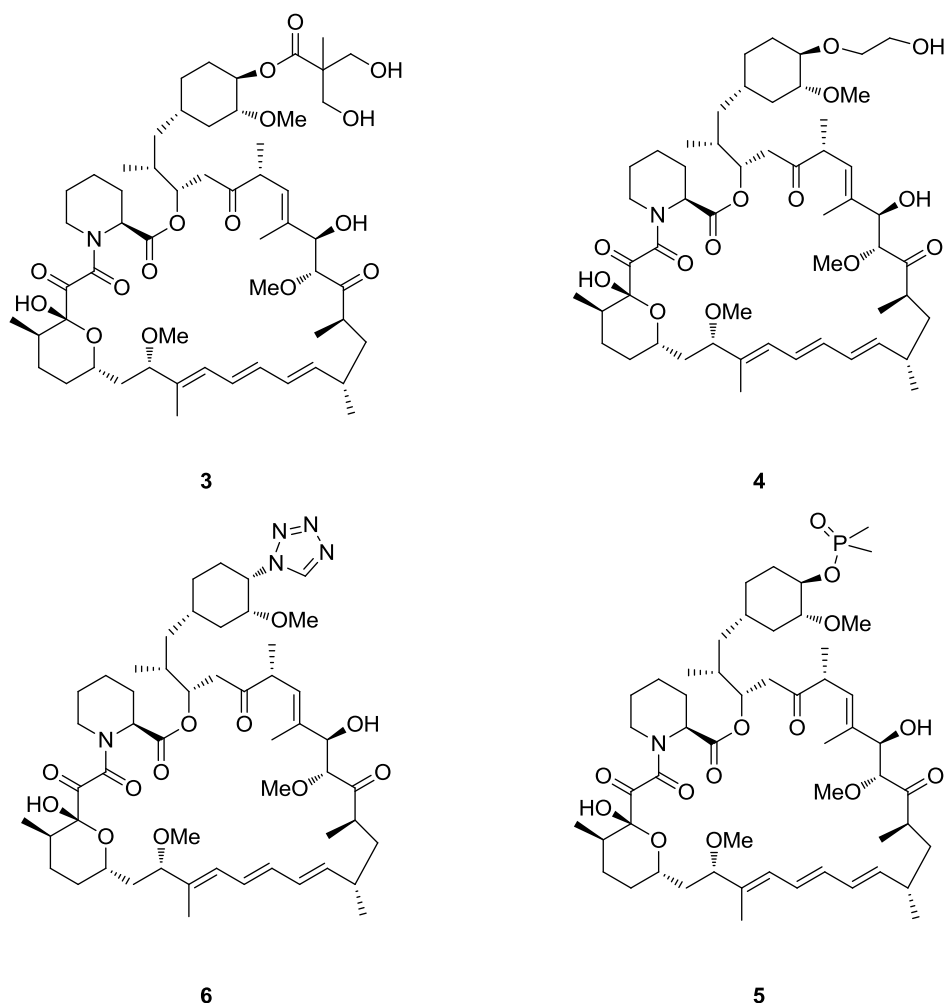


Figure 17

Temsirolimus (**3**) was the earliest analogue of rapamycin. It is a water-soluble ester analogue of rapamycin³⁴ and acts as a prodrug form of rapamycin.⁴⁵ It is rapidly hydrolysed, with intravenous administration rapamycin can be detected as quickly as 15 min with peak concentration between 0.5 h and 2 h.⁴⁵ Temsirolimus was licensed by the FDA in 2007 for use in the treatment of renal cell carcinoma and can be used as either an oral or intravenous administration.⁴⁵

Everolimus (**4**) is a hydroxyl ethyl ether analogue of rapamycin. It has immunosuppressive activity, can be used in a synergistic manner with cyclosporine and was approved in Europe for its immunosuppressant activity.⁴⁵ *In vitro* everolimus has immunosuppressive activity three times lower than of rapamycin, however *in vivo* activity is comparable, due to the improved pharmacokinetics.⁴³ Everolimus also has anti-cancer activity and was licensed in the US for treatment of kidney cancer in 2009.⁴⁷

Deforolimus (**5**) is a phosphinate analogue of rapamycin.³⁴ Deforolimus is the newest addition to the series of rapamycin analogues.⁴⁵ It is stable in organic solutions and aqueous solution at a range of pH. Deforolimus is also stable in both plasma and blood, indicating that **5** does not act as a prodrug *in vivo*.⁴³ Deforolimus had activity against a range of cell lines *in vitro*⁴³ and is currently in phase III clinical trials.⁴⁸

Zotarolimus (**6**) is a rapamycin analogue designed to be used as a drug to elute from coronary stents to prevent restenosis.⁴⁶ It replaces the C40 hydroxyl group with a tetrazole moiety.⁴⁴

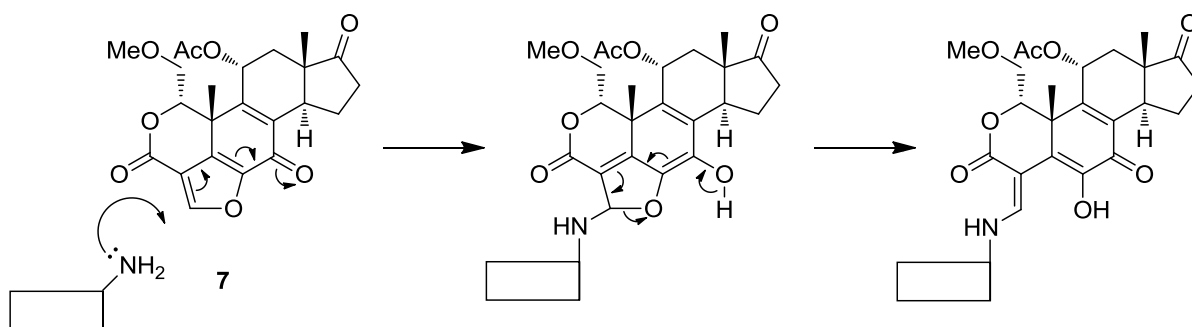
Rapamycin and its analogues are well tolerated and share similar side-effects.⁴⁵ However, identification of the correct subset of patients who will benefit from rapamycin or rapalog treatment is vital as within trials less than 10% of patients responded.³⁴ Rapamycin treatment can trigger an S6K1 dependant negative feedback loop which leads to increased signalling from IRS1/2, leading to increased activation of Akt, as well as MEK-ERK signalling.^{23,33} This reduces the usefulness of rapamycin and rapalogs as a treatment for cancer. Rapamycin and rapalogs have been found to be useful in mantle cell lymphoma, renal cell carcinomas and endometrial cancer, a small number of cancers, given that aberrant signalling within the PI 3-K/Akt pathway is very common.⁴⁹ However, it is thought that an ATP-competitive inhibitor of mTOR, which should in theory target equally both complexes of mTOR, will avoid this issue by targeting the pathway at two points, leading to a more pronounced effect on cellular growth and survival. An ATP-competitive inhibitor will also be useful as mTORC2 has been implicated in some cancers.³³

2.6 mTOR Inhibitors Targeting the Kinase Domain

The PI 3-K/Akt pathway is a key cellular pathway regulating cellular proliferation and growth, survival and protein synthesis.²⁹ The significance of this pathway within cancer lies within frequent mutation, such as mutation or amplification of the *PIK3CA* gene, which is mutated in around 15% of tumours, making it the most commonly mutated kinase within the human genome.²⁹ In view of the frequency with which the PI 3-K/AKT pathway has aberrant signalling in cancers, it is thought that targeting this pathway could have a wide range of therapeutic uses. There is a wide range of evidence validating kinases within this signalling cascade as therapeutic targets.²⁹ Applying Luo *et al*'s theory of oncogene and non-oncogene addiction,⁵ a number of tumours are 'addicted' to the PI 3-K/Akt pathway. Targeting this

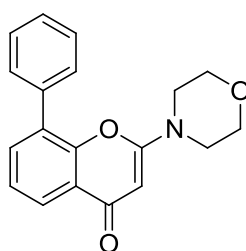
pathway on which the tumour is ‘addicted’ should selectively target tumour cells over normal cells. Crucially, mTOR itself, which is a key component of this pathway, is rarely mutated,³⁴ making mTOR a non-oncogene addiction. This can prove beneficial for the purpose of drug discovery as the tumour relies on this kinase for continual growth and replication but genetically mTOR is stable and unlikely to mutate, leading to small-molecule inhibitors becoming ineffective. For these reasons, mTOR has become an increasingly popular target within both academic and pharmaceutical drug discovery.

An early inhibitor of both complexes of mTOR was the natural product Wortmannin (**7**), which inhibits mTOR with an IC_{50} of 40 nM.⁵⁰ Wortmannin is a pan PI 3-K and PIKK inhibitor, which binds in the ATP-binding site and then covalently modifies the protein, through a reaction with a Lys residue (Lys833 in PI 3-K γ)⁵¹ and the C-21 position of Wortmannin in a Michael-type reaction.⁵² Wortmannin is unstable in solution, but has some uses as probe compound.⁵¹



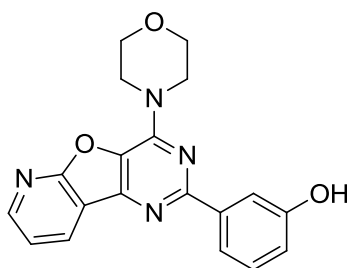
Scheme 1 Mechanism of covalent attack by the PI 3-K on Wortmannin

The first example of an ATP-competitive inhibitor of mTOR is the pan PI 3-K and PIKK ATP-competitive inhibitor LY294002 (**8**). The compound, developed by Lilly, inhibits mTOR with an IC_{50} of 5 μ M.⁵³



LY294002
8

The compound PI-103 was synthesised as part of a programme to develop isoform selective inhibitors of PI 3-K but was also found to have off-target activity including inhibition of mTOR.⁵⁴⁻⁵⁵ PI-103 inhibits mTORC1 89% at 0.50 μ M, but has greater activity against PI 3-K with an IC₅₀ of 2, 3 and 3 nM against α , β and γ isoforms respectively.⁵⁶ PI-103 also inhibits the PIKK family member DNA-PK, with an IC₅₀ of 14 nM.⁵⁶ PI-103 demonstrated a rapid effect, with phosphorylation of Akt at both Ser473 (mTORC2 site) and Thr308 (PDK1 site) inhibited within 15 min of treatment.⁵⁶ PI-103 also showed activity with human tumour xenografts with upregulation of the PI 3-K pathway.⁵⁶ However, PI-103 has a poor metabolic profile, with greater than 70% metabolism after 30 min incubation with human microsomes which combined with the ‘dirty’ inhibition profile of PI-103 would be undesirable as a drug.

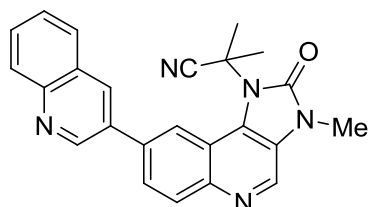


PI-103
9

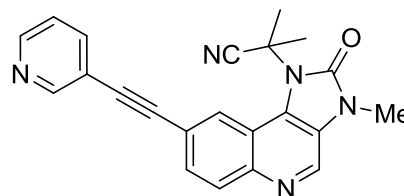
Stauffer *et al* have demonstrated that the imidazo[4,5-*c*] scaffold is a privileged scaffold for the development of ATP-competitive kinase inhibitors.⁵⁷ From this series two dual PI 3-K/mTOR inhibitors have been developed, NVP-BEZ235 (**10**) and NVP-BBD130 (**11**), are both potent and stable, orally administered agents.⁵⁸ NVP-BEZ235 has IC₅₀s of 4, 75, 7, 5 nM against PI 3-K isoforms α , β , δ and γ respectively. **10** also inhibits mTOR with an IC₅₀ of 20.7 nM within a KLISA assay and *in vitro* has an IC₅₀ of 6.5 nM measuring reduction of phosphorylation of S6 at Ser235.⁵⁹ NVP-BBD130 has IC₅₀s of 72, 2340, 201 and 382 nM against PI 3-K isoforms α , β , δ and γ respectively, and an IC₅₀ against mTOR of 7.7 nM determined by measuring phospho S6.⁵⁸ By measuring autophosphorylation of DNA-PK on treatment with NVP-BEZ235, inhibition of DNA-PK was observed, though only at high concentrations of NVP-BEZ235.⁵⁹

Docking of NVP-BEZ235 into a PI 3-K γ -based 3-D homology model of PI 3-K α kinase domain demonstrated that **10** forms three H-bonds with the protein. The core quinoline nitrogen forms one H-bond with PI 3-K α Val851, the quinoline substituent nitrogen forms a hydrogen bond with the backbone of Asp933 and the nitrile nitrogen interacts with the side-

chain of Ser774.⁵⁹ Hydrophobic interactions with Met772, Tyr836 and Met922 also contribute to binding.⁵⁹ Homology modelling with mTOR suggests similar binding, including replication of the H-bond to the Ser2165 (mTOR numbering) side chain.⁵⁹



NVP-BEZ235
10

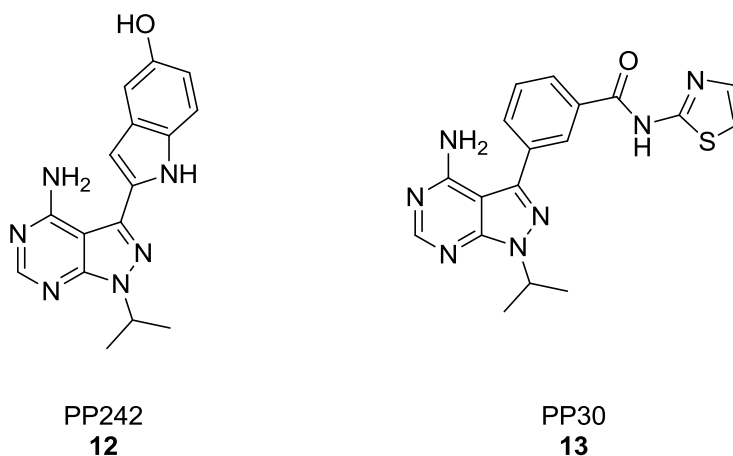


NVP-BBD130
11

Treatment of Pten-null cell-lines PC3M and U87MG with **10** demonstrated a dose-dependent effect on cell-proliferation, with a GI₅₀ of 10-12 nM.⁵⁹ NVP-BEZ235 has a cytostatic effect, inducing growth arrest at G₁ due to downregulation of cyclin D1. However **10** can increase the efficiency of anticancer drugs, such as temozolomide in combination.⁵⁹ Treatment of tumour-bearing mice with both NVP-BEZ235 and NVP-BBD130 reduced neovascularisation, without effecting pre-existing vessels.⁵⁸ Both NVP-BEZ235 and NVP-BBD130 have a good pharmacological profile, with high and prolonged cellular exposure.⁵⁸ Treatment of PC3M with a 50 mg/kg dose of NVP-BEZ235 resulted in a plasma C_{max} of 1.68 μM at 0.5 h and a C₂₄ of 0.03 μM. Within the tumour tissue a C_{max} of 2.05 nM was observed after 1 h, which after 24 h was decreased to 0.23 nM. NVP-BEZ235 is currently in phase I/II clinical trials in solid tumours.⁴⁹

During synthetic efforts to develop dual tyrosine and PI 3-K inhibitors a number of mTOR inhibitors were developed.⁶⁰ PP242 and PP30 share a pyrazolopyrimidine scaffold and inhibit mTOR with an IC₅₀ of 0.008 and 0.080 μM respectively.⁶⁰⁻⁶¹ PP242 also demonstrates a minimum of 10-fold selectivity over all isoforms of PI 3-K,⁶¹ and in a screen against 219 protein kinases at a concentration 100-fold above that of the mTOR IC₅₀, only demonstrated at 90% inhibition of one kinase and three at 75%.⁶⁰ Due to the selectivity of PP242 and PP30 over PI 3-Kα, the functions of mTOR within the PI 3-K/Akt can be explored and the different response to mTOR kinase domain inhibition and rapamycin can be explored.⁶¹ PP242 was shown to have a dose-dependent inhibition of proliferation, and inhibited phosphorylation of

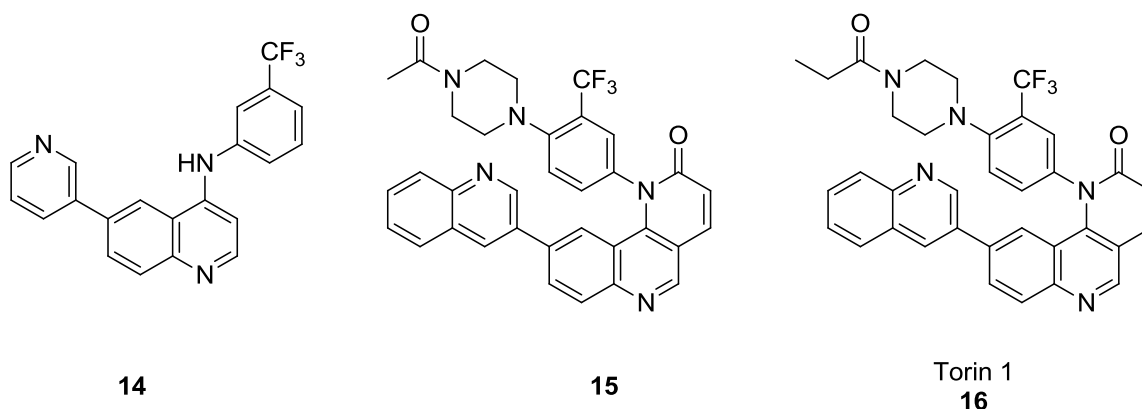
4E BP1 at Thr36, Thr45 and Ser65 to a greater extent than rapamycin, suggesting that some functions of mTORC1 are insensitive to rapamycin treatment.⁶¹



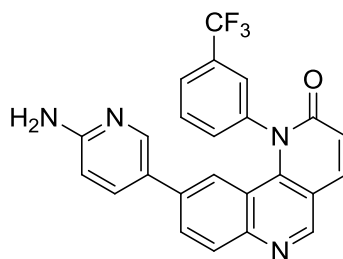
Development of the Torin series of inhibitors has resulted in a highly potent mTOR inhibitor. During SAR exploration of 6-(pyridin-3-yl)-*N*-(3-(trifluoromethyl)phenyl)quinolin-4-amine (**14**) it was observed that compound **10** contained a cyclic urea moiety which constrains substituents in the ideal conformation for biological activity. Luo *et al* decided to incorporate a six-membered lactam to hold the trifluoromethyl substituted aniline in the optimal position which after further optimisation, and addition of an acetyl substituted piperazine gave compound (**15**), which was observed to improve biological activity against mTOR from 5 μ M to 5.4 nM.⁶² Compound **15** was then docked into an mTOR homology model based on the crystal structure of PI 3-K γ . It was proposed that compound **15** forms a hydrogen bond between the quinoline nitrogen and Val2240 in the hinge, with the quinoline substituent positioning in an inner hydrophobic pocket consisting of Glu2190, Leu2192, Asp2195, Tyr2225, Asp2357, Phe2358, Gly2359 and Asp2360 and the substituent quinoline nitrogen is proposed to form a hydrogen bond with Tyr2225 side-chain. The phenyl piperazine substituent positioned below a loop consisting of residues 2183-2187 and the acyl carbonyl carbon is thought to form a hydrogen bond with the amine of Lys2186.⁶² Optimisation of the acyl substituent to a propyl amide increased activity to an IC₅₀ of 0.29 nM against mTOR, and a cellular IC₅₀ of 2 nM, this compound was named Torin1 (**16**) and subjected to further biochemical analysis.⁶²

Torin1 has 800-fold selectivity over PI 3-K and is highly selective over other PIKK enzymes with the exception of DNA-PK. Within LanthaScreen analysis **16** has an IC₅₀ against mTOR of 4.32 nM and against DNA-PK of 6.34 nM, however, within a radiometric kinase assay

against DNA-PK it has a IC_{50} of approximately 1 μM .⁶² Both human and mice microsomal stability studies revealed a half-life of 4 min, and *in vitro* studies demonstrated a half-life of 0.5 h, which is proposed to be due to high first-pass metabolism. Intraperitoneal dosing resulted in suppression of phosphorylation at Akt Ser473 for 2-3 h and phosphorylation of S6 (an indirect target of mTORC1 activity) was inhibited for 6 h in the lungs and 10 h within the lungs.⁶² A U87MG xenograft model, which is a Pten-null glioblastoma cell line, demonstrated 99% inhibition of growth inhibition after 10-days dosing, but growth returned after cessation of treatment, suggesting Torin1 is cytostatic.⁶²



Due to the pharmacokinetic problems, poor water solubility and low oral bioavailability of Torin1 further synthetic efforts were directed towards identification of a further compound with improved properties.⁶³ It was proposed that by reducing the molecular mass of **16** a more water-soluble compound could be developed, which would potentially reduce the sites for metabolism.⁶³ Removal of the piperazine moiety, and replacement of the substituent quinoline groups with amino-substituted pyridine resulted in compound **17** Torin2. Torin2 has an EC_{50} of 0.25 nM and is estimated to be 10-fold more potent than Torin1. Torin2 also maintains 800-fold selectivity over PI 3-K.⁶³ **17** is predicted to bind in a similar mode to compound **15**, with the hinge hydrogen bond maintained. The pyridine nitrogen forms a hydrogen bond to Tyr2225. The pyridine amino substituent forms two hydrogen bonds with Asp2195 and Asp2357.



Torin2
17

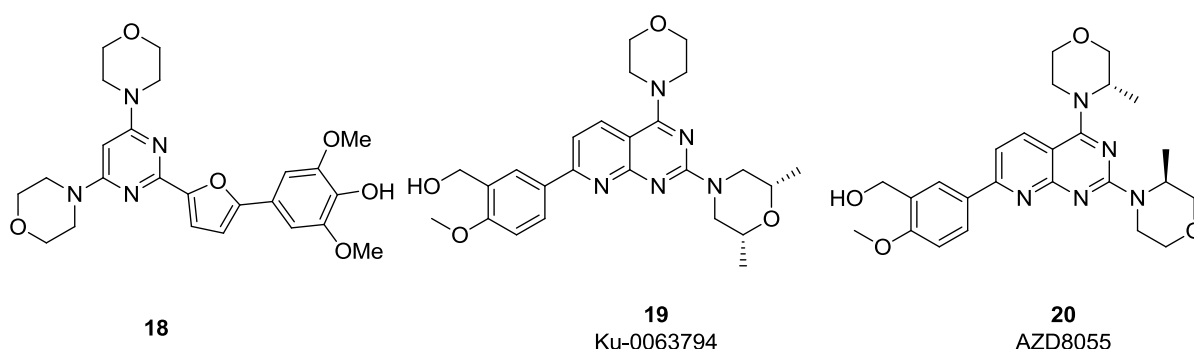
Torin2 displayed improved pharmacodynamics over Torin1, with over 95% inhibition of phosphorylation of S6K Thr389 and Akt Thr308 after 6 h in lung and liver tissue. **17** also has a $t_{1/2}$ of 11.7 min in liver microsomes and on intravenous and oral dosing in mice had a $t_{1/2}$ of less than 2 h. Torin2 has improved oral bioavailability of 51%.⁶³ LanthaScreen assay analysis of Torin2 has an IC_{50} of 2.81 nM (against mTOR) and 0.5 nM (against DNA-PK), though kinase assay activity of **17** against DNA-PK has not been reported.

Development of Torin1 has also supported the findings of Feldman *et al* who demonstrated that ATP-competitive inhibitors of mTOR inhibited a greater range of mTORC1 phosphorylations than rapamycin.⁶¹ Treatment of MEFs (mouse embryonic fibroblasts) with Torin1 reducing protein synthesis by 50%.⁶⁴

KuDOS pharmaceuticals published two series of ATP-competitive inhibitors of mTOR in 2009.⁶⁵⁻⁶⁶ The first series is based on either a pyrimidine or triazine scaffold, optimisation gave compound **18**, with an IC_{50} of 0.023 μ M, and selectivity over PI 3-K α , with an IC_{50} > 10 μ M. However, this series shown disappointing cellular activity, which was possibly due to poor cell permeability.⁶⁶ The second series was based on pyridopyrimidine scaffold, with optimisation leading to compound **19**.⁶⁵ Compound **19** (also known as Ku-0063794) has an IC_{50} of 0.016 μ M. Cell-line U87MG was treated with **19** for 2 h and inhibition of phosphorylation of S6 at Ser235 and Akt Ser473 was measured with IC_{50} s of 0.10 and 0.15 μ M observed for these targets respectively. Treatment of the T47D breast cancer cell line with **19** resulted in a GI_{50} of 0.35 μ M.⁶⁵ On treatment of 76 protein kinases with 1 μ M of **19**, no significant inhibition was observed and at 10 μ M only one kinase showed any significant degree of inhibition, the MAPK kinase-1, with 55% inhibition at 10 μ M. This panel also included PI 3-K α and β .⁶⁷

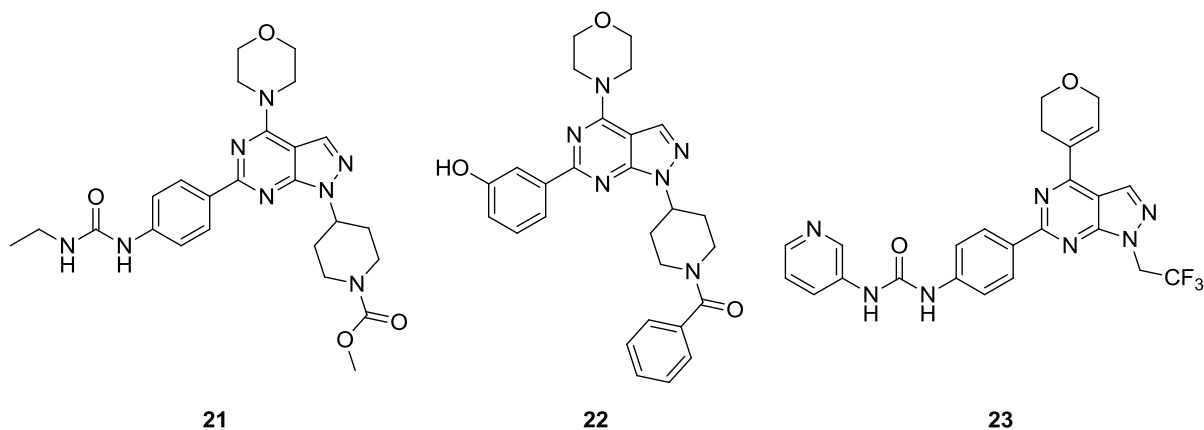
As with previous compounds Ku-0063794 has a greater effect on 4E BP1 phosphorylation than rapamycin and induces G₁ growth arrest. Treatment of HEK-293 (human embryonic kidney) cells with **19** resulted in almost complete loss of S6K activity, resulting in a decrease of phospho-S6. This effect was rapid, with maximal inhibition observed within 10 min. Inhibition of Akt phosphorylation at Ser473 was also observed, with a knock-on decrease in Akt target phosphorylations.⁶⁷ Garcia-Martinez *et al* also proposes that Ku-0063794 is more selective than PP242. At 1 μ M 22 out of 76 kinases were inhibited by PP242 at > 50%, and 46 out of 76 were inhibiting at > 50% at a concentration of 10 μ M, unlike Ku-0063794, which only inhibits one other kinase > 50% at 10 μ M.⁶⁷

Further development resulted in AZD8055 (**20**), a potent, selective and orally available ATP-competitive inhibitor of mTOR.⁶⁸ AZD8055, is currently in phase I/II clinical trials for solid tumours, including hepatocellular carcinoma.⁴⁹ **20** has an IC₅₀ of 0.13 nM against truncated mTOR, and 0.8 nM against mTOR extracted from HeLa cells. A range of ATP concentrations resulted in a linear IC₅₀, indicating **20** is ATP-competitive, and has a K_i of 1.3 nM. Counterscreening against class I and II PI 3-K, DNA-PK and ATM, demonstrated a 1000-fold selectivity for mTOR and a panel of 260 other kinases demonstrated no significant activity at 10 μ M.⁴⁹ In MDA-MB-468 cells an IC₅₀ of 24 nM and 27 nM was calculated for phosphorylation of Akt Ser473 and S6 Ser235.⁴⁹ Xenograft studies with U87-MG bearing mice observed that after a 10 mg/kg oral dose phosphorylation of Akt at Ser473 had decreased to 5% of control level after 20 min, and inhibition of phosphorylation was greater than 50% for at least 8 h. Phosphorylation of S6 at Ser235 was decreased to 21% of control level after 20 min, though after 8 h 63% of control level of phosphorylation was observed.⁴⁹

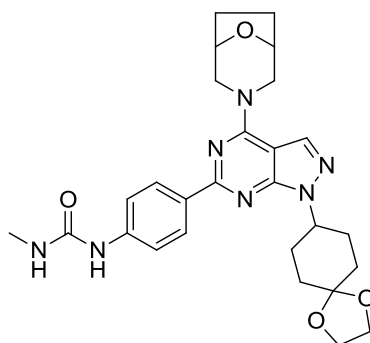


One of the most potent and selective mTOR inhibitors has been developed by Wyeth Pharmaceuticals, who have published a number of articles on the development of ATP-competitive inhibitors of mTOR.⁶⁹⁻⁷⁶ The Wyeth compounds e.g. 21-23 contain a pyrazolopyrimidine core, where potency was achieved with morpholine, piperidine and

aromatic substituents,⁷² but replacement of the morpholine moiety with a bridged morpholine groups in the 4-position achieved selectivity over PI 3-K α .⁷⁶ Docking of this series of compounds into an mTOR homology model, based on the crystal structure of PI 3-K γ suggested that the morpholine group forms a hydrogen bond with a hinge residue Val2240 backbone NH. The pocket the morpholine groups occupy is defined by Tyr867 and Cys885 (PI 3-K γ numbering), which limits the size of the substituent, tolerates an ethyl bridged morpholine, but not a dimethyl morpholine. Within mTOR, the bridged morpholine derivative can still interact with Val2240, however, within PI 3-K, this interaction cannot occur, resulting in a loss of PI 3-K activity. A single change in amino acid is thought to be the grounds for this selectivity. mTOR has a smaller Leu residue, which tolerates the bridged morpholine group, whilst PI 3-K has a Phe residue, which creates a smaller pocket, ensuring the bridged morpholine is not tolerated.^{71, 76}

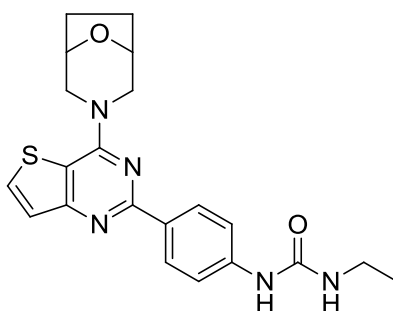


WYE-132 (**24**)⁷⁰ is the most potent and selective compound developed in this study, with an mTOR IC₅₀ of 0.21 nM and PI 3-K α IC₅₀ of 1180 nM, giving 5619 fold selectivity.⁶⁹ **23** has high selectivity over ATR, with an IC₅₀ of >10000 nM and hSMG1 (IC₅₀ = 1250 nM) and in a panel of 230 protein kinases was largely inactive.⁷⁰ **24** also has a LNCap cellular assay IC₅₀ of 2 nM and was shown to have metabolic stability with a half life of greater than 30 min in murine microsomes and 26 min in human microsomes.⁶⁹



WYE-132
24

The selectivity of WYE-132 was tested using biomarkers in a nude mouse MDA361 xenograft model. Treatment with WYE-132 showed complete inhibition of phosphorylation at the mTORC1 biomarker S6K Thr389, sustained suppression of the mTORC2 biomarker Akt Ser 473 and complete inhibition of the downstream biomarker S6 Ser 240/244 for 8 h at a dose of 25 mg/kg. No phosphorylation was observed at the PI 3-K biomarker Akt Thr308, demonstrating the selectivity of this compound.⁶⁹ Within the nude mouse model a dose of 25 mg/kg resulted in complete inhibition of growth of the tumour but with no significant weight loss within the mice.⁶⁹ WYE-132 has been demonstrated to induce a G₁ arrest, and like other compounds has been demonstrated to fully inhibit 4E BP1, unlike the rapalog CCI-779.⁷⁰ Treatment of an oral 5 mg/kg dose of **24** in a MDA361 tumour resulted in a growth delay in a dose-dependent manner, and within MDA361, BT474, LNCap and H1975 cell-lines, which all have both PI 3-K/mTOR and Her-2 hyperactivation, a significant apoptotic response was observed.⁷⁰

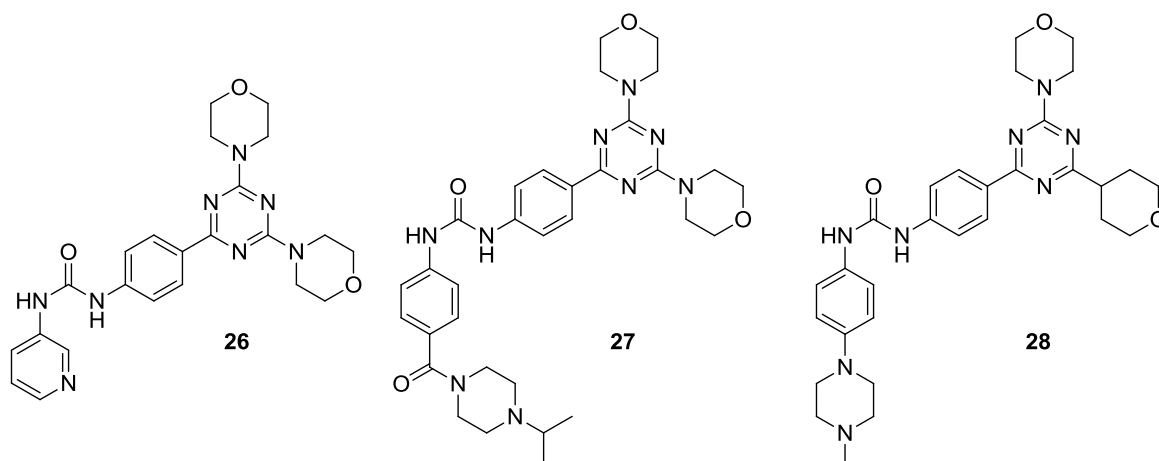


25

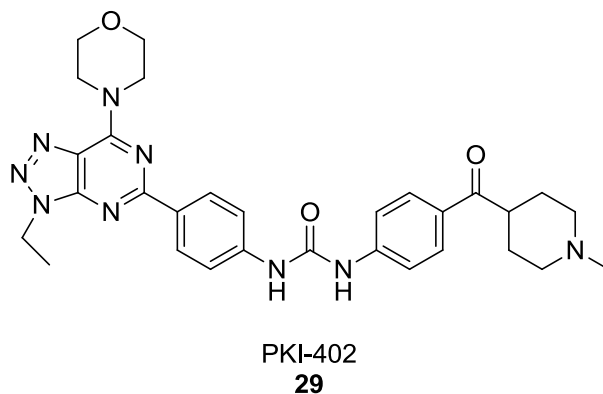
Wyeth also published on an alternative series of mTOR inhibitors which replace the pyrazolopyrimidine core with a thienopyrimidine core e.g. **25** (IC₅₀ = 0.7 nM).⁷⁷ Potency in this series of compound is good, as is selectivity, but cellular potency is slightly lower than in the pyrazolopyrimidine series.⁷⁷ Further work identified a dimorpholine substituted triazine moiety as having activity against mTOR.⁷⁸ Incorporation of bridged morpholines was shown

to increase selectivity for mTOR over PI 3-K α , and side chains at 4-position of the ureidophenyl type of previous molecules such as **24** increased potency.⁷⁸ Unfortunately, the bridged morpholine groups were seen to be the primary site of metabolism of these compounds.⁷⁹ Synthetic efforts were then directed towards identification of alternative groups for the 2- and 6-position, that maintains potency and selectivity over PI 3-K α , as well as identification of the optimal position of the 4-position.⁷⁹⁻⁸⁰ The optimal replacement for the bridged morpholine groups were found to be either a tetrahydropyran group or a (*R*)-3-methylmorpholine.⁸⁰ For the 4-position substituent, a basic group was found to improve cellular activity, though selectivity was reduced in comparison with previous analogues (e.g. **24**), a range of compounds were synthesised, including **26** with an IC₅₀ of 0.2 nM, **27** with an IC₅₀ of 0.7 nM and **28** with an IC₅₀ of 0.7 nM.⁸⁰

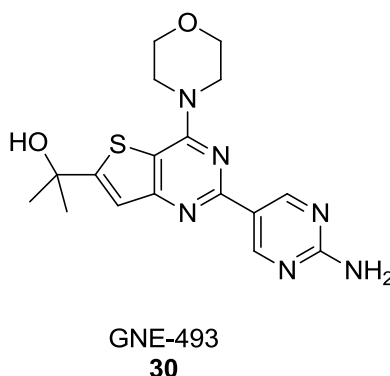
27 has the poorest selectivity over PI 3-K α , only 131-fold, with both **26** and **28** having at least 400-fold selectivity for mTOR over PI 3-K α . The highest cellular IC₅₀ were observed for **27** with values < 0.8 nM in both LNCaP and MDA468 cell-lines.⁸⁰



Along with these series of selective ATP-competitive inhibitors of mTOR, Wyeth have also published a number of dual PI 3-K/mTOR inhibitors, including PKI-402 (**29**).⁸¹ These dual PI 3-K/mTOR inhibitors have a triazolopyridimidine core and have a morpholine group on the 4-position of the pyrimidine. The structure of PKI-402 is shown below. PKI-402 has an IC₅₀ of 1.4, 9.2 and 1.7 nM for PI 3-K α , γ and mTOR respectively and an IC₅₀ of 8 nM in MDA-361 cell lines. Compound **29** was also shown to induce cleaved PARP enzymes, a marker of apoptosis.⁸¹



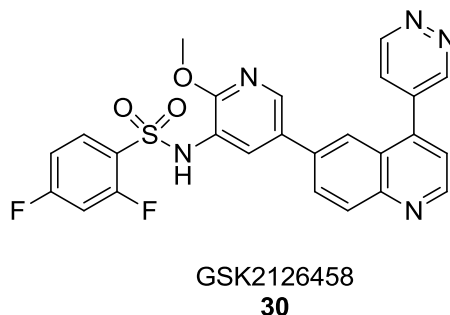
Sutherlin *et al* have also developed a dual mTOR/PI 3-K inhibitor. GNE-493 (**30**) is an orally available inhibitor and has good selectivity over other kinases.⁸² Compound **30** has an IC_{50} of 3.4 and 30 nM for PI 3-K α and mTOR respectively and in nude mice has a half life of 3.6 h.⁸² GNE-493 was also shown to be 0.5-2 more potent within PC3 and MCF7 cell lines than a PI 3-K inhibitors alone.⁸²



The dual PI 3-K/mTOR inhibitor GSK2126458 (**30**), is currently in phase I clinical trials for solid tumours or lymphomas.⁴⁹ **30** was originally developed as a potent PI 3-K inhibitor and has a PI 3-K α IC_{50} of 0.04 nM, but is also active against other isoforms of PI 3-K. **30** was also found to have both mTOR and DNA-PK activity, with a K_i of 0.18 and 0.3 nM against mTORC1 and mTORC2 respectively, and a DNA-PK of 0.28 nM.⁸³ GSK2126458 was crystallised with PI 3-K γ , which demonstrates that the pyridyl nitrogen forms a H-bond with a conserved water molecule, the sulphonamide interacts with Lys833, the difluorophenyl group sits within a hydrophobic pocket and the quinoline nitrogen forms a hydrogen bond to Val882 within the hinge.⁸³

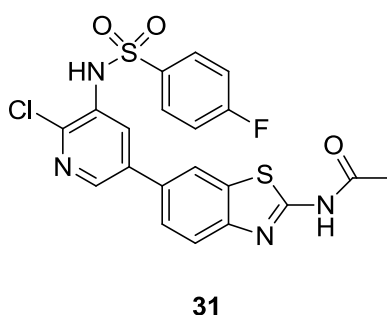
In cellular assays, **30** induces G_1 arrest and *in vivo* has good oral bioavailability and low clearance. Monitoring of pharmacodynamic response indicated that a single dose of 300 $\mu\text{g/mL}$ resulted in a decrease in phosphorylation of Akt for 10 h, with a return to control

levels after 24 h. Within a BT474 xenograft model treatment with **30** resulted in dose-dependent decrease in tumour growth.



D'Angelo *et al* have described the synthesis of a series of benzothiazole-based dual PI 3-K/mTOR inhibitors.⁸⁴ Compound **31** has an IC_{50} against mTOR of 2.0 nM and a K_i against PI 3-K α of 1.2 nM, though **31** also inhibits PI 3-K β , γ and δ with an $K_i < 5$ nM, DNA-PK with an IC_{50} of 3 nM and hVsp34 with a K_i of 31 nM.⁸⁴

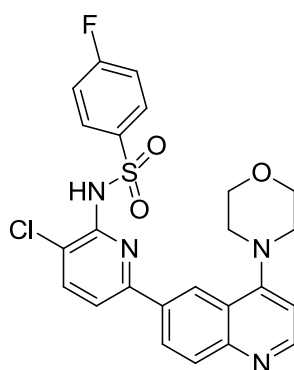
Crystallisation of **31** with PI 3-K γ identified that the *N*-acetylbenzothiazole forms two hydrogen bonds with Val882 backbone, and a hydrogen bond with Tyr867 and Asp841 *via* a water molecule to the pyridine ring nitrogen.⁸⁴ **31** displayed stability to both human liver microsome and rat liver microsomes of greater than 50 (μ L/min)/mg, and *in vivo*, after intravenous administration had clearance of 0.007 (L/h)/kg and a half life of 19 h. Given orally to rats, **31** has an oral bioavailability of 103%.⁸⁴ Pharmacodynamic analysis of **31** identified a dose dependant decrease in the phosphorylation of Akt Ser473, and significant inhibition was observed for 24 h after dosing.



However, further investigation revealed that *in vivo* compound **31** is metabolised to the deacetylated compound.⁸⁵ To avoid this two approaches were taken. In the first, the *N*-acetyl amino benzothiazole moiety was replaced with a range of 6,6-heterocycles, which negated the requirement for the acetamide moiety of compound **31**.⁸⁵ The second approach replaced the benzothiazole moiety with a range of 6,5-bicyclic heterocycles, with the aim of identifying a more stable acetamide moiety.⁸⁶

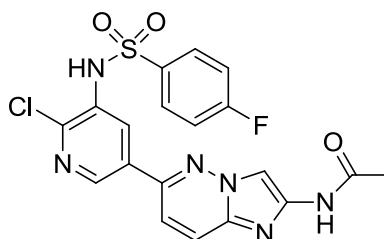
The *N*-acetyl 2-aminobenzothiazole moiety forms two key hydrogen bonds with Val882 backbone, the benzothiazole nitrogen interactions with Val882 NH and the amino hydrogen atom interacts with the carbonyl of Val882.⁸⁵ It is these interactions which any 6,6 heterocycle must reproduce to maintain activity. It was also postulated that substitution from either the 3- or 4-position of a 6,6-heterocycle could probe the ribose pocket and lead to a further increase in potency.⁸⁵ After synthesis of a range of heterocycles a quinoline was found to maintain potency comparable to the *N*-acetyl 2-aminobenzothiazole analogue. Substitution with a morpholine group at the 4-position of the quinoline ring which lead to a further increase in potency, gave **32**, with an IC₅₀ against PI 3-K α of 0.6 nM, and *in vitro* activity of 4.6 nM against PI 3-K α and 3.9 nM against mTOR. Compound **32** is also active against all isoforms of PI 3-K, hVsp34 and DNA-PK.⁸⁵

X-ray crystallography of compound **32** bound in PI 3-K γ active site revealed that the quinoline nitrogen forms a hydrogen bond with Val882 backbone NH, the hydrogen bond formed between the pyridyl nitrogen Asp841 and Tyr867 in compound **31** is maintained, though the morpholine ring points out towards solvent, rather than toward the ribose pocket as predicted.⁸⁵ **32** has good metabolic stability in both rat liver microsomes and human liver microsomes, *in vivo* clearance was good (0.17 L/kg/h) and good bioavailability (92%).⁸⁵ *In vivo* pharmacodynamic modelling demonstrated that after 3 h, a 3 mg/kg dose resulted in 97% inhibition of Akt Ser473 phosphorylation. In a Pten-null U-87 MG glioblastoma model oral dosing of 10 mg/kg daily reduced growth to 28% of control.⁸⁵

**32**

Design of alternative 5,6-heterocycles to replace the benzothiazole moiety identified imidazopyridazines as having good potency. Compound **33** has a K_i of 1.4 nM against PI 3-K α (with activity also observed against other isoforms), an IC₅₀ of 0.4 nM against mTOR and

an IC_{50} of 13 nM for the phosphorylation of Akt within U87 MG.⁸⁶ Incubation with hepatocytes and microsomes revealed the acetyl group of compound **33** was stable, with only trace amounts of deacetylation observed.⁸⁶ *In vivo* **33** had low clearance 0.04 L/h/kg and an oral bioavailability of 46%. A xenograft model with U87 MG, demonstrated that 3mg/kg once a day dosing resulted in tumour stasis.

**33**

The mTORC1/2 inhibitor OSI027 is currently in phase I clinical trials for solid tumours and lymphomas. The structure of OSI027 has not currently been revealed, but synthetic efforts directed towards the discovery of OSI027 have recently been published. Crew *et al* describe the optimisation of a series of imidazo[1,5-*a*]-pyrazine compounds.⁸⁷ Several other inhibitors of mTOR are currently in clinical trials but the structure of these compounds has not been disclosed. These include XL765, a dual mTOR (IC_{50} = 157 nM) and PI 3-K α (IC_{50} = 39 nM) inhibitor in phase I clinical trials for solid tumours, non-small-cell lung cancer and malignant glioma and phase I/II for breast cancer, and GDC0980 a further dual inhibitor with an IC_{50} of 17.3 nM (against mTOR) and 4.8 nM (against PI 3-K α). GDC0980 is currently in phase I trials for non-Hodgkin's lymphomas and solid tumours. An mTOR selective inhibitor currently in phase I trials is INK128, with an IC_{50} against mTOR of 1 nM.⁴⁹

All ATP-competitive inhibitors of mTOR are either selective for mTOR or dual PI 3-K/mTOR inhibitors. Whether an mTOR selective inhibitor or a dual PI 3-K/mTOR will be optimal has yet to be established. Inhibition of both mTORC1 and mTORC2 is well tolerated within adult tissue. During mouse models of leukaemia with PP242, only a mild effect was observed on normal lymphocytes. However, selective mTOR inhibitors can potentially suffer from problems due to the S6K negative feedback loop. Lack of mTORC1 signalling results in continued signalling from IRS-1, which results in the conversion of PtdIns (4,5) P₂ to PtdIns (3,4,5) P₃ recruiting PDK1. As PDK1 phosphorylation is not inhibited by selective mTOR inhibitor, loss of mTORC1 signalling results in PDK1 phosphorylation of Akt, which if a suboptimal dose of an mTOR selective inhibitor is used, can result in full Akt activation.³⁵

Rodrik-Outmezguine *et al* have observed that treatment of a number of cell lines with AZ8055 resulted in inhibition of phosphorylation of Akt Ser473, S6K and 4E BP1 for greater than 24 h.⁸⁸ Inhibition of Akt Thr308 was also observed, although after 4 h phosphorylation levels began to return to baseline levels, as well as the phosphorylation levels of Akt targets including PRAS40 and FOXO1/3, inhibition of Akt Thr308 is only temporary. Treatment of PP242 was also observed to have the same effect, and this effect was identified as being due to reactivation of Akt as a result of AZ8055 and PP242 activation of PI 3-K. However, cotreatment with either an Akt inhibitor or an HER kinase inhibitor, the phosphorylation of PRAS40 and FOXO1/3 was not observed. In cells treated with both a Akt inhibitor and AZ8055 an increase in the level of apoptotic cells was observed, as well as an increase in levels of cleaved PARP and caspase-3.⁸⁸

A PI 3-K/Akt inhibitor would avoid the activation of Akt but may prove more toxic to normal cells. In studies with PI-103, a toxic effect on normal lymphocytes was also observed,³⁵ however, this could be due to the slightly promiscuous profile of PI-103. The current clinical trials should illuminate which class of inhibitor is optimal for tumours addicted to the PI 3-K/Akt pathway.

3. MDM2/p53: An Anti-Cancer Target

3.1 Inhibitors of Protein-protein Interaction

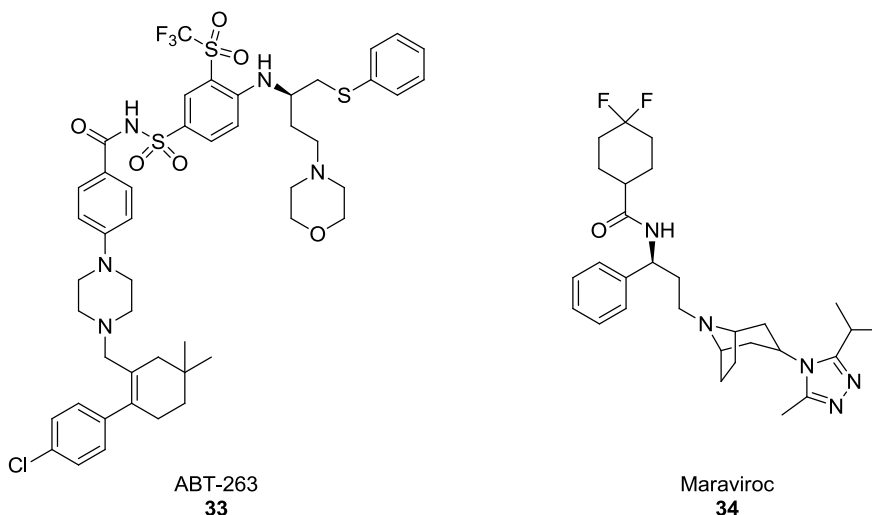
Inhibition of protein-protein interactions is an important area within medicinal chemistry. Protein-protein interactions control a number of cellular processes including mammalian immune response, recognition between cells, signal transduction and transcription. These interactions are not random but the result of the particular structures of each protein involved.⁸⁹

The development of small molecule protein-protein inhibitors faces a number of challenges. Unlike enzymes, where the active site is small and frequently shielded from solvent,⁹⁰ protein-protein interactions occur over large areas (750 -1500Å on each protein)⁸⁹ and are relatively flat. Interactions can also occur over non-adjacent binding domains.⁹⁰ Small-molecules require pockets into which they can bind. In enzymes, small molecules can exploit the active site. However, with protein-protein interactions identifying a small pocket may be more difficult.⁸⁹ For some protein-protein interactions, although the area of the interaction may be large, the binding may be due to a small number of high affinity interactions between a small number of residues and any disruption of the binding could result in a biochemical effect.⁸⁹ These areas of high affinity residues are known as a 'hot spots', and were identified in 1995⁹¹ by Wells and Clackson using mutagenesis studies.⁹² These studies involved a process known as alanine scanning, in which residues at the face of the protein-protein interaction are mutated to alanine, to identify the individual contribution to the binding energy of each residue.⁹³ This analysis identified that residues contributed unevenly to the binding interaction, with some labelled 'hot spots' strongly contributing to the binding interaction. To be defined as a 'hot spot' a residue must cause an increase in free binding energy of 8.37 kJ/mol on mutation to an alanine.⁹³ The average number of 'hot spots' at the face of a protein-protein interaction is 9.5%.⁹³ They are usually hydrophobic regions with buried charged regions. 'Hot spots' are complementary to each other, with residues on one protein fitting into a pocket on the other protein.⁹¹

Therapeutic proteins and antibodies have shown success in inhibiting extracellular protein-protein interactions, however, as these are not usually cell permeable or orally bioavailable there is a need for small-molecules to disrupt cellular protein-protein interaction.⁹⁴ To

develop inhibitors of the protein-protein interaction compounds must mimic protein surfaces, such as α -helices and β -sheets, and are known as *surface mimetics* or *proteomimics*.⁹¹ These challenges ensure not all protein-protein interactions are druggable, and attempts to develop small molecules to inhibit interactions are very dependent on the unique structure of each protein; those with ‘hot-spots’ are most likely to be druggable. Each protein-protein interaction must be carefully chosen before beginning development.⁹⁵ Blundell *et al* proposed that interactions between one rigid component, and one more flexible component, which only forms a secondary structure on binding to the partner, may prove to be the most druggable protein-protein interactions.⁹⁶ The p53 MDM2 protein-protein interaction is an example of a protein-protein interaction of this type and is discussed in more detail in chapter 3.2. The use of peptides may aid the identification of druggable protein-protein interactions. If a small fragment of peptide from one of proteins is able to bind to the second this suggests a suitable pocket exists for the targeting of small molecules.⁹⁴

The ‘rules’ for designing small molecule inhibitors of protein-protein may be different to typical enzyme inhibitors. Ligand efficiency may be much lower as the binding region is a large hydrophobic region. Abbott’s compound ABT-263 (**33**) fails Lipinski’s criteria, with a molecular mass of well over 500 Da but is orally available and has good cellular activity.⁹⁵ There is currently only one non-natural protein-protein inhibitor on the market.⁹⁵ Maraviroc (**34**) is an anti-HIV agent developed by Pfizer;⁹⁷ however, this molecule does obey Lipinski’s rule.⁹⁵ Maraviroc is a chemokine co-receptor 5 antagonist, antagonism of CCR5 (a GPCR)⁹⁸ by Maraviroc inhibits HIV binding, preventing virus entry into the cell.⁹⁷ Targeting protein-protein interactions are becoming an increasing area of interest within drug discovery with the emergence of new techniques for drug discovery.



3.2 p53, MDM2 and MDMX

p53 is a tumour suppressor that was simultaneously discovered in 1979 by a number of groups. Named after its apparent mass of 53 kDa, p53 acts as a tumour suppressor through its ability to act as a transcription factor and instigator of apoptosis.⁹⁹ p53 acts as the cells' regulator of growth arrest, cell cycle senescence and apoptosis as a response to cellular stress. Under stress conditions, cellular levels of p53 rapidly increase to prevent proliferation of cells containing damaged DNA.¹⁰⁰ It is highly conserved throughout, over both vertebrates and invertebrates, underlining its crucial cellular function.¹⁰¹ The importance of p53 as a tumour suppressor is underlined by one in two cancers carrying a mutation of p53, and remaining cancers negate p53 by inactivation of associated pathways.¹⁰²

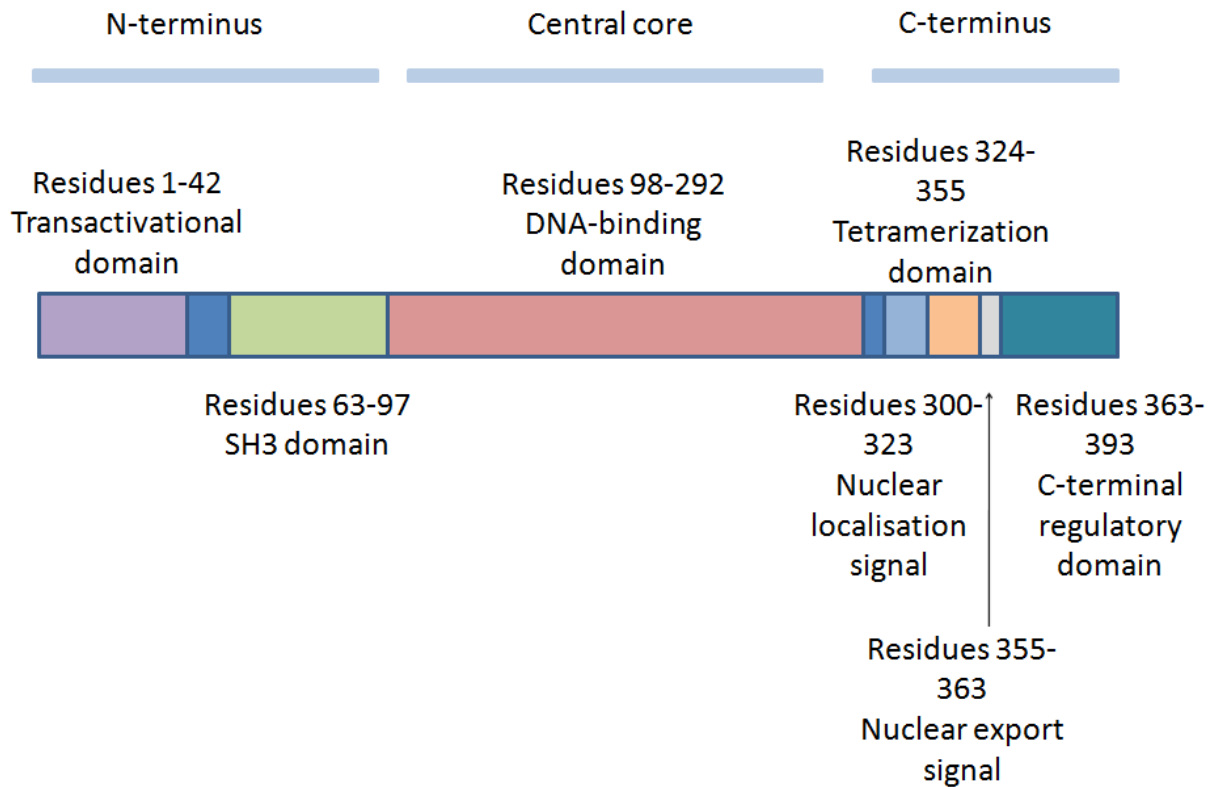


Figure 19 Structure of p53

The tumour suppressor p53 is a 393-residue protein, consisting of a number of domains (see Fig 19) including a transactivational domain, an unfolded acidic region which acts as a promiscuous binding site for proteins such as MDM2 and p300/CBP (which are discussed in more detail later). A short section of this domain (residues 15-29) is able to form an α -helix

on binding to MDM2.¹⁰² The DNA-binding domain is a structured region which interacts with DNA in a sequence specific manner.¹⁰² It interacts with both the minor and the major groove of DNA, the minor groove *via* two loops which contain a Zn²⁺, co-ordinated to His179, Cys176, Cys238 and Cys242 and the major *via* loop-sheet-helix motif.¹⁰²

Although p53 is a monomer under low concentrations, under stressed conditions it can form a tetramer. p53 is transcriptionally active as a tetramer, monomeric p53 can bind to DNA but its affinity is 10-100 times lower than that of tetrameric p53.¹⁰³ The tetramer is made up of four identical p53 chains – 393 residues in length.¹⁰² The tetramer is formed by residues 325-356, which form the tetramerization domain. The quaternary structure is made up of a dimer of dimers, with each monomer consisting of a short β -strand (residues 326-335) and an α -helix (335-355) linked by Gly334.¹⁰³ The monomer forms a V shape, with hydrophobic residues Ile332, Phe338 and Phe341 forming an hydrophobic cluster at the hinge of the V structure.¹⁰³ Two monomers interact *via* β -sheets, forming an anti-parallel double strand, with the two helices forming a double helical bundle.¹⁰³ The anti-parallel β -sheet has eight backbone H-bonds. The two dimers interact through the α -helices,¹⁰³ forming a four-helix bundle.¹⁰² The tetramer is stabilised by hydrophobic interactions.¹⁰² The formation of tetramers also aids accumulation of p53 within the nucleus. The leucine-rich nuclear export signal located between residues 340-351 is on the monomer surface but is hidden when the tetramer is formed. For nuclear export to occur the tetramer must dissociate.¹⁰²⁻¹⁰³

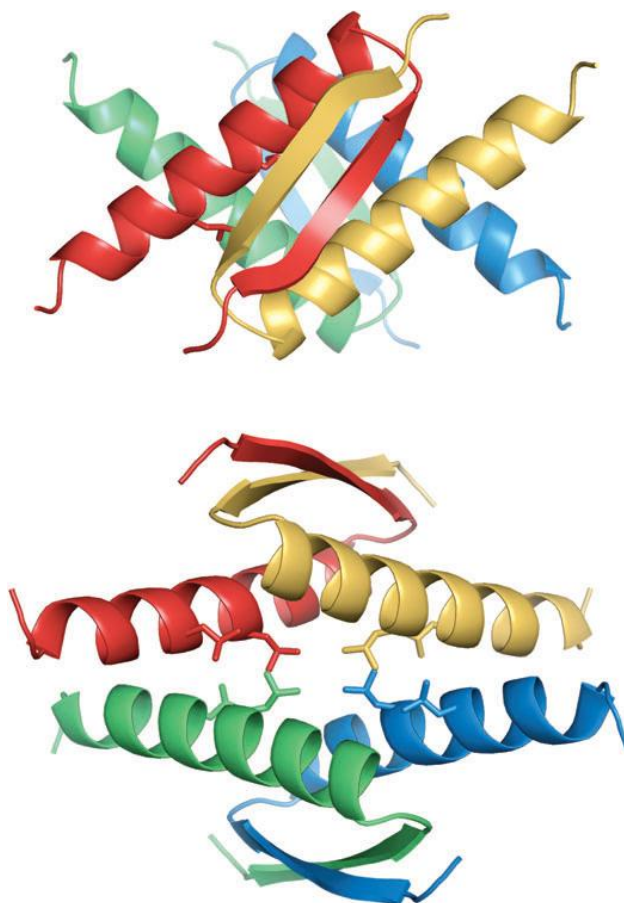


Figure 20 Tetramer of p53 – each colour represents a monomer unit (Taken from reference 102)

Murine double minute gene 2 (MDM2) is a 90 kDa protein, with human MDM2 containing 491 amino acids.¹⁰⁴ MDM2 was first discovered in mouse chromosomes from abnormal chromosomes known as double minutes, and a human homolog was later discovered.¹⁰⁵⁻¹⁰⁶ In 1992, MDM2 was discovered to interact with p53, blocking the biological activity of p53. MDM2 achieves this by firstly blocking the transactivation domain of p53 and secondly acting as a p53 specific E3 ubiquitin ligase.¹⁰⁷ The E3 ubiquitin ligase activity of MDM2 catalyses the ubiquitylation of p53, which in turn labels the protein for degradation by proteasomes. MDM2 is one of the target genes of p53 transcriptional activity and as MDM2 inhibits and marks p53 for degradation, these two proteins are locked in a negative feedback loop.⁹⁹ The negative feedback mechanism allows p53 to be kept at low cellular concentration under unstressed conditions. When the stress pathway is activated, p53 is stabilised and cellular concentrations increase. As a response, MDM2 levels are also increased, which will bring the level of p53 back down to its previous low concentrations after the stress signalling has been removed. MDM2 has a number of different domains which are shown below.

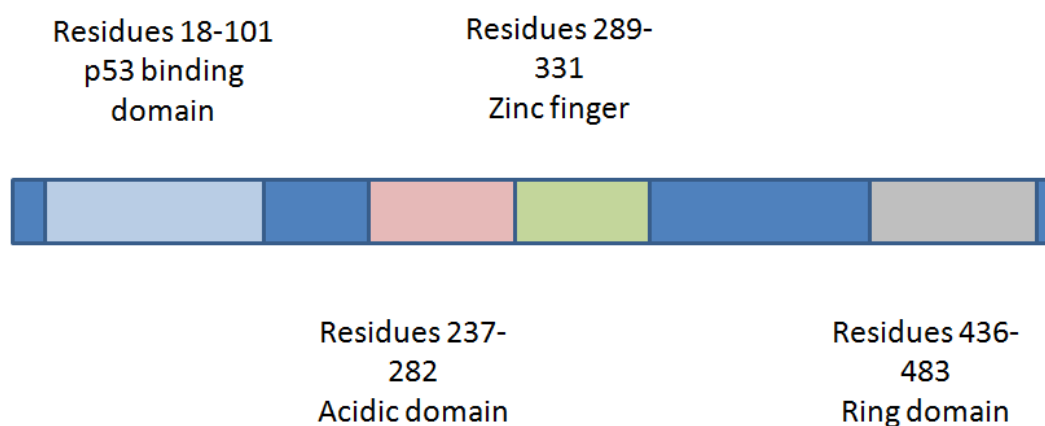


Figure 21 Structure of MDM2

The proteins MDM2 and p53 interact *via* a hydrophobic region on MDM2, which lies towards the amino terminus of MDM2. The hydrophobic region forms a deep cleft made up of residues 19-102.¹⁰⁴ These residues form two structurally similar sections which fold to form a pocket lined by 14 highly conserved hydrophobic and aromatic amino acids. Residues Gly58, Glu68, Val75 and Cys77 are important for p53 binding, as MDM2 with mutations at any of these sites does not interact with p53.¹⁰⁰ p53 interacts with this region through an amphipathic α -helix found within the amino terminal domain, the area also responsible for p53 transcription abilities. The α -helix is formed by 15 amino acids, those crucial for binding are residues 18-26, whilst Thr18 is thought important in stabilising the α -helix. Phe19, Trp23 and Leu26 of p53 insert into the cleft formed by MDM2.^{100, 108} The strength of the interaction between these two proteins is thought to have an IC_{50} of between 60 -700 nM (dependent on length of the p53 peptide used) but the interactions are predominantly hydrophobic, with only 3 H-bonds thought to be formed; the most deeply buried being formed with Trp23 on p53.¹⁰⁰

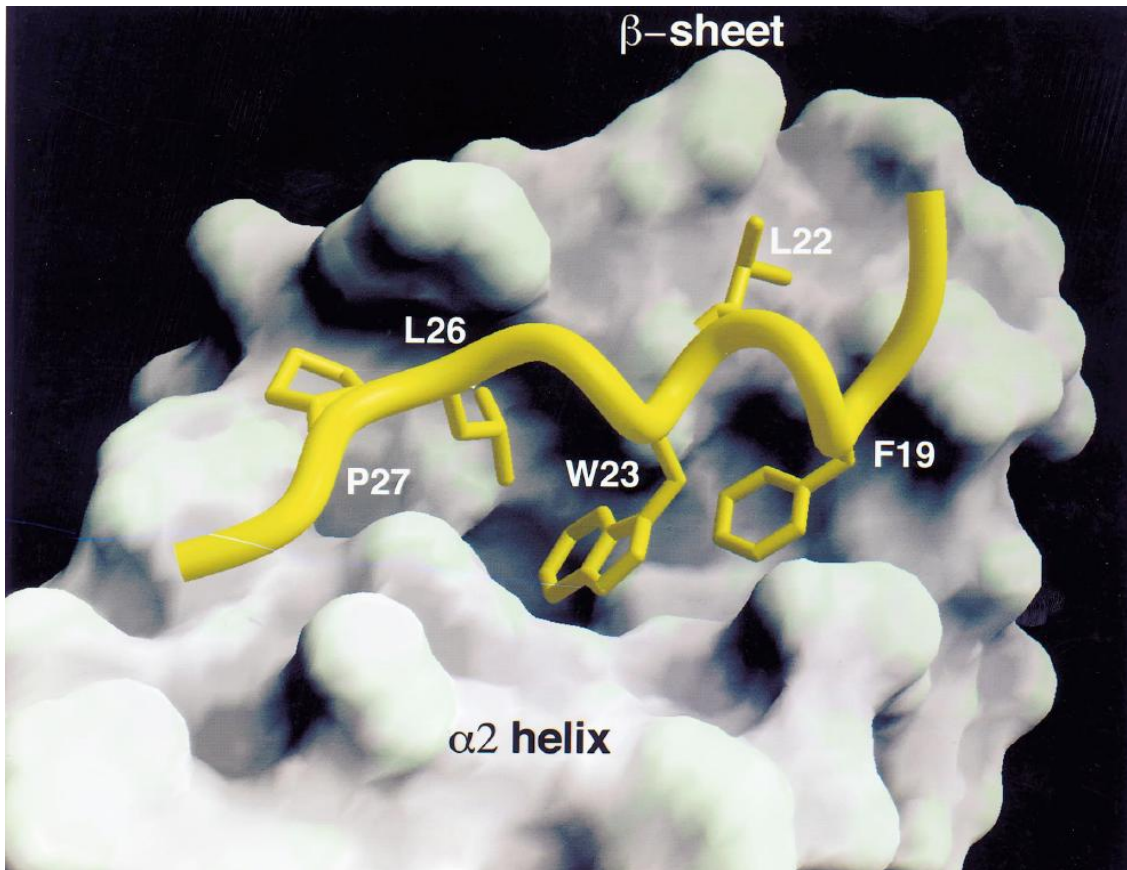


Figure 22 The MDM2 protein (in grey) with the p53 amino acids which interact with this region shown in yellow (Taken from reference 108)

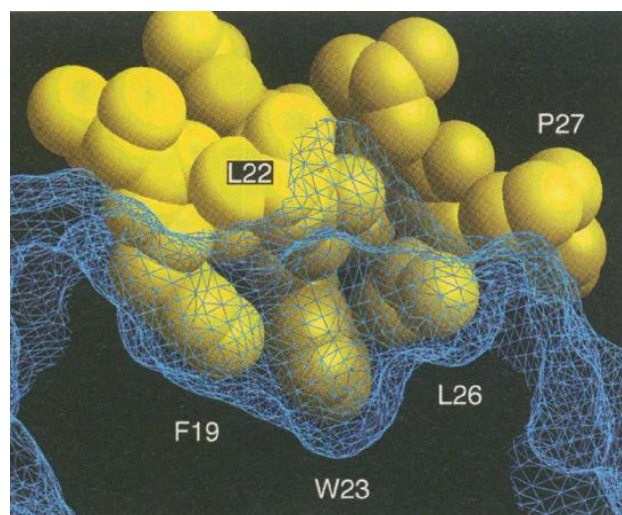


Figure 23 p53 amino acids as space-filling models demonstrating that p53 is complementary to MDM2 (Taken from reference 108)

In unstressed cells p53 is a very unstable protein with a half life of 5-30 minutes as a result of being constantly degraded by MDM2, and is therefore found in low cellular concentrations under normal conditions. As a response to DNA damage, hypoxia, telomere shortening or

oncogene activation p53 is stabilized *via* the blocking of p53 degradation.¹⁰⁰ MDM2 inhibits p53 activity in two ways. The first is by physically blocking the domain p53 uses for transcriptional activation. p53 requires L22 and W23 for transcriptional activity but these amino acid residues are found within α helix through which p53 and MDM2 interact.¹⁰⁴ The second approach by which MDM2 deactivates p53 is through its E3 ligase activity.

The protein MDM2 has both self and p53 ligase activity, due to its highly conserved C-terminal RING finger domain.¹⁰⁰ The RING domain (Really Interesting New Gene) has a C2H2C4 motif, which chelates Zn^{2+} , important for ligase activity.¹⁰¹ Modification of proteins by ubiquitin conjugation is a cellular mechanism which marks proteins for degradation by protease.¹⁰⁰ MDM2 monoubiquitinates lysine residues, predominantly within the C-terminal domain of p53, by transferring ubiquitin from E2 conjugating enzymes.¹⁰¹ When the MDM2-p53 complex is in a further complex with p300/CREB binding protein,¹⁰⁰ which acts as a scaffold, p53 can then be polyubiquitinated. It is the polyubiquitination which marks p53 for degradation by cellular proteases.¹⁰⁰ Before the proteasome can degrade p53, it must be exported from the nucleus into the cytoplasm of the cell. The exact mechanism of this export is unclear, but the MDM2 mediated ubiquitination is thought to be important. The ubiquitination of one or more lysines residues within a group of six lysines found between residues 370-386 at the C-terminal of p53 is thought to be a vital requirement.¹⁰⁹ The nuclear export of p53 also requires the p53 C-terminal nuclear export signal (NES), found at residues 345 to 355.¹⁰⁹ Nie *et al* propose that the ubiquitination of the lysine residues is vital as it induces a conformational change which can then activate or expose the NES, resulting in p53 nuclear export.¹⁰⁹

The relationship between p53 and MDM2 was further complicated by the discovery in 1996 of MDMX (also known as MDM4). MDM2 and MDMX are descended from a common ancestor gene and share significant sequence similarity.¹⁰¹ The N-terminal domain of MDMX has highest sequence similarity with MDM2 (53.6%).¹¹⁰ MDMX can also bind to the N-terminal of p53, therefore also blocking the translational activity of p53. However, the Leu54 (of MDM2) is replaced by a methionine in MDMX, resulting in a smaller binding site.¹¹¹ The central domain of MDMX has 41.9% sequence similarity and the C-terminal domain has 51.3% sequence similarity,¹¹⁰ but MDMX does not have the E3 ligase activity of MDM2.⁹⁹ Instead MDMX acts to stabilise and increase the ligase activity of MDM2. *In vivo*, MDM2 is not particularly stable, and by formation of a heterodimer with MDMX through the RING

domain on both proteins, MDM2 is stabilised. MDMX is in turn labelled with ubiquitin by MDM2 and marked for degradation.^{104, 111}

Due to the role of p53 as a tumour suppressor, the interaction between p53, MDM2 and MDMX is important within cancer. p53 is either lost or mutated in either 50% of cancers¹¹² with MDM2 amplified in around 7% of all cancers.¹¹³ However, within some cancer types this figure rises. Within brain tumours or nervous system cancers (including astrocytomas, oligodendriomas, glioblastomas, gliosarcomas, medulloblastomas, ependymomas and neuroblastomas) the figure rises to 10.4%, within HCC it rises to 44.4%, within soft tissue tumours 30.9% and in Hodgkins disease to 66.7%.¹¹⁴ However, these two mutations rarely happen simultaneously. In most tumours with amplified levels of MDM2, the cell has retained wild type p53, but because of the high levels of MDM2, the protein is rapidly degraded, allowing the cell to replicate unrestricted. If the MDM2 function was restricted, the p53 could function normally, placing the cell into senescence or beginning a programme of apoptosis. This makes the MDM2 a highly attractive target for the development of new anti-cancer therapeutics within medicinal chemistry.

3.3 p53 Cellular Function

The tumour suppressor p53 is activated as a response to genotoxic stress or oncogenic activation through two distinct pathways. These two pathways act to release p53 from the inhibitory activity of MDM2, allowing p53 to act as a transcriptional initiator. Through this, the cell cycle is halted allowing either cellular repair or apoptosis if the damage cannot be repaired.

The first pathway is activated as a response to genotoxic stress. The genotoxic stress includes irradiation, x-rays, ultraviolet radiation, ionising radiation (IR), cytotoxic chemotherapeutic drugs and carcinogens.¹¹⁵ The signal from genotoxic stress is transmitted to p53 through a pathway of 'stress kinases'.¹⁰⁰ As a response to IR and double strand breaks,¹¹⁶ ataxia telanglectasia mutated (ATM)¹¹⁷ kinase is activated. ATM phosphorylates p53 at serine 15 as well as MDM2 at Ser395. ATM also acts on the checkpoint kinase CHK2, phosphorylating CHK2 at threonine 68. This activates CHK2 allowing the DNA-damage signal to be amplified, resulting in the phosphorylation of a number of targets including p53 at serine 20 as well as other sites within p53.^{116, 118}

In the case of DNA-damage caused by UV radiation, single strand breaks and bulky lesions, ATR is activated.^{116, 119} ATR can also phosphorylate Ser15,¹¹⁶ as well as activating CHK1. Activation of CHK1 results in the phosphorylation of p53 at Ser20. Therefore whether activated by DNA-damage resulting in single strand breaks or double strand breaks, p53 will be phosphorylated at both sites Ser15 and Ser20.

p53 can be further phosphorylated by other kinases including DNA-PK.¹²⁰ One crucial site of phosphorylation is Thr18 by CK1. Phosphorylation at Ser15, Ser20 and Thr18 of p53 and sites on MDM2 are thought to destabilise the interaction between p53 and MDM2. Ser15, Ser20 and Thr18 lie on the α -helix which interacts with MDM2 – Thr18 is especially important as it can destabilise the α -helix – altering its structure.¹¹⁴ Phosphorylation of MDM2 at a site close to the RING domain by ATM or an ATM-dependant kinase also acts to switch the MDM2 ligase activity from p53 to MDM2/MDMX, leading to increased accumulation of p53.¹⁰¹

Phosphorylation at multiple sites destabilises the interaction between p53 and MDM2, releasing p53 from the inhibitory activity of MDM2. This results in the increase in the half-life of p53 and its accumulation in the nucleus. In addition, p53 can also be stabilised as a response to oncogene activation.

Acute renal failure (ARF) is the result of the alternative transcription of the gene for the inhibitor of cyclin dependent kinase 4a.¹²¹ ARF (p14^{ARF} in humans)¹¹⁵ is a tumour suppressor and is activated by oncogenes including Ras.¹⁰⁰ It acts by sequestering MDM2,¹¹⁵ physically releasing p53 from its interaction. ARF inhibits the E3 ligase activity of MDM2 by binding to the RING finger domain of MDM2,¹⁰⁰ stabilising the cellular level of p53. Over the process of the development of a tumour, the boundary between these two methods of p53 activation can blur. Continuous replicative cycles as a result of oncogene activation results in replicative stress. The resulting DNA damage will activate the stress kinase cascade.

After p53 has been freed from the inhibitory activity of MDM2, it can then undertake its transcriptional activity. p53 acts as a transcription initiator, initiating the transcription of a large number of genes. p53 can undergo a range of post-translational modifications including phosphorylation, acetylation, methylation, ubiquitination, sumoylation and neddylation.¹²²

The degree of modification can control which genes are translated and the level of translation.¹²² Phosphorylation of p53 increases the affinity for transcriptional co-activators, including histone acetyl transferases (HATs) p300 and CREB binding protein (CRB).¹¹⁴ These HATs acetylate p53 at sites within the carboxyl terminal of p53, sites which are usually ubiquitinated, therefore contributing to the further stabilisation of p53 as well as increasing the site specificity of p53.¹²³ p53 and p300 can then form a DNA-binding complex.

The C-terminal of p53 interacts with DNA through a 26 amino acid sequence.¹²⁴ The 26 amino acid sequence contains nine basic residues which interact with DNA/RNA. Residues K120, S241, R273, A276 and R283 interact with the phosphate backbone in the major groove; residues K120, C277, R283 form H-bonds with DNA-bases and R248 interacts with the minor groove, forming multiple H-bonds. p53 binds with DNA in a sequence specific manner.¹²⁴ p53 binds to areas of DNA known as responsive elements (REs).¹²³ The RE sequence consists of RRRCWWGYYY and 0-21 spacer and RRRCWWGYYY where R = purine W = A or T and Y = pyrimidine.¹²⁴ Genes whose transcription is initiated by p53 have a RE within the DNA close to or within the gene. p53 binding to one of these RE either activates or represses transcription.¹²³ p53 binds to RE and for genes whose transcription is activated by p53 will recruit general transcription proteins through protein-protein interaction.¹²³ However, for genes which are repressed by its binding, p53 either blocks the gene through overlap of the binding site, by squelching of the transcriptional activator or by recruiting p53 histone deacetylases. Proteins whose transcription is inhibited by p53 includes Bcl-2,¹²³ an anti-apoptotic protein which will be discussed later.

The transcription of number of proteins is initiated by p53. These proteins include those responsible for initiating apoptosis, preventing angiogenesis, growth arrest and DNA repair.¹²⁵ A few examples of p53 target genes and the cellular processes they are involved in are listed below.

- PUMA – Apoptosis
- DRAM – Autophagy
- p21 – Cell cycle arrest
- R2 – DNA repair
- LIF – Embryo Implantation

- TSP1 – Inhibition of Angiogenesis
- TIGAR – Inhibition of ROS/survival
- ICAM-1 – Innate immunity
- SCO2 – Metabolism
- MDM2 – p53 Regulation
- PAI-1 – Senescence¹²⁶

Some of these translation targets will be discussed in more detail. p21, which acts to prevent cell cycle progression by inhibiting cyclin E and CDK2, is required for progression from G1 to S phase.¹¹⁶ The expression of p21 is induced by very low cellular levels of p53. This allows a temporary pause of the cell cycle as a response to mild DNA damage or stress, allowing the issue to be resolved and the cell to survive.¹²⁶

Two further proteins also play a vital role in halting the cell cycle and DNA-repair. GADD45 (Growth Arrest DNA Damage) is proposed to have a role in halting the cell cycle at the G1 to S phase transition – possible through an interaction with p21.¹²⁷ Better understood is the role of GADD45 in G2 to M arrest. GADD45 can interact with the Cdc2 (also known as CDK1)/cyclin B complex, causing it to dissociate. As the CDK1/cyclin B complex induces the G2 to M transition, this dissociation halts the cell-cycle before it enters mitosis.¹²⁷ G2 arrest is also instigated by the 14-3-3 protein, a further transcriptional target of p53 which acts in two ways. 14-3-3 acts upstream of cyclin B/Cdc2, preventing activation, which is required for the G2/M transition.¹²⁸ CHK1 and 2 phosphorylate Cdc25, and phospho-Cdc25 can then bind to 14-3-3. The 14-3-3 sequesters Cdc25 in the cytoplasm, preventing activation of Cdc2 (by dephosphorylation). The phospho-Cdc2 binds to 14-3-3 σ (one member of the 14-3-3 family), which also anchors it in the nucleus, preventing the inducement of the G2 to M transition.¹²² The halting of the cell cycle allows repair of DNA damage or the stress-signalling to abate. GADD45 is also implicated in DNA damage repair. GADD45 interacts with PCNA, a protein which is involved in the nucleotide excision repair pathway.¹²⁷ However, if this DNA damage cannot be repaired, the cell commits to apoptosis, programmed cell death, to prevent the continuing proliferation of damaged genetic material.

There are two major routes to apoptosis, the intrinsic and extrinsic pathway.¹¹⁵ p53 plays a role within both of these pathways, as well as a family of proteins called the Bcl-2 (B

lymphoma 2) family. The Bcl-2 family contain both pro and anti-apoptotic members. The anti-apoptotic members block apoptosis and include Bcl-2, Bcl-XL, Bcl-w, Mcl-1 and A1 whilst the pro-apoptosis members block inhibitors of apoptosis. The proapoptotic members can be divided further into two subfamilies: the BAX family comprising of BAX, BAK and BOK and the BH3-only subfamily comprising of BID, BIM, BAD, BIK, BMF, PUMA, NOVA; and HRK. Both the intrinsic and extrinsic pathways result in the activation of proteases known as caspases, but *via* a differing route. The extrinsic pathway is also known as the death receptor pathway whilst the intrinsic pathway is also known as the mitochondrial pathway.¹¹⁵

The extrinsic pathway is activated by members of the tumour necrosis factor (TNF) including TNF α , FAS/CD95 ligand and APO2 ligand. These activate death receptors including TNF/NGF receptor family¹¹⁵ resulting in activation of the cell surface receptor FAS. This interacts with FADD protein (Fas associated death domain) forming the complex DISC (death-inducing signalling complex). The complex activates caspase 3 and caspase 7 which in turn results in apoptosis.¹¹⁵ p53 initiates the transcription of a number of proteins within this pathway.¹¹⁵

The intrinsic pathway results in the release of cytochrome c from the mitochondria into the cytoplasm through the activity of the Bcl-2 family.¹¹⁵ Bcl-2 is found within the outer membrane of the mitochondria and is thought to safeguard the integrity of the mitochondrial membrane, but other anti-apoptosis members such as Bcl-XL and BCL-W only associate with the mitochondria after a cytotoxic event.¹²⁹ The anti-apoptotic proteins are found in complex with the BAX family proteins BAX and BAK under unstressed condition. Both are both activated by BID, a member of the BH3 only family. As BID is, in turn, activated by TNF α and FAS ligand, a link is formed between the extrinsic and the intrinsic pathway.¹¹⁵

Bcl-associated protein (BAX)¹²¹ is found within the cytoplasm under normal conditions in complex with anti-apoptotic conditions,¹¹⁵ however, as a result of apoptotic signalling it is replaced in this complex by BAD and other BH3 only members which inhibit the BH3-only proteins by binding to them. The anti-apoptotic proteins include proteins PUMA and NOXA which are translated as a result of p53 activity.^{129,115} BAX then changes conformation and is incorporated into the outer membrane of mitochondria.¹²⁹ Unlike BAX, BAK (Bcl-homologous antagonist-killer)¹²¹ is always found within the mitochondrial membrane but

during apoptosis changes conformation.¹²⁹ Both BAX and BAK are responsible for making the membrane of the mitochondria permeable, forming channels which allows the efflux of cytochrome c.¹²¹

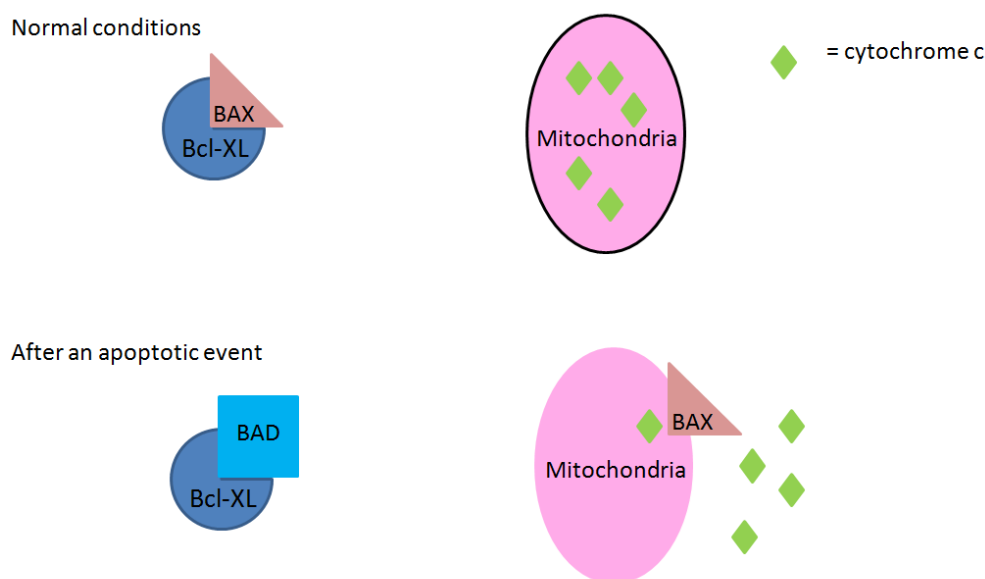


Figure 24 Cellular changes after an apoptotic event

Once cytochrome c is released from the mitochondria it binds to Apaf-1 (Apoptotic protease activating factor 1) forming apoptosome.¹¹⁵ Apoptosome acts on procaspase 9, resulting in its activation which in turn activates caspase 3 and 7, these in turn activate other caspases beginning what is known as a ‘caspase cascade’ resulting in cell death.¹¹⁵ Caspases (Cysteine aspartic acid proteases) are selective proteases. There are 14 caspases, which organize all steps of apoptosis.¹¹⁵ They are found within the cell as inactive precursors, which are known as procaspases and are activated during apoptosis. The caspases act to break down cellular molecules and DNA, condense chromatin and result in the changes of an apoptotic cell.¹³⁰

A further aspect of the apoptosis pathway directly links p53 to apoptosis. During apoptosis a small portion of the free p53 migrates to the membrane of the mitochondria.¹²¹ p53 then interacts with Bcl-XL, freeing Bax from its complex with Bcl-XL. This results in Bax releasing cytochrome c from the mitochondria.

3.4 Drug-like Inhibitors of the MDM2-p53 Protein-protein Interaction

The tumour suppressor p53 protects the integrity of the genome and prevents the development of tumours. In 7% of all tumours the cell retains wild type functional p53 but is essentially p53-null due to an over expression of MDM2.¹¹³ The highest frequency of amplification occurs in soft-tissue cancer, osteosarcomas and oesophageal carcinomas.¹¹³ Therefore, small drug-like molecules which inhibit the protein-protein interaction between p53 and MDM2 are an attractive target for the treatment of cancer. The interaction between MDM2 and p53 is an ideal target for the development of small molecule inhibitors. The area of interaction is relatively small, calculated to be 660\AA^2 surface area on MDM2 and 809\AA^2 surface area on p53, and forms a 'hot spot', an area of intense interaction formed by an α -helices of p53 and a hydrophobic cleft on MDM2 (discussed in chapter 3.2).¹¹³

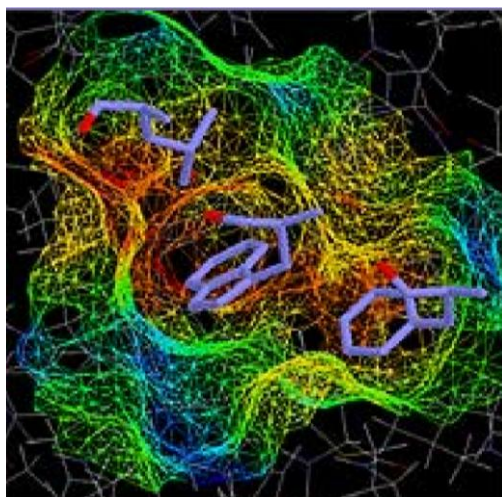


Figure 25 X-ray Structure of MDM2 with p53 bound, crucial residues for the interaction are shown in purple

Inhibition of the protein-protein interaction was first demonstrated by the use of peptides such as the 12mer peptide (Ac-Met-Pro-Arg-Phe-Met-Asp-Tyr-Trp-Glu-Gly-Leu-Asn-NH₂) that demonstrated an IC₅₀ of 0.3 μM .¹¹³ Introduction of unnatural amino acids further increased potency, by inducing the correct conformation before binding to the MDM2 pocket. Experimentation with unnatural amino acids also identified that the replacement of tryptophan (which mimics Trp23) with 6-chlorotryptophan fills a small hydrophobic cavity unfilled by the wild type p53, thus leading to a 60-fold increase in potency between the two comparable peptides.¹¹³ However, peptides are not appropriate for use as drugs and extensive

medicinal chemistry efforts have resulted in a number of small-molecule inhibitors of the p53/MDM2 interaction.

3.4.1. Nutlins

One of the first series of potent, small molecule inhibitors of the MDM2 p53 protein-protein interaction were the Nutlins, developed by scientists at Hoffman la Roche.¹³¹ A screen of a diverse library of chemicals identified a class of *cis*-imidazolines as lead compounds for the inhibition of the MDM2 p53 interaction. These compounds, named Nutlins (for the Nutley inhibitors) (**35-37**) have activity within the range of IC₅₀ 100-300 nM range.¹³¹

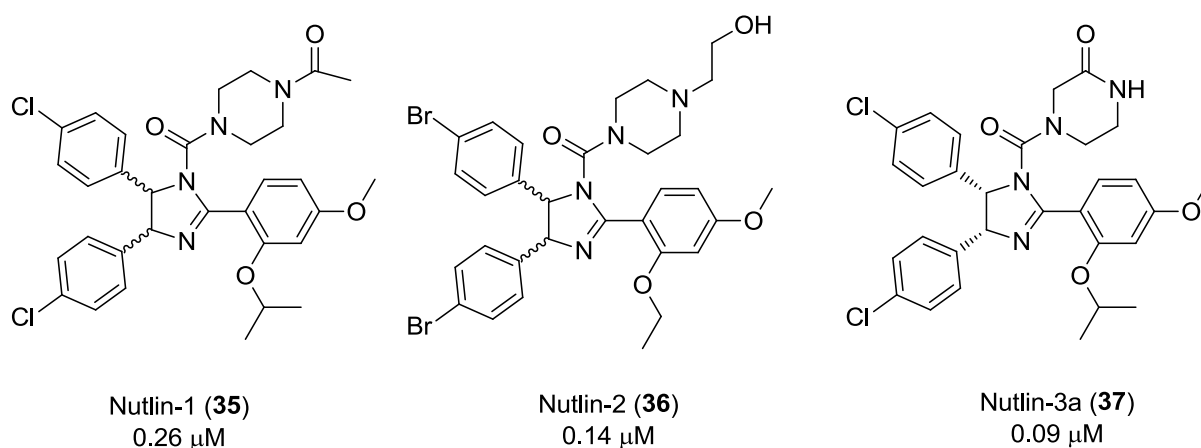


Figure 26

The IC₅₀ values for the compounds were identified as 0.26 μ M and 0.14 μ M for Nutlin-1 and -2 respectively, with these two compounds tested as a racemic mixture. Nutlin-3 was separated into its two enantiomers using chiral HPLC. The IC₅₀ for these two enantiomers initially arbitrarily named Nutlin-3a (**37**) and Nutlin-3b were 0.09 μ M and 13.6 μ M respectively.¹³¹⁻¹³²

The crystal structure of Nutlin-2 bound to human MDM2 shows that it closely mimics the interaction of p53 and MDM2. The *cis*-imidazolidine scaffold mimics the α -helix backbone of p53. One bromophenyl group sits in the pocket occupied by Trp23 of p53; the second bromophenyl group sits in the Leu26 pocket, and the ethyl ether side chain points towards the Phe19 pocket.¹³¹

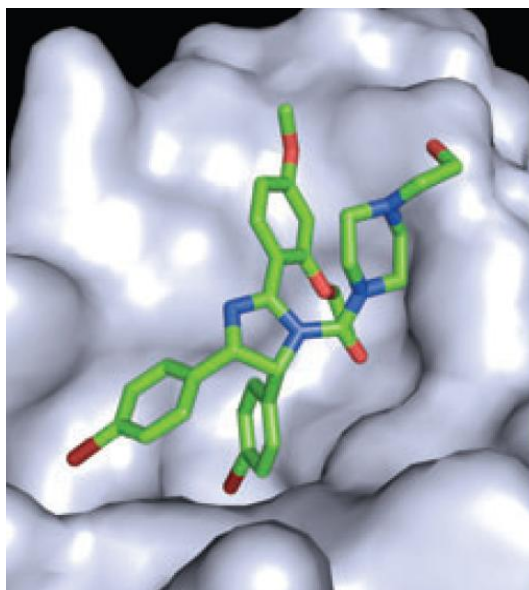
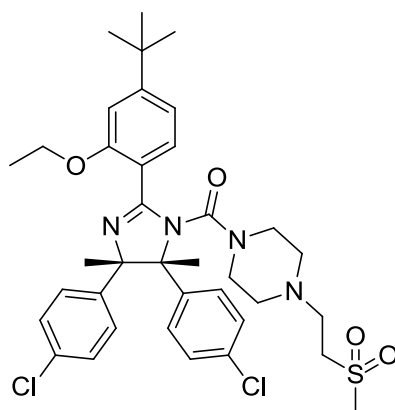


Figure 27 Nutlin 2 bound to MDM2 PBD code 1RV1 (Taken from reference 102)

As Nutlins target the MDM2 p53 interaction stabilising p53, treatment of cells with these compounds should result in an increase in levels of p53, MDM2 and p21 (as both MDM2 and p21 are transcriptional targets of p53). However, this effect should only be observed in cells with wild type p53 and not those with mutated or deleted copies of the gene. Nutlin-1 was tested against human cancer cell lines with wild type p53 (colon cancer cell lines HCT116 and RKO) and also cell lines with inactive p53 (SW480 (colon), MDA-MB-435 (breast) and PC3 (prostate)) to act as a negative control. HCT116 was treated with Nutlin-1 for 8h. A dose dependent increase in levels of p53, MDM2 and p21 was observed. SW480 was treated under similar conditions and whilst basal levels of p53 were observed, no increase in MDM2 or p21 was observed.¹³¹ To ensure that the HCT116 response was a post-translational response to treatment with the Nutlin, the gene expression of both p53 and p21 was monitored. Treatment with Nutlin-1 had no effect on p53 expression but p21 increased in a dose-dependent manner, suggesting that the Nutlins were acting purely by inhibiting the MDM2 p53 protein-protein interaction to upregulate p53 cellular levels.¹³¹

A recent patent has been published from the Nutlin series suggesting increase in activity and an improvement in the physical properties of the series.¹³³ The Nutlin analogue RG7112 (**38**) is currently in clinical trials. The hydrogen atoms in the imidazolidine ring of the early Nutlin compounds have been replaced by methyl groups and the piperazine ring has a further *N*-propyl methyl sulfone group. This additional change may possibly be forming further H-bond interaction between the sulfone oxygen atoms and Tyr67 and Asn72.¹³⁴

RG7112 (**38**)

3.4.2. Spirooxindoles

A series of spirooxindoles are also potent small molecule inhibitors of the MDM2 p53 protein-protein interaction. Crystal structures of the MDM2 p53 interaction showed that the indole side chain of Trp23 from the p53 peptide forms a hydrogen bond with a carbonyl of the MDM2 protein backbone.¹³⁵

Ding *et al* then identified compounds which could imitate this interaction. Oxindoles were found to mimic this interaction and a screen of natural products was undertaken to identify compounds which contained this motif. A number of alkaloids were identified, including spirotryprostatin A and Alstonisine, and although these did not inhibit the protein-protein interaction the spiro (oxindole-3,3'-pyrrolidone) motif was used as a starting point.¹³⁵ The spiro pyrrolidine ring provides a rigid scaffold from which group to mimic the Phe19 and Leu26 can be added. Molecules were designed using the docking program GOLD by altering the R¹, R² and R³ around the ring. This process, followed by further optimisation resulted in compound **39**, which has a K_i of 86 nM in a fluorescence polarisation assay.¹³⁵

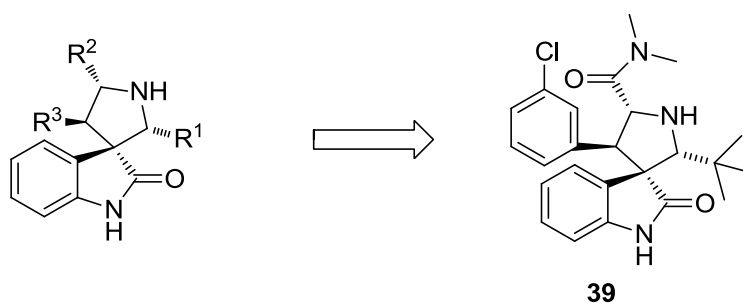


Figure 28 Spirooxindoles core, following optimisation gave **39**

To test the cell activity of the spirooxindoles series the compounds were tested against LNCaP human prostate cancer cells, which have wild type p53. Compound **39** had an IC_{50} of 0.83 μ M. The compounds were also shown to be selective for cell lines with wild type p53 and for cancer cells. Treatment of normal human prostate epithelial cell, with wild type p53, had an IC_{50} of 10.5 μ M.¹³⁵

Although the preliminary compounds showed good potency, comparison with the p53 inhibitory peptides suggested that additional interactions may be accessible to gain additional activity. X-ray crystallography identified a fourth interaction between MDM2 and Leu22 of p53.¹³⁶ The 5' carbonyl of **39** is predicted to lie within 2 Å of the position of carbonyl backbone of Leu22 in p53, suggesting that expanding the compound from the 5' carbonyl may pick up further interaction with MDM2. As Leu22 is partially solvent exposed the additional functionalities may also act to improve solubility. Ding *et al* used the docking program GOLD to predict that the *N,N*-dimethylamine group of **39** can be replaced with 2-morpholin-4-yl-ethylamine group.¹³⁶ The oxygen within the morpholine was proposed to lie close to the positively charged amine of Lys90 of MDM2. The resulting compound has a K_i of 13 nM.¹³⁶

Further optimisation of the *m*-chlorophenyl ring resulted in incorporation of a fluorine in the 2-position. Combination of the two changes resulted in the development of MI-63 (**40**) with a K_i of 3 nM. Compound **40** has four chiral centres, and as binding to MDM2 is stereospecific, identification of the most active stereoisomer (shown below) is important. A further isomer with the opposite stereochemistry has a K_i of 4 μ M.¹³⁶

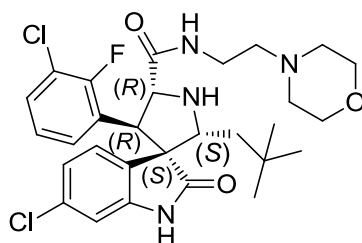


Figure 29 The structure of MI-63 (**40**)

Other protein-protein interactions have a similar binding interaction to MDM2-p53 i.e one partner forms an α -helix which fits into a complementary pocket on the other partner.¹³⁶ This

manner of binding is seen for the Bcl-2/Bcl-XL anti-apoptotic proteins with a pro-apoptotic protein such as BID, BAD, or BAX, and was studied to see if compound **40** inhibits this binding. No significant inhibition was observed at concentrations up to 50 μM , suggesting that the spirooxindoles are selective for the MDM2-p53 interaction. Compound **40** was also tested to ensure that it was only active in cells with wild type p53, which supports the believed mode of action, as well as minimally toxic to normal cells.¹³⁶

Although compound **40** is a potent inhibitor of the MDM2-p53 protein-protein interaction it has a poor pharmacokinetic profile and modest oral availability. MI-63 is therefore not a good drug candidate. The morpholine group is partially solvent exposed so there is no selectivity for the functionality at this position, and therefore the substituent was altered without loss of activity. Replacement with either a methylpiperazinyl or a methyl-piperadinyl group resulted in a K_i of 1.5 and 20 nM respectively.¹³⁷ Both the *N*-methyl-piperazinyl and *N*-methyl-piperadinyl substitutions resulted in improved pharmacokinetic profile but the maximum concentration within the plasma and the area under the curve remained low.¹³⁷ The morpholine, methylpiperadine and methylpiperazine are all protonated and positively charged at physiological pH, contributing to the low bioavailability. The synthesis of a butyl-1,2-diol group improved the K_i to 0.6 nM, and also improved pharmacokinetics, as well as higher concentration within the plasma and improved area under the curve. The compound (**41**), known as MI-147, became the new lead compound.¹³⁷ A further compound, MI-219 (**42**) was also synthesised, without the fluorine atom on the phenyl ring, instead it lies on the oxindole ring. MI-219 has an IC_{50} of 162 nM, but in cellular assays is only slightly less growth inhibitory in SJSA-1 and HCT-116 cell lines than MI-147.¹³⁷ MI-219 has improved oral bioavailability than MI-147 (from 21% to 65%) and a 25 mg/kg oral dose achieve a C_{max} of 3751 ng/mL and an area under the curve of 7677 h·mg/L.¹³⁷

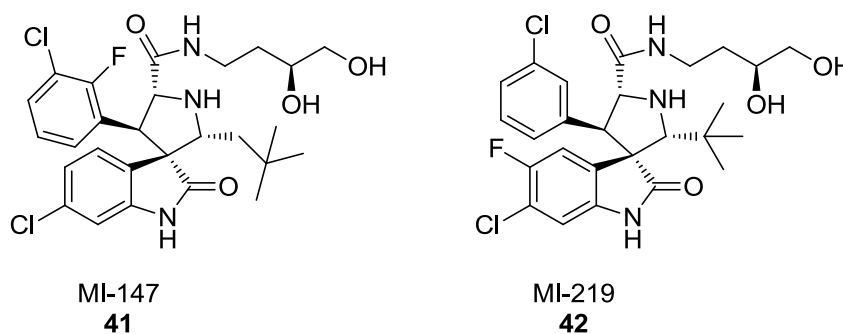


Figure 30

SJSA-1 cell lines, with wild type p53 MDM2 amplified, were treated with compound **41**. A dose dependent activation of p53 was observed, with increasing levels of MDM2 and p21. Compound **41** also induces a dose dependent increase in BAX, PUMA, and NOVA.¹³⁷ A two day treatment of SJSA-1 cell line with 1.25 μ M dose of compound **41** resulted in cell death in 50% of cells. Compound **41** was confirmed to be acting in a p53-dependant manner as minimal effects were seen on a SAOS-2 cell line which has deleted p53. In xenograft models animals were treated with either **41** alone or **41** in combination with irinotecan and was growth inhibitory. Compound **41** is potentially the most potent, orally available, cell permeable, specific inhibitor of the MDM2 p53 protein-protein interaction.¹³⁷

3.4.3. 1,4-Benzodiazepine-2,5-diones

From a screen of MDM2 binding of 338, 000 compounds designed using directed diversity software, 1216 compounds were selected for further investigation by Grasberger *et al.*¹³⁸ From these 1216, 116 compounds had a benzodiazepinedione core. The benzodiazepinedione compounds have two chiral centres and were screened as a mixture of four stereoisomers, with the most active compounds used as a guide for further elaboration of this scaffold. Separation of the most active pair of enantiomers revealed the active compound to be the (*S*, *S*) diastereoisomer.¹³⁸

The benzodiazepinediones were screened using a novel affinity-based assay named 'Thermofluor'. The assay uses fluorescent dye to monitor the unfolding of protein on heating. Compounds which bind to the MDM2 protein increase the thermal stability of the protein and will increase the temperature at which the protein unfolds. The value was quantified by change in the mid-point transition temperature. The initial 116 benzodiazepinedione compounds had a change in the midpoint transition temperature of 1.0 - 4.9 $^{\circ}$ C,¹³⁸ with any hit being a compound with a change of greater than three times the standard deviation. The change in stability of the MDM2 protein over a range of concentrations allowed a dissociation constant (K_d) to be calculated.¹³⁹

Further characterisation of the hits was undertaken using a fluorescence polarisation (FP) assay. This assay used fluorescein-labelled p53 peptide which undergoes excitation at 485 nm and emits at 530 nm. On the binding of a compound to the MDM2, the p53 peptide will be

displaced and the polarisation will be altered. This change was expressed as a percentage with respect to the p53 control.¹³⁹

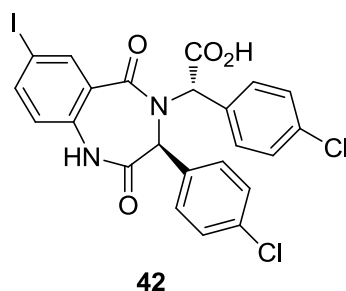


Figure 31

Optimisation around the benzodiazepinedione ring resulted in compound **42**, with a K_d of 67 nM and an IC_{50} of 420 nM.¹³⁹ Incorporation of an *ortho* amino group on the benzylic ring improved the IC_{50} value for the compound but reduced cellular potency, probably due to the compound behaving as a zwitterion.¹⁴⁰ The amino group is thought to form a hydrogen bond with Val93 on MDM2,¹⁴⁰ and can be replaced with a hydroxyl group which can form a similar H-bond. A methyl group on the benzylic carbon maintains good potency in the *R*-enantiomer, with a 3-fold increase in potency.¹⁴¹

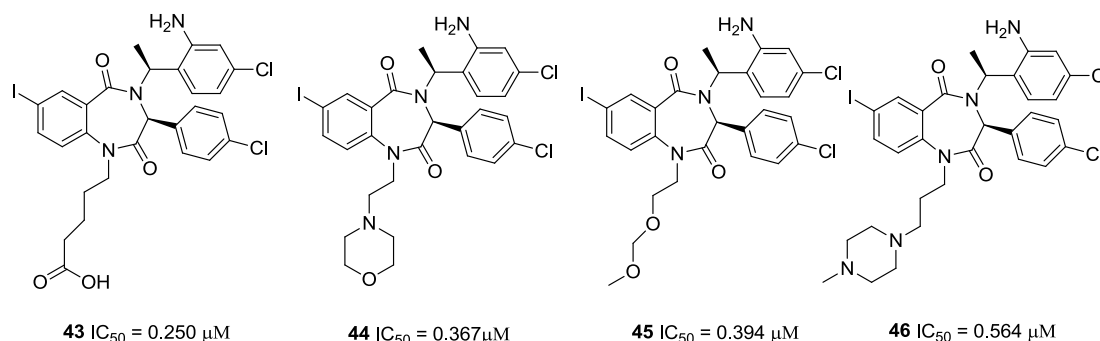


Figure 32 Structure of compounds **43**, **44**, **45** and **46**

Groups on the 1-amino position are relatively solvent exposed, and were therefore varied to improve water solubility. A valeric acid group (**43**), whilst increasing solubility and potency can form a zwitterion which resulted in poorer cell activity when compared to a morpholin-4-ylethyl group (**44**), a 2-(2-methoxyethoxy)ethyl (**45**) and 1-methyl-4-propylpiperazine (**46**), although these compounds had somewhat reduced potency.¹⁴⁰ This series are amongst the most potent inhibitors of the MDM2 p53 protein-protein interaction published. The benzodiazepinedione scaffold acts as an α -helix mimic to orientate the aromatic groups into the correct positions to interact with MDM2.¹⁴²

3.4.4. Chromenotriazolopyrimidines

A further class of inhibitors of the MDM2/p53 protein-protein interaction has been published by Allen *et al.*¹⁴³ From a high-throughput screen of 1.4 million compounds, compound **47** (shown below) was identified as binding to MDM2. Compound **47** was initially tested as a racemic mixture of *syn* and *anti* diastereoisomers and had an IC_{50} of 3.88 μ M.¹⁴³ On chiral separation the active compound was shown to be the *syn* 6*R*, 7*S* configuration (**48**) with an IC_{50} of 1.23 μ M.¹⁴³

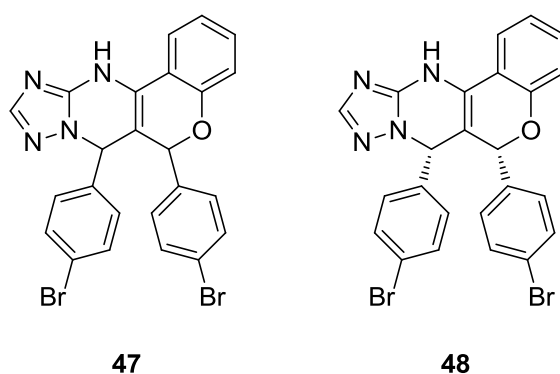


Figure 33

Compound **48** was cocrystallised with MDM2. The crystal structure shows the C7 bromophenyl group occupies the Leu26 pocket, forming a weak π -stacking interaction with His96 which lies 4.0-4.9Å away. The C6 bromophenyl group lies within the Trp23 pocket and the aromatic ring of the chromenone lies within the Phe19 pocket.¹⁴³

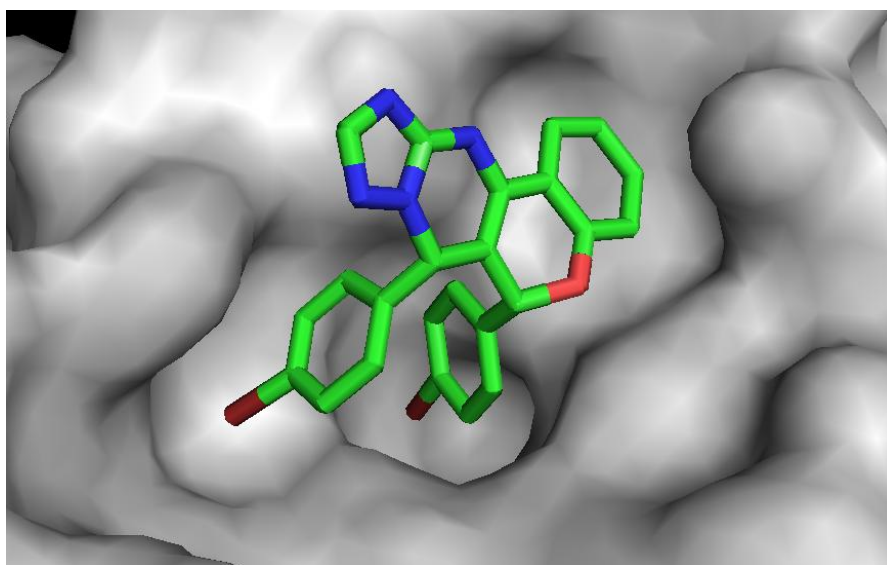
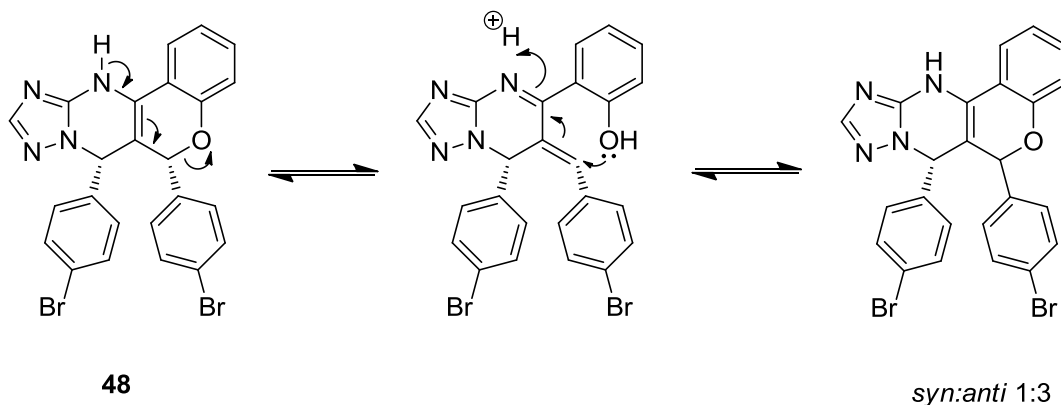


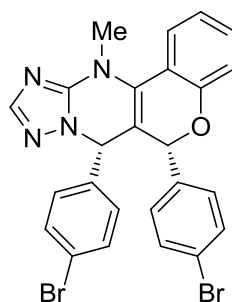
Figure 34

However, compound **48** has a number of problems as a lead structure. It has a high molecular weight (536.22 Da), although the ligand efficiency is comparable with other protein-protein inhibitors. The isomers of compound **47** are poorly soluble in DMSO and at room temperature solutions of enantiomerically pure *syn* diastereoisomers racemise to the *anti* configuration.¹⁴³ The racemisation only occurs at the 6-position and is thought to proceed *via* the mechanism shown below.



Scheme 2

To prevent racemisation the N11 position was methylated (**49**), preventing formation of the enamine, the intermediate in the racemisation process. *N*-methylation increases stability in solution, and improved organic solubility. Crucially, *N*-methylation maintained good potency with an IC_{50} of 1.17 μ M.¹⁴³



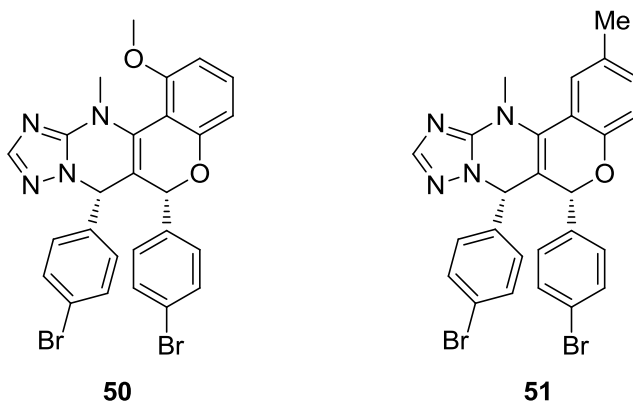
49

The *N*-methylated compound was then used as a starting point for further development. In an attempt to reduce the molecular mass the dibromo motif was replaced by either difluoro which was not tolerated, or dichloro which was equipotent, $IC_{50} = 1.21 \mu$ M for 89 Da reduction in molecular mass. The Trp23 pocket was probed by a series of larger substituents on the C6 aryl group. Of these, the linear groups with some π -character maintained some

activity, with the nitrile analogue the most active at 2.08 μM . These substituents are thought to interact with aromatic residues Phe86 and Phe91 of MDM2.¹⁴³

Synthetic efforts were directed at optimising the substituents for the Leu26 pocket demonstrated that the fluorophenyl analogue was better tolerated as the C6 substituent, however, no improvements in potency were observed.¹⁴³ The aromatic ring of the chromenone was then probed. In the C1 position a methoxy group was shown to be favourable, with a 3.9-fold increase in potency observed for the racemic mixture. The 6*R*,7*S* enantiomer of the methoxy compound (**50**) has an IC_{50} of 0.20 μM . The improvement in potency is thought to be due to the twist induced in the molecule due to clashes between the methoxy group and the N11 methyl group. This induces an improved in the position of the two bromophenyl groups within the Trp23 and Leu26 pockets.¹⁴³

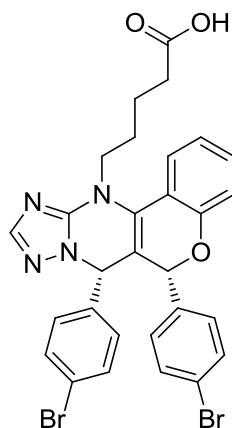
At the C2 position of the chromenone a methyl substituent improved potency 2-fold, with an IC_{50} of 0.44 μM (0.39 μM for the 6*R*,7*S* enantiomer (**51**)).¹⁴³ The crystal structure of **51** showed a small pocket which could be probed by a small group, as demonstrated by tolerance for an ethyl group. No further increase in potency was observed by substitution at either the C3 or C4 position around the ring. However, addition of the C1 methoxy group and C2 methyl group failed to have an additive effect with an IC_{50} 3.94 μM .¹⁴³



Biochemical analysis demonstrated that the chromenotriazolopyrimidines are cell permeable, though the level varied between different compounds. Treatment of HCT116 cells with **51** showed a dose-dependent increase in p21 mRNA although not in p53 knockout cells indicating chromenotriazolopyrimidines acts *via* MDM2 inhibition.¹⁴³ However, compound **49** has high clearance (2.4 L/h/kg) and an oral bioavailability of only 23%. On incubating with rat liver microsomes less than 5% remained after 30 min and on intravenous administration significant levels of des-methyl enantiomers were detectable within the plasma.¹⁴⁴ Oxidative

N-demethylation and isomerisation were thought to occur, resulting in the formation of the inactive enantiomers therefore a more metabolically stable substituent was required.

A series of *N*-alkyl carboxylic acid were synthesised. Of these the *N*-pentyl carboxylic acid analogue (**52**) was shown to maintain good potency with an IC₅₀ of 0.76 μM for the racemic mixture and 0.35 μM for the (6*R*,7*S*) enantiomer. **52** showed low *in vivo* clearance and modest oral bioavailability of 54%.¹⁴⁴



52

Figure 35

3.4.5. Imidazoindoles

Imidazoindole scaffold for MDM2-p53 inhibition was discovered simultaneously by a number of groups including Novartis and Popwicz *et al.*¹⁴⁵ The imidazoindole scaffold is also the only scaffold to also have MDMX inhibitory activity. The imidazoindole scaffold comprises an imidazole ring with a phenyl substituent at the 4-position, a 2-carboxy-6-chloroindole substituent at the 5-position and a 4-chlorobenzyl substituent at position 1.¹⁴⁶

Novartis 101(WW298) (**53**) has an IC₅₀ of 0.19 μM against MDM2 and 19.7 μM against MDMX.¹⁴⁵ The indole group of WW298 sits within the Trp23 pocket with the indole N forming an H-bond to Leu54 of MDM2. However, in the Trp23 pocket of MDMX binding of WW298 induces an energetically unfavourable change in conformation.¹⁴⁵⁻¹⁴⁶ The phenyl ring occupies the Phe19 pocket, orientated perpendicular to the ring of Phe19 and the Leu26 pocket is filled by the chlorobenzyl group.¹⁴⁶ Within the MDMX crystal structure the *N,N*-dimethylaminopropyl moiety folds over the Phe19 pocket, shielding the pocket from solvent

and providing additional hydrophobic interactions.¹⁴⁶ However, the crystal structure of WW298 with MDM2 is not currently available to confirm whether this occurs with MDM2. The *N,N*-dimethylaminopropyl pyrrolidine moiety also improves the water solubility of WW298.

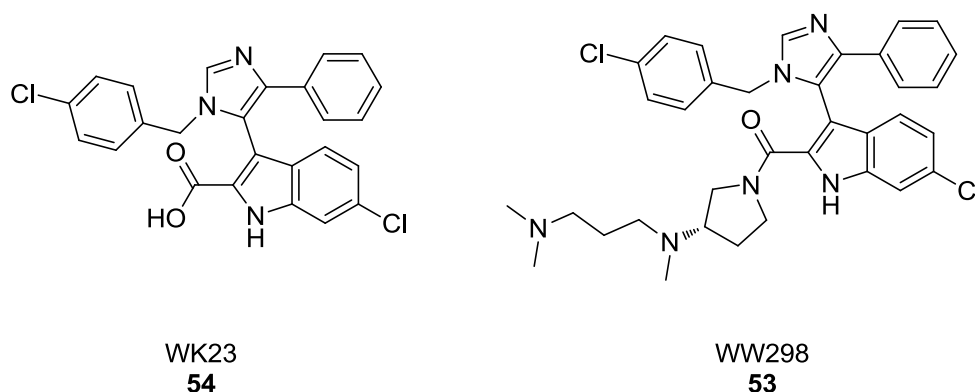


Figure 36

Compound **54** (WK23) developed by Popwicz *et al*¹⁴⁵ is essentially the core of WW298. It lacks the dimethylamino pyrrolidine moiety, instead replacing the amide linker with a carboxylic acid group. WK23 has significantly lower activity, with an IC_{50} of 1.71 μ M. A crystal structure of WK23 bound to MDM2 demonstrates that it binds in a similar manner to WW298 (Figure 37).¹⁴⁵

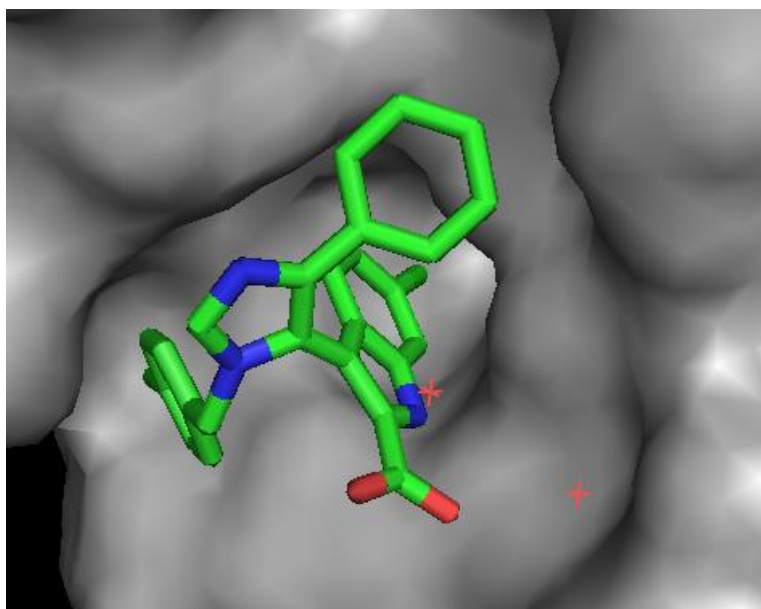


Figure 37 WK23 bound to MDM2 (PDB 3LBK)

To date no MDM2 p53 protein-protein inhibitor has been approved for clinical use. R7112 (**38**) from Hoffman – La Roche is undergoing clinical evaluation, and R7112 is currently in phase I trials for haematological neoplasm (from May 2008 to March 2012)¹³⁴ and advanced

solid tumours (from December 2007 to November 2011)¹³⁴ and is an orally available compound.¹³² A Johnson and Johnson MDM2 inhibitor with a non-p53 mechanism JNJ00676910 underwent clinical trials from November 2006 to February 2010 for advanced/refractory solid tumours. However, no results have been published and there is currently no evidence of this compound going forward into phase II trials.¹³⁴ AT-219 is undergoing late preclinical development. It is an optimised member of the spirooxindoles family of compounds.¹³²

4. The Development of ATP-competitive Inhibitors of mTOR

4.1 Pyrimidines as mTOR Inhibitors

A high-throughput screen of pyrimidine-based compounds carried out by KuDOS Pharmaceuticals identified a number of O^4 -substituted pyrimidines as having inhibitory activity against mTOR. Three series were identified and are shown below.¹⁴⁷⁻¹⁵¹ The compounds were originally synthesised within a CDK2 project of the NICR drug discovery laboratories and all compounds had exhibited some degree of activity against this target. The structures of compounds and their inhibitory activity against both mTOR and CDK2 are shown below (Table 1).

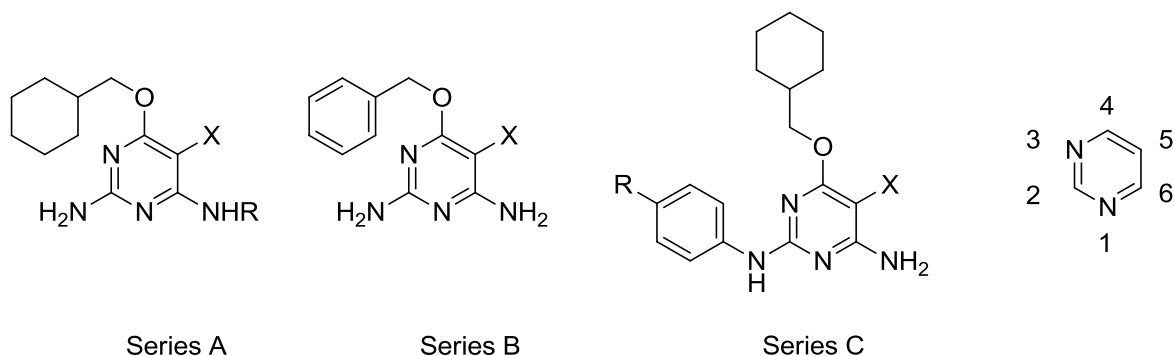


Table 1

Compound	Series	X	R	Kinase Inhibition (IC ₅₀ μM)	
				mTOR	CDK2
55	A	H	H	>50	>50
56	A	NO	H	2.6	2.2
57	A	CHO	H	3.1	6.2
58	A	NO ₂	H	1.5	8.3
59	A	CN	H	1.5	62
60	A	NO	COMe	>50	28
61	A	NO	COEt	11	~100
62	B	NO	-	2.0	27
63	C	NO	SO ₂ NH ₂	4.7	0.001
64	C	NO	OH	3.1	0.016

In the O^4 -cyclohexylmethoxy series substituents are required at the 5-position for activity against both mTOR and CDK2. Modest activity is observed for those compounds bearing

electron withdrawing, H-bond accepting substituents at the 5-position. However, with the exception of compound **59** no selectivity for mTOR is observed. For the acyl analogues the propionyl derivative (**61**) shows significant selectivity for mTOR, in contrast to the acetyl and unsubstituted derivatives (**60**) and (**56**), although the latter is much more potent against mTOR than **61**.

Compound **62** shows that a benzyl substituent is tolerated for mTOR activity but not for CDK2. The *N*²-anilino series also maintains good potency against mTOR. However, these compounds are highly selective for CDK2 over mTOR, suggesting that pursuing compounds of this type would be unwise. The most promising starting points from the HTS were NU6027 (**56**) and NU6227 (**59**) that showed the best potency for mTOR and offered the possibility of selectivity over CDK2.

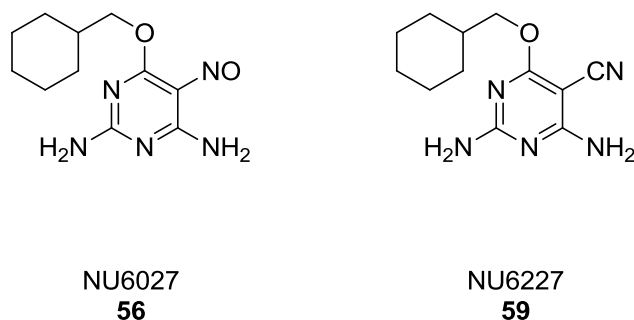
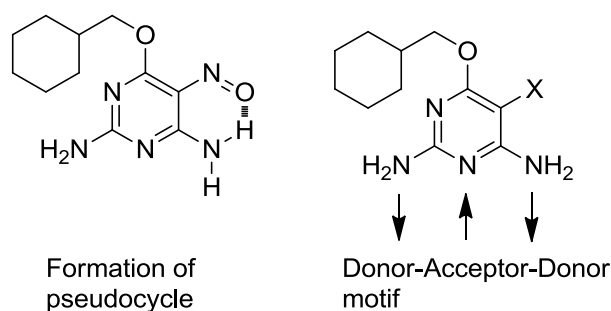
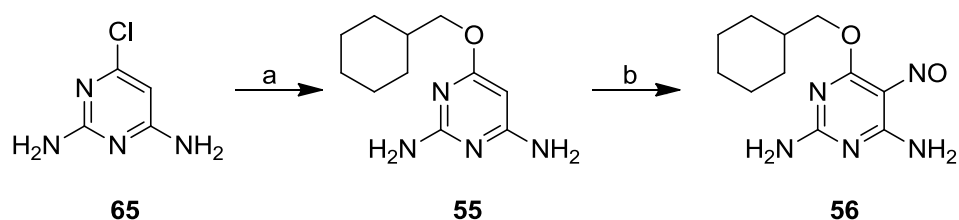


Figure 38

The CDK2 inhibitory activity of compounds **55-64** has been described previously.¹⁴⁷⁻¹⁵¹ All maintain a crucial triplet of hydrogen bonds with the CDK2 protein, forming a donor-acceptor-donor motif. The 5-nitroso-6-aminopyrimidines were found to form a pseudo-cycle between the nitroso group and one proton on the 6-amino group (Figure 39) and therefore act as a purine-mimetic.¹⁴⁹ Detailed structure-activity relationships have been deduced for CDK2 inhibition by 2,6-diamino-4-alkoxy-pyrimidines and so synthetic efforts were first directed towards generating a SAR for mTOR inhibition. This is particularly important given the lack of an available crystal structure of the ATP-binding site of mTOR. A detailed understanding of the SAR should aid the development of a potent inhibitor, but also aid in the separation of mTOR inhibitory activity from that of CDK2.

**Figure 39****4.2 Synthesis of NU6027 and NU6227**

As a prelude to further studies, compounds NU6227 and NU6027 were prepared using the described synthetic route.¹⁵² The first step in both synthetic schemes requires generation of cyclohexylmethoxide formed by heating sodium in cyclohexylmethanol. On addition of 4-chloro-2,6-diaminopyrimidine (**65**) the 4-chloro group is displaced by the cyclohexylmethoxide to generate 4-(cyclohexylmethoxy)pyrimidine-2,6-diamine (**55**). The reaction utilises the electron-deficient nature of pyrimidines to facilitate an S_NAr addition-elimination reaction displacing the chloride with the alkoxide.

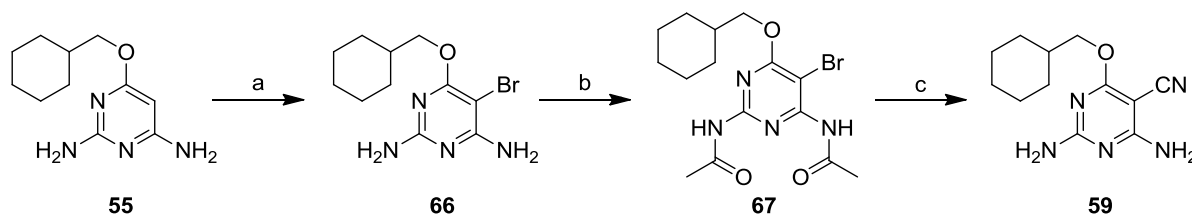


Scheme 3 Reagents and conditions; a) Na, cyclohexylmethanol, 90 min, 180 °C, 20%;
b) $\text{NaNO}_2(\text{aq})$, $\text{AcOH}(\text{aq})$, 40 min, 80 °C, 86%

The 5-nitroso substituent was installed by nitrosation with sodium nitrite in aqueous acetic acid at 80 °C in 86% yield. The electron-donating nature of the substituents on the pyrimidine counteracts the electron deficient nature of the pyrimidine ring, allowing electrophilic substitution to occur at the activated 5-position of the pyrimidine under mild conditions.

The synthetic route to NU6227 is shown below (Scheme 4). Bromination at the 5-position was achieved using *N*-bromosuccinimide in acetic acid at 60 °C in 80% yield. Previously the nitrile moiety had been incorporated using CuCN after protection of the amino groups.¹⁵² Protection of the amino groups by acetylation prevents chelation to the copper but may also have activated the ring, by reducing the electron-donating nature of the amino groups.

Protection of the amino groups was achieved in a 53% yield using a 1:1 mixture of acetic acid and acetic anhydride. Incorporation of the nitrile group was achieved using CuCN in DMF for 5 h. Ethylenediamine was then added to chelate the remaining copper, allowing it to be removed on aqueous work-up, but also as a useful side reaction resulted in the removal of the acetyl protecting groups, giving the desired final compound in 70% yield.



Scheme 4 Reagent and conditions; a) NBS, AcOH, 1 h, 60 °C, 80%; b) AcOH, Ac₂O, overnight, reflux, 53%; c) i. CuCN, DMF, 5 h, reflux; ii. Ethylenediamine, overnight, 70%

4.3 Modifications to the *O*⁴-Position of NU6227

4.3.1. Synthesis of *O*⁴-Alkyl Substituted Analogues of NU6227

To develop the *O*⁴ structure activity relationship a series of *O*⁴-alkyl analogues were synthesised. The 5-cyano analogue has some selectivity for mTOR over CDK2 and as a number of 5-nitroso analogues had previously been synthesised, the substitution at the 5-position was fixed as the nitrile group. A range of substituents was selected covering alkyl and cycloalkyl groups, all smaller than a cyclohexylmethyl group.

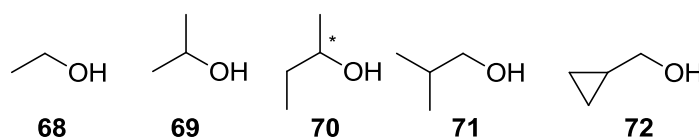
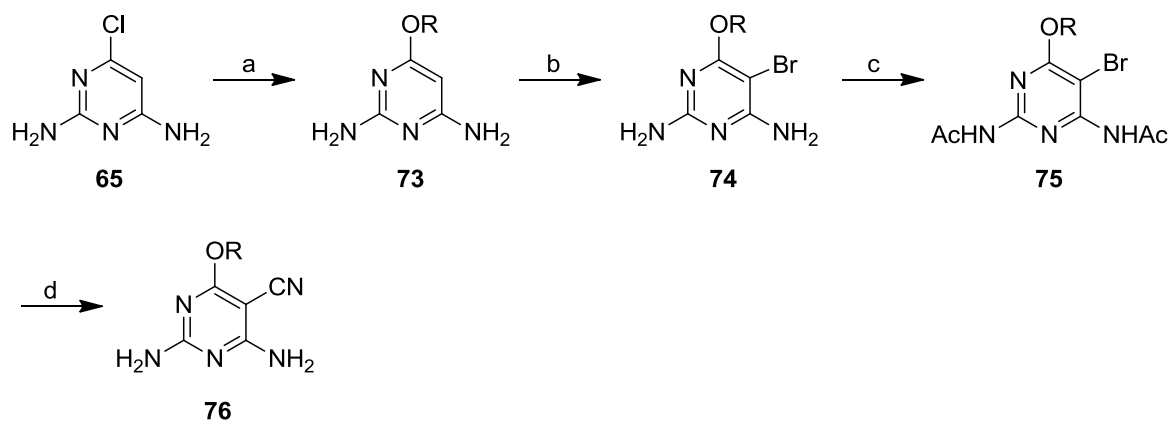
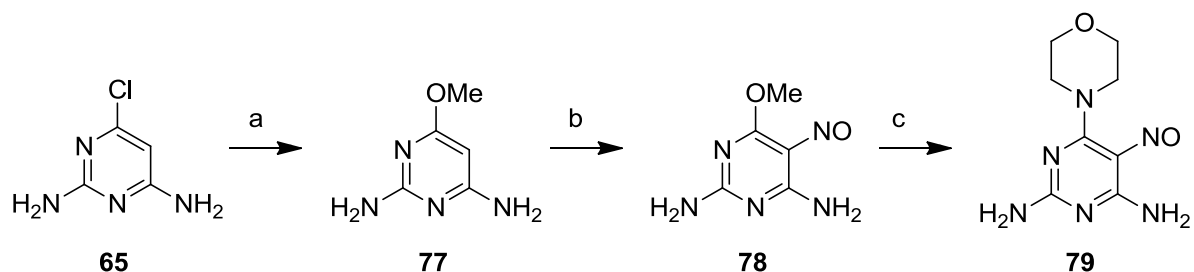


Figure 40

The desired compounds were synthesised using a similar synthetic route to that of NU6227 (Scheme 5). Previous work suggested that whilst the 5-nitroso substituted compounds were sufficiently electron deficient to allow incorporation of a 4-methoxy substituent, followed by displacement with the desired 4-substituent (Scheme 6), this does not occur with 5-nitrile analogues.¹⁵³ As a result the *O*⁴-substituent must be incorporated in the first step of the synthetic scheme. Consequently, five linear syntheses were undertaken, rather than one divergent route.

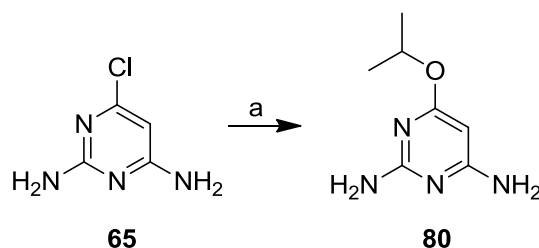


Scheme 5 Reagents and conditions; a) Na, ROH, 20 min – 5 h, 98-160 °C; b) NBS, AcOH, 15–60 min, RT-60 °C; c) AcOH, Ac₂O, reflux, 17-48 h; d) i. CuCN, DMF, 2-7 h, 120 °C; ii. Ethylenediamine, overnight



Scheme 6 Reagents and conditions: a) Na, MeOH, 1 h, 50 °C, 96%; b) NaNO_{2(aq)}, AcOH_(aq), 20 min, 80 °C, 84% c) Morpholine, 10 min 120 °C, 76%¹⁵⁴

Each sodium alkoxide was generated from sodium in the neat alcohol with conventional heating, followed by the addition of 4-chloro-2,6-diaminopyrimidine (**65**). However, a search of the literature suggested that microwave heating may also be appropriate for the S_NAr reaction,¹⁵⁵ and a slight improvement was achieved in this way (Table 2). For alcohols that did not react readily with sodium, microwave heating proved impractical as the metal cannot remain in the reaction mixture when heating in the microwave.



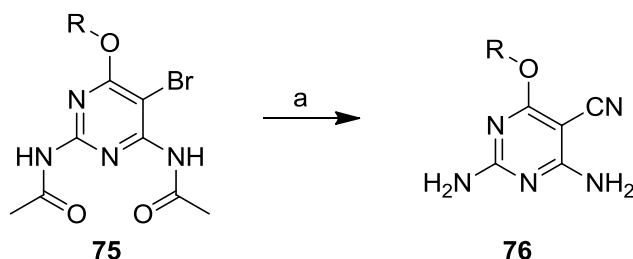
Scheme 7 Reagents and conditions; a) Na, isopropanol

Table 2

Heating type	Temperature (°C)	Time	Yield (%)
Conventional	125	14 h	55
Microwave	160	20 min	67

Bromination was achieved in an analogous manner to NU6227 (**59**) using *N*-bromosuccinimide. However, for the isopropyl, *sec*-butyl and isobutyl analogues the reaction required less vigorous conditions. The desired products were obtained in 15 min at room temperature in good yields (58% for the isopropyl analogue, 72% for the *sec*-butyl analogue and 86% for the isobutyl analogue). Indeed, heating the isopropyl, *sec*-butyl and isobutyl analogues gave only poor yields (~ 20%).

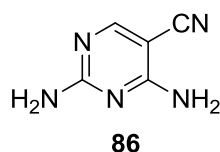
Acetylation of the amino groups was achieved using a 1:1 mixture of acetic acid and acetic anhydride, though further addition of acetic anhydride and longer reaction times were required to increase conversion to the product, compared to those required for the cyclohexylmethyl compound (**67**). Displacement of the bromo substituent was achieved using CuCN in DMF. It was found that reducing the temperature to 120 °C (from 160 °C) gave cleaner conversion to the product. Reaction conditions are summarised below.

**Scheme 8** Reagents and conditions; a) i. CuCN, DMF ii. Ethylenediamine**Table 3** Conditions and yields for conversion to nitrile product

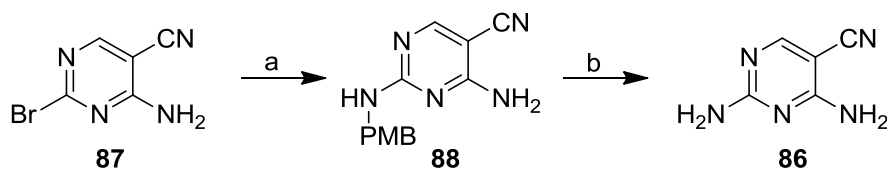
Number	<i>O</i> ⁴ -substituent	Temperature (°C)	Reaction time (h)	Yield (%)
81	Ethyl	160	3.5	75
82	Isopropyl	120	2	25
83	<i>sec</i> -butyl	120	6	61
84	isobutyl	120	7	30
85	cyclopropylmethyl	120	4	82

Compounds **82** and **85** required additional purification by semi-preparative HPLC before achieving appropriate purity for biological testing. The impurity was likely to be bromo-substituted compound **74**, which is generated from remaining starting material on addition of ethylenediamine. To try and avoid this problem, further equivalents of CuCN were added to try to ensure complete conversion of **74** to **75**, but this approach was not successful.

4.3.2. 4-Unsubstituted Analogues of NU6227



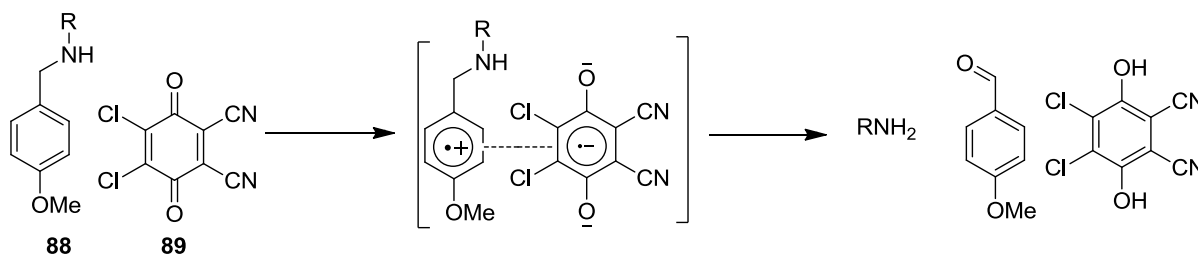
Previously a number of 4-substituted pyrimidines had been prepared (see chapter 4.3.1 and Payne¹⁵⁴). The synthesis of the unsubstituted analogues was explored to expand the SAR. Compound **86** maintains all substituents found in NU6227, other than the 4-position substituent. The analogous 5-nitroso analogue cannot be prepared as the nitrosation reaction requires a highly activated pyrimidine ring, and nitrosations without either the 4-alkoxy or 6-amino groups have previously proved impossible.¹⁵³ Feuer *et al* suggest that the reaction occurs *via* initial nitrosation on the amino group, followed by a rearrangement to give the 5-nitroso compound, a variation of the Fischer-Hepp reaction.¹⁵⁶



Scheme 9 Reagents and conditions; a) *p*-methoxybenzylamine, DMF, 3 h, 100 °C, 91%; b) TFA, DCM, 18 h, reflux, 77%

The synthesis of compound **88** is possible from bromo compound **87**. Displacement of the 2-bromo substituent was achieved employing *para*-methoxybenzylamine, which was used as a convenient source of the amino group. A number of methods of deprotection of the amine groups was then attempted. The deprotection was first attempted using 2,3-dichloro-5,6-dicyanobenzoquinone (DDQ) (**89**) in DCM. The use of the oxidant DDQ requires a 2-electron transfer from the electron rich methoxybenzyl group to the DDQ *via* a charge transfer complex (Scheme 10).¹⁵⁷ However, treatment of compound **88** with DDQ failed to remove the PMB group. Hydrogenation using 10% Pd/C in acidic methanol also failed to

remove the PMB group. Finally **88** was treated with 70% TFA in DCM at reflux overnight to give **86** in a 77% yield.



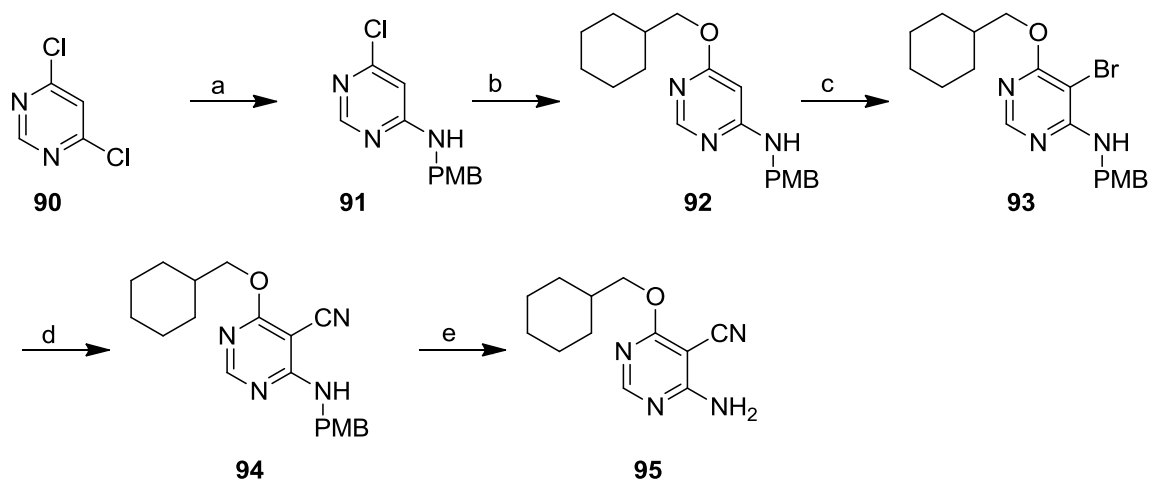
Scheme 10

4.4 Structure-Activity-Relationships Around the Amino Groups

4.4.1. Synthesis of Pyrimidine Derivatives Lacking a 2-Amino Group

The three hydrogen bonds formed by the 2,6-diamino groups and the N^1 of the pyrimidine ring has been shown to be essential for CDK2 inhibitory activity.¹⁴⁹ A 2-unsubstituted analogue of NU6227 and NU6027 would establish whether this is also true for mTOR inhibitory activity. If mTOR inhibitory activity does not require the 2-amino group, mTOR inhibitory activity could be separated from CDK2 activity and the 2-position may provide an interesting position for further substitution.

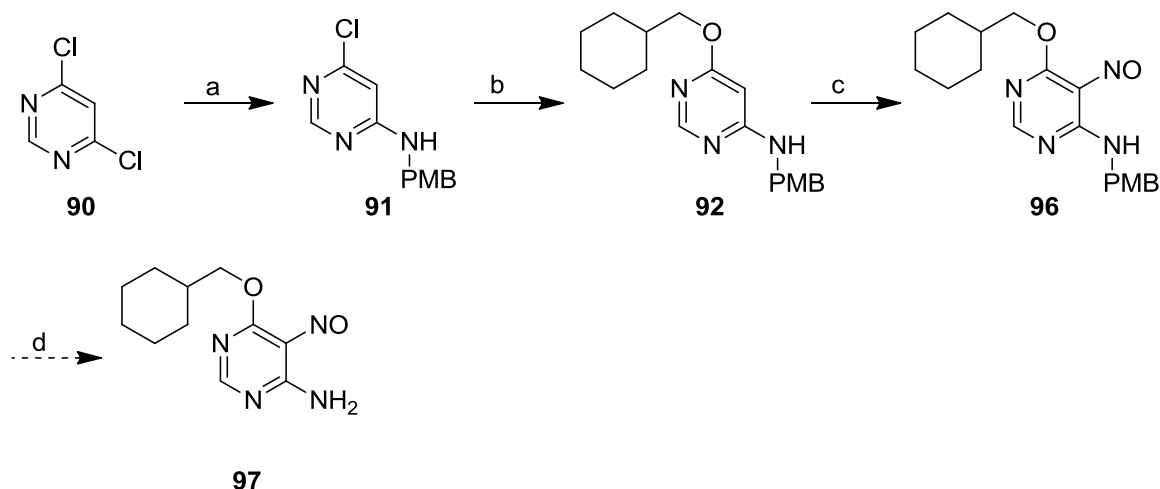
Luo *et al* generated a series of 6-aminosubstituted-4-chloropyrimidines from 4,6-dichloropyrimidine using microwave heating.¹⁵⁸ *para*-Methoxybenzylamine can be used as a convenient source of the amino group, and due to the electron-rich nature of the *p*-methoxybenzyl group, it can be easily removed, leaving the desired amino group in place. Compound **91** was formed by treating 4,6-dichloropyrimidine with *para*-methoxybenzylamine, in the presence of Hünig's base in isopropanol, in 83% yield. Despite the dichloro-motif no formation of the di-amino compound was observed. Only 0.9 eq of the *p*-methoxybenzylamine was used and the pyrimidine ring is deactivated toward $\text{S}_{\text{N}}\text{Ar}$ reactions after the first displacement.



Scheme 11 Reagents and conditions; a) *p*-methoxybenzylamine, DIPEA, isopropanol, 20 min, 120 °C, 83%; b) Na, cyclohexylmethanol, 180 °C, 30 min, 76% or NaH, cyclohexylmethanol, THF, 18 min, 120 °C, 72%; c) NBS, AcOH, 1 h, 69%; d) i. CuCN, DMF, 3 days, 120 °C; ii. Ethylenediamine, 3 days, 28%; d) TFA, DCM, 18 h, reflux, 50%

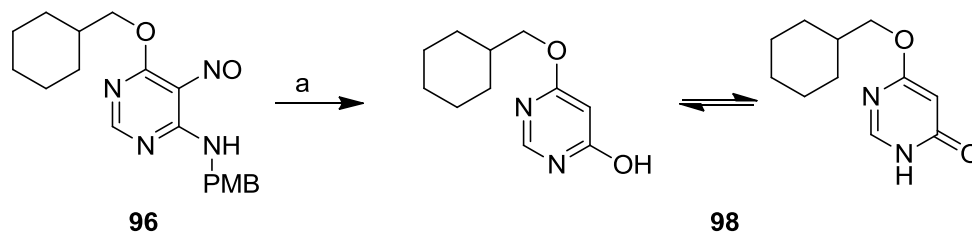
Two alternative reaction conditions were developed for the formation of compound **92**. The first reaction uses the published methodology, i.e. sodium in neat cyclohexylmethanol with conventional heating, giving **92** in 76% yield. The second uses microwave heating. Previous work had suggested that formation of O^4 -alkoxy derivatives with microwave heating is feasible, though impractical for derivatives where formation of the sodium alkoxide requires heating. A series of O^4 -benzyl derivatives were also synthesised using microwave heating from sodium hydride and the appropriate benzyl derivative in THF.¹⁵³ Therefore, this methodology was also applied to the formation of compound **92** in 72% yield.

Bromination of **93** was achieved with NBS in AcOH using the conditions previously optimised for the formation of the O^4 -alkyl derivatives (**81-85**). Slightly longer reaction times were required, as the lack of the 2-amino group results in a less-activated ring towards electrophilic aromatic substitution. The nitrile group was incorporated using CuCN in DMF at 120 °C to give **94**. The PMB group was removed from compound **94** using 30% TFA in DCM at reflux to give compound **95** in 50% yield.



Scheme 12 Reagents and conditions; a) *p*-methoxybenzylamine, DIPEA, isopropanol, 20 min, 120 °C, 83%; b) Na, cyclohexylmethanol, 180 °C, 30 min, 76% **or** NaH, cyclohexyl methanol, THF, 18 min, 120 °C, 72%; c) NaNO_{2(aq)}, AcOH_(aq), 1 h, 80 °C, 79%; d) TFA, 60 °C, 1 h

A similar synthetic route to scheme 11 was developed for the synthesis of the 2-unsubstituted analogue of NU6027 (**56**) (Scheme 12). Compound **96** was synthesised from compound **92** using sodium nitrite in aqueous acetic acid in an analogous reaction to the synthesis of NU6027. Deprotection of the PMB group was attempted using neat TFA, a reaction which had previously been successful for more electron-rich pyrimidine systems.¹⁵⁹ However, multiple products were observed by TLC and the major component was only isolated in poor yield (Scheme 12). The ¹H NMR spectrum of the isolated compound was initially thought to correspond to that of the expected product **97**. However, mass spectrometry showed an *m/z* of 208, which corresponded to a chemical formula of C₁₁H₁₆N₂O₂, presumed to be 6-hydroxypyrimidine **98** (Scheme 13).



Scheme 13 Reagent and conditions; a) TFA, 1 h, 60 °C

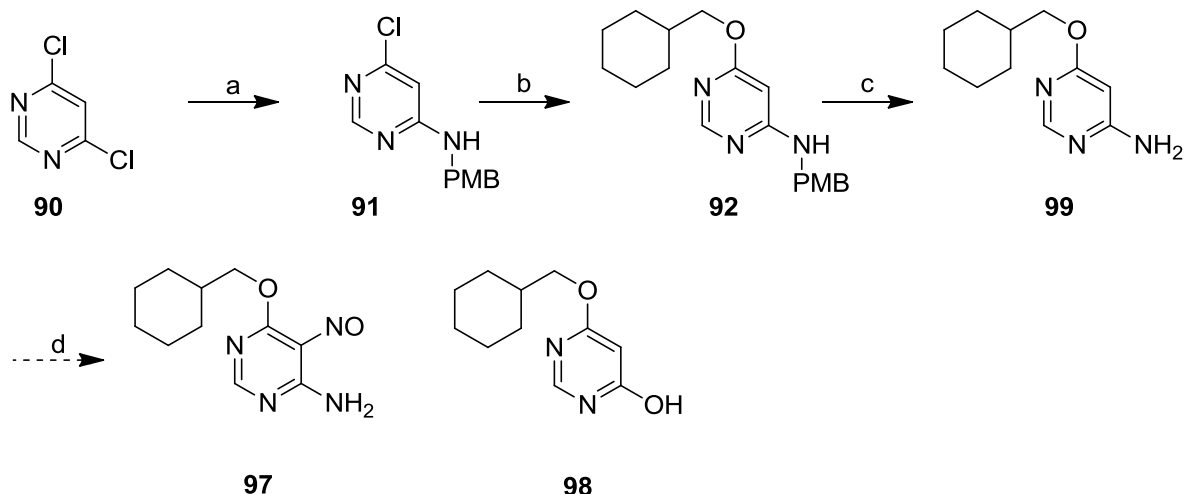
Compound **98** can be formed *via* a diazonium reaction; thus the reaction of TFA with the 5-nitroso group of **96** liberates nitrous acid forming the diazonium intermediate. Reaction with water will produce the 6-hydroxy compound **98**.

In light of the above results a milder deprotection of the PMB group was attempted (Table 4). Oxidative conditions were attempted including CAN, both in a buffered reaction with sodium tetraborate/ borax buffer, in an analogous reaction to Marko *et al.*,¹⁶⁰ and in a dual phase reaction as described by Fürstner *et al.*¹⁶¹ The ‘dual phase’ reaction was achieved using a mixture of chloroform and water, with either 1,2-dimethoxyethane or camphorsulfonic acid as phase-transfer agent to aid the reaction (Table 4).

Table 4

Reagents	Conditions	Observations
TFA	0 °C	Pyrimidinone compound observed after 15 min
1.5 eq TFA in DCM	0 °C	Slow conversion to pyrimidinone compound
DDQ	RT	No reaction
CAN, aqueous acetonitrile	RT	Loss of nitroso group
CAN, buffered solution	RT, pH 8	Mixture of products
CAN, dual phase conditions, DME	RT	No reaction
CAN, dual phase conditions, DME (5% of solvent total)	RT, vigorous stirring	No reaction
CAN, dual phase conditions, DME and camphorsulfonic acid	RT, vigorous stirring	No reaction

The failure of the PMB route required an alternative approach to compound **97**. As the nitroso group had proved especially sensitive, it was decided to remove the *para*-methoxybenzyl group before nitrosation.

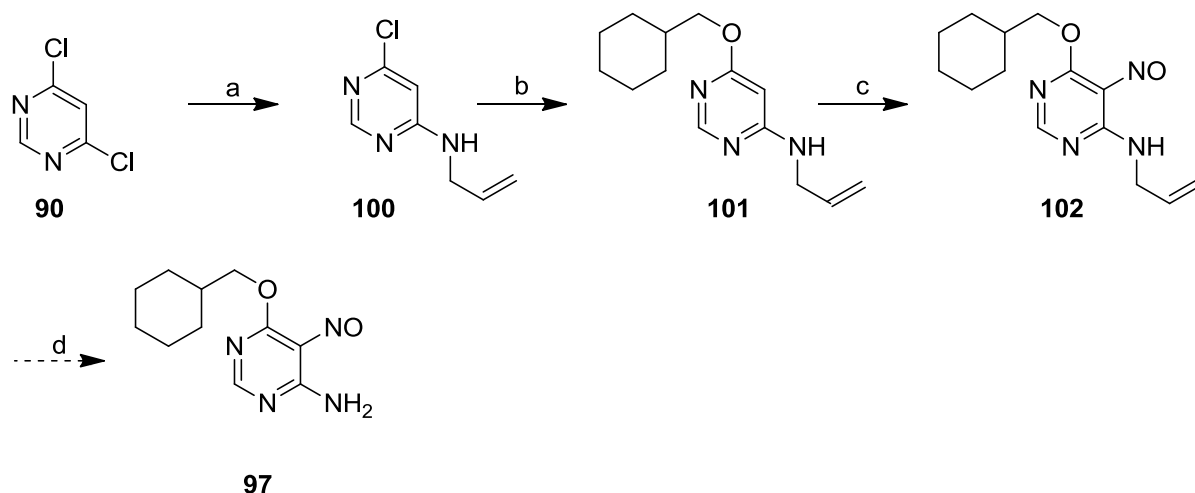


Scheme 14 Proposed reagents and conditions; a) 4-methoxybenzylamine, DIPEA, isopropanol, 83 min, 120 °C, 83%; b) sodium, cyclohexylmethanol, 30 min, 160 °C, 76%; c) trifluoroacetic acid, DCM, 24 h, reflux 87%; d) NaNO_2 (aq), AcOH (aq), 80 °C

Aminopyrimidine **99** was prepared from PMB protected **92** (prepared as discussed for Scheme 11) using 30% TFA in DCM at reflux overnight in good yield. Attempts to nitrosate **99** using the previous conditions failed, instead forming pyrimidinone **98**. The failure of the reaction may be explained by the lack of activation of amino pyrimidine **99** relative to the diamine **56**. Alternative conditions were then investigated. Previous work had identified nitrosation conditions appropriate for electron-deficient pyrimidines.¹⁵⁹ Compound **99** was treated with sodium nitrite in trifluoroethanol with stoichiometric equivalents of TFA at reflux. This reaction proceeded at a slower rate than previous nitrosation reactions and a small percentage of the 5-nitroso **97** was observed by LCMS, but the predominant observed product was compound **98**.

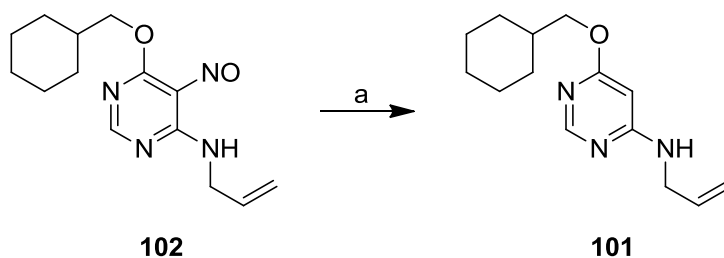
Marchal *et al* used isoamyl nitrite in DMSO as nitrosating reagent on a series of alkoxy, amino pyrimidines.¹⁶² However, for the example which correlates with the desired compound, (4-methoxy-6-aminopyrimidine) they also observed failure of the nitrosation. Instead, they isolated the pyrimidinone formed by diazotation and hydrolysis.¹⁶² The result obtained by Marchal *et al* demonstrated that the nitrosation cannot be performed with a free amino group in place. The nitrosating agent always forms nitrous acid, and without an activating group *para*- to the 5-position, this preferentially forms the diazonium ion instead of nitrosating the pyrimidine ring.

It was proposed that an alternative protecting group, which is removed under different conditions to PMB, may allow access to compound **97**, therefore, the synthesis of **97** via an allyl protected amino group was attempted. The S_NAr reaction on 4,6-dichloropyrimidine with allylamine proceeded cleanly at room temperature for 24 h, with good conversion to give **100**. The second displacement of the chloro from the pyrimidine heterocycle with cyclohexylmethoxide was undertaken as previously with NaH, cyclohexylmethanol in THF and microwave irradiation at 120 °C. However, conversion to the product was incomplete, and using medium pressure column chromatography separation of the starting material and product was not possible. Increasing the time of heating from 15 min to 20 min resulted in total conversion to the product. Compound **101** was then nitrosated using standard conditions, in a 66% yield.



Scheme 15 Proposed reagents and conditions; a) allylamine, Et_3N , THF, 24 h, 98%; b) cyclohexylmethanol, NaH, THF, 20 min, 120 °C, 75%; c) $NaNO_{2(aq)}$, acetic acid $_{(aq)}$, 75 min, 80 °C, 66%; d) deprotection

Deprotection of the allyl group to give the free amine group and the desired 5-nitroso **97** was then required. The deallylation was initially attempted using Wilkinson's catalyst and DABCO. These conditions isomerize the allyl double bond, allowing extraction using DABCO as a nucleophile.¹⁶³ Allyl **102** was treated with Wilkinson's catalyst and DABCO in refluxing ethanol. However, the allyl group remained in place but the nitroso group had been removed giving allyl **101**.



Scheme 16 Reagent and Conditions; a) DABCO, Rh(PPh₃)₃Cl, EtOH, 80 °C, 4 h

Ueda *et al* used palladium triphenylphosphine and *N,N*-barbituric acid to remove allyl groups during the total synthesis of (+)-haplophytine.¹⁶⁴ Treatment of **102** with Pd(PPh₃)₄, 1,3-dimethylbarbituric acid in refluxing DCM failed to remove the allyl group. However, replacing the DCM with the higher boiling ethanol resulted in the generation of a number of products. ¹H NMR identified these two products as **101** and **99**, one lacking the 5-nitroso group **101** and the other lacking the 5-nitroso and the allyl group **99**.

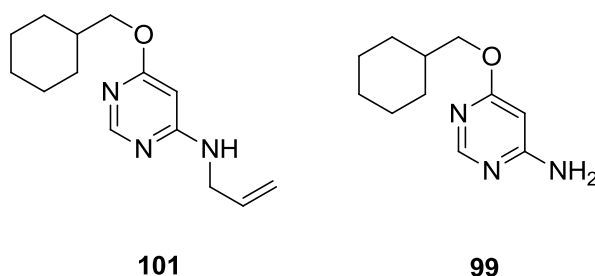


Figure 41

Karpf *et al* removed allyl groups in their azide free synthesis of oseltamivir using 10% palladium on carbon and ethanolamine in ethanol.¹⁶⁵ However, under these conditions, the nitroso group was rapidly removed. In view of these unsuccessful results and time-constraints it was decided to discontinue work on the synthesis of **97**.

4.4.2. Synthesis of 6-Hydroxylamino Pyrimidines

The high-throughput screen which identified pyrimidine-based compounds as having mTOR inhibitory activity also identified a number of 6-amino acyl derivatives with mTOR inhibitory activity e.g. **60** and **61**. A range of acyl and carbamates derivatives were therefore synthesised. These derivatives may be unstable under assay conditions, and HPLC monitoring showed decomposition over time.¹⁵⁴ A more stable substituent was required to

probe the region around the 6-amino position, such as the methyl (**103**) and the benzyl (**104**) aminoxy analogues.

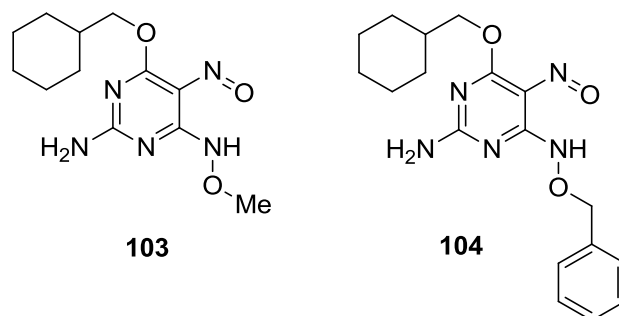
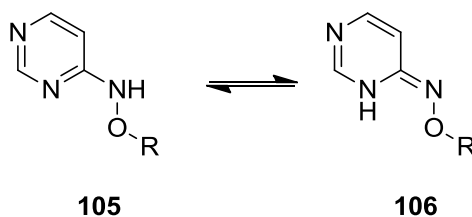
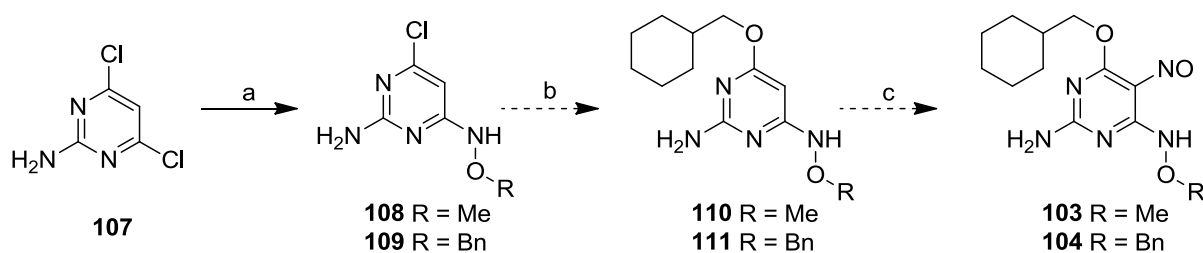


Figure 42

Too *et al* proposed that with electron-withdrawing methoxy or benzyloxy groups on the 6-amino groups an alternative tautomer may be observed, whereby the amino tautomer (**105**) interconverts with the imino tautomer (**106**), which would disrupt the triplet of hydrogen bonds to the protein.¹⁶⁶ However, with the 5-nitroso group forming a hydrogen bond to the 6-amino proton the equilibrium may favour the desired tautomeric form.



The synthetic route to access compounds **103** and **104** is shown below.



Scheme 17 Proposed reagents and conditions; a) R = Me methylamine hydrochloride, DIPEA, DMSO, 16 h, 130 °C, 52%; R = Bn *O*-benzyloxyamine, DIPEA, DMSO, 6 h, 130 °C, 66%; b) Na, cyclohexylmethanol; c) NaNO_{2(aq)}, AcOH_(aq)

Too *et al* prepared aminoxy-substituted purines by treating chloro-substituted purines with 10 equivalents of the appropriate alkyl substituted hydroxylamines in the presence of Hünig's base.¹⁶⁶ To avoid using such a large excess of reagent, conditions were adapted from the synthesis of compound **91** to synthesise **109**. However, multiple products were formed.

Therefore, optimisation of this reaction was undertaken. The conditions and results are summarised below.

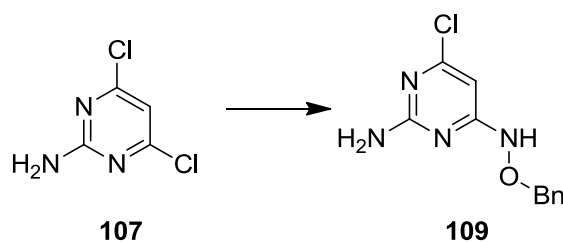
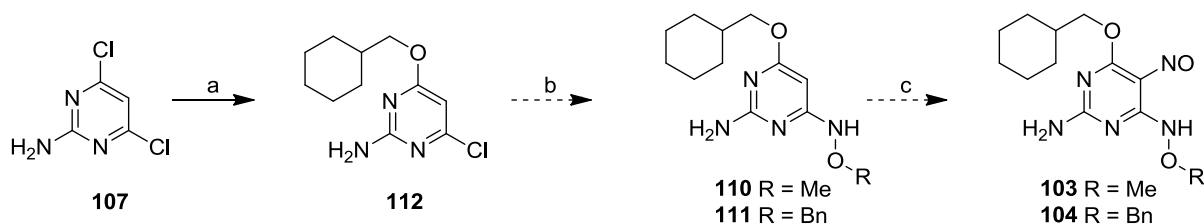


Table 5 Results and conditions for the synthesis of **109**

Solvent	Heating type	Equivalents of <i>O</i> -benzyl hydroxylamine	Temperature (°C)	Time	Yield
Isopropanol	microwave	1	140	75 min	27 %
<i>n</i> -Butanol	microwave	1	160	90 min	39%
Trifluoro-ethanol	microwave	1	170	-	0%
DMSO	microwave	1	170	40 min	29%
DMSO	microwave	1	180	15 min	17%
DMSO	microwave	1	170	30 min	29%
DMSO	conventional	1	130	8 h	42%
DMSO	conventional	1.5	130	6 h	66%

Conventional heating for longer times at a low temperature was shown to be higher yielding, along with increasing the equivalents of *O*-benzylhydroxylamines. These conditions were then applied to the synthesis of compound **108**, though the reaction time was slightly longer for the methyl compound and slightly lower yielding (52%). However, on attempting formation of cyclohexylmethoxy compound **111**, the sensitive nature of hydroxylamine **109** again proved problematic. Treatment of compound **109** with either sodium in cyclohexylmethanol or sodium hydride with cyclohexylmethanol in THF at 120 °C with both microwave and conventional heating resulted in decomposition of the starting material and the formation of by-products. Under similar conditions the analogous methyl compound was also seen to decompose. Multiple products may be formed as a result of nucleophiles attacking the benzyl and methyl group. Therefore, incorporation of the hydroxylamine

functionality at a later step may be advantageous. An alternative synthetic route was devised which reversed the order of substitution. The synthetic route is shown below (Scheme 18).



Scheme 18 Proposed reagents and conditions; a) Na, Cyclohexylmethanol, 20 min, 100 °C, 62%; b) R = Me, methoxyamine hydrochloride, DIPEA, DMSO, 130 °C; R = Bn, *O*-benzylhydroxylamine, DIPEA, DMSO, 130 °C; c) NaNO_{2(aq)}, AcOH_(aq)

Conventional introduction of the cyclohexylmethoxide group (180 °C, Na) resulted in disubstitution forming **113**. Optimisation of this reaction was therefore undertaken. Optimal conditions were found to 0.9 eq. of sodium at 100 °C, resulting in the formation of compound **112** in a 62% yield. However, attempts to incorporate the amino-oxy functionality proved unsuccessful. In view of their instability it was decided to discontinue work on these compounds.

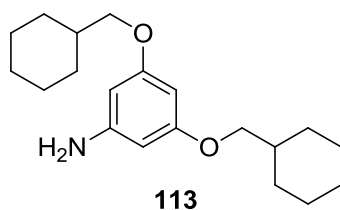


Table 6

Equivalents of sodium	Temperature (°C)	Product
Excess	180	113
Excess	120	113
0.9	100	112

Unfortunately, modification to either of the amino groups proved either unsuccessful, or abolished activity. Alternative areas of the molecule were then addressed to develop further the SAR.

4.4 Modifications to the 5-Position

Potent compounds identified from the high throughput screen all maintained an electron-withdrawing substituent capable of accepting a hydrogen-bond at the 5-position. Compounds bearing electron-withdrawing substituents, which cannot form hydrogen bonds, have also been synthesised, including the acetylene derivative shown below, but this modification resulted in a loss of biological activity against mTOR.

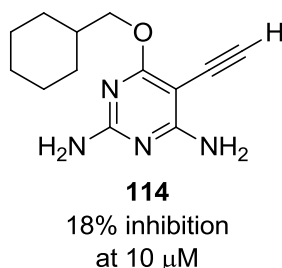
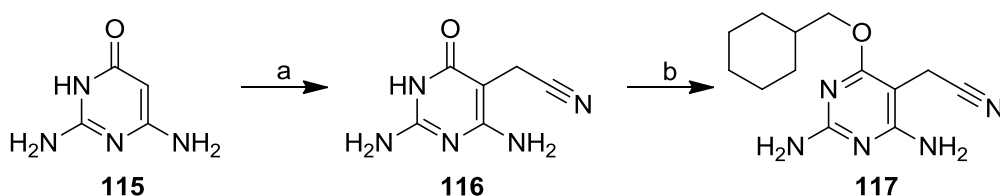


Figure 43

To examine further the structure-activity relationships around the 5-position a series of analogues was therefore designed. Compound **117**, which introduces a CH_2 unit between the aromatic ring and the nitrile group, was synthesised. Hockova *et al* alkylated at the 5-position by treating 2,6-diaminopyrimidinone with bromoacetonitrile in the presence of base.¹⁶⁷ Using this synthetic route compound **117** was synthesised in an unoptimised yield of 9% (Scheme 19).



Scheme 19 Reagents and conditions; a) bromoacetonitrile, NaHCO_3 , DMF, 4 days, 9%; b) (bromomethyl)cyclohexane, K_2CO_3 , DMF, 15 h, 100 $^\circ\text{C}$, 22%

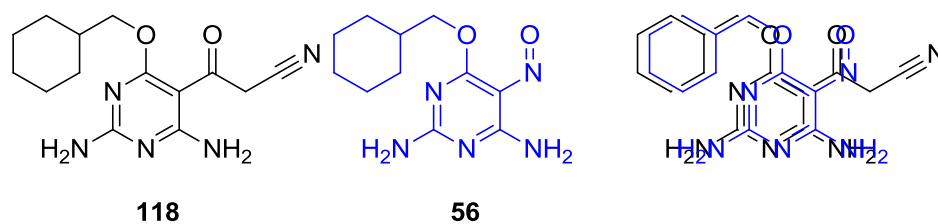
Formation of the desired final compound requires alkylation of the pyrimidine oxygen. The attempted conditions are shown below (Table 7). The alkylation reaction with (bromomethyl)cyclohexane proved successful, although purification of compound **117** proved difficult, requiring multiple rounds of medium pressure chromatography, followed by recrystallisation giving compound **117** in 22% yield.

Table 7

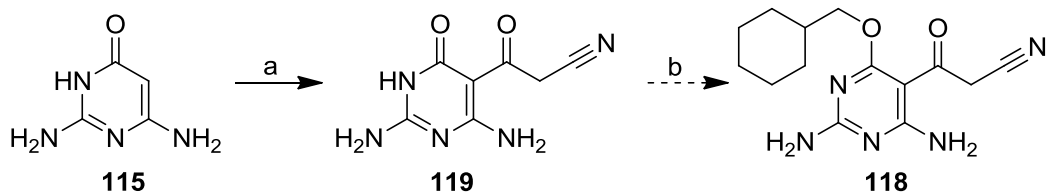
Reagents	Conditions	Yield (%)
DEAD, PPh ₃ , Cyclohexylmethanol, THF	RT	No reaction
DEAD, PPh ₃ , Cyclohexylmethanol, DMF	RT	No reaction
DIAD, PPh ₃ , Cyclohexylmethanol, DNF	100 °C	No reaction
(Bromomethyl)cyclohexyl, K ₂ CO ₃ , DMF	100 °C	22

Both the *N*-alkylated product and *O*-alkylated product are possible results of this reaction. The ¹³C NMR spectrum of the major product suggested *O*-alkylation. The predicted values for the methylene carbon adjacent to either the pyrimidine N or the exocyclic O are 44 or 72 ppm respectively. The observed value for the methylene carbon was 70.3 ppm, suggesting that the desired *O*-alkylated compound has been formed. Unlike the compounds where the nitrile group is directly attached to the aromatic ring, which have a strong absorption peak in the IR at around 2000 cm⁻¹, compound **117** had a weak CN absorption, as expected for an alkyl nitrile as this is known to be a weaker absorption.

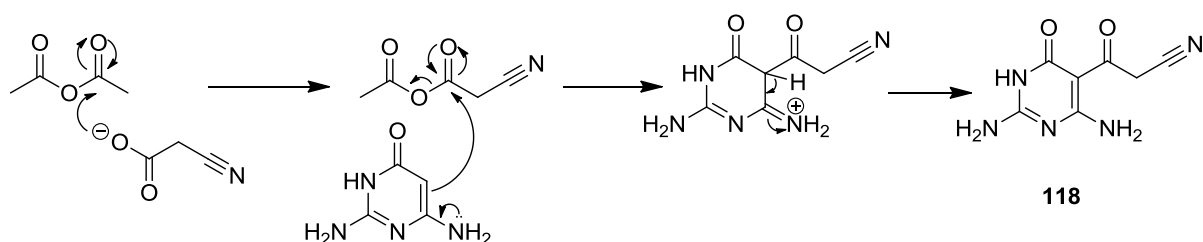
Compound **118** extends the nitrile further from the 5-position and retains a hydrogen bond acceptor at a similar position to that of the nitroso group in NU6027.

**Figure 44**

Quiroga *et al* cyanoacetylated a series of pyrimidinone compounds by forming a mixed anhydride from cyanoacetic acid and acetic anhydride. Pyrimidinones are required starting materials, as the use of pyrimidines as the starting material resulted in acylation at the exocyclic amino group.¹⁶⁸



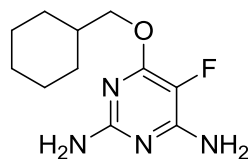
Scheme 20 Reagents and conditions; a) Ac_2O , $\text{NCCH}_2\text{CO}_2\text{H}$, $80\text{ }^\circ\text{C}$; b) (bromomethyl)cyclohexane, K_2CO_3 , DMF, 15 h, $100\text{ }^\circ\text{C}$



Scheme 21

The mixed anhydride was formed from acetic anhydride and cyanoacetic acid at $80\text{ }^\circ\text{C}$. Pyrimidinone (**115**) was then added to the reaction mixture to form compound **119**. As the cyano-substituted portion of the acetic anhydride is more electron-deficient, attack from the pyrimidinone ring should occur on this moiety. However, the crude product obtained from this reaction proved to be very insoluble, and no purification or NMR analysis was possible. Therefore the synthesis of this molecule was delayed until the biological results of compound **117** were obtained. Subsequently, as **117** showed a loss of activity, no further synthetic efforts were directed towards **118**.

It has been proposed that the biological potency of derivatives with electron-withdrawing groups at the 5-position is due to the acidification of the two amino protons, leading to the formation of stronger hydrogen bonds with the protein. A fluorine group at the 5-position of the pyrimidine ring would also act to acidify the 2-amino protons. The 5-fluoropyrimidine derivative **119** might identify whether the 5-substituent is required to act as a hydrogen-bond acceptor or to acidify the 2-amino substituents.



119

Fluorinating agents have become an area of interest due to their increasing use within medicinal chemistry.¹⁶⁹ A class of reagents known as N-F reagents are becoming increasingly popular, as they are a stable and easy to handle source of 'F⁺'.¹⁶⁹ Selectfluor™ is one of the commonest reagents of this class, and there are examples within the literature of electrophilic substitution of aromatic rings using Selectfluor™, including the fluorination of pyrimidine compounds.¹⁷⁰⁻¹⁷¹ The structure of Selectfluor™ (**120**) is shown below.

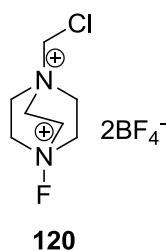
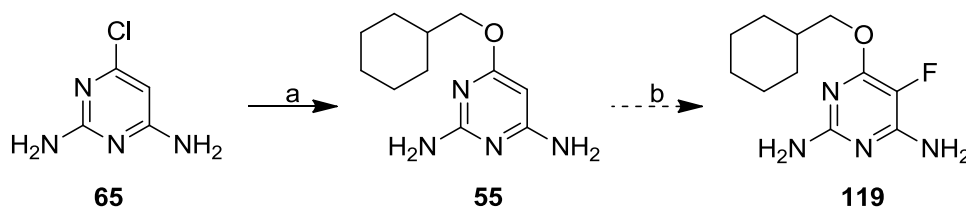


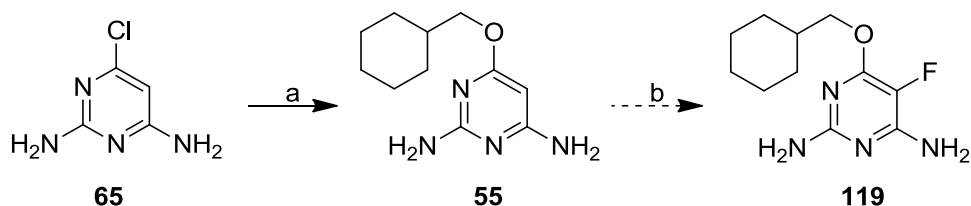
Figure 45

Compound **55** was treated with Selectfluor™ in acetonitrile at temperature up to 80 °C. LCMS monitoring indicated the formation of a new product. However, the reaction did not go to completion and on work-up and purification, no new product was obtained.



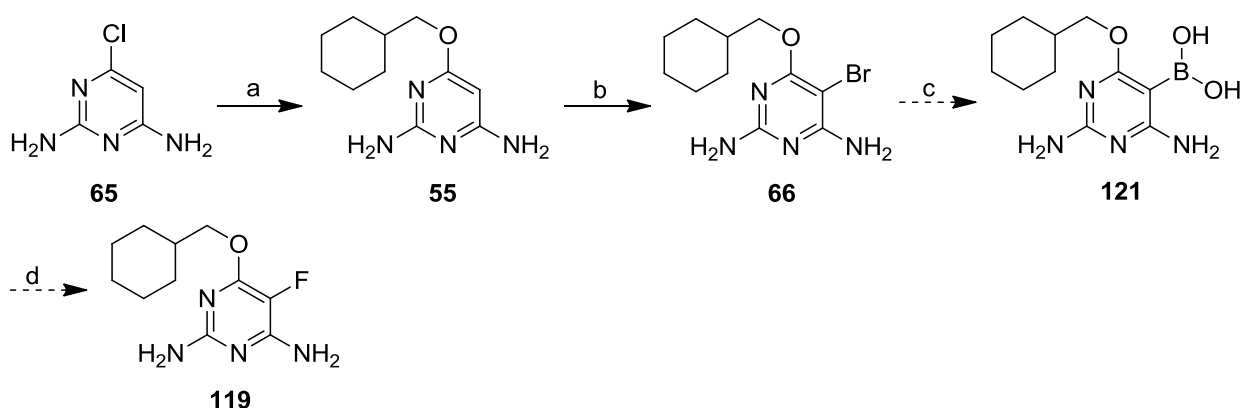
Scheme 22 Proposed reagents and conditions; a) Cyclohexylmethanol, sodium, 160 °C, 2h, 20 %; b) Selectfluor™, MeCN, 80 °C

A further group of reagents within the N-F class of reagents, which also includes Selectfluor™, are the *N*-fluoropyridinium salts, which also act as a source of electrophilic fluorine. On treating **55** with 1-fluoro-2,4,6-trimethylpyridinium salt, LCMS monitoring of the reaction suggested a new product was formed. However, after work-up and attempted purification only starting material was isolated (Scheme 23).



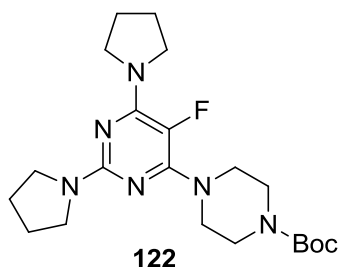
Scheme 23 Proposed reagents and conditions; a) Cyclohexylmethanol, Na, 160 °C, 2h, 20 %; b) 1-fluoro-2,4,6-trimethylpyridinium salt, MeCN, 18 h

Furuya *et al* have reported the fluorination of aromatic species from boronic acids,¹⁷² using silver triflate and Selectfluor™. The reaction proceeds *via* transmetallation of the aromatic species from the boronic acid to silver, which is then followed by fluorination of the aromatic ring. To follow the synthetic procedure developed by Furuya *et al*, the 5-boronic acid analogue **121** was required. The bromo derivative **66** was accessed from 4-cyclohexylmethoxy-2,6-diaminopyrimidine on treatment with NBS (Scheme 24). However, attempts to form the boronic acid, *via* the boronic ester, using bis(pinacolato)diboron, palladium acetate and potassium acetate¹⁷³ in DMF rapidly resulted in protodeboronation. In view of these results the synthesis of **119** was abandoned.



Scheme 24 Proposed reagents and conditions; a) Cyclohexylmethanol, sodium, 160 °C, 2h 20 %; b) NBS, AcOH, 1 h 80 %; c) Bis(pinacolato)diboron, Pd(OAc)₂, KOAc, DMF, 90 °C; d) AgOTf, NaOH, Selectfluor™

Cabaj *et al* have synthesised compound **122** using Selectfluor™, but no experimental procedure was given. The compound is described as ‘moderately stable’ and only a crude yield is provided, suggesting that 5-fluoropyrimidines, with three electron-donating substituents are not especially stable.



4.5 Pyridine Analogues of mTOR Inhibitory Pyrimidines

To separate mTOR inhibitory activity from CDK2 inhibitory activity, and to develop the structure-activity relationships for the pyrimidine ring, two pyridine-based analogues were synthesised. Each of these analogues probes the role of both of the pyrimidine nitrogens.

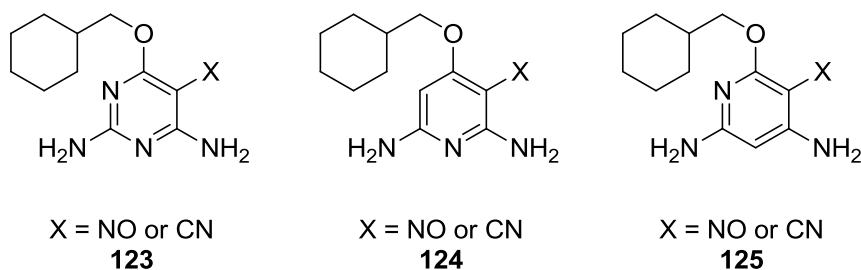
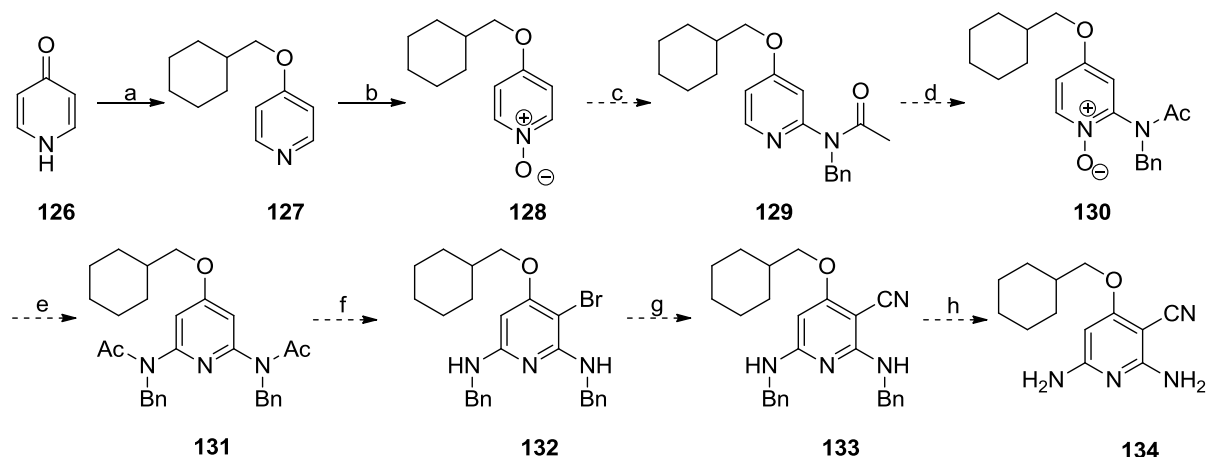


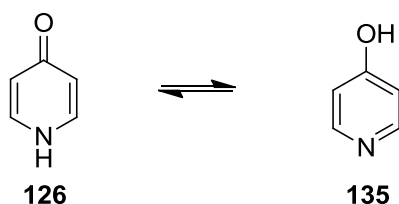
Figure 46

The first pyridine analogue **134** is capable of maintaining the triplet of hydrogen bonds, shown to be essential for CDK2 inhibitory activity but replaces the *N3* nitrogen with CH. The proposed synthetic route utilises a reaction described by Manley *et al*, which attaches secondary amides α to pyridine *N*-oxides (Scheme 25).¹⁷⁴



Scheme 25 Proposed reagents and proposed conditions; a) Conditions discussed below; b) *m*-CPBA, CH₂Cl₂; c) *N*-benzylacetamide, oxalyl chloride, 2,6-lutidine, CH₂Cl₂; d) *m*-CPBA, CH₂Cl₂; e) *N*-benzylacetamide, oxalyl chloride, 2,6-lutidine, CH₂Cl₂

The first step of the reaction is formation of the 4-cyclohexylmethoxypyridine (**126**). It was proposed to achieve formation of this product *via* a Mitsunobu reaction between cyclohexylmethanol and 4-pyridone (**126**) (the preferred tautomer of 4-hydroxypyridine (**135**)).



On treating 4-pyridone in THF with DEAD, PPh₃ and cyclohexylmethanol the highest isolated yield was 16%. Further analysis of the product also revealed that the compound was not the desired *O*-alkylated product, but instead the *N*-alkylation product. Although there are numerous examples within the literature of a Mitsunobu reaction performed on 2-pyridone, there are few examples of the Mitsunobu reaction with 4-pyridone.¹⁷⁵ Comins *et al* suggest that THF is an appropriate solvent to form the *O*-alkylated product in a Mitsunobu reaction with 2-pyridone. However, in our hands 4-pyridone in THF forms the *N*-alkylated product. The p*K*_a of 2-pyridone (11.62)¹⁷⁵ is similar to that of 4-pyridone (p*K*_a of 11.09)¹⁷⁶, so should not influence the reaction outcome. However, Schlegel *et al* suggest that a weak interaction can occur between the 2-hydroxy and pyridine nitrogen in 2-hydroxypyridine, stabilising the hydroxy form slightly, and it could be this form which reacts in the Mitsunobu reaction.¹⁷⁷ However, in view of the disappointing yield an alternative method of formation of 4-cyclohexylmethoxypyridine was investigated.

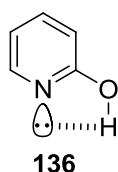
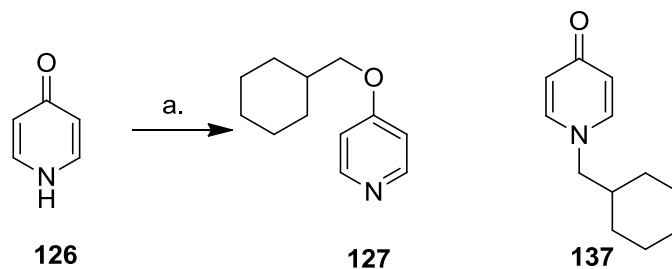


Figure 47 Proposed interaction between 2-hydroxy group and nitrogen of 2-hydroxypyridine

Alkylation of 4-pyridone with (bromomethyl)cyclohexane in the presence of a base was investigated. Two products are possible from this reaction, the *N*-alkylated product and the *O*-alkylated product. By altering the reaction conditions the reaction could be tuned to provide the desired *O*-alkylated product (Table 8). All the reactions used 1 equivalent of 4-pyridone, 1.5 equivalents of base, 5 equivalents of cyclohexylmethyl bromide and if used, 2 equivalents of 18-crown-6 and followed the procedure as described for 1-(cyclohexylmethyl)pyridin-4(1*H*)-one (**137**).



Scheme 26 Reagent and conditions; a) (bromomethyl)cyclohexane, base and solvent

18-Crown-6 was used as an additive to the reaction as previous work within the laboratory suggested that this would increase the yield of the *O*-alkylated product.¹⁷⁸ Crownethers ‘shield’ the cation allowing delocalisation of the negative charge. But in our hands this did not aid formation of the desired product. Both CsF and Cs₂CO₃ were used as a larger, softer cation may allow delocalisation of the negative charge, therefore resulting in *O*-alkylation. Caesium carbonate did result in formation of the greatest percentage of the desired product (**127**) but still a 1:1 ratio of product and unwanted isomer was formed. Both Hopkins *et al* and Comins *et al* suggest that silver salts favour formation of *O*-alkylated products in alkylation reactions of 2-pyridone,^{175, 179} and Hopkins *et al* also demonstrated selective *O*-alkylation by using pentane as a solvent.¹⁷⁹ In our case, silver salts gave particularly poor yields of any alkylated products.

Table 8 Conditions and yield for the 4-pyridone alkylation reaction

Solvent	Base	Additive	Conditions	<i>N</i> -alkylation yield	<i>O</i> -alkylation yield
DMSO	NaH	-	18 h, RT	46%	26%
DMSO	K ₂ CO ₃	-	26 h, RT	71%	24%
DMSO	NaH	18-crown-6	48 h, RT	49%	5 %
DMSO	K ₂ CO ₃	18-crown-6	26h, RT	41%	14%
DMSO	Cs ₂ CO ₃	-	5h, RT	42%	46%
DMF	Cs ₂ CO ₃	-	21 h	38%	41%
DMSO	CsF	-	28 h RT, 4 days, 30 °C	48%	7%
DMF	CsF	-	28 h RT, 4 days, 30 °C	45%	8%
DMF	Ag ₂ CO ₃	-	2 days, RT, 60 °C, 16 h	17%	-
Pentane	Ag ₂ CO ₃	-	2 days, RT, 60 °C, 16 h	-	-

Identification of the two isomers was possible *via* the ¹³C NMR spectrum and by comparison with the 4-methoxypyridine ¹³C spectrum. The NMR spectrum of the *N*-alkylated product has a signal at 179 ppm, which corresponds to the pyridone carbonyl carbon, whilst the *O*-alkylated product has a signal at 166 ppm which corresponds with the pyridine C-O carbon.

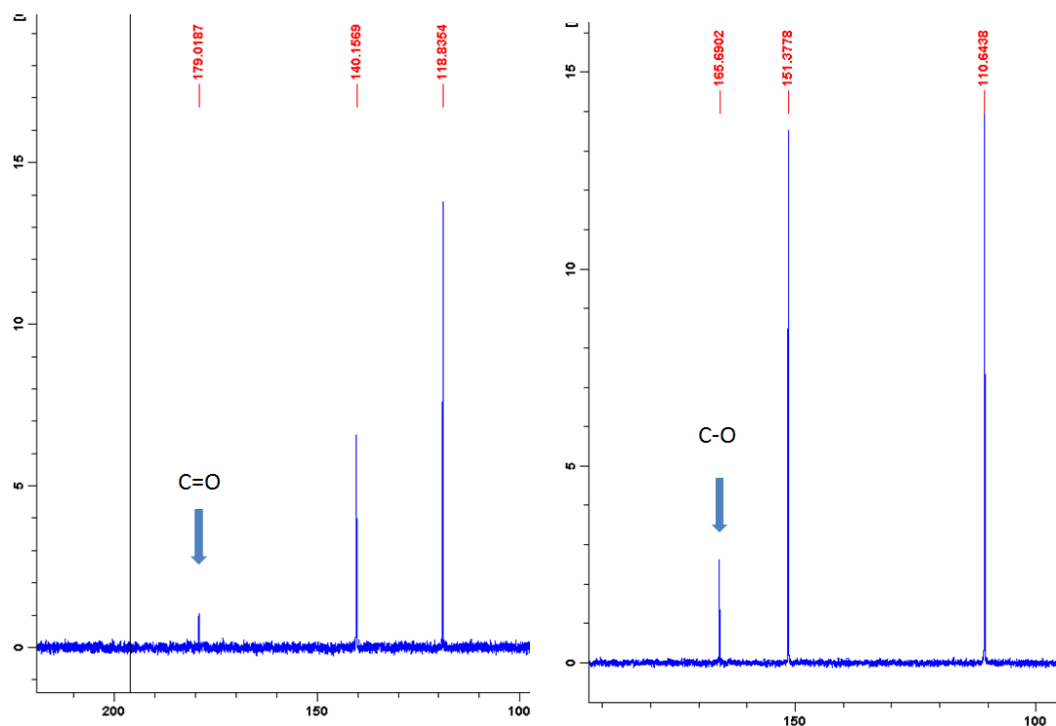


Figure 48 ^{13}C NMR spectrum of the *N*-alkylated (left) and the *O*-alkylated product (right)

To confirm the identity of the two possible isomers a crystal structure of the putative *O*-alkyl product was obtained. The *N*-alkylated product did not give appropriate crystals for X-ray crystallography.

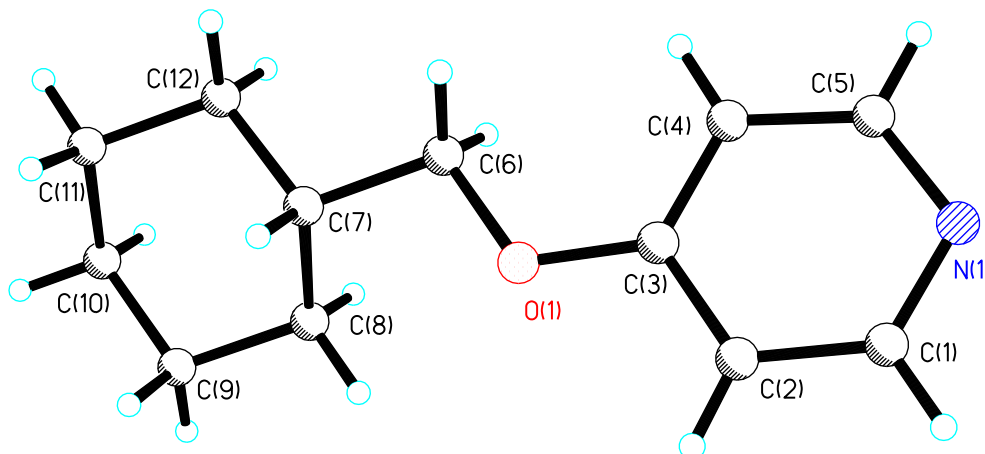
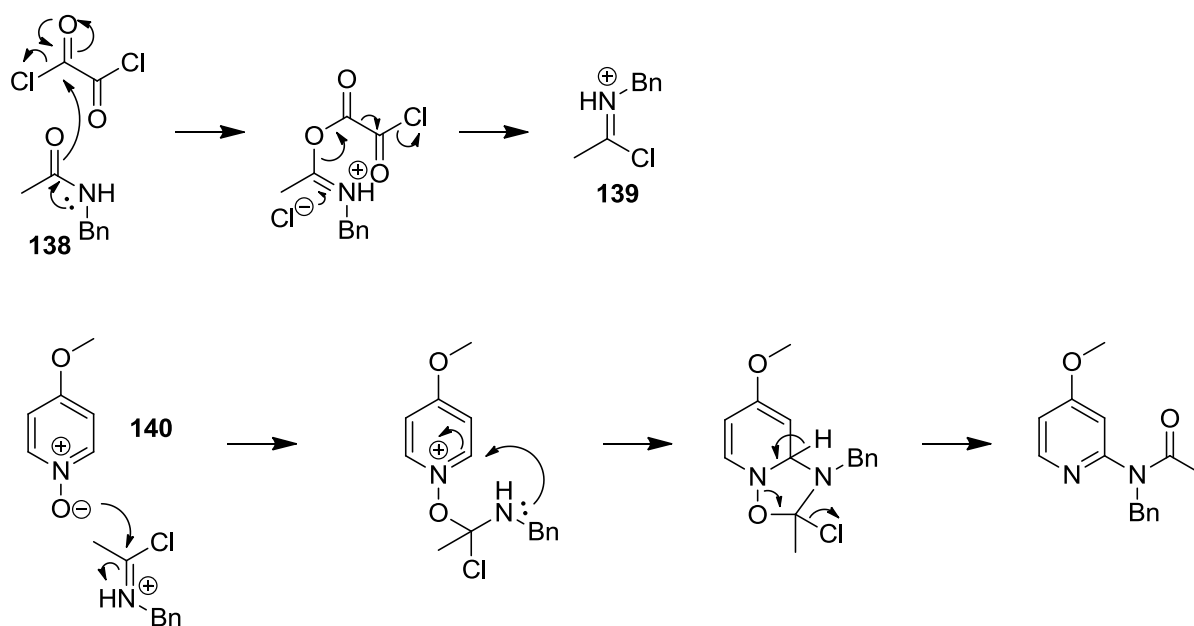


Figure 49 X-ray structure of the *O*-alkylated product (**127**)

To avoid the formation of the undesired *N*-alkylated an alternative route to the desired 4-cyclohexylmethoxypyridine was developed. Utilising a similar approach to pyrimidine derivatives the chloro group can be displaced from 4-chloropyridine by sodium alkoxide. To

o vercome the less electron-deficient nature of the pyridine ring the reaction temperature was increased to 200 °C, and resulted in good conversion to the product in 3.5 h.

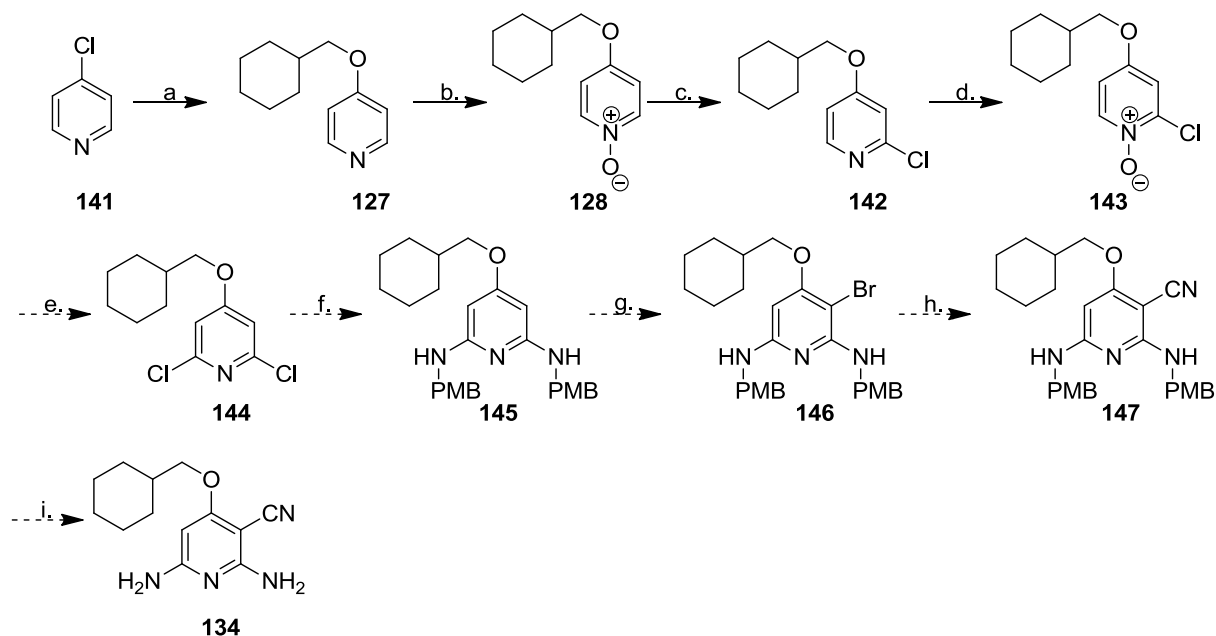
To utilise the synthetic route developed by Manley *et al* the pyridine *N*-oxide must first be formed. This was achieved using *m*-CPBA at room temperature in good yield. 4-Methoxypyridine was also used as a model compound for this reaction and was converted to pyridine *N*-oxide **140** in good yield. Manley *et al* formed imidoyl chloride (**139**) *in situ* from a secondary amide on treatment with oxalyl chloride and 2,6-lutidine.¹⁷⁴ It is the imidoyl chloride species which then reacts with the pyridine *N*-oxide.



Scheme 27

N-benzylacetamide (**138**) was synthesised by treating benzylamine with acetic anhydride in 27% yield. **138** was then treated with oxalyl chloride and 2,6-lutidine in DCM at 0 °C, and after 15 min 4-methoxypyridine *N*-oxide was added and the reaction was warmed to RT. Unfortunately, during the model reactions no reaction was observed, and so an alternative method to incorporate the desired 2,6-diamino motif was required. Treatment of pyridine *N*-oxides with phosphorous oxychloride results in chlorination α to the nitrogen atom. The phosphorous oxychloride firstly reacts with the *N*-oxide which results in the loss of a chloride ion. This chloride ion can then attack the ring, which has been activated towards nucleophilic attack by formation an intermediate *N*-oxy species, which makes the ring more electron-deficient.

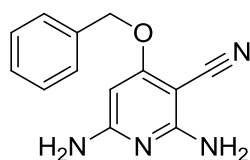
The new proposed scheme is shown below (Scheme 28). Each reaction of the *N*-oxide will result in the addition of one chloro group. Therefore, the molecule must be re-oxidised to incorporate the second chloro group. After both chloro-groups have been incorporated they can be displaced using *p*-methoxybenzylamine, which can act as a protected form of the amino groups for the synthetic route.



Scheme 28 Proposed reagents and conditions; a) Na, cyclohexylmethanol, 3.5 h, 200 °C, 53%; b) *m*-CPBA, DCM, 2 days, 97%; c) POCl₃, MeCN, 30 min, 160 °C, 56%; d) *m*-CPBA, DCM, 94%; e) POCl₃, MeCN

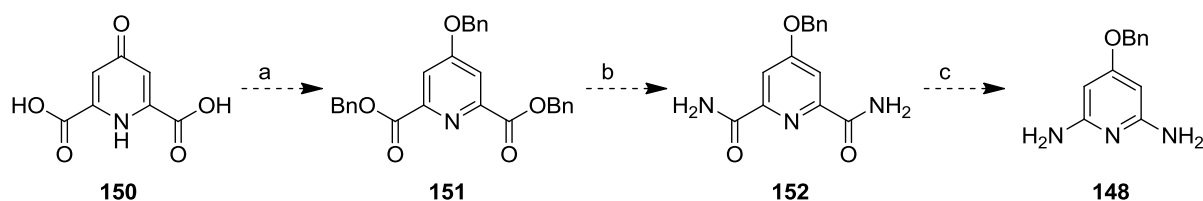
The optimal conditions for the chlorination were found to be with POCl₃ in MeCN and microwave heating at 160 °C for 30 min giving compound **142** in a 56% yield. Conventional heating resulted in lower yields and required overnight heating. Re-oxidising to the *N*-oxide was achieved using *m*CPBA in good yield 94%. However, the second chlorination failed to occur, both with microwave and conventional heating and continual heating resulted in the formation of a number of by-products.

An alternative synthetic route to the desired pyridine analogue was required. Braxmeier *et al* has synthesised 4-benzyloxy-2,6-diaminopyridine (**148**) in three steps from chelidamic acid, by utilising a Hofmann rearrangement to convert amide groups to amine groups (Scheme 29).¹⁸⁰ The benzyloxy pyrimidine derivatives are equipotent as mTOR inhibitors, so to allow direct comparison with the literature compounds, it was decided to synthesise compound **149**.



149

The first step of the synthetic scheme is an alkylation of both carboxylic acid groups and the pyridine oxygen, followed by conversion to the amide, prior to the Hofmann rearrangement. In our hands these alkylation conditions resulted in the formation of multiple products, making it difficult to identify the desired products



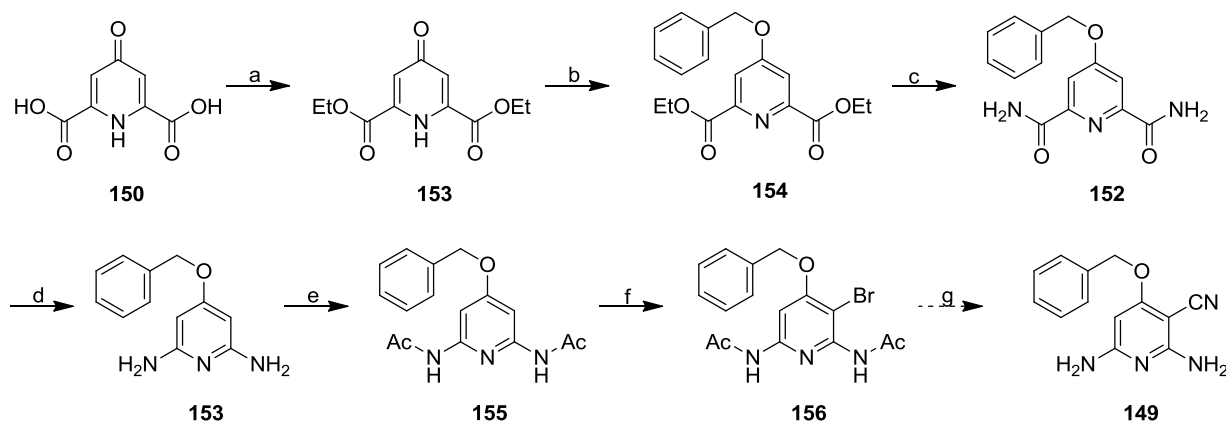
Scheme 29 Reagents and conditions; a) BnBr, K₂CO₃, acetone, 3 days, reflux, 71%; b) ammonia, methanol, 3 h, 93%; c) 5 M KOH_(aq), Br₂, 5 h, 90 °C, 76%¹⁸⁰

However, alternative procedures to dialkyl 4-alkoxy-pyridine-2,6-dicarboxylate rely on formation of the esters before alkylation.¹⁸¹ Conversion of chelidamic acid (**150**) to ethyl ester (**153**) followed by alkylation of the pyridine ring proved to be more reliable, with the alkylation achieved in particularly high yield (96%) (Scheme 31). The solvent was changed for the alkylation reaction, using DMF rather than acetone suggested by Kruizinga *et al.*¹⁸² Conversion of the ester groups to amide was achieved using 7 M ammonia in methanol in good yield (Scheme 30).

The Hofmann rearrangement was achieved using bromine in 5 M KOH, which proceeds *via* a nitrene species, which can rearrange to an amine, *via* an isocyanate. The desired 2,6-diamino functionality was now in place. The amino groups were then protected using acetic acid and acetic anhydride at room temperature in 91% yield. The pyrimidine-based synthesis of nitrile analogues suggested that the motif must be protected to prevent chelation to the copper cyanide.¹⁵² As the pyridine ring has two potential sites of electrophilic addition it was decided the ring should be deactivated slightly to prevent over-substitution. Therefore, the acetyl protection was incorporated before the bromination. Bromination was achieved using NBS in acetic acid in a 77% yield. However, on treating the brominated pyridine with CuCN in DMF at 120 °C no product was formed. Increasing the temperature only resulted in decomposition.

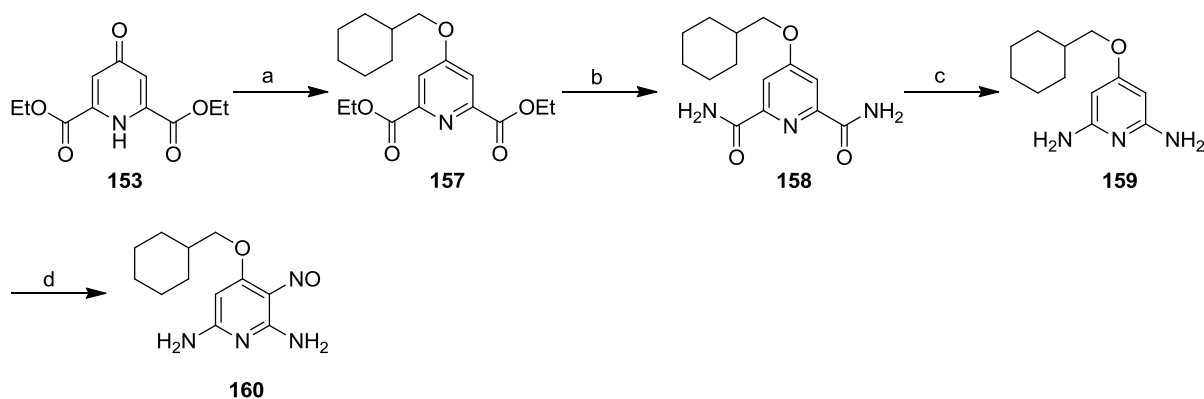
The reaction was then repeated at higher temperatures using microwave irradiation, with *N*-methylpyrrolidinone as solvent. Under the conditions, only slight traces of the product were observed, with the majority of the starting material decomposing. The reaction was repeated with further equivalent of CuCN, with similar results, as well as with the deprotected compound, but no compound was isolated.

Nitrile groups can also be incorporated using a palladium-catalysed method. Maligres *et al* used Pd(dba)₂ to catalyse the formation of aromatic nitriles from aromatic bromines using Zn(CN)₂.¹⁸³ However, under these conditions no reaction occurred. Replacing the catalyst with Pd(PPh₃)₄ also failed to give any product. It was therefore decided to halt the attempted synthesis of this molecule.



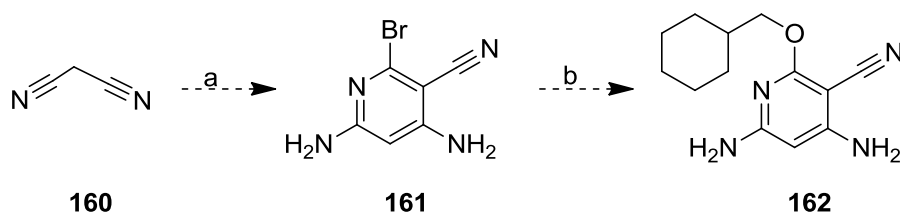
Scheme 30 Proposed reagents and conditions; a) SOCl₂, EtOH, 2 h, reflux, 46%; b) benzyl bromide, K₂CO₃, DMF, 30 min, 80 °C, 96%; c) 7 M methanoic ammonia, 3.5 h, 88%; d) Br₂, 5 M KOH_(aq), 2 h, 90 °C, 71%; e) Ac₂O, AcOH, 3 days, 92%; f) NBS, AcOH, 30 min, 77%; g) i. CuCN, DMF; ii. ethylenediamine

Whilst this work was ongoing the direct pyridine analogue of NU6027 was also synthesised. Using the previously developed methodology, compound **160** was synthesised using the route shown below. Formation of **160** proceeded cleanly in 30 min using standard nitrosating condition of NaNO₂ in 30 % acetic acid in water to give the direct pyridine analogue of NU6027.



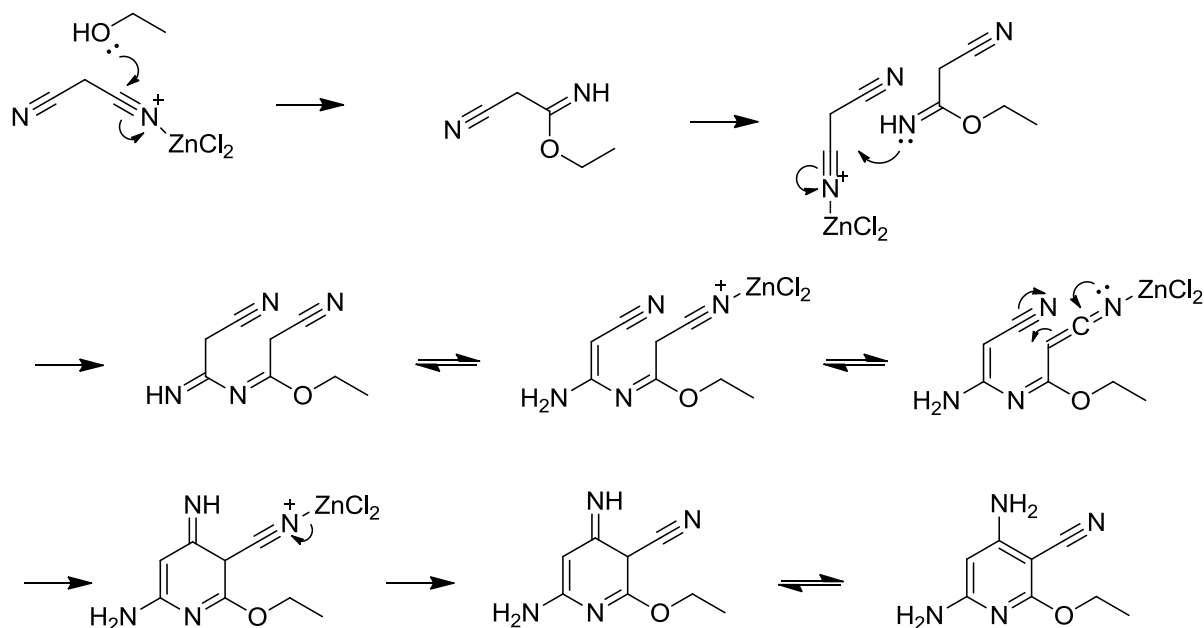
Scheme 31 Reagents and conditions; a) (bromomethyl)cyclohexane, K_2CO_3 , DMF, 16 h, 80 °C, 70%; b) 7 M NH_3 in MeOH, 1 h, 47%; c) Br_2 , 5M KOH, 90 °C, 2 h, 47%; d) $NaNO_2(aq)$, $AcOH(aq)$, 30 min, 80 °C, 47%

The alternative pyridine analogue of the ‘hit’ compounds was also required. Szczepankiewicz *et al* synthesised 2-alkoxy-3-carbonitrile-4,6-diaminopyridines from a bromo-substituted pyridine ring, with a sodium alkoxide to displace the bromo group.¹⁵⁵ Szczepankiewicz *et al* synthesised the bromo-substituted pyridine ring (**162**) in a one-step cyclisation step as described by Carboni *et al* by treating malononitrile with gaseous hydrogen bromide.¹⁸⁴ For safety reasons, the reaction was replicated using a liquid solution of 45% HBr in acetic acid, resulting in multiple products by TLC, and it was not possible to isolate the desired intermediate.

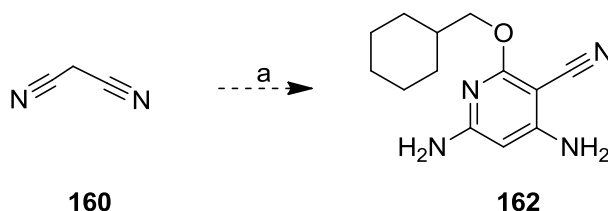


Scheme 32 Proposed reagents and conditions; a) 48% HBr in AcOH; b) Na, cyclohexylmethanol

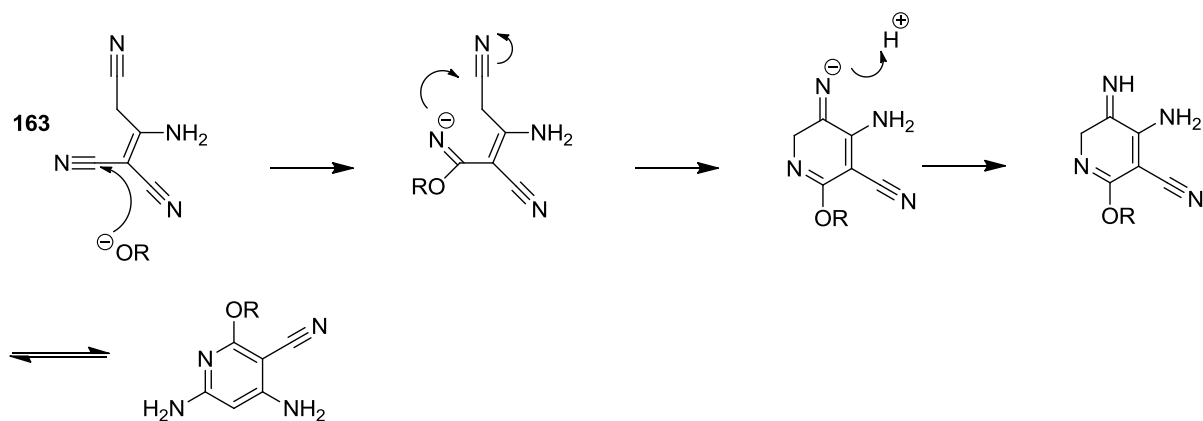
Silver *et al* treated malononitrile with zinc chloride in the presence of ethanol to synthesise 3-carbonitrile-4,6-diamino-2-ethoxypyridine.¹⁸⁵ A proposed mechanism of formation of the pyridine ring is shown below.

**Scheme 33**

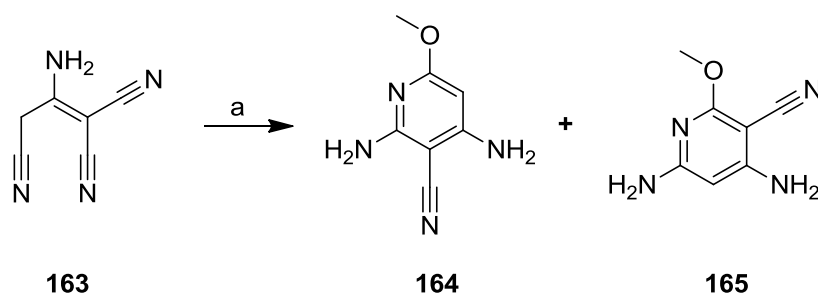
The synthesis of compound **162** by treating malononitrile with ZnCl_2 in the presence of cyclohexylmethanol was attempted. A number of products was observed by TLC, and although the LCMS suggested that the correct product had been formed, it was not possible to isolate the desired compound. The reaction was repeated using ethanol as described in the literature, but multiple products were formed.

**Scheme 34** Proposed reagents and conditions; a) ZnCl_2 , cyclohexylmethanol, $100\text{ }^\circ\text{C}$

Junek *et al* treated 2-amino-1,1,3-tricyanopropene (**163**) with sodium alkoxide, synthesising a pyridine ring with the desired functionality.¹⁸⁶ 2-Amino-1,1,3-tricyanopropene is also known as malononitrile dimer and is proposed as the intermediate in the synthesis of the substituted pyridine described by Carboni *et al*, suggesting that this reaction may proceed by a similar mechanism, which is shown below.¹⁸⁴

**Scheme 35**

Nitrile **163** was treated with sodium methoxide for 48 h at reflux forming two products, as described by Junek *et al.*¹⁸⁶ The two compounds had similar R_f to those described in the paper (0.3 and 0.6 in 4:1 diethyl ether to petrol). The major compound, with an R_f of 0.3, was isolated in 20%. It is this compound which Junek *et al* identified as being the desired isomer. The minor compound has an R_f of 0.6 and was produced in 5% yield.

**Scheme 38** Reagents and conditions; a) Na, MeOH, 48 h, reflux, **164** = 20%, **165** = 5%

NMR experiments were undertaken to confirm the identity of the compounds. The proton NMR spectrum was insufficient to identify the compounds. A 1D nOe (Nuclear Overhauser Effect) experiment was undertaken to observe interactions between the protons within the molecule. By the irradiation of a known proton (in this case the aromatic proton), an effect should be observed on protons which lie close within space to this proton. For the desired isomer an interaction should be seen between the aromatic proton and both amino groups, and for the unwanted isomer an interaction should be seen between one amino group and the methyl group. On running the 1D nOe experiment on the major compound an interaction was seen between the aromatic proton and both amino groups. These results suggest the major compound is the desired isomer. However, when the same experiments were run on the minor compound no interaction was seen. As a result a new ^1H NMR experiment was run, which

revealed significant decomposition of the compound, suggesting this compound is unstable in deuterated chloroform. This degradation would explain the apparent lack of interaction between protons in the nOe experiment.

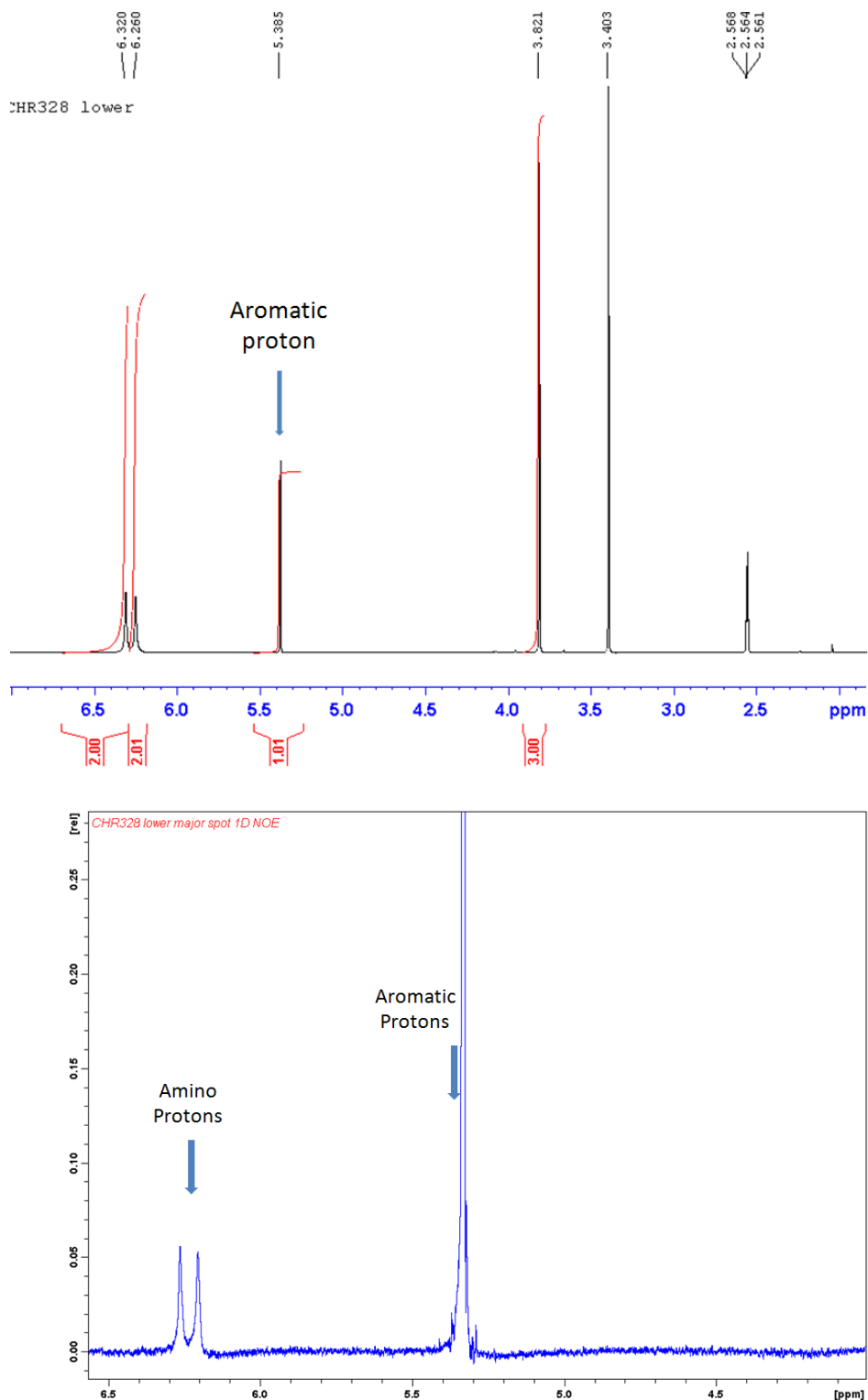


Figure 50 ^1H NMR spectrum and 1D nOe experiment performed on compound 165

A further experiment was therefore run to confirm the identity of **165**. A ^{15}N HMBC looks at the interaction between nitrogen atoms and the protons. The interaction between a proton and the nitrogen atoms can occur only over a distance of four bonds. With the desired compound the aromatic proton will interact with three nitrogen atoms, however the other isomer will only interact with 2 nitrogen atoms. After running the ^{15}N HMBC experiment on the major product the aromatic proton was seen to interact with 3 nitrogen atoms, confirming that the major product is the desired isomer (**165**).

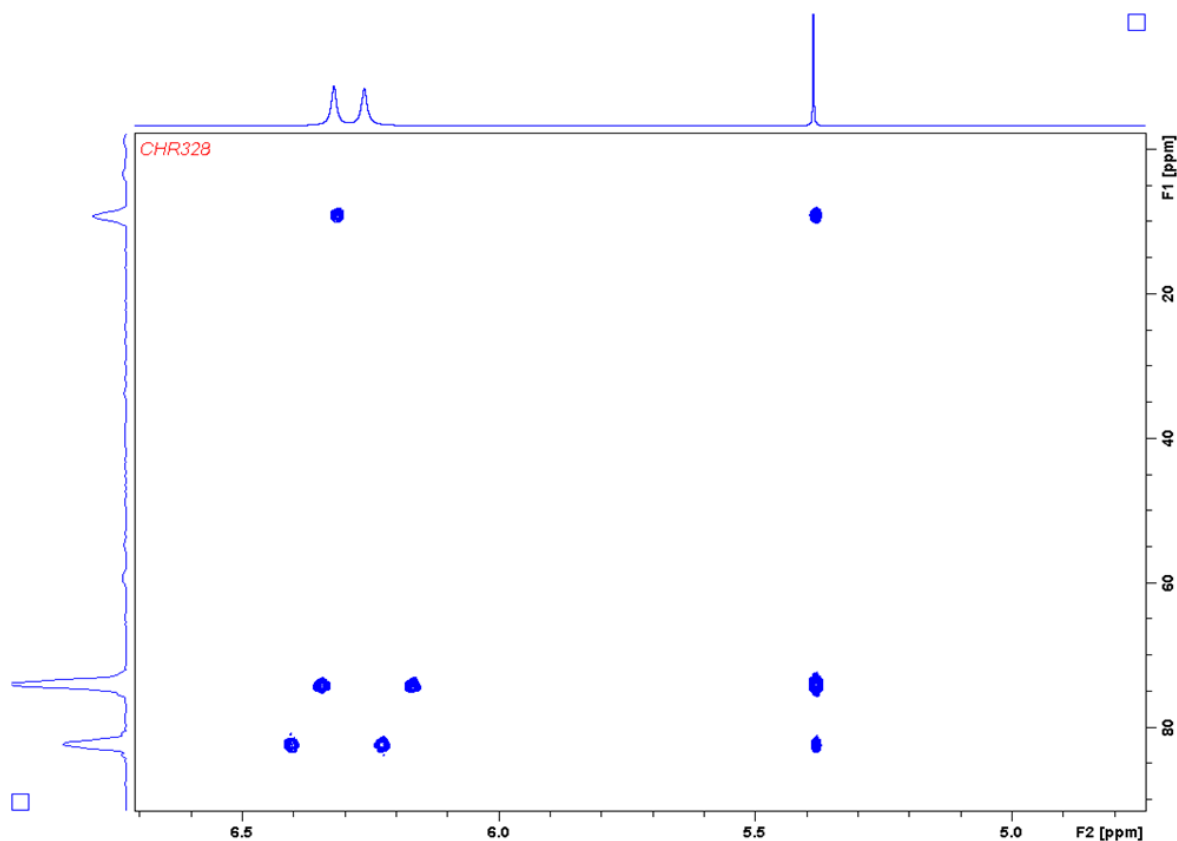
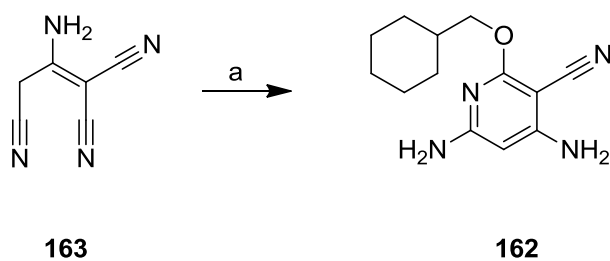


Figure 51



Scheme 37 Reagents and condition: a) Na, cyclohexylmethanol, 48 h, 120 °C, 4%

After successfully forming the methoxy analogue (**165**), synthesis of the direct pyridine analogue of NU6227 was undertaken using cyclohexylmethanol. The reaction mixture was heated at 120 °C for two days resulting in a complex mixture which required prep. HPLC. The 1D nOe experiment was not conclusive as irradiation at the frequency of the aromatic proton resulted in signal in both the diamino protons and the cyclohexylmethoxy CH₂ protons. However, the ¹⁵N HMBC showed that the aromatic proton interacts with three nitrogen nuclei, both amino nitrogens and the pyridine nitrogen. As this interaction occurs over a maximum of three bonds the aromatic proton must lie between the amino groups for this to occur. This suggests that the synthesised compound is the desired substance.

The synthesis of both pyridine isomers of the modestly active pyrimidine compounds unfortunately failed to maintain activity against mTOR; therefore no further investigation of this heterocycle was undertaken.

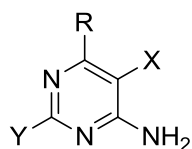
4.6 Biological Results

4.6.1. Assay details

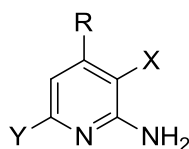
Biological analysis was carried out at the Northern Institute for Cancer Research by Lan Zhen Wang. Testing was undertaken with a KLISA assay using a recombinant human mTOR protein, recombinant p70S6K-GST protein, ATP, an anti p70S6K-T389 antibody and a secondary antibody with immobilised horse radish peroxidase.

A solution of p70S6K protein was added to a 96 well plate and incubated for 1 h at room temperature. Excess solution was then poured away and the plate dried. A solution of tris buffered solution (TBS) was used three times to wash the wells. The mTOR standard (protein and ATP) and the compound (dissolved in DMSO) were then added to the wells with a buffer solution; the plate was then covered and shaken for 30 seconds by a plate shaker, then incubated for 30 min at 30 °C. The kinase stop solution was then added and the plates washed. The anti p70S6K-T389 antibody solution was added and the plate incubated at room temperature for 1 h. The plate was washed and the horse radish peroxidase conjugate antibody added, then again incubated for 1 h and washed. A 3,3',5,5'-tetramethylbenzidine (TMB) solution was added and the mixture was incubated for 10 min at room temperature, followed by the ELISA stop solution (2.5 M H₂SO₄). The plate was read at 450 nm.

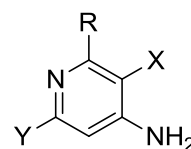
4. The Development of ATP-competitive Inhibitors of mTOR



Series A



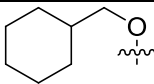
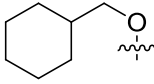
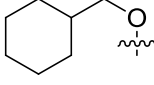
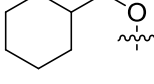
Series B



Series C

Table 9 Biological results * indicates compounds first synthesised by other chemists

Number	Series	R	X	Y	mTOR inhibition (% inhibition at 10 μ M)
56*	A		NO	NH ₂	80
59*	A		CN	NH ₂	64
166*	A		NO	NH ₂	23
81	A		CN	NH ₂	12
82	A		CN	NH ₂	34
167*	A		NO	NH ₂	42
83	A		CN	NH ₂	42
84	A		CN	NH ₂	40
168*	A		NO	NH ₂	43
85	A		CN	NH ₂	N. D.
169*	A		CN	NH ₂	29
170*	A		NO	NH ₂	44

86	A	H	CN	NH ₂	37
95	A		CN	H	17
118	A		CH ₂ CN	NH ₂	0
160	B		NO	NH ₂	34
162	C		CN	NH ₂	0

None of the new compounds that have been synthesised showed improved activity compared to the parent compounds. All newly synthesised compounds were weakly active, with an IC₅₀ against mTOR > 10 μM. The 5-nitroso or nitrile substituent has been demonstrated as important for activity, as is the triplet of hydrogen bonds.

The series of *O*⁴-alkyl substituents demonstrated that the further the alkyl group is from the cyclohexylmethyl group, in both size and shape, the greater the loss of activity. A series of aromatic *O*⁴-derivatives have been synthesised and demonstrated a tolerance for large lipophilic groups – suggesting the alkyl groups are too small to fill the lipophilic pocket in which the *O*⁴-substituent sits. Complete removal of the substituent at the 4-position, interestingly, has increasing biological activity over smaller alkoxy derivatives, suggesting that the oxygen atom itself is not forming an interaction with the protein, but is only acting as a link between the pyrimidine ring and the alkyl substituent. No substituent at the 4-position appears to be preferred over a small alkoxy substituent.

Insertion of a CH₂ group between the pyrimidine ring and the nitrile group in compound **117** abolished activity. The binding site around the 5-position may be very narrow, and does not tolerate the additional chain length. Or, the additional CH₂ group positions the nitrile group in the incorrect alignment to form a hydrogen bond with the protein. Removal of the 2-amino groups also abolished activity, underlining the importance of the triplet of hydrogen bonds, for not only CDK2 inhibition but also for mTOR inhibitory activity.

For both pyridine-based compounds, activity was significantly reduced. For compound **157**, activity was approximately halved. Though the triplet of hydrogen bonds is maintained, a

nitrogen atom at the 3-position of the pyrimidines is deleted, which may be forming an interaction with the protein. However, the change from pyrimidine to pyridine heterocycles will also result in a change in pK_a . This may result in a change of protonation state under assay conditions, which removes the acceptor moiety of the donor-acceptor-donor motif. Compound **160** completely abolishes mTOR inhibitory activity. Removal of the acceptor moiety of the triplet of hydrogen bonds resulted in a complete loss of activity.

Interestingly, though mTOR activity is significantly reduced by the modification from the pyrimidine to the pyridine heterocycle, CDK2 activity does not follow the same trend. Compound **157**, which retains the triplet of hydrogen bonds maintains biological activity, but compound **160**, which lacks the triplet of hydrogen bonds has significantly reduced biological activity.

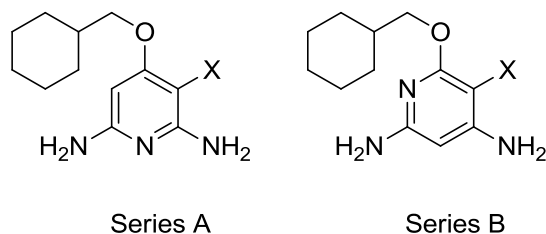


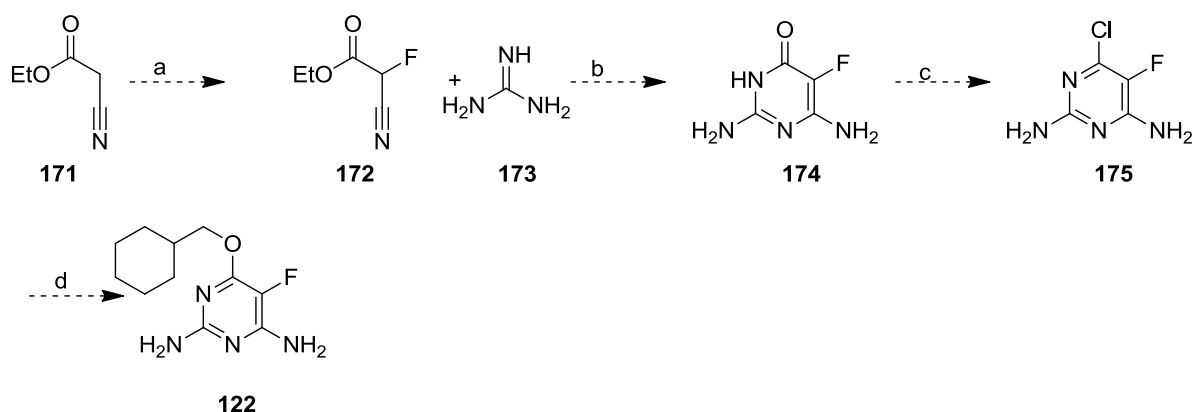
Table 10 Biological activity against CDK2

Number	Series	X	CDK2 inhibition % inhibition at 100 μ M (IC_{50} (μ M))
160	A	NO	(5.2)
162	B	CN	43

4.7 Future Work for the Development of Pyrimidine-based mTOR Inhibitors

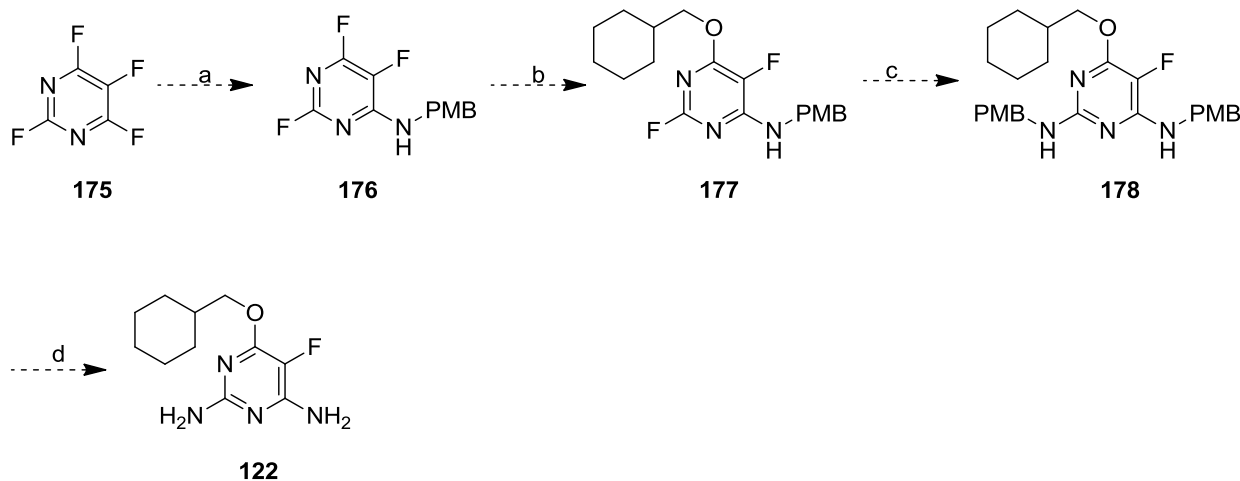
A 5-fluorinated pyrimidine was desired to determine the role of the 5-substituent, specifically the requirement to form an intermolecular hydrogen bond, or as an electron withdrawing group. Due to time constraints it was not possible to explore fully the alternative routes to access compound **122**. One approach would involve the building of the pyrimidine ring with the 5-fluoro substituent in place.

Joule *et al* proposed that the use of ethyl-2-cyanoacetate would allow the 6-amino group to be incorporated during the building up of the pyrimidine heterocycle.¹⁸⁷ Protons which lie between the nitrile group and the ester groups are acidic, with a p*K*_a value of ca. 13.¹⁸⁸ Deprotection followed by quenching the anion with a source of F⁺ should result in generation of compound **172**. Formation of the pyrimidine from guanidine would allow incorporation of the 2-amino group. After chlorination of the oxo group with POCl₃ and displacement with cyclohexylmethoxide the desired compound **119** would be obtained.



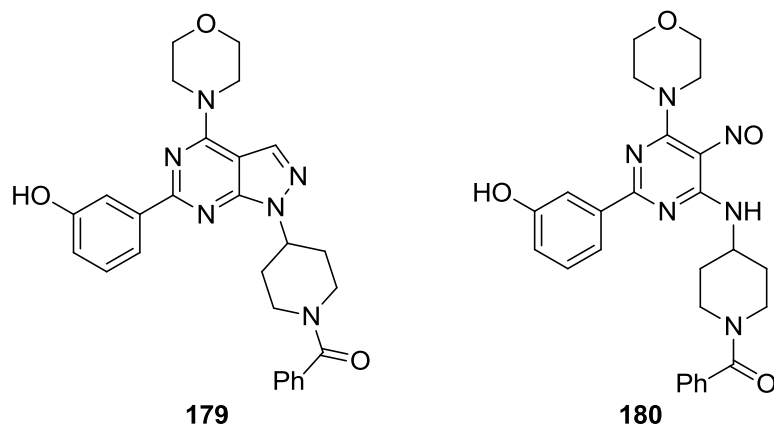
Scheme 38 Proposed reagents and conditions; a) KOH, Selectfluor, THF; b) Na, methanol; c) POCl₃ d) Na, cyclohexylmethanol

Parks *et al* have reported the regiospecific displacement of fluorine atoms by nucleophiles from tetrafluoropyrimidine.¹⁸⁹ Using a similar approach, the desired fluoro compound could be synthesised. The displacements are thought to occur first at the 4- and 6-position, followed by the 2-position. Therefore, adapting the synthetic route shown below, compound **122** could be synthesised. Hünig's base was added by Parks *et al* to all reactions to neutralise any formed HF.¹⁸⁹



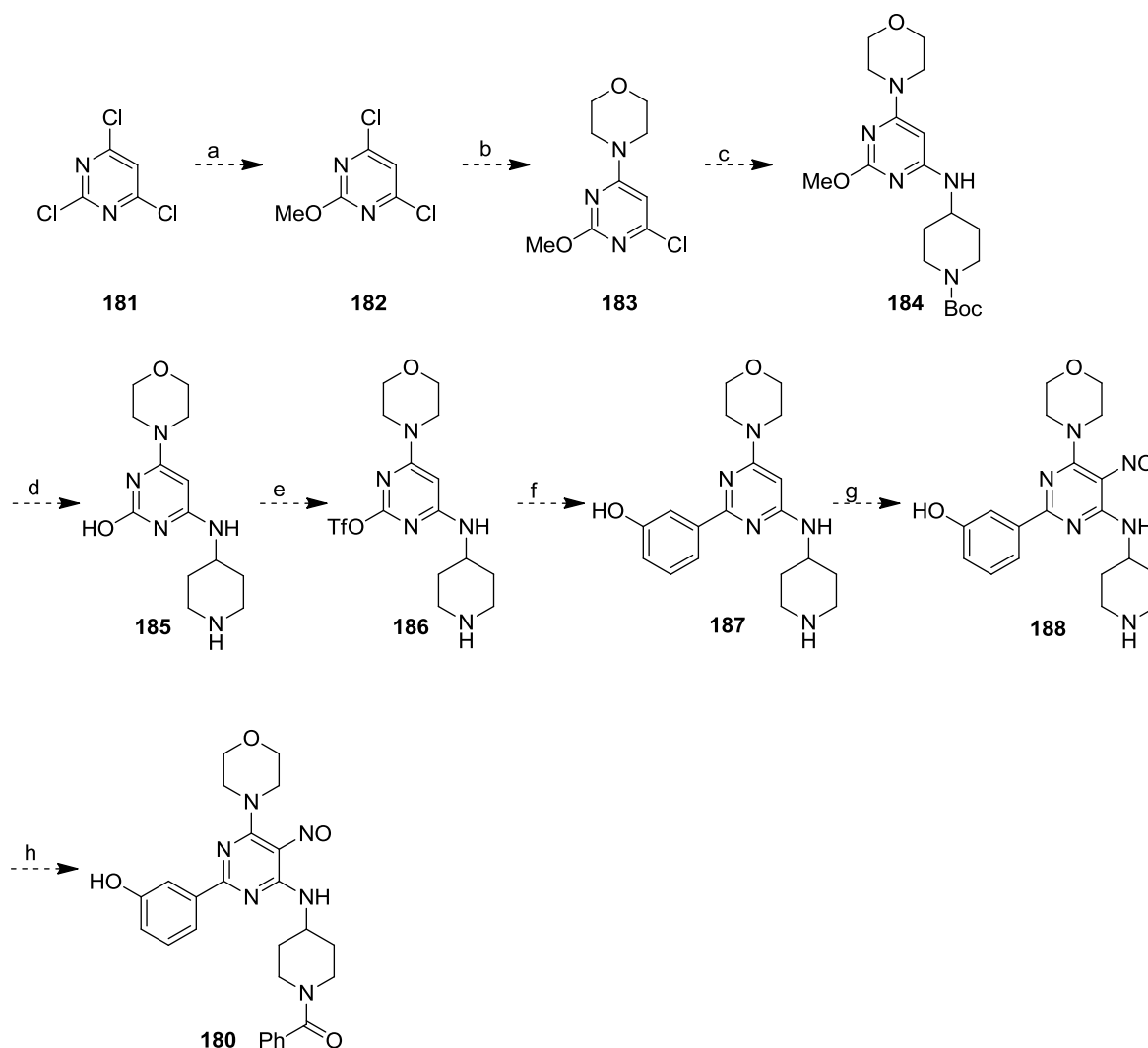
Scheme 39 Proposed reagents and conditions; a) *p*-methoxybenzylamine, DIPEA, THF, 0 °C; b) Cyclohexylmethanol, NaH, THF, DIPEA, room temperature; c) *p*-methoxybenzyl amine, DIPEA, THF, 140 °C

Nowak *et al* have described the synthesis of pyrazolopyrimidine-based potent mTOR inhibitors such as **179**, with an IC₅₀ of 4 nM.⁷² The 5-nitroso compound (**180**) has been demonstrated to form a hydrogen bond between the 5-nitroso substituents and the proton on the 6-amino group forming a pseudocycle. Therefore a pyrimidine with a 5-nitroso substituent may act as a mimetic for a pyrazolopyrimidine, and a scaffold-hopping approach will identify active substituents for the pyrimidine ring such as **180**.



A S_NAr reaction between sodium methoxide and trichloropyrimidine will result in substitution at the 2-position, the most reactive position. Two further S_NAr reactions with morpholine and *N*-benzyl protected 4-aminopiperidine, will incorporate the desired functionality at both the 4- and 6-position. Removal of the methyl group with the Lewis acid boron tribromide, will also result in removal of the Boc protecting group. Triflation of the resulting hydroxyl group will generate the appropriate substituent for a Suzuki reaction,

which followed by nitrosation and treatment with benzoyl chloride should result in the formation of the desired compound.



Scheme 40 Proposed reagents and conditions; a) Na, MeOH; b) Morpholine, DIPEA, THF; c) 4-amino-1-Boc-piperidine, DIPEA, THF; d) 1 M BBr₃ in DCM, DCM; e) Tf₂O, Et₃N, THF; f) (3-hydroxyphenyl)boronic acid, Pd(PPh₃)₄, Na₂CO₃, dioxane, water; g) NaNO₂, AcOH, water; h) Benzoyl chloride, Et₃N, THF

4.8 Conclusion

mTOR is an attractive anti-cancer target due to its function within the PI 3-K/Akt pathway, which frequently suffers from aberrant signalling within cancer. Our work on ATP-competitive inhibitors of mTOR began with a series of pyrimidines with modest activity against mTOR. Synthetic efforts have identified the importance of the pyrimidine heterocycle through the synthesis of two pyridine analogues. The synthesis of a 2-unsubstituted analogue

of NU6227 has also identified the importance of the triplet of hydrogen bonds formed with the protein. Modifications to the O^4 -substituent with a series of alkyl derivatives reduced activity, alkyl groups such as the *sec*-butyl which had comparable shapes and size to the cyclohexylmethyl group were shown to be the most active of the newly synthesised analogues, whilst smaller groups, such as the ethyl analogue, were shown to be less active than complete removal of the 4-substituent. A series of substituted benzyl analogues have also been synthesised and showed a flat SAR, suggesting that the O^4 -substituent sits within a large lipophilic pocket, which is not fully utilised by the alkyl substituents. The initial screen of compound which identified the 2,6-diaminopyrimidine scaffold, demonstrated that 5-substituents capable of forming a hydrogen bond gave activity. An additional methylene group between the pyrimidine ring and the hydrogen bond forming substituent essentially abolished activity. Therefore, despite the extensive synthetic efforts no compound was synthesised with improved activity over the initial compound within the screen.

Since work began at the NICR on the development of ATP-competitive inhibitors of mTOR a number of highly potent and selective inhibitors of mTOR have been published, and a number of these have progressed into clinical trials. Many of these inhibitors are, like the NICR series, based on nitrogen containing heterocycles. The compound space has been covered extensively in this area, suggesting that continued synthetic efforts may not result in the synthesis of a novel compound.

5. Isoindolinone-Based Inhibitors of the MDM2-p53 Protein-protein Interaction

5.1 Development of Isoindolinone Based Inhibitors of the MDM2 p53 Protein-protein Interaction

The Northern Institute for Cancer Research programme to discover inhibitors of the MDM2-p53 protein-protein interaction was initiated by the identification of a number of isoindolinone-based compounds, by a preliminary screen of compounds using an *in vitro* binding assay.¹⁹⁰ Compounds **189**, **190** and **191** were identified as weak inhibitors with IC₅₀s of around 200 μ M, were shown to have growth inhibitory activity in NCI 60 cell line screen and were classed as COMPARE negative against known classes of antitumour agents.¹⁹⁰

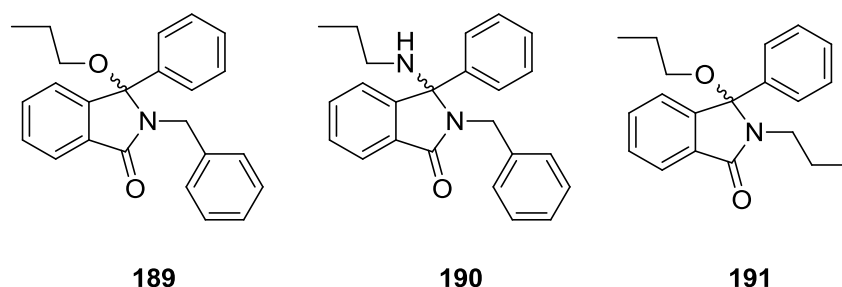


Figure 52 Structure of the initial isoindolinone hits

A programme of library synthesis was undertaken, guided by a virtual screening to suggest desired compounds.¹⁹⁰ Compounds **189** and **191** were docked into MDM2 to identify a single, low energy binding mode using the program easyDOCK.¹⁹⁰ Both stereoisomers of the isoindolinones were docked into the 1YCR crystal structure of MDM2. However, due to the lipophilicity of both the compounds and the MDM2 binding site, along with the open shape of the compounds a large number of potential binding modes were identified.¹⁹⁰

A number of further compounds were synthesised, some suggested from ‘virtual screening’ by the selection of a single binding mode from those identified, others suggested by the availability of starting material during the synthesis of the isoindolinones. However, those suggested by the ‘virtual screening’ were found to be no more potent than those synthesised without docking.¹⁹⁰ These results suggested that there may be multiple experimental binding modes for isoindolinones and MDM2, and that the use of multiple binding modes within computational chemistry may increase possibility of accurately predicting the experimental binding mode. This approach was used to identify a more diverse group of seed compounds which were used by to aid the identification of the experimental binding mode.¹⁹⁰

Six seed compounds were selected and synthesised with activities ranging from 27 to 92 μM .¹⁹⁰ These compounds were again docked into the MDM2 crystal structure using both the easyDOCK and GOLD program which again generated a large number of solutions. 24 high scoring, unique binding modes were chosen as a starting point for further work. These 24 modes were generated from the six seed compounds, one per stereoisomer of each compound per docking program. In each mode the position of the isoindolinone was preserved and unique compounds generated by varying R^1 or R^2 using commercial reagents.

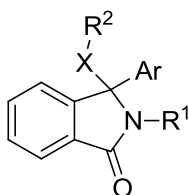


Figure 53 Structure of the isoindolinone core

The interaction between the ligand and MDM2 protein was further explored using the program Skelgen.¹⁹⁰ This explores the interaction of a ligand with that of the active site of a protein, defined as a rectangular box with selected fragments included. Ligands were selected which formed at least one interaction with the target residues within the MDM2 protein. The target residues included Leu54 O, Phe55 O, Gln59 NE2, Gln72 O and OE1, Val93 O, His96 ND1 and Tyr100 OH.¹⁹⁰ The parameters suggested 57 ‘virtual hits’ and of the 57, 43 were synthesised. These 43 compounds covered 14 of the 24 potential modes, with substituents selected which appeared in only one binding mode chosen to aid identification of the preferred binding mode.¹⁹⁰

Of the 43 synthesised compounds, five showed no appreciable inhibitory activity, approximately half showed inhibitory activity in the region of 100-400 μM , a further 12 showed activity in the 50-100 μM range, similar to the initial six seed compounds.¹⁹⁰ Two compounds had activity that improved on the most potent of the seed compounds. From these compounds a number of binding modes were proposed, dependent on the R^1 and R^2 substituents, the most important being those associated with the two most active compounds.¹⁹⁰

The first binding mode has the isoindolinone lying in the Trp23 pocket, with an N-ethylacetamide group (R^1) forming an H-bond interaction to Gln72 within the Phe19 pocket.

A *tert*-butylbenzyl group (R^2) overlays the surface.¹⁹⁰ The second binding mode has the isoindolinone overlying the surface with the Trp23 pocket occupied by the 3-phenyl group, syringic alcohol (3,5-dimethoxy-4-hydroxybenzyl alcohol) (R^2) in the Leu26 pocket which forms an H-bond to Trp100 and an *N*-benzyl group (R^1) in the Phe19 pocket.¹⁹⁰

A combinatorial approach was then undertaken using the most favourable substituents which are summarized below.¹⁹⁰ This resulted in the design of 36 isoindolinones, with the number reduced as synthesis proved problematic or preliminary biological results proved disappointing. The 4-SEM group was found to be a poor substituent, suggesting that previously the group was forming a non-specific hydrophobic interaction. 4-Chlorophenyl was the preferred aromatic substituent, with the presence of this substituent suggesting that the compounds are making a favourable interaction with the hydrophobic Trp23 pocket.¹⁹⁰ This correlates with the second mode described. The most active compounds identified are shown below.¹⁹⁰

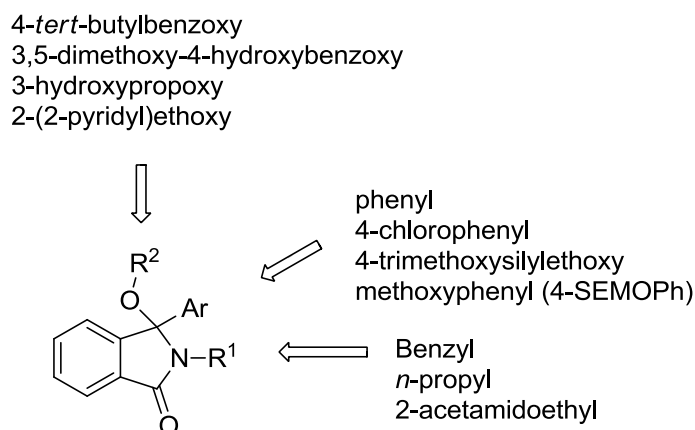


Figure 54 The isoindolinone scaffold with favoured substituents in each position

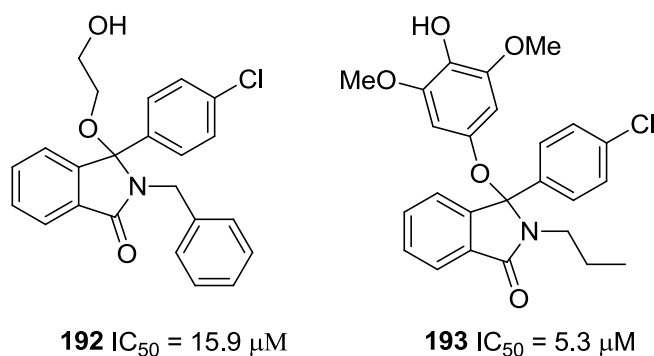


Figure 55

Selected isoindolinones had also been shown to behave in a dose-dependent manner, with p53 related gene transcription increasing with increasing dose within a MDM2 amplified SJS human sarcoma cell line.¹⁹¹ However, combinatorial chemistry and molecular docking were not providing sufficient increases in potency. Additional information about how the isoindolinone binds to MDM2 would validate the structure-activity relationships and suggest areas for further modification. Due to the moderate potency of these protein-protein inhibitors it can be difficult to gain further structural information. Computational methods are limited when interaction is due to hydrophobic interactions rather than H-bonds. Crystallography can also potentially prove difficult due to the weak affinities, poor solubility of the inhibitors and the flexibility of the protein. NMR studies would also prove difficult as the protein must be saturated and a micromolar affinity would result in line broadening.¹⁹¹

A different approach uses 2D HSQC-NMR chemical shifts to determine the location of a ligand binding by observing changes in the chemical shift. The binding mode is determined by comparing the experimentally observed chemical shifts with those predicted for each of the suggested binding modes.¹⁹¹

The 12 isoindolinones that were subjected to NMR analysis were divided into groups that differed in only one area of their chemical structure, either the isoindolinone *N*-substitution or substitution in the 3 position. The 3-position aromatic was fixed as a *p*-chlorophenyl moiety. The active site of the MDM2, in which the isoindolinone binds, can be summarised as 4 main sub-pockets.¹⁹¹

- The pocket in which Trp23 of p53 binds is a shallow pocket, with the Trp23 forming a H-bond with Leu54 on MDM2
- The Leu26 pocket formed by the residues Ile99 and Ile103 of MDM2
- The Phe19 pocket around residue Ile61
- A deep pocket in which the Trp23 side chain lies

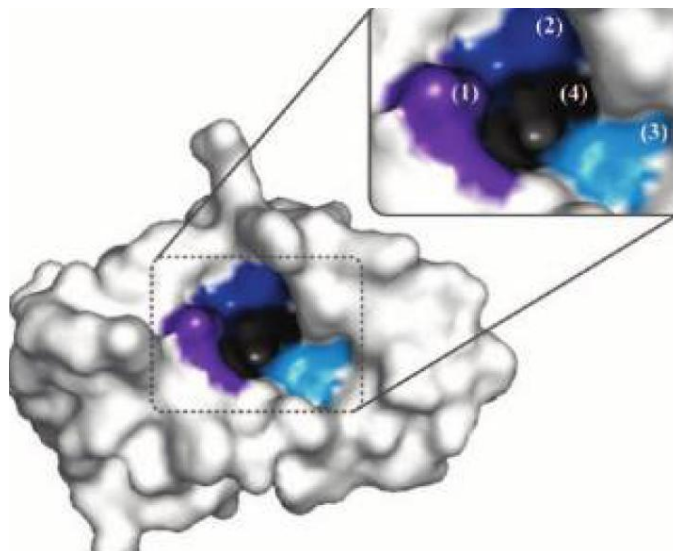


Figure 56 Surface representation of MDM2 (1YCR) with the 4 sub-pocket highlighted. (1) Trp23 sub-pocket (2) Leu26 sub-pocket (3) Phe19 sub-pocket (4) Trp23 side chain sub-pocket (Taken from reference 190)

For the NMR studies 38 residues surrounding the isoindolinone binding site were monitored. The 38 residues were the most likely to be affected by the binding:

- helix $\alpha 2$ (residues 50 to 63 and 67 to 75)
- helix $\alpha 1'$ (residues 82 to 86)
- helix $\alpha 2'$ (residues 91-106)

Cluster analysis was then performed on each residue per group of compound, with closely clustered peaks suggesting similar binding. As each group only differs chemically in one area, the area of unclustered peaks will be the area of different binding. This was used to show which amino acid residue lies near each area of the isoindolinone.¹⁹¹

As a result of these NMR studies the isoindolinones are thought to bind with either the isoindolinone or the 4-chlorophenyl group pointing into the deep pocket of MDM2, the Ile99 pocket is thought to prefer aromatic groups, while both Leu54 and Ile 61 pockets are not selective for the type of group.¹⁹¹ NMR studies with compound **184** identified a significant shift in the signal for the Leu54 region, which was thought to be due to an interaction between Leu54 and the hydropropoxy chain. It was proposed that by introducing rigidity to the propyl chain activity could be improved. Replacement of the propyl chain with a cyclopropyl derivative increased activity to 3.0 μM .¹⁹²

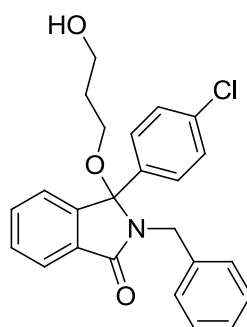
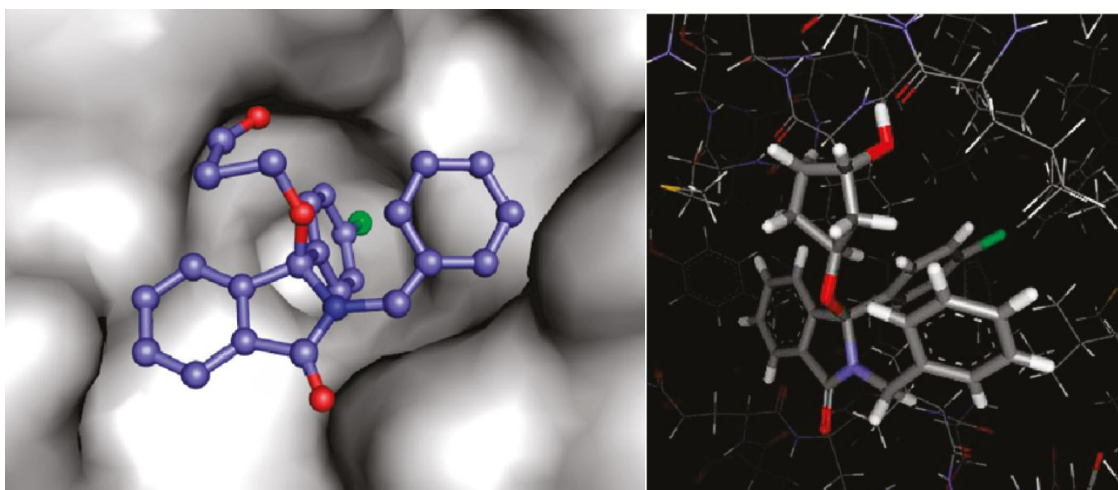
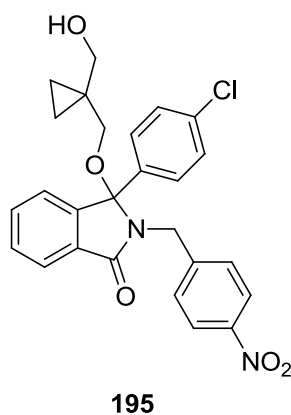
**194**IC₅₀ = 16 μM

Figure 57 Structure of (*R*)-NU8165 (**194**) bound to MDM2 deduced from HSQC NMR studies (left) and modelling of a cyclopropyl derivative (Taken from reference 193)

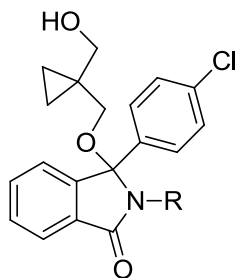
Further SAR studies with the 3-hydroxyisoindolinone identified small lipophilic groups at the 4-position of the *N*-benzyl group as improving potency. Inclusion of a chlorine atom at this position resulted in a compound 17 times more potent than an initial parent compound. However, it was then found that inclusion of a nitro group at this position increased potency further, with activity 30 times greater than that of the parent.¹⁹²

Combining the optimal nitrobenzyl substituent with a racemic cyclopentyl ether side-chain was discovered to have an additive effect with an IC₅₀ of 0.70 μM, and on synthesis of the *cis*-derivative gave an IC₅₀ of 0.30 μM. A range of alkoxy derivatives were then incorporated to probe the SAR around this region, that identified the 1,1-bis(hydroxymethyl)cyclopropyl derivative as the optimal substituent at this position.¹⁹² Interestingly, in NMR studies with cyclopropyl derivative (**195**) the 2-cyclopropylpropanol chain is seen to interact with an area, which is not exploited by either the Nutlin series or the benzodiazepinedione series.¹⁹²



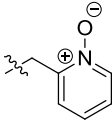
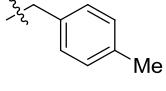
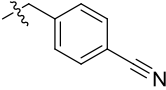
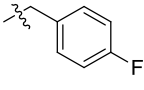
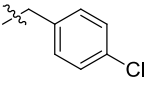
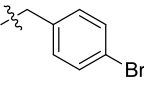
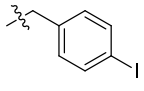
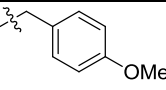
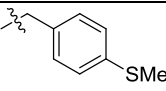
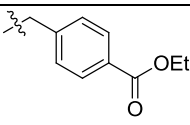
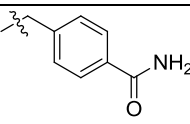
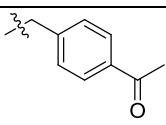
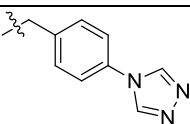
NMR studies were undertaken comparing isoindolinone, Nutlin-3 and p53 peptide binding to MDM2. The ‘footprint’ of isoindolinone, Nutlin-3 and p53 binding was then characterised.¹⁹³ A 2D NMR ¹H ¹⁵N-heteronuclear single-quantum coherence (HSQC) titration was undertaken with a range of concentration of each inhibitor. The binding of ligands resulted in a shift in signal in the primary sequence of MDM2, apart from the C-terminal 10 residues. The average chemical shift is 0.045 to 0.083 ppm. Nutlin-3 has an average shift of 0.076 ppm, p53 peptide has an average shift of 0.22 ppm and compound **195**, the most potent isoindolinone compounds analyzed had an average shift of 0.075 ppm.¹⁹³ The greatest observed shift was seen in the hydrophobic pocket, which is in direct contact with the ligands. The greatest shift was observed between the helix 2 α (residues 51-63), the area surrounding β -strands β 3 and β 1’ (residues 66-77) and the region connecting β 2’ to α 2’ (residues 89-104). The N-terminal also has larger shift, due to the change in conformation from the closed to open position.¹⁹³ Nutlin-3 was seen to induce a larger chemical shift on the beta sheet β 3, while isoindolinone **195** has a greater effect on residues at the opposite side of the pocket helix α 2’ and the back of Trp23 pocket.¹⁹³ This underlines that whilst all MDM2/p53 inhibitors are acting as p53 α -helix mimetics; there are differences between binding modes of the inhibitors.

As the nitro group is undesirable within drug molecules, due to the possibility of forming toxic metabolites, a number of classical and non-classical isosteres for the nitro group have previously been investigated. A table of the previously synthesised compounds and their activity is shown below.¹⁹⁴⁻¹⁹⁵ Compounds all have the structure type shown below

Table 11 Classical and non-classical isosteres attempted for replacement after the nitro benzyl group

Compound number	Structure of R group	IC ₅₀ of activity against MDM2 (μM)
195		0.23 ± 0.11
196		23 ^a
197		>10
198		210 ^a
199		180
200		8.9 ± 3.8
201		8.8 ± 4.2
202		250 ^a
203		> 200 ^a
204		29 ± 6.0
205		>200
206		11 ± 0.8

5. Isoindolinone-Based Inhibitors of the MDM2 p53 Protein-protein Interaction

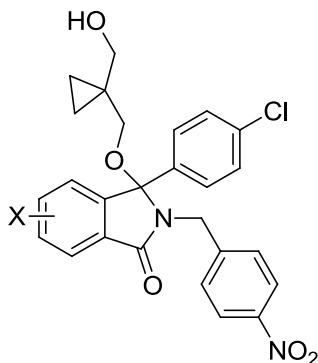
207		32 ± 5.2
208		2.3 ± 0.059
209		1.8 ± 1.3
210		1.7 ± 0.73
211		2.3 ± 1.1
212		1.2 ± 1.2
213		1.0 ± 0.39
214		2.5 ± 0.86
215		180^a
216		$> 20^a$
217		> 50
218		15 ± 1.4
219		> 20

^a indicates n = 1

Previous SAR studies around the 'A'-ring showed that substitution around the isoindolinone further improved potency. A chloro-substituent in the 4-position was found to be optimal (**220**), increasing potency to 143 nM. A *tert*-butyl group in the 6-position was also shown to

be favourable, with an IC_{50} value of 152 nM. Some of the previously synthesised compounds are shown below.

Table 12 Substitution patterns around the ‘A’ ring and the resulting activity against MDM2



Compound Number	‘A’-ring and substituent	IC_{50} of activity against MDM2 (μ M)
195	H	0.23 ± 0.11
220	4-Cl	0.095 ± 0.096
221	4-Me	0.30 ± 0.17
222	5- ^t Bu	0.89 ± 0.29
223	5-Br	0.90 ± 0.071
224	6- ^t Bu	0.19 ± 0.10
225	6-F	0.85 ± 0.090
226	6-Br	1.0 ± 0.068
227	5,6 Cl	3.7 ± 1.2
228	4-Cl,5-F	0.31 ± 0.15

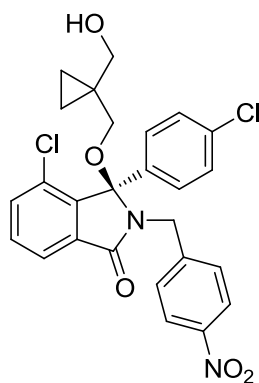
Interestingly, the addition of the chlorine in the 4-position reduces the difference between the different benzyl substitutions. When the ‘A’-ring is unsubstituted the difference between the benzyl NO_2 analogue and the bromo benzyl analogue is 5-fold. However, when the 4-chloro is placed on the ‘A’-ring the difference is less than 2 fold. These results are summarised below.

Table 13 Comparison activity of substituted isoindolinone with varying benzyl substitution

Compound No.	'A'-ring substitution	Benzyl substitution	IC ₅₀ of activity against MDM2 (μM)
125	H	NO ₂	0.23 ± 0.11
212	H	Br	1.2 ± 1.2
209	H	CN	1.8 ± 0.67
220	4-Cl	NO ₂	0.095 ± 0.096
229	4-Cl	Br	0.17 ± 0.003
230	4-Cl	CN	0.18 ^a

^a indicated n = 1

The values for all of the above compounds are for the racemic mixtures. When the most active compound **220** was separated into its two enantiomers, one was found to have an activity of 44 nM, with the alternative enantiomer shown to be significantly less potent. The inactive enantiomer was successfully crystallised, and the structure of the active enantiomer is that shown below. Treatment of SJSA-1 cell line with the active enantiomer of **220** produced a concentration dependent inducement of MDM2, p53 and p21, treatment with the inactive enantiomer and resulted in a response at the highest dose of 20 μM. The dose-dependent inducement of p21, p53 and MDM2 verifies that isoindolinones are acting *via* inhibition of the p53 MDM2 protein-protein interaction.¹⁹²

**Figure 58** Active isomer of **220**

A final step forward in potency was discovered when attempting to add water-solubilising groups. A succinic ester group was added to the isoindolinone core *via* the diol side chain. Initially, the succinic ester group was added as a cleavable pro-drug, but the compound (**231**) displayed an increase in potency, with an activity of 11 nM.

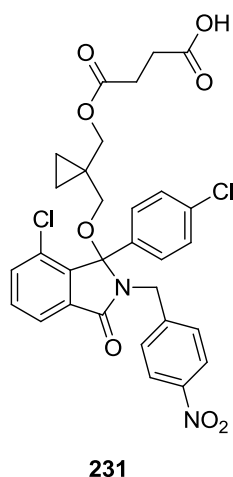
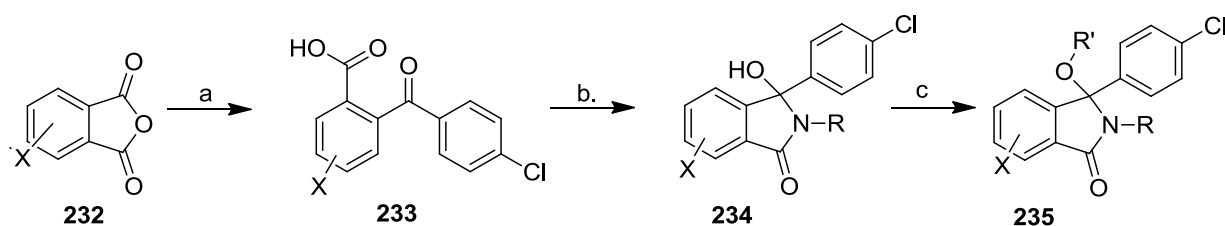


Figure 59 The structure of **231**

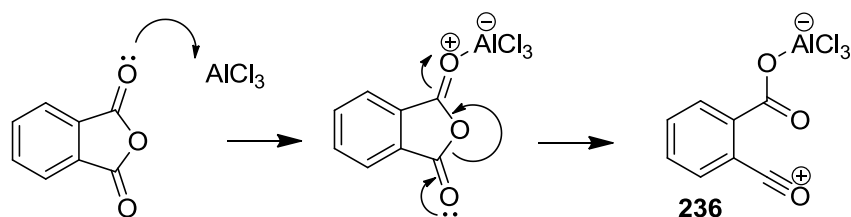
The two compounds (**220**, **231**) were the leads for the development of inhibitors of the MDM2-p53 protein-protein interaction described herein.

5.2. Isoindolinone Formation

The isoindolinone series of compounds were synthesised using methodology previously developed within the laboratory (Scheme 41).¹⁹² The first step of the synthetic route is a Friedel-Crafts reaction between the appropriate phthalic anhydride and chlorobenzene to give the benzoyl benzoic acid (**233**). The Friedel-Crafts reaction can be omitted when X = H as the required 2-(4-chlorobenzoyl)benzoic acid is commercially available. For compounds which require substitution around the 'A' ring of the isoindolinone, the initial step is synthesis of the benzoyl benzoic acid. The Friedel-Crafts reaction between the appropriate phthalic anhydride and chlorobenzene is mediated by aluminium chloride, generating the reactive acylium ion (**236**) *via* the mechanism below (Scheme 42). Stoichiometric amounts of AlCl₃ must be used as it remains complexed to the oxygen and must be removed by hydrolysis at the end of the reaction.¹⁹⁶

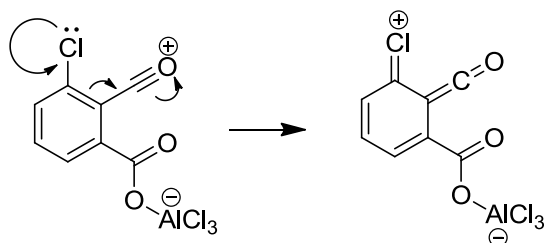


Scheme 41 Reagents and conditions; a) PhCl, AlCl₃, 90 °C, 2h; b) i. SOCl₂, DMF, THF, 4 h; ii. Appropriate amine, Hünig's base, THF, overnight; c) i. SOCl₂, DMF, THF, 4 h; ii. Appropriate alcohol, K₂CO₃, THF, overnight



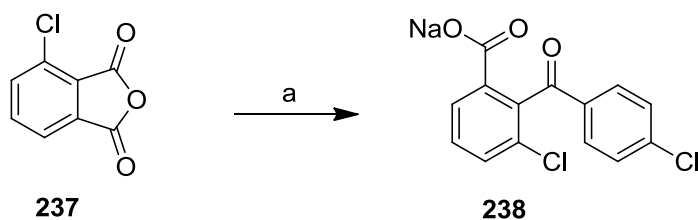
Scheme 42 Proposed mechanism of formation of the acylium ion

In the case of substituted phthalic anhydrides, two possible isomers of the acylium ion may be formed, resulting in a mixture of isomers. For 3-chlorophthalic anhydride the major product formed is 3-chloro-2-(4-chlorobenzoyl)benzoic acid. The predominant formation of one isomer suggests that the chlorine atom plays a significant role in the reaction. One proposal is that the chlorine atom stabilises the acylium ion *via* conjugation (Scheme 43).¹⁹⁶



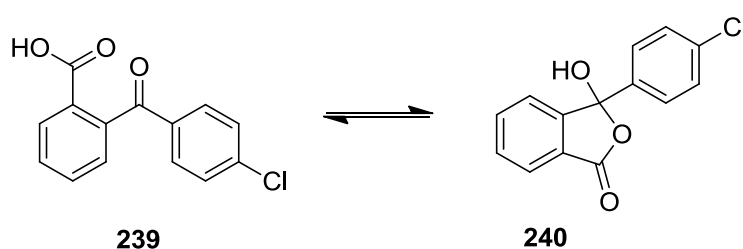
Scheme 43 Potential stabilisation of acylium ion

Newman *et al* observed the same effect when performing a Friedel-Crafts reaction with 3-chlorophthalic anhydride and benzene, with only the carbonyl alpha to the chloro atom reacting.¹⁹⁷ Allahdad *et al* suggests that the aluminium chloride preferentially reacts with the most electron rich carbonyl group.¹⁹⁸ For 3-chlorophthalic anhydride the most electron-rich carbonyl group lies *meta* to the chloro group. If AlCl₃ reacts with the *meta* carbonyl group, the acylium ion will be formed on the carbonyl group alpha to the chlorine atom. Both of these two different theories support formation of the acylium ion alpha to the chloro, which gives rise to the 3-chloro-2-(4-chlorobenzoyl)benzoic acid as the major product.¹⁹⁷



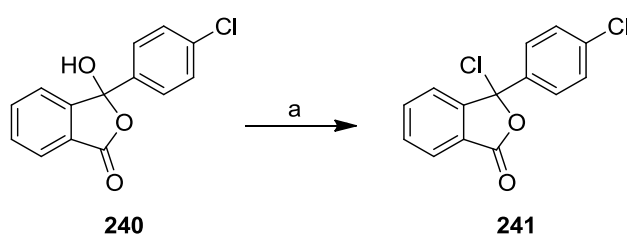
Scheme 44 Reagents and conditions; a) AlCl₃, 2 h, 90 °C, 91%

The first work-up to the Friedel-Crafts reaction of 3-chlorophthalic anhydride and chlorobenzene an acidic solution resulted in the isolation of both possible isomers as a precipitate. However, on subsequent attempts the precipitate did not always occur and a further extraction into organic solvent was required, but re-extraction into organic solvent also resulted in the extraction of further impurities which were inseparable from the desired product. A simple alteration to the work-up avoided this problem. The benzoyl-benzoic acid was isolated as the sodium salt that precipitated reliably in good yield and purity (91 %). At this point the two isomers cannot be separated; the second step of the reaction is performed on the mixture of isomers. After formation of the isoindolinones the two isomers can then be separated.



Scheme 45 The equilibrium between the open and cyclised form of *ortho*-benzoylbenzoic acids

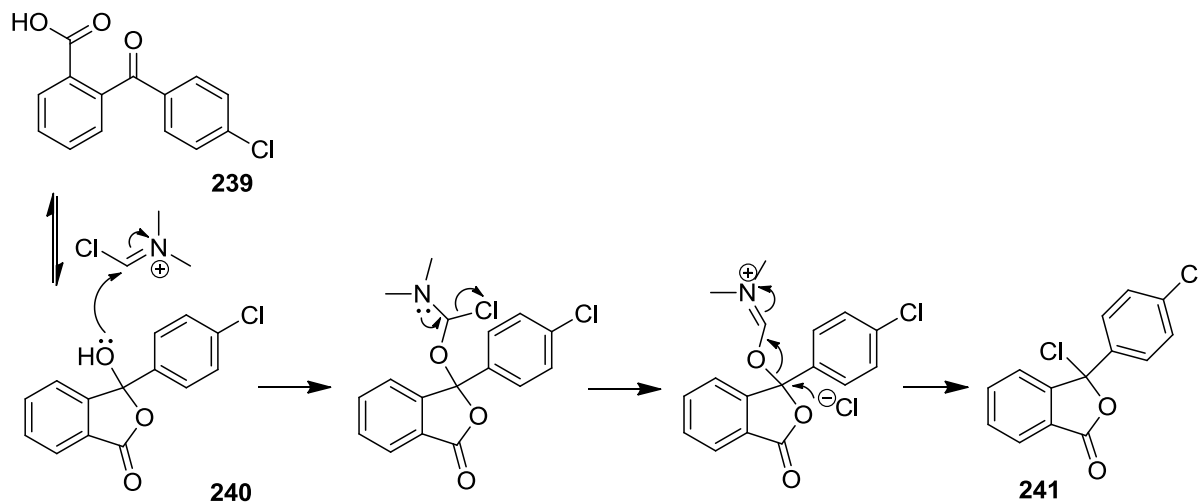
The second step of the synthetic route requires formation of the isoindolinone heterocycle *via* the formation of a ψ -acid chloride,¹⁹⁹ as the reactive intermediate. *Ortho*-benzoylbenzoic acids are found in an open state (**229**) as a solid but in solution are in equilibrium between the open form and a cyclic form (**230**) (Scheme 45).²⁰⁰



Scheme 46 Reagents and conditions; a) SOCl_2 , DMF, THF, 4 h

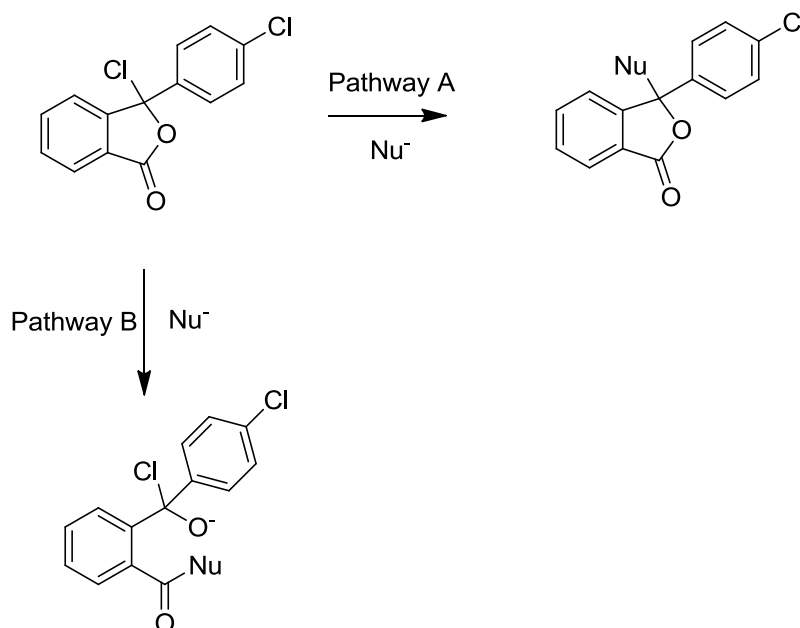
Treatment of the cyclised form the benzoylbenzoic acids with the Vilsmeier reagent, synthesised from two equivalents of thionyl chloride and catalytic *N,N*-dimethylformamide, results in the synthesis of ψ -acid chloride (**241**)(Scheme 46). The 3-hydroxy group can attack the Vilsmeier reagent, which results in the formation of the chloride ion, which can then

attack the acetal, liberating DMF and forming the pseudo-acid chloride. The ψ -acid chloride (**231**) is an unstable intermediate and must be used immediately. Treatment with the appropriate benzylamine (either as the hydrochloride salt or the free amine) in the presence of Hünig's base generates the isoindolinone.



Scheme 47 Mechanism of formation of ψ -acid chloride

The amine has a choice of two sites to attack, either the carbonyl carbon or the carbon substituted with the chlorine atom. Bhatt *et al* describes these two routes as pathway A or pathway B.²⁰¹ Pathway A is a S_N2 reaction at the chloro-substituted atom, replacing the chloro atom with the nucleophile, whilst pathway B has the nucleophile attacking at the carbonyl, and ring opening the lactone.



Scheme 48

Route A is preferred by weaker nucleophiles whereas route B is preferred by stronger nucleophiles including amines.²⁰¹ Sloan *et al* also found that the reaction of primary amines resulted in the formation of amides, rather than displacement of the halide.²⁰² Sloan *et al* suggest that all nucleophiles attack initially at the chloro-substituted carbon but stronger nucleophiles form a looser transition state whilst weaker nucleophiles form tighter transition states.²⁰² The looser transition state allows for delocalisation of the partial positive charge towards the carbonyl carbon, resulting in formation of the amide. The formation of this transition state may also be applied to the formation of the isoindolinone. A proposed mechanism is shown in Scheme 49. Formation of the isoindolinone is only possible *via* route B. Secondary attack on the ketone, formed by opening the lactone will result in the formation of the five-membered isoindolinone ring. If this step is attempted using the mixture of isomers from the previous step, two isomeric products will be synthesised. However, at this point the two isomers are separable by column chromatography.

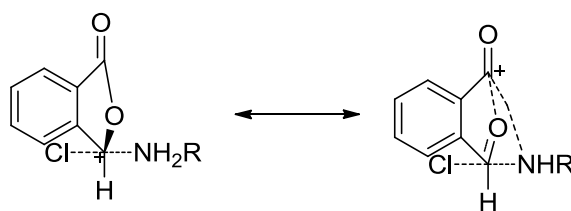
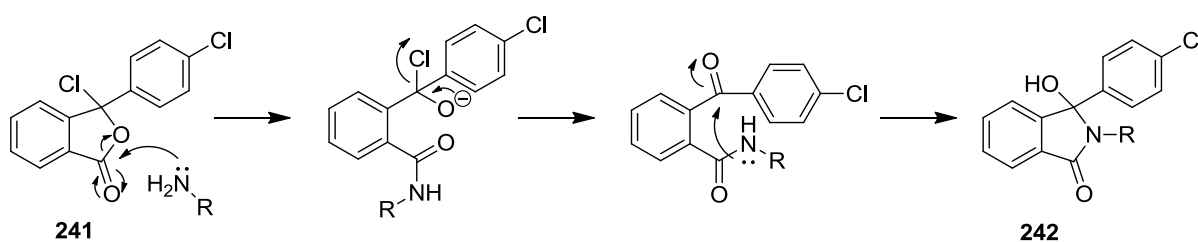


Figure 60 Proposed looser transition state formed during the nucleophilic attack, allowing delocalisation of the transition state



Scheme 49 Mechanism of formation of the 3-hydroxyisoindolinone from the ψ -acid chloride of the benzoyl-benzoic acid

Treatment of the benzoyl benzoic acid (**239**) with thionyl chloride and DMF for 4 h results in the formation of the pseudo acid chloride. This must be immediately treated with a nucleophile, for formation of an *N*-benzyl substituted isoindolinone a substituted benzylamine is used, in the presence of Hünig's base. The reaction is then stirred overnight.

Substitution of the 'A'-ring can play a significant role in the yield of this reaction. Synthesis of the 4-chloro isoindolinone can be low yielding.

Formation of the isoindolinone gives rise to a characteristic ^1H NMR spectrum. The diastereotopic benzyl methylene protons are expected to exhibit two pairs of doublets, at approximately δ 4-5. Each methylene protons only couples to the other methylene proton with geminal coupling constants of around 15 Hz.¹⁹⁶

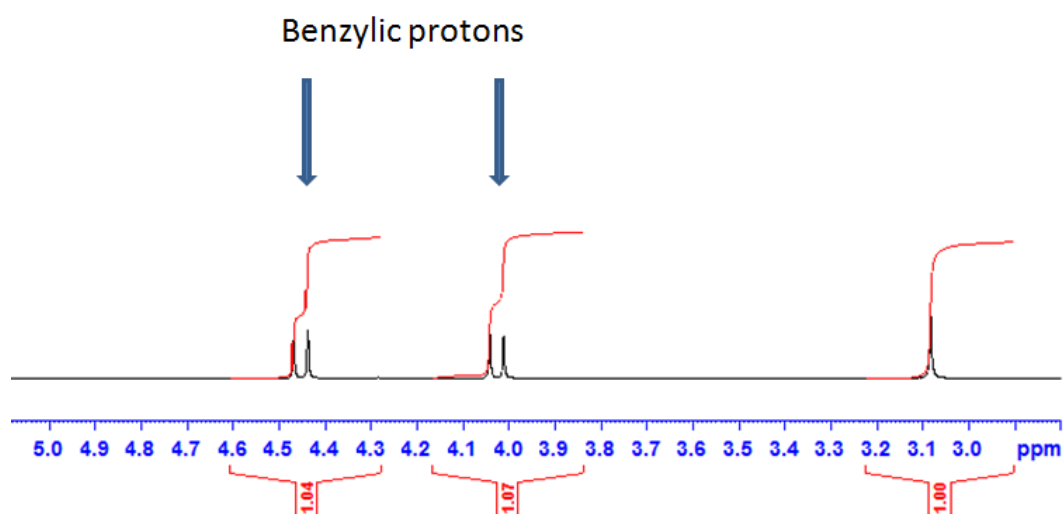
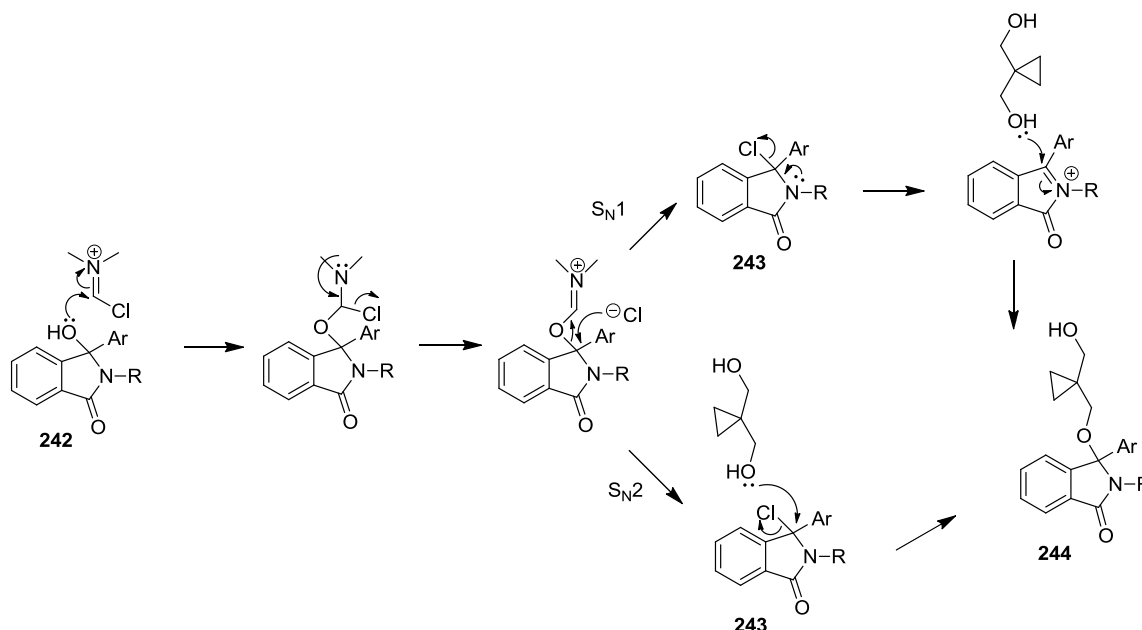


Figure 61

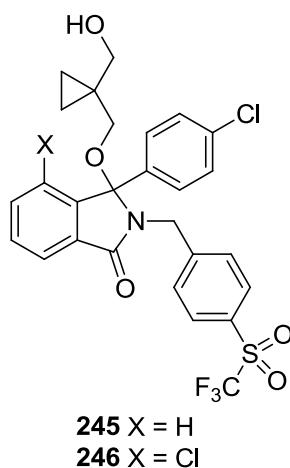
The standard final step of the synthetic route is formation of the ether linkage. The optimal substituent at this position has been shown previously to be the (1-hydroxymethylcyclopropyl)methoxy ether group.¹⁹² The ether linkage is formed by using two equivalents of thionyl chloride with catalytic *N,N*-dimethylformamide in anhydrous THF. These reagents generate the Vilsmeier reagent *in situ*, resulting in chlorination at the 3-position of the isoindolinone (**243**) (Scheme 50). The resulting halide species must be used immediately to generate the ether, by treatment with 1,1 bis-(hydroxymethane)cyclopropane with potassium carbonate. The lone pairs of the oxygen of the 3-hydroxyisoindoline attacks the Vilsmeier reagent which rearranges to reform the iminium ion and kick out the chloride ion, which then attacks the hemi-aminal carbon to displace DMF. The ether can then be formed either *via* an $\text{S}_{\text{N}}1$ reaction or an $\text{S}_{\text{N}}2$ reaction. In the $\text{S}_{\text{N}}1$ reaction the chloride ion is displaced forming an iminium species, which is then attacked by the lone-pairs of the hydroxyl group of 1,1-bis(hydroxymethyl)cyclopropane. In the $\text{S}_{\text{N}}2$ reaction, the chloride ion

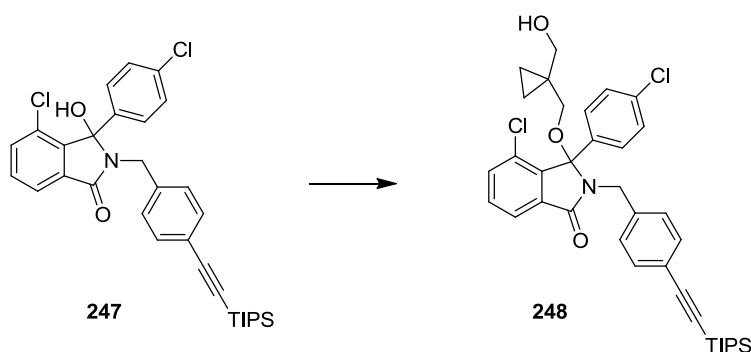
is displaced by the hydroxy groups of 1,1-bis(hydroxymethyl)cyclopropane. The formation of the ether is thought to occur *via* the S_N2 pathway.



Scheme 50 Mechanism of formation of the ether linkage

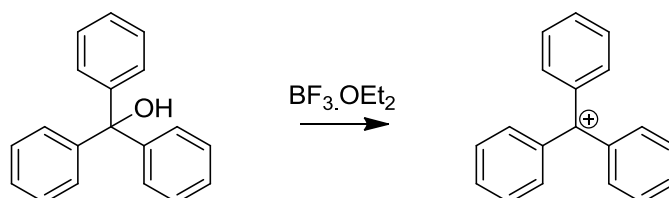
An alternative method for the formation of the ether linkage uses $\text{BF}_3 \cdot \text{OEt}_2$ and 10 equivalents of the required diol. Lejkowski *et al*²⁰³ use this method for the formation of an allyl ether group alpha to the oxygen in a tetrahydropyran ring. This methodology proved useful for the synthesis of compounds without the chlorine in the 4-position, with reactions taking approximately 2.5 hours, in good yields. The formation of **245** was achieved in 2.5 h in 62% yield using the $\text{BF}_3 \cdot \text{OEt}_2$ chemistry. However, for the 4-chloroisoindolinone (**246**), the reaction was much slower, taking over 24 h, and the longer exposure to the harsher reagent resulted in a number of by-products were also generated. For comparison of reaction times between the two different reagents see Table 14



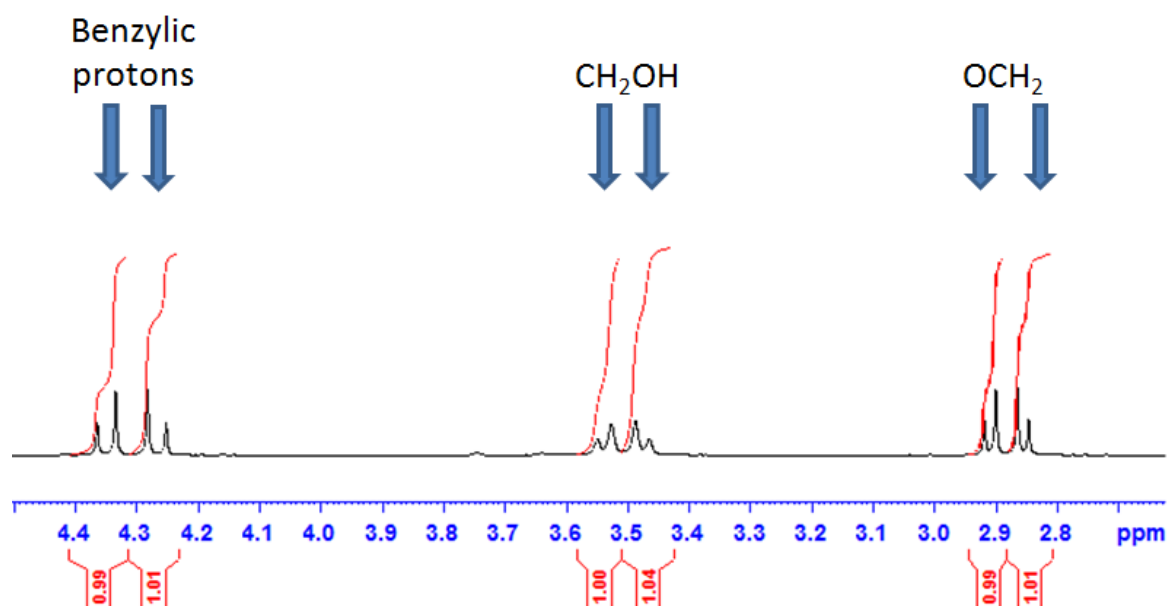
**Table 14** Reagents and conditions for formation of **248**

Reagents	Time (h)	Yield
SOCl ₂ /DMF + diol (2 eq)	16	24%
BF ₃ .OEt ₂ (2.5 eq + 2.5 eq) + diol (10 eq)	42	86%

The mechanism of formation of the ether differs when using the BF₃.OEt₂ from the chlorination method. The Lewis acid is thought to generate a cation at the 3-position, which is then quenched with the diol. Carey *et al.*²⁰⁴ used BF₃ to generate a trityl cation, and the cation on the 3-position of the isoindolinone could be considered to be equivalent to the trityl cation.

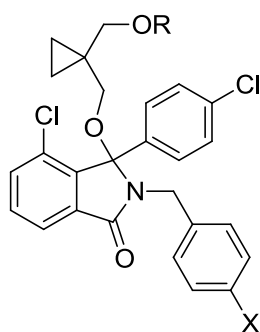
**Scheme 51** Formation of trityl cation achieved using BF₃.OEt₂²⁰⁴

A distinctive pattern is again observed for the ¹H NMR resonances from the ether side-chain. Each of the CH₂ moieties within the side chain give a pair of doublets, with one proton coupling to the other within each CH₂ unit, again displaying geminal coupling. The OCH₂ resonances typically lie between δ 2-3 whilst the CH₂OH unit typically shows peaks between δ 3-4, and is occasionally observed to couple to the hydroxyl proton.

**Figure 62**

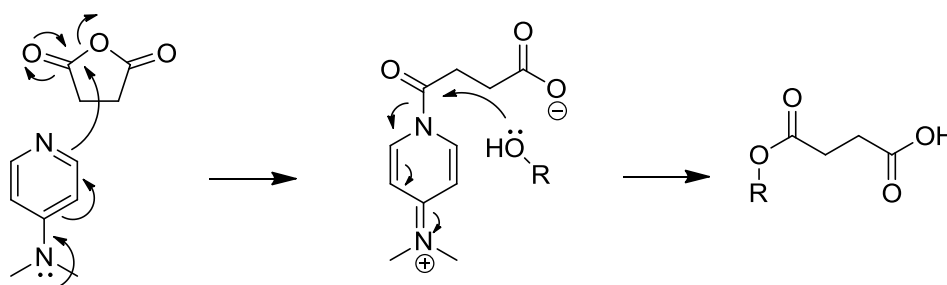
Formation of the succinic ester group

To improve the solubility of the isoindolinones a succinic half ester group was added to the ether side chain. The succinate group was initially added to the isoindolinone as a prodrug water-solubilising group. However, the addition of the succinate group was found to improve potency from an IC₅₀ of 143 nM (**220**) to 11 nM (**231**). Therefore, for selected compounds the succinate esters have been prepared for comparison.

Table 15 IC₅₀ values for the succinic ester derivatives

Number	X	R	IC ₅₀ (μM)
220	NO ₂	H	0.95
230	CN	H	0.18
229	Br	H	0.17
231	NO ₂	C(O)CH ₂ CH ₂ CO ₂ H	0.020
249	CN	C(O)CH ₂ CH ₂ CO ₂ H	0.097
250	Br	C(O)CH ₂ CH ₂ CO ₂ H	0.118

The succinate group is added using succinic anhydride, with catalytic 4-dimethylaminopyridine (DMAP) and pyridine in refluxing THF. The DMAP activates the succinic anhydride to attack from the isoindolinone hydroxyl group. The addition of the succinate group proceeds cleanly in around 15 h in refluxing THF.

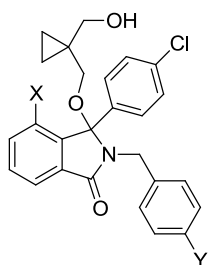
**Scheme 52** Mechanism of formation of the succinic ester

5.3 Modifications to the *N*-benzyl Group

The most potent compound identified within the isoindolinone series contains the 4-nitrobenzyl group (**210**) with an IC₅₀ of 143 nM. However, a nitro functionality is undesirable in a drug as it can be metabolised to a number of toxic metabolites. The metabolism can proceed *via* a nitro radical anion, the nitroso, the nitroxyl radical, the hydroxylamine and then

the primary amine. Hydroxylamines may cause methaemoglobinaemia and mutagenicity. Carcinogenic effects of nitro groups may be a result of nitro radicals, nitroso derivatives and hydroxylamines.²⁰⁵ A number of replacements for the nitro group have been synthesised previously. However, none of these have displayed equivalent potency to the nitro compound. Therefore the aim of this work was to find a nitro group replacement which is appropriate for use in a drug.

Table 16 Key alternatives for the nitro group

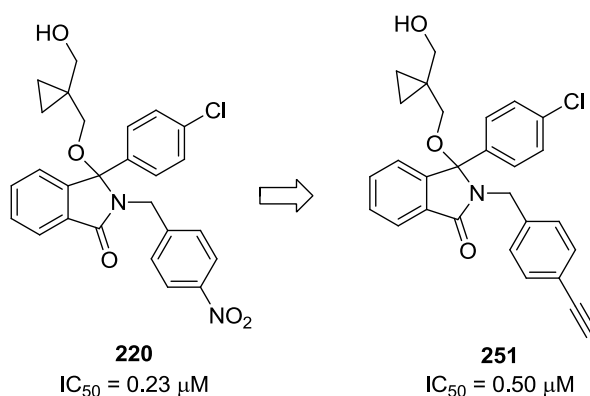


Number	X	Y	IC ₅₀ (μM)
220	Cl	NO ₂	0.095 ± 0.096
230	Cl	CN	0.18 ^a
229	Cl	Br	0.17 ^a
251	H	CCH	0.50 ^a

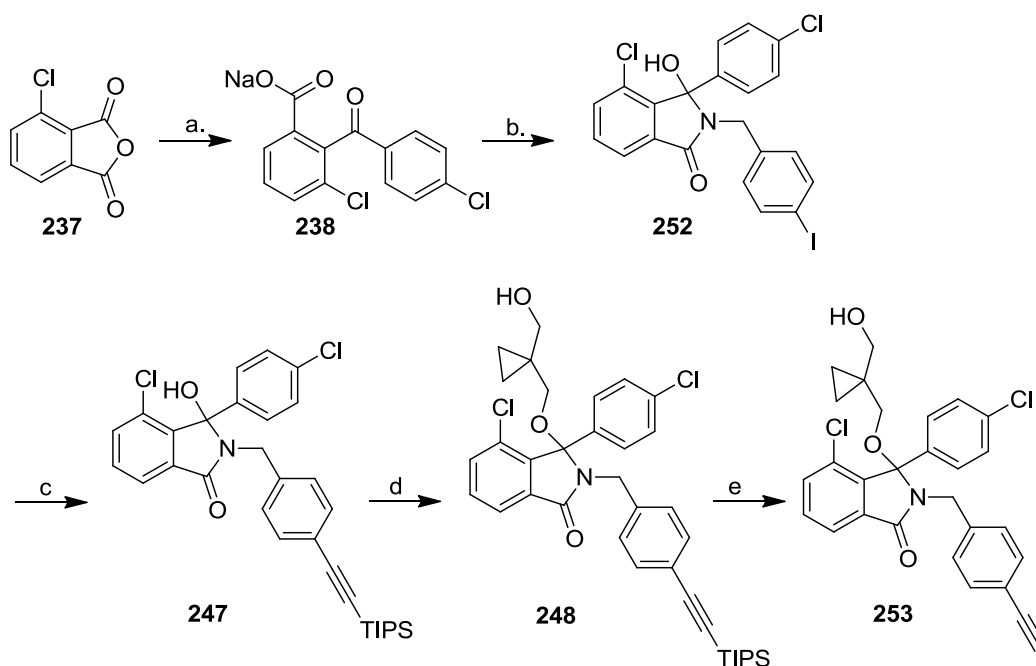
^a n = 1

5.3.1 Ethynyl Replacement of the Nitro Group

An isoindolinone with an ethynyl group in the 4-benzyl position has previously been synthesised within the group. The ethynyl compound (**250**), with no substituent at the 4-position, showed a 2-fold loss in potency compared with **220**.



As addition of the chloro group at the 4-position of the isoindolinone has been shown to improve potency, synthesis of the chloro analogue of the ethynyl isoindolinone was desired. The synthetic route of the ethynyl compound is shown below (Scheme 53).



Scheme 53 Reagents and conditions; a) AlCl_3 , chlorobenzene, $90\text{ }^\circ\text{C}$, 2h, 91%; b) i. SOCl_2 , DMF, THF, 4 h; ii. 4-iodobenzylamine hydrochloride, Hünig's base, THF, overnight, 36%; c) $\text{Pd}(\text{PPh}_3)_2\text{Cl}_2$, CuI, Et_3N , TIPS-acetylene, THF, 15 h, 88%; d) i. SOCl_2 , DMF, THF, 4h ii. 1,1-bis-(hydroxymethyl)-cyclopropane, K_2CO_3 , THF, overnight, 24%; e) 1M TBAF in THF, THF, 75 min, 41%

The 4-iodobenzyl substituted isoindolinone (**252**) was synthesised following the published synthetic route from 3-chlorophthalic anhydride and 4-iodobenzyl amine hydrochloride,¹⁹² with the ethynyl functionality incorporated using a Sonogashira coupling reaction to give **247** in a 88% yield.

The Sonogashira reaction cross-couples an aryl iodo species and triisopropylsilyl protected acetylene using a palladium catalyst and a copper (I) species. The reaction was achieved using 0.03 equivalents of $\text{Pd}(\text{PPh}_3)_2\text{Cl}_2$ and 0.02 equivalents of copper iodide. To improve conversion to the ethynyl product, the number of equivalents of TIPS-acetylene was increased from 1.1 to 1.3. Although this made little difference to the overall yield (95% conversion to 100% by LCMS) this resulted in significantly simpler purification as both the starting material and the product were close running during purification with medium

pressure column chromatography on silica. When using 1.3 equivalent of TIPS-acetylene the reaction proceeded cleanly and was readily purified in good yield (88%).

The catalytic cycle of a Sonogashira reaction is shown below. The first step of the catalytic cycle is formation of the Pd (0) species from Pd (II). The Pd (0) species then undergoes oxidative insertion with the aryl-iodo species, returning to Pd (II). The TIPS-acetylene initially forms a copper species *via* deprotonation with triethylamine. Chelation of the copper to the alkyne activates the triisopropylacetylene to deprotonation, without the presence of the copper the alkyne would not be deprotonated by Et₃N (p*K*_a of 10.7)¹⁹⁶ as acetylene has a p*K*_a of ~25¹⁹⁶ and usually requires a strong base to deprotonate. The acetylene-copper species then undergoes transmetallation resulting in formation of a palladium acetylene species, with the acetylene group and the aryl group are *trans* to each other, which isomerizes to give the *cis* species and then undergoes reductive elimination, giving rise to the aryl acetylene species and regenerating the Pd (0) species.²⁰⁶

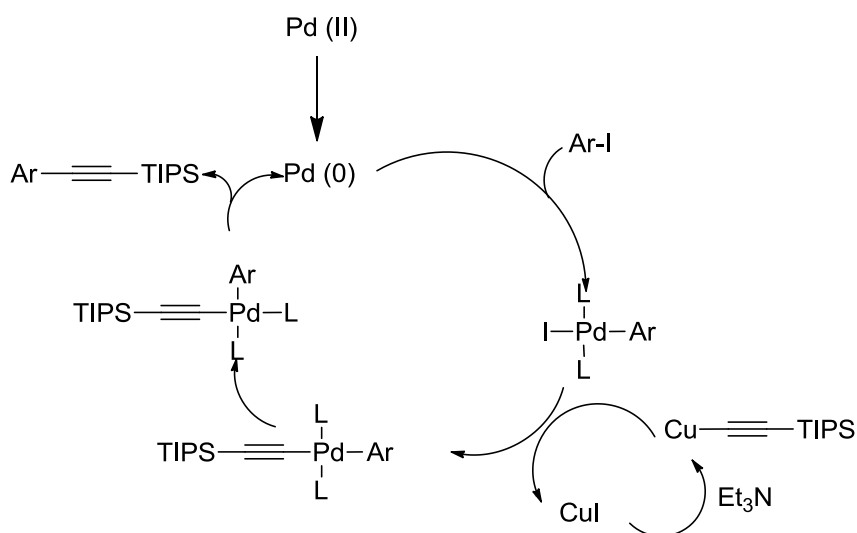


Figure 63 The catalytic cycle for a Sonogashira reaction

Once the ethynyl group had been incorporated, the TIPS protecting group was left in place until the final step of the synthesis. The ether linkage was formed using the standard reaction conditions to give **248**. Deprotection was achieved using a 1M solution of TBAF in THF at room temperature to give the desired product. The first batch of **253** was synthesised using the 3-chloro-2-(4-chlorobenzoyl)-benzoic acid which contained an inseparable impurity, which persisted through the synthetic route, purification by HPLC was required to obtain the 95% purity required for testing. However, on resynthesis starting from the sodium salt of 3-

chloro-2-(4-chlorobenzoyl)-benzoic acid no addition HPLC purification was required and the final compound **253** was achieved in a higher yield (88%).

All isoindolinones are synthesised as racemic mixtures. Due to the favourable biological results compound **242** was resynthesised for separation of the enantiomers by chiral HPLC using a Daicel Chiralpak AD-H column, using 92.5:7.5 hexane:ethanol. Chiral separation gave two enantiomers, peak 1 (NCL-00018225, **254**) with $[\alpha] = -9.16^\circ$ and peak 2 (NCL-00018226, **255**) with $[\alpha] = +11.4^\circ$. NCL-00018225 is expected to be the R-enantiomer by analogy with NU8354 and NCL-00008406, and has the structure shown below.

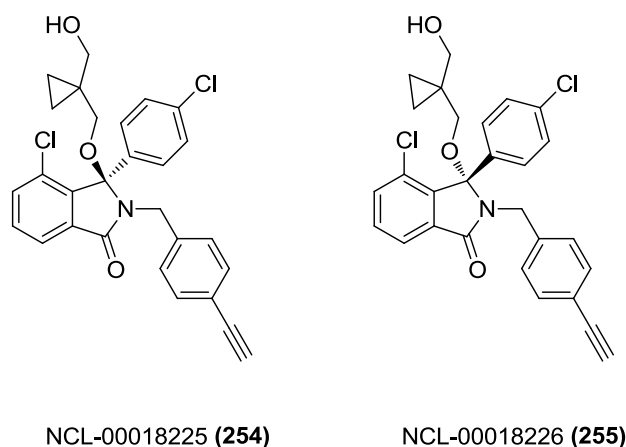
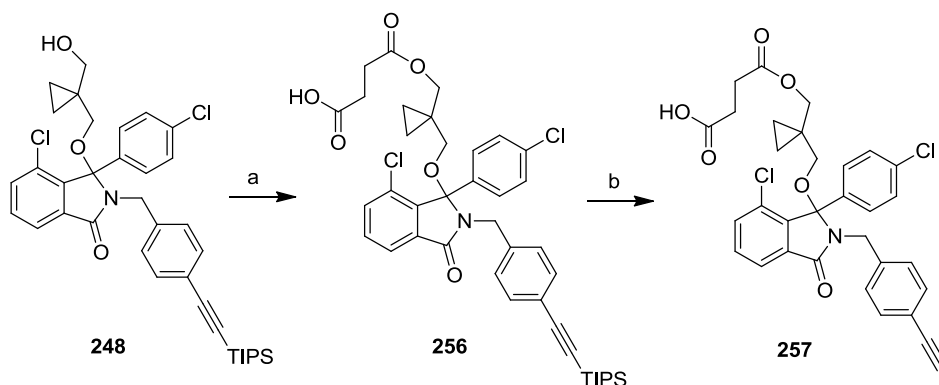


Figure 64

As the ethynyl compound has already been shown to be potent, the succinate ester was also synthesised *via* a DMAP catalysed esterification. The TIPS protecting group was left in place to protect the ethynyl group until the final step of the synthesis route before removing *via* 1 M TBAF (Scheme 54).



Scheme 54 Reagents and conditions; a) Succinic anhydride, pyridine, DMAP, THF, reflux, overnight, 94%; b) 1M TBAF in THF, THF, 2 h 45 min, 81%

Succinic ester **257** is acid sensitive. An aliquot of the compound, left in deuterated chloroform, which is relatively acidic, resulted in decomposition, with loss of the succinate group. Acidic chloroform was catalysing hydrolysis of the ester linkage. Succinic ester groups are easily cleaved which might explain the compounds relative sensitivity. The compound was therefore resynthesised before testing.

5.3.2 Trifluoromethylsulfone Replacement of the Nitro Group

An alternative non-classical isostere for the nitro group is a trifluoromethylsulfonyl group. The trifluoromethylsulfonyl group has been used by Abbott pharmaceuticals as a replacement for the nitro group within their series of inhibitors of the Bcl-2 anti-apoptotic family protein-protein interaction.²⁰⁷⁻²⁰⁸ The trifluoromethylsulfonyl group (**259**), which is slightly more electron withdrawing than the nitro group, was tolerated as a replacement for the nitro (**258**), whilst the methyl sulfonyl group (**261**) and the trifluoromethyl group (**260**) were not.²⁰⁷⁻²⁰⁸ A trifluoromethyl analogue of the isoindolinone has previously been synthesised and was not tolerated, a trifluoromethylsulfonyl may prove to be an ideal replacement for the nitro group.

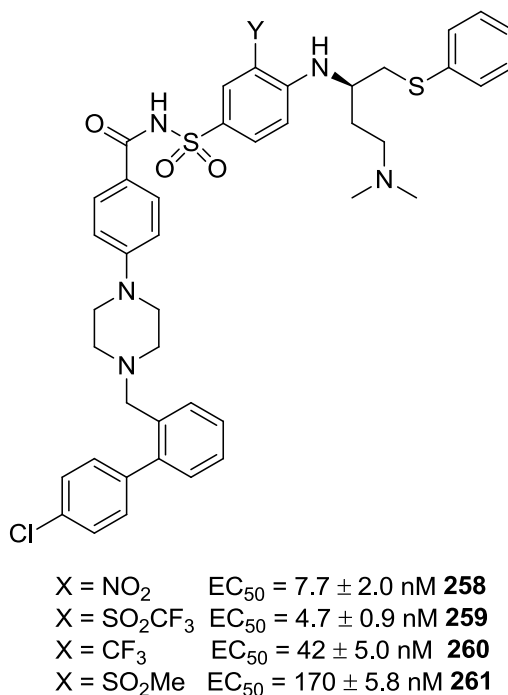
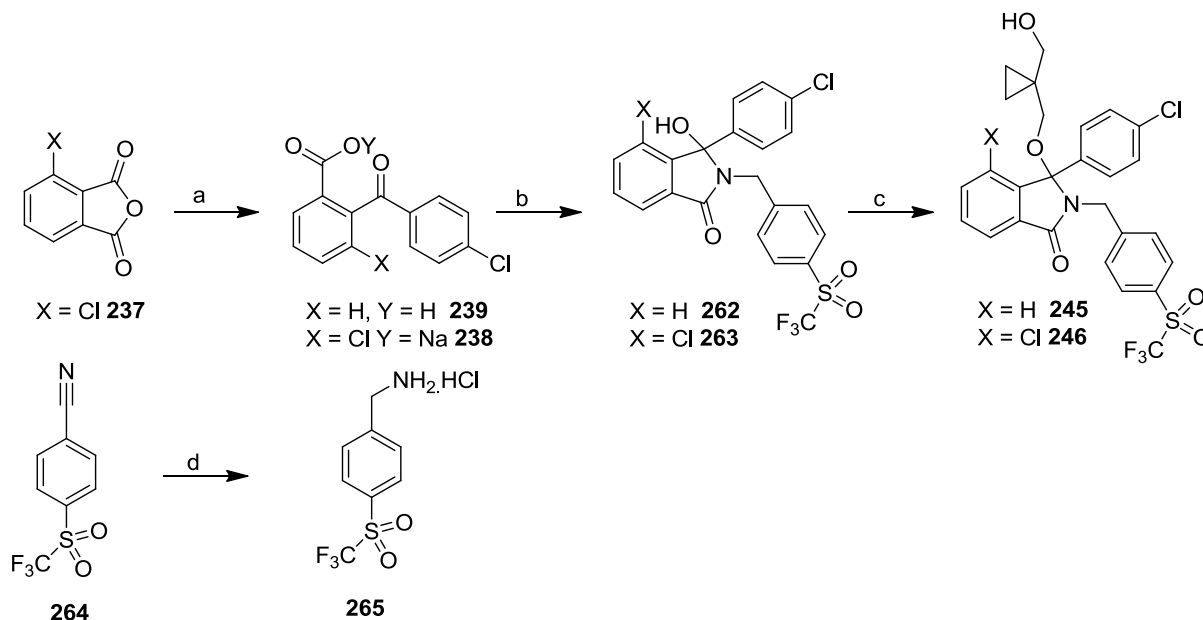


Figure 65 Replacement of the nitro group with trifluoromethylsulfonyl group in the Abbott pharmaceuticals compounds

The trifluoromethylsulfonyl analogue of the isoindolinone was synthesised using the published route.¹⁹² The required benzylamine was not commercially available, so it was

prepared from 4-(trifluoromethylsulfonyl)benzonitrile by reduction with a 1M solution of $\text{BH}_3\cdot\text{THF}$ complex in THF as described Leach *et al.*²⁰⁹ The compound was stored and used as a hydrochloride salt, as on standing as the free amine, the benzylamine converted from a solid to an oil.



Scheme 55 Reagents and conditions; a) AlCl_3 , chlorobenzene, 90 °C, 2 h, 91%; b) i. SOCl_2 , DMF, THF, 4 h ii. **265**, Hünig's base, THF, $\text{X} = \text{Cl}$ 35%, $\text{X} = \text{H}$ 87%; c) $\text{X} = \text{Cl}$ i. SOCl_2 , DMF, THF 4 h; ii. 1,1-bis(hydroxymethyl)cyclopropane, K_2CO_3 , THF, overnight, 29%; $\text{X} = \text{H}$ $\text{BF}_3\cdot\text{OEt}_2$, 1,1-bis(hydroxymethyl)cyclopropane, DCM 0 °C-RT 2.5 h, 69%; d) i. 1M $\text{BH}_3\cdot\text{THF}$ in THF, THF, reflux, 4 days ii. 1M $\text{HCl}_{(\text{aq})}$, 51%

For compound **245** the ether linkage was formed using $\text{BF}_3\cdot\text{OEt}_2$ in good yield (69%). As the ether formation using $\text{BF}_3\cdot\text{OEt}_2$ reaction has previously been shown to proceed slowly when the 4-Cl is in place, the Vilsmeier reaction was instead used to chlorinate, followed by displacement with 1,1-bis(hydroxymethyl)cyclopropyl to form **246**, which previous experience had shown to take 24 h, though with lower yields.

5.3.3. 3-Fluoro-4-Halo Benzyl Analogues

3,4-Difluorobenzyl may mimic both the space-filling capacity of the nitro group and the electron-withdrawing nature of the nitro group. A single fluoro atom is less electron withdrawing than a nitro group. The σ value for a 4-fluoro group is 0.06 whilst for a 4-nitro group the σ value is 0.78.²¹⁰ However if the values for a 3-fluoro group (0.34) and 4-fluoro

(0.06) are combined (0.40) the value becomes closer to that of the nitro group.²¹⁰ Previous work has shown that a number of 4-halo compounds have been moderately potent; therefore a series of 3-fluoro-4-halo compounds may aid identification of a compound with similar potency to the 4-nitro compound. As a result of the favourable potency of the 4-ethynyl analogue, a 3-fluoro, 4-ethynyl analogue was also synthesised. The combined Hammett values for each analogue are shown below. 3-Substitution has not previously been tolerated around the benzyl ring, a fluoro group should be sufficiently small to be tolerated.

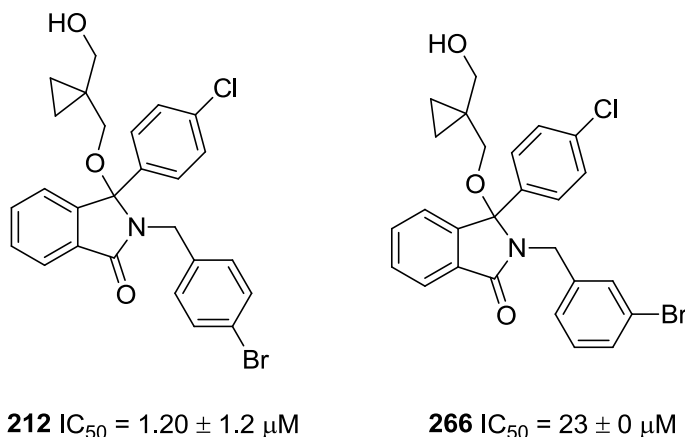
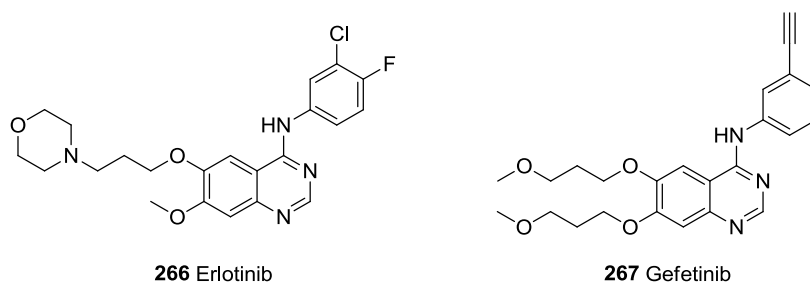


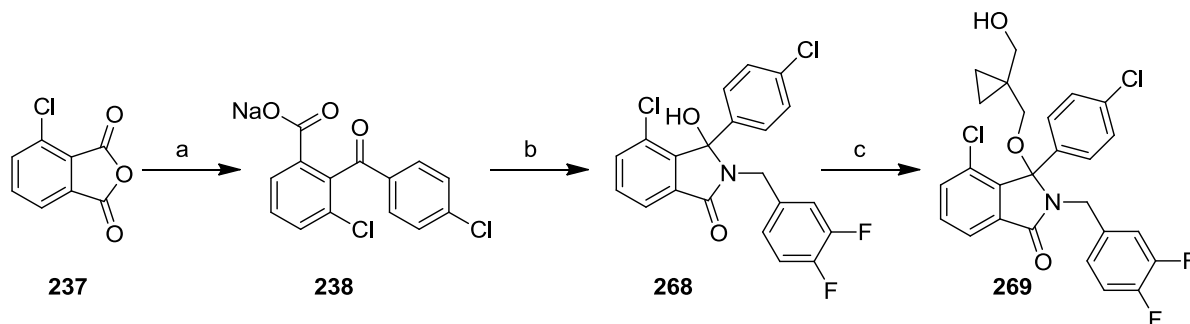
Table 17 Literature σ values for 3 and 4 substituents²¹⁰ and calculated combined values

Substituent	3-Substituent Value	4-Substituent Value	Total value
4-NO ₂	-	0.78	0.78
3-F,4-F	0.34	0.06	0.40
3-F,4-Cl	0.34	0.23	0.57
3-F,4-Br	0.34	0.23	0.57
3-F,4-I	0.34	0.18	0.52
3-F, 4-CCH	0.34	0.23	0.57

The 4-chloro-3-fluoro analogue was particularly interesting in view of the activity of compound **253** as the literature has shown these groups can be interchangeable. The two EGFR kinase inhibitors Gefetinib and Erlotinib share significant structural similarities.⁷



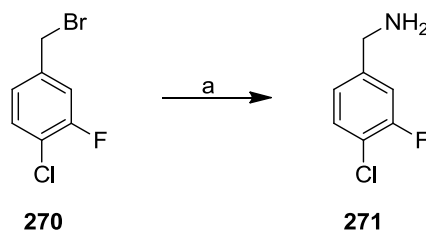
The 3,4-difluoro analogue was synthesised from 3,4-difluorobenzylamine following the previously described isoindolinone synthetic route as shown in Scheme 56.



Scheme 56 Reagents and Conditions; a) AlCl_3 , PhCl, 90°C , 2 h, 91%; b) i. SOCl_2 , DMF, THF, 4 h; ii. 3,4-Difluorobenzylamine, Hünig's base, THF, overnight, 39%; c) i. SOCl_2 , DMF, THF, 4 h; ii. 1,1-bis(hydroxymethyl)cyclopropane, K_2CO_3 , THF, overnight, 23%

For the remaining compounds in the series the required benzylamine was not commercially available. Both the 4-bromo-3-fluorobenzonitrile and 3-fluoro-4-iodobenzonitrile were commercially available and could be reduced following the previously developed methodology. Unfortunately, the 4-chloro-3-fluorobenzonitrile was considerably more expensive than for the bromo and iodo analogues. Therefore, it was decided instead to access the benzylamine *via* the 4-chloro-3-fluorobenzyl bromide.

A search of the literature suggested that benzyl bromides could be converted to benzyl amines using methanolic ammonia at high temperatures.²¹¹ A table of the conditions used is shown below.



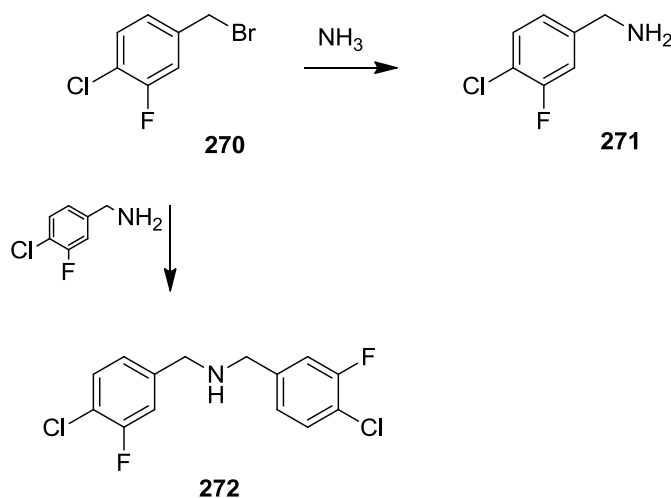
Scheme 57 Reagents and conditions; a) 7 M methanoic ammonia, methanol, conditions and yield as described below

Table 18 Summary of conditions used in attempted synthesis of **271**

Concentration of benzyl bromide	No. of equivalents	Heating type	Temperature (°C)	Time	Yield
0.45 M	16	Conventional	80	3 h	-
0.23 M	32	Conventional	80	3 h	-
0.15 M	16	Conventional	80	5 h	28%
0.23 M	16	-	RT	2.5 days	15%
0.23 M	16	Microwave	120	5 min	~ 35%

The best yield (28%) was achieved using conventional heating at 80 °C for 5 h. LCMS monitoring of the microwave irradiated reaction suggest that 35% conversion was achieved, though the product was not isolated.

The reactions all resulted in the formation of multiple products alongside the desired benzylamine. It was hypothesised that this is due to desired product (**271**) reacting with the starting material synthesising further compounds, as (**270**) may be highly reactive, due to the electron withdrawing substituents on the benzyl ring.



Scheme 58 Reagents and conditions; 7 M methanoic ammonia, methanol, RT-120 °C, 3 h - 2.5 days

An alternative route was therefore required. To reduce the reactive nature of the synthesised benzylamine, it was proposed to initially form a tertiary amine, which should reduce the reactivity of the amine group, the primary amine could then be released under mild conditions. Both a modified Gabriel with sodium diformylamide, an alternative reagent to

potassium phthalamide, which requires mild hydrolysis conditions and a Staudinger reaction have been attempted.²¹²⁻²¹⁵

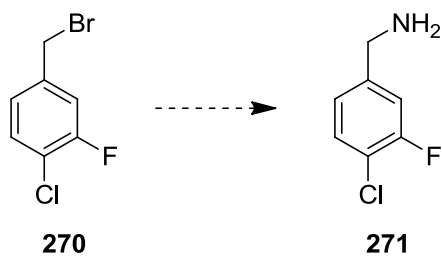
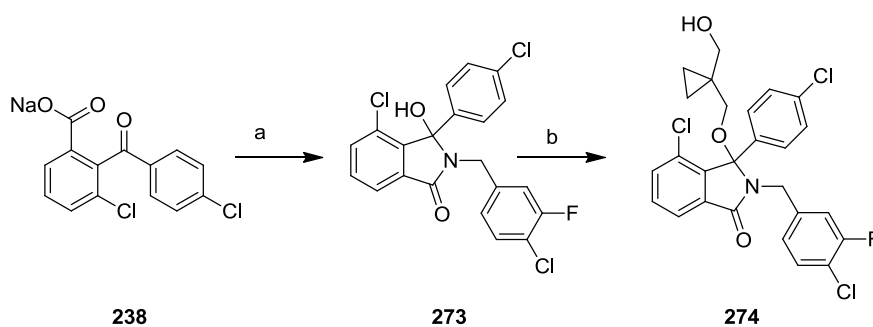


Table 19

Reagents	Conditions	Observed outcome
i. Sodium diformylamide, 18-crown-6, MeCN; ii. 5% ethanoic HCl	Reflux, then room temperature	No product observed
i. NaN ₃ , DMF; ii. PPh ₃ , H ₂ O	100 °C, then room temperature	Major isolated product PPh ₃ O

While the displacement reactions with both sodium diformylamide and sodium azide were in progress it was observed that the TLC fraction of the starting material, which was stood at room temperature in solvent (EtOAc), began to degrade forming multiple products, suggesting that the starting material itself may not be especially stable, leading to the disappearance of starting material by TLC but without conversion to the product.

While the above work was in progress, the commercial price for 4-chloro-3-fluorobenzonitrile significantly reduced, and it was purchased and reduced to the desired product using 1 M BH₃.THF in 63% yield using the optimised conditions developed in the synthesis of **277**.



Scheme 59 Reagents and Conditions; a) i. SOCl_2 , DMF, THF 4 h; ii. **271**, Hünig's base, THF, overnight, 37%; b) i. SOCl_2 , DMF, THF, 4 h; ii. 1,1-bis(hydroxymethyl)cyclopropane, K_2CO_3 , THF, overnight, 18%

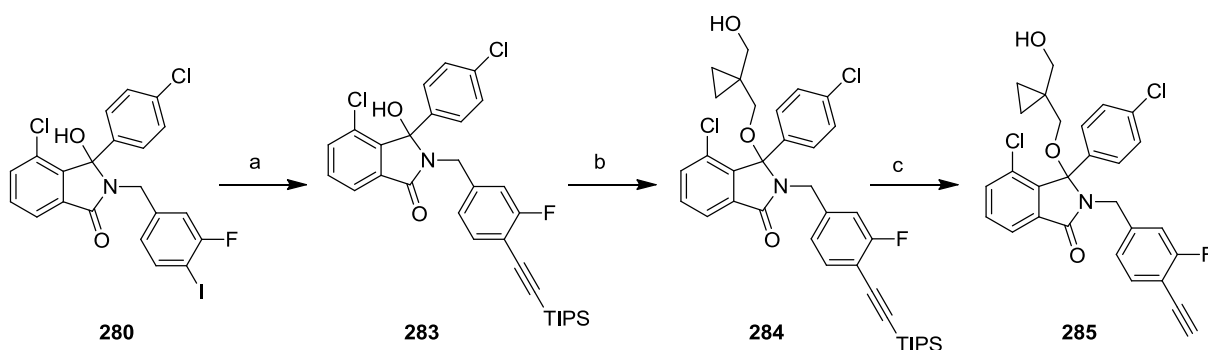
Once **271** had been synthesised in sufficient yield, isoindolinone **273** was synthesised from the sodium salt of 3-chloro-2-(4-chloro-benzoyl)-benzoic acid and **271**, using the standard conditions, followed by the chlorination at the 3-hydroxy position and displacement with 1,1-bis(hydroxymethyl)cyclopropane to give isoindolinone **274**. Unfortunately LCMS analysis showed that **274** contained a minor impurity which require multiple rounds of medium pressure column chromatography and reverse phase chromatography before an appropriate level of purity was obtained leading to a slightly lower than anticipated yield.

Both the 3-fluoro-4-iodo and 4-bromo-3-fluoro benzonitrile compounds were commercially available and previous work suggested that the nitrile group could be reduced using borane. However reductions of both the 3-fluoro-4-iodobenzonitrile (**275**) and 4-bromo-3-fluorobenzonitrile (**276**) with BH_3 .THF, the reaction proceeded very slowly (up to 5 days) so a series of alternative reduction agents were investigated (Table 20).

Table 20 Alternative reagents and conditions for reduction of **275**

Reaction No.	Reagent	Conditions	Observations
1	LiAlH_4	$0\text{ }^\circ\text{C}$ for 15 min then warmed to RT	Multiple spots by TLC
2	LiAlH_4	$0\text{ }^\circ\text{C}$ for 2 h	Multiple spots by TLC
3	$\text{Li}(\text{Et})_3\text{BH}$	RT to $70\text{ }^\circ\text{C}$	No significant change from starting material

The 4-ethynyl benzyl analogue (**253**) has proved to be potent so the 4-ethynyl-3-fluoro analogue was synthesised to explore the effects of the electronic of the ring. The 3-fluoro-4-iodo compound (**280**) was used as a precursor in a Sonogashira reaction, as described for the 4-iodo compound (**223**). Fluoro groups are poor leaving groups in palladium catalysed reactions, so selectivity problems were not anticipated. Compound **280** was instead as the precursor to **284** rather than compound **282** to allow incorporation of a range of alternative ether groups.



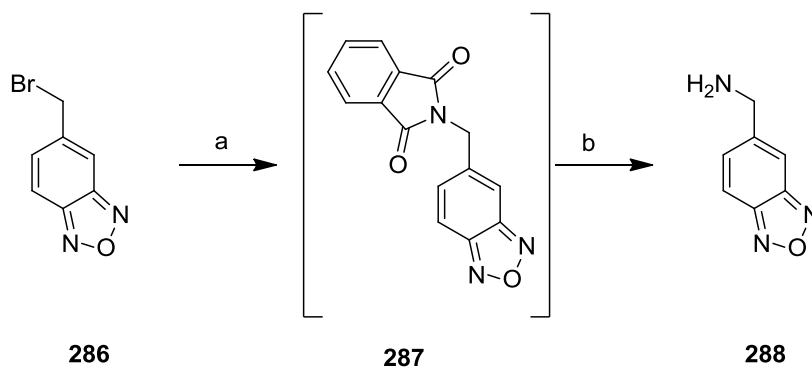
Scheme 62 Reagents and conditions; a) Triisopropylsilylacetylene, Et_3N , $\text{Pd}(\text{PPh}_3)_2\text{Cl}_2$, CuI , THF, 15 h, 95%; b) i. SOCl_2 , DMF, THF, 4 h; ii. 1,1-bis(hydroxymethyl)cyclopropyl, K_2CO_3 , THF, overnight, 26%; c. 1M TBAF in THF, THF, 1 h, 62%

Compound **283** was synthesised using the previously optimised Sonogashira conditions from triisopropylsilylacetylene and compound **280** in excellent yield (95%). Vilsmeier conditions were used to incorporate the ether linkage and the TIPS group removed using 1 M TBAF in THF to give **285**.

5.3.4. Benzoxadiazoles as Isosteres for the Nitro Group

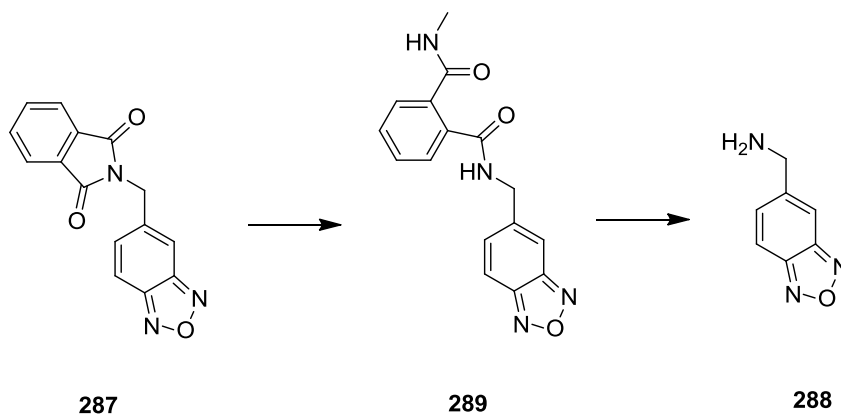
The benzoxadiazole group has been reported as a replacement for a nitrophenyl group,^{205, 216-217} as it maintains a number of atoms in similar positions from the nitro group.

Benzo[*c*]oxadiazol-5-ylmethanamine (**288**) is not commercially available but 5-(bromomethyl)-2,1,3-benzoxadiazole (**276**) is available and the patent literature suggest that compound **288** could be formed from **286** via a Gabriel reaction. In this case hydrazine was not used to liberate the amine, instead, Ohlmeyer *et al* used an excess of methylamine to open the phthalamide ring and liberate the free amine.²¹⁸



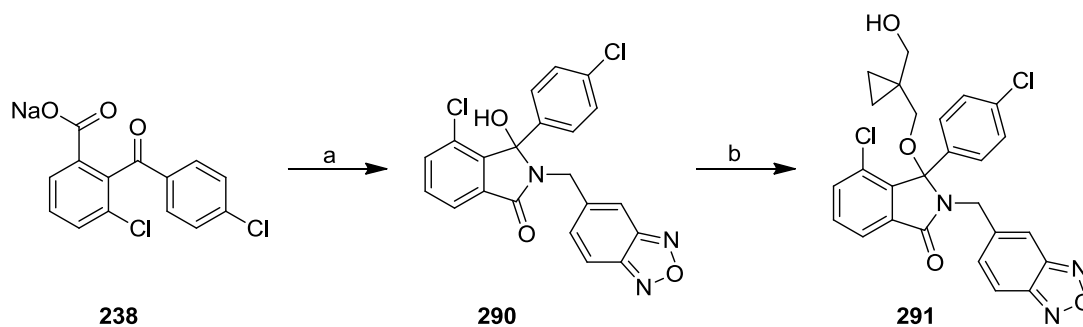
Scheme 63 Reagents and conditions; a) potassium phthalimide, DMF, 16 h; b) 40% MeNH₂(aq), EtOH, 25 h, 53%

Treatment of bromide **286** with potassium phthalimide gave **287**. A ¹H NMR showed that **286** formed the phthalimide **287** on treatment with potassium phthalimide in DMF. The crude material was worked up and used immediately in the second step. However, on addition of methylamine, the intermediate **287** rapidly disappeared within 30 min, but only a low yield of 25% product was obtained. A repeat reaction with LCMS monitoring demonstrated that after 1 h phthalimide **287** had completely disappeared but the product (**288**) had not been formed as the major product. Phthalimide **287** is rapidly converted to ring opened amide **289**, however, the attack from the second molecule of methylamine is much slower, with the reaction requiring approximately 24 h.



Scheme 64

The reaction gave a modest yield of amine **288** (53%), which was then used to synthesise compound **290** (Scheme 65).



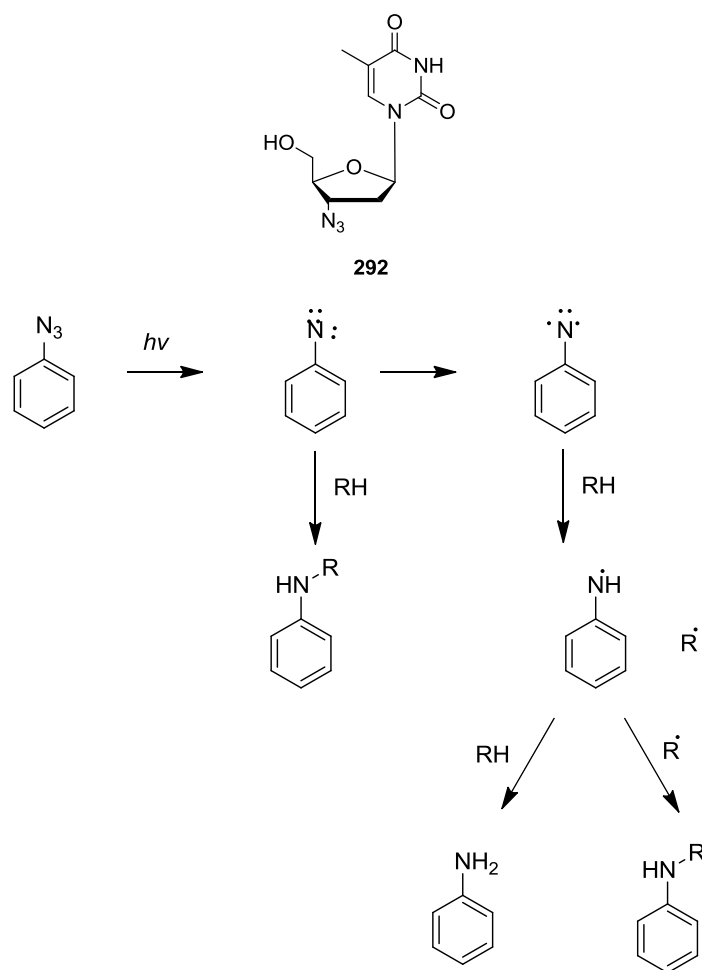
Scheme 65 Reagents and conditions; a) i. SOCl_2 , DMF, THF, 4 h; ii. **277**, Hünig's base, THF, overnight, 15 %; b) $\text{BF}_3 \cdot \text{OEt}_2$, DCM, 0 °C-RT, 3 days, 36%

Synthesis of **290** from sodium 3-chloro-2-(4-chlorobenzoyl)benzoate occurred in poor yield, due to being an unoptimised reaction and the product required multiple rounds of medium pressure column chromatography. This resulted in the loss of further material before compound **290** could be used in the next synthetic step.

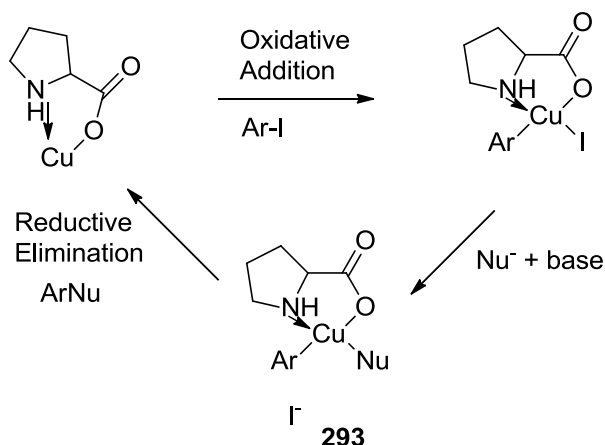
As only around 100 mg of compound **290** had been synthesised it was decided rather than using the SOCl_2 /DMF methodology for incorporation of the ether linkage, the $\text{BF}_3 \cdot \text{OEt}_2$ synthetic route would be used instead. The use of the $\text{BF}_3 \cdot \text{OEt}_2$ methodology would lead to a longer reaction time but these reagents usually have a higher yield, necessary in this case. Treatment of **290** with $\text{BF}_3 \cdot \text{OEt}_2$ for 3 days gave **291** as a colourless oil, which required both medium pressure column chromatography and semi-preparative HPLC before reaching the required purity for biological testing.

5.3.5. Replacement of the 4-Nitro Group with 4-Azide

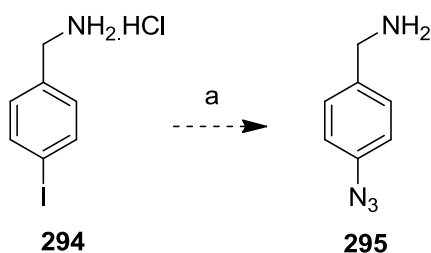
A further proposed replacement of the nitro group is an azido group. The azido group is only thought to be featured in one drug on the market (AZT (**292**), an antiretroviral drug).²¹⁹ However, azido groups can be used in labelling studies. Parang *et al* have used azido groups to observe protein cross linking with azido labelled ATP. Irradiation of the azido group with UV light results in release of N_2 and formation of a nitrene.²²⁰ The reactive nitrene species then react with C-H bonds within the protein, labelling the residues at the binding site.²²¹ Singlet nitrenes are thought to react *via* addition and rearrangement with aryl CH and triplet nitrenes insert in alkyl C-H bonds *via* hydrogen abstraction.²²²

**Scheme 66**

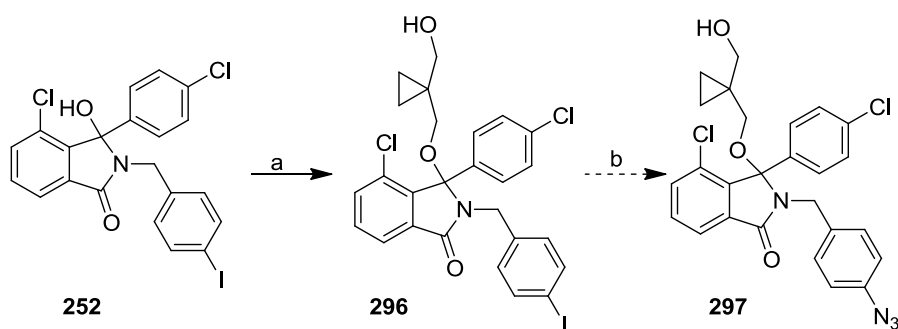
Zhu *et al*²²¹ describe the CuI catalysed synthesis of aryl azides from aromatic iodides. The formation of the azide requires L-proline (0.2 eq) and sodium hydroxide (0.2 eq) alongside sodium azide (1.2 eq) and copper iodide (0.1 eq). The sodium hydroxide and L-proline form the sodium salt of L-proline which then forms a complex with the copper, resulting in the active species *via* **293**.²²¹ The copper species can then couple the azide with the aromatic iodide species. Ma *et al*²²³ suggest that the formation of the aryl azide species occur *via* an Ullman-type reaction. However, traditional Ullman reactions require high temperatures, but with Zhu *et al* copper-catalysed reaction the temperature is lower as the reaction is promoted by the use of amino acids.²²³ Ma *et al* propose the reaction occurs via oxidative insertion of the iodoaryl species to the copper/amino acid complex. The formation of this amino acid/copper complex activates the copper to oxidative insertion and is also thought to stabilise the product of the oxidative addition, which allows the coupling reaction to occur.²²³

**Scheme 67**

To form the azido isoindolinone the copper catalysed reaction was initially attempted with 4-iodobenzylamine hydrochloride (**294**). The reaction was heated in DMSO for 20 h at 60 °C. However, the progress of the reaction was difficult to observe, even using amino TLC plates. IR analysis of the crude mixture suggested that the aromatic azido product had been formed, as a strong peak at around 2000 cm^{-1} was observed. However, on purification the product was not isolated.

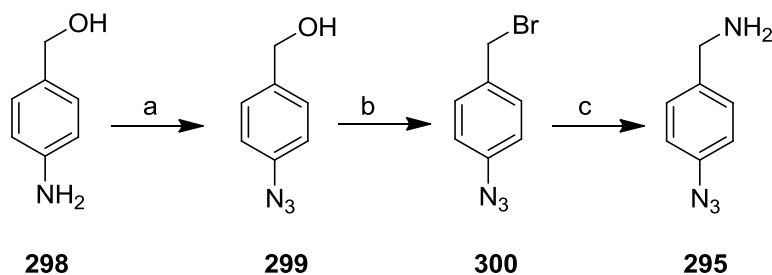
**Scheme 68** Reagents and conditions; a) L-proline, CuI, NaOH, DMSO, 60 °C

The basic nature of the benzylamine prevent monitoring and purification of the benzylamine it was decided to form the isoindolinone with the 4-iodobenzyl group in place. This should reduce the basicity of the azido-incorporated product, which should make monitoring and purifying the reaction easier, but will also mean that the potentially sensitive azido group will not be carried through a number of steps through the formation of the isoindolinone and incorporation of the ether but can instead be added in the final step. However, attempts to synthesise the desired product (**295**) proved unsuccessful, after heating overnight in the presence of CuI and L-proline, only starting material was observed.



Scheme 69 Proposed reagents and conditions; a) i. SOCl_2 , DMF, THF, 4 h; ii. 1,1-bis(hydroxymethyl) cyclopropane, K_2CO_3 , THF, overnight, 52%; b) L-proline, NaOH, CuI, DMSO, 60 °C

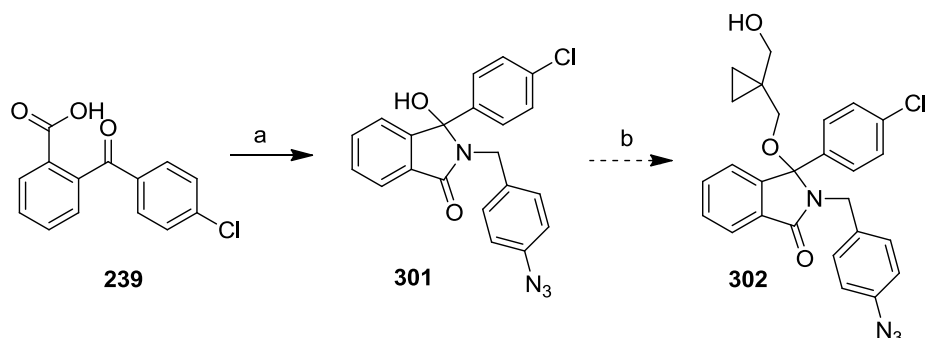
Given the unreactivity of the isoindolinone to this methodology and inherent safety issues of using azide species with copper, which would prevent scaling up of reactions it was decided to access this molecule *via* an alternative route. Griffin *et al* prepared 4-azidobenzyl alcohol from 4-aminobenzyl alcohol *via* a diazonium intermediate,²²⁴ which could then potentially be converted to 4-azidobenzylamine *via* the bromide.



Scheme 70 Reagents and conditions; a) 5M $\text{HCl}_{(\text{aq})}$, NaNO_2 , NaN_3 , 0-5 °C, 1 h, 86%; b) PBr_3 , Et_2O , 45 min, 0 °C-RT, 73%; c) i. $\text{NaN}(\text{CHO})_2$, 18-crown-6, MeCN, 95 °C, 24 h; ii. 5% ethanolic HCl, 3 days, 96%

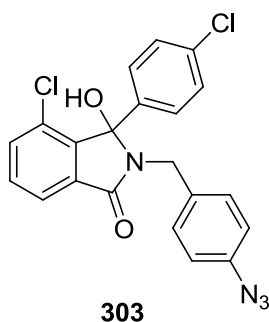
Using the literature method 4-azidobenzyl alcohol **299** was successfully synthesised. The benzyl alcohol was then converted to the benzyl bromide using PBr_3 following the procedure developed by Takatori *et al*²²⁵ which used 0.4 eq of PBr_3 at 0 °C-RT. However, in our hands 0.8 eq of PBr_3 was required to give full conversion to the benzyl bromide in good yield (73%). The modified Gabriel reaction, using sodium diformylamide,²¹³⁻²¹⁴ with the milder conditions than the traditional Gabriel reaction was used to convert the benzyl bromide to the benzylamine. Treatment of 4-azidobenzyl bromide in MeCN with 2.7 eq of sodium diformylamide with 18-crown-6 (0.1 eq) at 95 °C for 24 h resulted in complete conversion to the intermediate, and hydrolysis of the formyl groups was achieved using 5% ethanoic HCl

overnight, with an overall yield of 96%. As the azido group is light sensitive all reactions with either sodium azide or with molecules which incorporated the azido group were carried out in the dark and were stored at 4 °C in the dark. However, the azide group did appear to be robust enough to allow formation of the benzylamine, and compounds were stable for up to 1 year when stored at 4 °C in the dark.



Scheme 71 Proposed reagents and conditions; a) i. SOCl_2 , DMF, THF, 4 h; ii. **284**, Hünig's base, THF, overnight, 78%; b) i. SOCl_2 , DMF, THF, 4 h; ii. 1,1-bis(hydroxymethyl)cyclopropane, K_2CO_3 , THF, overnight

4-Azidobenzyl amine was then used to synthesise hydroxy isoindolinone **290**. When repeating these conditions to synthesis the 4-chloro analogue (**292**), the ^1H NMR spectrum of the isolated product did not correlate with the structure of the isoindolinone. However, as this reaction was only attempted once, the incorrect product simply may have been isolated.

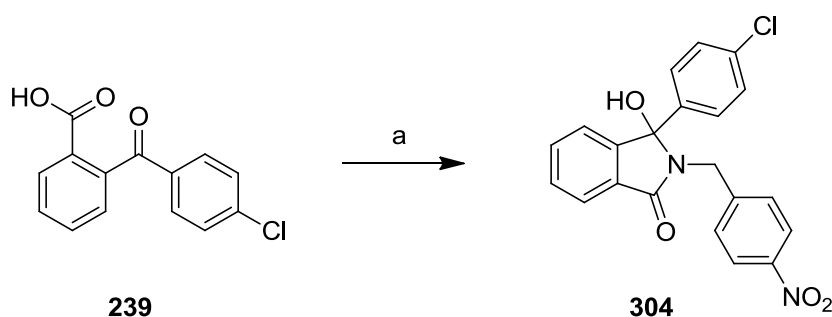


When attempting to form compound (**291**) using the SOCl_2/DMF synthetic route, no product was observed, instead two new compounds which were not isoindolinones as they lacked the characteristic isoindolinone pair of doublets for the benzyl protons.

We doubted whether the sensitive azide group would survive the $\text{BF}_3 \cdot \text{OEt}_2$ conditions for forming the ether. Therefore, the reaction with $\text{BF}_3 \cdot \text{OEt}_2$ was attempted on a small scale, and after stirring at room temperature overnight with 2.5 eq of $\text{BF}_3 \cdot \text{OEt}_2$, no reaction or significant degradation was observed. In previous examples with the 4-H isoindolinone the

$\text{BF}_3 \cdot \text{OEt}_2$ reaction quickly proceeds to completion, but with the more hindered 4-Cl reactions, several additions of 2.5 eq and a longer reaction time is required. As the azido group does not appear as sensitive to $\text{BF}_3 \cdot \text{OEt}_2$ a further 2.5 eq was added to try and push the reaction. Unfortunately, after stirring the reaction for a further 5 h no reaction was observed.

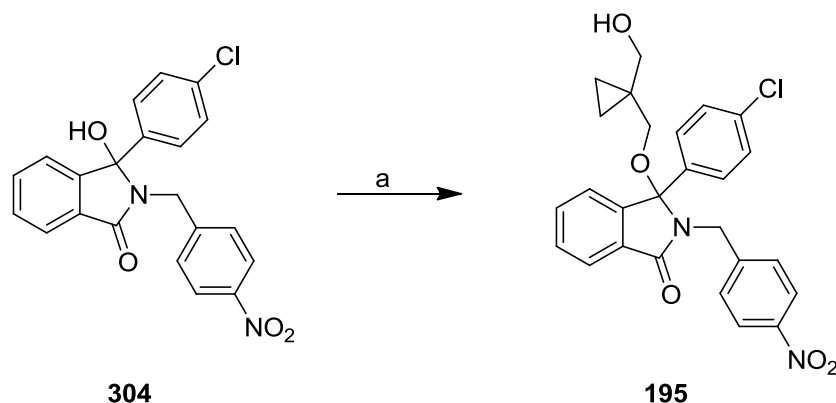
The lack of success in these reactions prompted the search for alternative methods. Compound **293** was synthesised to be used as a model compound for alternative methods in these reactions. The alternative methodologies used can be broadly divided into two classes, the first is alternative methods of chlorinating the 3-OH group of the isoindolinone, the second looks at alternative methods of activating the 3-OH to displacement by the 1,1-bis(hydroxymethyl)cyclopropane.



Scheme 72 Reagents and conditions; a). i. SOCl_2 , DMF, THF, 4 h; ii. 4-nitrobenzylamine hydrochloride, Hünig's base, THF, overnight, 63%

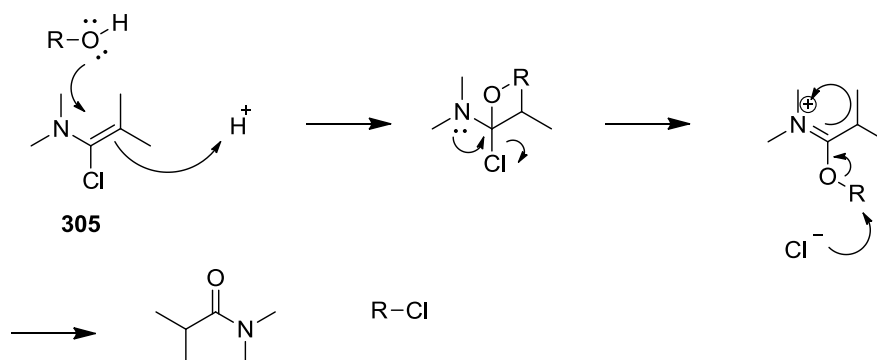
The first question to address is why the SOCl_2/DMF method of chlorination, which is used in the formation of the azido isoindolinone and tolerated, when used to chlorinate the 3-hydroxy isoindolinone results in some degradation but no reaction? When forming the isoindolinone the SOCl_2/DMF reagents are used in the first step. For the second step of the reaction, the Hünig's base is always added before the benzylamine, so any HCl generated will be neutralised before the addition of the benzylamine. For the azido analogue this could be vital as azides are known to be sensitive to acid.²²² In the second step, however, the azido functionality is present in the starting isoindolinone, and it must survive the SOCl_2/DMF conditions before the base (K_2CO_3) is added. The first alternative chlorination method attempted was the use of a commercial source of the Vilsmeier reagent. Thus, isoindolinone (**293**) was treated with (chloromethylene)dimethyliminium chloride (Vilsmeier reagent) in THF and the standard experimental procedure followed. This gave compound **195** in a poor

yield (22%). Reaction of the azido analogue **301**, under the same conditions resulted in no reaction.



Scheme 73 Reagents and conditions; a) i. (chloromethylene)dimethyliminium chloride, THF, 4 h; b) 1,1-bis(hydroxymethyl)cyclopropyl, K_2CO_3 , THF, overnight, 22%

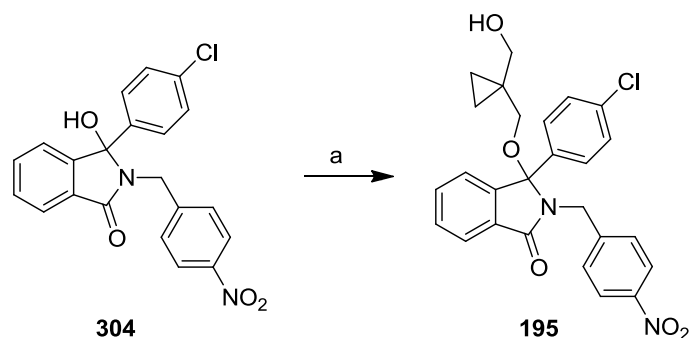
An alternative chlorination, using Ghosez reagent (1-chloro-*N,N*,2-trimethylpropenamine) (**305**) was also attempted. Ghosez reagent have been used for the synthesis of acid chlorides from carboxylic acids and maintains essentially neutral conditions.²²⁶ Bendall *et al* also described the use of Ghosez reagent for the chlorination of primary, secondary and tertiary alcohols.²²⁶ The mechanism of Ghosez reagent is shown below (Scheme 74). The first step of the mechanism is attack of the hydroxyl group on the carbon alpha to the chloro atom, the lone pair of electron on the nitrogen then forms the iminium ion, breaking the C-Cl bond. The chloride ion can then attack the alkyl group to form the alkyl halide species.



Scheme 74

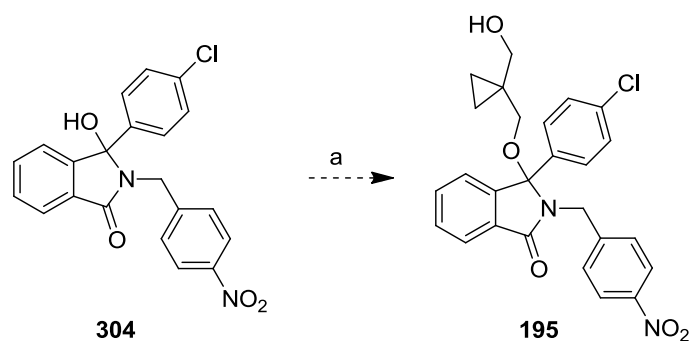
3-Hydroxyisoindolinone (**304**) was treated with Ghosez reagent at -78 °C. No reaction was observed at room temperature or at 60 °C. The failure in this case may be due to the hindered nature of the isoindolinone OH, in comparison to the literature examples.

Therefore, an alternative less bulky chlorination methodology may prove more effective. Oka *et al* used oxalyl chloride to chlorinate tertiary alcohols, where each alkyl group is a phenyl ring.²²⁷ 3-Hydroxy isoindolinone (**304**) was treated with oxalyl chloride giving **195** in 62% yield. These same conditions were applied to the azido analogues with the addition of 1 eq. of Hünig's base. However, on addition of the oxalyl chloride to the solution of isoindolinone (**301**) the reaction mixture rapidly changed colour from pale yellow to black and significant decomposition of the isoindolinone was observed by TLC.



Scheme 75 Reagents and conditions; a) i. $(\text{COCl})_2$, DCM, 2 h; ii. 1,1-bis(hydroxymethyl)cyclopropane, Hünig's base, DCM, 15 h, 62%

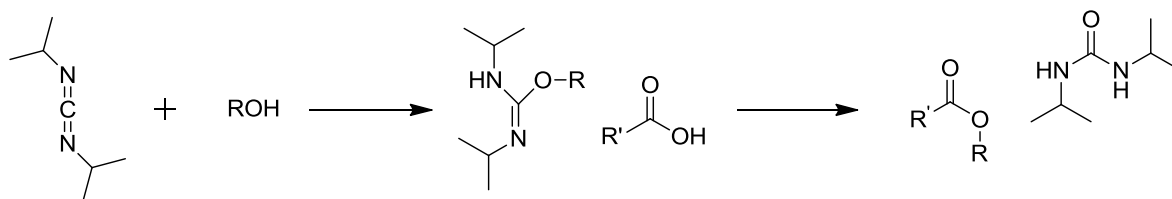
Alternative methods of activating the 3-hydroxy to displacement were explored. Firstly, triflation of the 3-OH group was attempted using *N*-phenyltriflimide. However on heating the 3-hydroxyisoindolinone (**304**) with *N*-phenyltriflimide and Hünig's base, no reaction was observed.



Scheme 76 Proposed reagents and conditions; a) i. *N*-phenyltriflimide, Hünig's base, THF, RT-70 °C, ii) 1,1-bis(hydroxymethyl)cyclopropane, Hünig's base, THF, overnight

An alternative methodology for activating hydroxyl groups to displacement is to convert them to isoureas,²²⁸ commonly by reacting the hydroxyl group with *N,N*-dialkyl carbodiimide in the presence of $\text{Cu}(\text{OTf})_2$ or CuCl .²²⁹ Attack of a nucleophile will generate urea, thus driving the reaction.²²⁸ Formation of an isourea followed by attack of a nucleophile

is commonly used to form esters^{228, 230-232} however Liu suggests that it can be used to form ethers.²²⁹ The reaction proceeds *via* attack of the *N,N*-dialkyl carbodiimide by the hydroxy species forming the isourea, which activates the hydroxy species to attack by a nucleophile forming the urea and in this example the ester species (Scheme 77).



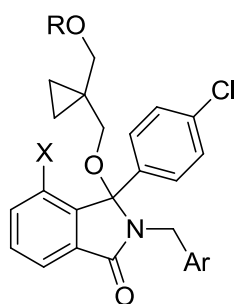
Scheme 77

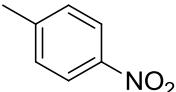
Treatment of 3-hydroxyisoindolinone **304** with diisopropylcarbodiimide and Cu(OTf)₂ in MeCN with microwave heating failed to give a new product on quenching aliquots with methanol. The reaction order was switched, first reacting 1,1-bis(hydroxymethyl)cyclopropyl with DIC, however no new product was formed. In view of these unsuccessful results, and the time restraints it was decided to discontinue work on the synthesis of the azido analogue.

5.3.6. Biological Results for Benzyl Analogues

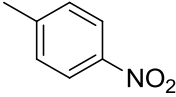
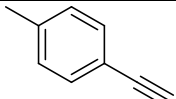
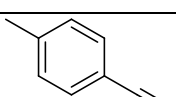
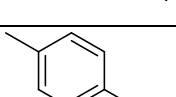

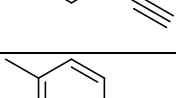
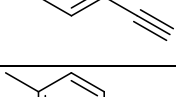
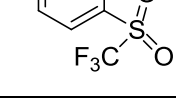
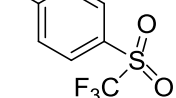
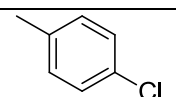
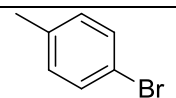
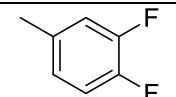
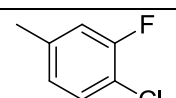
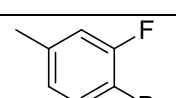
All final compounds from the benzyl series were submitted for biological testing. For assay details see chapter 5.9.

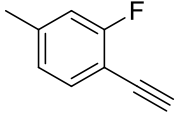
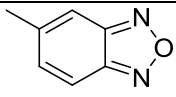
Table 21 Biological results for modifications to the benzyl group * indicate compounds synthesised by other chemists



Number	Rotation	X	R	Ar	Biological Activity IC ₅₀ (μM)
195*	(+/-)	H	H		0.23 ± 0.11

5. Isoindolinone-Based Inhibitors of the MDM2 p53 Protein-protein Interaction

220*	(+/-)	Cl	H		0.095 ± 0.096
251*	(+/-)	H	H		0.50 ^a
253	(+/-)	Cl	H		0.15 ± 0.084
257	(+/-)	Cl	C(O)CH ₂ C H ₂ CO ₂ H		0.053 ^a
254	(-)	Cl	H		0.041 ± 0.022
255	(+)	Cl	H		2.4 ± 1.5
245	(+/-)	H	H		43% inhibition at 5 μM
246	(+/-)	Cl	H		9.0 ^a
306*	(+/-)	Cl	H		0.13 ± 0.016
229*	(+/-)	Cl	H		0.17 ^a
258	(+/-)	Cl	H		0.41 ± 0.021
274	(+/-)	Cl	H		0.20 ^a
281	(+/-)	Cl	H		0.19 ± 0.069
282	(+/-)	Cl	H		0.53 ± 0.083

285	(+/-)	Cl	H		0.19 ± 0.026
291	(+/-)	Cl	H		0.28 ± 0.13

^a indicates n = 1

The ethynyl compound **253** has similar potency to the nitro group. It is structurally dissimilar to the nitro group, suggesting that the nitro group is not forming a direct electrostatic interaction which a replacement must replicate. Instead, it is the size and electron-withdrawing nature of the nitro group which must be replicated. The 4-ethynyl des-chloro analogue (**251**) was relatively potent ($IC_{50} = 0.50 \mu\text{M}$), few analogues have potency in the nanomolar range without the 'A'-ring 4-chloro group, but a greater increase in potency is observed when going from the (**251**) to (**253**) than from (**195**) to (**220**). This suggests that compound **253** shifts slightly in relation to compound **220** which positions the 4-chloro of the isoindolinone 'A'-ring in a slightly more optimal position.

The crystal structure of an isoindolinone bound to MDM2 (see chapter 5.7.1) suggests that the 4-chloro forms a halogen bond to the protein. This acts to pull the isoindolinone into a slightly different position in comparison to des-chloro analogues. In this position it would appear that the ethynyl substitution is positioned in a more optimal arrangement, than in comparison to the des-chloro analogue.

The proposed shift in position is supported by the biological activity of compound **257**. When converting **220** to the succinic ester analogue **231** an increase in potency of around 130 nM is observed, however, when adding the succinic ester to compound **253** an increase in potency of only around 30 nM is observed. In optimally positioning the ethynyl group within the pocket, the succinic group is shifted from its optimal position.

Separation of the enantiomers (**254** and **255**) demonstrates that the biological activity resides in the (-) isomer. The residual activity observed for the opposite enantiomer suggests that potency is strongly controlled by the benzyl group and substituent choice. The absolute stereochemistry of **254** is yet to be determined. It is anticipated to be the *R*-enantiomer by comparison with NU8354 and NU8604.

The trifluoromethylsulfone substituent appears to be too large to be tolerated within the MDM2 pocket. However, the increase in potency is still observed on addition of the 4-chloro group to the isoindolinone 'A'-ring. By comparing the Cresset Fieldview modelling of the negative field (areas which like to interact with positive areas or electron-deficient of the protein) of the nitro (**220**) and the trifluoromethylsulfone (**246**) compounds, we can see that these compounds are similar. However, observing the compounds for an alternative angle we can see that this is not the case. The negative field for the benzyl group is disrupted by the presence of the trifluoromethyl group.

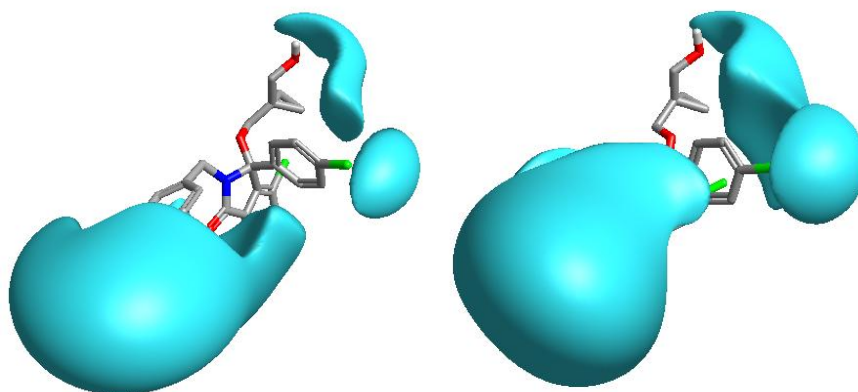


Figure 66 Cresset Fieldview modelling of the nitro (**220**) (left) and trifluoromethylsulfone (**246**) right, the blue surface represents the negative field

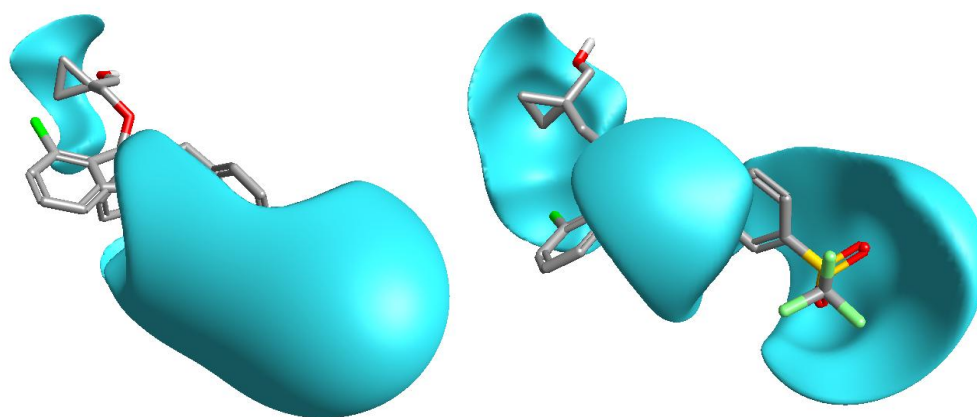


Figure 67 Cresset Fieldview modelling of nitro (**220**) (left) and trifluoromethylsulfone (**246**) (right) compounds showing the negative field

The series of 3-fluoro-4-halo or ethynyl compounds shows some interesting results. For both the 4-chloro and the 4-ethynyl compounds, which both have similar levels of potency to

compound **220**, addition of the fluoro group reduces activity. However, for compound **281**, which without the fluoro is slightly less potent than the nitro analogue, although within the range of error, there is little change in the potency. The addition of the fluoro group can adjust the electronic of the benzyl ring sufficiently but any change is within the margin of error. The 3,4-fluoro motif appear to be small to fulfil the shape filling requirement whilst the 3-fluoro-4-iodo appears to be slightly too large to be the optimal substituent.

The benzoxadiazole substituent (**291**) is tolerated, with a small decrease in potency from that of the nitro substituent. This demonstrates that this substituent can be effective as a replacement for the nitro group in both steric and electronic properties. The Fieldview modelling of the negative field of compound **220** and **291** shows a similar distribution between both compounds.

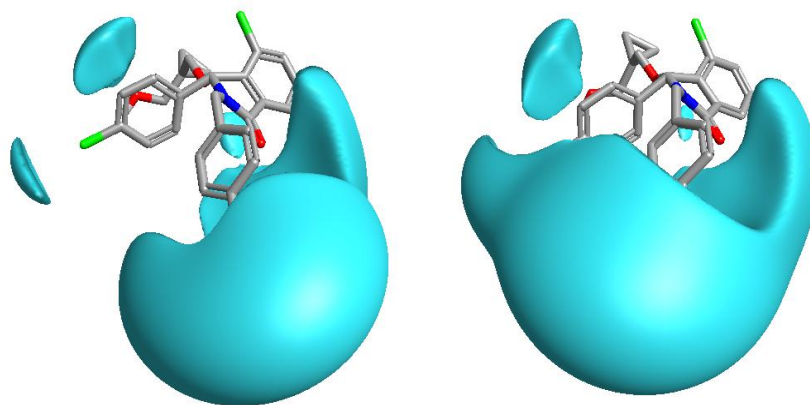
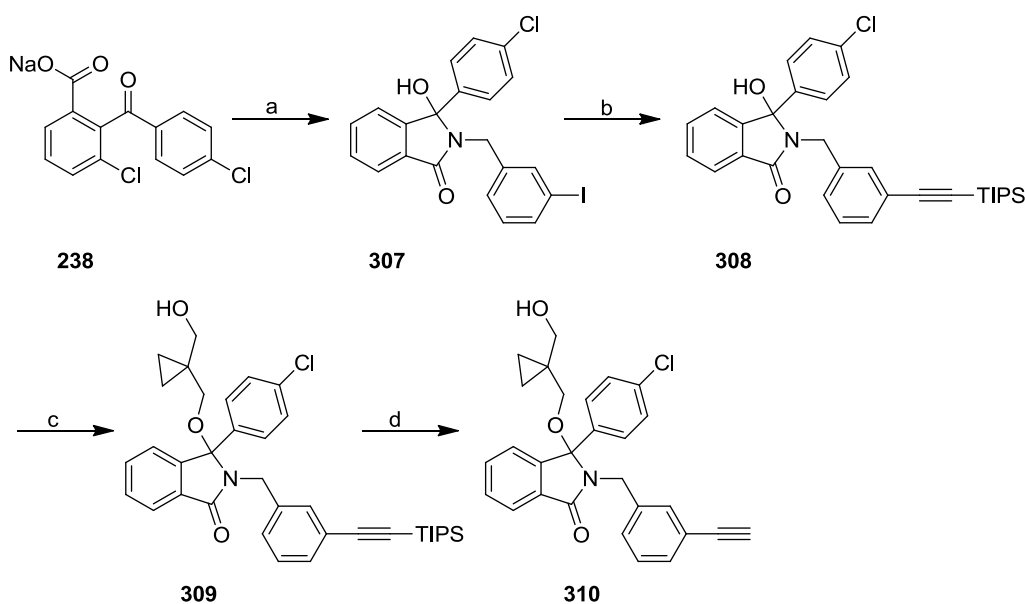


Figure 68 Comparison of the negative field of **220** (left) and **291** (right)

5.4 Analogues of the Ethynyl Group

Due to the potency of 4-chloroisoindolinone (**253**) a series of analogues were synthesised to develop the structure-activity relationships around the ethynyl analogue. Previously synthesised analogues have shown that substitution at the 3-position is not tolerated, to confirm this is also true for the benzyl ethynyl analogues, the 3-ethynyl analogue was synthesised *via* 3-iodobenzyl precursor. The 3-ethynyl analogue can be synthesised following a similar synthetic route to 4-ethynyl analogue, which is shown below in Scheme 78. Synthesis of **310** was achieved in similar yields to the synthesis of **253** in an overall yield of 6%.



Scheme 78 Reagents and conditions; a) i. SOCl_2 , DMF, THF, 4 h; ii. 3-iodobenzylamine hydrochloride, Hünig's base, THF, overnight, 37%; b). Triisopropylsilylacetylene, Et_3N , CuI , $\text{Pd}(\text{PPh}_3)_2\text{Cl}_2$, THF, 16 h, 80%; c) i. SOCl_2 , DMF, THF, 4 h ii. 1,1-bis(hydroxymethyl) cyclopropyl, K_2CO_3 , THF, overnight, 37% v. 1 M TBAF in THF, THF, 61%

Based on previous models the ethynyl group was thought to sit close to the bottom of the pocket of MDM2, leaving little room for further substitution. To probe whether any further substitution on the ethynyl group is tolerated two compounds were synthesised i.e. **311**, which adds a methyl group to the terminal end of the ethynyl group and compound **312**, which adds a phenyl ring to the terminal end of the ethynyl

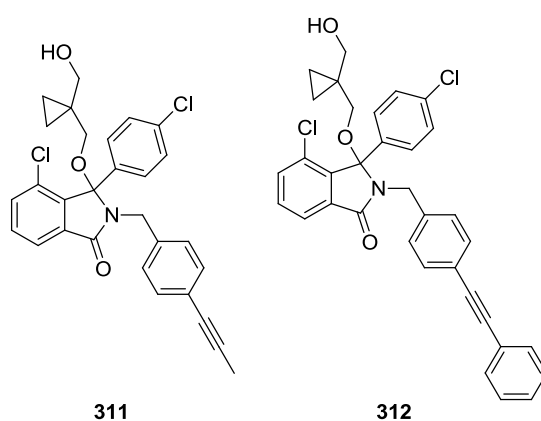
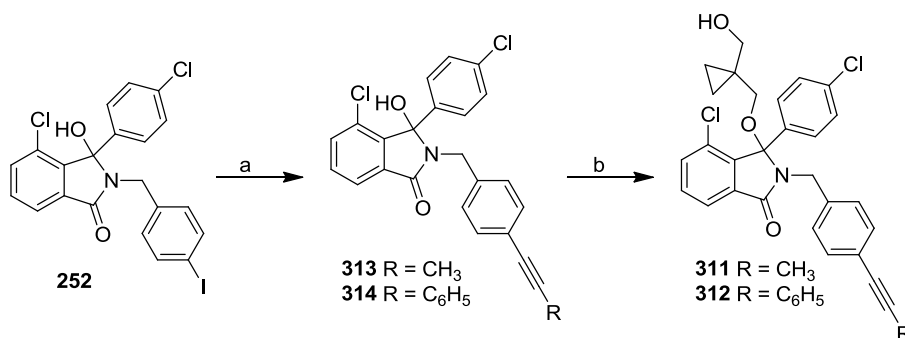


Figure 69

The synthesis of compound **313** was achieved using a Sonogashira reaction between the 4-iodobenzyl substituted isoindolinone (**252**) and propyne. Unfortunately, unlike

triisopropylacetylene, propyne is not a liquid but a gas, and therefore requires an alternative set-up of the reaction. The reaction mixture was prepared and degassed and cooled to $-78\text{ }^{\circ}\text{C}$ before the addition of the condensed propyne from a cold finger and the reaction gradually warmed to room temperature. As propyne is a gas at room temperature, it was not possible to measure 1.3 equivalents as the propyne boils within the needle syringe, therefore a large excess (as measured by the change in solvent level) was added. The general reaction scheme for the synthesis of **311** and **312** is shown below (Scheme 79).

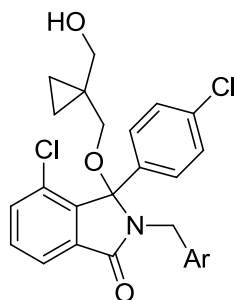


Scheme 79 Reagents and conditions; a) $\text{R} = \text{CH}_3$ $\text{Pd}(\text{PPh}_3)_2\text{Cl}_2$, CuI , Et_3N , propyne, THF, 18 h, 94%; $\text{R} = \text{C}_6\text{H}_{11}$ $\text{Pd}(\text{PPh}_3)_2\text{Cl}_2$, CuI , Et_3N , phenyl acetylene, THF, 17 h, 91%; iv. 1. SOCl_2 , DMF, THF, 4 h 2. 1,1-bis(hydroxymethyl)cyclopropyl, K_2CO_3 , THF, overnight, $\text{R} = \text{CH}_3$ 20%, $\text{R} = \text{C}_6\text{H}_5$ 36%

Using the optimised Sonogashira conditions compound **314** was synthesised in excellent yield (91%), the complete synthetic route to synthesise the final compound is shown above.

5.4.1. Biological Results for Ethynyl Analogues

Table 22 Biological activity for the ethynyl analogues



Number	Structure	Biological Activity IC ₅₀ (μM)
310		2.0 ± 0.75
311		0.7 ^a
312		2.9 ^a

^a indicates results where n = 1

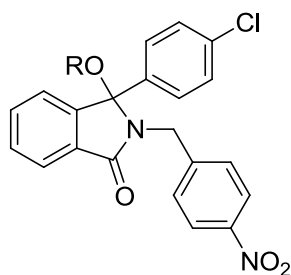
Compound **310** demonstrates the narrow structure activity relationships for the benzyl substituents. No tolerance is observed for substituents larger than a fluoro group in the 3-benzyl position, suggesting that the benzyl group sits in a narrow deep pocket, ideal for a 4-ethynyl group, but intolerant of a change in position. Both compounds **311** and **312** demonstrate that there is insufficient space for any further extension from the ethynyl group, suggesting that the terminal hydrogen of the ethynyl sits close to the bottom of the pocket. Interesting, compound **312** has a smaller loss of potency than expected, suggesting that compound **312** may adopt an alternative binding mode.

A number of compounds have now been synthesised with a variety of substituents on the benzyl ring. Several highly activity substituents have been identified; to increase activity attention has been directed to alternative areas of the molecule.

5.5 Further SAR for the Isoindolinone Ether-Groups

Previous work with the Northern Institute for Cancer Research drug discovery laboratories identified the oxymethyl-cyclopropyl methanol substituent optimal for the C3 position of the isoindolinone e.g. NU8604 (**220**). The addition of the cyclopropyl group to the ether side-chain significantly increased potency over the *n*-propoxy derivative the improvement was rationalised by the ability of the cyclopropyl to restrict the freedom of rotation of the propyl chain thus removing an entropic penalty to binding. However, addition of the cyclopropyl ring increases the *clogP* which is unfavourable for solubility and can cause more metabolic liability and the ether side chain may be a site for metabolic attack of the molecule *in vivo*.

Table 23 Ether derivatives with IC₅₀ values and *clogP* values



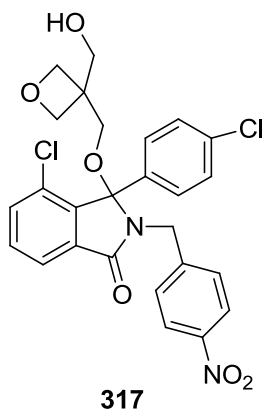
Number	R	IC ₅₀ (μM)	<i>clogP</i>
315		0.52 ± 0.14	4.4
316		0.34 ± 0.26	5.2
185		0.23 ± 0.11	4.8

The *gem*-dimethyl group also improved activity, whilst commonly used to block metabolism, also increases the lipophilicity of molecules which can in turn place molecules at higher risk of metabolism.

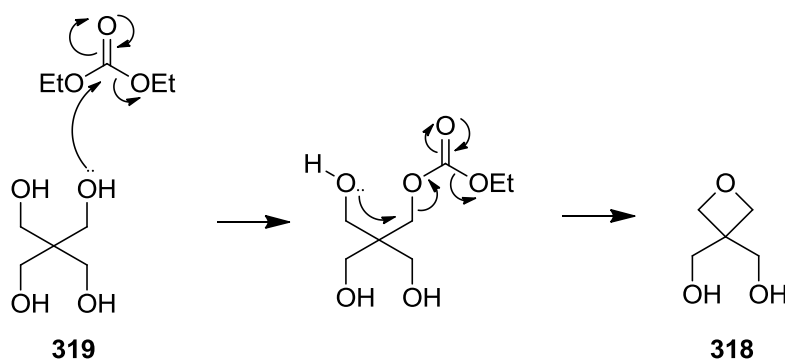
Wuitschik *et al*²³³⁻²³⁵ have replaced a *gem*-dimethyl group with an oxetane ring. The van der Waals volumes of the *gem*-dimethyl group and the oxetane ring are thought to be similar but the oxetane ring is more hydrophilic. Within simple model systems the replacement of a *tert*-

butyl group with a 3-methyl-oxetanyl group improved the solubility of the compounds and reduced the $\log D$ value by one unit. The oxetane ring was also shown to have good stability within human and mice microsomes, a potential indicator of metabolic stability.²³⁵

As the isoindolinone molecules have poor solubility (with a $\text{clog}P$ of 5.7 for **253**), making aqueous formulation difficult and leaving the molecule prone to metabolism, the inclusion of an oxetane ring may be beneficial. Therefore, the synthesis of oxetane **317** was proposed.



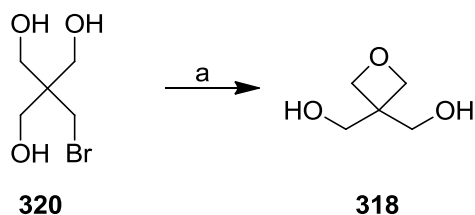
Oxetane **317** required the synthesis of the 3,3-bis(hydroxymethyl)oxetane (**318**). The synthesis of 3,3-bis(hydroxymethyl)oxetane from pentaerythritol (2-bis-hydroxymethylpropane-1,3-diol) (**319**) using diethyl carbonate and potassium carbonate in ethanol has been reported.²³⁶ The reaction employs a catalytic amount of potassium hydroxide, as the reaction generates ethoxide ions to act as a base for further reactions (Scheme 80). The reaction was repeated following literature procedure. However, no product was observed using this reaction.



Scheme 80 Proposed mechanism for formation of oxetane ring using diethyl carbonate

An alternative route, used by Issidorides *et al*²³⁷ proved more successful, this route uses 2-(bromomethyl)-2-(hydroxymethyl)propan-1,3-diol (**320**) with potassium hydroxide in ethanol. **320** was stirred at room temperature for 2 h, then heated to reflux. The length of

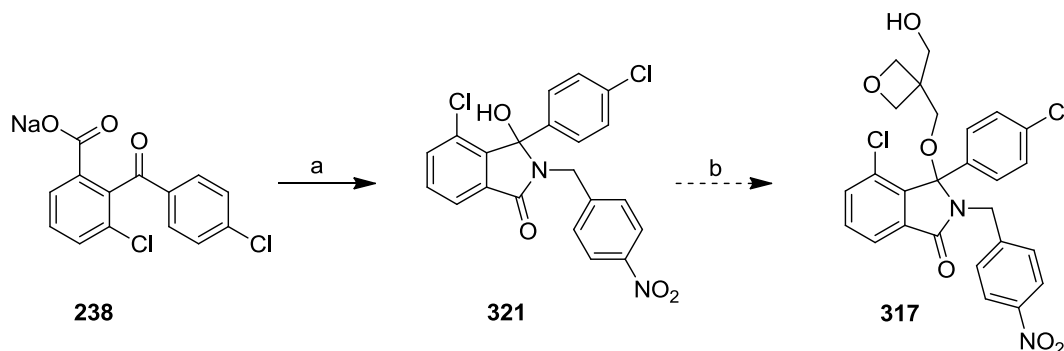
time the reaction was at reflux was gradually increased to optimise the yield of the reaction, the time and yield is shown below (Scheme 81 and Table 24).



Scheme 81 Reagents and conditions; a) KOH, Ethanol, RT-reflux

Table 24 Comparison of reaction time with yield

Length of time at reflux (min)	Yield (%) of 318
7	26
10	26
15	78
20	62
1.5 h	62



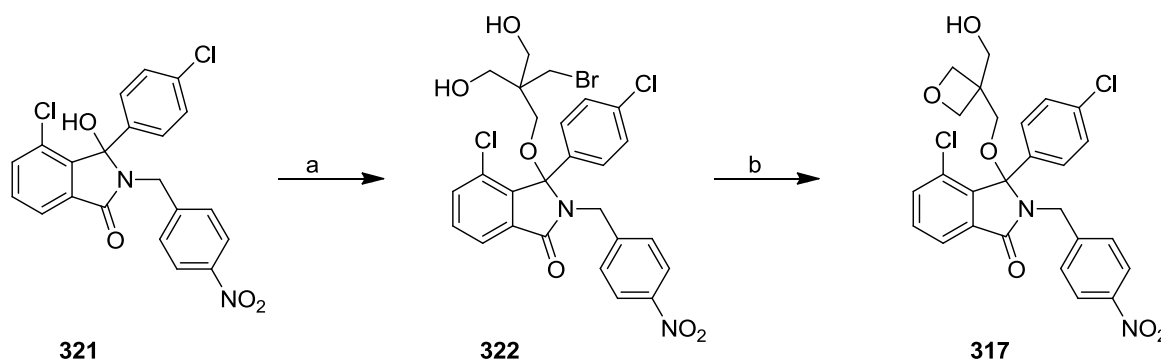
Scheme 82 Proposed reagents and conditions; a) i. SOCl_2 , DMF, THF, 4 h ii. 4-nitrobenzylamine hydrochloride, Hünig's base, THF, overnight, 28%; c) i. SOCl_2 , DMF, THF, 4 h ii. 3,3-bis(hydroxymethyl)oxetane, K_2CO_3 , THF, overnight or $\text{BF}_3 \cdot \text{OEt}_2$, 3,3-bis(hydroxymethyl)oxetane, DCM 0 °C-RT

Formation of the ether linkage was then attempted using 3,3-bis(hydroxymethyl) oxetane in the standard synthetic procedure, with thionyl chloride and DMF. However, the synthesis of the desired product did not proceed as cleanly as previously seen when using bis(hydroxymethyl) cyclopropane and two minor spots were observed by TLC. Therefore the

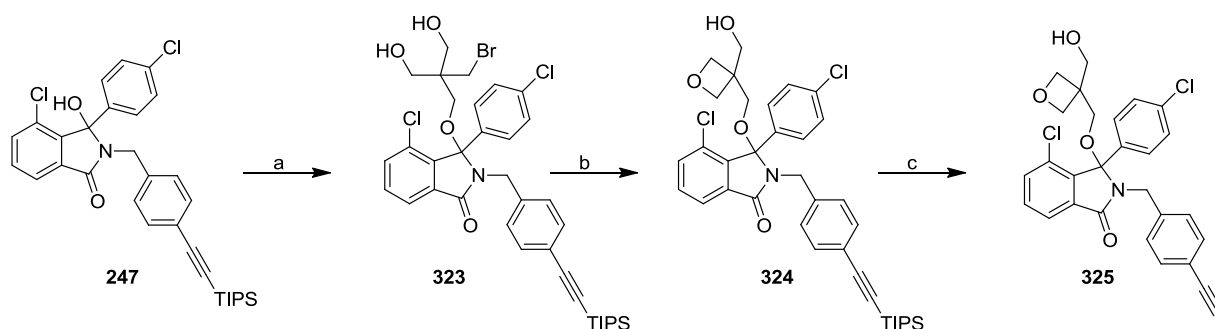
reaction time was extended by 24 h, but no significant change was observed. On workup and purification of the reaction both compounds were isolated, but, only small amounts of each compound were isolated and the NMR spectrum of indicated poor purity. Both spectrum contained characteristic isoindolinone resonances. Full assignment was not possible.

The alternative $\text{BF}_3 \cdot \text{OEt}_2$ route to ether formation was then attempted. 3,3-Bis(hydroxymethyl)oxetane is not soluble in DCM so the solvent was switched to THF. However, rather than forming a yellow solution on addition of the $\text{BF}_3 \cdot \text{OEt}_2$ and a colourless solution on addition of the alcohol as is usually observed, a precipitate was instead observed, and no reaction occurred. The reaction was repeated, DCM was used as the main solvent, with 3,3-bis(hydroxymethyl)oxetane dissolved in the minimum of THF and added to the reaction, still no reaction was observed.

2-(Bromomethyl)-2-(hydroxymethyl)-propan-1,3-diol (**320**), which is used as the precursor to 3,3-bis(hydroxymethyl)oxetane is a white solid which is soluble in THF. It was decided to try and form the ether with **309** and then form the oxetane ring *in situ*. The cyclisation to form the oxetane ring should occur as previously seen, with compound **322** behaving as a monoprotected bromomethyl analogue. Formation of the ether was achieved in good yield under Vilsmeier conditions (42%) and cyclisation was achieved by stirring for 2 h at room temperature in the presence of potassium hydroxide in ethanol followed by 1 h at reflux in 68% yield (see Scheme 83). The 4-ethynyl derivative was prepared by the same route in an overall 13% yield (Scheme 84)



Scheme 83 Reagents and conditions; a) i. SOCl_2 , DMF, THF, 4 h; ii. 2-(bromomethyl)-2-(hydroxymethyl)-propan-1,3-diol, K_2CO_3 , THF, overnight, 42%; b) KOH, EtOH, 3 h, RT-reflux, 68%



Scheme 84 Reagent and conditions a) i. SOCl_2 , DMF, THF, 4 h; ii. 2-(bromomethyl)-2-(hydroxymethyl)propan-1,3-diol, K_2CO_3 , THF, overnight; 31% b) KOH, EtOH, 3 h, RT-reflux, 63%; c) 1 M TBAF in THF, THF, 1 h, 89%

Both compounds separated by chiral HPLC. Compound **317** was separated using a Daicel Chiralpak AD-H using hexane:ethanol 85:15 to give two compounds, both a foamy solid. NCL-00018566 (peak 1, **326**) with $[\alpha] = -10.7^\circ$ and NCL-00018565 (peak 2, **327**) with $[\alpha] = +30.3^\circ$. Compound **325** was separated using *tert*-butyl methyl ether:isopropanol 95:5. Peak 1 (NCL-00018710, **328**), was a fluffy solid with optical rotation of with $[\alpha] = -7.74^\circ$, whilst peak 2 (NCL-00018711, **329**) was a colourless oil which gradually solidified to a white solid. **329** had an optical rotation of $[\alpha] = +4.65^\circ$. Assignment of the absolute stereochemistry has not been possible as the compounds fail to give suitable crystals. The faster eluting peaks are expected to have an (*R*)-configuration by analogy with NU8354.¹⁹² A chiral HPLC trace is shown below (Figure 70) demonstrating the clear separation between compound **326** and **327** on the chiral column.

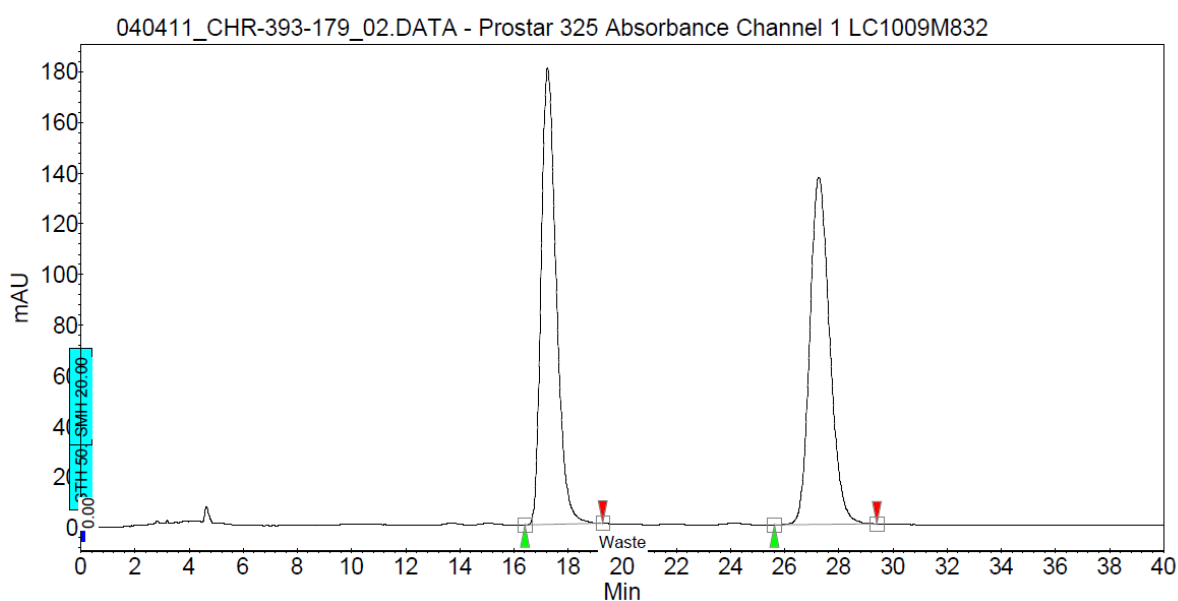


Figure 70

5.5.1. Biological Results for Isoindolinone Ether Groups

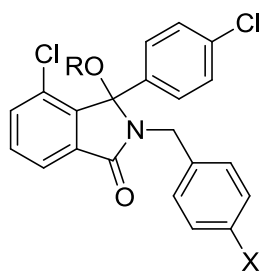


Table 25 Biological results for ether derivatives * indicates compounds synthesised by other chemist'

Number	Rotation	X	R	Biological Activity IC ₅₀ (μM)	clogP	Measured Solubility (midpoint)
220*	(+/-)	NO ₂		0.095 ± 0096	5.6	6.5 μM
317	(+/-)	NO ₂		0.048 ± 0.0091	4.7	18.75 μM
326	(-)	NO ₂		0.025 ± 0.0061	4.7	-
327	(+)	NO ₂		0.83 ± 0.12	4.7	-
253	(+/-)	CCH		0.15 ± 0.084	6.1	3.75 μM
325	(+/-)	CCH		0.090 ± 0.032	5.2	11.5 μM
328	(-)	CCH		0.12 ± 0.096	5.2	-
329	(+)	CCH		3.5 ± 1.7	5.2	-

The replacement of the cyclopropyl ring with an oxetane is calculated to give an improvement in the physical properties of the molecule, reducing the clogP by one unit. In the case of the **220** to **317** an increase in potency is also observed. Wuitschik *et al* describes 3-disubstituted oxetanes as possessing significant influence over the conformation of the carbon chain to which it is joined. With a *gem*-dimethyl substituted chain a staggered

conformation is adapted, however, with a oxetane the chain form a gauche conformation.²³³ The introduction of the oxetane ring may therefore be holding the propyl chain in the ideal conformation, accounting for the increase in potency.

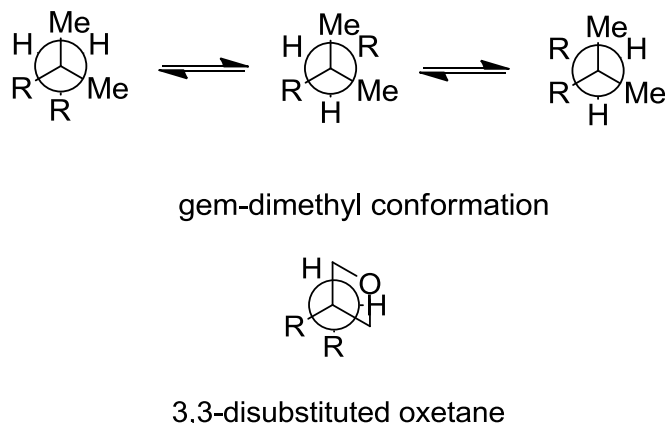


Figure 71

When changing from the cyclopropyl ring to the oxetane ring with compound **253** to **325**, the two compounds are essentially equipotent suggests that the isoindolinone adopts a somewhat different binding mode in MDM2 when substituted with an ethynyl group in comparison to the nitro analogues. When separating compound **317** into the two enantiomers **326** and **327**, the (-)-enantiomer (**326**) improves activity beyond the parent compound. However, with compound **328**, the (-)-enantiomer of compound **325**, the activity is lower than the parent compound. It should be noted that this is the result of initial testing, and has a large error within the results, so further testing may result in improved activity.

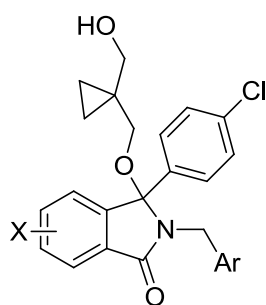
The oxetane confers good properties without compromising the potency of the analogues. Consequently, it should be included in subsequent series of a future isoindolinones.

5.6 *tert*-Butyl ‘A’-Ring Analogues

The isoindolinone series has poor aqueous solubility, well below the target solubility for an orally available drug of 50 μM . Measurements of the aqueous solubility of a number of compounds by Cyprotex, a company which specialises in the measuring of physical properties of molecules developed by academia and pharmaceutical industry, observed that a significant difference could be seen within molecules of the isoindolinone series. Table 26 shows some of the results of a number of compounds below. The solubility was measured

using a turbidimetric solubility assay, which measures kinetic solubility by a diluting DMSO solution of the drug with an aqueous buffer at a pH of 7.4 and a temperature of 37 °C. Turbidity was measured at 620 nm.²³⁸ Results are quoted as start point, midpoint and end point of precipitation. The solubility midpoint was obtained by measuring the first concentration at which precipitation is observed and the concentration where complete precipitation is observed. From this a midpoint is calculated.

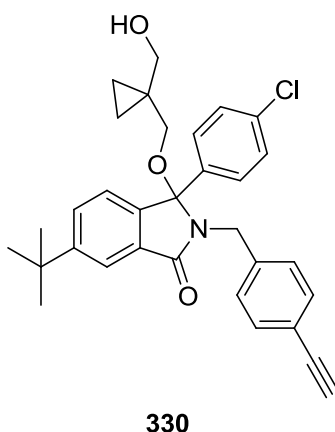
Table 26 Structure and related midpoint of solubility



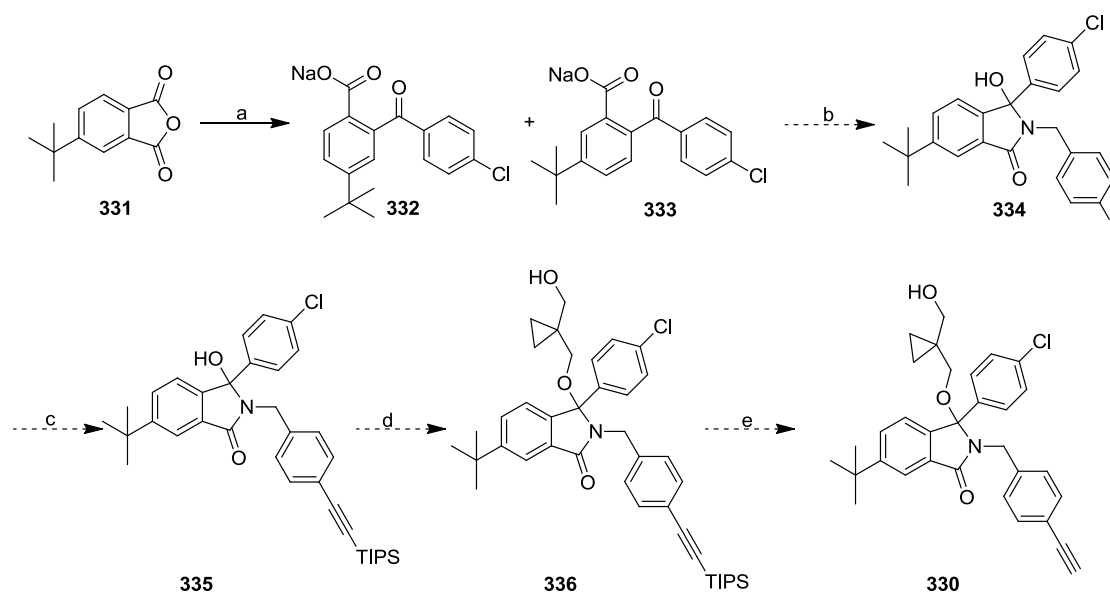
Number	X	Ar	Lower Solubility point (μM)	Upper Solubility point (μM)	Solubility Midpoint (μM)
253	4-Cl		1	6.5	3.75
185	-		1	3	2
220	4-Cl		3	10	6.5
224	6- ^t Bu		10	30	20

From Table 26 compound **253** can be seen to have particularly poor solubility. Interestingly, the change from compound **220** to compound **224** has a 3-fold change in solubility, which is a large difference for simply changing the 'A'-ring 4-chloro to a 6-^tBu. A *tert*-butyl group would be expected to decrease the aqueous solubility, as it increases lipophilicity. In terms of dissolution from a solid into a solution *tert*-butyl groups are known to have an interesting affect on solubility. Law describes *tert*-butyl as increasing organic solubility within a series of compounds.²³⁹ The *tert*-butyl increases steric hindrance, which reduces the interaction between molecules thus increasing solubility, a principle which can also be applied to aqueous solubility.

Compound **224**, whilst having essentially equipotent biological activity ($IC_{50} = 194$ nM) as compound **220** has significantly improved aqueous solubility. Compound **330**, which maintains the favourable ethynyl substitution of the benzyl ring, and incorporates the solubilising *tert*-butyl group on the isoindolinone 'A'-ring was therefore synthesised.



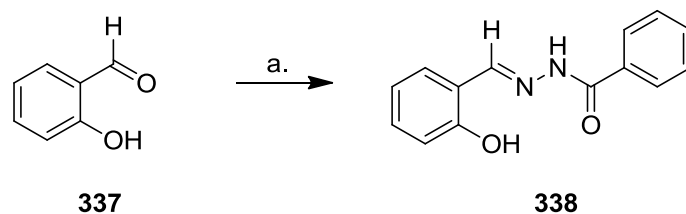
Compound **224** was synthesised starting from 4-*tert*-butylphthalic anhydride, forming the benzoyl benzoic acid *via* a Friedel-Crafts acylation analogous to 4-chloro analogues.²⁴⁰ Therefore, we hoped to utilise this synthetic route to access compound **330**. The proposed synthetic route is shown below.



Scheme 85 Proposed reagents and conditions; a) AlCl₃, PhCl, 2 h, 90 °C; b) i. SOCl₂, DMF, THF, 4 h ii. 4-iodobenzylamine hydrochloride, Hünig's base, THF, overnight; c) Triisopropylsilyl acetylene, Pd(PPh₃)₂Cl₂, CuI, Et₃N, THF; d) i. SOCl₂, DMF, THF, 4 h ii. 1,1-bis(hydroxymethyl)cyclopropyl, K₂CO₃, THF, overnight e) 1 M TBAF in THF, THF, 1 h

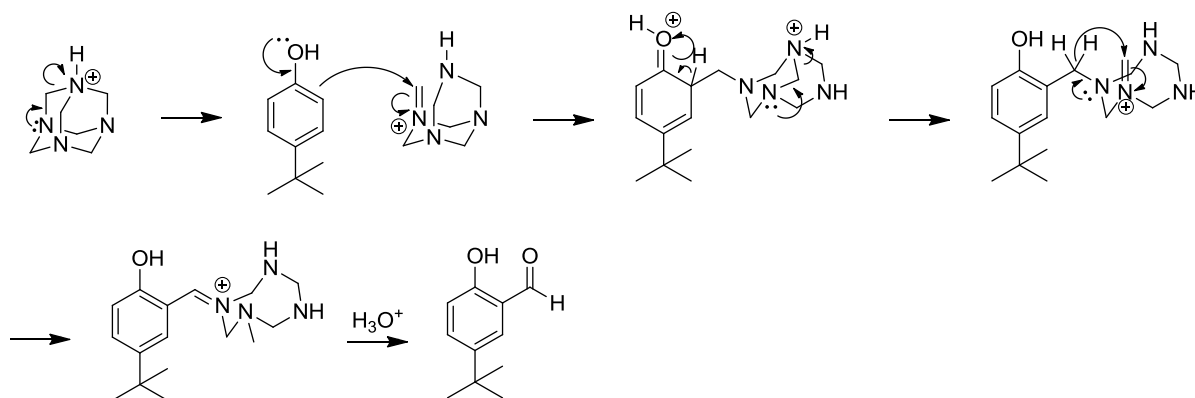
Previous work undertaken within the laboratory identified that the Friedel-Crafts reaction between 3-*tert*-butyl phthalic anhydride and chlorophenyl would give approximately 1:1 mixture of the 5- and 6- isomers of the substituted benzoyl benzoic acid.²⁴⁰ The preparation was repeated as described and unfortunately, it proved to be very erratic in yield, and also very difficult to dry the product to a suitable level for the following reaction in the scheme. Therefore, an alternative method for formation of the benzoyl benzoic acid was sought.

An alternative synthetic route to the benzoyl benzoic acid had recently been developed in-house.²⁴¹ It utilises a lead tetraacetate mediated rearrangement to form a benzoyl benzaldehyde from 2-hydroxyhydrazide.²⁴² To utilise this new synthetic method the correctly substituted 2-hydroxyhydrazine was required. Jacq *et al* synthesised 2-hydroxyhydrazine from 2-hydroxybenzaldehydes and hydrazides,²⁴² a protocol which should provide access to the desired intermediates for synthesis of the desired final compound.



Scheme 86 Reagents and conditions; a) benzhydrazide, AcOH, 15 min, RT, 91%²⁴²

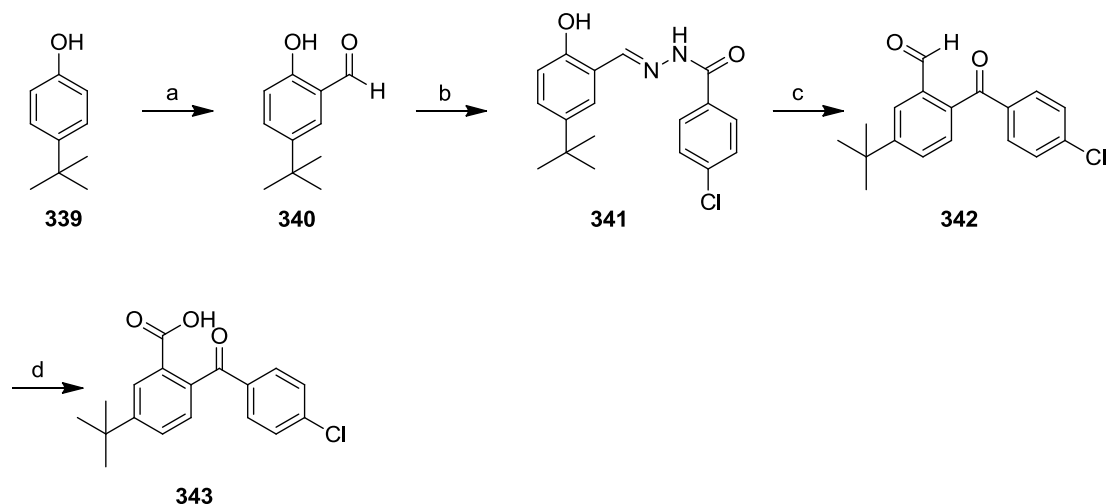
Synthesis of the 6-*tert*-butylsubstituted isoindolinones following this synthetic scheme requires use of 5-*tert*-butyl-2-hydroxybenzaldehyde (**340**), which can be synthesised in one step from 4-*tert*-butyl phenol (**339**). The Duff reaction is a method of installing aromatic formyl groups *via* electrophilic aromatic substitution.²⁴³ The reaction uses hexamethylenetetramine (HMTA) as a formaldehyde equivalent, which, when catalysed by trifluoroacetic acid will formylate an aromatic ring.¹⁹⁶ The mechanism of is shown below. Acid catalysis results in formation of an iminium species, which is then attacked by the aromatic ring, to form the Wheland intermediate, a further iminium species then extracts a hydride from the benzylic position, forming a further iminium species, which on aqueous work-up will result in formation of the desired aldehyde.



Scheme 87

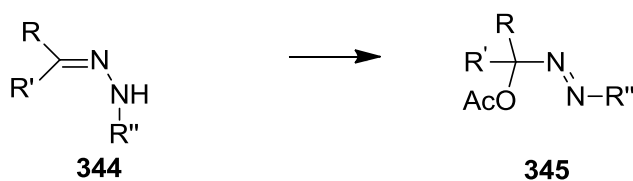
Lindoy *et al* have synthesised 5-*tert*-butyl-2-hydroxybenzaldehyde (**340**) from HMTA and 4-*tert*-butylphenol in refluxing TFA for in 29%.²⁴³ In-house development of this reaction suggested microwave heating was appropriate for this reaction. A solution of 4-*tert*-butylphenol and HMTA in TFA was heated at 120 °C for 30 min in a yield of 46%. LCMS monitoring of this reaction suggested no starting material remained, but the lower yield suggests a large number of minor impurities are formed.

Benzaldehyde **340** was converted to hydrazone **341** on treatment with 4-chlorobenzhydrazide in acetic acid in excellent yield (94%) following the procedure described by Jacq *et al.*²⁴² The correct substituents for the rearrangement reaction to give the benzoyl benzaldehyde were now in place. The synthetic scheme to give key intermediate benzoyl benzoic acid is shown below.

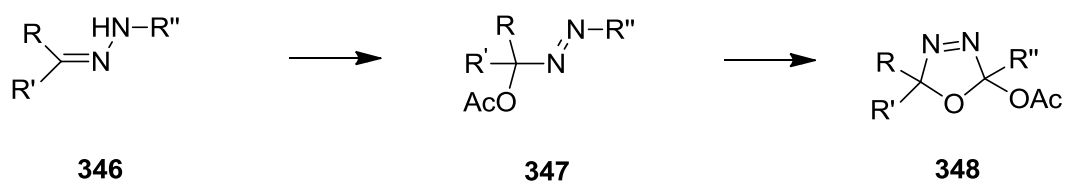


Scheme 88 Reagents and conditions; a) HMTA, TFA, 120 °C, 30 min, 46%; b) 4-chlorobenzhydrazide, AcOH, 15 min, 94%; c) $\text{Pb}(\text{OAc})_4$, THF, 2 h, 0 °C, 73%; d) NaClO_2 , $\text{H}_2\text{NSO}_3\text{H}$, MeCN, 1.5 h, 85%

The mechanism of the lead tetraacetate induced rearrangement has been extensively explored by Katritzky *et al.*²⁴⁴ Treatment of monosubstituted hydrazones (e.g. **344**) leads to formation of acetoxyazo compounds like **345** (where $\text{R}'' = \text{H}$). However, when $\text{R}'' = \text{COAr}$ e.g. **346** a cyclisation can occur to give 1,3,4-oxadiazolines such as **338**.

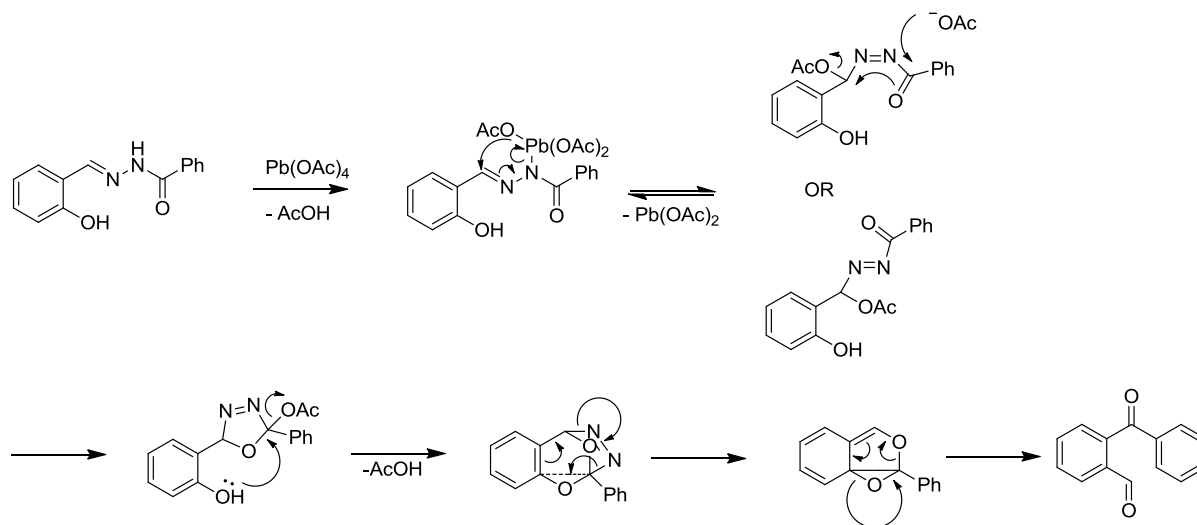


Scheme 89



Scheme 90

When $R' = 2$ -phenol further rearrangement can occur, with the hydroxyl group replaced with the acyl substituent. This rearrangement leads to the formation of the desired benzoyl benzaldehydes. Katritzky *et al* demonstrated that the benzoyl benzaldehyde is formed *via* an intramolecular reaction, and proved that $Pb(OAc)_4$ does not act as an acid catalyst *via* minor contamination with acetic acid.²⁴⁴ Instead, the proposed mechanism is shown below (Scheme 91). Co-ordination to lead (IV) acetate is followed by attack of an acetate ion on the imine, with displacement of lead (II) acetate. This can result in either a *cis* or *trans* double bond, with the *cis* required for the following mechanism to proceed. However this step of the mechanism may be reversible, allow reformation of the imine, preventing the loss of the *trans* product. Attack of the carbonyl with an acetate ion breaks the double bond, with the electrons displacing the first acetate ion and forming a 1,3,4-oxadiazolines. The second acetate ion is then displaced by the lone pair of electron of the phenol oxygen, this species then rearranges to extrude nitrogen and rearomatises to the benzoyl benzaldehyde. Labelling studies undertaken by Katritzky *et al* demonstrated that the acyl group oxygen eventually becomes the aldehyde oxygen, rather the hydroxyl oxygen atom *via* formation of 1,3,4-oxadiazolines as was seen previously.

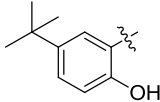
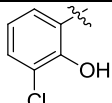
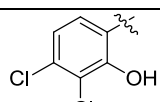
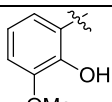
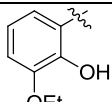
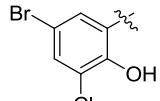


Scheme 91 Mechanism of $Pb(OAc)_4$ induced rearrangement of 2-hydroxyacyl hydrazones to benzoyl benzaldehyde²⁴⁴

The benzoyl benzoic aldehyde (**342**) was synthesised following the procedure described by Jacq *et al.*²⁴² The yield of this reaction was observed to be somewhat inconsistent, ranging from 54-73% and producing numerous minor side-products. A number of analogues with a range of substituents on the 'A'-ring have been synthesised and a general trend has been observed, electron-donating substituents on the phenolic ring lowers the yield of the reaction

(Table 27). The few examples of electron-donating phenolic substituents reported also have a lower yield (e.g. 46% for a methoxy analogue).²⁴² Benzoyl benzaldehyde (**342**) was oxidised to benzoyl benzoic acid (**343**) following the procedure of Lampe *et al*²⁴⁵ which, after recrystallisation gave **343** as a fluffy white solid.

Table 27 Yields for lead (IV) acetate mediated rearrangement with a variety of phenolic substituents, * indicates results obtained by other chemists

Phenolic ring substituents	Yields (%)
	73
	91*
	94*
	56*
	30*
	74*

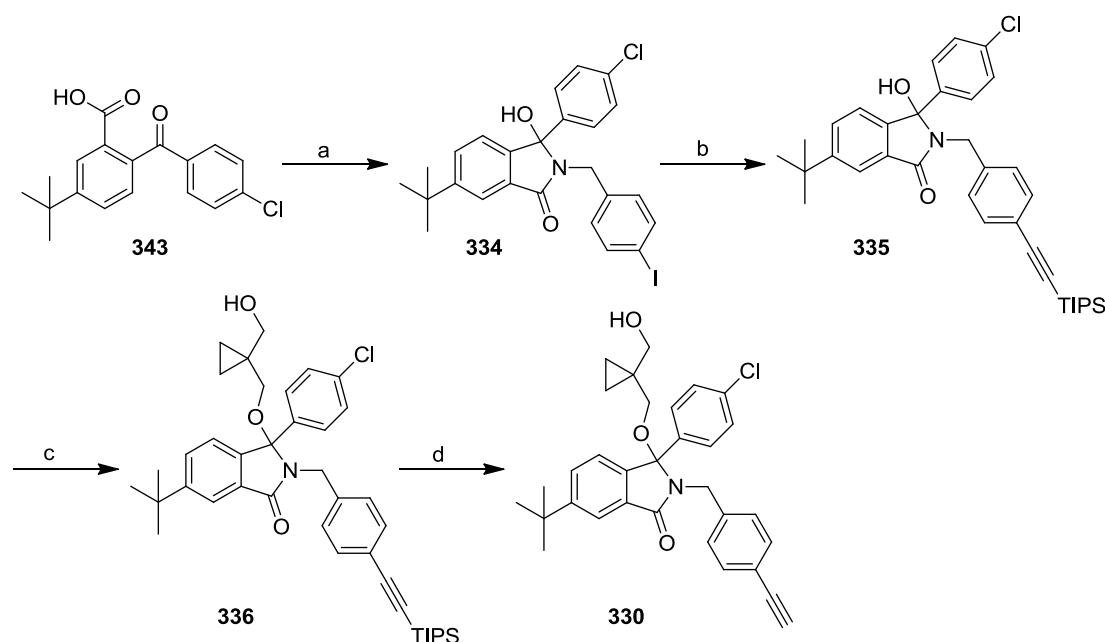
Compound **343**, which had previously been synthesised in one step from a Friedel-Crafts reaction (in 92% yield, mixture of isomers) has now been synthesised in 4-step route an overall yield of 26%. Although this scheme adds further synthetic steps to the synthesis of benzoyl benzoic acid (**343**), the regioselectivity removes the need for the difficult separation of isomers, as used in the Friedel-Crafts route. The desired final compound **330** can now be synthesised (Scheme 92).

Formation of the isoindolinone, using SOCl_2/DMF , is achieved in significantly higher yield when using 5-*tert*-butyl-2-(4-chlorobenzoyl)benzoic acid (**323**) (86%) rather than 36% for 4-chloro **241**, (even allowing for the mixture of isomers). The 4-chloro atoms appears to hinder

formation of the isoindolinone, either sterically, perhaps hindering formation of the Ψ acid chloride or electronically, due to the electron withdrawing nature of the chloro substituent.

The acetylene moiety was incorporated using the optimised Sonogashira conditions in excellent yield (91%). Formation of the ether linkage *via* the Vilsmeier chemistry was achieved in moderately higher yield for compound **336** in comparison to the 4-Cl analogue (**238**) (50% versus 24%), influenced by the change in steric and electronic factors.

Deprotection of acetylene groups with TBAF gave compound **330** in 80% yield.

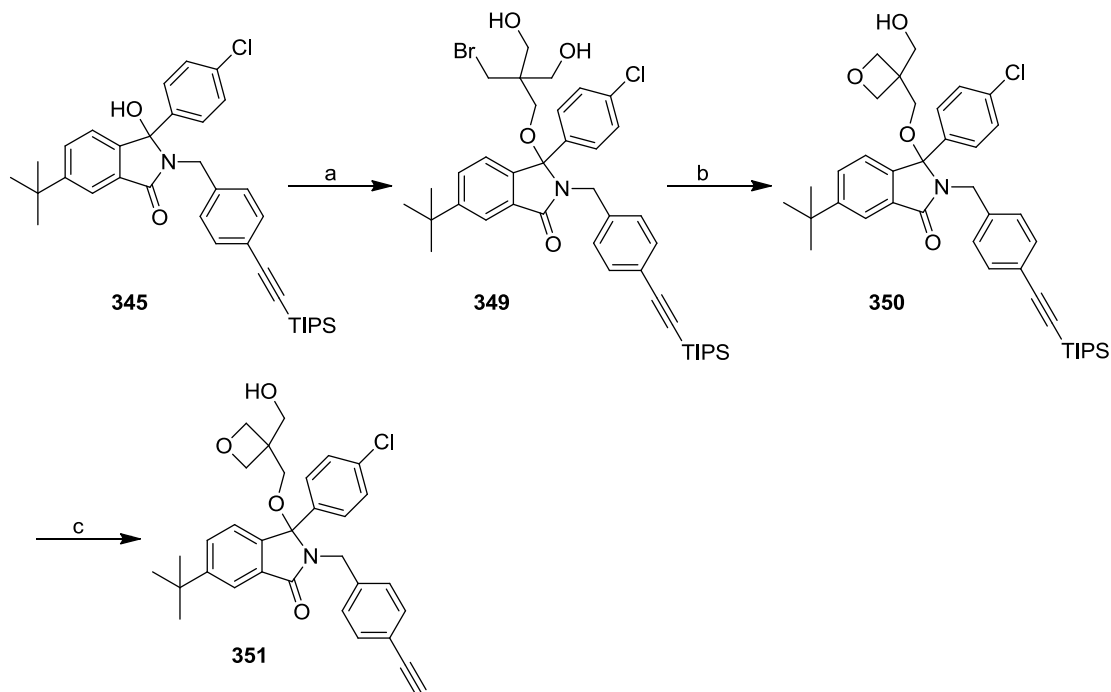


Scheme 92 Reagents and conditions; a) i. SOCl_2 , DMF, THF, 4 h; ii. 4-iodobenzylamine hydrochloride, Hünig's base, THF, overnight, 86%; b) $\text{Pd}(\text{PPh}_3)_2\text{Cl}_2$, CuI, Et_3N , triisopropylsilylacetylene, THF, 16 h, 91%; c) i. SOCl_2 , DMF, THF, 4 h ii. 1,1-bis(hydroxymethyl)cyclopropyl, K_2CO_3 , THF, overnight, 50%; d) 1 M TBAF in THF, THF, 1 h, 80%

Previous results showed that compound **224** displayed similar biological activity to the 4-Cl analogue, the replacement of the (hydroxymethyl)cyclopropylmethoxide side chain, with the alternative (hydroxymethyl)oxetanemethoxide side chain, with the aim of improving physical properties, was desired. The synthetic route is shown below and utilises the methodology of incorporating the bromomethyl species and forming the oxetane *in situ*.

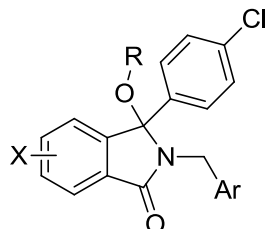
It was decided to use the $\text{BF}_3 \cdot \text{OEt}_2$ reaction to incorporate the 2-(bromomethyl)-2-(hydroxymethyl)-propan-1,3-diol as it lacked the steric hindrance of the 4-Cl analogue.

Formation of the ether **349** was achieved in 4.5 h and as previously observed, conversion to the ether using $\text{BF}_3 \cdot \text{OEt}_2$ is high yielding, forming **349** in 87%. The cyclisation to form the oxetane ring was achieved in 78% yield on treatment with KOH in ethanol, and deprotection of the acetylene group gave the desired final compound (**351**).

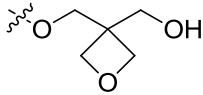
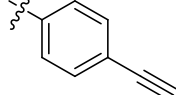


Scheme 93 Reagents and conditions; a) 2-(bromomethyl)-2-(hydroxymethyl)propan-1,3-diol, $\text{BF}_3 \cdot \text{OEt}_2$, THF, 4.5 h 0 °C-RT, 87%; b) KOH, EtOH, 3 h, RT-reflux, 78%; c) 1 M TBAF in THF, THF, 1 h, 59%

Both compounds **351** and **330** were selected for separation of the two enantiomers for chiral HPLC and are currently awaiting separation.

5.6.1. Biological Results for *tert*-Butyl Analogues**Table 28** Biological activity for *tert*-butyl analogues * indicates compounds synthesised by other chemists

Number	R	X	Ar	Rotation	Biological Activity IC ₅₀ (μM)
220*		4-Cl		(+/-)	0.095 ± 0.096
224*		6- <i>t</i> Bu		(+/-)	0.19 ± 0.10
253		4-Cl		(+/-)	0.15 ± 0.083
330		6- <i>t</i> Bu		(+/-)	0.078 ^a
325		4-Cl		(+/-)	0.090 ± 0.032
351		6- <i>t</i> Bu		(+/-)	0.028 ^a
352*		4-Cl, 6- <i>t</i> Bu		(+/-)	0.14 ± 0.055

353*		4-Cl, 6- ^t Bu		(+/-)	0.27 ± 0.015
------	---	--------------------------	--	-------	--------------

^a indicates n = 1

A change in 'A'-ring substituent from the 4-chloro **253** to 6-*tert*-butyl **330** gives equipotent compounds. However, when the oxetane side chain is also incorporated, an increase in potency is observed for the ^tBu **351** suggesting that the 4-chloro substituted isoindolinone and the 6-^tBu substituted isoindolinone are slightly shifted in position within MDM2 pocket, allowing the oxetane to adopt a more favourable position. Interestingly, when the 4-Cl, 6-^tBu A-ring substituents, which are active when combined with the cyclopropyl-substituted ether side-chain, is not when combined with the oxetane-substituted ether side-chain. This supports the evidence for a slightly different binding mode for the *tert*-butyl substituted isoindolinone, which adopts the optimal position for the oxetane substituted, whilst the chloro substituted isoindolinone does not.

5.7 Protein Crystallography of Isoindolinone-based Inhibitors of p53/MDM2 Protein-protein Interaction

Protein crystallography is an important aid for the drug discovery process. Although a number of MDM2/p53 inhibitors have been crystallised bound to the protein, no crystal structure of the isoindolinone has previously been available. Collaborators at the University of Oxford Biochemistry Department have previously identified the binding mode of isoindolinones through NMR studies,¹⁹¹ and suggested proposed which would lead to further increases in potency,¹⁹² a crystal structure would give further insights into the interactions between the isoindolinones and the protein.

Protein crystallography is traditionally used in lead optimisation to guide chemical modification.⁹⁶ For X-ray crystallography to successfully obtain a structure a well-ordered crystal must first be grown. Protein crystals are less ordered than small molecule crystals, and frequently contain channels of disordered solvent.²⁴⁶ Protein crystallisation requires the synthesis of sufficient volumes of purified protein to screen a variety of crystallisation conditions. The development of molecular biology has aided that production of larger volumes of protein. Bacteria, such as E-coli, can be used to express the desired protein in

large quantities, through the introduction of plasmids containing the gene of the target protein. Within crystal structure of MDM2 the protein is stabilised by other molecules of MDM2 resulting in a number of molecules of MDM2 per unit cell. The crystal structure of Nutlin-2a (PDB code 1RV1) contains three molecules of MDM2 (Figure 72).

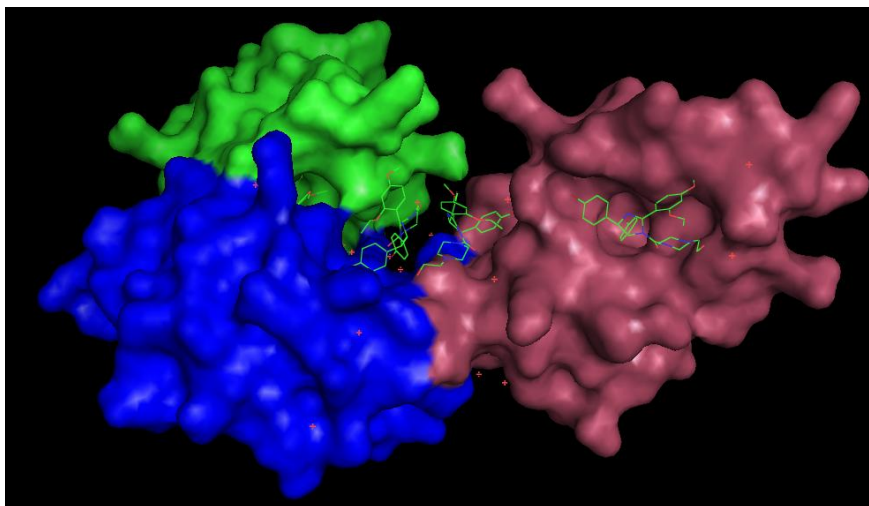


Figure 72

To gain understanding of the processes behind protein crystallography a period of four months was spent working alongside colleagues at the University of Oxford working on protein purification and protein crystallography. Both mutants and wild type samples of the MDM2 binding site were purified, of either residues 17-109 or 17-125 of MDM2. Removal of residues 110-125 removes an unstructured loop which may prevent crystallisation. A number of mutants were developed which replace either one, two or three residues with alanine residues. Crystals develop when good contacts are formed between protein molecules, and two residues, lysine and glutamic acid, have been shown to be prone to preventing the formation of good contacts between protein molecules. Therefore, Lys and Glu residues which commonly lie on the surface of proteins can be replaced by Ala to aid crystallography.²⁴⁷

A number of wild type and mutant MDM2 protein samples were then purified using the methodology shown below, all included a Glutathione S-Transferase tag to aid purification. E-coli bacteria were employed to grow the protein in 1 L cultures, centrifuged and the supernatant removed. The remaining pellet was resuspended in PBS buffer (40 mL) and flash

frozen by co-workers in Oxford before my work began. For methodology for protein purification see appendix one.

A number of MDM2 samples were prepared and are summarised below.

K94A (17-109)

K94E95A (17-109)

MDM2 (17-109)

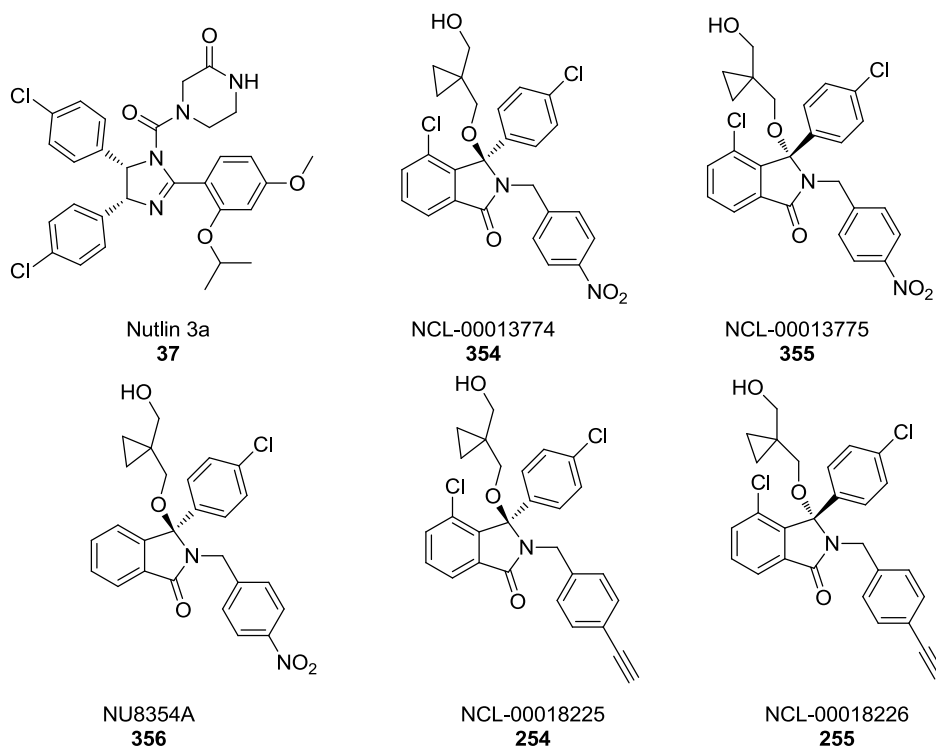
E69K70A (17-109)

E69A (17-109)

E69K70E94A (17-125)

E69A (17-125)

All mutants were expressed in sufficient volumes for crystallography with the exception of K94E95A, and E69K70E94A which only allowed a small volume of crystallography tray to be set up. After purification the purified protein was concentrated to approximately 2 mg/mL and incubated overnight with a series of inhibitors – Nutlin-3a, NU8354a, NCL00013774, NCL00013775, NCL00018225 and NCL00018226, which includes the most active compound synthesised at the NICR, the less active opposite enantiomers, and Nutlin-3a, the classical example of an MDM2/p53 inhibitor. 1.5 equivalents of the inhibitor in DMSO was incubated at 4 °C overnight, followed by washing with Hepes buffer and concentrating to a concentration of approximately 12 mg/mL.

**Figure 73**

The protein and inhibitor mix was then set up into crystallisation trays. These were either purchased trays, to give a range of conditions to identify which conditions give crystals or custom trays, with a narrower range of conditions, with the aim of identifying optimal conditions for crystallisation. Purchased trays were dispensed in a 96-well plate using liquid handling robots and had a range of protein concentrations within each well. Trays were then sealed and stored in a fridge with automated image collection at 4 °C to allow monitoring of each well. Custom trays were alternatively set up in 24 well plates and the crystallisation conditions were prepared by hand to give a much smaller range of conditions, all based around conditions which had previously been identified from purchased screens as leading to crystals. Previous work undertaken at Oxford at identified polyethylene glycol (PEG) containing conditions as optimal for MDM2 crystallisation, therefore all custom trays were based either around PEG4000, PEG5000 or PEG8000. Each well contained a 500 μ L reservoir and the raised well for the protein. Each reservoir was made up to 500 μ L with water (volume determined by percentage of PEG used). Both ammonium sulphate and sodium acetate (from a 1 M stock of each) were used as additives to the solution, with the pH of the sodium acetate solution adjusted in some cases to pH 4.6. To the raised well was added 1 μ L of the protein and inhibitor solution and 1 μ L of the reservoir solution. These were also sealed and stored at 4 °C for crystallisation. All custom trays were prepared in this manner

with the exception of the E69K70A mutant. Previous work had resulted in the growth of small spike-like crystals which were too small to be useful for X-ray structure determination. Therefore, a custom tray was prepared with only NCL-00018225 and NCL-00013775 as only these inhibitors had formed crystals, stored to two days at 4 °C before being seeded with fragments of these small needle-like crystals. Seeding provides a surface for crystallisation to occur and can result in the formation of larger crystals. A summary of crystallisation conditions is shown in appendix one. An illustrative example of the set up of a 24 well plate is also shown in appendix one.

From the crystallography tray seeded with the E69K70A mutant, a needle-like crystal was isolated. X-ray crystallography undertaken at the diamond synchrotron in Oxford with a 3 GeV electron beam, with a micro focus beamline under the supervision of Dr Ed Lowe and obtained a diffraction pattern of sufficiently high resolution to give a crystal structure which is shown below.²⁴⁸ The crystal structure was obtained with a resolution of 2.9 Å and the structural insights gained by this crystal structure will be discussed in more detail below.

To validate the use of mutants as a more crystallisable form of MDM2, we must firstly confirm that the isoindolinone bind to a similar manner to both the mutants and wild-type MDM2. For this confirmation two assay types were selected, a ThermoFluor assay and a fluorescence anisotropy assay. Assays were initially run on the wild-type MDM2 and the E69K70A mutant, the only mutant at this point to crystallise in the presence of an isoindolinone ligand.

ThermoFluor was a technique originally developed as high-throughput manner of identifying ligands for drug discovery targets.²⁴⁹ It requires a hydrophobic fluorescent probe or dye to distinguish between folded and unfolded proteins.²⁴⁹⁻²⁵⁰ When the protein is folded the probe is exposed to the aqueous environment, which quenches fluorescence. On heating, the protein will begin to unfold, exposing its hydrophobic core, to which the probe can then bind, and the fluorescence will no longer be quenched. This allows a measurement of unfolding as a function of temperature.²⁴⁹ This process can be undertaken using a real-time PCR machine in a 96-well plate. By introducing ligands to the wells, those which bind to the protein will stabilise it, and increase the thermal stability, increasing the melting temperature. This can be used to measure affinity of the ligand for the protein, a greater affinity will lead to a greater

increase in temperature. Results obtained should be consistent with results gained from other assays such as enzymatic assays.²⁵¹

The Thermofluor assay was used to compare the melting of wild-type and mutant MDM2 in the presence of ligands. The hydrophobic probe used was sypro orange, a fluorescent dye. Firstly the optimal conditions for fluorescence were identified using a range of protein concentration and dye concentrations. Sypro orange is sold at a concentration of 2000 x, so was therefore diluted with Hepes buffer to create a range of concentration 5 x, 10 x, 15 x and 20 x. The set up of the plate is shown in appendix one.

From this experiment, optimal conditions for monitoring of the protein melting was determined as 10 x dye concentration and after further optimisation the protein concentration was maintained at 9 μ M. The inhibitor was added in a 2:1 inhibitor to protein ratio, with the inhibitor concentration maintained at 18 μ M. To measure the inhibitor's affinity, each plate contained 7.5 μ L of 10 x dye, 1.76 μ L protein at 77 μ M and 0.54 μ L inhibitor (from 500 μ M DMSO stocks) and each well was made up to 15 μ M with Hepes buffer. As a control, another well was run with identical conditions, with 0.54 μ L of DMSO, and as a second control a well contained just dye and protein. A second row acted as a control for each inhibitor – each well contained 7.5 μ L of 10 x dye and 0.54 μ L inhibitor (or DMSO). For comparison a p53 peptide (sequence SQETFSDLWKLLPEN) was also included in these studies.

For the wild-type protein optimal concentrations were identified as 20 x concentration of sypro dye, 5 μ M concentration of dye and 10 μ M concentration of dye. With plates made up of 10 μ L of 20x sypro dye, 0.56 μ L protein (178 μ M), 0.4 μ L of inhibitor (500 μ M) and were made up to 20 μ L with Hepes buffer.

For both proteins fluorescence was measured over a temperature range of 25-89 °C, with three readings taken at each temperature, with each temperature maintained for one minute. The observed melting points are shown below for each protein; average change in melting point was calculated using DMSO as the blank for all inhibitors except the p53 peptide. As the peptide was an aqueous solution the buffer solution was used as the blank for this well.

Table 29 Melting point for E69K70A protein with inhibitors

Inhibitor	Melting point repeat 1 (°C)	Melting point repeat 2 (°C)	Average change in melting point from control (°C)
No Inhibitor	59	50	-
DMSO	58	54	-
NU8354a	70	69	13
NCL-00013774	75	64	14
NCL-00013775	71	68	13
NCL-00018225	77	77	21
NCL-00018226	72	74	17
Nutlin-3a	79	77	22
p53 peptide	63	59	3.7

Table 30 Melting point for wt MDM2 17-109 protein with inhibitors

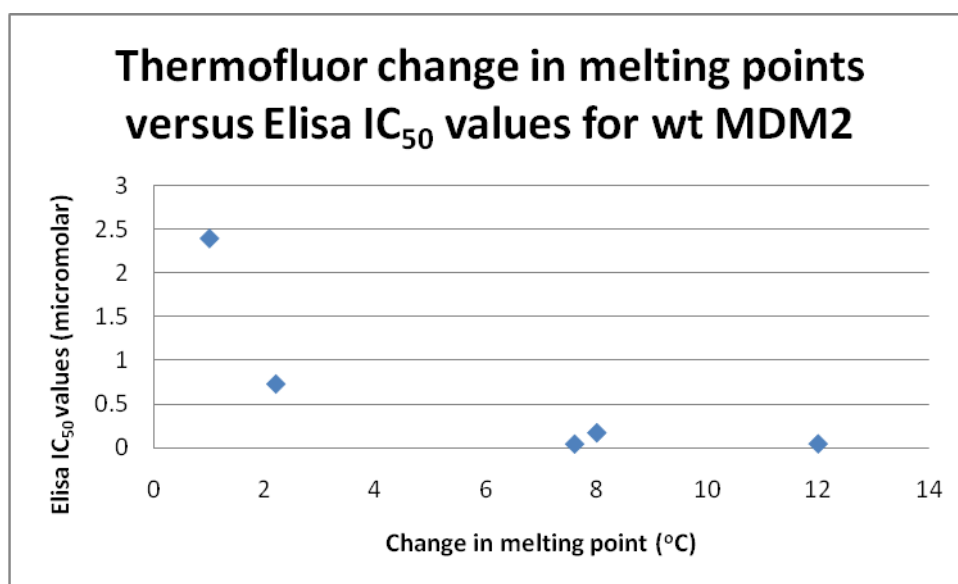
Inhibitor	Melting point repeat 1 (°C)	Melting point repeat 2 (°C)	Melting point repeat 3 (°C)	Average change in melting point from control (°C)
No inhibitor	62	64	63	-
DMSO	68	64	67	-
NU8354a	72	75	76	8.0
NCL-00013774	75	79	76	12
NCL-00013775	64	71	70	2.2
NCL-00018225	76	70	77	7.6
NCL-00018226	65	68	68	1.0
Nutlin-3a	90	82	80	20
Peptide	67	70	68	5.1

A comparison of the change in melting point between the E69K70A and wild-type protein is shown below, along with the ELISA assay IC₅₀ values for each isoindolinone.

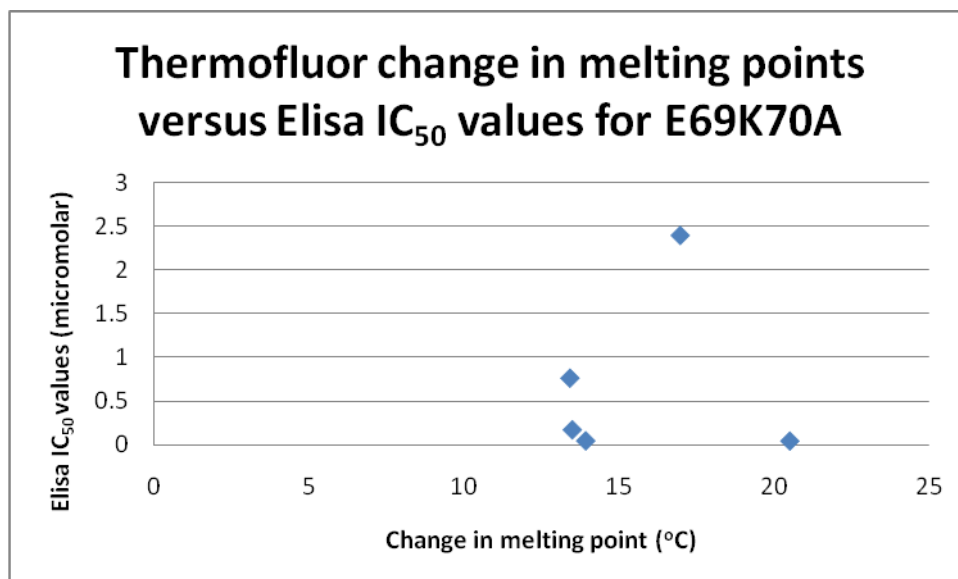
Table 31 Comparison of change in melting point between each protein and ELISA assay values for the wild-type protein

Inhibitor	E69K70A change in melting point	Wt MDM2 change in melting point	ELISA assay IC ₅₀ (μM)
NU8354a	13	8.0	0.17
NCL-00013774	14	12	0.044
NCL-00013775	13	2.2	0.73
NCL-00018225	21	7.6	0.041
NCL-00018226	17	1.0	2.4
Nutlin-3a	22	20	-
peptide	3.7	5.1	-

By drawing a graph comparing the change in melting point against the IC₅₀ value it can be observed that for wild-type MDM2 some correlation can be observed between the thermofluor values and IC₅₀ values



However, when looking at the graph for the E69K70A mutant little correlation is observed between the change in melting points and the IC₅₀. For the (+)-isomers NCL-00013775 and NCL-00018226, a significant change in melting point is observed, unlike the wild-type protein.



The fluorescence anisotropy assay was then undertaken to give a further comparison between the mutant and wild-type protein. Fluorescence anisotropy uses a fluorescently labelled p53 peptide and monitors the displacement from MDM2 on titration of increasing concentration of inhibitor.

A fluorescent molecule, if excited by polarized light, will emit polarized light. However, in solution, the polarized light will be randomized, due to the rotation of the molecule in solution. Fluorescence anisotropy is based on the observation that the size of molecules can affect the polarization of fluorescence. A larger molecule results in less scattering of the polarized light than a smaller molecule.²⁵² Therefore, when the p53 fluorescently labelled peptide is in complex with MDM2, the fluorophore behaves as a large molecule, but on titration of increasing concentrations of inhibitors, the p53 will be displaced from the p53/MDM2 complex and will behave as a smaller fluorophore. By monitoring the degree of scattering, the increasing levels of displacement can be observed. By plotting concentration of inhibitor against levels of polarization, a sigmoidal curve should be observed, of the type shown below, measured by Zhang *et al.*²⁵³

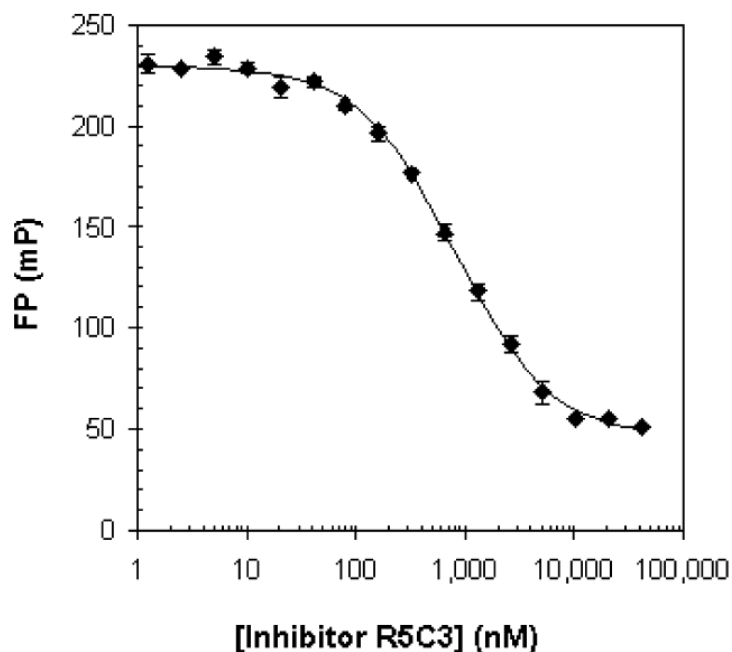


Figure 74 A graph monitoring fluorescence polarisation (FP) against inhibitor concentration (Taken from reference 252)

Firstly the optimised concentrations without inhibitor were identified using a range of MDM2 and fluorescently labelled p53 concentrations (Table 35 Appendix one). Each well was made up to a final concentration of 20 μ L with HEPES buffer.

For each concentration of MDM2 an increase in intensity of fluorescence was observed with increasing concentration of fluorescently labelled peptide. A MDM2 concentration of 10 nM was identified as the optimal concentration to use for the titration of inhibitor and a fluorescently labelled peptide concentration of 2 nM was used. NU8354a (**345**) was used as the inhibitor, and due to the extensive pipetting involved in the preparation of each experiment; conditions were optimised using a single inhibitor first. The concentration of inhibitor ranged from 2-57 nM from a DMSO solution, and to maintain a constant DMSO concentration each well was made up to a DMSO volume of 1.2 μ L along with a blank well containing just DMSO. The volume for each well was maintained at 20 μ L using HEPES buffer. However, on measuring the polarization no curve was observed.

After discussion with co-workers it was decided to alter the range of inhibition concentration, to give a range of 1-256 nM to give a range of values either side of the IC_{50} value. On measuring the polarization, no curve was obtained. It was proposed that a greater

concentration of fluorescently labelled peptide was required. At low concentration of inhibitor, there are sufficient binding sites on MDM2 for both peptide and inhibitor; therefore the displacement of the peptide may not occur. By increasing the concentration of the peptide, the peptide should be displaced by the inhibitor of the peptide at a lower concentration, which should be observed by a change in fluorescence polarization.

Therefore, whilst both the MDM2 concentration and the range of inhibitor concentrations were maintained, the peptide concentration was increased to 5 nM. However, no curve was again observed. The experiment was repeated with Nutlin-3a to verify that the isoindolinone was not affecting the experiment, but this gave identical results. Work on this assay was therefore stopped. However, colleagues at Oxford, who continued to optimise this assay after my placement was completed, suggested that by saturating the MDM2 binding site with peptide, a curve can be observed on addition of the inhibitor.

The inhibitor may induce a change of behaviour of the MDM2 protein when in solution. To monitor this an analytical size S75 size exclusion column was used. Size exclusion columns separate proteins according to size, with larger proteins coming off the column quicker. A sample of protein in HEPES buffer was run through the column, and the trace showed a peak at 12 min. The protein was then incubated with NU8354a (**356**) for 1 h in a 1:1 ratio of protein to inhibitor and the size exclusion column was then repeated. The trace showed two peaks, one at 12 min which corresponds to the protein in solution, and another peak at 4.2 min. This suggests that in the presence of the inhibitor the MDM2 protein forms a complex of a number of units of the protein. To identify the size of the complex a calibration column of proteins of known mass must be used. Two proteins; bovine serum albumin (66 kDa) and carbonic anhydrase (29 kDa) were mixed together and ran through the size exclusion column. The largest of these two proteins appeared on the trace at 4.2 min, which agrees with the time of the MDM2 complex, suggesting a mass of 66 kDa. The wt MDM2 (17-109) has a mass of approximately 11 kDa, therefore six molecules of MDM2 form the complex.

The unusual behaviour of the MDM2 protein in the presence of inhibitors may influence the results of the fluorescence anisotropy and ThermoFluor assay leading to the unusual results. Coworkers at Oxford are continuing work on assay optimisation.

5.7.1. Crystal Structure of NCL00013774

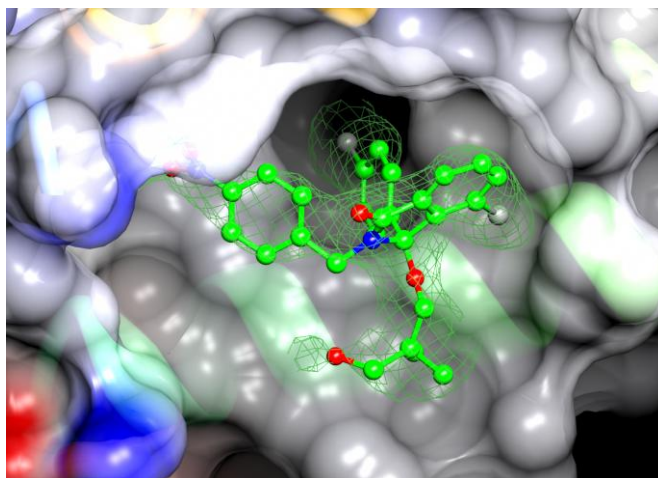


Figure 75 X-ray crystallography of NCL-00017734 modelled using CCP4MG, the electron density map of the isoindolinone is shown

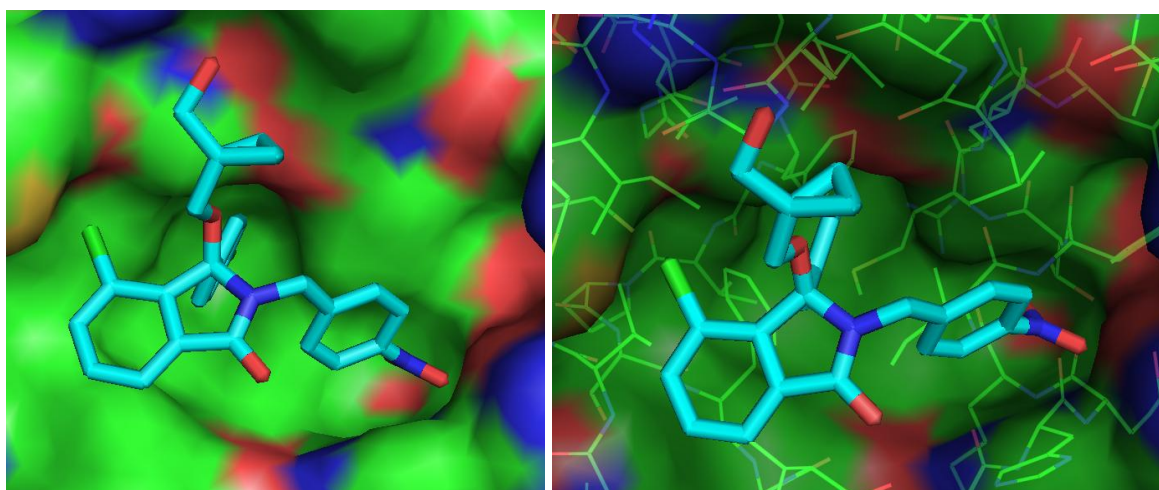


Figure76 Image of NCL-00013774 in MDM2 binding site modelled in PyMOL and (right) with surrounding residues displayed

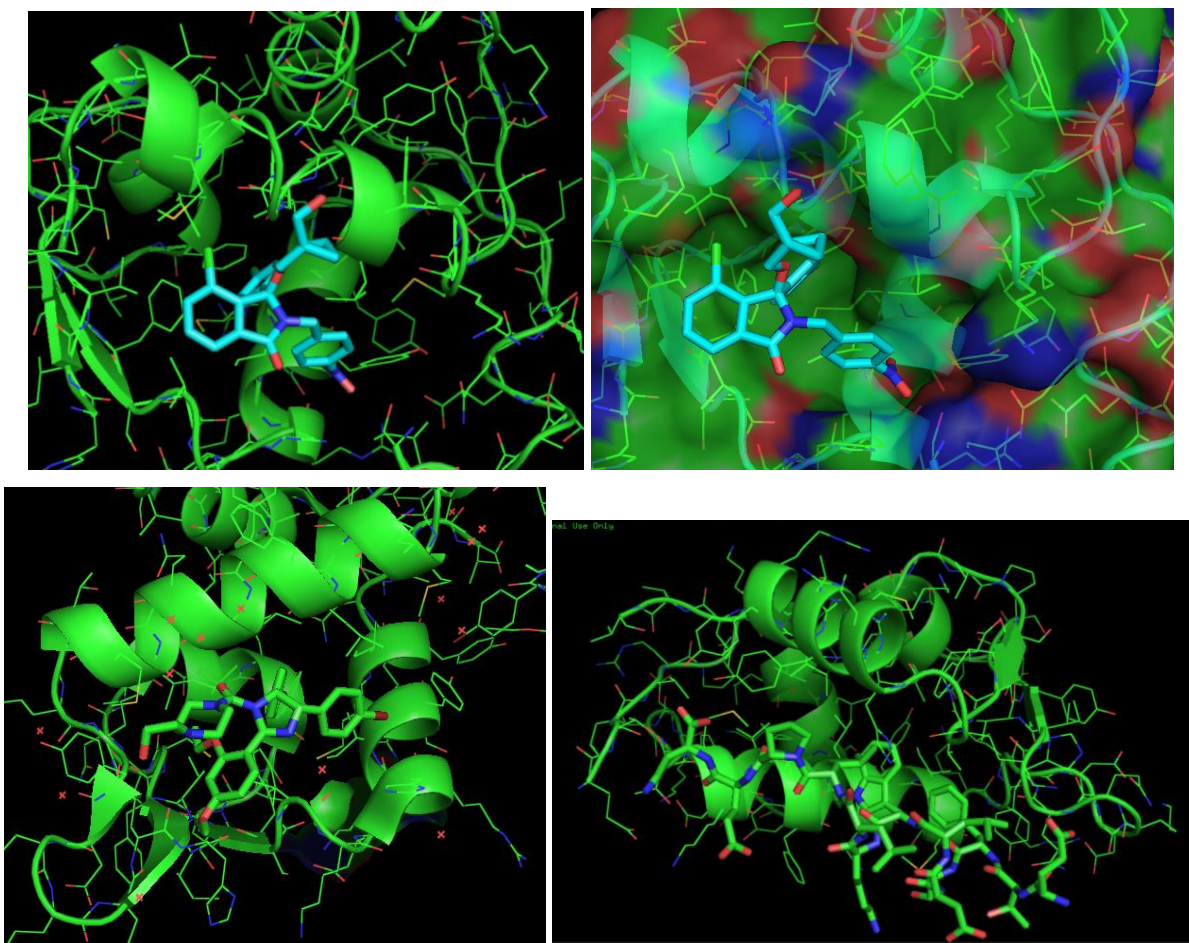


Figure 77 Modelling of crystal structure of NCL00013774 (top) and Nutlin-2a (bottom left) and p53 (bottom right), with the MDM2 protein represented as ribbons

A crystal structure of an isoindolinone was achieved using E69K70A mutant of MDM2 17-109 with a resolution of 2.9Å. From the crystal structure it can be observed that the chlorophenyl ring lies within the Trp23 pocket, the nitrobenzyl ring sits within the Leu26 pocket and the isoindolinone moiety lies over the Phe19 pocket.

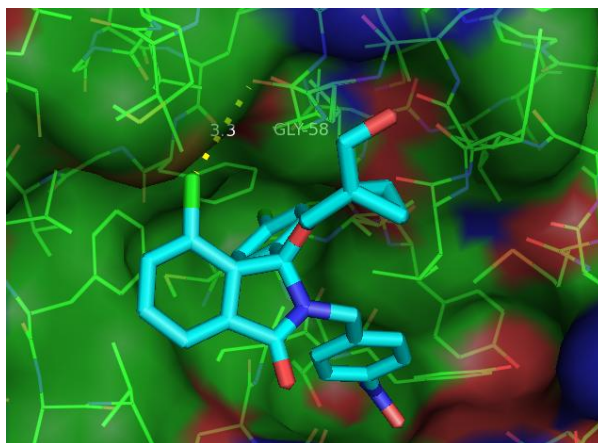


Figure 78 Halogen bond between 4-Cl and Gly58 of MDM2

The 'A'-ring 4-Cl is observed to a halogen bond with a backbone carbonyl group of a glycine residue, with a length of 3.3Å. The electron cloud surrounding the chloro atom interacts with the lone pair of the carbonyl. Chlorine, bromine and iodine atoms attached to either aryl or electron withdrawing alkyl groups can form bonds to electrophiles, nucleophiles and other halogens,²⁵⁴ dependent on direction of the interaction.²⁵⁵ A σ -hole is formed when halogen atoms are attached to either aryl or electron withdrawing alkyl groups. A σ -hole is a positive area within electron density, which lies opposite the carbon-halogen bond and is formed by the three pairs of unpaired electrons on the halogen, forming a ring of electron density surrounding the centre of the halogen atom, while any remaining electrons are involved in bonding to the carbon.²⁵⁴ A representation of the different interactions is shown below. Halogen bonds lie approximately 180 ° to the C-X bond, though this angle can be as little as 155 °.²⁵⁶ Halogen bonds are weaker than H-bonds but the larger the halogen atom the stronger the halogen bond.²⁵⁴ They can be increased in strength by increasing the electron-withdrawing nature of the substituents on the aromatic ring. The halogen bond acts to pull the isoindolinone in closer to the protein into a slightly different binding mode to the unsubstituted isoindolinone 'A'-ring. This may account for differing degrees of activity between unsubstituted and substituted analogues.

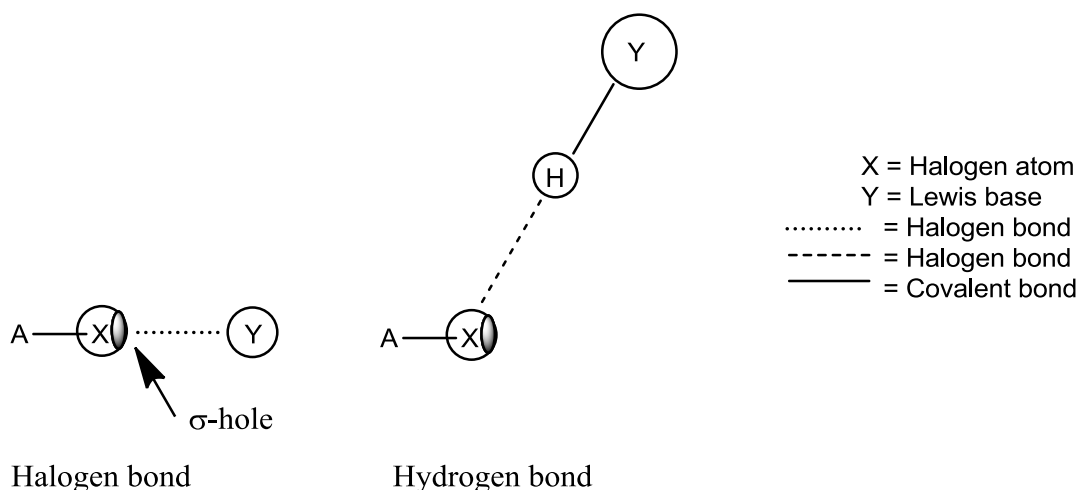


Figure 79 Representation of halogen and hydrogen bonds formed by a halogen atom (X) and hydrogen atom (H) (Taken from reference 254)

An edge-face stacking interaction is observed between the protons at the 5- and 6-position of the 'A'-ring and Tyr67 within MDM2, an interaction which would not be observed when the 6-

tert-butyl group is in place. The 7-position of the isoindolinone points out into solvent and should prove an interesting area to incorporate solubilising groups.

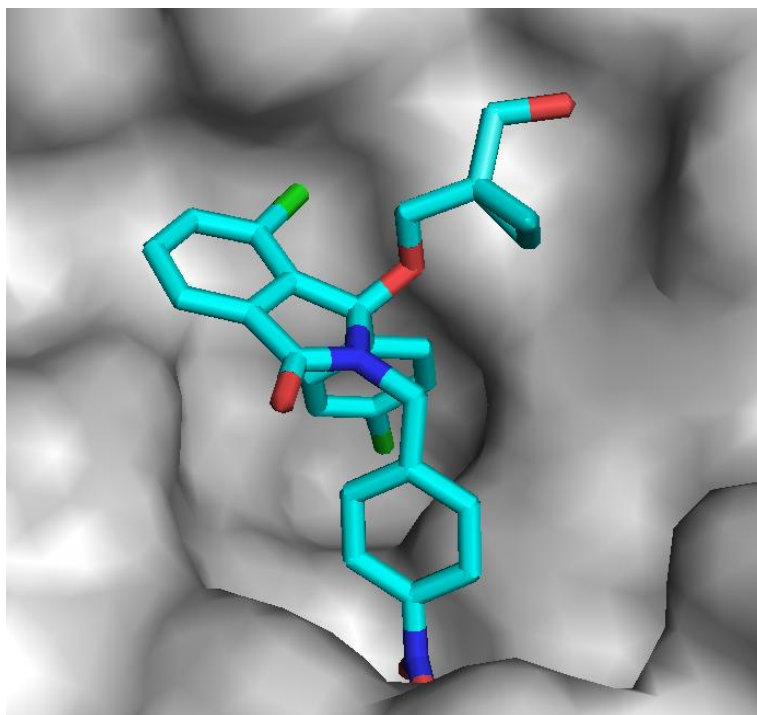


Figure 80 The crystal structure demonstrates that the cyclopropyl substituted ether group lies along the surface of the protein

The cyclopropyl group of the ether side-chain was initially incorporated to restrict rotational freedom of the propyl ring.¹⁹² However, the protein crystallography (Figure 80) suggests that the cyclopropyl ring nestles up to the protein, contributing to the binding energy. The hydroxyl group itself points out into solution and does not form an interaction with the protein.

From the crystal structure it is unclear what role the nitro group is fulfilling. A direct interaction is not observed between the protein and the nitro group. Similarly, a clear role for the ethynyl functionality cannot be proposed, although His and Tyr residues are present at the bottom of the pocket, so this may be the ideal environment for the ethynyl group. The preference for the ethynyl over the nitro functionality in **253** and **220** may be a result of the halogen bond. By pulling the isoindolinone 'A' ring closer to the protein, the benzyl ring is pulled out of the Leu26 pocket. However, with the longer ethynyl substituent this may be counteracted.

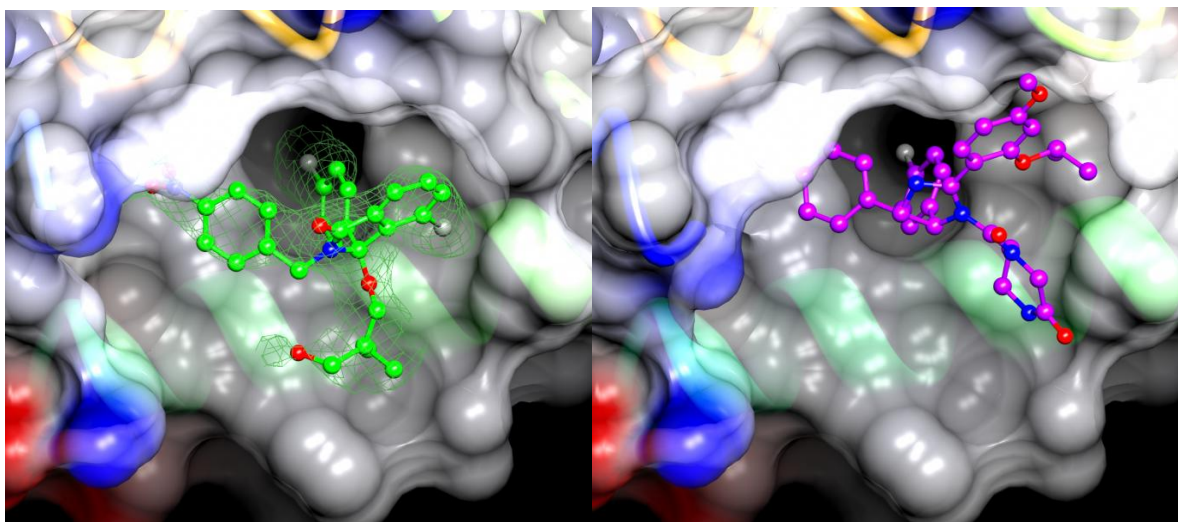


Figure 81 X-ray crystallography of NCL00013774 (left) and Nutlin-3a modelled using CCP4MG

From Figure 81 we can see that the benzyl aromatic ring of **354** does not protrude as deeply into the Leu26 pocket as Nutlin-3a. The ‘lid’ component, which partially covers the aromatic ring of Nutlin-3a does not cover NCL00013774, an area which could potential be utilised by isoindolinone to give a further increase in potency.

The Tyr23 pocket of MDM2 is filled with a chlorophenyl ring on MDM2 binding. An overlay of a number of inhibitors of the MDM2/p53 interaction suggests that this ring is always filled with a chlorophenyl ring, suggesting the optimal substituent for this position has been identified. The crystal structure of **354** bound to MDM2 will guide the direction of synthetic efforts and a number of potential compounds designed as a result of this crystal structure will be discussed in chapter 5.8.

5.8 Future Work for MDM2/p53

The crystal structure of NCL-00013774 identified a number of areas to address to attempt to improve potency. A series of compounds designed to exploit these areas should result in an improvement in potency. NCL-00013774 was shown to -

- Form a halogen bond with the protein
- Form an edge-face interaction with a tyrosine residue
- C^7 position of the isoindolinone points into solution

Halogen bonds and edge-face interactions can be enhanced by an electrodeficient aromatic ring.²⁵⁴ As the C^7 position points out into solution, replacement of the isoindolinone phenyl ring with a pyridine ring may be tolerated, and should strengthen the halogen bond. The inclusion of a pyridine ring will also reduce the $clogP$ from 6.6 for **253** to 5.6 for **357**. Compound **357** may prove a useful compound to synthesise.

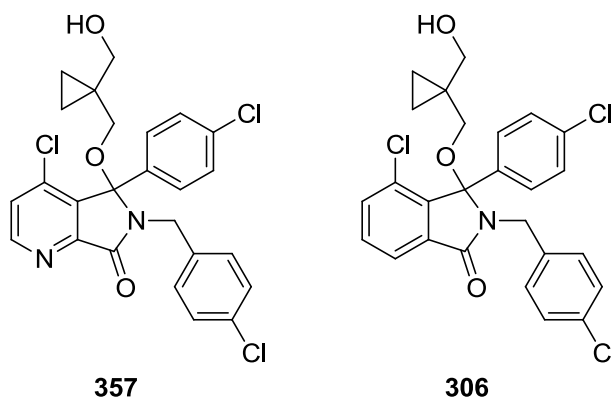
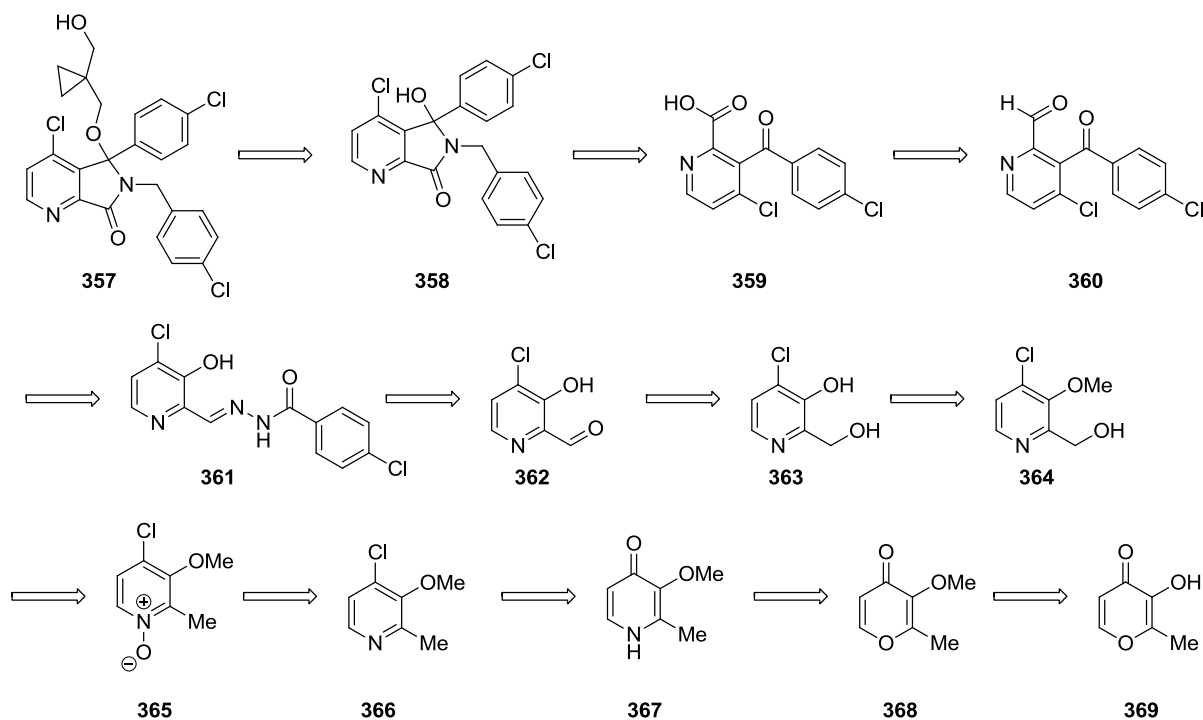


Figure 82

An ‘isoindolinone’ type molecule in which the pyridine ring replaced the phenyl ring has previously been synthesised from the furo[3,4-*b*]pyridine-5,7-dione, however no chloro substituted analogue is available. Spaeth *et al* forms the chloro substituted anhydride from 4-chloroquinoline *via* the diacid.²⁵⁷ However, formation of the benzoyl benzoic acid from the anhydride allows no control over which isomer is formed. Alternatively, the lead (IV) acetate mediated chemistry could be employed to synthesise the desired isomer of the benzoyl benzoic acid (**359**) (Scheme 93).

The retrosynthesis of this molecule is shown below. To utilise this synthetic route 4-chloro-2-formyl-3-hydroxypyridine must first be synthesised. Belley *et al* synthesised 4-chloro-2-formyl-3-methoxypyridine from (4-chloro-3-methoxypyrid-2-yl)methanol oxidising the hydroxymethyl group to an aldehyde using Dess-Martin periodinate.²⁵⁸ Masaaki *et al* synthesised (4-chloro-3-methoxypyrid-2-yl)methanol (**364**) from 4-chloro-3-methoxy-2-methylpyridine (**366**) *via* the *N*-oxide (**365**). Treatment of the pyridine *N*-oxide (**354**) with acetic anhydride followed by potassium hydroxide can incorporate the hydroxymethyl functionality. Formation of the *N*-oxide acidifies the alkyl protons, allowing deprotonation with potassium hydroxide. To access 4-chloro-3-methoxy-2-methylpyridine (**366**), 3-methoxy-2-methylpyridin-4(1*H*)-one (**367**) can be chlorinated using $POCl_3$ as described by Kohl *et al*.²⁵⁹ To synthesise the pyridone ring methyl maltol can be treated with a methylating

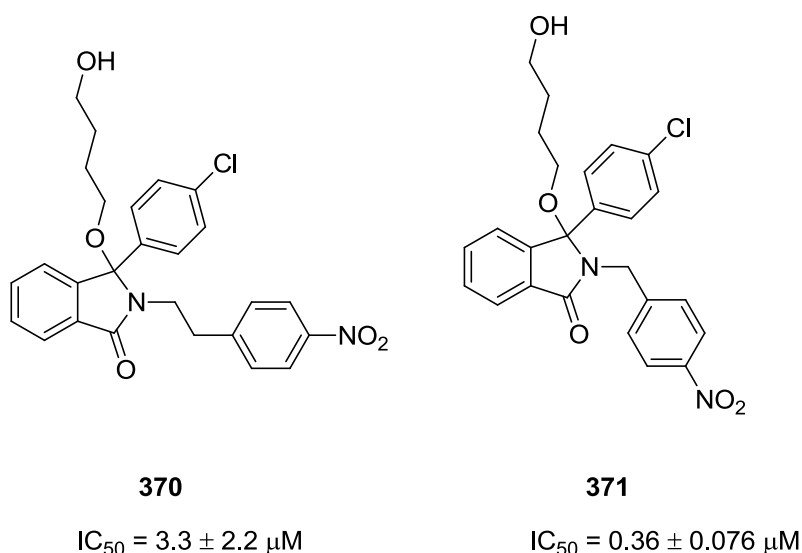
agent, followed by heating with ammonia as described by Ma *et al* will access compound **367**.



Scheme 93

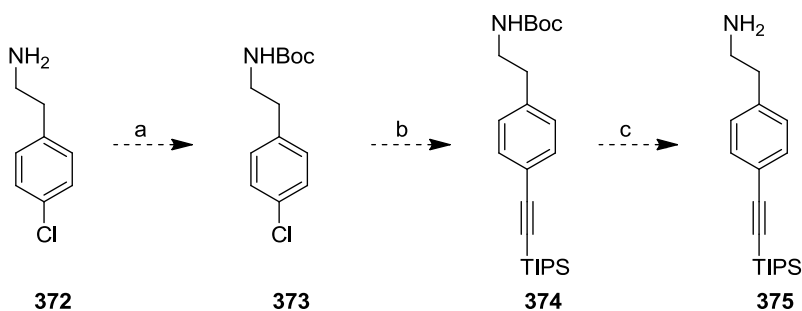
The proposed synthetic route should allow access to compound **361** from which the lead (IV) acetate mediated chemistry can be utilised to form the desired isomer of the 3-(4-chlorobenzoyl)picolinaldehyde. Electron-withdrawing groups have shown to improve the yield of the $\text{Pb}(\text{OAc})_4$ mediated rearrangement, suggesting that the electron-deficient nature of the pyridine ring will not hinder rearrangement.

The crystal structure of NCL-00013774 also demonstrates that the isoindolinones fail to exploit the depth of the Leu26 pocket as fully as the Nutlin-type molecules. It was proposed that by replacing the benzyl moiety with phenylethyl moiety, the aromatic ring would sit deeper within the Leu26 pocket, mimicking the Nutlin series. Previously compound **370**, failed to improved potency, compound **371** has an IC_{50} of $0.36 \mu\text{M}$ whilst compound **370** with the addition CH_2 unit has an IC_{50} of $3.3 \mu\text{M}$. However, with the 'A'-ring 4-chloro substituent forming a halogen bond, the molecules are expected to have a slightly different binding mode which may result in tolerance for the addition CH_2 moiety.

**Figure 83**

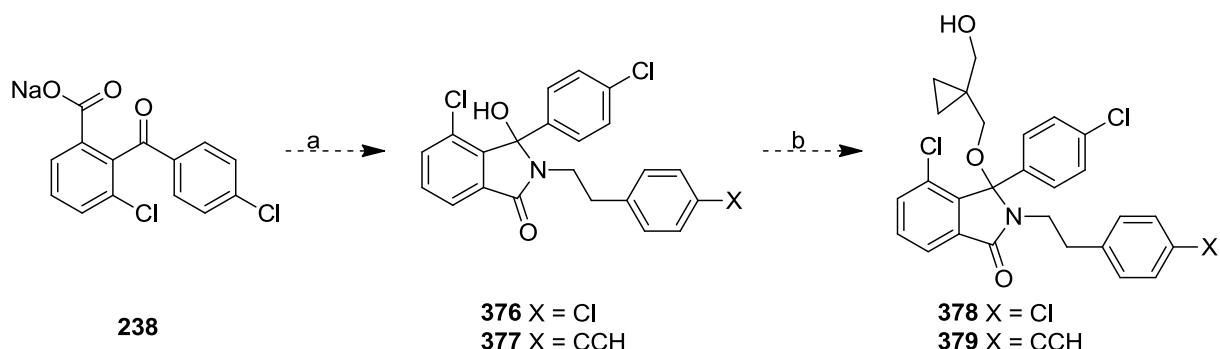
Both compounds **378** and **379** can be synthesised as analogues of the most potent non-nitro compounds. 4-Chloro substituted phenylethyl compound **372** can be purchased and *via* Buchwald-type Sonogashira reaction can be used to access **375** using chemistry optimised in-house.²⁶⁰ This utilises the chemistry developed by Gelman *et al* to couple acetylene-derivative to aromatic chloro species.²⁶¹

However, the different vector of the substituent due to the addition CH₂ may lead to the aromatic ring not taking the optimal position within the pocket – resulting in a loss of potency. The addition flexibility of the chain may overcome this. The loss of potency that occurs in changing from the ethylene to the propylene substituent on the aromatic ring also suggests that the addition of the CH₂ to the *N*-benzyl substituent may not result in an increase in potency. However, by synthesising these two compounds **378** and **379** the SAR around the *N*-benzyl substituent will be developed further.



Scheme 94 Proposed reagents and conditions; a) Boc₂O, Amberlyst, 3 min; b) PdCl₂(CH₃CN)₂, XPhos, CsCO₃, MeCN, 110 °C, overnight; c) TFA, DCM, 1 h

The isoindolinone compounds **375** and **376** can be synthesised using the previously discussed synthetic route.



Scheme 95 Proposed reagents and conditions; a) i. SOCl₂, DMF, THF, 4 h; ii. X = Cl, **369**, Hünig's base, THF, overnight, X = CCH, **375**, Hünig's base, THF, overnight; b) i. SOCl₂, DMF, THF, 4 h ii. 1,1-bis(hydroxymethyl)cyclopropane, K₂CO₃, THF, overnight

An overlay of the crystal structures of NCL-00013774 and a number of published inhibitors identified that the spirooxindole series occupies a unique area of the binding pocket, in which a number of water-solubilising groups are located. This area lies between the isoindolinone phenyl ring and the benzyl groups as shown below. However, the published crystal structure of the spirooxindole series is not the same diastereoisomer as the preclinical candidates 2'*R*,3*R*,4'*S*,5'*R* for the crystallised form rather than 2'*R*,3*S*,4'*R*,5'*R*. In the preclinical candidates the water-solubilising groups lies in a similar orientation as the Nutlin-3a water solubilising group. However, there are only slight differences in biological activity between the two diastereoisomers.¹⁴⁶

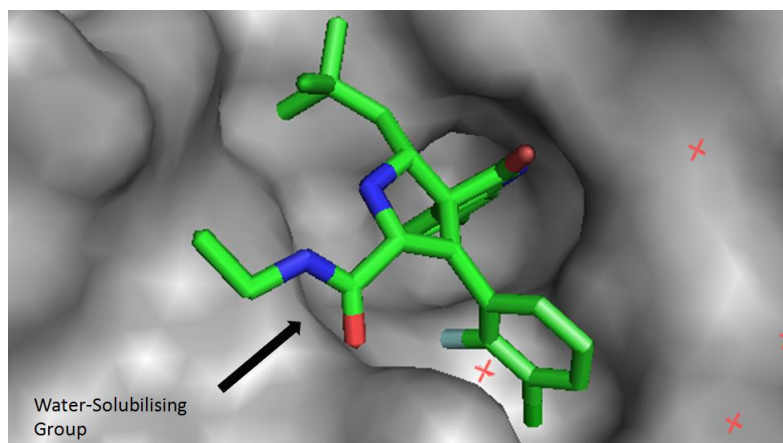
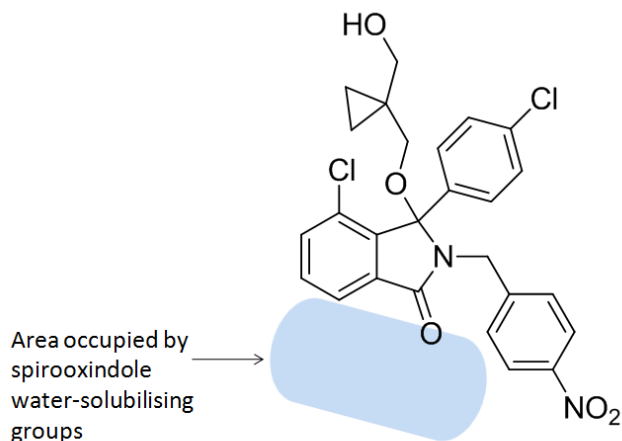
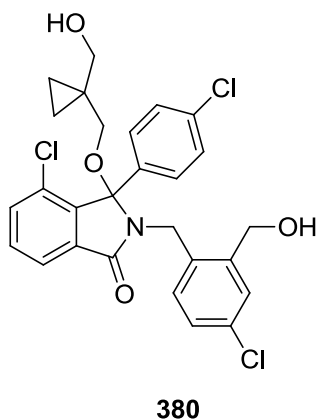


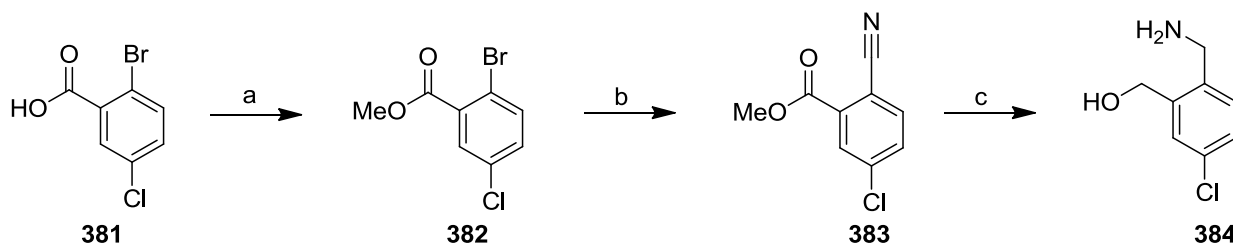
Figure 84 Crystal structure of an analogue of MI-63

**Figure 85**

This area of the pocket could be accessed by substituents from the *ortho*-position of the benzyl ring. To confirm that substituents at this position are tolerated compound **377** could be synthesised. If compound **380** retains potency the alcohol group could provide synthetic access to a range of substituents at this position.



Nelson *et al* have synthesised (2-(aminomethyl)-5-chlorophenyl)methanol (**384**) from methyl 5-chloro-2-cyanobenzoate (**383**) by reducing the ester and nitrile group simultaneously with $\text{Zn}(\text{BH}_4)_2$. Copper cyanide was used to form methyl 5-chloro-2-cyanobenzoate from methyl 2-bromo-5-chlorobenzoate,²⁶² and the analogous carboxylic acid is commercially available (Scheme 96). Following this synthetic scheme will allow formation of the required benzylamine, from which isoindolinone **380** can be synthesised.



Scheme 96 Proposed reagents and conditions; a) H_2SO_4 , MeOH; b) CuCN, DMF; c) 1 M BH_3 .THF in THF

Compounds **357**, **378**, **379** and **380** can act as a series of probes investigated areas suggested by the crystal structure of NCL-00013774. This will develop the SAR further for the isoindolinones, and potentially lead to a further increase in potency and improve physical and chemical properties.

5.9 p53/MDM2 Assay Details

Biological testing of compounds was undertaken by bioscientists at the NICR using an ELISA assay.¹⁹⁰ A 96-well plate was incubated overnight at 96°C with streptavidin in a coating buffer. Plates were then rinsed 5 times with dissociation enhanced lanthanide immunoassay buffer, then incubated for 3 h at room temperature with a saturation buffer to block non-specific protein binding. After removal, plates were dried in sterile fumehood at room temperature before incubating at 4°C for 1 h with biotinylated IP3 peptide²⁶³ in 0.05% DMSO in PBS buffer, then plates were washed three times with PBS.

For initial testing compounds and controls were plated out in triplicate to give final concentrations of $500\ \mu\text{M}$, $100\ \mu\text{M}$ and $20\ \mu\text{M}$. Controls were 5% DMSO as a negative control and $100\ \text{nM}$ active peptide as a positive control.²⁶⁴ Compounds and controls that were aliquoted in 96-well plate were preincubated with for 20 min at 20°C with $190\ \mu\text{L}$ aliquots of concentrated of *in vitro* translated MDM2, then transferred to the streptavidin coated plates and incubated at 4°C for 90 min. Plates were then washed three times with PBS buffer, incubated for 1 h at 20°C with TBS-Tween buffered solution of mouse monoclonal anti-MDM2 antibody, then washed three times with TBS-Tween solution, then incubated for 45 min at 20°C with goat-antimouse house radish peroxidase conjugate secondary antibody. Unbound secondary antibody was removed by washing three times with TBS-Tween

solution. HRP activity measured using oxidation of diacylhydrazide substrate luminal. The IC_{50} were calculated using plot of % MDM2 inhibition versus concentration.¹⁹⁰

5.10 Conclusion

The p53/MDM2 protein-protein interaction is an important anti-cancer target. Isoindolinones have proved to be a valuable scaffold for the development of small molecules targeting the p53/MDM2 interaction, allowing elaboration of the scaffold in a number of positions. Modifications to the isoindolinone have led to a significant increase in potency from inhibitors with activity in the micromolar range to low nanomolar range.

The lead compound NCL-00008406 contains an undesirable nitro substituent on the benzyl group, however, synthetic efforts have identified appropriate replacements for the nitro group, which either improve or maintain activity against MDM2. The SAR around the benzyl group has been shown to be very narrow, substitution at the 3-position of the benzyl ring is only tolerated with small substituents, such as a fluoro group. Substituents at the 4-position of the benzyl ring have also demonstrated that the benzyl ring sits close to the bottom of the pocket. An ethylene group is tolerated, but addition of a terminal methyl group to the ethylene group is not tolerated, suggesting that this substituent is too large. The SARs around the isoindolinone A-ring have been developed and demonstrate that a number of substituents around the A-ring confer activity. Further investigation is required. Synthesis of an alternative ether chain, incorporating an oxetane ring has also shown to be tolerated.

An alternative regioselective synthesis of the important benzoyl benzoic acid intermediate has also been developed which is proving more versatile in the synthesis of new molecules. Although adding a number of steps to the synthetic route, the new synthetic route results in only the desired isomer and the additional steps are mostly trivial and high yielding.

The crystal structure of an isoindolinone bound to MDM2 has been solved recently. This will guide the synthesis of more potent molecules, as well as allowing the incorporation of groups to improve the properties to the molecules, without disrupting the interaction with MDM2.

Several potent inhibitors of the MDM2/p53 interaction have been published, and the biological activity of lead isoindolinone compounds is comparable to those in the public

domain. Interesting, biological studies have suggested that both Nutlin-3a and MI-63 are both substrates for PGP transporters, whereas isoindolinones series are not. It was demonstrated that isoindolinones induced p21 in a cell-line in which PGP is upregulated, unlike Nutlin-3a and MI-63 which failed to induce p21.²⁶⁵ Zhang *et al* have also observed that Nutlin-3a is an inhibitor of the breast cancer resistance protein efflux pump, by inhibition of the ATPase activity of BCRP.²⁶⁶ Nutlin-3a was shown to inhibit the efflux of the anti-cancer agent Mitoxantrone. The inhibition of efflux-pumps may impact on the pharmacokinetic, pharmacodynamic and safety profile of any anti-cancer agents which are substrates for efflux pumps. As isoindolinones do not appear to be either a target of efflux pumps or an inhibitor of efflux pumps, these safety fears can be negated.

Isoindolinones have proved a versatile scaffold for the development of inhibitors of the MDM2/p53 protein-protein interaction. Synthetic efforts have successfully identified a replacement for the toxic nitro group of the lead compound NCL-00008406. The SAR has also been developed further around the isoindolinone 'A'-ring and an alternative ether chain has been identified. The recent solving of the crystal structure of NCL-00013774 will guide further synthetic effort and the incorporation of groups to improve solubility. Isoindolinones are not substrates for cellular transporters which is unique amongst potent inhibitors of the p53/MDM2 interaction.

6. Overall Conclusion

Anti-cancer drug discovery has moved away from the development of broad spectrum cytotoxic agents towards the development of targeted agents, inhibiting a number of targets including receptors, kinases and protein-protein interactions. The drug discovery process entails a number of steps, and medicinal chemists are involved in a number of these steps, including hit and lead identification, hit validation and lead optimisation. The importance of the compound series has been demonstrated by the synthetic efforts towards the development of small molecule inhibitors of both mTOR and MDM2.

The pyrimidine-based series was shown to inhibit mTOR after a small screen of compounds. The molecules were originally developed as CDK2 inhibitors, so had modest activity against both mTOR and CDK2, and the pyrimidine heterocycle was already substituted at all available position around the pyrimidine. Design of a potent and selective inhibitor of mTOR required both the optimisation of mTOR activity and reduction of CDK2 activity around a ring which was already optimally substituted.

Alternatively, the isoindolinone series of inhibitors were identified as having cellular inhibitory activity and were then identified as inhibitors of the MDM2/p53 interaction, ensuring from the outset that compounds had cellular activity. As the isoindolinone scaffold was largely unsubstituted wide-ranging SAR studies have been undertaken to identify optimal substituents and position. As the isoindolinone compound were not part of a compound series directed at an alternative biological target, efforts were solely directed towards identification of active compounds.

The importance of hit compounds within the drug discovery process has lead to the development of a wide-range of techniques for the identification of compounds with activity against a particular biological target. Early techniques such as the use of natural compounds, screens of existing compounds and a me-too approach are being joined by more innovative techniques such as fragment-based drug discovery and computer-based techniques, making the drug discovery process increasingly efficient.

7. Experimental

Commercially available starting materials were purchased from fine chemical vendors and used as purchased unless otherwise stated. *N,N,N,N*-tetramethylethylenediamine was distilled over potassium hydroxide before use. Anhydrous THF, DMF, methanol, ethanol, DCM, acetonitrile and pyridine were obtained from Aldrich in SureSeal™ bottles or Acros in AcroSeal™. Petrol refers to petroleum ether with the boiling range of 40-60 °C. All reactions, unless otherwise stated were carried out under an inert atmosphere of nitrogen or argon. Palladium and rhodium catalysed reactions were degassed by bubbling N₂ through the reaction for the specified length of time.

All microwave assisted synthesis was performed using an Initiator Sixty Biotage apparatus. Hold temperature mode was used in all experiments.

LC-MS spectra were recorded either using a Micromass Platform LC in combination with a Waters 996 Photodiode Array Detector, a Waters 600 Controller and a Waters 2700 Sample Manager. Separation was achieved on a Waters Symmetry C18 column (4.6 x 20 nm) or Waters Atlantis C18 column (4.6 x 50 nm) using gradient elution with (A) 0.1% aqueous formic acid and (B) acetonitrile. The gradient used was A: B 95:5 to 5:95 over 3.5 min for the Symmetry column and 4.0 min for the Atlantis column. The Symmetry column had an overall time of 5.00 min and is referred to as (1) within experimental procedures. The Atlantis column has an overall time of 12.00 min and is referred to as (2) within experimental procedures. Alternatively, samples were run using a Waters Acquity UPLC system with PDA and ELSD. Separation was achieved using an Acquity UPLC BEH C18, 1.7 μM, 2.1 50 mm column. With a mobile phase of (A) 0.1% v/v aqueous formic acid and (B) 0.1% formic acid in acetonitrile A:B 95:5 to 5:95 over 1.5 min, overall times were either 2.00 min (3), 2.50 min (4) or 3.00 min (5) achieved with a range of hold times.

Thin-layer chromatography (TLC) was performed using precoated silica gel 60 F₂₅₄ or NH₂F_{254s} plates (amino silica) with aluminium backing and was visualised with ultra-violet (UV) light or potassium permanganate. Column chromatography was performed either on DAVISIL silica gel 40-63 μm or on automated medium pressure chromatography apparatus, a Biotage SP4 system running a graduated system as

specified with either Biotage flash prepaclet column KP-Sil, KP-NH (amino silica) and KP-C18 or Agilent Si 50 or 35 and NH (amino silica). Chromatography refers to medium pressure column chromatography or Biotage SP4 under the given conditions unless otherwise stated.

Chiral semi-preparative HPLC was performed using a Varian Prostar instrument equipped with a Daicel Chiralpak AD-H250 x 10mm column eluting with solvent (as specified), at a flow rate of 4.0 mL/min, monitoring by UV at $\lambda = 254$ nm. Analytical HPLC was performed using Waters XTerra RP185 μm (4.6 x 150 mm) column at 1 mL/min, with either (A) 0.1% aqueous ammonia and acetonitrile (B) 0.1% aqueous formic acid and acetonitrile (B), with a gradient of 5-100% acetonitrile over 25 min with the lowest purity quoted.

NMR spectra were recorded on a Bruker Spectrospin AC 300E spectrometer (^1H at 300 MHz, ^{13}C at 75 MHz) or using a Bruker Ultrashield 500 plus (^1H at 500 MHz, ^{13}C at 125 MHz) with CDCl_3 , d_6 -DMSO or d_3 -MeCN as the solvent. Chemical shifts (δ_{H}) are reported in parts per million (ppm) downfield from tetramethylsilane (TMS). Multiplicities are indicated by s (singlet), d (doublet), t (triplet), q (quartet), m (multiplet), br (broad); or combinations thereof. Coupling constants (J) were measured in Hertz (Hz).

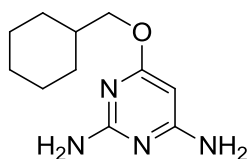
Melting points were measured on either Stuart Scientific melting point apparatus (SMP3) or Stuart automatic melting point apparatus (SMP40) and are uncorrected.

IR spectra were recorded on a Bio-Rad FTS 3000MX diamond ATR as a neat sample. UV spectra were recorded on a Hitachi U-2800A spectrophotometer and were performed in ethanol.

High resolution mass spectra were performed by the EPSRC National mass spectrometry service, University of Wales, Swansea, Singleton Park, Swansea, SAZ 8PP. Elemental analyses were performed by The School of Pharmacy, Analytical Facility, University of London, WC1N 1AX.

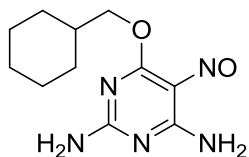
7.1 mTOR Experimental Procedures

4-(Cyclohexylmethoxy)pyrimidine-2,6-diamine (**55**)



Sodium (0.40 g, 17 mmol, 1.3 eq) was added, in portions, to cyclohexylmethanol (20.0 mL, 189 mmol, 14 eq) and the mixture was heated to 160 °C until the sodium had dissolved. 4-Chloro-2,6-diaminopyrimidine (2.00 g, 13.8 mmol, 1 eq) was added to the solution and the temperature was increased to 180 °C. After 90 min the reaction mixture was cooled to room temperature and neutralised with acetic acid. Methanol (10 mL) was added and the solution was allowed to cool to 4 °C and then left overnight. The resulting white solid was filtered and recrystallised (methanol). Additional precipitation of crude product was brought about by the addition of methanol to the remaining crude oil to give **55** as a white powder (0.55 g, 20%). $R_f = 0.38$ (100% EtOAc); mp = 137.5-138.8 °C (lit. 142 °C)¹⁴⁷; UV λ_{max} (EtOH): 266.5 nm; IR ν_{max} 3344 (NH), 2920, 2850, 1589 cm^{-1} ; δ_H (500 MHz d_6 -DMSO) 0.93-1.00 (2H, m, C_6H_{11}), 1.34-1.23 (3H, m, C_6H_{11}), 1.63-1.73 (6H, m, C_6H_{11}) 3.88 (2H, d, $J = 6.6$ Hz, CH_2), 5.04 (1H, s, H^5), 5.83 (2H, s, N^1H_2), 5.99 (2H, s, N^2H_2); δ_C (125 MHz, d_6 -DMSO): 25.2 (C_6H_{11}), 26.0 (C_6H_{11}), 29.3 (C_6H_{11}), 36.9 (CCH_2O), 69.7 (OCH_2), 76.0 (C^5), 162.9 (C^2), 165.9 (C^6), 170.3 (CO); LCMS $R_t = 2.31$ min, (1); MS (ESI+) m/z 223.15 $[M+H]^+$

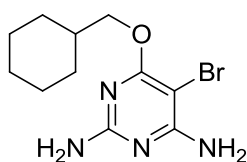
4-Cyclohexylmethoxy-5-nitrosopyrimidine-2,6-diamine (**56**)



4-(Cyclohexylmethoxy)pyrimidine-2,6-diamine (100 mg, 0.45 mmol, 1 eq) was dissolved in acetic acid (30% in water, 5 mL) at 80 °C. Sodium nitrite solution (40 mg in 0.8 mL of water, 0.58 mmol, 1.3 eq) was added dropwise to the solution, resulting in a purple solution being formed instantly which was stirred at 80 °C for 40 min and then cooled to room temperature. The resulting purple precipitate was filtered and recrystallised in ethanol to give a purple powder (97 mg, 86%). $R_f = 0.41$ (15:85

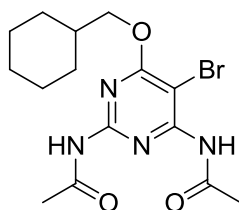
MeOH:DCM); mp = 247.8-248.5 °C (lit. 254 °C)¹⁴⁷; UV λ_{\max} (EtOH): 334.5, 235.0 nm; IR ν_{\max} 3499 (NH), 3161, 1570, 1508 (NO), 1262 cm^{-1} ; δ_{H} (300 MHz d_6 -DMSO): 0.99-1.33 (5H, m, C₆H₁₁), 1.64-1.86 (6H, m, C₆H₁₁), 4.29 (2H, d, J = 6.3 Hz, CH₂) 7.77 (1H, s, N¹H₂), 7.82 (1H, s, N¹H₂), 8.00 (1H, s, N²HH), 10.09 (1H, s, N²HH); δ_{C} (75 MHz d_6 -DMSO): 25.5 (C₆H₁₁), 26.3 (C₆H₁₁), 29.5 (C₆H₁₁), 37.2 (CCH₂O), 71.9 (CH₂O), 140.1 (C⁶), 164.0; LCMS R_t = 2.94 min, (1); MS (ESI+) m/z 252.20 [M+H]⁺

5-Bromo-4-(cyclohexylmethoxy)pyrimidine-2,6-diamine (**66**)



To a solution of 4-(cyclohexylmethoxy)-pyrimidine-2,6-diamine (300 mg, 1.35 mmol, 1eq) in acetic acid (5.0 mL, 87 mmol, 64 eq) was added *N*-bromosuccinimide (240 mg, 1.35 mmol, 1 eq) and the mixture heated to 60 °C for 1 h then and diluted with water (10 mL) giving a white suspension and neutralised with 2.5M aqueous NaOH solution. The resulting white precipitate was filtered and redissolved in DCM (20 mL). The solution was dried over Na₂SO₄ and evaporated *in vacuo*. Chromatography (silica, 15% MeOH, DCM) gave **66** as a white solid (326 mg, 80 %). R_f = 0.58 (100% EtOAc); mp = 193.7 – 194.5 °C (193-194 °C)¹⁴⁸; UV λ_{\max} (EtOH): 338.5, 327.5, 273.5, 233.5 nm; IR ν_{\max} 3497 (NH), 3472, 1053 cm^{-1} ; δ_{H} (300 MHz d_6 -DMSO): 0.93-1.29 (5H, m, C₆H₁₁), 1.62-1.72 (6H, m, C₆H₁₁), 3.98 (2H, d, J = 6.3 Hz, CH₂), 6.09 (2H, s, N¹H₂), 6.25 (2H, s, N²H₂); δ_{C} (75 MHz d_6 -DMSO) 25.6 (C₆H₁₁), 26.4 (C₆H₁₁), 29.5 (C₆H₁₁), 37.3 (CCH₂O), 71.1 (CH₂O) 161.5 (CNH₂), 162.2 (CNH₂), 165.4 (CO); LCMS R_t = 2.99 min, (1); MS (ESI+) m/z 301.23 [M+H]⁺

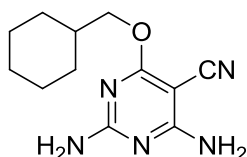
N,N'-(5-Bromo-4-(cyclohexylmethoxy)pyrimidine-2,6-diyl)diacetamide (**67**)



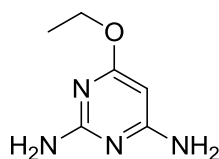
5-Bromo-4-(cyclohexylmethoxy)pyrimidine-2,6-diamine (200 mg, 0.66 mmol, 1 eq) was added to a mixture of acetic acid (2.5 mL, 44 mmol, 66 eq) and acetic anhydride (2.5 mL, 26 mmol, 40 eq) under nitrogen. The solution was heated to reflux overnight

resulting in a colour change from yellow to pale brown, then cooled to room temperature and poured into water (10 mL), resulting in a white precipitate, neutralised with concentrated ammonia and extracted into ethyl acetate (3 x 20 mL). The combined organic layers were then washed with NaHCO₃ (3 x 30 mL) and then water (3 x 30 mL) dried over Na₂SO₄, filtered and evaporated *in vacuo*. Recrystallised (acetonitrile) gave **67** as a white solid (135 mg, 53%). $R_f = 0.5$ (100% EtOAc); mp = 178.4-178.8 °C (lit. 179-182)¹⁴⁸; UV λ_{max} (EtOH): 388.0, 228.0, 205.5 nm; IR ν_{max} 3389 (NH), 1671 (C=O), 1258, 1111, 1067, 1036 cm⁻¹; δ_H (300 MHz, *d*₆-DMSO): 0.98-1.31 (5H, m, C₆H₁₁), 1.69-1.79 (6H, m, C₆H₁₁), 2.17 (3H, s, COCH₃), 2.20 (3H, s, COCH₃), 4.20 (2H, d, $J = 6.3$ Hz, CH₂), 9.98 (1H, s, NH), 10.48 (1H, s, NH); δ_C (75 MHz *d*₆-DMSO): 24.2 (CH₃), 25.1 (CH₃), 25.5 (C₆H₁₁), 26.3 (C₆H₁₁), 29.4 (C₆H₁₁), 37.1 (CCH₂O), 73.0 (CH₂O), 157.5 (C-N), 166.9 (CO), 169.5 (C=O), 169.6 (C=O); LCMS $R_t = 3.21$ min, (1); MS (ESI+) m/z 385.35 [M+H]⁺

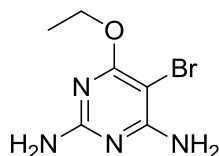
2,6-Diamino-4-(cyclohexylmethoxy)pyrimidine-5-carbonitrile (**59**)



To a solution of *N,N'*-(5-bromo-4-(cyclohexylmethoxy)pyrimidine-2,6-diyl)diacetamide (100 mg, 0.26 mmol, 1 eq) in DMF (5 mL) CuCN (28 mg, 0.31 mmol, 1.2 eq) was added, the mixture was heated to reflux for 5 h, then cooled to room temperature, ethylenediamine (1.4 mL, 20 mmol, 77 eq) was added and stirred overnight at room temperature. The mixture was filtered through Celite and washed with DMF (2 x 5 mL), water (10 mL) was added to the filtrate and the product extracted into ethyl acetate (3 x 20 mL). The combined organic layers were washed with brine (50 mL), dried over Na₂SO₄ and evaporated under vacuum. Recrystalliation (ethyl acetate / petrol) gave **59** as cream crystals (45 mg, 70%). $R_f = 0.64$ (100 % EtOAc); mp = 187.5 – 188.3 °C (lit. 186-188 °C)¹⁴⁸; UV λ_{max} (EtOH): 367.5, 267.0, 251.5, 234.5 nm; IR ν_{max} 3512 (NH), 3381, 2210 (CN), 1549, 1226 cm⁻¹; δ_H (300 MHz *d*₆-DMSO): 0.96-1.26 (5H, m, C₆H₁₁), 1.63-1.75 (6H, m, C₆H₁₁), 4.06 (2H, d, $J = 6.3$ Hz, CH₂), 6.90 (2H, d, $J = 15.3$ Hz, N¹H₂) 7.95 (2H, s, N²H₂); δ_C (75 MHz *d*₆-DMSO): 25.5 (C₆H₁₁), 26.3 (C₆H₁₁), 29.4 (C₆H₁₁), 35.2 (CCH₂O), 71.1 (CH₂O), 163.8 (CNH₂), 166.3 (CNH₂), 177.9 (CO)

4-Ethoxypyrimidine-2,6-diamine (**385**)

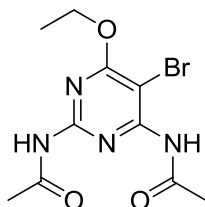
Ethanol (15 mL, 260 mmol, 19 eq) was added slowly to sodium (0.50 g, 22 mmol, 1.5 eq). Once the gas evolution had stopped the solution was heated to 80 °C until all the sodium had dissolved. 4-Chloro-2,6-diaminopyrimidine (2.00 g, 13.8 mmol, 1 eq) was added and the temperature increased to 98 °C for 5 h before cooling to room temperature, neutralising with acetic acid and evaporated *in vacuo*. The residue was suspended in water and extracted into ethyl acetate (3 x 20 mL). The combined organic layers were dried over Na₂SO₄, filtered and evaporated *in vacuo* resulting in cream crystals. Recrystallised (ethyl acetate /petrol) gave **385** as a white solid (1.25g, 58%). $R_f = 0.44$ (1:9 MeOH:EtOAc); mp = 134.7 – 136.1 °C, (lit. 167-169 °C)¹⁴⁸; UV λ_{\max} (EtOH): 366.5, 284.5, 279.5, 267.0, 204.0 nm; IR ν_{\max} 3426 (NH), 1344, 1208, 1040 cm⁻¹; δ_H (300 MHz, *d*₆-DMSO): 1.21 (3H, t, $J = 7.0$, CH₃), 4.12 (2H, q, $J = 7.0$ Hz, CH₂), 5.01 (1H, s, H^5), 5.85 (2H, s, N¹H₂), 5.99 (2H, s, N²H₂); δ_C (75 MHz *d*₆-DMSO): 16.0 (CH₃), 61.5 (CH₂), 77.8 (C⁵), 167.4 (CNH₂), 171.5 (CNH₂), 173.1 (CNH₂); LCMS $R_t = 2.16$ min, (2); MS (ESI+) m/z 155.20 [M+H]⁺

5-Bromo-6-ethoxypyrimidine-2,6-diamine (**386**)

To a solution of 4-ethoxypyrimidine-2,6-diamine (1.00 g, 6.49 mmol, 1eq) in acetic acid (8.0 mL, 140 mmol, 22 eq) was added *N*-bromosuccinimide (1.17 g, 6.57 mmol, 1 eq) and the solution heated to 60 °C for 90 min, cooled to room temperature, diluted with water (45 mL) and neutralised with 2.5 M aqueous NaOH solution. Solution then extracted with ethyl acetate (3 x 50 mL) and combined organic layers were then dried over Na₂SO₄, filtered and evaporated *in vacuo*. Recrystallisation (methanol) to give **386** as a pale yellow powder which was then dried over P₂O₅ before further use (0.724 g, 48%). $R_f = 0.35$ (100% EtOAc); mp = 179.7-180.5 °C; UV λ_{\max} (EtOH): 353.5, 275.5, 235.5 nm; IR ν_{\max} 3426 (NH), 3344, 1206, 1047 cm⁻¹; δ_H (300 MHz, *d*₆-DMSO): 1.25 (3H, t, $J = 7.1$ Hz, CH₃), 4.23 (2H, q, $J = 7.1$ Hz, CH₂) 6.09 (2H, s,

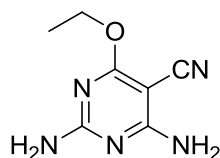
N^1H_2), 6.27 (2H, s, N^2H_2); δ_C (75 MHz d_6 -DMSO): 14.9 (CH₃), 62.0 (CH₂), 72.4 (C⁵), 161.5 (CNH₂), 162.2 (CNH₂), 179.3 (CO); LCMS R_t = 5.53 min, (2); MS (ESI+) m/z 233.06 [M+H]⁺

N,N'-(5-Bromo-4-ethoxypyrimidine-2,6-diyl)diacetamide (**387**)



A solution of 5-bromo-6-ethoxypyrimidine-2,6-diamine (500 mg, 2.15 mmol, 1 eq) in acetic acid (5.5 mL, 96 mmol, 45 eq) and acetic anhydride (7.5 mL, 68 mmol, 32 eq) was heated to reflux for 48 h, then cooled to room temperature, diluted with water (20 mL) and neutralised with concentrated ammonia, and extracted with ethyl acetate (3 x 30 mL). The combined organic extracts were washed with saturated NaHCO₃ (3 x 50 mL) followed by water (3 x 50 mL) and dried (Na₂SO₄). Recrystallised (methanol) gave **387** as off-white solid (0.19 g, 27%). R_f = 0.48 (100% EtOAc); mp = 181.4 – 182.8 °C; UV λ_{max} (EtOH): 353.0, 256.0, 227.5, 207.0 nm; IR ν_{max} 3362 (NH), 1676 (C=O), 1261, 1097, 1023 cm⁻¹; δ_H (300 MHz, d_6 -DMSO): 1.35 (3H, t, J = 7.1, Hz, CH₂CH₃), 2.17 (3H, s, COCH₃), 2.21 (3H, s, COCH₃), 4.44 (2H, q, J = 7.0 Hz, CH₂CH₃), 9.96 (1H, s, N¹H), 10.49 (1H, s, N²H); δ_C (75 MHz d_6 -DMSO): 14.5 (CH₂CH₃), 24.1 (CH₃), 25.1 (CH₃), 64.3 (CH₂), 155.2 (CNH₂), 157.5 (CNH₂), 166.7 (CO), 169.4 (C=O), 169.6 (C=O); LCMS R_t = 6.55 min, (2); MS (ESI+) m/z 247.07 [M+H]⁺

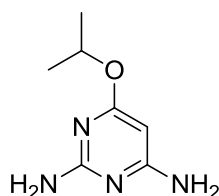
2,6-Diamino-4-ethoxypyrimidine-5-carbonitrile (**81**)



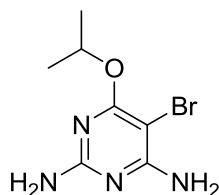
To a solution of *N,N'*-(5-bromo-4-ethoxypyrimidine-2,6-diyl)diacetamide (110 mg, 0.35 mmol, 1 eq) in DMF (5 mL) was CuCN (48 mg, 0.54 mmol, 1.5 eq). The resulting green solution was heated to reflux for 3.5 h the solution before cooling to room temperature and ethylene diamine (2.5 mL, 37 mmol, 106 eq) added. The dark blue solution was stirred overnight, filtered through Celite and washed with further

DMF (8 mL). Water (25 mL) was added to the filtrate and the product was extracted into ethyl acetate (3 x 50 mL), dried over Na₂SO₄ and concentrated *in vacuo*. Chromatography (silica, 100% EtOAc) followed by recrystallisation (methanol) gave **81** as an off-white solid (0.047 g, 75%). *R*_f = 0.66 (100% EtOAc); mp = 226.7-227.1 °C; UV λ_{max} (EtOH): 251.5, 216.5 nm; IR ν_{max} 3433 (NH), 3372, 3093, 2199 (CN), 1668, 1615, 1539 cm⁻¹; δ_H (300 MHz, d₆-DMSO): 1.27 (3H, t, *J* = 7.1 Hz, CH₃), 4.30 (2H, q, *J* = 7.1 Hz, CH₂), 6.88 (2H, s, N¹H₂), 6.93 (2H, s, N²H₂); δ_C (75 MHz d₆-DMSO): 14.8 (CH₃), 62.2 (CH₂), 116.1 (CN), 163.4 (CNH₂), 166.3 (CNH₂), 171.2 (CO); LCMS *R*_t = 1.29 min, (1); MS (ESI+) *m/z* 180.12 [M+H]⁺; HRMS *m/z*; Calc. for C₇H₁₀N₅O: 180.0880 [M+H]⁺. Found 180.0880 [M+H]⁺. Analytical HPLC: 98.2% purity

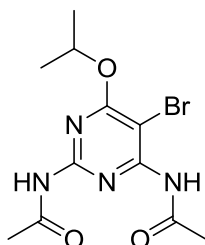
4-Isopropoxyppyrimidine-2,6-diamine (**80**)



To isopropanol (4.8 mL, 62 mmol, 18 eq) under constant flushing with nitrogen was gradually added sodium (0.13 g, 5.65 mmol, 1.6 eq). Once all gas evolution had stopped the solution was heated at 50 °C until all sodium had dissolved. 4-Chloro-2,6-diaminopyrimidine (0.50 g, 3.46 mmol, 1 eq) was added, which was sealed and irradiated for 20 min at 160 °C, then neutralised using acetic acid and evaporated. The resulting white solid was suspended in water (20 mL) and extracted with ethyl acetate (3 x 20 mL) and the resulting organic layers were dried over Na₂SO₄ and evaporated. Recrystallisation (ethyl acetate /petrol) gave **80** as a white solid (0.39 g, 68%). *R*_f = 0.31 (100% EtOAc); mp = 112.8-113.0 °C; UV λ_{max} (EtOH): 379.0, 267.0 nm; IR ν_{max} 3356 (NH), 1317, 1208 cm⁻¹; δ_H (300 MHz d₆-DMSO): 1.19 (6H, d, *J* = 6.2 Hz, 2 x CH₃), 4.97 (1H, s, H⁵), 5.10 (1H, septet, *J* = 6.2 Hz, CH) 5.81 (2H, s, N¹H₂), 5.94 (2H, s, N²H₂); δ_C (75 MHz d₆-DMSO): 22.4 (CH₃), 66.7 (OCH), 77.5 (C⁵), 163.4 (CNH₂), 166.4 (CNH₂), 172.0 (CO); LCMS *R*_t = 4.59 min, (2); MS (ESI+) *m/z* 169.21 [M+H]⁺

5-Bromo-4-isopropoxy pyrimidine-2,6-diamine (**388**)

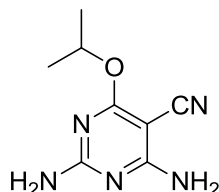
To a solution of 4-isopropoxy pyrimidine-2,6-diamine (250 mg, 1.49 mmol, 1 eq) in acetic acid (5 mL, 87 mmol, 59 eq) was added *N*-bromosuccinimide (265 mg, 1.49 mmol, 1 eq), and the mixture was stirred at RT for 45 min, then diluted with water (10 mL) and neutralised using 2.5 M aqueous solution of NaOH. The resulting white precipitation was filtered, redissolved in methanol (15 mL), dried over Na₂SO₄, and evaporated. Recrystallisation (methanol) gave **388** as a white solid (21 mg, 58%). *R*_f = 0.74 (100% EtOAc); mp = 160.9 – 161.2 °C; UV λ_{max} (EtOH): 379.0, 274.5, 232.0, 205.0 nm; IR ν_{max} 3426 (NH), 1335, 1206, 1047 cm⁻¹; δ_H (300 MHz *d*₆-DMSO): 1.24 (6H, d, *J* = 6.2 Hz, CH₃), 5.19 (1H, septet, *J* = 6.3 Hz, CH) 6.05 (2H, s, N¹H₂), 6.23 (2H, s, N²H₂); δ_C (75 MHz *d*₆ DMSO) 29.9 (CH₃), 73.2 (OCH), 161.6 (CNH₂), 162.3 (CNH₂), 179.5; LCMS *R*_t = 6.20 min, (2); MS (ESI+) *m/z* 247.10 [M+H]⁺; CHN Calculated C 34.03 H 4.49 N 22.67 Found C 34.65 H 4.18 N 21.78

N,N'-(5-Bromo-4-isopropoxy pyrimidine-2,6-diyl)diacetamide (**389**)

To a solution of 5-bromo-4-isopropoxy pyrimidine-2,6-diamine (150 mg, 0.61 mmol, 1 eq) in acetic acid (2.5 mL, 44 mmol, 72 eq) was added acetic anhydride (5 mL, 53 mmol, 86 mmol). The mixture heated to 160 °C for 16 h followed by 170 °C for a further 8 h, diluted with water (10 mL) and neutralised with concentrated ammonia. The solution was then extracted into ethyl acetate (3 x 20 mL). The combined organic layers washed with saturated NaHCO₃ solution (1 x 50 mL) dried over Na₂SO₄, evaporated *in vacuo*. The residue was redissolved in petrol and evaporated to give **389** as a cream solid (184 mg, 91%). *R*_f = 0.71 (100% EtOAc); mp = 174.4 – 174.9 °C; UV λ_{max} (EtOH): 367.0, 254.5, 227.5, 204.0 nm; IR ν_{max} 3375 (NH), 1669 (C=O), 1313, 1262, 1221, 1096 cm⁻¹; δ_H (300 MHz, *d*₆-DMSO): 2.69 (6H, d, *J* = 6.3 Hz,

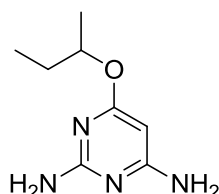
CH(CH₃)₂), 2.15 (3H, s, COCH₃), 2.20 (3H, s, COCH₃), 5.31 (1H, septet, *J* = 6.3 Hz, CH), 10.0 (1H, s, N¹H), 10.45 (1H, s, N²H); δ_C (75 MHz *d*₆-DMSO): 22.0 (COCH₃), 22.3 (COCH₃), 25.0 (CH(CH₃)₂), 71.7 (OCH), 99.6 (C⁵), 157.7 (C²), 166.8 (C⁶), 168.5 (CO), 169.5 (C=O), 169.9 (C=O); LCMS R_t = 3.01 min, (1), MS (ESI+) *m/z* 331.22 [M+H]⁺

2,6-Diamino-4-isopropoxyypyrimidine-5-carbonitrile (**82**)



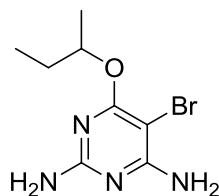
To a solution of *N,N'*-(5-bromo-4-isopropoxyypyrimidine-2,6-diyl)diacetamide (200 mg, 0.60 mmol, 1 eq) in DMF (5 mL) was added CuCN (73 mg, 0.81 mmol, 1.4 eq). The reaction mixture was heated at 120 °C for 2 h, to room temperature and ethylenediamine (5 mL, 75 mmol, 125 eq) added and the mixture stirred overnight. The resulting blue solution was filtered through Celite, washed with DMF (10 mL) and diluted with water (50 mL). Solution was extracted with ethyl acetate (3 x 70 mL). The combined organic extracts were washed with brine (150 mL), dried (Na₂SO₄) and evaporated *in vacuo*. Chromatography (silica, 10% MeOH, EtOAc) followed by (SP4, silica, 15-100% EtOAc, PE). Final purification using HPLC (0.1% NH₃ aqueous solution: acetonitrile 75:25) to give **82** as a white solid (29 mg, 25%). *R*_f = 0.64 (1:9 MeOH:EtOAc); mp = 190.5-190.8 °C; UV λ_{max} (EtOH): 267.0, 252.0, 217.5 nm; IR ν_{max} 3381 (NH), 3129, 2208 (CN), 1669, 1614 cm⁻¹; δ_H (300 MHz, *d*₆-DMSO): 1.26 (6H, d, *J* = 5.1 Hz, CH₃), 5.27 (1H, septet, *J* = 6.3 Hz, CH), 6.84 (2H, s, N¹H₂), 6.89 (2H, s, N²H₂); δ_C (75 MHz, *d*₆-DMSO): 22.2 (CH(CH₃)₂), 69.2 (OCH(CH₃)₂), 116.2 (CN), 163.5 (C²), 166.4 (C⁶), 170.9 (CO); LCMS R_t = 2.59 min, (1); MS (ESI+) *m/z* 194.04 [M+H]⁺; HRMS *m/z*: Calc. for C₈H₁₂N₅O: 194.1036 [M+H]⁺. Found 194.1035 [M+H]⁺. Analytical HPLC: 99.7% purity

4-*sec*-Butoxyypyrimidine-2,6-diamine (**390**)

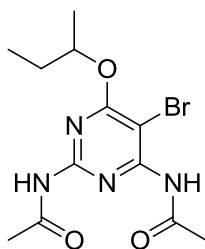


To sodium (0.45 g, 19.6 mmol, 1.4 eq) under nitrogen was slowly added *sec*-butanol (18 mL, 196 mmol, 14 eq) and heated to 120 °C and until all sodium has dissolved. 4-Chloro-2,6-diaminopyrimidine (2.00 g, 13.8 mmol, 1 eq) was added and the mixture heated to reflux for 5.5 hours, then cooled to room temperature, neutralised with acetic acid and concentrated *in vacuo*. Crude was suspended in water (20 mL) and extracted into ethyl acetate (3 x 30 mL), combined organic layers were dried over Na₂SO₄, concentrated *in vacuo* resulting in a yellow solid. This crude product was recrystallised (ethyl acetate /petrol) to give **390** as a cream solid (1.20 g, 48%). $R_f = 0.44$ (100% EtOAc); mp = 92.7-93.1 °C; UV λ_{max} (EtOH): 265.5, 234.5, 206.0 nm; IR ν_{max} 3356 (NH), 1315, 1208, 1098 cm⁻¹; δ_H (300 MHz *d*₆-DMSO): 0.86 (3H, t, $J = 7.4$, CH₂CH₃), 1.16 (3H, d, $J = 6.2$ Hz, CHCH₃), 1.47 -1.62 (2H, m, CH₂), 4.88- 4.98 (1H, m, OCH), 5.01 (1H, s, H^5), 6.00 (2H, s, N¹H₂), 6.12 (2H, s, N²H₂); δ_C (75 MHz *d*₆-DMSO): 9.8 (CH₃CH₂), 18.9 (CH₃CH), 29.0 (CH₃CH₂), 71.3 (OCH₂), 77.4 (C⁵), 163.4 (CNH₂), 166.5 (CNH₂), 170.5 (CO); LCMS $R_t = 5.39$ min, (2), MS (ESI+) m/z 183.18 [M+H]⁺

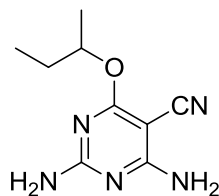
5-Bromo-4-*sec*-butoxypyrimidine-2,6-diamine (**391**)



To a solution of 4-*sec*-butoxypyrimidine-2,6-diamine (250 mg, 1.37 mmol, 1 eq) in acetic acid (5 mL, 87 mmol, 64 eq), was added *N*-bromosuccinimide (249 mg, 1.39 mmol, 1 eq). After 15 min of stirring at room temperature the yellow solution was diluted with water (10 mL) and neutralised with 2.5M aqueous NaOH solution. The product was extracted into ethyl acetate (3 x 30 mL), dried over Na₂SO₄, concentrated *in vacuo* giving **391** as a cream solid (257 mg, 72%) which was used without further purification. $R_f = 0.76$ (100% EtOAc); mp = 103.7 – 104.2 °C; UV λ_{max} (EtOH): 344.0, 274.0, 234.5, 204.0 nm; IR ν_{max} 3451 (NH), 3411, 3357, 1043 cm⁻¹; δ_H (300 MHz *d*₆-DMSO): 0.88 (3H, t, $J = 7.4$ Hz, CH₂CH₃), 1.20 (3H, d, $J = 6.2$ Hz, OCHCH₃), 1.53-1.59 (2H, m, CH₂CH₃), 4.97-5.07 (1H, m, OCH), 6.06 (2H, s, N¹H₂), 6.26 (2H, s, N²H₂); δ_C (75 MHz *d*₆-DMSO): 9.6 (CH₃CH₂), 19.8 (CH₃CH), 28.9 (CH₃CH₂), 73.1 (OCH), 161.5 (CNH₂), 162.3 (CNH₂), 165.1 (CO); HRMS m/z : Calc. for C₈H₁₄⁷⁹BrN₄O: 261.0346 [M+H]⁺. Found 261.0343 [M+H]⁺.

N,N'-(5-Bromo-4-*sec*butoxypyrimidine-2,6-diyl)diacetamide (**392**)

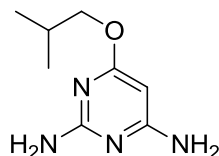
A solution of **391** (2.38 g, 9.65 mmol, 1 eq) in AcOH (23 mL, 405 mmol, 42 eq) and Ac₂O (58 mL, 1.01 mol, 105 eq) was heated to 170 °C for 40 h, cooled to room temperature, water (60 mL) and basified using conc. ammonia, the beige precipitate was collected by filtration, dissolved in DCM (30 mL) and dried over Na₂SO₄ and concentrated *in vacuo*. Chromatography (silica, 100% EtOAc) gave **392** as a white solid (0.86 g, 26%). *R*_f = 0.66 (100% EtOAc); mp = 139.3-142.0 °C; UV λ_{max} (EtOH): 253.5, 228.0 nm; IR ν_{max} 3215 (NH), 2974, 1677 (C=O), 1571, 1311 cm⁻¹; δ_H (500 MHz, *d*₆-DMSO): 0.92 (3H, t, *J* = 7.4 Hz, CH₃CH₂), 1.32 (3H, d, *J* = 6.1 Hz, CHCH₃), 1.65-1.74 (2H, m, CH₂CH₃), 2.18 (3H, s, COCH₃), 2.21 (3H, s, COCH₃), 5.15-5.19 (1H, m, OCHCH₃), 9.89 (1H, s, NH), 10.4 (1H, s, NH); δ_C (125 MHz, *d*₆-DMSO): 9.4 (CH₃CH₂), 19.0 (CH₃CH), 23.7 (COCH₃), 24.7 (COCH₃), 28.2 (CH₃CH₂), 75.9 (CH₃CHO), 90.3 (C⁵), 154.8 (C²), 157 (C⁶), 166.1 (C-O), 168.9 (C=O), 169.2 (C=O)

2,6-Diamino-4-*sec*-butoxypyrimidine-5-carbonitrile (**83**)

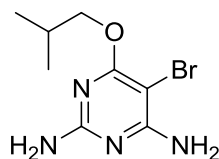
To a solution of *N,N'*-(5-bromo-4-*sec*-butoxypyrimidine-2,6-diyl)diacetamide (300 mg, 0.87 mmol, 1 eq) in DMF (5 mL) was added CuCN (99 mg, 1.1 mmol, 1.3 eq) and the reaction mixture was heated to 120 °C for 6 h, then cooled to room temperature. Ethylenediamine (5 mL, 75 mmol, 86 eq) was added and the reaction mixture was stirred for 4 h, and the resulting blue solution was filtered through Celite, washed with DMF (8 mL) and diluted with water (30 mL). The filtrate was then extracted with ethyl acetate (3 x 50 mL) and the combined organic layers washed with brine (2 x 100 mL), dried over Na₂SO₄ and concentrated *in vacuo*. The residue was suspended in water (100 mL), extracted in to ethyl acetate (3 x 70 mL), dried over

Na₂SO₄ and concentrated *in vacuo*. Recrystallisation (methanol / petrol) gave **83** as a white solid (0.093 mg, 51%). $R_f = 0.71$ (7:3 EtOAc:PE); mp = 165.6-166.4 °C; UV λ_{\max} (EtOH): 265.5, 251.5, 218.0, 202.5 nm; IR ν_{\max} 3380 (NH), 3125, 2199 (CN), 1660, 1628, 1572 cm⁻¹; δ_H (300 MHz, *d*₆-DMSO): 0.88 (3H, t, $J = 7.5$ Hz, CH₂CH₃), 1.23 (3H, d, $J = 6.0$ Hz, CHCH₃), 1.54-1.66 (2H, m, CH₂CH₃), 5.07-5.16 (1H, m, CHCH₃), 6.83 (2H, s, N¹H₂), 6.89 (2H, s, N²H₂); δ_C (75 MHz, *d*₆-DMSO): 9.6 (CH₃CH₂), 19.6 (CH₃CH), 28.8 (CH₃CH₂), 73.6 (OCH), 116.1 (CN), 163.6 (CNH₂), 166.4 (CNH₂), 171.3 (CO); LCMS $R_t = 3.11$ min, (1), MS (ESI+) m/z 208.18 [M+H]⁺; HRMS m/z : Calc. for C₉H₁₅N₅O: 208.1193 [M+H]⁺. Found 208.1191 [M+H]⁺. Analytical HPLC: 96.8% purity

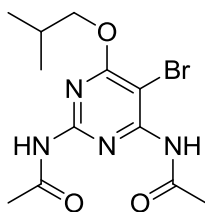
4-Isobutoxypyrimidine-2,6-diamine (**393**)



Sodium (0.45 g, 19.6 mmol, 1.4 eq) was added to (2-methyl-1-propanol (16 mL, 173 mmol, 13 eq) then heated to 80 °C until all the sodium had dissolved resulting in a yellow solution. 4-Chloro-2,6-diaminopyrimidine (2.00 g, 13.7 mmol, 1 eq) was added and the temperature increased to 120 °C for 1 h then 140 °C for 3 h, then cooled to room temperature, neutralised with acetic acid and evaporated. The resulting yellow solid was suspended in water (30 mL), and extracted in ethyl acetate (3 x 30 mL). The organic layers were dried over Na₂SO₄, evaporated resulting in a yellow oil that was triturated to form a cream solid. Recrystallisation (ethyl acetate /petrol) gave a sticky white solid which was dried over P₂O₅, then covered in diethyl ether (20 mL) which was allowed to slowly evaporate giving **393** as a white solid (1.31 g, 53%). $R_f = 0.39$ (100% EtOAc); mp = 81.8-82.8 °C; UV λ_{\max} (EtOH): 379.0, 266.5, 205.5 nm; IR ν_{\max} 3439 (NH), 3323, 1213, 1027 cm⁻¹; δ_H (300 MHz *d*₆-DMSO): 0.90 (6H, d, 6.6 Hz, 2 x CH₃), 1.87-1.96 (1H, m, CH), 3.84 (2H, d, $J = 6.6$ Hz, CH₂), 5.03 (1H, s, H⁵), 5.88 (2H, s, N¹H₂), 6.01 (2H, s, N²H₂); δ_C (75 MHz *d*₆-DMSO): 19.4 (2 x CH₃), 27.3 (CH), 71.2 (CH₂), 76.8 (C⁵), 163.3 (CNH₂), 166.4 (CNH₂), 170.9 (CO); LCMS $R_t = 5.70$ min, (2); MS(ESI+) m/z 183.18 [M+H]⁺

5-Bromo-4-isobutoxypyrimidine-2,6-diamine (**394**)

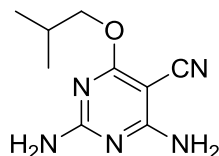
To 4-isobutoxypyrimidine-2,6-diamine (250 mg, 1.37 mmol, 1 eq) in acetic acid (5 mL, 87 mmol, 64 eq) was added *N*-bromosuccinimide (255 mg, 1.43 mmol, 1 eq). After stirring at room temperature for 15 min the reaction was diluted with water (10 mL) and the neutralised with 2.5M aqueous NaOH solution, resulting in a white precipitate which was collected by filtration. The precipitation was redissolved in water (50 mL) and extracted into ethyl acetate (3 x 50 mL), dried over Na₂SO₄ and evaporated *in vacuo* giving **394** as a cream solid used without any further purification (309 mg, 86 %). $R_f = 0.77$ (100% EtOAc); mp = 136.3 – 136.7 °C; UV λ_{\max} (EtOH): 379.0, 274.5, 234.0, 204.0 nm; IR ν_{\max} 3451 (NH), 3406, 1292, 1048 cm⁻¹; δ_H (300 MHz *d*₆-DMSO): 0.93 (6H, d, $J = 6.6$ Hz, CH₃), 1.89-2.02 (1H, m, CH), 3.95 (2H, d, $J = 6.6$ Hz, CH₂), 6.10 (2H, s, N¹H₂), 6.29 (2H, s, N²H₂); δ_C (75 MHz *d*₆-DMSO): 19.2 (CH₃), 27.9 (CH), 72.2 (CH₂), 161.5 (CNH₂), 162.2 (CNH₂), 165.3 (CO); LCMS $R_t = 2.83$ min, (1); MS (ESI+) m/z 261.10 [M]⁺; CHN Calculated C 36.80, H 5.02, N 21.45 Found C 36.81 H 4.81 N 21.49

N,N'-(5-Bromo-6-isobutoxypyrimidine-2,6-diyl)diacetamide (**395**)

A mixture of 5-bromo-4-isobutoxypyrimidine-2,6-diamine (150 mg, 0.57 mmol, 1 eq) in acetic acid (2.5 mL, 44 mmol, 76 eq) and acetic anhydride (5 mL, 52.9 mmol, 92 mmol) was heated to 150 °C for 28 h then to 160 °C for 11 h., then cooled to room temperature, diluted with water (10 mL) and neutralised with concentrated ammonia, then extracted into ethyl acetate (3 x 70 mL). The combined organic extracts were dried over Na₂SO₄, filtered and evaporated. Recrystallisation (methanol) gave **395** as a beige solid which was washed with petroleum ether (3 x 5 mL) (0.16 g, 79%). $R_f = 0.61$ (100% EtOAc); mp = 129.7-130.4 °C; UV λ_{\max} (EtOH): 254.5, 216.5 nm; IR ν_{\max} 3395 (NH), 1670 (C=O), 1142, 1310, 1142, 1001 cm⁻¹; δ_H (300 MHz *d*₆-DMSO):

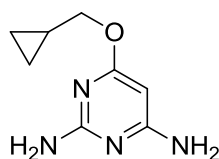
0.98 (6H, d, $J = 6.9$ Hz, 2 x CH_3), 1.98-2.13 (1H, m, CH), 2.17 (3H, s, COCH_3), 2.02 (3H, s, COCH_3), 4.17 (2H, d, $J = 6.6$ Hz, CH_2), 9.97 (1H, s, N^1H), 10.48 (1H, s, N^2H); δ_{C} (75 MHz d_6 -DMSO): 19.1 ($\text{CH}(\text{CH}_3)_2$), 24.2 (COCH_3), 25.1 (COCH_3), 27.7 (CH), 75.0 (CH_2), 155.2 (CNH_2), 157.5 (CNH_2), 166.8 (CO), 169.4 (C=O), 169.5 (C=O); LCMS $R_t = 3.16$ min, (1); MS (ESI+) m/z 345.13 $[\text{M}+\text{H}]^+$

2,6-Diamino-4-isobutoxypyrimidine-5-carbonitrile (**84**)



To a solution of *N,N'*-(5-bromo-4-isobutoxypyrimidine-2,6-diyl) (200 mg, 0.58 mmol, 1 eq) in DMF (5 mL) was added CuCN (70 mg, 0.78 mmol, 1.3 mmol) and the reaction heated to 120 °C for 7 h. The mixture was then cooled to room temperature, ethylenediamine (4 mL, 60 mmol, 103 eq) added and the reaction stirred for 17 h, filtered through Celite, washing with DMF (10 mL), the filtrate was diluted with water (30 mL) and extracted with ethyl acetate (3 x 50 mL). The combined organic layers were washed with brine (100 mL), dried over Na_2SO_4 and evaporated *in vacuo* resulting in a cream solid. Recrystallisation (MeOH/petrol). Chromatography (SP4, silica, 10-80% EtOAc, petrol) gave **84** as a white solid (36 mg, 30%). $R_f = 0.58$ (100% EtOAc); mp = 197.4-198.2 °C; UV λ_{max} (EtOH): 266.0, 251.0, 217.5 nm; IR ν_{max} 3344 (NH), 3204, 2207 (CN), 1628 cm^{-1} ; δ_{H} (300 MHz, d_6 -DMSO): 0.93 (6H, d, $J = 6.6$ Hz, $\text{CH}(\text{CH}_3)_2$), 1.89-2.04 (1H, m, CH), 4.03 (2H, d, $J = 6.6$ Hz, OCH_2), 6.87 (2H, s, N^1H_2), 6.93 (2H, s, N^2H_2); δ_{C} (75 MHz, d_6 -DMSO): 19.1 (CH_3), 27.9 (CH), 72.3 (CH_2), 163.5 (CNH_2), 166.3 (CNH_2), 171.6 (CO); HRMS m/z : Calc. for $\text{C}_9\text{H}_{14}\text{N}_5\text{O}$: 208.1193 $[\text{M}+\text{H}]^+$. Found 208.1193 $[\text{M}+\text{H}]^+$. Analytical HPLC: 97.1% purity

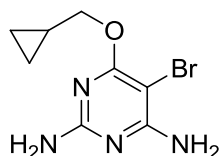
4-Cyclopropylmethoxypyrimidine-2,6-diamine (**396**)



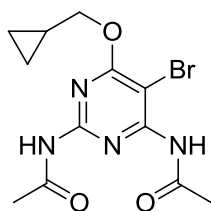
Sodium (0.55 g, 23.9 mmol, 1.7 eq) was added in portions to a flask containing cyclopropylmethanol (20 mL, 247 mmol, 18 eq) and heated to 60 °C until all the

sodium had dissolved. 4-Chloro-2,6-diaminopyrimidine (2.00g, 13.8 mmol, 1 eq) was added to the solution and the mixture was heated to 120 °C for 90 min, cooled to RT, neutralised with acetic acid, and evaporated. The resulting brown oil was suspended in water (50 mL) and extracted with EtOAc (3 x 70 mL). The combined organic layers were dried over Na₂SO₄ and concentrated *in vacuo*. Chromatography (silica, 100% Ethyl acetate) gave **396** as a yellow oil (1.90 g, 77%). $R_f = 0.33$ (100% EtOAc); UV λ_{\max} (EtOH): 265.0, 233.0, 206.0 nm; IR ν_{\max} 3338 (NH), 3188, 1564 cm⁻¹; δ_H (300 MHz, *d*₆-DMSO): 0.22-0.27 (2H, m, CH₂), 0.47-0.53 (2H, m, CH₂), 1.15-1.20 (1H, m, CH), 3.91 (2H, d, $J = 6.9$ Hz, OCH₂), 5.01 (1H, s, H⁵), 5.84 (2H, s, N¹H₂), 5.98 (2H, s, N²H₂); δ_C (75 MHz, *d*₆-DMSO): 3.4 (cyclopropyl), 10.6 (cyclopropyl), 69.4 (OCH₂), 76.9 (C⁵), 163.3 (CNH₂), 166.5 (CNH₂), 170.7 (CO); LCMS $R_t = 0.33$ min, (1); MS (ESI+) m/z 181.15 [M+H]⁺

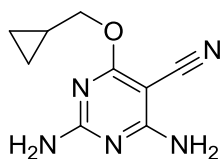
5-Bromo-4-cyclopropylmethoxypyrimidine-2,6-diamine (**397**)



A mixture 4-cyclopropylmethoxypyrimidine-2,6-diamine (0.72 g, 4.00 mmol, 1 eq) and *N*-bromosuccinimide (0.72 g, 4.06 mmol, 1.01 eq) was dissolved in acetic acid (8.0 mL, 130 mmol, 32 eq) was stirred at room temperature for 15 min neutralised using 2.5 M aqueous solution of NaOH resulting in a white precipitate which was filtered, redissolved in DCM (50 mL) and dried over Na₂SO₄ giving **397** as a white solid (1.03 g, 99%). $R_f = 0.8$ (100% EtOAc); mp = 147.6-147.8 °C; UV λ_{\max} (EtOH): 274.0, 236 nm; IR ν_{\max} 3447 (NH), 3407, 3349, 3152, 1634, 1549 cm⁻¹; δ_H (300 MHz, *d*₆-DMSO) 0.27-0.32 (2H, m, CH₂), 0.49-0.54 (2H, m, CH₂), 1.15-1.25 (1H, m, CH), 4.03 (2H, d, $J = 7.2$ Hz, OCH₂), 6.09 (2H, s, N¹H₂), 6.28 (2H, s, N²H₂); δ_C (75 MHz, *d*₆-DMSO): 3.3 (cyclopropyl), 10.5 (cyclopropyl), 70.4 (cyclopropyl), 161.4 (CNH₂), 162.2 (CNH₂), 165.3 (CO); LCMS $R_t = 2.34$ min, (1); MS (ESI+) m/z 259.91 [M+H]⁺ HRMS m/z : Calc. for C₈H₁₂⁷⁹BrN₄O: 259.0192 [M+H]⁺. Found 259.0192 [M+H]⁺. Analytical HPLC: 98.5% purity

N,N'-(5-Bromo-4-cyclopropylmethoxypyrimidine-2,6-diyl)diacetamide (**398**)

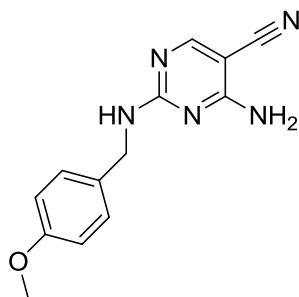
A mixture of 5-bromo-4-cyclopropylmethoxypyrimidine-2,6-diamine (1.03 g, 3.97 mmol, 1 eq) in acetic acid (12 mL, 207 mmol, 53 eq) and acetic anhydride (10 mL, 106 mmol, 27 eq) was heated to 80 °C for 17 h, cooled to room temperature and basified concentrated ammonia resulting in a white precipitate. The suspension was extracted into ethyl acetate (3 x 100 mL) and the combined organic layers washed with a saturated aqueous solution of NaHCO₃ (250 mL), dried over Na₂SO₄ and evaporated *in vacuo*. Chromatography (silica, EtOAc) gave **398** as a white solid (0.75g, 54%). *R_f* = 0.60 (100% EtOAc); mp = 191.3-192.5 °C; UV λ_{max} (EtOH): 256.0, 227.0 nm; IR ν_{max} 3207 (NH), 3140, 3003, 2925, 1674 (C=O), 1574, 1498 cm⁻¹; δ_H (300 MHz, *d*₆-DMSO): 0.35-0.41 (2H, m, CH₂), 0.52-0.60 (2H, m, CH₂), 1.24-1.37 (1H, m, CH), 2.17 (3H, s, COCH₃), 2.19 (3H, s, COCH₃), 4.25 (2H, d, *J* = 7.2 Hz, OCH₂), 9.96 (1H, s, N¹H), 10.49 (1H, s, N²H); δ_C (75 MHz, *d*₆-DMSO) 3.4 (cyclopropyl), 10.1 (cyclopropyl), 24.3 (COCH₃), 25.1 (COCH₃), 72.7 (CH₂), 169.5, 157.5; LCMS *R_t* = 3.07 min, (1); MS (ESI+) *m/z* 247.91 [M+H]⁺

2,6-Diamino-4-(cyclopropylmethoxy)pyrimidine-5-carbonitrile (**85**)

To a solution of **384** (80 mg, 0.23 mmol, 1 eq) in DMF (3 mL) was added CuCN (42 mg, 0.49 mmol, 2 eq) and the reaction heated to 120 °C for 4 h. After cooling to room temperature, ethylenediamine (1.20 mL, 18.0 mmol) was added and stirring continued for 20 h. The mixture was before diluted with water (10 mL), filtered through Celite and washed with further water (2 x 5 mL). The filtrate solution was extracted with EtOAc (3 x 30 mL), and the combined organic extracts washed with brine (40 mL), dried over Na₂SO₄ and concentrated *in vacuo*. Chromatography (SP4, silica, 18-100% EtOAc, PE) gave **85** as a white solid (39 mg, 82%). *R_f* = 0.55 (7:3 EtOAc:PE); mp = 216.2-217.7 °C; UV λ_{max} (EtOH): 265.5, 251.0, 216.5 nm; IR ν_{max} 3500 (NH), 3437,

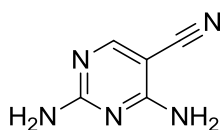
3379, 3096, 2202 (CN), 1666 cm^{-1} ; δ_{H} (500 MHz, d_6 -DMSO): 0.05-0.08 (2H, m, cyclopropyl), 0.30 (2H, ddt, $J = 4.2, 5.8$ and 7.9 Hz, cyclopropyl CH_2), 0.94-1.00 (1H, m, cyclopropyl), 3.87 (2H, d, $J = 7.2$ Hz, OCH_2), 6.60 (2H, s, N^1H_2), 6.65 (2H, s, N^2H_2); δ_{C} (125 MHz, d_6 -DMSO): 3.09 (cyclopropyl), 9.90 (cyclopropyl), 62.7 (C^5), 70.4 (OCH_2), 116.1 (CN), 162.9 (C^2), 165.8 (C^6), 170.8 (C^4); LCMS $R_t = 1.01$ min (3); MS (ESI+) $m/z = 206.3$ $[\text{M}+\text{H}]^+$; HRMS m/z : Calc. for $\text{C}_9\text{H}_{11}\text{N}_5\text{O}$: 206.1036 $[\text{M}+\text{H}]^+$. Found 206.1034 $[\text{M}+\text{H}]^+$.; Analytical HPLC: 98.6% purity

6-Amino-2-(4-methoxybenzylamino)pyrimidine-5-carbonitrile (**88**)



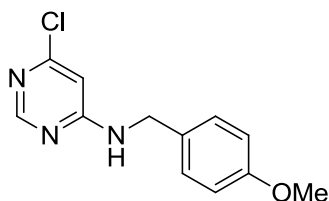
6-Amino-2-chloropyrimidine-5-carbonitrile (250 mg, 1.25 mmol, 1 eq) was dissolved in DMF (10 mL) and 4-methoxybenzylamine (0.54 mL, 3.88 mmol, 2.4 eq) was added. The reaction temperature was increased to 100 $^{\circ}\text{C}$. After 3 h the reaction mixture was cooled to room temperature and diluted with water (40 mL) resulting in a white precipitate which was collected by filtration to give **88** as a white solid used without further purification (375 mg, 91%). $R_f = 0.50$ (1:1 EtOAc:PE); mp = 227.6-228.2 $^{\circ}\text{C}$; UV λ_{max} (EtOH): 220.0, 257.5; IR ν_{max} 3431 (NH), 3337 (NH), 3206, 2210 (CN), 1641, 1578, 1504 cm^{-1} ; δ_{H} (300 MHz d_6 -DMSO): 3.72 (3H, s, OCH_3), 4.39 (2H, d, $J = 5.5$ Hz, NHCH_2), 6.86-6.88 (2H, m, Ar-H), 7.13 (1H, s, NH^1), 7.23-7.25 (2H, m, Ar-H), 7.82 (1H, s, NH^2), 8.00 (1H, s, NH), 8.17 (1H, s, H^4); δ_{C} (125 MHz d_6 -DMSO): 43.1 (CH_2), 55.0 (OCH_3), 77.7 (C^5), 113.7 (benzyl Ar-H), 117.5 (CN), 128.6 (benzyl Ar-H), 131.6 (CCH_2), , 158.1 (COCH_3), 162.2 (CH), 162.2 (CNH), 163.2 (CNH $_2$); LCMS $R_t = 2.10$ min, (1); MS (ESI+) $m/z = 256.06$ $[\text{M}+\text{H}]^+$

2,6-Diaminopyrimidine-5-carbonitrile (**86**)

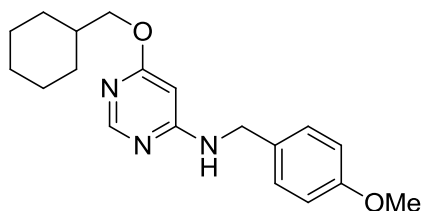


6-Amino-2-(4-methoxybenzylamino)pyrimidine-5-carbonitrile (**88**) (334 mg, 1.31 mmol, 1 eq) was suspended in DCM (4.5 mL) was TFA (10.5 mL) added slowly and the mixture heated to reflux for 18 h, then cooled room temperature, neutralised using saturated sodium bicarbonate, and extracted using DCM (4 x 100 mL). The combined organic layers were concentrated *in vacuo*. The resulting white solid was redissolved in THF (300 mL) and dried over Na₂SO₄ and evaporated. Chromatography (100% EtOAc) gave the title compound as a white solid (138 mg, 77%). $R_f = 0.35$ (100% EtOAc); mp > 300 °C (lit. 318 °C)²⁶⁷; UV λ_{max} (EtOH): 284.5; IR ν_{max} 3430 (NH), 3082, 2201 (CN), 1647, 1582, 1545 cm⁻¹; δ_H (500 MHz *d*₆-DMSO): 6.93 (1H, s, NH¹), 7.03 (1H, s, NH²), 7.15 (2H, s, NH₂), 8.20 (1H, s, H⁴); δ_C (125 MHz *d*₆-DMSO): 78.3 (C⁵), 162.3 (CH), 163.2 (CNH₂), 163.6 (CNH₂); HRMS m/z : Calc. for C₅H₆N₅: 136.0618 [M+H]⁺. Found 136.0617 [M+H]⁺.; Analytical HPLC: 98.9% purity

4-Chloro-N-(6-methoxybenzyl)pyrimidin-4-amine (**91**)



A mixture of 4,6-dichloropyrimidine (103 mg, 0.69 mmol, 1 eq), 4-methoxybenzylamine (0.078 mL, 0.60 mmol, 0.86 eq) and DIPEA (0.23 mL, 1.34 mmol, 1.9 eq) in 2-propanol (2.5 mL) was heated by microwave for 20 min at 120 °C. After cooling to room temperature the solvent was evaporated *in vacuo*. Chromatography (silica, 30% EtOAc, PE) gave the title compound as a white solid (140 mg, 83%). $R_f = 0.31$ (3:7 EtOAc:PE); mp = 132.3-133.0 °C (lit. 118-120 °C)²⁶⁸; UV λ_{max} (EtOH): 248.5 nm; IR ν_{max} 3221 (NH), 3077, 1595, 1561, 1506 cm⁻¹; δ_H (300 MHz CDCl₃): 3.82 (3H, s, CH₃), 4.44 (2H, broad s, CH₂), 6.35 (1H, s, H⁵), 6.90 (2H, d, $J = 8.4$ Hz, Ar-H), 7.25 (2H, d, $J = 8.4$ Hz, Ar-H), 8.23 (1H, s, H²); δ_C (125 MHz CDCl₃): 45.2 (CH₂), 55.3 (CH₃), 114.3 (Benzyl CH), 128.9 (benzyl CH), 158.4 (C²), 159.4 (CCl), 163.2 (CNH); LCMS $R_t = 2.77$ min, (1); MS (ESI+) m/z 250.0 [M+H]⁺

4-(Cyclohexylmethoxy)-N-(4-methoxybenzyl) pyrimidin-6-amine (**92**)

Method A: using conventional heating

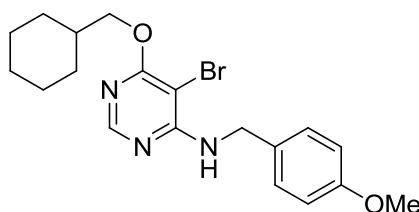
To cyclohexylmethanol (5.0 mL, 40 mmol, 20 eq) was added sodium (0.06 g, 2.6 mmol, 1.3 eq) in portions, the reaction mixture was heated at 160 °C until all sodium had dissolved, 4-chloro-*N*-(6-methoxybenzyl) pyrimidin-4-amine (**91**) (500 mg, 2.0 mmol, 1 eq) was added and the temperature increased to 180 °C for 30 min, then cooled to room temperature and neutralised using acetic acid. Petrol (30 mL) was added and the solution cooled to 4 °C overnight. The resulting precipitate was collected by filtration and the filtrate evaporated. Further petroleum ether (20 mL) was added to this filtrate and the solution cooled to 4 °C. This was repeated until no further solid formed. Recrystallisation (methanol) gave **92** as a white solid (500 mg, 76%).

Method B: using microwave assisted heating

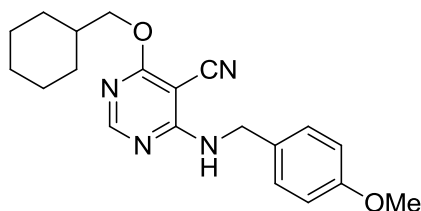
To a solution of cyclohexylmethanol (1.30 mL, 10.6 mmol, 5.3 eq) in THF (10 mL) was added . NaH (140 mg, 5.83 mmol, 2.9 eq) and the mixture stirred at room temperature for 45 min. 4-Chloro-*N*-(6-methoxybenzyl)pyrimidin-4-amine (**91**) (500 mg, 2.00 mmol, 1 eq) was added and the reaction mixture was stirred for 20 min at room temperature. The vial was then heated at 120 °C for 18 min then cooled to room temperature and neutralised using acetic acid. The solvent was evaporated to give a cream coloured oily solid. Petroleum ether (100 mL) was added to the residue and it was then cooled to 4 °C. The resulting white precipitate was then filtered. The filtrate was then evaporated and further petrol (100 mL) was added and cooled to 4 °C any further precipitate was then collected by filtration. The combined solid was recrystallised (methanol) to give **92** as a white solid (471 mg, 72%).

$R_f = 0.79$ (8:2 EtOAc:PE); mp = 112.4-113.2 °C; UV λ_{\max} (EtOH): 245.5, 356.0 nm; IR ν_{\max} 3216 (NH), 2917, 2850, 1588, 1561, 1510 cm^{-1} ; δ_{H} (300 MHz CDCl_3) 0.97-1.31 (5H, m, C_6H_{11}), 1.60-1.85 (6H, m, C_6H_{11}), 3.83 (3H, s, CH_3), 4.07 (2H, d, $J = 6.3$ Hz, OCH_2), 4.39 (2H, d, $J = 5.4$ Hz, NHCH_2), 5.15 (1H, s, NH), 5.66 (1H, s, H^5), 6.90 (2H, d, $J = 8.4$ Hz, 2 x Ar-H), 7.25-7.28 (m, 2 x Ar-H), 8.27 (1H, s, H^2); δ_{C} (125 MHz CDCl_3): 25.8 (C_6H_{11}), 26.5 (C_6H_{11}), 29.8 (C_6H_{11}), 37.4 (CHCH_2O), 45.3 (NCH_2), 55.3 (OCH_3), 85.1 (OCH_2), 114.2 (benzyl Ar-H), 128.7 (benzyl Ar-H), 129.7 (CCH_2NH), 157.8 (COCH_3), 159.1 (CH), 164.1 (CNH), 170.3 (CO); LCMS $R_t = 3.17$ min, (1); MS (ESI+) m/z 328.25 $[\text{M}+\text{H}]^+$

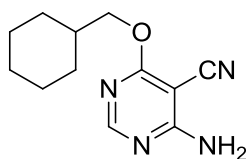
5-Bromo-4-(cyclohexylmethoxy)-N-(6-methoxybenzyl)pyrimidin-4-amine (**93**)



To a solution of 4-(cyclohexylmethoxy)-N-(4-methoxybenzyl)pyrimidin-6-amine (**92**) (100 mg, 0.31 mmol, 1 eq) in acetic acid (5 mL) was added *N*-bromosuccinimide (59 mg, 0.33 mmol, 1 eq) and the reaction stirred at room temperature for 1 h, then neutralised using 2.5 M aqueous solution of NaOH and extracted with ethyl acetate (3 x 30 mL). The combined organic extracts were dried over MgSO_4 and evaporated. Chromatography (silica, 30% EtOAc, PE) gave **93** as a white solid (87 mg, 69%). $R_f = 0.86$ (3:7 EtOAc:PE); mp = 62.4-63.7 °C; UV λ_{\max} (EtOH): 213.5, 251.0 nm; IR ν_{\max} 3417 (NH), 2922, 2843, 1578, 1503 cm^{-1} ; δ_{H} (300 MHz CDCl_3): 1.02-1.37 (5H, m, C_6H_{11}), 1.68-1.88 (6H, m, C_6H_{11}), 3.28 (3H, s, CH_3), 4.19 (2H, d, $J = 6$ Hz, OCH_2), 4.65 (2H, d, $J = 5.4$ Hz, NHCH_2), 5.53 (1H, s, NH), 6.90 (2H, d, $J = 8.7$ Hz, 2 x Ar-H), 7.28 (2H, d, $J = 8.7$ Hz, 2 x Ar-H), 8.22 (1H, s, H^2); δ_{C} (75 MHz CDCl_3): 26.1 (C_6H_{11}), 26.9 (C_6H_{11}), 30.1 (C_6H_{11}), 37.9 (CHCH_2O), 45.4 (CH_2NH), 55.7 (COCH_3), 72.7 (OCH_2), 86.6 (C^5), 114.7 (benzyl Ar-H), 129.2 (benzyl Ar-H), 131.2 (CCH_2NH), 155.9 (COCH_3), 159.7 (CH), 160.3 (CNH), 165.3 (CO); LCMS $R_t = 4.51$ min, (1); MS (ESI+) m/z 406.26 $[\text{M}+\text{H}]^+$

4-(Cyclohexylmethoxy)-6-(4-methoxybenzylamino)pyrimidine-5-carbonitrile (**94**)

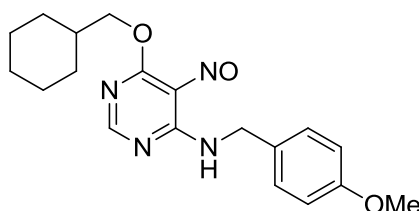
To a solution of 5-bromo-4-(cyclohexylmethoxy)-*N*-(6-methoxybenzyl)pyrimidin-4-amine (**93**) (280 mg, 0.69 mmol, 1 eq) in DMF (5 mL) was added CuCN (79 mg, 89 mmol, 1.3 eq) and the reaction heated to 120 °C. After 3 days the reaction was cooled to room temperature and ethylenediamine (5 mL, 75 mmol, 108 eq) added. After stirring at room temperature for 3 days the mixture was filtered through Celite, washed with further DMF (15 mL), diluted with water (30 mL) and extracted with EtOAc (3 x 100 mL). The combined organic layers were then dried (MgSO₄) and evaporated to give a brown oil. Chromatography (silica, 20% EtOAc, PE) gave the title compound as a white solid (68 mg, 28%). *R*_f = 0.59 (2:8 EtOAc:PE); mp = 119.8-120.4 °C; UV λ_{max} (EtOH): 228.0, 249.0, 296.5 nm; IR ν_{max} 3337 (NH), 2925, 2855, 2218 (CN), 1582, 1512 cm⁻¹; δ_H (500 MHz CDCl₃): 0.92-1.24 (5H, m, C₆H₁₁), 1.60-1.76 (6H, m, C₆H₁₁), 3.74 (3H, s, OCH₃), 4.14 (2H, d, *J* = 6.5 Hz, OCH₂), 4.59 (2H, d, *J* = 5.5 Hz, NHCH₂), 6.81 (2H, d, *J* = 8.5 Hz, 2 x Ar-H), 7.18 (2H, d, *J* = 8.5 Hz, 2 x Ar-H), 8.29 (1H, s, *H*²); δ_C (125 MHz CDCl₃): 25.7 (C₆H₁₁), 26.4 (C₆H₁₁), 29.5 (C₆H₁₁), 37.2 (CHCH₂O), 44.8 (CH₂NH), 55.4 (OCH₃), 72.8 (OCH₂), 114.2 (benzyl Ar-H), 129.2 (benzyl Ar-H), 159.3 (COCH₃), 159.9 (CH), 163.5 (CNH), 170.5 (CO)

4-Amino-6-(cyclohexylmethoxy)pyrimidine-5-carbonitrile (**95**)

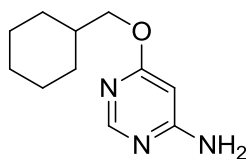
4-(Cyclohexylmethoxy)-6-(4-methoxybenzylamino)pyrimidine-5-carbonitrile (**94**) (63.9 mg, 0.18 mmol, 1 eq) was dissolved in DCM (3.5 mL) and TFA (1.5 mL) added dropwise. The reaction was heated to reflux for 18 h then neutralised using saturated sodium bicarbonate and extracted using DCM (3x 40 mL). The combined organic layers were dried over Na₂SO₄ and concentrated *in vacuo*. Chromatography (silica, 50% EtOAc, PE) gave white solid, compound (**95**) (21 mg, 50%). *R*_f = 0.64 (1:1 EtOAc:PE); mp = 133.1-134.0 °C; UV λ_{max} (EtOH): 283.5, 343.0, 384.0 nm; IR ν_{max}

3378 (NH), 3336, 3211, 2919, 2847, 2220 (CN), 1666, 1574, 1551 cm^{-1} ; δ_{H} (500 MHz CDCl_3): 0.93-1.26 (5H, m, C_6H_{11}), 1.61-1.77 (6H, m, C_6H_{11}), 4.16 (2H, d, $J = 3.6$ Hz, OCH_2), 5.62 (2H, broad s, NH_2), 8.23 (1H, s, H^2); δ_{C} (125 MHz CDCl_3): 25.7 (C_6H_{11}), 26.4 (C_6H_{11}), 29.7 (C_6H_{11}), 37.1 (CHCH_2O), 73.1 (CH_2O), 113.5 (CN), 160.0 (C^2), 165.0 (CNH), 170.6 (CO); LCMS $R_t = 3.25$ min, (1); MS (ESI+) m/z 232.90 $[\text{M}+\text{H}]^+$; HRMS m/z : Calc. for $\text{C}_{12}\text{H}_{17}\text{N}_4\text{O}$: 233.1397 $[\text{M}+\text{H}]^+$. Found 233.1395 $[\text{M}+\text{H}]^+$.
Analytical HPLC: 95.5% purity

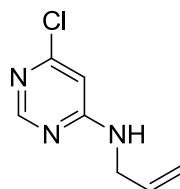
4-(Cyclohexylmethoxy)-N-(6-methoxybenzyl)-5-nitrosopyrimidin-4-amine (**96**)



To a solution of 4-(cyclohexylmethoxy)-N-(4-methoxybenzyl)pyrimidin-6-amine (**96**) (100 mg, 0.31 mmol, 1 eq) in 30% acetic acid in water (5 mL) at 80 °C. Sodium nitrite (30 mg, 0.43 mmol, 1.3 eq) in water (0.56 mL, resulting in a 0.7 M solution) was added dropwise and the mixture was stirred at 80 °C for 1 h, cooled to room temperature and neutralised using a 2.5 M aqueous solution of NaOH, then extracted with ethyl acetate (3x 50 mL). The combined organic layers were dried over MgSO_4 and concentrated *in vacuo*. Chromatography (silica, 50% EtOAc, PE) gave **96** as a yellow oil (87 mg, 79%). $R_f = 0.95$ (8:2 EtOAc:PE); UV λ_{max} (EtOH): 224.5, 275.0 nm; IR ν_{max} 3007 (NH), 2933, 2917, 2849, 1585, 1562 (NO), 1510 cm^{-1} ; δ_{H} (300 MHz CDCl_3): 1.04-1.32 (5H, m, C_6H_{11}), 1.75-1.86 (6H, m, C_6H_{11}), 3.76 (3H, s, CH_3), 4.21 (2H, d, $J = 6$ Hz, OCH_2), 5.31 (2H, s, NHCH_2), 6.79 (2H, d, $J = 8.7$ Hz, 2 x Ar-H), 7.25 (2H, d, $J = 8.4$ Hz, 2 x Ar-H), 7.32 (1H, s, NH), 8.71 (1H, s, H^2); δ_{C} (125 MHz CDCl_3): 25.7 (C_6H_{11}), 26.4 (C_6H_{11}), 29.7 (C_6H_{11}), 37.3 (CHCH_2O), 43.1 (CH_2NH), 55.2 (OCH_3), 72.5 (CH_2O), 93.5 (C^5), 113.8 (benzyl Ar-H), 127.0 (benzyl Ar-H), 130.0 (CCH_2NH), 157.9 (COCH_3), 159.0 (C^2), 161.6 (CNH), 171.0 (CO); LCMS $R_t = 4.22$ min, (1); MS (ESI+) m/z 357.28 $[\text{M}+\text{H}]^+$

4-(Cyclohexylmethoxy)pyrimidin-6-amine (**99**)

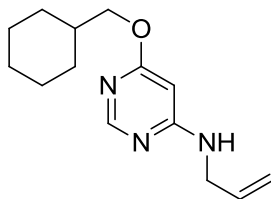
4-(Cyclohexylmethoxy)-N-(4-methoxybenzyl) pyrimidin-6-amine (**92**) (500 mg, 1.53 mmol, 1 eq) was dissolved in DCM (13.5 mL) and TFA (6 mL) was added dropwise. The reaction was heated to reflux for 41 h, then neutralised using a saturated sodium bicarbonate, then extracted using DCM (3x 40 mL). The combined organic layer were dried over MgSO₄ and evaporated. Chromatography (silica, 70% EtOAc, PE) gave compound (**99**) a white solid (245 mg, 77%). $R_f = 0.33$ (7:3 EtOAc:PE); mp = 179.6-180.1 °C; UV λ_{max} (EtOH): 283.5, 343.0, 384.0 nm; IR ν_{max} 3378 (NH), 3336, 3211, 2919, 2847, 2220, 1666, 1574, 1551 cm⁻¹; δ_H (300 MHz *d*₆-DMSO): 0.95-1.24 (5H, m, C₆H₁₁) 1.67-1.74 (6H, m, C₆H₁₁), 3.97 (2H, d, $J = 6.3$ Hz, OCH₂), 5.66 (1H, s, H^5), 6.58 (2H, s, NH₂), 8.06 (1H, s, H^2); δ_C (75 MHz *d*₆-DMSO): 25.6 (C₆H₁₁), 26.4 (C₆H₁₁), 29.6 (C₆H₁₁), 37.3 (CHCH₂O), 70.7 (CH₂O), 86.0 (C⁵), 158.0 (C²), 165.9 (CNH₂), 169.7 (CO); LCMS $R_t = 2.60$ min, (1); MS (ESI+) m/z 240.03 [M+H]⁺

N-Allyl-4-chloropyrimidin-6-amine (**100**)

To a solution of 4,6-dichloropyrimidine (500 mg, 3.36 mmol, 1 eq) in THF (10 mL) was added triethylamine (0.49 mmol, 3.52 mmol, 1.05 eq) and allylamine (264 μ L, 3.52 mmol, 1.05 eq). The reaction was stirred at room temperature for 24 h then the solvent was evaporated *in vacuo*. The resulting solid was suspended in water (40 mL) and extracted using DCM (3 x 50 mL). The combined organic layers were dried (MgSO₄) and evaporated *in vacuo*. Chromatography (SP4, silica, 15-100% EtOAc, PE) gave **100** as a colourless oil which solidified to a white solid (560 mg, 98%). $R_f = 0.52$ (1:1 EtOAc:PE) mp = 87.4-88.1 °C; UV λ_{max} (EtOH): 340.5, 246.0 nm; IR ν_{max} 3233 (NH), 3054 (alkene C-H), 3015, 2965, 1598 (alkene C-C), 1568, 1531 cm⁻¹; δ_H (500 MHz CDCl₃): 3.89 (2H, s, NHCH₂), 5.16-5.22 (2H, m, NHCH₂CHCH₂), 5.79-7.5.86 (1H, m, NHCH₂CHCH₂), 6.29 (1H, s, H^5), 8.28 (1H, s, H^2) δ_C (125 MHz

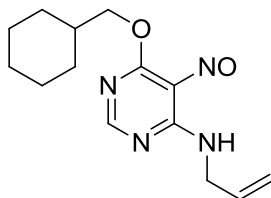
CDCl₃): 43.9 (NHCH₂), 117.3, (NHCH₂CHCH₂), 132.8 (NHCH₂CHCH₂), 158.2 (C²), 163.2 (C-Cl)

N-Allyl-4-(cyclohexylmethoxy)pyrimidin-6-amine (**101**)



Cyclohexylmethanol (1.01 mL, 8.84 mmol, 5 eq) was added to a microwave vial followed by THF (4mL) and NaH (0.13 mg, 3 eq). The reaction was stirred at rt for 30 min before *N*-allyl-4-chloropyrimidin-6-amine (300 mg, 177 mmol, 1 eq) was added, and the reaction irradiated at 120 °C for 20 min. The solvent was removed *in vacuo*. Chromatography (SP4, silica, 12-100 % EtOAc, PE) followed by SPE (C18 isoeolute, 20-80% MeOH with 0.1 % formic acid, 0.1 % formic acid_(aq)) gave **101** as a white solid (331 mg, 75%). *R*_f = 0.78 (1:1 EtOAc:PE); mp = 62.4-63.5 °C; UV λ_{max} (EtOH): 340.5, 245.0, 211.0 nm; IR ν_{max} 3231 (NH), 3080 (Alkene C-H), 2918, 2849, 1596 (Alkene C-C), 1573 cm⁻¹; δ_H (500 MHz CDCl₃): 0.94-1.24 (5H, m, C₆H₁₁), 1.60-1.77 (6H, m, C₆H₁₁), 3.79-3.81 (2H, m, NHCH₂), 4.00, (2H, d, *J* = 6.6 Hz, OCH₂), 5.13 (1H, dd, *J* = 10.3 and 1.3 Hz, 1 x NHCH₂CHCH₂), 5.20 (1H, dd, *J* = 17.2 and 1.3, 1 x NHCH₂CHCH₂), 5.57 (1H, s, H⁵), 5.85-5.78 (1H, m NHCH₂CH₂), 8.16 (1H, s, H²); δ_C (125 MHz CDCl₃): 25.7 (C₆H₁₁), 26.6 (C₆H₁₁), 29.8 (C₆H₁₁), 37.4 (CCH₂O), 44.1 (NHCH₂), 71.6 (OCH₂), 85.1 (C⁵), 116.8 (NHCH₂CHCH₂), 133.5 (NCH₂CHCH₂), 157.5 (C²), 163.8 (CNH), 170.4 (CO); LCMS *R*_t = 2.82 min; (ESI+) *m/z* 248.13 [M+H]⁺

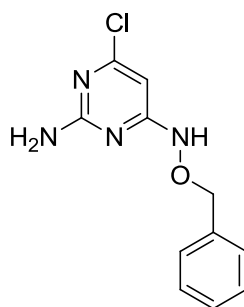
N-Allyl-4-(cyclohexylmethoxy)-5-nitrosopyrimidin-6-amine (**102**)



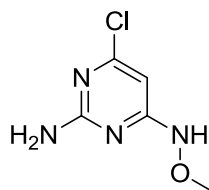
To a solution of *N*-allyl-4-(cyclohexylmethoxy)pyrimidin-6-amine (50 mg, 0.20 mmol, 1 eq) in acetic acid (1.5 mL) and water (3.5 mL) was added NaNO₂ (15 mg, 0.22 mmol, 1.1 eq) in water (1 mL) and the reaction heated to 80 °C for 75 min before then neutralised with a saturated NaHCO₃, and extracted with DCM (3 x 25 mL). The

combined organic layers dried (MgSO_4) and evaporated *in vacuo*. Chromatography (silica, 50% EtOAc, PE) gave **102** as a yellow oil (37 mg, 66%). $R_f = 0.94$ (1:1 EtOAc:PE); UV λ_{max} (EtOH): 340.5 nm; IR ν_{max} 2922, 1656 (Alkene C-C), 1588 (NO) cm^{-1} ; δ_{H} (500 MHz CDCl_3): 0.96-1.26 (5H, m, C_6H_{11}), 1.61-1.79 (6H, m, C_6H_{11}), 4.14 (2H, d, $J = 6.3$ Hz, OCH_2), 4.70-4.71 (2H, m, NHCH_2), 4.98-5.08 (1H, m, $\text{NHCH}_2\text{CHCH}_2$), 5.03-5.06 (1H, m, $\text{NHCH}_2\text{CHCH}_2$), 5.60-5.68 (1H, m, $\text{NHCH}_2\text{CHCH}_2$), 8.60 (1H, d, $J = 0.9$ Hz, H^2); δ_{C} (125 MHz CDCl_3): 25.5 (C_6H_{11}), 25.7 (C_6H_{11}), 26.4 (C_6H_{11}), 37.2 (CCH_2O), 42.6 (NHCH_2), 72.5 (OCH_2), 93.3 (C-NO), 118.1 ($\text{NHCH}_2\text{CHCH}_2$), 129.5 ($\text{NHCH}_2\text{CHCH}_2$), 158.0 (CNH), 161.4 (CO), 171.0 (C^2); LCMS $R_t = 3.98$ min (1); MS (ESI+) m/z 277.14 $[\text{M}+\text{H}]^+$

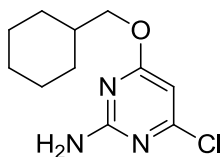
6-(Benzyloxyamino)-4-chloropyrimidin-2-amine (**109**)



A mixture of 2-amino-4,6-dichloropyrimidine (100 mg, 0.61 mmol, 1 eq), DMSO (5 mL), DIPEA (0.35 mL, 2.01 mmol, 3.3 eq) and *O*-benzylhydroxylamine (0.11 mL, 0.91 mmol, 1.5 eq) was heated to 130 °C for 6 h then cooled to room temperature, diluted with water (30 mL) and extracted using ethyl acetate (3 x 40 mL). The organic layers were dried over Na_2SO_4 and evaporated. Chromatography (silica, 30-50% EtOAc, PE) gave **109** as a white solid (101 mg, 66%). $R_f = 0.14$ (3:7 EtOAc:PE); mp = 172.3-172.9 °C; UV λ_{max} (EtOH): 208.5, 288.0, 341.5; IR ν_{max} 3470 (NH), 3298 (NH), 3173, 2918, 1632, 1593, 1546 cm^{-1} ; δ_{H} (500 MHz d_6 -DMSO): 4.84 (2H, s, OCH_2), 5.97 (1H, s, H^5), 6.73 (2H, s, NH_2), 7.44-7.46 (5H, m, Ar-H), 10.28 (1H, s, NH); δ_{C} (125 MHz d_6 -DMSO): 77.0 (CH_2), 90.2 (C^5), 128.4 (Ar-H), 128.9 (Ar-H), 136.0 (Ar-H), 159.5 (CCl), 162.5 (CNH_2), 167.0 (CNH); LCMS $R_t = 2.66$ min, (1); MS (ESI+) m/z 251.03 $[\text{M}+\text{H}]^+$

4-Chloro-6-(methoxyamino)pyrimidin-2-amine (**108**)

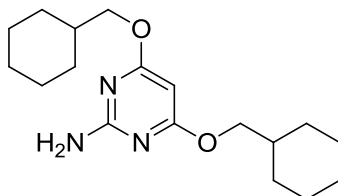
A solution of methoxyamine hydrochloride (229 mg, 2.7 mmol, 4.5 eq) and DIPEA (0.90 mL, 7.3 mmol, 12 eq) in DMSO (5 mL) was stirred at room temperature for 30 min. 2-Amino-4,6-dichloropyrimidine (100 mg, 0.61 mmol, 1 eq) was added and the mixture heated to 130 °C for 16 h then diluted with water (30 mL) and extracted with EtOAc (3 x 70 mL). The combined organic layers were dried over Na₂SO₄ and evaporated. Chromatography (silica, 50% EtOAc, PE) gave the title compound as a white solid (55 mg, 52%). $R_f = 0.38$ (1:1 EtOAc:PE); δ_H (500 MHz d_6 -DMSO): 3.61 (3H, s, CH₃), 5.93 (1H, s, H^5), 6.66 (2H, s, NH₂), 10.17 (1H, s, NH); LCMS $R_t = 0.72$ min, (1); MS (ESI+) m/z 174.93 [M+H]⁺

4-Chloro-6-(cyclohexylmethoxy)pyrimidin-2-amine (**112**)

To cyclohexylmethanol (15 mL, 122 mmol, 10 eq) was added sodium (0.25 g, 11.0 mmol, 0.9 eq) in portions, and the mixture heated to 100 °C until all sodium had dissolved. 2-Amino-4,6-dichloropyrimidine (2.00 g, 12.2 mmol, 1 eq) was added and the mixture stirred at 100 °C for 20 min, then cooled to room temperature, neutralised using acetic acid, diluted with petroleum ether (30 mL) and cooled to 4 °C. The precipitated solid was collected and purified using chromatography (silica, 30% EtOAc, PE). The filtrate was evaporated, diluted with petroleum ether and cooled to 4 °C. The collected solid was recrystallised from boiling methanol. The products were combined to give compound (**112**), a white solid (1.83 g 62%). $R_f = 0.61$ (3:7 EtOAc:PE); mp = 108.6-109.3 °C; UV λ_{max} (EtOH): 233.0, 278.0; IR ν_{max} 3349 (NH), 3221, 2926, 2849, 1653, 1538 cm⁻¹; δ_H (300 MHz d_6 -DMSO): 0.92-1.30 (5H, m, C₆H₁₁), 1.63-1.74 (6H, m, C₆H₁₁), 4.03 (2H, d, $J = 6.3$ Hz, OCH₂), 6.08 (1H, s, H^5), 7.04 (2H, s, NH₂); δ_C (75 MHz d_6 -DMSO): 25.8 (C₆H₁₁), 26.5 (C₆H₁₁), 29.8 (C₆H₁₁),

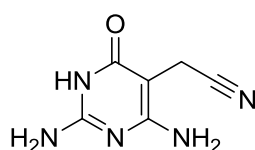
37.4 (CHCH₂O), 71.8 (CH₂O), 162.2 (Ar), 172.3 (CO); LCMS R_t = 3.36 min, (1); MS (ESI+) *m/z* 242.01 [M+H]⁺

4,6-Bis(cyclohexylmethoxy)pyrimidin-2-amine (**113**)



To cyclohexylmethanol (4.5 mL, 36 mmol, 60 eq) was added sodium (0.08, 3.49 mmol, 5.7 eq) in portions. The reaction mixture was heated to 120 °C and until all sodium had dissolved, 2-amino-4,6-dichloropyrimidine (100 mg, 0.61 mmol, 1 eq) was added and stirring continued at 120 °C followed by neutralisation using acetic acid. The mixture was diluted with petroleum ether (30 mL) cooled to 4 °C, and the white precipitate collected by filtration. Recrystallisation (methanol) gave the title compound as a white solid (65 mg, 33%). *R_f* = 0.70 (3:7 EtOAc:PE); mp = 114.0-114.7 °C; UV λ_{max} (EtOH): 299.5, 260.5; IR ν_{max} 3350 (NH), 3235, 2920, 2820, 1644, 1566 cm⁻¹; δ_H (500 MHz *d*₆-DMSO): 0.88-1.18 (10H, m, C₆H₁₁), 1.54-1.65 (12H, m, C₆H₁₁), 3.88 (4H, d, *J* = 3.6 Hz, 2 x OCH₂), 5.21 (1H, s, *H*⁵), 6.36 (2H, s, NH₂); δ_C (125 MHz CDCl₃): 25.8 (C₆H₁₁), 26.5 (C₆H₁₁), 29.8 (C₆H₁₁), 37.4 (CHCH₂O), 71.8 (CH₂O), 79.6 (C⁵), 162.2 (CNH₂), 172.4 (CO); LCMS R_t = 3.86 min, (1); MS (ESI+) *m/z* 320.23 [M+H]⁺

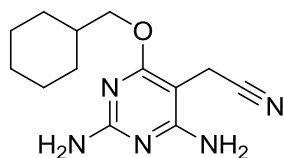
2-(2,4-Diamino-6-oxo-1,6-dihydropyrimidin-5-yl)acetonitrile (**116**)



To a solution of 2,6-diaminopyrimidone (250 mg, 1.98 mmol, 1 eq) and NaHCO₃ (366 mg, 4.36 mmol, 2.2 eq) in DMF (5 mL) was added bromoacetonitrile (0.30 mL, 4.36 mmol, 2.2 eq). The reaction was stirred at room temperature for 4 days, then concentration *in vacuo*, and water (40 mL) was added and the resulting precipitate was collected by filtration. Recrystallisation (ethanol) gave the title compound as beige needles (46 mg, 9%). *R_f* = 0.63 (3:7 MeOH:EtOAc); mp = dec; UV λ_{max} (EtOH): 211.5, 269.5; IR ν_{max} 3437 (NH), 3363 (Amide NH), 2903, 2829, 2712, 2246

(weak, CN), 1630 (C=O), 1591 (Amide C-N) cm^{-1} ; δ_{H} (300 MHz d_6 -DMSO) 3.36 (2H, CH₂), 6.23 (4H, m, 2 x NH₂), 10.08 (1H, s, NH); δ_{C} (75 MHz d_6 -DMSO): 11.9 (CH₂), 78.1 (C⁵), 119.7 (CN), 154.4 (CNH₂), 162.2 (CNH₂), 162.4 (C=O); LCMS R_t = 1.99 min, (2); MS (ESI+) m/z 166.12 [M+H]⁺

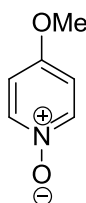
2-(2,4-Diamino-6-(cyclohexylmethoxy)pyrimidin-5-yl)acetonitrile (**117**)



A solution of **116** (244 mg, 1.48 mmol, 1 eq) and K₂CO₃ (230 mg, 1.63 mmol, 1.1 eq) in DMF (5 mL) was stirred at room temperature for 90 min, then (bromomethyl) cyclohexane (0.68 mL, 7.39 mmol, 5 eq) was added and the solution heated to 100 °C for 15h, cooled to room temperature, and poured into ice. The aqueous solution was extracted with EtOAc (4 x 70 mL), dried (Na₂SO₄) and concentrated *in vacuo*.

Chromatography (silica, 100% EtOAc) and crystallisation gave **117** as a brown solid (84 mg, 22%). R_f = 0.6 (100 % EtOAc); mp = 172.6-173.4 °C; UV λ_{max} (EtOH): 267.0, 234.5; IR ν_{max} 3438 (NH), 3355, 3140, 2932, 2854, 2251 (weak, CN), 1624, 1569 cm^{-1} ; δ_{H} (500 MHz d_6 -DMSO): 1.04-1.35 (6H, m, C₆H₁₁), 1.70-1.85 (5H, m, C₆H₁₁), 3.54 (2H, s, CH₂CN), 4.05 (2H, d, J = 6.0 Hz, OCH₂), 6.05 (2H, s, N¹H₂), 6.32 (2H, s, N²H₂); δ_{C} (500 MHz d_6 -DMSO): 25.3 (C₆H₁₁), 26.0 (C₆H₁₁), 29.1 (C₆H₁₁), 36.9 (CHCH₂O), 70.3 (CH₂O), 77.9 (C⁵), 119.0 (CN), 161.7 (CNH₂), 162.9 (CNH₂), 167.2 (CO); LCMS R_t = 2.29 min, (1); MS (ESI+) m/z 262.12 [M+H]⁺; HRMS m/z : Calc. for: C₁₃H₂₀N₅O 262.1662 [M+H]⁺. Found 262.1666 [M+H]⁺.; Analytical HPLC: 96.0% purity

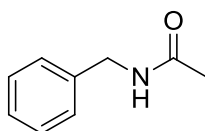
4-Methoxypyridine 1-oxide (**140**)



To 4-methoxypyridine (0.50 mL, 4.92 mmol, 1 eq) in DCM (10 mL) was added *m*-CPBA (1.28 g, 7.41 mmol, 1.5 eq) in portions, and the mixture stirred for 20 h, then evaporated. Chromatography (silica, 30% MeOH, EtOAc) gave **140** as a cream solid

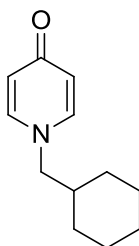
(0.48g, 79%). $R_f = 0.14$ (3:7 MeOH:EtOAc); mp = 101.7-102.3 °C (lit. 82-84 °C)²⁶⁹; UV λ_{\max} (EtOH): 205.0, 268.0; IR ν_{\max} 1561, 1286, 1207 cm^{-1} ; δ_{H} (300 MHz, d_6 -DMSO): 3.82 (3H, s, CH₃), 7.02 (2H, d, $J = 7.8$ Hz, Ar-H), 8.1 (2H, d, $J = 7.8$ Hz, Ar-H); δ_{C} (75 MHz d_6 -DMSO): 56.6 (CH₃), 112.7 (Ar-H), 139.8 (CO), 156.7 (CHN)

N-Benzylacetamide (**138**)



Benzylamine (2.0 mL, 18.3 mmol, 1 eq) and acetic anhydride (2.6 mL, 28 mmol, 1.5 eq) were heated to 150 °C for 2 h then cooled to room temperature, neutralised using 2.5 M NaOH solution, and extracted into ethyl acetate (3 x 50 mL). The combined organic layers were dried over MgSO₄ and concentrated *in vacuo*, resulting in a yellow oil which then crystallised. Chromatography (100% ethyl acetate) gave **138** as a white solid (0.74 g, 27%). $R_f = 0.33$ (100% EtOAc); mp = 62.9 – 63.8 °C (lit. 149.19 °C)²⁷⁰; UV λ_{\max} (EtOH): 379.5, 278.0, 244.5; IR ν_{\max} 3289 (NH), 1635 (C=O) cm^{-1} ; δ_{H} (300 MHz, d_6 -DMSO): 1.87 (3H, s, CH₃), 4.24 (2H, d, $J = 5.1$ Hz, CH₂), 7.23-7.32 (5H, m, 5 x Ar-H), 8.35 (1H, s, NH); δ_{C} (75 MHz d_6 -DMSO): 22.9 (COCH₃), 42.6 (CH₂), 127.0, 127.6, 128.5, 140.0 (CCH₂), 169.4 (C=O)

1-(Cyclohexylmethyl)pyridin-4(1H)-one (**137**)

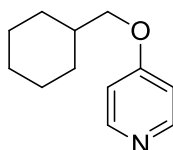


4-Pyridone (100 mg, 1.05 mmol, 1 eq) was added to a microwave vial in the dark, then DMSO (2 mL) was added, followed by the potassium carbonate (218 mg, 1.58 mmol, 1.5 eq) and the mixture was stirred for 1h at room temperature.

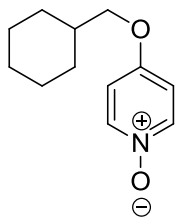
Cyclohexylmethanol (0.5 mL, 5.26 mmol, 5 eq) was added and the reaction then stirred at rt for 26 h. The mixture was added to ice water (50 mL) and extracted using DCM (3 x 50 mL). The combined organic layers were dried over MgSO₄ and evaporated. Chromatography (SP4, silica, 7-60% MeOH, EtOAc) gave the title compound as a colourless oil which solidified on standing (82 mg, 41%). $R_f = 0.5$ (3:7

MeOH:EtOAc); mp = 132.2-133.4 °C; UV λ_{\max} (EtOH): 263.5; IR ν_{\max} 3427 (NH), 3366, 3427, 3366, 3289, 2918, 2849, 1638 (C=O), 1531 cm^{-1} ; δ_{H} (300 MHz CDCl_3) 0.82-1.24 (5H, m, C_6H_{11}), 1.56-1.72 (6H, m, C_6H_{11}), 3.51 (2H, d, $J = 6.9$ Hz, NCH_2), 6.30 (2H, d, $J = 7.5$ Hz, CHCO), 7.17 (2H, d, $J = 7.5$ Hz, CHN); δ_{C} (75 MHz CDCl_3): 25.8 (C_6H_{11}), 26.4 (C_6H_{11}), 39.6 (C_6H_{11}), 41.5 (CHCH_2N), 63.5 (CH_2N), 118.9 (CHC=O), 140.2 (CHN), 179.1 (C=O), LCMS $R_t = 1.76$ min, (1); MS (ESI+) m/z 192.09 $[\text{M}+\text{H}]^+$

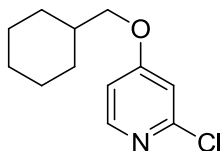
4-(Cyclohexylmethoxy)pyridine (**127**)



To cyclohexylmethanol (30 mL, 244 mmol, 18 eq) was added to sodium (1.30 g, 56.5 mmol, 4.3 eq) in portions and the mixture heated to 140 °C until all the sodium had dissolved the solution. The solution was allowed to cool for 10 min then 4-chloropyridine hydrochloride (2.00 g, 13.3 mmol, 1 eq) was added and the reaction temperature increased to 200 °C with vigorous stirring for 3.5 h. The reaction mixture was cooled to room temperature and neutralised using acetic acid, diluted with petroleum ether (100 mL) and the precipitate filtered. The filtrate was concentrated *in vacuo*, diluted with DCM (100 mL) and extracted using 1 M HCl (6 x 70 mL). The combined acidic layers were basified using 2.5 M NaOH, and extracted using DCM (12 x 100 mL). The combined organic layers were dried over MgSO_4 and evaporated to give a yellow oil. Chromatography (silica, 80% EtOAc, PE) gave **127** as a pale yellow solid (1.02 g, 53%). $R_f = 0.47$ (8:2 EtOAc:PE); mp = 60.2-61.6 °C; UV λ_{\max} (EtOH): 218.0, 328.0; IR ν_{\max} 2923, 2847, 1586, 1567 cm^{-1} ; δ_{H} (300 MHz CDCl_3): 1.01-1.32 (5H, m, C_6H_{11}), 1.72 -1.90 (6H, m, C_6H_{11}), 3.81 (2H, d, $J = 5.4$ Hz, CH_2), 6.80 (2H, d, $J = 4.8$ Hz, 2 x Ar-H), 8.42 (2H, d, $J = 4.8$ Hz, 2 x Ar-H); δ_{C} (75 MHz CDCl_3): 26.1 (C_6H_{11}), 26.8 (C_6H_{11}), 30.2 (C_6H_{11}), 37.9 (CHCH_2O), 73.6 (CH_2O), 110.7 (CHCO), 151.4 (CHN), 165.7 (CO); LCMS $R_t = 1.24$ min, (1); MS (ESI+) m/z 192.08 $[\text{M}+\text{H}]^+$

4-(Cyclohexylmethoxy)pyridine-1-oxide (**128**)

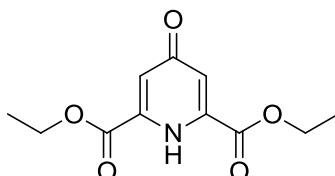
To a solution of 4-cyclohexylmethoxypyridine (1.52 g, 7.93 mmol, 1 eq) in DCM (15 mL) was added *m*CPBA (2.29 g of 65% purity, 18.0 mmol, 1.5 eq) with stirring at room temperature for 2 days. The reaction mixture was then diluted with DCM (20 mL) and washed with a sat. NaHSO₃ (3 x 50 mL). The organic layer was then dried over MgSO₄ and evaporated. Chromatography (silica, 3-30% MeOH, EtOAc) to give the title compound as a white solid (1.59 g, 97%). *R*_f = 0.17 (1:9 MeOH:EtOAc); UV λ_{max} (EtOH): 202.0, 208.0, 261.0, 265.0, 268.5, 276.0; IR ν_{max} 3105, 3028, 2924, 2850, 1611, 1553 cm⁻¹; δ_H (300 MHz CDCl₃): 0.99-1.33 (5H, m, C₆H₁₁), 1.75-1.85 (6H, m, C₆H₁₁), 3.79 (2H, d, *J* = 6 Hz CH₂), 6.80 (2H, d, *J* = 7.5 Hz, 2 x Ar-H), 8.13 (2H, d, *J* = 7.5 Hz, 2 x Ar-H); δ_C (75 MHz CDCl₃): 26.0 (C₆H₁₁), 26.7 (C₆H₁₁), 30.0 (C₆H₁₁), 37.8 (CHCH₂O), 75.0 (CH₂O), 112.5, 140.4; LCMS *R*_t = 9.40 min, (2); MS (ESI+) *m/z* 208.19 [M+H]⁺

2-Chloro-4-(cyclohexylmethoxy)pyridine (**142**)

A solution of 4-(cyclohexylmethoxy)pyridine 1-oxide (**128**) (0.646 g, 3.11 mmol, 1 eq) in acetonitrile (6 mL) was added phosphorus oxychloride (7.5 mL, 107 mmol, 34 eq) was added and the mixture was heated at 160 °C for 30 min in a microwave, then poured into ice (2 x 20 mL) and stirred overnight. The aqueous solution was basified using 1M aqueous KOH solution and extracted using DCM (9 x 100 mL). The combined organic layers were then dried over MgSO₄ and concentrated *in vacuo* to give a brown oil. Chromatography (silica, 100% EtOAc) gave the title compound as a brown oil (0.40 g, 56%). *R*_f = 0.87 (100% EtOAc); mp = 49.2-49.8 °C; UV λ_{max} (EtOH): 217.5; IR ν_{max} 3073, 2922, 2846, 1730, 1584, 1551 cm⁻¹; δ_H (300 MHz CDCl₃) 0.78-1.25 (5H, m, C₆H₁₁), 1.62-1.78 (6H, m, C₆H₁₁), 3.72 (2H, d, *J* = 6.0 Hz, CH₂), 6.66 (1H, dd, *J* = 2.4 and 6.0 Hz, CHCO), 6.74 (1H, d, *J* = 2.1 Hz, CHCCL),

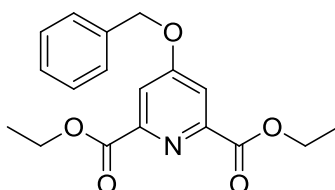
8.09 (1H, d, $J = 6.0$ Hz, NCH); δ_C (75 MHz CDCl_3): 26.0 (C_6H_{11}), 26.7 (C_6H_{11}), 30.1 (C_6H_{11}), 37.8 (CHCH_2O), 74.3 (CH_2O), 110.3 (C^2), 110.4 (C^1), 150.5 (CCl), 153.1 (C^3), 167.4 (CO); LCMS $R_t = 3.93$ min, (1); MS (ESI+) m/z 226.11 $[\text{M}+\text{H}]^+$

Diethyl 4-oxo-1,4-dihydropyridine-2,6-dicarboxylate (**153**)



To a solution of chelidamic acid monohydrate (500 mg, 2.73 mmol, 1 eq) in ethanol (15 mL) was added thionyl chloride (0.8 mL, 10.9 mmol, 4 eq) dropwise. The reaction heated to reflux for 2 h, then cooled to room temperature and the solvent evaporated. The mixture was neutralised using a saturated sodium bicarbonate solution, and the solvent evaporated. The residue was diluted with water (15 mL) and extracted using EtOAc (3 x 40 mL). The combined organic extracts were dried over MgSO_4 and concentrated *in vacuo*. Chromatography (SP4, silica, 12-100% EtOAc, PE) gave the title compound as a white solid (0.30 g, 46%). $R_f = 0.38$ (100% EtOAc); mp = 118.2-118.8 °C (lit 115-116 °C)²⁷¹; UV λ_{max} (EtOH): 214.5; IR ν_{max} 2985, 1722 (Ester C=O), 1603 (Pyridone C=O), 1568 cm^{-1} ; δ_H (500 MHz CDCl_3): 1.29 (6H, t, $J = 7.5$ Hz, CH_3), 4.34 (4H, q, $J = 7.5$ Hz, CH_2), 7.49 (2H, s, Ar-H); δ_C (125 MHz CDCl_3): 14.1 (CH_3), 63.0 (CH_2), 118.7 (Ar-H), 162.6 (COOEt); LCMS $R_t = 2.34$ min, (1); MS (ESI+) m/z 240.01 $[\text{M}+\text{H}]^+$

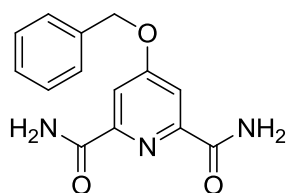
Diethyl 4-(benzyloxy)pyridine-2,6-dicarboxylate (**154**)



To a solution of diethyl 4-oxo-1,4-dihydropyridine-2,6-dicarboxylate (**153**) (500 mg, 2.09 mmol, 1 eq) in DMF (5 mL) was added K_2CO_3 (318 mg, 2.30 mmol, 1.1 eq) and benzyl bromide (0.255 mL, 2.14 mmol, 1.03 eq). The reaction was heated to 80 °C for 30 min, then cooled to room temperature and water (20 mL) was added, and extracted using EtOAc (3 x 50 mL). The combined organic layers were dried over Na_2SO_4 and evaporated. Chromatography (silica, 40% EtOAc, PE) gave compound **154** a white

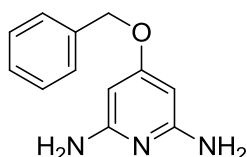
solid (659 mg, 96%). $R_f = 0.46$ (4:6 EtOAc:PE); mp = 74.6-75.2 °C; UV λ_{\max} (EtOH): 215.5; IR ν_{\max} 3075, 2975, 1712 (Ester C=O), 1592, 1567 cm^{-1} ; δ_{H} (300 MHz CDCl_3): 1.35 (6H, t, $J = 7.2$ Hz, CH_3), 4.37 (4H, q, $J = 7.2$ Hz, CH_2), 5.13 (2H, s, OCH_2), 7.26-7.34 (5H, m, C_6H_5), 7.78 (2H, s, Ar-H); δ_{C} (75 MHz CDCl_3): 13.2 (CH_3), 61.2 (CH_2CH_3), 69.9 (OCH_2), 113.6 (Ar-H), 126.7 (benzyl Ar-H), 127.7 benzyl (Ar-H), 127.9 (benzyl Ar-H), 134.1 (CCH_2), 149.7 (CCO_2Et), 163.7 (C-O), 165.7 (C=O); LCMS $R_t = 3.81$ min, (1); MS (ESI+) m/z 330.14 $[\text{M}+\text{H}]^+$

4-(Benzyloxy)pyridine-2,6-dicarboxamide (**152**)



A solution of diethyl 4-(benzyloxy)pyridine-2,6-dicarboxylate (**150**) (290 mg, 0.88 mmol, 1 eq) in 7 N methanolic ammonia in methanol (10 mL, 70 mmol, 80 eq) was stirred for 3.5 h. The white precipitate was collected by filtration and used without further purification. The filtrate was concentrated *in vacuo*. Chromatography (SP4, silica, 2-20% MeOH, EtOAc) gave a white solid compound (**152**) (212 mg, 88%) in total. $R_f = 0.26$ (100% EtOAc); mp = 271.3-272.1 °C (lit: > 220 °C)¹⁸⁰; UV λ_{\max} (EtOH): 214.0 nm; IR ν_{\max} 3076 (NH), 1711, 1663 (Amide C=O), 1591, 1564 (NH) cm^{-1} ; δ_{H} (500 MHz d_6 -DMSO): 5.29 (2H, s, OCH_2), 7.28-7.42 (5H, m, Ar-H), 7.65 (2H, s, NH), 7.67 (2H, s, Ar-H), 8.77 (2H, s, NH); δ_{C} (125 MHz d_6 -DMSO): 69.8 (CH_2), 110.5 (Ar-H), 127.7 (benzyl Ar-H), 128.1 (benzyl Ar-H), 128.8 (benzyl Ar-H), 135.8 (CCH_2O), 151.2 (CCONH_2), 165.1 (CO), 166.7 (C=O); LCMS $R_t = 3.04$ min, (1); MS (ESI+) m/z 272.00 $[\text{M}+\text{H}]^+$

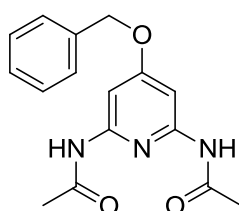
4-Benzyloxy-2,6-diaminopyridine (**153**)



To an aqueous solution of 5M KOH (60 mL, 300 mmol, 55 eq) was added bromine (700 μL , 13.6 mmol, 2.5 eq) followed by 4-benzyloxy-2,6-diaminopyridine (1.48 g, 5.45 mmol, 1 eq). The mixture was heated to 90 °C for 2 h, cooled to room temperature, and extracted with DCM (6 x 100 mL), and THF (3 x 60 mL). The

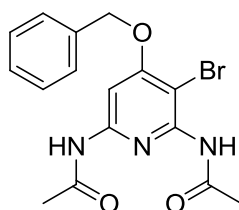
combined organic layers were dried (MgSO_4). Chromatography (SP4, silica, 3-20% MeOH, EtOAc) gave **153** as a white solid (837 mg, 71%). $R_f = 0.2$ (1:9 MeOH:EtOAc); mp. = 166.2 -167.0 °C (lit. 164-166 °C)¹⁸⁰; UV λ_{max} (EtOH): 289.0, 248.0 nm; IR ν_{max} 3372 (NH), 3188, 2198, 1590, 1559 cm^{-1} ; δ_{H} (500 MHz d_6 -DMSO): 5.02 (2H, s, OCH_2), 5.39 (2H, s, Ar-H), 5.40 (4H, s, NH_2), 7.38-7.45 (5H, m, benzyl); δ_{C} (125 MHz d_6 -DMSO): 68.3 (OCH_2), 82.3 (Ar-H), 127.4 (benzyl Ar-H), 127.7 (benzyl Ar-H), 128.4 (benzyl Ar-H), 137.1 (CCH_2O), 159.7 (CNH_2), 167.1 (CO); LCMS $R_t = 2.00$ min (1); MS (ESI+) m/z 216.04 $[\text{M}+\text{H}]^+$

N,N'-(4-Benzyloxy-2,6-diylo)diacetamide (**155**)



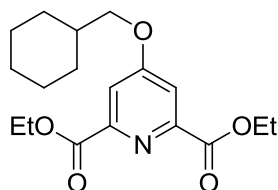
A mixture of 4-benzyloxy-2,6-diaminopyridine (193 mg, 0.90 mmol, 1 eq), acetic acid (3 mL) and acetic anhydride (3 mL) was stirred at room temperature for 3 days, then diluted with water (15 mL) and neutralised with ammonia. The resulting precipitate was collected by filtration, dissolved in DCM (20 mL), dried (MgSO_4) and the solvent removed *in vacuo*. Chromatography (silica, 10% MeOH, EtOAc) gave **155** as a white solid (247 mg, 92%). $R_f = 0.66$ (1:9 MeOH:EtOAc) mp.= 116.6-117.3 °C; UV λ_{max} (EtOH): 340.5, 283.0, 218.5 nm; IR ν_{max} 3322 (NH), 1663 (C=O), 1618, 1580, 1521 cm^{-1} ; δ_{H} (500 MHz CDCl_3): 2.08 (6H, s, 2 x CH_3), 5.05 (2H, s, OCH_2), 7.25-7.36 (5H, m, benzyl), 7.55 (2H, Ar-H), 7.70 (2H, s, NH); δ_{C} (125 MHz CDCl_3): 23.7 (CH_3), 69.4 (OCH_2), 95.5 (Ar-H), 126.7 (benzyl Ar-H), 127.2 (benzyl Ar-H), 127.6 (benzyl Ar-H), 134.7 (CCH_2O), 149.5 (CNH), 167 (CO); LCMS $R_t = 2.49$ min; MS (ESI+) m/z 300.16 $[\text{M}+\text{H}]^+$

N,N'-(4-Benzyloxy-3-bromopyridine-2,6-diylo)diacetamide (**156**)

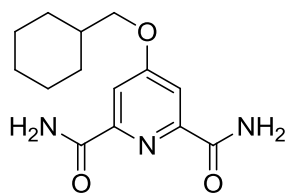


To a solution of *N,N'*-(4-benzyloxypyridine-2,6-diyl)diacetamide (117 mg, 0.39 mmol, 1 eq) and acetic acid (7 mL), *N*-bromosuccinimide (69 mg, 0.39 mmol, 1 eq) was added, then stirred at room temperature for 30 min and neutralised with NaOH (2.5 M). The resulting precipitate was collected by filtration, dissolved in DCM (30 mL), dried (MgSO₄) and evaporated *in vacuo*. Chromatography (silica, 10% MeOH, EtOAc) to give **156** as a white solid (0.115 mg, 77%). $R_f = 0.7$ (1:9 MeOH:EtOAc) mp. = 212.0-212.6 °C; UV λ_{\max} (EtOH): 340.5, 257.5, 221.5 nm; IR ν_{\max} 3327 (NH), 1669 (C=O), 1590, 1590, 1559, 1511 cm⁻¹; δ_H (500 MHz *d*₆-DMSO): 2.06 (3H, s, CH₃), 2.13 (3H, s, CH₃), 5.31 (2H, s, OCH₂), 7.41-7.7.56 (5H, m, benzyl), 7.95 (1H, s, Ar-H), 9.97 (1H, s, NH), 10.68 (1H, s, NH); δ_C (125 MHz *d*₆-DMSO): 22.8 (CH₃), 24.0 (CH₃), 70.4 (OCH₂), 96.5(Ar-H), 127.6 (benzyl Ar-H), 128.2 (benzyl Ar-H), 128.5 (benzyl Ar-H), 135.6 (CCH₂O), 148.6 (CNH₂), 151.1 (CNH₂), 163.1 (carbonyl), 168.5 (carbonyl), 169.6 (CO); LCMS $R_t = 2.80$ min (1); MS (ESI+) m/z 378.06 [M+H]⁺

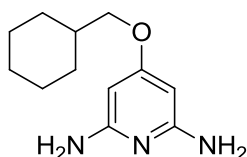
4-Cyclohexylmethoxypyridine-2,6-dicarboxylic acid diethyl ester (**157**)



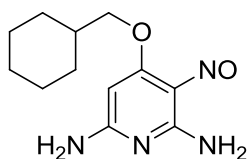
A mixture of diethyl 5-oxocyclohexa-3,6-diene-1,3-dicarboxylate (1.00 g, 4.18 mmol, 1 eq), DMF (7 mL), K₂CO₃ (0.64 g, 4.60 mmol, 1.1 eq) and (bromomethyl) cyclohexane (0.70 mL, 5.02 mmol, 1.2 eq) was heated to 80 °C for 16 h, cooled to room temperature, diluted with saturated NaHCO₃ (20 mL) and extracted using DCM (3 x 30 mL). The combined organic layers were dried (MgSO₄) and evaporated *in vacuo*. Chromatography (silica, 50% EtOAc, PE) gave **157** as a colourless oil (491 mg, 70%). $R_f = 0.75$ (1:1 EtOAc:PE); UV λ_{\max} (EtOH): 340.5, 213.5 nm; IR ν_{\max} 2926, 2853, 1717 (Ester C=O), 1593 cm⁻¹; δ_H (500 MHz CDCl₃): 1.00 (5H, m, C₆H₁₁), 1.38 (6H, t, 7.2 Hz, OCH₂CH₃), 1.62-1.81 (6H, m, C₆H₁₁), 3.85 (2H, d, $J = 6.0$ Hz, OCH₂), 4.40 (4H, q, $J = 7.2$ Hz, OCH₂CH₃), 7.70 (2H, s, Ar-H); δ_C (125 MHz CDCl₃): 14.1 (CH₃), 25.6 (C₆H₁₁), 26.3 (C₆H₁₁), 29.6 (C₆H₁₁), 37.4 (CCH₂O), 62.4 (OCH₂CH₃), 74.3 (OCH₂), 114.4 (Ar-H), 150.1 (CCO₂Et), 164.8 (CO), 167.2 (C=O)

4-Cyclohexylmethoxypyridine-2,6-dicarboxamide (**158**)

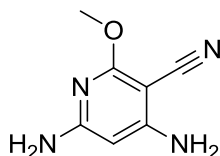
4-Cyclohexylmethoxypyridine-2,6-dicarboxylic acid diethyl ester (270 mg, 0.80 mmol, 1 eq) was dissolved in 7 M methanoic ammonia (7 mL, 49 mmol, 61 eq) and stirred at room temperature for 1h. The white precipitate was collected by filtration and recrystallised from boiling methanol to give the title compound as a white solid (105 mg, 47%). $R_f = 0.68$ (1:9 MeOH:EtOAc) mp = 269.0-269.9 °C; UV λ_{max} (EtOH): 340.5, 212.0 nm; IR ν_{max} 3447 (NH), 3341, 3181, 2921, 2845, 1672 (C=O), 1588 (NH) cm^{-1} ; δ_H (500 MHz d_6 -DMSO) 1.08-1.35 (5H, m, C_6H_{11}), 1.69-1.86 (6H, m, C_6H_{11}), 4.05 (2H, d, $J = 5.9$ Hz, OCH_2), 7.68 (2H, s, Ar-H), 7.76 (2H, d, $J = 1.8$ Hz, NH), 8.89 (2H, d, $J = 1.75$ Hz, NH) δ_C (125 MHz d_6 -DMSO): 25.1 (C_6H_{11}), 25.9 (C_6H_{11}), 28.9 (C_6H_{11}), 39.0 (CCH_2O), 73.3 (OCH_2), 110.0 (Ar-H), 151.2 (CCONH_2), 165.2 (CO), 167.2 (C=O); LCMS $R_t = 2.73$ min (1); ESI+ m/z 278.12 [$\text{M}+\text{H}$] $^+$

4-Cyclohexylmethoxy-2,6-diaminopyridine (**159**)

To an aqueous solution of 5M KOH (3.96 mL, 19.8 mmol, 55 eq) was added bromine (46 μL , 0.90 mmol, 2.5 eq) followed by 4-cyclohexylmethoxypyridine-2,6-dicarboxylic acid diamine (100 mg, 0.36 mmol, 1 eq). The reaction mixture was heated to 90 °C for 2 h, cooled to room temperature, extracted with DCM (3 x 25 mL). The combined organic layers were dried (MgSO_4) and evaporated. Chromatography (SP4, silica, 3-20% MeOH, EtOAc) to give 4-cyclohexylmethoxy-2,6-diaminopyridine as a white solid (35 mg, 44%). $R_f = 0.18$ (1:9 MeOH:EtOAc); mp = 152.0-152.8 °C; UV λ_{max} (EtOH): 289.5, 246.5 nm; IR ν_{max} 3435 (NH), 3363, 3333, 3187, 2926, 2854, 1626, 1578 cm^{-1} ; δ_H (500 MHz d_6 -DMSO): 0.97-1.25 (5H, m, C_6H_{11}), 1.64-1.76 (6H, m, C_6H_{11}), 3.65 (2H, d, $J = 6.5$ Hz, OCH_2), 5.27 (2H, s, Ar-H), 5.42 (4H, s, NH_2); δ_C (125 MHz d_6 -DMSO): 25.2 (C_6H_{11}), 26.0 (C_6H_{11}), 29.2 (C_6H_{11}), 36.9 (CCH_2O), 71.9 (OCH_2), 82.1 (Ar-H), 159.2 (CNH_2), 167.6 (CO); LCMS $R_t = 2.33$ min (1); MS (ESI+) m/z 222.16 [$\text{M}+\text{H}$] $^+$

4-Cyclohexylmethoxy-3-nitrosopyridine-2,6-diamine (**160**)

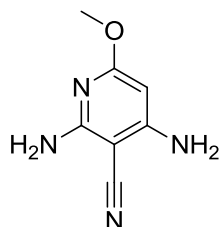
A solution of 4-cyclohexylmethoxy-2,6-diaminopyridine (50 mg, 0.23 mmol, 1 eq), in acetic acid (1.5 mL) and water (3.5 mL) was heated to 80 °C and NaNO₂ (17 mg, 0.25 mL, 1.1 eq) in water (1 mL) was added. The brown solution was stirred at 80 °C for 30 min, cooled to room temperature, neutralised using a saturated NaHCO₃ and extracted using DCM (4 x 25 mL). The combined organic layers were dried (Na₂SO₄), and evaporated *in vacuo*. Chromatography (silica, 10% MeOH, EtOAc), followed by recrystallisation (methanol) gave **160** as a purple solid (24 mg, 42%). *R*_f = 0.57 (1:9 MeOH:EtOAc); mp = 253.0-254.2 °C; UV λ_{max} (EtOH): 365.0, 323.5, 247.5, 204.0 nm; IR ν_{max} 3151 (NH), 2920, 2848, 1608, 1506 (NO) cm⁻¹; δ_H (500 MHz, d₆-DMSO): 1.04-1.31 (5H, m, C₆H₁₁), 1.66-1.85 (6H, m, C₆H₁₁), 3.91 (2H, d, *J* = 6.05 Hz, OCH₂), 5.62 (1H, s, *H*³), 7.46 (1H, s, N¹H¹), 7.06 (1H, s, N¹H²), 7.66 (1H, d, *J* = 5.25 Hz, N²H¹), 11.14 (1H, d, *J* = 5.2 Hz, N²H²); δ_C (125 MHz, d₆-DMSO): 25.2 (C₆H₁₁), 25.9 (C₆H₁₁), 29.1 (C₆H₁₁), 37.8 (CCH₂O), 73.3 (OCH₂), 83.3 (Ar-H), 142.3 (Ar-NO), 148.8 (CNH₂), 165.0 (CNH₂), 166.0 (CO); LCMS *R*_t = 2.16 min (1); MS (ESI+) *m/z* 251.10 [M+H]⁺ HRMS *m/z*: Calc. for C₁₂H₁₉N₄O₂: 251.1503 [M+H]⁺. Found: 251.1506 [M+H]⁺; Analytical HPLC: 97.0% purity

4,6-Diamino-2-methoxynicotinitrile (**165**)

Sodium (0.72 g, 30.0 mmol, 3 eq) was added in portions to methanol (30 mL, 698 mmol, 70 eq), after all the sodium had dissolved 2-amino-1,1,3-tricyanopropene (1.32 g, 9.99 mmol, 1 eq) was added and the reaction heated to reflux for 48 h, then cooled to room temperature and the solvent removed *in vacuo*. The resulting oil was diluted with ice water (5 mL) and chilled to 4 °C for 2 days. The precipitate was collected by filtration and purified by chromatography (silica, 4:1 Et₂O:PE) to give the title compound as a white solid (0.33 g, 20%). *R*_f = 0.26 (4:1 Et₂O:PE); mp. = 183.3-183.8 °C (lit. 176 °C)¹⁸⁶; UV λ_{max} (EtOH): 267.5, 220.5 nm; IR ν_{max} 3511 (NH), 3398, 3337,

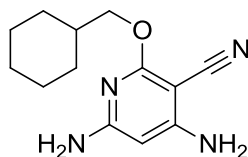
3240, 2197 (CN), 1638, 1597, 1547 cm^{-1} ; δ_{H} (500 MHz d_6 -DMSO): 3.82 (3H, s, CH_3), 5.39 (1H, s, Ar-H), 6.26 (2H, s, NH_2), 6.32 (2H, s, NH_2); δ_{C} (125 MHz d_6 -DMSO): 53.0 (CH_3), 67.5 (CCN), 82.5 (Ar-H), 116.7 (CN), 158.4 (CNH_2), 160.2 (CNH_2), 165.7 (CO); LCMS R_t = 1.56 min (1); MS (ESI+)+ m/z 164.98 [$\text{M}+\text{H}$] $^+$

4,6-Diamino-2-methoxynicotinitrile (**164**)



The title compound was synthesised as a by-product of the above reaction as a pale yellow solid (77 mg, 5%). R_f = 0.53 (4:1 Et_2O :PE); mp = 139.5-140.9 $^{\circ}\text{C}$; UV λ_{max} (EtOH): 341.0, 293.5, 225.5 nm; IR ν_{max} 3357 (NH), 3232, 2195 (CN), 1626, 1569 cm^{-1} ; δ_{H} (500 MHz CDCl_3): 3.74 (3H, s, CH_3), 4.52 (2H, s, NH_2), 4.87 (2H, s, NH_2), 5.36 (1H, s, Ar-H); δ_{C} (125 MHz CDCl_3): 53.7 (CH_3), 70.4 (CCN), 83.8 (Ar-H), 116.5 (CN), 157.6 (CNH_2), 160.3 (CNH_2), 167.0 (CO); LCMS R_t = 2.45 min (1); MS (ESI+) m/z 165.06 [$\text{M}+\text{H}$] $^+$

4,6-Diamino-2-cyclohexylmethoxynicotinitrile (**162**)



Sodium (0.73 g, 31.2 mmol, 3.2 eq) was added in portions to cyclohexylmethanol (30 mL, 244 mmol, 24 eq) and the reaction heated to 160 $^{\circ}\text{C}$ until the sodium had dissolved, the reaction mixture was cooled to 120 $^{\circ}\text{C}$ and 2-amino-1-propene-1,1,3-tricarbonitrile (1.32 g, 10.0 mmol, 1 eq) added. The temperature was maintained at 120 $^{\circ}\text{C}$ for 48 h before cooling to room temperature. The solvent was removed *in vacuo*. The resulting solid was dissolved in DCM (250 mL) and the precipitate was removed by filtration. The filtrate was purified using repeated rounds of medium pressure column chromatography (silica, 80% Et_2O , PE) followed by (silica, 40% EtOAc , PE). The crude product was then purified by semi-preparative HPLC (60:40 0.1% formic acid in MeCN :0.1 % aqueous formic acid) to give **162** as a off-white solid (0.11g, 4%). R_f = 0.8 (6:4 EtOAc :PE); mp = 85.2-86.0 $^{\circ}\text{C}$; UV λ_{max} (EtOH):

341.5, 268.0, 223.0 nm; IR ν_{\max} 3442 (NH), 3327, 3215, 2922, 2849, 2203 (C=N), 1599, 1552 cm^{-1} ; δ_{H} (500 MHz CDCl_3): 0.93-1.21 (5H, m, C_6H_{11}), 1.59-1.77 (6H, m, C_6H_{11}), 3.98 (2H, d, $J = 6.6$ Hz, OCH_2), 4.45 (2H, s, NH_2), 4.54 (2H, s, NH_2), 5.28 (1H, s, Ar-H); δ_{C} (125 MHz CDCl_3): 25.8 (C_6H_{11}), 26.5 (C_6H_{11}), 29.7 (C_6H_{11}), 37.8 (CCH_2O), 71.2 (CCN), 71.7 (OCH_2), Ar-H (OCH_2), 116.8 (CN), 158.0 (CNH_2), 159.5 (CNH_2), 166.3 (CO); LCMS $R_t = 3.18$ min (1); MS (ESI+) m/z 247.04 $[\text{M}+\text{H}]^+$; HRMS m/z : Calc. for $\text{C}_{13}\text{H}_{19}\text{N}_4\text{O}$: 247.1553 $[\text{M}+\text{H}]^+$. Found 247.1554 $[\text{M}+\text{H}]^+$.; Analytical HPLC: 98.1% purity

7.2 MDM2 Experimental Procedures

General Procedure A – Freidel-Crafts Reaction

To the appropriate phthalic anhydride (1 eq) was added chlorobenzene (8 eq) and AlCl_3 (2.4 eq) under N_2 . The reaction mixture was heated to 90 °C for 2 h before cooling to room temperature and quenching with ice. Concentrated HCl (1 mL per 3 mmol of anhydride) was added and the solution extracted with DCM (3 x 3 mL per mmol of anhydride). The combined organic layers were washed using 20 % Na_2CO_3 aqueous solution (3 mL per mmol of anhydride). On standing a precipitate formed which was collected by filtration, giving the desired 2-(4-chlorobenzoyl) benzoic acid as the sodium salt.

General procedure B – Formation of the 2-aryl-3-(4-chlorophenyl)-3-hydroxyisoindolin-1-one

To the appropriate 2-benzoyl benzoic acid (1 eq) in THF was added thionyl chloride (2 eq) followed by DMF (4 drops) under N_2 . The reaction mixture was stirred at room temperature for 4 h before then concentrated *in vacuo*. The residue was dissolved in THF and DIPEA (2.2 eq) and the appropriate benzylamine or benzylamine hydrochloride salt (1.1 eq) was added. The reaction mixture was stirred for 16 h at room temperature, then the solvent removed *in vacuo*. The residue was partitioned between ethyl acetate (1 mL per 0.1 mmol of benzoyl benzoic acid) and water (1 mL per 0.1 mg). The aqueous layer was extracted with ethyl acetate (2 x 1 mL per 0.1 mmol of benzoyl benzoic acid). The combined organic layers were washed with brine (1 mL per 0.1 mmol of benzoyl benzoic acid), dried (MgSO_4), filtered and evaporated *in vacuo*. Chromatography (silica, with appropriate solvents) gave the desired 3-hydroxyisoindolinone.

General procedure C – Synthesis of the alkoxy isoindolinones via 3-chloride

To the appropriate 3-hydroxy isoindolinone (1 eq) in THF was added thionyl chloride (2 eq) and DMF (4 drops) under N_2 and stirred for 4 h at room temperature, then concentrated *in vacuo*. The residue was dissolved in THF and K_2CO_3 (2 eq) and the

appropriate diol (2 eq) were added and the reaction stirred at room temperature for 16 h then concentrated *in vacuo* and the residue partitioned between ethyl acetate (1 mL per 0.1 mmol of isoindolinone) and water (1 mL per 0.1 mmol of isoindolinone). The aqueous layer extracted using ethyl acetate (2 x 1 mL per 0.1 mmol of isoindolinone). The combined organic layers were washed with brine (1 mL per 0.1 mmol of isoindolinone), dried over Na₂SO₄ and evaporated *in vacuo*. Chromatography (silica, appropriate solvents) gave the desired compound.

General procedure D – Synthesis of alkoxy isoindolinone via Lewis acid catalysis

To a solution of the appropriate 3-hydroxyisoindolinone (1 eq) in either DCM (1.5 mL per 100 mg of isoindolinone) at 0 °C was added BF₃·OEt₂ (2.5 eq) under N₂. After stirring at 0 °C for 15 min, the appropriate diol (10 eq) in DCM (1 mL per 10 mmol of diol) was added dropwise to the reaction mixture. After stirring at 0 °C for 1.5 h the reaction was warmed to room temperature and stirred until the reaction is complete. Saturated NH₄Cl (10 mL per 1 mmol of isoindolinone) was then added and extracted using DCM (3 x 40 mL per mmol of isoindolinone). The combined organic layers were dried over Na₂SO₄ and evaporated *in vacuo*. Chromatography (silica, appropriate solvents) gave the desired compounds.

General procedure E – Formation of alkoxy isoindolinone succinic esters

To a solution of the required 2-(4-aryl)-3-(4-chlorophenyl)-3-((1-(hydroxymethyl)cyclopropyl)methoxy)isoindolin-1-one in THF (3 mL per mmol) was added DMAP (0.2 eq), pyridine (2 eq) and succinic anhydride (2 eq) and the mixture was heated to reflux for 14 h, cooled to room temperature and concentrated *in vacuo*. The residue was partitioned between ethyl acetate (5 mL per and 0.01 mmol) and water (10 mL per 0.01 mmol). The aqueous layer was extracted with ethyl acetate (2 x 5 mL per 0.01 mmol). The combined organic layers were washed with brine (10 mL per 0.01 mmol), dried over Na₂SO₄ evaporated *in vacuo*. Chromatography (silica, appropriate solvent) gave the title compound.

General procedure F- Sonogashira Reaction

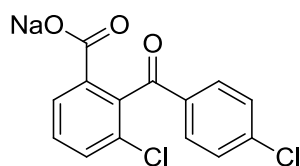
To a solution of the required 3-(4-chlorophenyl)-3-hydroxy-2-(4-iodobenzyl)isoindolin-1-one (1 eq) in THF (4 mL per mmol) was added Pd(PPh₃)₂ (0.03 eq) and CuI (0.02 eq) and the solution degassed for 5 min. Et₃N (2.5 eq) and appropriate substituted acetylene (1.3 eq) were added and the solution degassed for a further 15 min, before stirring overnight in the dark, filtering through Celite and washing with MeOH (60 mL per mmol of isoindolinone). Crude product concentrated *in vacuo* and purified (Chromatography, silica, appropriate solvent).

General procedure G – Triisopropylsilyl group deprotection

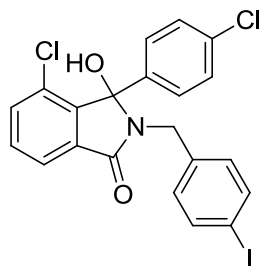
To 3-(alkoxy)-3-(4-chlorophenyl)-2-(4-((triisopropylsilyl)ethynyl)benzyl)isoindol-1-one (1 eq) in THF (mL per mmol) was added 1M tetrabutylammonium fluoride in THF (1.5 eq) and the reaction stirred at room temperature for 1 h. The solvent was removed *in vacuo* and the crude product purified using chromatography (silica, appropriate solvents).

General procedure H – Formation of the oxetane ring

To a solution of 3-(3-bromo-2,2-bis(hydroxymethyl)propoxy)isoindolinone (1 eq) in ethanol (10 mL per mmol) was added powdered potassium hydroxide (1.5 eq) and the reaction mixture stirred at room temperature for 2 h, then heated to reflux for 1 h. The reaction mixture was then cooled to room temperature and neutralised using 1 M aqueous HCl and concentrated *in vacuo*. The residue was partitioned between water (30 mL per mmol) and EtOAc (100 mL per mmol). The aqueous solution was extracted further with EtOAc (2 x mL per mmol) and the combined organic layers dried over Na₂SO₄ and evaporated *in vacuo*. Chromatography (silica, appropriate solvents) gave the desired compound.

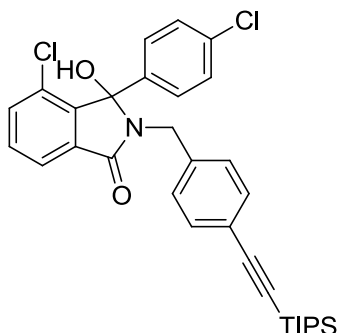
Sodium 3-chloro-2-(4-chlorobenzoyl)benzoate (**238**)

General procedure A: 3-chlorophthalic anhydride (5.00 g, 27.00 mmol). White solid (7.85 g, 91%). Dried over P₂O₅ before use. $R_f = 0.5$ (100 % EtOAc); mp > 350 °C; UV λ_{\max} (EtOH): 256 nm; IR ν_{\max} 2163, 1975, 1666 (Acid C=O), 1608 (Ketone C=O), 1583, 1556 cm⁻¹; δ_H (500 MHz *d*₆-DMSO) 7.40-7.49 (4H, m, 4 x Ar-H), 7.54-7.57 (2H, m, 2 x Ar-H), 7.87 (1H, dd, $J = 1.3$ and 7.4 Hz, CHCOOH); δ_C (125 MHz *d*₆-DMSO): 128.3, 128.4, 128.9, 129.4, 129.7, 129.8, 136.4, 137.0, 138.9, 141.7 (H^7), 167.0 (acid carbonyl), 193.0 (ketone carbonyl); LCMS $R_t = 3.18$ min, (1); MS (ESI+) m/z 295.02 [M+H]⁺

4-Chloro-3-(4-chlorophenyl)-3-hydroxy-2-(4-iodobenzyl)isoindolin-1-one (**252**)

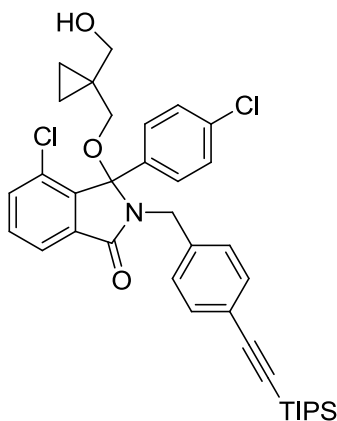
General procedure B: sodium 3-chloro-2-(4-chlorobenzoyl)benzoate (846 mg, 2.87 mmol) and 4-iodobenzylamine hydrochloride (850 mg, 3.15 mmol). Chromatography (SP4, silica, 7-60% EtOAc, petrol) gave **252** white solid (523 mg, 36%). $R_f = 0.35$ (3:7 EtOAc:PE); mp = 233.7-234.3 °C; UV λ_{\max} (EtOH): 340.5, 227.5 nm; IR ν_{\max} 3194, 2929, 1655 (C=O), 1587 (amide C-N) cm⁻¹; δ_H (500 MHz, *d*₆-DMSO): 4.20 (1H, d, $J = 15.7$ Hz, NCH₂), 4.32 (1H, d, $J = 15.7$ Hz, NCH₂), 6.92 (2H, d, $J = 8.3$ Hz, Ar-H), 7.22-7.7.29 (3H, m, Ar-H), 7.43 (1H, s, OH), 7.50 (2H, d, $J = 8.3$ Hz, Ar-H), 7.61-7.62 (2H, m, Ar-H), 7.77 (1H, dd, $J = 2.6$ and 5.8 Hz, H^7); δ_C (125 MHz *d*₆-DMSO): 41.5 (NCH₂), 89.8 (Ar-I), 92.4 (hemi-aminal carbon), 121.6, 128.0, 128.4, 128.6, 130.2, 131.8, 132.8, 133.2, 133.6, 136.5, 136.6, 137.5, 144.3 (CCCl), 165.3 (carbonyl); LCMS $R_t = 3.78$ min, (1); MS (ESI+) m/z 510.06 [M+H]⁺; HRMS m/z : Calc. for C₂₁H₁₅³⁵Cl₂INO₂: 509.9519 [M+H]⁺. Found 509.9507 [M+H]⁺.

3-Chloro-3-(4-chlorophenyl)-3-hydroxy-2-(4-((triisopropylsilyl)ethynyl)benzyl)isoindolin-1-one (**247**)



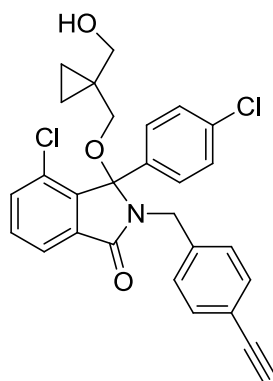
General procedure F: 4-chloro-3-(4-chlorophenyl)-3-hydroxy-2-(4-iodobenzyl)isoindolin-1-one (500 mg, 0.98 mmol) and triisopropylsilylacetylene (286 μL , 1.27 mmol). Chromatography (silica, 30% EtOAc, PE) to give **247** as an off-white solid (488 mg, 88%). $R_f = 0.54$ (3:7 EtOAc:PE); mp = 192.6-193.4 $^{\circ}\text{C}$; UV λ_{max} (EtOH): 266.5, 254.5, 232.0 nm; IR ν_{max} 3231, 2942, 2865, 2155 (Ethyne stretch), 1680 (C=O), 1587 (Amide C-N) cm^{-1} ; δ_{H} (500 MHz CDCl_3): 1.03 (18H, s, $\text{CH}(\text{CH}_3)_2$), 1.18 (3H, m, $\text{CH}(\text{CH}_3)_2$), 3.35 (1H, s, OH), 3.98 (1H, d, $J = 15.1$ Hz, NCH_2), 4.43 (1H, d, $J = 15.1$ Hz, NCH_2), 6.97 (2H, d, $J = 8.3$ Hz, Ar-H), 7.14-7.16 (6H, m, Ar-H), 7.33-7.35 (2H, m, Ar-H), 7.57 (1H, dd, $J = 3.1$ and 5.35, H^7); δ_{C} (125 MHz CDCl_3): 11.3 ($\text{CH}(\text{CH}_3)_2$), 18.7 (3 x $\text{C}(\text{CH}_3)_2$), 42.6 (NCH_2), 90.7 (hemi-aminal carbon), 91.0 (ethynyl), 106.8 (ethynyl), 122.0 (Ar-ethynyl), 122.4, 128.3, 128.5, 128.6, 129.6, 131.5, 131.9, 132.9, 134.0, 134.7, 134.9, 137.7, 143.9 (CCCl), 166.3 (carbonyl); LCMS $R_t = 4.74$ min; MS (ESI+) m/z 564.36 $[\text{M}+\text{H}]^+$; HRMS m/z : Calc. for $\text{C}_{32}\text{H}_{36}^{35}\text{Cl}_2\text{NO}_2\text{Si}$: 564.1887 $[\text{M}+\text{H}]^+$. Found: 564.1884 $[\text{M}+\text{H}]^+$.

4-Chloro-3-(4-chlorophenyl)-3-(((1-hydroxymethyl)cyclopropyl)methoxy)-2-(4-((triisopropylsilyl)ethynyl)benzyl)isoindolin-2-one (**248**)



General procedure C: 3-chloro-3-(4-chlorophenyl)-3-hydroxy-2-(4-((triisopropylsilyl)ethynyl)benzyl)-isoindolin-1-one (308 mg, 0.55 mmol) and 1,1-bis(hydroxymethyl)cyclopropane (0.11 mL, 1.15 mmol). Chromatography (SP4, silica, gradient 7-60% EtOAc, petrol) gave **248** as a colourless oil (85 mg, 24%). $R_f = 0.24$ (4:6 EtOAc:PE); UV λ_{\max} (EtOH): 340.5, 267.0, 254.5 nm; IR ν_{\max} 3388, 2940, 2862, 2157 (Ethyne stretch), 1682 (C=O), 1588 (Amide C-N) cm^{-1} ; δ_H (500 MHz CDCl_3): 0.15-0.17 (1H, m, cyclopropyl), 0.29-0.31 (1H, m, cyclopropyl), 0.44-0.46 (2H, m, cyclopropyl), 1.12 (18H, s, CH_3), 2.83 (1H, d, $J = 9.1$ Hz, OCH_2), 2.91 (1H, d, $J = 9.1$ Hz, OCH_2), 3.44 (1H, d, $J = 11.5$ Hz, CH_2OH), 3.52 (1H, d, $J = 11.5$ Hz, CH_2OH), 4.21 (1H, d, $J = 15.0$ Hz, NCH_2), 4.48 (1H, d, $J = 15.0$ Hz, NCH_2), 7.07 (2H, d, $J = 8.25$ Hz, Ar-H), 7.20-7.28 (6H, m, Ar-H), 7.46 (1H, dd, $J = 1$ and 7.9 Hz, H^5), 7.50-7.53 (2H, Ar-H), 7.81 (1H, dd, $J = 1.0$ and 7.4 Hz, H^7); δ_C (125 MHz CDCl_3): 8.6 (cyclopropyl), 8.6 (cyclopropyl), 18.7 ($\text{CH}(\text{CH}_3)_2$), 22.1 (cyclopropyl), 42.7 (NCH_2), 67.9 (CH_2OH), 68.1 (OCH_2), 90.9 (ethynyl), 94.6 (ethynyl), 106.7 (hemi-aminal carbon), 122.3, 122.6, 128.3, 128.5, 128.9, 129.7, 131.8, 133.9, 134.2, 134.7, 135.0, 137.2, 140.8, 166.7 (carbonyl); LCMS $R_t = 4.78$ min, (1); HRMS m/z : Calc. for $\text{C}_{37}\text{H}_{44}^{35}\text{Cl}_2\text{NO}_3\text{Si}$: 648.2462 $[\text{M}+\text{H}]^+$. Found: 648.2447 $[\text{M}+\text{H}]^+$.

4-Chloro-3-(4-chlorophenyl)-2-(4-ethynylbenzyl)-3-(((1-(hydroxymethyl)cyclopropyl)methoxy)isoindolin-1-one (**253**)



To a solution of 4-chloro-3-(4-chlorophenyl)-3-(((1-(hydroxymethyl)cyclopropyl)methoxy)-2-(4-((triisopropylsilyl)ethynyl)benzyl)isoindolin-2-one (99 mg, 0.15 mmol, 1 eq) in THF (2 mL) was added 1M TBAF in THF (0.23 mL, 0.23 mmol, 1.5 eq). The reaction was stirred at for 75 min, concentrated *in vacuo*. Chromatography (silica, EtOAc:PE), followed by semi-preparative HPLC (1:1 MeCN: 0.1% aqueous formic acid) gave **253** as a colourless oil (30 mg, 41%). $R_f = 0.44$ (1:1 EtOAc:PE);

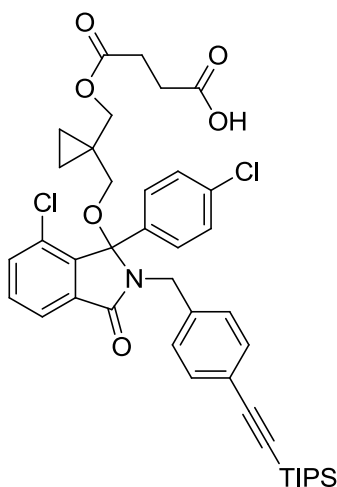
UV λ_{\max} (EtOH): 229.5 nm; IR ν_{\max} 3438 (OH), 3296, 2924, 2874, 1693 (C=O), 1588 (Amide C-N) cm^{-1} ; δ_{H} (500 MHz, CDCl_3) 0.05-0.11 (1H, m, cyclopropyl), 0.24-0.30 (1H, m, cyclopropyl), 0.40-0.44 (2H, m, cyclopropyl), 1.67 (1H, s, OH), 2.79 (1H, d, $J = 9.1$ Hz, OCH_2), 2.90 (1H, d, $J = 9.1$ Hz, OCH_2) 3.04 (1H, s, CCH), 3.40 (1H, d, $J = 11.4$ Hz, CH_2OH) 3.50 (1H, d, $J = 11.4$ Hz, CH_2OH), 4.16 (2H, d, $J = 15.0$ Hz, NCH_2), 4.50 (1H, d, $J = 15.0$ Hz, NCH_2), 7.11-7.30 (8H, m, Ar-H) 7.44-7.52 (2H, m, Ar-H), 7.85 (1H, dd, $J = 0.65$ and 7.3 Hz, H^7); δ_{C} (125 MHz, CDCl_3): 8.5, (cyclopropyl) 8.5 (cyclopropyl), 22.1 (cyclopropyl), 42.7 (NCH_2), 67.9 (OCH_2), 68.1 (CH_2OH), 83.3 (ethynyl CH), 94.7 (hemi-aminal carbon), 121.2 (C-ethynyl), 122.3, 128.3, 128.5, 129.0, 129.7, 131.9, 133.0, 134.0, 134.1, 134.7, 135.0, 137.9, 140.7, 166.7 (carbonyl carbon); LCMS $R_t = 3.71$ min, (1); MS (ESI+) m/z 492.24 $[\text{M}+\text{H}]^+$; HRMS m/z : Calc. for $\text{C}_{28}\text{H}_{24}^{35}\text{Cl}_2\text{NO}_3$: 492.1128 $[\text{M}+\text{H}]^+$. Found: 492.1124 $[\text{M}+\text{H}]^+$.; Analytical HPLC: 99.9% purity

Chiral Separation: mobile phase hexane:ethanol 92.5:7.5

254 Peak 1: (33.8 mg, 42%); Specific rotation $[\alpha] = -9.16^\circ$ (at 21.0°C , wavelength = 589 nm, tube length = 0.1 dm, concentration = 0.328 g per 100 mL);

255 Peak 2: (33.8 mg, 42%); Specific rotation $[\alpha] = +11.4^\circ$ (at 21.0°C , wavelength = 589 nm, tube length = 0.1 dm, concentration = 0.336 g per 100 mL)

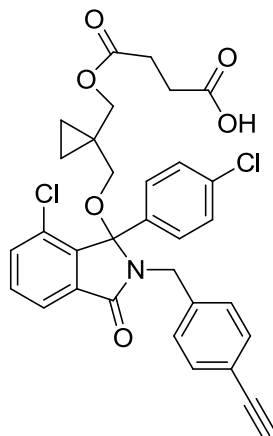
4-Chloro-3-(4-chlorophenyl)-3-(((1-methoxy(succinic ester))cyclopropyl)methoxy)-2-(((4-triisopropylsilyl)ethynyl)benzyl)isoindolin-1-one (**256**)



General procedure E: 4-chloro-3-(4-chlorophenyl)-3-(((1-hydroxymethyl)cyclopropyl)methoxy)-2-(4-((triisopropylsilyl)ethynyl)benzyl)isoindolin-2-one (**248**)

(84 mg, 0.13 mmol). Chromatography (silica, 50-85 % EtOAc, petrol) gave **256** as a pale yellow oil (92 mg, 94%). $R_f = 0.15$ (85:15 EtOAc:PE); UV λ_{\max} (EtOH): 266.5, 254.5 nm; IR ν_{\max} 2942, 2865, 2158 (Ethyne stretch), 1708 (Carboxylic acid C=O), 1608 (Amide C=O), 1582 (Amide C-N), 1556 cm^{-1} ; δ_{H} (500 MHz CDCl_3) 0.18-0.20 (1H, m, cyclopropyl), 0.29-0.36 (1H, m, cyclopropyl), 0.47-0.52 (2H, m, cyclopropyl), 1.11 (18H, s, CH_3), 1.24-1.27 (3H, m, $\text{CH}(\text{CH}_3)_2$), 2.55-2.64 (4H, m, succinic ester CH_2), 2.71 (1H, d, $J = 9.3$ Hz, OCH_2), 2.86 (1H, d, $J = 9.3$ Hz, OCH_2), 3.93 (1H, d, $J = 11.4$ Hz, CH_2OH), 4.21 (1H, d, $J = 11.4$ Hz, CH_2OH), 4.29 (1H, d, $J = 15.0$ Hz, NCH_2), 4.35 (1H, d, $J = 15.0$ Hz, NCH_2), 7.00 (2H, d, $J = 8.2$ Hz, Ar-H), 7.15-7.23 (6H, m, Ar-H), 7.43 (1H, dd, $J = 1.0$ and 8.0 Hz, H^5), 7.48-7.51 (1H, m, H^6), 7.84 (1H, dd, $J = 1.0$ and 7.4 Hz, H^7); δ_{C} (125 MHz CDCl_3): 8.9 (cyclopropyl), 11.3 (cyclopropyl), 18.7 ($\text{CH}(\text{CH}_3)_2$), 19.4 ($\text{CH}(\text{CH}_3)_2$), 28.8 ($\text{CH}_2\text{CO}_2\text{H}$), 28.9 (COCH_2), 42.6 (NCH_2), 66.5 (OCH_2), 68.4 (CH_2OH), 90.8 (ethynyl), 94.4 (ethynyl), 106.8 (hemi-aminal), 122.2 (Ar-ethynyl), 122.5, 128.3, 128.4, 128.9, 129.9, 131.7, 131.8, 133.8, 134.1, 134.6, 134.8, 137.1, 140.8, 167.0 (isoindolinone carbonyl), 172.1 (succinic ester carbonyl), 177.2 (succinic acid carbonyl)

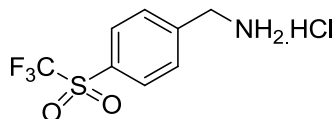
4-Chloro-3-(4-chlorophenyl)-2-(4-ethynylbenzyl)-3-(((1-methoxy(succinic ester))cyclopropyl)methoxy)isoindolin-1-one (**257**)



To 4-chloro-3-(4-chlorophenyl)-3-(((1-methoxy(succinic ester))cyclopropyl)methoxy)-2-(((4-triisopropylsilyl)ethynyl)benzyl)isoindolin-1-one (81 mg, 0.11 mol) in THF (2 mL) was added 1M TBAF in THF (162 μL , 0.16 mmol). The reaction was stirred for 165 min and concentrated *in vacuo*. Chromatography (SP4, silica, 3-20% MeOH, EtOAc) to give **257** as a colourless oil (53 mg, 81%). $R_f = 0.56$ (1:9 MeOH:EtOAc); UV λ_{\max} (EtOH): 228.5 nm; IR ν_{\max} 3295, 2927, 1706 (Carboxylic

acid C=O), 1588 (Amide C-N) cm^{-1} ; δ_{H} (500 MHz CDCl_3): 0.20-0.22 (1H, m, cyclopropyl), 0.36-0.39 (1H, m, cyclopropyl), 0.50-0.53 (2H, m, cyclopropyl), 2.57-2.64 (4H, m, succinic 2 x CH_2), 2.80 (1H, d, $J = 9.3$ Hz, OCH_2), 2.84 (1H, d, $J = 9.3$ Hz, OCH_2), 3.04 (1H, s, ethynyl), 4.00 (1H, d, $J = 11.5$ Hz, CH_2OH), 4.16 (1H, d, $J = 11.5$ Hz, CH_2OH), 4.32 (1H, d, $J = 15.0$ Hz, NCH_2), 4.39 (1H, d, $J = 15.0$ Hz, NCH_2), 7.06 (2H, d, $J = 8.3$ Hz, Ar-H), 7.18-7.28 (6H, m, Ar-H), 7.45 (1H, dd, $J = 1.0$ and 8.0 Hz, H^5), 7.49-7.52 (1H, m, H^6), 7.86 (1H, dd, $J = 1.0$ and 7.4 Hz, H^7); δ_{C} (125 MHz CDCl_3): 8.9 (cyclopropyl), 8.9 (cyclopropyl), 19.4 (cyclopropyl), 28.8 ($\text{CH}_2\text{CO}_2\text{H}$), 29.0 (COCH_2), 42.6 (NCH_2), 66.5 (OCH_2), 68.4 (CH_2O), 83.3 (ethynyl), 94.5 (ethynyl), 121.2 (Ar-ethynyl), 122.2, 128.3, 128.4, 129.0, 131.0, 131.9, 133.8, 134.2, 134.7, 134.9, 137.7, 140.8, 167.0 (isoindolinone CO), 172.0 (succinic ester carbonyl), 176.0 (succinic acid carbonyl); LCMS $R_t = 3.67$ min, (1); MS (ESI+) m/z 592.11 $[\text{M}+\text{H}]^+$ HRMS m/z : Calc. for $\text{C}_{32}\text{H}_{28}^{35}\text{Cl}_2\text{NO}_6$: 592.1288 $[\text{M}+\text{H}]^+$. Found: 592.1290 $[\text{M}+\text{H}]^+$; Analytical HPLC: 95.8% purity

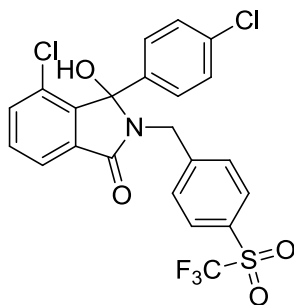
4-((Trifluoromethyl)sulfonyl)benzylamine hydrochloride (**265**)



To 4-((trifluoromethyl)sulfonyl)benzonitrile (400 mg, 1.70 mmol, 1 eq) in THF was added 1M BH_3 .THF complex in THF (13.6 mL, 13.60 mmol, 8 eq) and the reaction mixture stirred at room temperature for 1 h then heated to reflux for 4 days before cooling to room temperature. A 1:1 mixture of water (5 mL) and acetic acid (5 mL) was added slowly and stirred at room temperature for 15 min, then concentrated *in vacuo*. The resulting white solid was suspended in water (10 mL) cooled in an ice-bath, the pH was adjusted to 8 with a saturated sodium bicarbonate solution then extracted with ethyl acetate (3 x 50 mL). The combined organic layers were dried (MgSO_4), and concentrated *in vacuo*. Chromatography (SP4, silica, 3- 20% MeOH, EtOAc). The resulting yellow oil was redissolved in the minimum amount of methanol and 1M HCl (5 mL) added, then evaporated *in vacuo* to give **265** as a white solid (240 mg, 51%) and dried (P_2O_5). $R_f = 0.14$ (1:9 MeOH:EtOAc) mp. = 278.1-278.8 $^\circ\text{C}$; UV λ_{max} (EtOH): 271.0 nm; IR ν_{max} 2860, 2162, 1361 (Sulfone), 661 (C-F) cm^{-1} ; δ_{H} (500 MHz d_6 -DMSO): 4.26 (2H, s, CH_2), 7.97 (2H, d, $J = 8.5$ Hz, Ar-H), 8.24 (2H, d, $J = 8.5$ Hz, Ar-H), 8.68 (3H, s, NH_3); δ_{C} (125 MHz d_6 -DMSO): 41.2

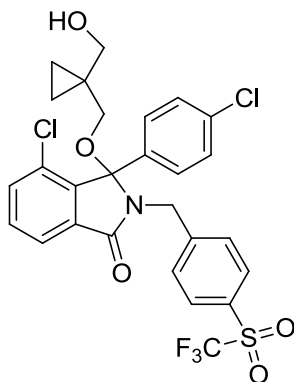
(CH₂), 120.7, 129.2, 130.9, 131.0, 144.6; δ_F (470 MHz *d*₆-DMSO): -78.4; LCMS R_t = 0.44 min, (1); MS (ESI+) m/z 239.99 [M+H]⁺

4-Chloro-3-(4-chlorophenyl)-3-hydroxy-2-(((4-(trifluoromethyl)sulfonyl)benzyl)benzyl)isoindolin-1-one (**263**)



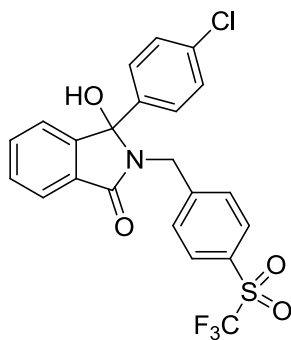
General procedure B: sodium 3-chloro-2-(4-chlorobenzoyl)benzoate (156 mg, 0.49 mmol) and 4-((trifluoromethyl)sulfonyl)benzylamine hydrochloride. Chromatography (SP4, silica, 12-100% EtOAc, petrol) to give **263** as an off-white solid (90 mg, 35%). R_f = 0.7 (1:1 EtOAc:PE); mp = 228.3-229.1 °C; UV λ_{max} (EtOH): 340.5 nm; IR ν_{max} 3269 (OH), 1682 (C=O), 1590 (Amide C-N), 1363 (sulfone) cm⁻¹; δ_H (500 MHz CDCl₃): 3.05 (1H, s, OH), 4.32 (1H, d, J = 15.5 Hz, NCH₂), 4.59 (1H, d, J = 15.5 Hz, NCH₂), 7.13-7.14 (4H, m, Ar-H), 7.39-7.45 (4H, m, Ar-H), 7.73-7.76 (3H, m, Ar-H); δ_C (125 MHz *d*₆-DMSO): 41.4 (NCH₂), 89.6 (hemi-aminal) 121.8, 123.2, 127.5, 127.9, 128.4, 128.7, 129.7, 130.3, 131.9, 132.8, 133.0, 133.8, 136.4, 144.2, 148.6, 165.5 (C=O); δ_F (470 MHz *d*₃-MeCN): -78.4; LCMS R_t = 3.74 min, (1); MS (ESI+) m/z 516.04 [M+H]⁺; HRMS m/z : Calc. for C₂₂H₁₄³⁵Cl₂F₃NO₄S: 514.9967 [M+H]⁺. Found: 514.9962 [M+H]⁺.

4-Chloro-3-(4-chlorophenyl)-3-(1-(hydroxymethyl)cyclopropyl)methoxy)-2-(4-((trifluoromethyl)sulfonyl)benzyl)isoindolin-one (**246**)



General procedure C: 4-chloro-3-(4-chlorophenyl)-3-hydroxy-2-(((4-trifluoromethyl)sulfonyl)benzyl)isoindolin-1-one **252** (162 mg, 0.31 mmol) and 1,1-bis(hydroxymethyl)cyclopropane (0.06 mL, mmol). Chromatography (SP4, silica, 12-100 % EtOAc, petrol) gave **246** as a colourless oil (55 mg, 29%). $R_f = 0.34$ (1:1 EtOAc:PE); UV λ_{\max} (EtOH): 225.5 nm; IR ν_{\max} 3457 (OH), 2925, 2877, 1703 (C=O), 1597 (Amide C-N), 1364 (Sulfone), 1194 (CF₃), 1139 cm⁻¹; δ_H (500 MHz *d*₃-MeCN): 0.04-0.06 (1H, m, cyclopropyl), 0.13-0.16 (1H, m, cyclopropyl), 0.19-0.23 (2H, m, cyclopropyl), 2.36 (1H, t, $J = 5.5$ Hz, OH), 2.56 (1H, d, $J = 9.1$ Hz, OCH₂), 2.89 (1H, d, $J = 9.1$ Hz OCH₂), 3.23 (1H, dd, $J = 5.0$ and 11.2 Hz, CH₂OH), 3.34 (1H, dd, $J = 5.0$ and 11.2 Hz, CH₂OH), 4.14 (1H, d, $J = 15.9$ Hz, NCH₂), 4.57 (1H, d, $J = 15.9$ Hz, NCH₂), 6.86-6.97 (4H, m, Ar-H), 7.19 (2H, d, $J = 8.0$ Hz, Ar-H), 7.35 (1H, dd, $J = 1.1$ and 8.0 Hz, H^5), 7.39-7.42 (1H, m, H^6), 7.55 (2H, d, $J = 8.5$ Hz, Ar-H), 7.63 (1H, dd, $J = 1.1$ and 7.4 Hz, H^7); δ_C (125 MHz *d*₃-MeCN): 7.3 (cyclopropyl), 7.4 (cyclopropyl), 21.6 (cyclopropyl), 41.2 (NCH₂), 64.9 (CH₂OH) 66.1 (OCH₂), 93.2 (hemi-aminal C), 120.7, 121.7, 127.6, 128.3, 128.4, 129.3, 129.8, 130.1, 132.0, 133.6, 133.6, 133.9, 135.5, 140.3, 147.6 (CF₃), 166.1 (C=O); δ_F (470 MHz *d*₃-MeCN) -93.9; LCMS $R_t = 3.78$ min, (1); HRMS m/z : Calc. for C₂₇H₂₅³⁵Cl₂F₃N₂O₅S: 617.0886 [M+NH₄]⁺. Found: 617.0884 [M + NH₄]⁺.; Analytical HPLC: 96.7% purity

3-(4-Chlorophenyl)-2-(4-(((trifluoromethyl)sulfonyl)benzyl)isoindolin-1-one (**262**)

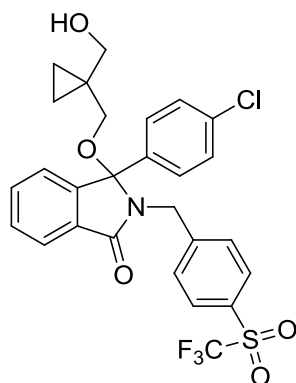


General procedure B: 2-(4-chloro-benzoyl)benzoic acid (56 mg, 0.21 mmol) and 4-(((trifluoromethyl)sulfonyl)benzylamine hydrochloride (65 mg, 0.24 mmol).

Chromatography (SP4, silica, 15-100 % EtOAc, petrol) gave the title compound as a white solid (88 mg, 87%). $R_f = 0.55$ (1:1 EtOAc:PE); mp = 208.8-209.2 °C; UV λ_{\max} (EtOH): 340.5 nm; IR ν_{\max} 2393, 1655 (C=O), 1598 (Amide C-N), 1365 (Sulfone) cm⁻¹; δ_H (500 MHz *d*₆-DMSO): 4.52 (1H, d, $J = 16.4$ Hz, NCH₂), 4.63 (1H, d, $J = 16.4$ Hz, NCH₂), 7.23-7.27 (4H, m, Ar-H), 7.31 (1H, d, $J = 7.2$ Hz, Ar-H), 7.41 (1H,

s, OH), 7.57-7.64 (4H, m, Ar-H), 7.81 (1H, dd, $J = 0.7$ and 6.8 Hz, Ar-H), 7.93 (2H, d, $J = 8.4$ Hz, H^7); δ_C (125 MHz d_6 -DMSO): 41.8 (NCH₂), 90.0 (hemi-aminal carbon), 122.8, 122.9, 127.4, 128.0, 128.2, 129.6, 129.8, 129.9, 130.4, 132.8, 133.1, 138.5, 148.9, 149.0, 166.9 (carbonyl); δ_F (470 MHz, d_6 -DMSO) -78.6; LCMS $R_t = 3.64$ min, (1); MS (ESI+) m/z 482.11 [M+H]⁺; HRMS m/z : Calc. for C₂₂H₁₆³⁵ClF₃NO₄S: 482.0435 [M+H]⁺. Found: 482.0431 [M+H]⁺.

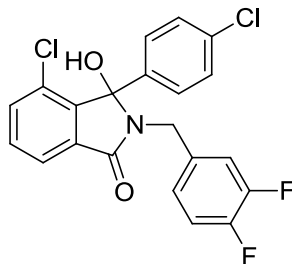
3-(4-Chlorophenyl)-3-(1-((hydroxymethyl)cyclopropyl)methoxy)-2-(((trifluoromethyl)sulfonyl)benzyl)isoindolin-1-one (**245**)



General procedure D: 3-(4-chlorophenyl)-2-(4-(((trifluoromethyl)sulfonyl)benzyl)isoindolin-1-one (209 mg, 0.43 mmol) and 1,1-bis(hydroxymethyl)cyclopropyl (0.27 mL, 4.34 mmol). The reaction was quenched after 1.5 h at 0 °C and 1 h at room temperature. Chromatography (SP4, silica, 15-100% EtOAc, petrol) gave **245** as a colourless oil (151 mg, 62%). $R_f = 0.43$ (1:1 EtOAc:PE); UV λ_{max} (EtOH): 203.0 nm; IR ν_{max} 3408 (OH), 2159, 1698 (C=O), 1597 (Amide C-N), 1364 (Sulfone), 1216 (CF₃), 1191 cm⁻¹; δ_H (500 MHz d_3 -MeCN): 0.15-0.18 (1H, m, cyclopropyl), 0.20-0.23 (1H, cyclopropyl), 0.36-0.38 (2H, m, cyclopropyl), 2.56 (1H, t, $J = 5.7$ Hz, OH), 2.82 (1H, d, $J = 9.3$ Hz, OCH₂), 2.87 (1H, d, $J = 9.3$ Hz, OCH₂), 3.41 (1H, dd, $J = 6.2$ and 11.2 Hz, CH₂OH), 3.47 (1H, dd, $J = 6.2$ Hz and 11.2 Hz, CH₂OH), 4.43 (1H, d, $J = 15.8$ Hz, NCH₂), 4.72 (1H, d, $J = 15.8$ Hz, NCH₂), 7.10 (2H, d, $J = 8.9$ Hz, Ar-H), 7.18-7.20 (3H, m, Ar-H), 7.46 (2H, d, $J = 8.6$ Hz, Ar-H), 7.59-7.61 (2H, m Ar-H), 7.79 (2H, d, $J = 8.4$ Hz, Ar-H), 7.86-7.88 (1H, m, H^7) δ_C (125 MHz d_3 -MeCN): 7.3, 7.3 (cyclopropyl), 21.6 (cyclopropyl), 41.4 (NCH₂), 64.9 (CH₂OH), 65.7 (OCH₂), 93.5 (hemi-aminal carbon), 122.9, 123.0, 127.8, 128.0, 128.5, 129.9, 130.1, 133.5, 137.3, 144.8, 148.0 (CCCl), 167.5 (carbonyl); δ_F (470 MHz d_3 -MeCN): -79.8;

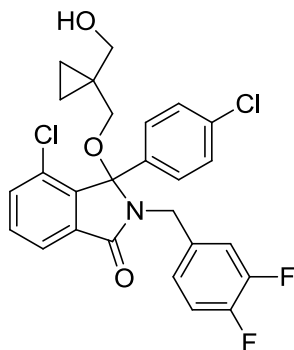
LCMS $R_t = 3.69$ min, (1); HRMS m/z : Calc. for $C_{27}H_{27}^{35}Cl_2F_3N_2O_5S$: 583.1261
 $[M+NH_4]^+$. Found: 583.1276 $[M + NH_4]^+$. ; Analytical HPLC: 99.6% purity

4-Chloro-3-(4-chlorophenyl)-2-(3,4-difluorobenzyl)-3-hydroxyisoindolinone (**268**)

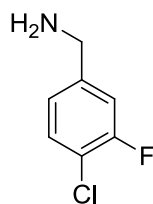


General procedure B: sodium 3-chloro-2-(4-chlorobenzoyl)benzoate (750 mg, 2.37 mmol) and 3,4-difluorobenzylamine (618 μ L, 5.22 mmol). Chromatography (SP4, silica, 7-60% EtOAc, PE) gave **268** as a white solid (390 mg, 39%). $R_t = 0.45$ (3:7 EtOAc:PE); mp = 147.3-149.1 $^{\circ}$ C; UV λ_{max} (EtOH): 210.0 nm; IR ν_{max} 3244 (OH), 2162, 1686 (C=O), 1588 (amide C-N), 1278 (C-F), 815, 757 (C-Cl) cm^{-1} ; δ_H (500 MHz $CDCl_3$): 3.83 (1H, s, OH), 4.03 (1H, d, $J = 14.7$ Hz, NCH_2), 4.33 (1H, d, $J = 14.7$ Hz, NCH_2), 6.71-6.74 (1H, m, benzyl Ar-H), 6.83 (1H, ap. dt, $J = 8.2$ and 10.2 Hz, benzyl Ar-H), 6.88 (1H, ddd, $J = 2.1, 7.7$ and 11.0 Hz, benzyl Ar-H), 7.15-7.19 (4H, m, Ar-H), 7.36-7.36 (2H, m, H^5 and H^6), 7.58-7.60 (1H, m, H^7); δ_C (125 MHz $CDCl_3$): 41.9 (NCH_2), 90.8 (hemi-aminal), 116.8 (d, $J = 17.1$ Hz, benzyl Ar-H), 117.7 (d, $J = 17.3$ Hz, benzyl Ar-H), 122.0, 124.8 (dd, $J = 3.6$ and 6.4 Hz, benzyl Ar-H), 128.2, 128.5, 129.7, 131.6, 134.1, 134.4 (dd, $J = 4.0$ and 5.3 Hz, benzyl Ar-H), 134.8, 134.9, 143.8, 148.7 (dd, $J = 12.6$ and 34.7 Hz, benzyl Ar-H), 150.7 (dd, $J = 12.6$ and 35.1 Hz, benzyl Ar-H), 166.3 (C=O); δ_F (470 MHz $CDCl_3$) -139.7 (d, $J = 20.7$ Hz), -137.7 (d, $J = 21.1$ Hz); LCMS $R_t = 1.63$ min, (4); MS (ESI+) m/z 420.2 $[M+H]^+$; HRMS m/z : Calc. for $C_{21}H_{13}^{35}Cl_2F_2NO_2$: 420.0364 $[M+H]^+$. Found 420.0365 $[M+H]^+$.

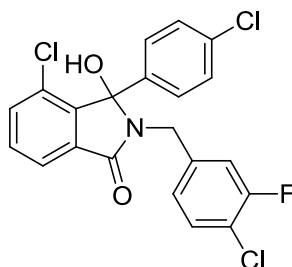
4-Chloro-3-(4-chlorophenyl)-2-(3,4-difluorobenzyl)-3-((1-(hydroxymethyl)cyclopropane)methoxy)isoindolin-1-one (**269**)



General procedure C: 4-Chloro-3-(4-chlorophenyl)-2-(3,4-difluorobenzyl)-3-hydroxyisoindolinone (210 mg, 0.50 mmol) and 1,1-bis(hydroxymethyl)cyclopropane (0.1 mL, 1.00 mmol). Chromatography (SP4, silica, 10-80% EtOAc, PE) gave **269** as a colourless oil (59 mg, 23%). $R_f = 0.24$ (4:6 EtOAc:PE); UV λ_{max} (EtOH): 232.0, 258.0 nm; IR ν_{max} 2925, 1694 (C=O), 1516 (Amide C-N), 1280 (C-F) cm^{-1} ; δ_H (500 MHz $CDCl_3$): 0.17-0.20 (1H, m, cyclopropyl), 0.32-0.35 (1H, m, cyclopropyl), 0.45-0.51 (2H, m, cyclopropyl), 1.78 (1H, s, OH), 2.86 (1H, d, $J = 9.2$ Hz, OCH_2), 2.92 (1H, d, $J = 9.2$ Hz, OCH_2), 3.49 (1H, d, $J = 11.4$ Hz, CH_2OH), 3.56 (1H, d, $J = 11.4$ Hz, CH_2OH), 4.28 (1H, d, $J = 15.0$ Hz, NCH_2), 4.34 (1H, d, $J = 15.0$ Hz, NCH_2), 6.79-6.82 (1H, m, Benzyl Ar-H), 6.91 (1H, ap. dt, $J = 8.3$ and 10.2 Hz, benzyl Ar-H), 6.97 (1H, ddd, $J = 2.1, 7.6$ and 10.7 , benzyl Ar-H), 7.18-7.19 (4H, m, Ar-H), 7.45 (1H, dd, $J = 1.0$ and 8.0 Hz, H^5), 7.49-7.52 (1H, m, H^6), 7.84 (1H, d, $J = 1.0$ and 7.4 , H^7); δ_C (125 MHz $CDCl_3$): 8.6 (cyclopropyl), 8.6 (cyclopropyl), 22.2 (cyclopropyl), 41.9 (NCH_2) 67.7 (CH_2OH), 68.0 (OCH_2), 94.4 (hemi-aminal), 116.8 (d, $J = 17.1$ Hz, benzyl Ar-H), 118.1 (d, $J = 17.3$, benzyl Ar-H), 122.3, 125.1 (dd, $J = 3.6$ and 6.2 , benzyl Ar-H), 128.3, 128.4, 129.8, 131.9, 134.0, 134.8, 135.0, 140.7, 148.8 (dd, $J = 6.4$ and 21.0 , benzyl Ar-F), 150.7 (dd, $J = 12.7$ and 21.3 , benzyl Ar-H), 166.7 (C=O); δ_F (470 MHz $CDCl_3$) -138.88 (d, $J = 21.9$), -137.62 (d, $J = 21.9$); LCMS $R_t = 1.66$ min, (3); HRMS m/z : Calc. for $C_{26}H_{22}^{35}Cl_2F_2NO_3$: 504.0939 $[M+H]^+$. Found: 504.0937 $[M+H]^+$; Analytical HPLC: 98.3% purity

4-Chloro-3-fluorobenzylamine (**271**)

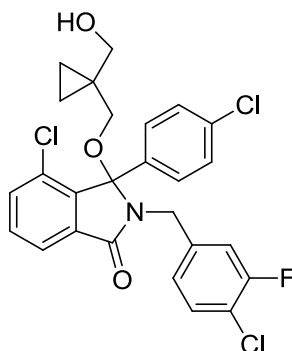
To a solution of 4-chloro-3-fluorobenzonitrile (500 mg, 3.21 mmol, 1 eq) in THF (1 mL) was added 1M BH₃.THF in THF (13 mL, 12.9 mmol, 4 eq) and the mixture stirred at room temperature for 15 min then heated to reflux for 16 h, cooled, and diluted by dropwise addition of a 1:1 solution of AcOH (10 mL) and water (10 mL). stirred at RT for 15 min, concentrated *in vacuo*. The residue was cooled in an ice-bath and basified to pH 9 by sat. NaHCO₃, then extracted using EtOAc (3 x 50 mL). Combined organic extracts were washed with brine (50 mL), dried over MgSO₄ and concentrated *in vacuo*. Chromatography (SP4, amino silica, 50-100% EtOAc, PE) gave **271** as a white solid (321 mg, 63%). $R_f = 0.71$ (1:4 EtOAc:PE, amino silica); mp = 93.5-95.9 °C; UV λ_{max} (EtOH): 253.5, 217.0 nm; IR ν_{max} 3295 (N-H), 2491, 2172, 1231 (C-F) cm⁻¹; δ_H (500 MHz CDCl₃): 1.48 (2H, s, NH₂), 3.86 (2H, s, CH₂), 7.04 (1H, d, $J = 8.0$ Hz, *CHCF*), 7.14 (1H, d, $J = 10.0$ Hz, *CHCCl*), 7.34 (1H, ap. t, $J = 8.0$ Hz, Ar-H); δ_C (125 MHz CDCl₃): 45.2 (CH₂), 115.2 (d, $J = 20.9$ Hz, *CHCF*), 119.0 (d, $J = 17.5$ Hz, CCl), 123.3 (d, $J = 14.1$ Hz, Ar-H), 130.5 (*CHCCl*), 144.1 (*CCH*₂), 158.2 (d, $J = 227.2$ Hz, CF); $^1\delta_F$ (470 MHz CDCl₃): -115.6; LCMS ($R_t = 0.81$ min, (3); MS (ESI+) m/z 160.1 [M+H]⁺; HRMS m/z : Calc. for C₇H₈³⁵ClFN: 160.0324 [M+H]⁺. Found 160.0320 [M+H]⁺.

4-Chloro-2-(4-chloro-3-fluorobenzyl)-3-(4-chlorophenyl)-3-hydroxyisoindolinone (**273**)

General procedure B: sodium 3-chloro-2-(4-chlorobenzoyl)benzoate (1.06 g, 3.34 mmol) and 4-chloro-3-fluorobenzylamine (587 mg, 3.63 mmol). Chromatography (SP4, silica, 7-60 % EtOAc, PE) gave **273** as a white solid (538 mg, 37%). $R_f = 0.39$

(3:7 EtOAc:PE); mp = 184.7-187.0 °C; UV λ_{\max} (EtOH): 231.0 nm; IR ν_{\max} 3217, 2158, 2028, 1683 (C=O), 1586 (amide C-N), 1093 (C-F), 814, 757 (C-Cl) cm^{-1} ; δ_{H} (500 MHz CDCl_3): 3.44 (1H, s, OH), 4.03 (1H, d, $J = 15.2$ Hz, NCH_2), 4.42 (1H, d, $J = 15.2$ Hz, NCH_2), 6.79 (1H, d, $J = 7.9$ Hz, CHCF), 6.88 (1H, d, $J = 9.8$ Hz, CHCCL), 7.09 (1H, ap. t, $J = 7.9$ Hz, benzyl Ar-H), 7.17-7.18 (4H, m, Ar-H), 7.37-7.40 (2H, m, H^5 and H^6), 7.64 (1H, dd, $J = 2.4$ and 5.8 Hz, H^7); δ_{C} (125 MHz CDCl_3): 42.0 (NCH_2), 90.8 (hemi-aminal), 116.9 (d, $J = 21.4$ Hz, CHCF), 119.8 (d, $J = 17.6$ Hz, CCL), 122.1, 125.1 (d, $J = 3.6$ Hz, benzyl Ar-H), 128.2, 128.6, 129.7, 130.2, 131.7, 132.8, 134.1, 134.9 (d, $J = 20.6$ Hz, CHCCL), 138.4 (d, $J = 25.8$ Hz, CCH_2), 143.7, 157.7 (d, $J = 247.4$ Hz, CF), 166.2 (C=O); δ_{F} (470 MHz CDCl_3): -115.3; LCMS $R_t = 1.68$ min, (4); MS (ESI+) m/z 436.2 $[\text{M}+\text{H}]^+$; HRMS m/z : Calc. for $\text{C}_{21}\text{H}_{14}^{35}\text{Cl}_3\text{FNO}_3$: 436.0069 $[\text{M}+\text{H}]^+$. Found 436.0068 $[\text{M}+\text{H}]^+$.

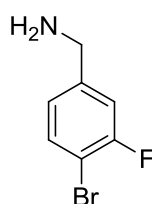
4-Chloro-2-(4-chloro-3-fluorobenzyl)-3-(4-chlorophenyl)-3-((1-(hydroxymethyl)cyclopropyl)methoxy)isoindolin-1-one (**274**)



General procedure C: 4-chloro-2-(4-chloro-3-fluorobenzyl)-3-(4-chlorophenyl)-3-hydroxyisoindolinone (501 mg, 1.15 mmol) and 1,1-bis(hydroxymethyl)cyclopropane (0.22 mL, 2.29 mmol). Chromatography (SP4, silica, 7-60% EtOAc, PE) followed by (SP4, C_{60} , 40-100% 0.1% HCOOH in MeCN, 0.1% HCOOH in water) to give **274** as a white oily solid (107 mg, 18%). $R_f = 0.25$ (3:7 EtOAc:PE); UV λ_{\max} (EtOH): 224.0 nm; IR ν_{\max} 3375 (OH), 2925, 2361, 1694 (C=O), 1585 (Amide C-N), 1489, 1063 (C-F) cm^{-1} ; δ_{H} (500 MHz CDCl_3): 0.17-0.20 (1H, m, cyclopropyl), 0.32-0.35 (1H, m, cyclopropyl), 0.45-0.51 (2H, m, cyclopropyl), 1.66 (1H, s, OH), 2.86 (1H, d, $J = 9.1$ Hz, OCH_2), 2.92 (1H, d, $J = 9.1$ Hz, OCH_2), 3.48 (1H, d, $J = 11.1$ Hz, CH_2OH), 3.56 (1H, d, $J = 11.1$ Hz, CH_2OH), 3.21 (1H, d, $J = 15.0$ Hz, NCH_2), 4.36 (1H, d, $J = 15.1$, NCH_2), 6.83 (1H, d, $J = 8.2$ Hz, Benzyl Ar-H), 6.93 (1H, dd, $J = 1.7$ and 9.8 Hz, benzyl Ar-H), 7.14-7.20 (5H, m, Ar-H), 7.47 (1H, d, $J = 7.9$ Hz, H^5), 7.50-7.53 (1H,

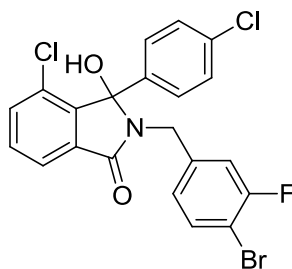
m, H^6), 7.85 (1H, d, $J = 7.4$ Hz, H^7); δ_C (125 MHz $CDCl_3$): 8.5 (cyclopropyl), 8.6 (cyclopropyl), 22.1 (cyclopropyl), 41.9 (NCH_2), 67.7 (CH_2OH), 67.9 (OCH_2), 94.4 (hemi-aminal), 117.3 (d, $J = 21.2$ Hz, $CHCF$), 120.0 (d, $J = 17.5$ Hz, CCl), 122.3, 125.4 (d, $J = 3.6$ Hz, benzyl Ar), 128.3, 128.5, 130.0, 130.2, 132.0, 134.0, 134.0, 134.9 (d, $J = 10.2$ Hz, benzyl Ar), 137.8 (d, $J = 6.4$ Hz, benzyl Ar), 140.6, 157.6 (d, $J = 247.9$ Hz, C-F), 166.7 C=O); δ_F (470 MHz $CDCl_3$): -115.2; LCMS $R_t = 1.74$ min, (3); MS (ESI+) m/z 520.3 $[M+H]^+$; HRMS m/z : Calc. for $C_{26}H_{22}^{35}Cl_3FNO_3$: 520.0644 $[M+H]^+$. Found 520.0643 $[M+H]^+$.; Analytical HPLC: 97.7% purity

4-Bromo-3-fluorobenzylamine (**278**)



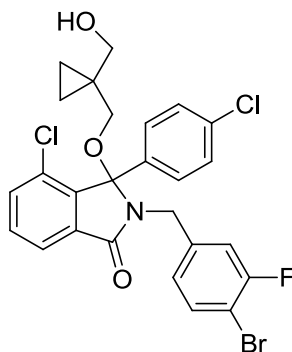
To a solution of 4-bromo-3-benzonitrile (500 mg, 2.50 mmol, 1 eq), in THF (1 mL) was added 1M BH_3 .THF in THF (10 mL, 10.0 mmol, 4 eq) and the reaction was stirred at RT for 20 min then heated to reflux for 14 h, cooled, and a 1:1 solution of AcOH(10 mL) and water (10 mL) was added dropwise with stirring for 15 min, concentrated *in vacuo*. The resulting solid was cooled in an ice-bath, suspended in water (10 mL) and basified to pH 9 with sat. $NaHCO_3$ solution, and extracted using EtOAc (3 x 70 mL). The combined organic extracts were washed with brine (50 mL), dried over $MgSO_4$ and concentrated *in vacuo*. Chromatography (SP4, amino silica, 60-100% EtOAc, PE) gave **278** as a white solid (432 mg, 84%). $R_f = 0.87$ (7:3 EtOAc:PE, amino silica); mp = 90.8-93.0 °C; UV λ_{max} (EtOH): 256.0 nm; IR ν_{max} 3297 (N-H), 2873, 1574, 1237 (C-F) cm^{-1} ; δ_H (500 MHz $CDCl_3$): 1.48 (2H, s, NH_2), 3.85 (2H, s, CH_2), 6.99 (1H, d, $J = 8.1$ Hz, $CHCF$), 7.12 (1H, d, $J = 9.5$ Hz, Ar-H), 7.48 (1H, s, ap. t, $J = 7.6$ Hz, Ar-H); δ_C (125 MHz $CDCl_3$): 45.5 (CH_2), 115.1 (d, $J = 22.1$ Hz, $CHCF$), 123.8 (d, $J = 13.1$ Hz, $CHCCH_2$), 133.4 ($CHCBr$), 145.2 (CCH_2), 159.2 (d, $J = 248.7$, CF); LCMS $R_t = 0.31$ min, (1) ; MS (ESI+) m/z 203.8 $[M+H]^+$; HRMS m/z : Calc. for $C_7H_8^{79}BrFN$: 203.9819 $[M+H]^+$. Found: 203.9822 $[M+H]^+$.

2-(4-Bromo-3-fluorobenzyl)-4-chloro-3-(4-chlorophenyl)-3-hydroxyisoindolinone
(**279**)



General procedure B: sodium 3-chloro-2-(4-chlorobenzoyl)benzoate (989 mg, 3.12 mmol) and 4-bromo-3-fluorobenzylamine (700 mg, 3.43 mmol). Chromatography (SP4, silica, 7-60% EtOAc, PE) gave **279** as an off-white solid (765 mg, 51%). $R_f = 0.43$ (3:7 EtOAc:PE); mp = 192.4-195.1 °C; UV λ_{max} (EtOH): 230.0 nm; IR ν_{max} 3236 (O-H), 2157, 1685 (C=O), 1587 (Amide C-N), 1400, 1093 (C-F), 818, 756 (C-Cl) cm^{-1} ; δ_H (500 MHz $CDCl_3$): 3.08 (1H, s, OH), 4.03 (1H, d, $J = 15.2$ Hz, NCH_2), 4.46 (1H, d, $J = 15.2$ Hz, NCH_2), 6.77 (1H, dd, $J = 1.8$ and 4.1 Hz, benzyl Ar-H), 6.89 (1H, dd, $J = 1.8$ and 9.4 Hz, $CHCF$), 7.18-7.19 (4H, m, Ar-H), 7.26 (1H, dd, $J = 7.3$ and 8.1 Hz, $CHCBr$), 7.37-7.42 (2H, m, H^5 and H^6), 7.68 (1H, dd, $J = 1.7$ and 6.7 Hz, H^7); δ_C (125 MHz $CDCl_3$): 42.0 (NCH_2), 90.8 (hemi-aminal), 107.8 (d, $J = 20.8$ Hz, C-Br), 116.8 (d, $J = 22.5$ Hz, $CHCF$), 122.2, 125.5 (d, $J = 3.5$ Hz, benzyl Ar-H), 128.2, 128.6, 129.6, 131.8, 132.8, 133.2, 134.2, 134.9 (d, $J = 26.7$ Hz, $CHCBr$), 139.3 (d, $J = 6.6$ Hz, benzyl CH_2C), 143.6, 158.7 (d, 246.2 Hz, CF), 166.1; δ_F (470 MHz $CDCl_3$): -107.2; LCMS $R_t = 1.70$ min, (4); MS (ESI+) m/z 579.4 $[M+H]^+$; HRMS m/z : Calc. for $C_{21}H_{13}^{79}Br^{35}Cl_2FNO_2$: 479.9564 $[M+H]^+$. Found 479.9551 $[M+H]^+$.

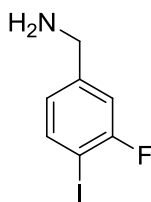
2-(4-Bromo-3-fluorobenzyl)-4-chloro-3-(4-chlorophenyl)-3-((1-(hydroxymethyl)cyclopropane)methoxy)isoindolin-1-one (**281**)



General procedure C: 2-(4-bromo-3-fluorobenzyl)-4-chloro-3-(4-chlorophenyl)-3-hydroxyisoindolinone (294 mg, 0.61 mmol) and 1,1-bis(hydroxymethyl)cyclopropane

(0.12 mL, 1.22 mmol). Chromatography (SP4, silica, 7-60% EtOAc, PE) followed by (SP4, silica, 20-100% EtOAc, PE) gave **281** as an oily white solid (65 mg, 19%). $R_f = 0.33$ (6:4 EtOAc:PE); UV λ_{\max} (EtOH): 260.0, 225.0, 205.0 nm; IR ν_{\max} 3458 (OH), 2925, 2872, 2360, 2159, 1694 (C=O), 1587 (Amide C-N), 1075 (C-F) cm^{-1} ; δ_{H} (500 MHz CDCl_3): 0.17-0.20 (1H, m, cyclopropyl), 0.32-0.35 (1H, m, cyclopropyl), 0.45-0.51 (2H, m, cyclopropyl), 1.67 (1H, s, OH), 2.86 (1H, d, $J = 9.2$ Hz, OCH_2), 2.92 (1H, d, $J = 9.2$ Hz, OCH_2), 3.48 (1H, d, $J = 11.4$ Hz, CH_2OH), 3.55 (1H, d, $J = 11.4$ Hz, CH_2OH), 4.27 (1H, d, $J = 15.1$ Hz, NCH_2), 4.36 (1H, d, $J = 15.1$ Hz, NCH_2), 6.78 (1H, dd, $J = 2.0$ and 8.2 Hz, benzyl Ar-H), 6.91 (1H, dd, $J = 2.0$ and 9.3 Hz, CHCF), 7.19-7.20 (4H, m, Ar-H), 7.31 (1H, dd, $J = 7.1$ and 8.2 Hz, CHCBr), 7.46 (1H, dd, $J = 1.1$ and 8.0 Hz, H^5), 7.50-7.53 (1H, m, H^6), 7.85 (1H, dd, $J = 1.1$ and 7.4 Hz, H^7); δ_{C} (125 MHz CDCl_3): 8.6 (cyclopropyl), 8.6 (cyclopropyl), 22.1 (cyclopropyl), 42.0 (cyclopropyl), 67.8 (CH_2OH), 68.0 (OCH_2), 94.4 (hemi-aminal), 107.9 (d, $J = 20.7$ Hz, C-Br), 117.2 (d, $J = 22.5$ Hz, CHCF), 122.4 (C^4), 125.6 (d, $J = 3.4$ Hz, benzyl Ar-H), 128.2, 128.5, 129.8, 132.0 (C^6), 133.1 (CHCBr), 134.0, 134.0, 138.7 (d, $J = 6.4$ Hz, benzyl C), 134.9, 134.9, 140.6, 158.6 (d, $J = 246.5$ Hz, C-F), 166.7 (C=O); δ_{F} (470 MHz CDCl_3): -107.2; LCMS $R_t = 1.75$ min, (3); HRMS m/z : Calc. for $\text{C}_{26}\text{H}_{22}^{79}\text{Br}^{35}\text{Cl}_2\text{FNO}_3$: 564.0139 $[\text{M}+\text{H}]^+$. Found 564.0137 $[\text{M}+\text{H}]^+$.; Analytical HPLC: 95.3% purity

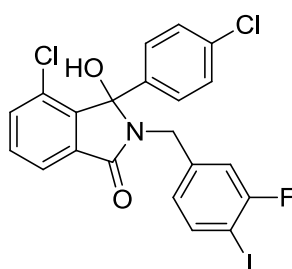
3-Fluoro-4-iodobenzylamine (**277**)



To a solution of 3-fluoro-4-iodobenzonitrile (500 mg, 2.02 mmol, 1 eq) in THF (1 mL) was added 1M $\text{BH}_3 \cdot \text{THF}$ in THF (8.1 mL, 8.10 mmol, 4 eq) and the reaction stirred at RT for 30 min then heated to reflux for 18 h, cooled, diluted with 1:1 AcOH (10 mL) and water (10 mL) added dropwise with stirring for 15 min before concentrated *in vacuo*. The resulting solid was cooled in an ice-bath, diluted with water (10 mL) and basified to pH 9 using sat. NaHCO_3 solution, and extracted using EtOAc (3 x 70 mL). The combined organic extracts were washed with brine (50 mL) and dried over MgSO_4 . Chromatography (SP4, amino silica, 60-100% EtOAc, PE) to give **277** as a white solid (414 mg, 82%). $R_f = 0.46$ (Amino silica) (9:1 EtOAc:PE);

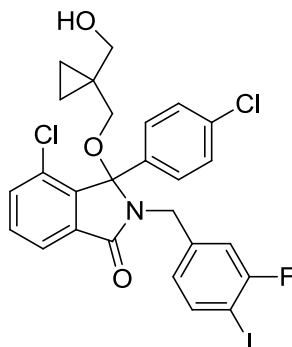
mp = 96.9-99.3 °C; UV λ_{\max} (EtOH): 230.0 nm; IR ν_{\max} 3283 (N-H), 2861, 2158, 1559, 1414, 1023 (C-F) cm^{-1} ; δ_{H} (500 MHz CDCl_3): 1.44 (2H, s, NH_2), 3.84 (2H, s, CH_2), 6.87 (1H, d, $J = 8.0$ Hz, CHCl), 7.06 (1H, d, $J = 8.7$ Hz, CHCF), 7.67 (1H, dd, $J = 6.7$ and 7.8 Hz, Ar-H); δ_{C} (125 MHz CDCl_3): 45.5 (CH_2), 78.6 (d, $J = 26.3$ Hz, Cl), 114.3 (d, $J = 24.0$ Hz, CHCF) 124.4 (d, $J = 3.8$ Hz, Ar-H), 139.2 (d, $J = 1.3$ Hz, CHCl), 146.4 (d, $J = 6.3$ Hz, CCH_2), 161.9 (d, 243.8 Hz, CF); δ_{F} (470 MHz CDCl_3): -94.2; LCMS $R_t = 0.61$ min, (3); MS (ESI+) m/z 252.0 $[\text{M}+\text{H}]^+$

4-Chloro-3-(chlorophenyl)-3-hydroxy-2-(3-fluoro-4-iodobenzyl)isoindolin-1-one
(**280**)



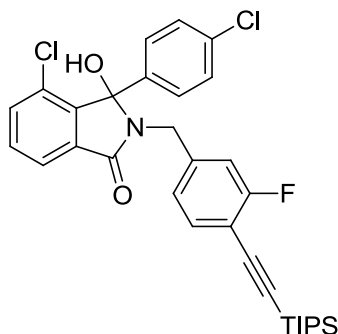
General procedure B: sodium 3-chloro-2-(4-chlorobenzoyl)benzoate (818 mg, 2.58 mmol) and 3-fluoro-4-iodobenzylamine (712 mg, 2.84 mmol). Chromatography (SP4, silica, 7-60% EtOAc, PE) to give **280** as a off-white solid (443 mg, 33%). $R_f = 0.48$ (3:7 EtOAc:PE); mp = 197.5-200.0 °C; UV λ_{\max} (EtOH): 227.0 nm; IR ν_{\max} 3264 (OH), 2362, 1683 (C=O), 1587 (Amide C-N), 1092 (C-F), 816, 757 (C-Cl) cm^{-1} ; δ_{H} (500 MHz CDCl_3): 3.32 (1H, s, OH), 4.02 (1H, d, $J = 15.2$ Hz, NCH_2), 4.43 (1H, d, $J = 15.2$ Hz, NCH_2), 6.63 (1H, dd, $J = 1.6$ and 8.1 Hz, benzyl Ar-H), 6.81 (1H, dd, $J = 1.6$ and 8.7 Hz, benzyl Ar-H), 7.17-7.7.41 (6H, m, Ar-H), 7.44 (1H, dd, $J = 6.7$ and 7.9 Hz, H^6), 7.65 (1H, dd, $J = 2.1$ and 6.3 Hz, H^7); δ_{C} (125 MHz CDCl_3): 42.0 (NCH_2), 90.8 (hemi-aminal), 116.0 (d, $J = 24.1$ Hz, benzyl Ar-H), 122.2, 126.1 (d, $J = 3.4$ Hz, benzyl Ar-H), 128.2, 128.6, 129.6, 131.7, 132.8, 132.2, 134.7, 135.0, 139.0, 140.5 (d, $J = 7.4$ Hz, benzyl Ar-H) 143.7, 161.4 (d, $J = 245.2$ Hz, C-F), 166.1 (C=O); δ_{F} (470 MHz CDCl_3): -93.9; LCMS $R_t = 1.72$ min, (4); MS (ESI+) m/z 528.1 $[\text{M}+\text{H}]^+$; HRMS m/z : Calc. for $\text{C}_{21}\text{H}_{14}^{35}\text{Cl}_2\text{FINO}_3$: 527.9425 $[\text{M}+\text{H}]^+$. Found 527.9411 $[\text{M}+\text{H}]^+$.

4-Chloro-3-(4-chlorophenyl)-3-((1-(hydroxymethyl)cyclopropane)methoxy)-2-(3-fluoro-4-iodobenzyl)isoindolin-1-one (**282**)



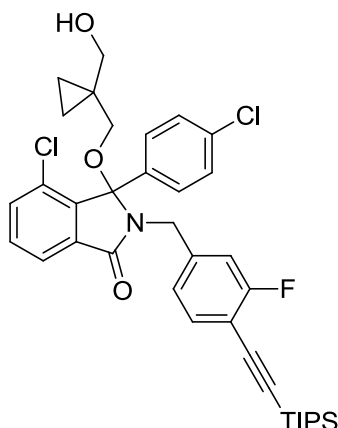
General procedure C: 4-chloro-3-(chlorophenyl)-3-hydroxy-2-(3-fluoro-4-iodobenzyl)isoindolin-1-one (332 mg, 0.63 mmol) and 1,1-bis(hydroxymethyl)cyclopropane (0.12 mL, 1.26 mmol). Chromatography (SP4, silica, 7-60 % EtOAc, PE) gave **282** as a colourless oil (138 mg, 36%). $R_f = 0.22$ (3:7 EtOAc:PE); UV λ_{\max} (EtOH): 227.5 nm; IR ν_{\max} 3481 (OH), 2924, 2876, 2158, 1693 (C=O), 1588 (Amide C-N), 1012 (C-F), 727 (C-Cl) cm^{-1} ; δ_{H} (500 MHz CDCl_3): 0.16-0.19 (1H, m, cyclopropyl), 0.31-0.34 (1H, m, cyclopropyl), 0.44-0.49 (2H, m, cyclopropyl), 1.73 (1H, s, OH), 2.86 (1H, d, $J = 9.1$ Hz, OCH_2), 2.91 (1H, d, $J = 9.1$ Hz, OCH_2), 3.48 (1H, d, $J = 11.4$, CH_2OH), 3.54 (1H, d, $J = 11.4$ Hz, CH_2OH), 4.27 (1H, d, $J = 15.1$, NCH_2), 4.35 (1H, d, $J = 15.1$ Hz, NCH_2), 6.65 (1H, dd, $J = 1.8$ and 8.1 Hz, benzyl Ar-H), 6.77 (1H, dd, $J = 1.8$ and 8.7 Hz, CHCF), 7.17-7.18 (4H, m, Ar-H), 7.45-7.52 (3H, m, H^5 , H^6 and CHCl), 7.84 (1H, dd, $J = 0.7$ and 7.4 Hz, H^7); δ_{C} (125 MHz CDCl_3): 8.5 (cyclopropyl), 8.6 (cyclopropyl), 22.1 (cyclopropyl), 41.9 (NCH_2), 67.1 (CH_2OH), 67.9 (OCH_2), 79.7 (d, $J = 25.4$ Hz, C-I), 94.4 (hemi-aminal), 116.4 (d, $J = 24.1$ Hz, CHCF), 122.4, 126.4 (d, $J = 3.2$ Hz, benzyl C-H), 128.3, 128.5, 129.8, 131.9, 134.0, 134.0, 134.9 (d, $J = 2.8$ benzyl CCH_2), 139.8 (d, $J = 6.6$ Hz, CHCl), 139.8, 139.9, 140.6, 161.3 (d, $J = 244.7$ Hz, C-F), 166.7 (C=O); δ_{F} (470 MHz CDCl_3): -93.8; HRMS m/z : Calc. for $\text{C}_{26}\text{H}_{22}^{35}\text{Cl}_2\text{FINO}_3$: 612.0000 $[\text{M}+\text{H}]^+$. Found 612.0001 $[\text{M}+\text{H}]^+$; Analytical HPLC: 99.2% purity

4-Chloro-3-(4-chlorophenyl)-2-(3-fluoro-4-((4-triisopropylsilyl)ethynyl)benzyl)-3-hydroxyisoindolin-1-one (**283**)



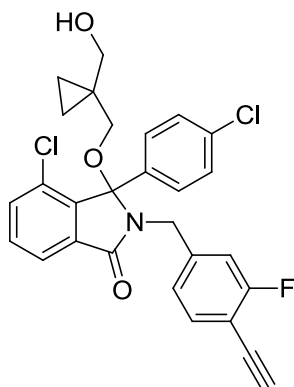
General procedure F: 4-chloro-3-(chlorophenyl)-3-hydroxy-2-(3-fluoro-4-iodobenzyl)isoindolin-1-one (250 mg, 0.47 mmol) and triisopropylsilylacetylene (138 μ L, 0.62 mmol). Chromatography (SP4, silica, 7-60% EtOAc, PE) to give **283** as an oily brown solid (261 mg, 95%). $R_f = 0.66$ (3:7 EtOAc:PE); mp = 180.0-182.2 $^{\circ}$ C; UV λ_{\max} (EtOH): 224.0 nm; IR ν_{\max} 3305 (OH), 2159 (Ethyne stretch), 1687 (C=O), 1588 (Amide C-N), 1092 (C-F), 757 (C-Cl) cm^{-1} ; δ_H (500 MHz CDCl_3): 1.04 (18H, s, CH_3), 3.51 (1H, s, OH), 3.99 (1H, d, $J = 15.3$ Hz, NCH_2), 4.45 (1H, d, $J = 15.3$ Hz, NCH_2), 6.76-6.79 (2H, m, Ar-H), 7.13-7.19 (5H, m, Ar-H), 7.35-7.40 (H^5 and H^6), 7.62 (1H, dd, $J = 2.2$ and 6.2 Hz); δ_C (125 MHz CDCl_3): 11.2 (CH_3), 18.6 ($\text{CH}(\text{CH}_3)_2$), 42.3 (NCH_2), 90.0 ($\text{CSi}(\text{C}_3\text{H}_7)_3$), 96.9 ($\text{CCSi}(\text{C}_3\text{H}_7)_3$), 99.9 ($\text{C}-\text{CCSi}(\text{C}_3\text{H}_7)_3$), 115.6 (d, $J = 21.3$ Hz, benzyl Ar-H), 122.1, 124.0, 124.0 (d, $J = 8.0$ Hz, benzyl Ar-H), 128.2, 128.6, 129.6, 131.6, 132.7, 133.5, 134.1, 134.8 (d, $J = 14.2$ Hz, benzyl Ar-H), 140.1 (d, $J = 7.2$ Hz, benzyl Ar-H), 143.8, 166.2 (C=O); δ_F (470 MHz CDCl_3): -109.6; LCMS $R_t = 2.25$ min, (4); MS (ESI+) m/z 582.4 $[\text{M}+\text{H}]^+$; HRMS m/z : Calc. $\text{C}_{32}\text{H}_{35}^{35}\text{Cl}_2\text{FNO}_2\text{Si}$: 582.1793 $[\text{M}+\text{H}]^+$. Found 582.1780 $[\text{M}+\text{H}]^+$.

4-Chloro-3-(4-chlorophenyl)-2-(3-fluoro-4-((triisopropylsilyl)ethynyl)benzyl)-3-(1-((hydroxymethyl)cyclopropane)methoxy)isoindolin-1-one (**284**)

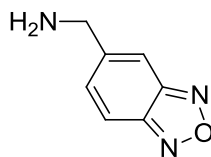


General procedure C: 4-chloro-3-(4-chlorophenyl)-2-(3-fluoro-4-((4-triisopropylsilyl)ethynyl)benzyl)-3-hydroxyisoindolin-1-one (261 mg, 0.45 mmol) and 1,1-bis(hydroxymethyl)cyclopropane (0.09 mL, 0.45 mmol). Chromatography (SP4, silica, 7-60% EtOAc, PE) gave **284** as a colourless oil (77 mg, 26%). $R_f = 0.23$ (3:7 EtOAc:PE); UV λ_{\max} (EtOH): 260.5 nm; IR ν_{\max} 3397, 2943, 2865, 2160, 1698 (C=O), 1588 (Amide C-N), 1013 (C-F), 760 (C-Cl) cm^{-1} ; δ_H (500 MHz CDCl_3): 0.13-0.16 (1H, m, cyclopropyl), 0.26-0.28 (1H, m, cyclopropyl), 0.37-0.41 (2H, m, cyclopropyl), 1.04 (18H, s, CH_3), 1.73 (1H, s, OH), 2.81 (1H, d, $J = 9.2$ Hz, OCH_2), 2.84 (1H, d, $J = 9.2$ Hz, OCH_2), 3.42 (1H, d, $J = 11.4$ Hz, CH_2OH), 3.48 (1H, d, $J = 11.4$ Hz, CH_2OH), 4.23 (1H, d, $J = 15.0$ Hz, NCH_2), 4.29 (1H, d, $J = 15.0$ Hz, NCH_2), 6.73 (1H, dd, $J = 1.4$ and 8.0 Hz benzyl Ar-H), 6.76 (1H, dd, $J = 1.4$ and 9.8 Hz, CHCF), 7.10-7.15 (5H, m, Ar-H), 7.38 (1H, dd, $J = 1.0$ and 8.0 Hz, H^5), 7.42-7.45 (1H, m, H^6), 7.78 (1H, dd, $J = 1.0$ and 7.4 Hz, H^7); δ_C (125 MHz CDCl_3): 7.5 (cyclopropyl), 7.6 (cyclopropyl), 10.2 (CH_3), 17.6 ($\text{CH}(\text{CH}_3)_2$), 21.1 (cyclopropyl), 41.2 (NCH_2), 66.7 (CH_2OH), 66.9 (OCH_2), 93.4 (ethynyl), 95.9 (d, $J = 3.2$ Hz, ethynyl), 98.5 (hemi-aminal), 110.1 (d, $J = 16.1$ Hz, C-CC), 115.0 (d, $J = 21.4$ Hz, CHCF), 121.3, 123.3 (d, $J = 3.3$ Hz, benzyl Ar-H), 127.2, 127.4, 128.7, 130.9, 132.4, 132.9, 133.0, 133.8 (d, $J = 6.8$ Hz, benzyl Ar-H), 138.4 (d, $J = 7.1$ Hz, benzyl Ar-H), 139.6, 161.7 (d, $J = 251.2$ Hz, C-F), 165.6 (C=O); δ_F (470 MHz CDCl_3): -109.6; LCMS $R_t = 2.33$ min, (5); MS (ESI+) m/z 666.5 $[\text{M}+\text{H}]^+$; HRMS m/z : Calc. for $\text{C}_{37}\text{H}_{43}^{35}\text{Cl}_2\text{FNO}_3\text{Si}$: 666.2368 $[\text{M}+\text{H}]^+$ Found 666.2362 $[\text{M}+\text{H}]^+$

4-Chloro-3-(4-chlorophenyl)-2-(4-ethynyl-3-fluorobenzyl)-3-(1-((hydroxymethyl)cyclopropane)methoxy)isoindolin-1-one (**285**)

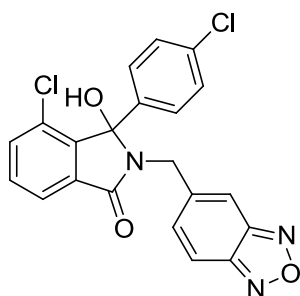


General procedure G: 4-chloro-3-(4-chlorophenyl)-2-(3-fluoro(4-((triisopropylsilyl)ethynyl)benzyl)-3-(1-((hydroxymethyl)cyclopropane)methoxy)isoindolin-1-one (90 mg, 0.14 mmol). Chromatography (SP4, silica, 7-60 % EtOAc, PE) gave the title compound as colourless oil (44 mg, 62%). $R_f = 0.22$ (3:7 EtOAc:PE); UV λ_{max} (EtOH): 230.0 nm; IR ν_{max} 3296 (OH), 2361 (Ethyne stretch), 1696 (C=O), 1588 (Amide C-N), 1012 (C-F), 761 (C-Cl) cm^{-1} ; δ_H (500 MHz CDCl_3): 0.15-0.18 (1H, m, cyclopropyl), 0.31-0.33 (1H, m, cyclopropyl), 0.44-0.49 (2H, m, cyclopropyl), 1.73 (1H, s, OH), 2.85 (1H, d, $J = 9.1$ Hz, OCH_2), 2.92 (1H, d, $J = 9.1$ Hz, OCH_2), 3.26 (1H, s, ethynyl), 3.47 (1H, d, $J = 11.3$ Hz, CH_2OH), 3.54 (1H, d, $J = 11.3$ Hz, CH_2OH), 4.26 (1H, d, $J = 15.1$ Hz, NCH_2), 4.40 (1H, d, $J = 15.1$ Hz, NCH_2), 6.64-6.88 (2H, m, benzyl Ar-H), 7.19-7.26 (5H, m, Ar-H), 7.46 (1H, dd, $J = 1.0$ and 8.0 Hz, H^5), 7.50-7.53 (1H, m, H^6), 7.85 (1H, dd, $J = 1.0$ and 7.4 Hz, H^7); δ_C (125 MHz CDCl_3): 8.5 (cyclopropyl), 8.6 (cyclopropyl), 22.1 (cyclopropyl), 42.2 (NCH_2), 67.7 (CH_2OH), 68.0 (OCH_2), 76.7 (ethynyl), 82.6 (d, $J = 3.2$ Hz, ethynyl), 94.5 (hemiaminal), 109.6 (d, $J = 15.6$ Hz, C-CCH), 116.1 (d, $J = 21.3$ Hz, CHCF), 122.4, 124.5 (d, $J = 3.3$ Hz, benzyl Ar-H), 128.3, 128.5, 129.8, 131.9, 133.6, 134.0, 134.0, 134.9 (d, $J = 3.6$ Hz, benzyl Ar-H), 140.3 (d, $J = 7.5$ Hz, benzyl Ar-H), 140.7, 162.9 (d, $J = 251.3$ Hz, C-F), 166.7 (carbonyl); δ_F (470 MHz CDCl_3): -110.0; HRMS m/z : Calc. for $\text{C}_{28}\text{H}_{22}^{35}\text{Cl}_2\text{FNO}_3$: 510.1034 $[\text{M}+\text{H}]^+$. Found 510.1034 $[\text{M}+\text{H}]^+$; Analytical HPLC: 98.1% purity

Benzo[*c*][1,2,5]oxadiazol-5-ylmethanamine (**288**)

To a solution of 5-(bromomethyl)-2,1,3-benzoxadiazole (500 mg, 2.35 mmol, 1 eq) in DMF (6 mL) was added potassium phthalamide (435 mg, 2.35 mmol, 1 eq) and the reaction was stirred at room temperature for 16 h. The solvent was removed *in vacuo*, and the resulting white solid was suspended in water (20 mL) and extracted into EtOAc (3 x 20 mL). The organic extracts were dried over MgSO₄, and concentrated *in vacuo*. The resulting solid was dissolved in EtOH (5 mL) and 40% aq. methylamine (5 mL) added and the reaction was stirred for 25 h, concentrating *in vacuo*, the white solid was suspended in water (50 mL) and extracting with EtOAc (3 x 50 mL). The combined organic extract was dried (MgSO₄) and concentrated *in vacuo*.

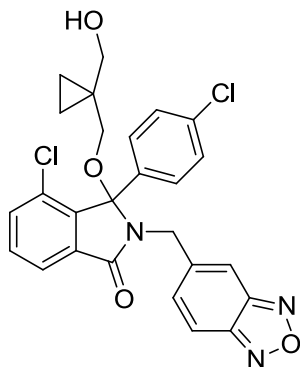
Chromatography (SP4, silica, 2-20% MeOH, EtOAc) gave **288** as an orange gummy solid (186 mg, 53%). $R_f = 0.07$ (1:9 MeOH:EtOAc); UV λ_{\max} (EtOH): 289.5 nm; IR ν_{\max} 2891, 2358, 2159, 1977, 1521 (Oxadiazole ring), 878, 800 cm⁻¹; δ_H (500 MHz CDCl₃): 1.55 (2H, s, NH₂), 4.02 (2H, s, CH₂), 7.40 (1H, dd, $J = 1.1$ and 9.2 Hz, CHCCH₂), 7.77-7.78 (1H, m, NCCHCCH₂), 7.80 (1H, d, $J = 14.3$, NCCHCH); δ_C (125 MHz CDCl₃): 46.2 (CH₂), 111.7 (NCCHCCH₂), 116.3 (NCCHCH), 132.7 (CHCCH₂), 147.0 (CCH₂), 148.9 (C=N), 149.5 (C=N)

2-(Benzo[*c*][1,2,5]oxadiazol-5-ylmethyl)-4-chloro-3-(4-chlorophenyl)-3-hydroxyisoindolin-1-one (**290**)

General procedure B: sodium 3-chloro-2-(4-chlorobenzoyl)benzoate (504 mg, mmol) and benzo[*c*][1,2,5]oxadiazol-5-ylmethanamine (261 mg, 1.75 mmol). Chromatography (SP4, silica, 7-60% EtOAc) and (silica, 1:1 EtOAc:PE) gave **290** as a gummy yellow solid (100 mg, 15%). $R_f = 0.61$ (1:1 EtOAc:PE); UV λ_{\max} (EtOH): 271.5 nm; IR ν_{\max} 3285 (OH), 2158, 2018, 1691 (C=O), 1665 (Oxadiazole ring), 1586

(Amide C-N), 820, 760 (C-Cl) cm^{-1} ; δ_{H} (500 MHz CDCl_3): 4.14 (1H, d, $J = 15.8$ Hz, NCH_2), 4.48 (1H, d, $J = 15.8$ Hz, NCH_2), 5.25 (1H, s, OH), 7.10-7.13 (3H, m, Ar-H), 7.17-7.19 (2H, m, Ar-H), 7.29-7.32 (2H, m, Ar-H), 7.35 (1H, dd, 1.0 and 7.9 Hz, H^5), 7.51 (1H, dd, $J = 0.6$ and 9.4 Hz, H^6), 7.53 (1H, dd, $J = 1.0$ and 7.3 Hz, H^7); δ_{C} (125 MHz CDCl_3): 42.7 (NCH_2), 91.0 (hemi-aminal), 114.3 (benzyl Ar-H), 116.1 (benzyl Ar-H), 121.9, 128.2, 128.6, 129.8, 131.6, 132.4, 132.9, 134.3, 134.8, 135.0, 141.4, 144.0, 148.3 (C=N), 148.7 (C=N), 166.7 (C=O); LCMS $R_t = 1.55$ min, (3); MS (ESI+) m/z 426.2 $[\text{M}+\text{H}]^+$ HRMS m/z : Calc. for $\text{C}_{21}\text{H}_{14}^{35}\text{Cl}_2\text{N}_3\text{O}_3$: 426.0407 $[\text{M}+\text{H}]^+$. Found 426.0405 $[\text{M}+\text{H}]^+$.

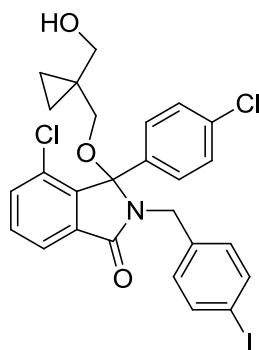
2-(Benzo[*c*][1,2,5]oxadiazol-5-ylmethyl)-4-chloro-3-(4-chlorophenyl)-3-((1-(hydroxymethyl)cyclopropyl)methoxy)isoindolin-1-one (**291**)



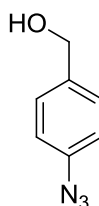
General procedure D: compound **290** (80 mg, 0.19 mmol) and 1,1-bis(hydroxymethyl)cyclopropane (0.18 mL, 1.88 mmol, 10 eq). Further additions of $\text{BF}_3 \cdot \text{OEt}_2$ at 0 °C occurred after 18 h and stirred for a further 2 days. Chromatography (SP4, silica, 17-100 % EtOAc, PE) followed by semi-preparative HPLC (95-0% acetonitrile, 0.1% formic acid (aq)) to give **291** as a colourless oil (35 mg 36%). $R_f = 0.55$ (3:7 EtOAc:PE); UV λ_{max} (EtOH) 268.0 nm; IR ν_{max} 3465 (OH), 2922, 2159, 2032, 1699 (C=O), 1588 (Amide C-N), 1011, 818, 760 (C-Cl) cm^{-1} ; δ_{H} (500 MHz CDCl_3): 0.17-0.24 (1H, m, cyclopropyl), 0.36-0.41 (1H, m, cyclopropyl), 0.43-0.48 (2H, m, cyclopropyl), 1.62 (1H, s, OH), 2.90 (1H, d, $J = 9.1$ Hz, CH_2OH), 4.60 (1H, d, $J = 9.1$ Hz, CH_2OH), 3.50-3.55 (2H, m, OCH_2), 4.41 (1H, d, $J = 15.3$ Hz, NCH_2), 4.57 (1H, d, $J = 15.3$ Hz, NCH_2), 7.07-7.26 (4H, m, Ar-H), 7.32 (1H, dd, $J = 1.1$ and 9.3 Hz, benzyl CHCCH_2), 7.37 (1H, s, benzyl CCHCN), 7.27 (1H, dd, $J = 0.6$ and 7.9 Hz, H^5), 7.31-7.34 (1H, m, H^6), 7.40 (1H, $J = 9.3$ Hz, benzyl CHCN), 7.66 (1H, dd, $J = 0.6$ and 7.4 Hz, H^7); δ_{C} (125 MHz CDCl_3): 8.5 (cyclopropyl), 8.7 (cyclopropyl),

22.2 (cyclopropyl), 42.6 (NCH₂), 67.5 (CH₂OH), 67.7 (OCH₂), 94.3 (hemi-aminal), 115.3 (benzyl CCHCN), 116.4 (CHCN), 122.4 (C⁷), 128.2, 128.5, 129.9, 132.1 (C⁶), 133.1 (benzyl CHCCH₂), 133.8, 134.2 (C⁵), 135.0, 140.6, 140.7, 148.2 (C=N), 148.8 (C=N), 166.8 (C=O); LCMS R_t = 1.58 min, (3); MS (ESI+) m/z 510.3 [M+H]⁺; HRMS m/z: Calc. for C₂₆H₂₂³⁵Cl₂N₃O₄: 510.0982 [M+H]⁺. Found: 510.0979 [M+H]⁺.; Analytical HPLC: 98.1% purity

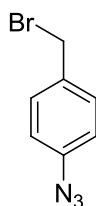
4-Chloro-3-(4-chlorophenyl)-2-(4-iodobenzyl)-3-((1-(hydroxymethyl)cyclopropyl)methoxy)isoindolin-1-one (**296**)



General procedure C: 4-chloro-3-(4-chlorophenyl)-2-(4-iodobenzyl)-3-(1-((hydroxymethyl)cyclopropyl)methoxy)isoindolin-1-one (120 mg, 0.24 mmol) and 1,1-bis(hydroxymethyl)cyclopropane (0.045 mL, 0.47 mmol). Chromatography (SP4, silica, 7-60% EtOAc, petrol) gave **296** as a colourless oil (75 mg, 52%). R_f = 0.33 (7:3 PE:EtOAc); UV λ_{max} (EtOH): 227.0 nm; IR ν_{max} 2360, 2160, 1684 (C=O), 1588 (Amide C-N) cm⁻¹; δ_H (500 MHz CDCl₃): 0.11-0.13 (1H, m, cyclopropyl), 0.28-0.32 (1H, m, cyclopropyl), 0.42-0.47 (2H, m, cyclopropyl), 2.80 (1H, d, J = 9.1 Hz, OCH₂), 2.89 (1H, d, J = 9.1 Hz, OCH₂), 3.43 (1H, d, J = 11.2 Hz, CH₂OH), (1H, d, J = 11.2 Hz, CH₂OH), 4.16 (1H, d, J = 15.0 Hz, NCH₂), 4.41 (1H, d, J = 15.0 Hz, NCH₂), 6.88 (2H, d, J = 8.3 Hz, Ar-H), 7.18-7.20 (4H, m, Ar-H), 7.44-7.52 (4H, m, Ar-H), 7.84 (1H, dd, J = 7.4 and 0.8 Hz, H⁷) δ_C (125 MHz CDCl₃): 8.6 (cyclopropyl), 22.1 (cyclopropyl), 42.4 (NCH₂), 67.0 (CH₂OH), 68.8 (OCH₂), 92.9 9 (Ar-I), 94.6 (hemi-aminal C), 122.3, 128.3, 128.5, 129.7, 131.0, 131.8, 133.9, 134.1, 134.8, 135.0, 136.7, 137.3, 140.7, 166.7 (carbonyl)

4-Azidobenzyl amine (**299**)

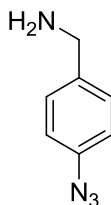
To a solution of 4-aminobenzyl alcohol (100 mg, 0.81 mmol, 1 eq) in 5 M aqueous HCl (3 mL) at 0 °C was added dropwise over 30 min an aqueous solution of NaNO₂ (71 mg, 1.03 mmol, 1.27 eq in 2 mL of water), followed by NaN₃ (CAUTION) (228 mg, 3.51 mmol, 4.3 eq) in portions over a further 30 min. The reaction mixture was stirred at 0 °C for a further 1 h before diluting with water (15 mL) and basifying with saturated aqueous solution of NaHCO₃ to around pH 8, then extracted into EtOAc (3 x 25 mL), dried over MgSO₄ and concentrated *in vacuo*. Chromatography (SP4, silica, 7-60% EtOAc, PE) gave the title compound as a colourless oil which solidified on standing to give a white solid which was stored in the dark at 4 °C (118 mg, 98%). $R_f = 0.43$ (3:7 EtOAc:PE); UV λ_{max} (EtOH): 251.5 nm; IR ν_{max} 3300 (OH), 2927, 2863, 2415, 2103 (very strong, N₃), 1505 cm⁻¹; δ_H (500 MHz CDCl₃): 1.84 (1H, s, OH), 4.58 (2H, s, CH₂), 6.94 (2H, d, $J = 8.5$ Hz, *CHCN*₃), 7.27 (2H, d, $J = 8.5$ Hz, *CHCCH*₂); δ_C (125 MHz CDCl₃): 64.7 (CH₂), 119.1 (*CHCCH*₂), 128.5 (*CHCN*₃), 137.6 (CN₃), 139.4 (CCH₂)

4-Azidobenzyl bromide (**300**)

To a solution of 4-azidobenzyl alcohol (334 mg, 2.24 mmol, 1 eq) in diethyl ether (2mL) at 0°C was added PBr₃ (168 μ L, 1.79 mmol, 0.8 eq) in diethyl ether (2 mL) over 30 min. The reaction was stirred for 15 min at 0 °C, then room temperature for 30 min, diluted with water (10 mL) and extracted with EtOAc (3 x 15 mL). The combined organic extracts were washed with sat. NaHCO₃ (30 mL) and brine (30 mL), dried over MgSO₄ and concentrated *in vacuo*. Chromatography (SP4, silica, 1-10% EtOAc, PE) gave **300** as a colourless oil (363 mg, 76%). $R_f = 0.75$ (1:9 EtOAc:PE); UV λ_{max} (EtOH): 379.0, 262.0, 209.0 nm; IR ν_{max} 2104 (very strong, N₃),

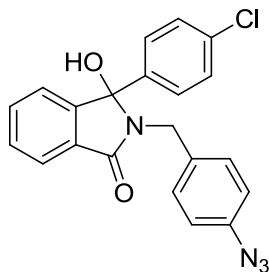
1606, 1504 cm^{-1} ; δ_{H} (500 MHz CDCl_3): 4.40 (2H, s, CH_2), 6.92 (2H, d, $J = 8.5$ Hz, CHCN_3), 7.30 (2H, d, $J = 8.5$ Hz, CHCCH_2); δ_{C} (125 MHz CDCl_3): 32.9 (CH_2), 119.4 (CHCCH_2), 130.6 (CHCN_3), 134.5 (CN_3), 140.2 (CCH_2)

4-Azidobenzylamine (**295**)



To benzyl bromide **289** (91 mg, 0.43 mmol, 1 eq) in acetonitrile (4 mL) was added 18-crown-6 (14 mg, 0.05 mmol, 1 eq) and the reaction was stirred at room temperature for 30 min, then sodium diformylamide (110 mg, 1.16 mmol, 2.7 eq) was added and the reaction heated to 95 °C for 24 h before cooling to room temperature. 5% HCl in EtOH (3 mL) was added and the reaction stirred for 3 days, then concentrated *in vacuo*. The residues were diluted with sat. NaHCO_3 (15 mL) and extraction with EtOAc (3 x 25 mL). The combined organic extracts were dried (MgSO_4) and concentrated *in vacuo*. Chromatography (SP4, silica, 7-60% EtOAc, PE) gave **295** as a white oily solid (61 mg, 96%). $R_f = 0.41$ (3:7 EtOAc:PE); UV λ_{max} (EtOH): 251.5 nm; IR ν_{max} 3307 (NH), 2101 (very strong, N_3), 1506, 1279 cm^{-1} ; δ_{H} (500 MHz CDCl_3): 4.66 (2H, s, CH_2), 7.03 (2H, d, $J = 8.5$ Hz, CHCN_3), 7.36 (2H, d, $J = 8.5$ Hz, CHCCH_2); δ_{C} (125 MHz CDCl_3): 64.7 (CH_2), 119.1 (CHCCH_2), 128.6 (CHCN_3), 137.6 (CN_3), 139.4 (CCH_2)

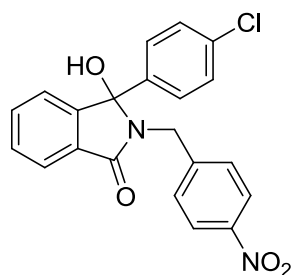
2-(4-Azidobenzyl)-3-(4-chlorophenyl)-3-hydroxyisoindolinone (**301**)



General procedure B: 2-(4-chlorobenzoyl)benzoic acid (185 mg, 0.71 mmol, 1 eq) and 4-azidobenzyl amine (116 mg, 0.78 mmol). The reaction was undertaken in the dark. Chromatography (SP4, silica, 7-60% EtOAc, PE) gave the title compound as a yellow oil (216 mg, 78%). $R_f = 0.79$ (3:7 EtOAc:PE); UV λ_{max} (EtOH): 252.5, 225.5

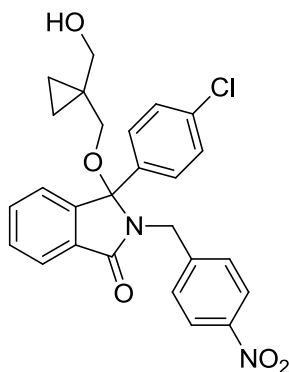
nm; IR ν_{\max} 2110 (very strong, N₃), 1775 (C=O), 1606 (Amide C-N), 1092 cm⁻¹; δ_{H} (500 MHz CDCl₃): 4.28 (1H, d, J = 11.1 Hz, NCH₂), 4.45 (1H, d, J = 11.1 Hz, NCH₂), 4.45 (1H, d, J = 11.1 Hz, NCH₂), 6.89 (2H, d, J = 8.6 Hz, CHCN₃), 7.19 (2H, dt, J = 2.5 and 8.6 Hz, benzyl Ar-H), 7.28 (2H, dt, J = 2.0 and 8.8 Hz, Ar-H), 7.39 (1H, d, J = 7.7 Hz, H⁴), 7.46 (2H, dt, J = 2.0 and 8.8 Hz, Ar-H), 7.52 (1H, ap. td, J = 0.9 and 7.5 Hz, H⁵), 7.60 (1H, ap. td, J = 1.1 and 7.5 Hz, H⁶), 7.86 (1H, ap. td, J = 0.8 and 7.6 Hz, H⁷); δ_{C} (125 MHz CDCl₃): 108.1 (hemi-aminal), 119.1, 123.3, 125.8, 126.3, 127.3, 129.0, 129.5, 130.9, 133.3, 135.5, 136.3, 139.8 (C-N₃), 147.9, 168.1 (C=O)

3-(4-Chlorophenyl)-3-hydroxy-2-(4-nitrobenzyl)isoindolin-1-one (**304**)



General procedure B: 2-(4-chlorobenzoyl)benzoic acid (750 mg, 2.88 mmol) and 4-nitrobenzylamine hydrochloride (597 mg, 3.16 mmol). Chromatography (silica, 1:1 EtOAc:PE) gave **304** as a white solid (714 mg, 63%). R_f = 0.66 (1:1 EtOAc:PE); mp = 178.3-182.1 °C (lit 148-149 °C)¹⁹²; UV λ_{\max} (EtOH): 257.5 nm; IR ν_{\max} 3190 (OH), 2928, 1679 (C=O), 1608 (Amide C-N), 1342 (NO₂ stretch), 709, 693 (C-Cl) cm⁻¹; δ_{H} (500 MHz CDCl₃): 3.40 (1H, s, OH), 4.16 (1H, d, J = 15.4 Hz, NCH₂), 4.58 (1H, d, J = 15.4 Hz, NCH₂), 7.13-7.20 (5H, m, Ar-H), 7.25 (2H, d, J = 8.7 Hz, benzyl Ar-H), 7.43 (2H, ap. dtd, J = 1.3, 7.4 and 18.2 Hz, H⁵ and H⁶), 7.71 (1H, d, J = 6.9 Hz, H⁷), 7.91 (2H, d, J = 8.7 Hz, CHCNO₂); δ_{C} (125 MHz CDCl₃): 42.3 (NCH₂), 91.1 (hemi-aminal), 122.8, 123.4 (CHCNO₂), 123.7 (H⁷), 127.8, 128.8, 129.5, 129.8 (benzyl Ar-H), 130.1, 133.4, 134.9, 136.4, 145.2, 147.0, 148.3, 167.8 (C=O); LCMS R_t = 1.52 min, (3); MS (ESI+) m/z 395.3 [M+H]⁺

3-(4-Chlorophenyl)-3-((1-(hydroxymethyl)cyclopropyl)methoxy)-2-(4-nitrobenzyl)isoindolin-1-one (**195**)



Using commercial Vilsmeier reagent

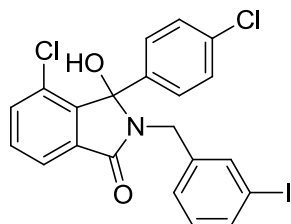
To a solution of **304** (100 mg, 0.25 mmol, 1 eq) in THF (3 mL) was added (chloromethylene)dimethyliminium chloride (44 mg, 0.38 mmol, 1.5 eq) and the reaction stirred for 4 h at room temperature, then concentrated *in vacuo*. The residue was dissolved in THF (3 mL) and K_2CO_3 (74 mg, 0.54 mmol, 2.1 eq) and 1,1-bis(hydroxymethyl)cyclopropane (0.05 mL, 0.51 mmol, 2 eq) added. The reaction was stirred for 16 h then concentrated *in vacuo*. The residue was suspended in water (30 mL) and extracted with EtOAc (3 x 50 mL). The combined organic extracts were washed with brine and dried (Na_2SO_4) and concentrated *in vacuo*. Chromatography (SP4, silica, 12-100% EtOAc, PE) gave **195** as a white oily solid (26 mg, 22%).

Using oxalyl chloride

To a solution of **304** (100 mg, 0.25 mmol, 2 eq) in DCM (2 mL) was added $(COCl)_2$ (0.11 mL, 1.27 mmol, 5 eq) dropwise, and the mixture was stirred for 2 h, then concentrated *in vacuo*. The residue was redissolved in DCM (2 mL), K_2CO_3 (73 mg, 0.55 mmol, 2.2 eq) and 1,1-bis(hydroxymethyl)cyclopropane (0.05 mL, 0.51 mmol, 2 eq) was added and the reaction stirred for 15 h, then concentrated *in vacuo*. The residue was suspended in water (30 mL) before extracting with EtOAc (3 x 30 mL). The combined organic extracts were washed with Na_2SO_4 , and concentrated *in vacuo*. Chromatography (SP4, silica, 12-100% EtOAc, PE) gave **195** as an oily solid (74 mg, 62%).

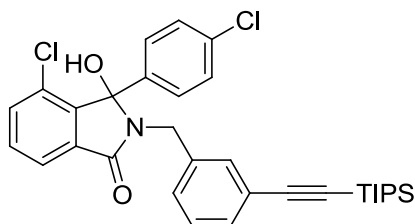
$R_f = 0.56$ (1:1 EtOAc:PE); UV λ_{\max} (EtOH): 267.5 nm; IR ν_{\max} 3445 (OH), 2923, 2875, 1689 (C=O), 1605 (Amide C-N), 1341 (NO₂) cm⁻¹; δ_H (500 MHz CDCl₃): 0.14-0.16 (1H, m, cyclopropyl), 0.19-0.21 (1H, m, cyclopropyl), 0.41-0.46 (2H, m, cyclopropyl), 1.57 (1H, t, $J = 2.4$ Hz OH), 2.80 (1H, d, $J = 9.5$ Hz, OCH₂), 2.82 (1H, d, $J = 9.5$ Hz, OCH₂), 3.45 (1H, dd, $J = 2.4$ and 11.2 Hz, CH₂OH), 3.50 (1H, dd, $J = 2.4$ and 11.2 Hz, CH₂OH), 4.47 (1H, d, $J = 15.2$ Hz, NCH₂), 4.52 (1H, d, $J = 15.2$ Hz, NCH₂), 7.15-7.17 (4H, m, Ar-H), 7.32 (2H, d, $J = 6.9$ Hz, Ar-H), 7.53-7.57 (2H, m, Ar-H), 7.91-7.93 (1H, m, H^7), 8.01 (1H, d, $J = 8.8$ Hz, CHCNO₂); δ_C (125 MHz CDCl₃): 8.6 (cyclopropyl), 8.7 (cyclopropyl), 22.3 (cyclopropyl), 42.3 (cyclopropyl), 67.5 (CH₂OH), 67.7 (OCH₂), 94.5 (hemi-aminal), 123.1, 123.4, 123.9, 127.9, 128.7, 129.8, 130.2, 131.2, 133.3, 134.8, 136.8, 144.7, 145.0 (C-NO₂), 147.1, 168.3; LCMS $R_t = 1.59$ min, (3); MS (ESI+) m/z 479.2 [M+H]⁺

4-Chloro-3-(4-chlorophenyl)-3-hydroxy-2-(3-iodobenzyl)isoindolin-1-one (**307**)



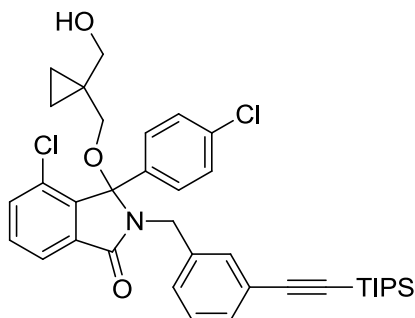
General procedure B: sodium 3-chloro-2-(4-chlorobenzoyl)benzoate (440 mg, 1.39 mmol) and 3-iodobenzylamine hydrochloride (750 mg, 2.78 mmol). Chromatography (SP4, silica, 7-60 % EtOAc, PE) gave **307** as a white solid (263 mg, 37%). $R_f = 0.5$ (3:7 EtOAc:PE); mp = 183.9-185.3 °C; UV λ_{\max} (EtOH): 225.0 nm; IR ν_{\max} 3278 (OH), 1679 (C=O), 1587 (Amide C-N), 813, 764 (C-Cl) cm⁻¹; δ_H (500 MHz CDCl₃): 3.56 (1H, s, OH), 4.10 (1H, d, $J = 15.1$ Hz, NCH₂), 4.31 (1H, d, $J = 15.1$ Hz, NCH₂), 7.07 (1H, d, $J = 7.8$, benzyl Ar-H), 7.13-7.19 (4H, m, Ar-H), 7.22-7.23 (1H, m, Ar-H), 7.36-7.40 (3H, m, Ar-H), 7.61-7.65 (1H, m, H^7); δ_C (125 MHz CDCl₃): 42.0 (NCH₂), 90.8 (Cl), 95.1 (hemi-aminal), 122.2, 128.1, 128.2, 128.5, 129.7, 129.9, 131.6, 132.8, 134.1, 134.7, 134.8, 136.2, 137.6, 139.6, 143.8, 166.2 (C=O); LCMS $R_t = 1.72$ min, (5); MS (ESI+) m/z 510.1 [M+H]⁺; HRMS m/z : Calc. for C₂₁H₁₅³⁵Cl₂INO₂: 509.9519 [M+H]⁺. Found 509.9515 [M+H]⁺.

4-Chloro-3-(4-chlorophenyl)-3-hydroxy-2-(3-((triisopropylsilyl)ethynyl)benzyl)isoindolinone (**308**)



General procedure F: 4-chloro-3-(4-chlorophenyl)-3-hydroxy-2-(3-iodobenzyl)isoindolin-1-one (263 mg, 0.52 mmol, 1 eq) and triisopropylsilylacetylene (150 μ L, 0.67 mmol). Chromatography (SP4, silica, 7-60% EtOAc, PE) gave the title compound as a white solid (234 mg, 80%). $R_f = 0.51$ (3:7 EtOAc:PE); mp = 206.9-208.8 $^{\circ}$ C; UV λ_{max} (EtOH): 262.0, 250.5 nm; IR ν_{max} 3373 (C=O), 2943, 2864, 2159 (Ethyne), 1695 (C=O), 1587 (Amide C-N), 760 (C-Cl) cm^{-1} ; δ_H (500 MHz $CDCl_3$): 1.05 (18H, s, CH_3), 3.59 (1H, s, OH), 4.05 (1H, d, $J = 15.1$ Hz, NCH_2), 4.39 (1H, d, $J = 15.1$ Hz, NCH_2), 6.78-7.05 (3H, m, Ar-H), 7.09-7.18 (5H, m, Ar-H), 7.34-7.35 (2H, m, H^5 and H^6), 7.60-7.62 (1H, m, H^7); δ_C (125 MHz $CDCl_3$): 11.3 (CH_3), 18.7 (CH), 42.4 (NCH_2), 90.6 (ethynyl), 90.9 (ethynyl), 106.7 (hemi-aminal), 122.0 (C-ethynyl), 123.5, 128.1, 128.2, 128.4, 129.7, 131.0, 131.5, 132.0, 132.9, 134.0, 134.7, 134.8, 137.5, 143.9, 166.2 (C=O); LCMS $R_t = 2.26$ min, (5); MS (ESI+) m/z 564.4 $[M+H]^+$; HRMS m/z : Calc. for $C_{32}H_{36}^{35}Cl_2NO_2Si$: 564.1887 $[M+H]^+$. Found 562.1883 $[M+H]^+$.

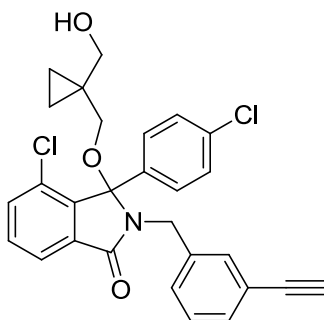
4-Chloro-3-(4-chlorophenyl)-3-(1((hydroxymethyl)cyclopropane)methoxy)-2-(3-((triisopropylsilyl)ethynyl)benzyl)isoindolin-1-one (**309**)



General procedure C: 4-chloro-3-(4-chlorophenyl)-3-hydroxy-2-(3-((triisopropylsilyl)ethynyl)benzyl)isoindolinone (167 mg, 0.30 mmol) and 1,1-bis(hydroxymethyl)cyclopropane (0.06 mL, 0.59 mmol). Chromatography (SP4, silica, 7-60% EtOAc, PE) gave the title compound as a colourless oil (67mg, 37%). $R_f = 0.29$ (3:7 EtOAc:PE); UV λ_{max} (EtOH): 262.0, 250.5 nm; IR ν_{max} 2942, 2864, 2158

(Ethyne), 1708 (C=O), 763 (C-Cl) cm^{-1} ; δ_{H} (500 MHz CDCl_3): 0.11-0.14 (1H, m, cyclopropyl), 0.26-0.28 (1H, m, cyclopropyl), 0.38-0.45 (2H, m, cyclopropyl), 1.74 (1H, s, OH), 2.78 (1H, d, $J = 9.2$ Hz, OCH_2), 2.94 (1H, d, $J = 9.2$ Hz, OCH_2), 3.42 (1H, d, $J = 11.4$ Hz, CH_2OH), 3.54 (1H, d, $J = 11.4$ Hz, CH_2OH), 4.14 (1H, d, $J = 15.0$ Hz, NCH_2), 4.48 (1H, d, $J = 15.0$ Hz, NCH_2), 7.09-7.19 (6H, m, Ar-H), 7.29 (1H, d, $J = 7.5$ Hz, benzyl Ar-H), 7.44 (1H, d, $J = 7.9$ Hz, H^5), 7.48-7.51 (1H, m, H^6), 7.86 (1H, d, $J = 7.3$ Hz, H^7); δ_{C} (125 MHz CDCl_3): 8.5 (cyclopropyl), 8.5 (cyclopropyl), 11.3 (CH_3), 18.7 ($\text{CH}(\text{CH}_3)_2$), 22.1 (cyclopropyl), 42.6 (NCH_2), 67.8 (CH_2OH), 67.9 (OCH_2), 90.8 (ethynyl), 94.7 (ethynyl), 106.6 (hemi-aminal), 122.3, 123.5, 128.2, 128.3, 128.4, 129.1, 129.7, 131.2, 131.8, 132.2, 133.9, 134.2, 134.7, 135.0, 137.1, 140.8, 166.7 (C=O); LCMS $R_t = 2.36$ min, (5); HRMS m/z : Calc. for $\text{C}_{37}\text{H}_{44}^{35}\text{Cl}_2\text{NO}_3\text{Si}$: 648.2462 $[\text{M}+\text{H}]^+$. Found 648.2463 $[\text{M}+\text{H}]^+$.

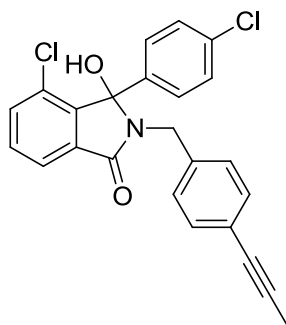
4-Chloro-3-(4-chlorophenyl)-2-(3-ethynylbenzyl)-(1-((hydroxymethyl)cyclopropane) methoxy)isoindolin-2-one (**310**)



General procedure G: 4-chloro-3-(4-chlorophenyl)-3-(1((hydroxymethyl) cyclopropane)methoxy)-2-(3-((triisopropylsilyl)ethynyl)benzyl)isoindolin-1-one (76 mg, 0.12 mmol). Chromatography (SP4, silica, 7-60% EtOAc, PE) gave **310** as a colourless oil (36 mg, 61%). $R_f = 0.2$ (3:7 EtOAc:PE); UV λ_{max} (EtOH): 246.0, 225.0, 211.0 nm; IR ν_{max} 3300 (OH), 2927, 2874, 2361, 2160 (Ethyne), 1695 (C=O), 1587 (Amide C-N), 1074 cm^{-1} ; δ_{H} (500 MHz CDCl_3): 0.10-0.12 (1H, m, cyclopropyl), 0.26-0.29 (1H, m, cyclopropyl), 0.39-0.45 (2H, m, cyclopropyl), 1.70 (1H, t, $J = 5.6$, OH), 2.80 (1H, d, $J = 9.2$ Hz, OCH_2), 2.93 (1H, d, $J = 9.2$ Hz, OCH_2), 3.04 (1H, s, ethynyl), 3.43 (1H, dd, $J = 4.2$ and 11.4 Hz, CH_2OH), 4.43 (1H, dd, $J = 4.2$ and 11.4 Hz, CH_2OH), 4.18 (1H, d, $J = 14.9$ Hz, NCH_2), 4.46 (1H, d, $J = 14.9$ Hz, NCH_2), 7.11-7.19 (7H, m, Ar-H), 7.30 (1H, d, $J = 7.6$ Hz, Ar-H), 7.45 (1H, dd, $J = 0.9$ and 7.9, H^5), 7.49-7.52 (1H, m, H^6), 7.85 (1H, dd, $J = 0.8$ and 7.4 Hz, H^7); δ_{C} (125 MHz

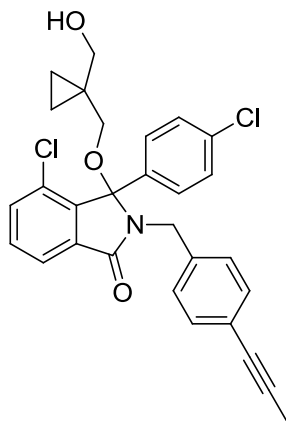
CDCl₃): 8.5 (cyclopropyl), 22.1 (cyclopropyl), 42.5 (NCH₂), 67.8 (CH₂OH), 67.9 (OCH₂), 77.4 (ethynyl), 83.1 (ethynyl), 96.6 (hemi-aminal), 122.1, 122.3, 128.3, 128.3 128.5, 129.6, 129.7. 131.0, 131.8, 132.6, 133.9, 134.1, 134.7, 135.0, 137.3, 140.8, 166.7 (carbonyl); LCMS R_t = 1.67 min, (4); HRMS *m/z*: Calc. for C₂₈H₂₄³⁵Cl₂NO₃: 492.1128 [M+H]⁺. Found 492.1123 [M+H]⁺.; Analytical HPLC: 98.7% purity

4-Chloro-3-(4-chlorophenyl)-3-hydroxy-2-(4-(prop-1-ynyl)benzyl)isoindolin-1-one
(**313**)



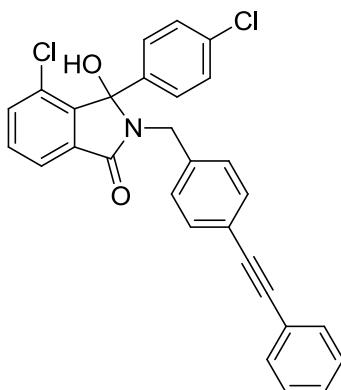
To a solution of **252** (383 mg, 0.75 mmol, 1 eq) in THF (4 mL) was added CuI (9 mg, 0.05 mmol, 0.06 eq) and Pd(PPh₃)₂Cl₂ (16 mg, 0.02 mmol, 0.03 eq) and the solution degassed for 5 min. Et₃N (0.26 mL, 1.88 mmol, 2.5 eq) was added and the solution degassed for a further 15 min and the reaction flask sealed. The reaction mixture was cooled to -78 °C and propyne (in excess) was added *via* cannula, then gradually warmed to room temperature and stirred for 18 h, filtered through Celite, washed with methanol (2 x 10 mL) and concentrated *in vacuo*. Chromatography (SP4, silica, 7-60% EtOAc, PE) gave **313** as an off-white solid (294 mg, 94%). R_f = 0.5 (3:7 EtOAc:PE); mp = 224.0-225.7 °C; UV λ_{max} (EtOH): 232.0 nm; IR ν_{max} 3178 (OH), 2159 (Ethyne), 1979, 1676 (C=O), 1658 (Amide C-N), 1406, 815, 770 (C-Cl) cm⁻¹; δ_H (500 MHz CDCl₃): 2.05 (3H, s, CH₃), 3.30 (1H, s, OH), 4.05 (1H, d, *J* = 15.1 Hz, NCH₂), 4.62 (1H, d, *J* = 15.1 Hz, NCH₂), 7.11 (2H, d, *J* = 8.3 Hz, benzyl Ar-H), 7.19 (2H, d, *J* = 8.3 Hz, benzyl Ar-H), 7.27-7.28 (4H, m, Ar-H), 7.45-7.47 (2H, m, *H*⁵ and *H*⁶), 7.76 (1H, dd, *J* = 1.8 and 6.7 Hz, *H*⁷); δ_C (125 MHz CDCl₃): 4.4 (CH₃), 42.6 (NCH₂), 79.5 (ethynyl), 86.0 (ethynyl), 91.0 (hemi-aminal), 122.1, 122.9, 128.3, 128.5, 128.6, 129.6, 131.4, 131.6, 133.0, 134.0, 134.7, 134.9, 137.0, 143.8, 166.1; LCMS R_t = 1.68 min, (4); MS (ESI+) *m/z* 422.2 [M+H]⁺; HRMS *m/z*: Calc. for C₂₄H₁₈³⁵Cl₂NO₂: 422.0709 [M+H]⁺. Found: 422.0711 [M+H]⁺.

4-Chloro-3-(4-chlorophenyl)-3-(1-((hydroxymethyl)cyclopropane)methoxy)-2-(4-(prop-1-ynyl)benzyl)isoindolin-1-one (**311**)



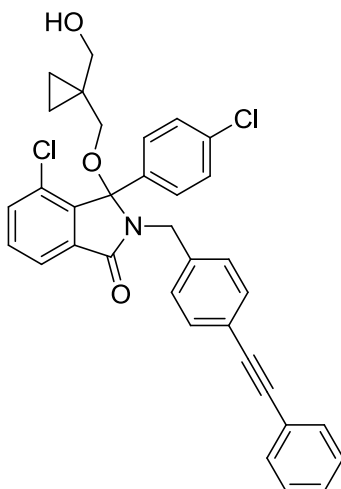
General procedure C: 4-chloro-3-(4-chlorophenyl)-3-hydroxy-2-(4-(prop-1-ynyl)benzyl)isoindolin-1-one (294 mg, 0.70 mmol) and 1,1-bis(hydroxymethyl)cyclopropane (0.14 mL, 1.39 mmol). Chromatography (SP4, silica, 6-70% EtOAc, PE) followed by (SP4, silica, 12-100% EtOAc, PE) gave **311** as a colourless oil (72 mg, 20%). $R_f = 0.21$ (3:7 EtOAc:PE); UV λ_{max} (EtOH): 229.0 nm; IR ν_{max} 3423 (OH), 2920, 2159 (Ethyne), 1703 (C=O), 1587 (Amide C-N), 760 (C-Cl) cm^{-1} ; δ_H (500 MHz CDCl_3): 0.02-0.08 (1H, m cyclopropyl), 0.22-0.28 (1H, m, cyclopropyl), 0.38-0.42 (2H, m, cyclopropyl), 1.67 (1H, s, OH), 2.02 (3H, s, CH_3), 2.77 (1H, d, $J = 9.1$ Hz, OCH_2), 2.87 (1H, d, $J = 9.1$ Hz, OCH_2), 3.38 (1H, dd, $J = 3.5$ and 11.4 Hz, CH_2OH), 3.47 (1H, dd, $J = 4.8$ Hz and 11.4 Hz, CH_2OH), 4.06 (1H, d, $J = 15.0$ Hz, NCH_2), 4.53 (1H, d, $J = 15.0$ Hz, NCH_2), 7.09 (2H, d, $J = 8.2$ Hz, benzyl Ar-H), 7.19-7.26 (6H, m, Ar-H), 7.44 (1H, dd, $J = 1.0$ and 8.0 Hz, H^5), 7.48-7.51 (1H, m, H^6), 7.90 (1H, dd, $J = 1.0$ and 7.4 Hz, H^7); δ_C (125 MHz CDCl_3): 4.4 (CH_3), 8.5 (cyclopropyl), 8.6 (cyclopropyl), 22.1 (cyclopropyl), 42.7 (NCH_2), 67.8 (CH_2OH), 68.0 (OCH_2), 79.4 (CCCH_3), 86.1 (CCCH_3), 94.8 (hemi-aminal), 122.3, 123.3, 128.4, 128.9, 129.1, 129.7, 131.3, 133.9, 134.7, 135.0, 136.4, 140.8, 166.8 (C=O); LCMS $R_t = 1.73$ min, (3); MS (ESI+) m/z 506.2 [$\text{M}+\text{H}$] $^+$; HRMS m/z : Calc. for $\text{C}_{29}\text{H}_{26}^{35}\text{Cl}_2\text{NO}_3$: 506.1284 [$\text{M}+\text{H}$] $^+$. Found: 506.1285 [$\text{M}+\text{H}$] $^+$.; Analytical HPLC: 95.3% purity

4-Chloro-3-(4-chlorophenyl)-3-hydroxy-2-(4-(phenylethynyl)benzyl)isoindolin-1-one
(**314**)

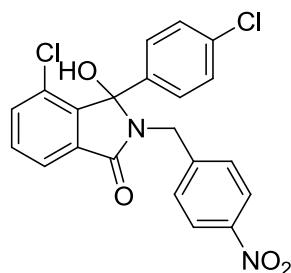


General procedure F: 4-chloro-3-(4-chlorophenyl)-3-hydroxy-2-(4-iodobenzyl)-isoindolin-1-one (241 mg, 0.47 mmol) and phenylacetylene (67 μ L, 0.61 mmol). Chromatography (SP4, silica, 7-60% PE, EtOAc) and (silica, 3:7 EtOAc:PE) gave **314** as a white solid (208 mg, 91%). $R_f = 0.43$ (3:7 EtOAc:PE); mp = 210.2-214.0 $^{\circ}$ C; UV λ_{max} (EtOH): 302.0, 284.0 nm; IR ν_{max} 3186 (OH), 2158 (Ethyne), 1657 (CO), 1589 (Amide C-N), 1406, 751 (C-Cl) cm^{-1} ; δ_H (500 MHz CDCl_3): 3.22 (1H, s, OH), 4.02 (1H, d, $J = 15.1$ Hz, NCH_2), 4.54 (1H, d, $J = 15.1$ Hz, NCH_2), 7.08 (2H, d, $J = 8.2$ Hz, benzyl Ar-H), 7.18-7.28 (9H, m, Ar-H), 7.35-7.740 (2H, m, H^5 and H^6), 7.41-7.44 (2H, m, Ar-H), 7.66 (1H, dd, $J = 1.7$ and 6.7 Hz, H^7); δ_C (125 MHz CDCl_3): 42.7 (NCH_2), 89.1 (alkyne), 89.5 (alkyne), 100.0 (hemi-aminal), 122.1 (C-alkyne), 122.2 (C-alkyne), 123.2, 128.3, 128.3, 128.3, 128.6, 128.7, 129.6, 131.5, 131.6, 131.6, 133.0, 134.0, 134.8, 134.9, 137.8, 143.8, 166.1 (C=O); LCMS $R_t = 1.82$ min, (3); MS (ESI+) m/z 484.2 $[\text{M}+\text{H}]^+$; HRMS m/z : Calc. for $\text{C}_{29}\text{H}_{20}^{35}\text{Cl}_2\text{NO}_2$ 484.0866 $[\text{M}+\text{H}]^+$. Found 484.0861 $[\text{M}+\text{H}]^+$.

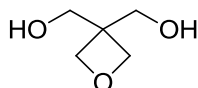
4-Chloro-3-(4-chlorophenyl)-3-(1-((hydroxymethyl)cyclopropane)methoxy)-2-(4-(phenylethynyl)benzyl)isoindolin-1-one (**312**)



General procedure C: 4-chloro-3-(4-chlorophenyl)-3-hydroxy-2-(4-(phenylethynyl)benzyl)isoindolin-1-one (208 mg, 0.43 mmol) and 1,1-bis(hydroxymethyl)cyclopropane (0.08 mL, 0.86 mmol). Chromatography (SP4, silica, 7-60 % EtOAc, PE) followed by (SP4, silica, 12-100 % EtOAc, PE) gave **312** as a colourless oil (89 mg, 36%). $R_f = 0.21$ (3:7 EtOAc:PE); UV λ_{max} (EtOH): 302.0, 284.0 nm; IR ν_{max} 3465 (OH), 2919, 1704 (C=O), 1587 (Amide C-N), 755 (C-Cl) cm^{-1} ; δ_H (500 MHz): 0.09-0.13 (1H, m, cyclopropyl), 0.27-0.29 (1H, m, cyclopropyl), 0.40-0.45 (2H, m, cyclopropyl), 1.70 (1H, s, OH), 2.82 (1H, d, $J = 9.1$ Hz, OCH₂), 2.90 (1H, d, $J = 9.1$ Hz, OCH₂), 3.40-3.41 (1H, m, CH₂OH), 3.50 (1H, dd, $J = 3.9$ and 11.4 Hz, CH₂OH), 4.14 (1H, d, $J = 15.1$ Hz, NCH₂), 4.54 (1H, d, $J = 15.1$ Hz, NCH₂), 7.15 (2H, d, $J = 8.2$ Hz, Ar-H), 7.22-7.7.35 (9H, m, Ar-H), 7.45 (1H, dd, $J = 1.0$ and 8.0 Hz, H^5), 7.49-7.52 (3H, m, Ar-H), 7.86 (1H, dd, $J = 1.0$ and 7.4 Hz, H^7); δ_C (125 MHz): 8.6 (cyclopropyl), 8.6 (cyclopropyl), 22.1 (cyclopropyl), 42.8 (NCH₂), 67.9 (CH₂OH), 68.2 (OCH₂), 89.0 (ethynyl), 89.6 (ethynyl), 95.8 (hemi-aminal), 122.3, 122.4, 123.2, 128.3, 128.3, 128.5, 129.0, 129.7, 131.5, 131.6, 131.9, 133.9, 134.4, 134.7, 135.0, 137.2, 140.8, 156.8, 166.8 (C=O); LCMS $R_t = 1.91$ min, (4); MS (ESI+) m/z 568.3 [M+H]⁺; HRMS m/z : Calc. for C₃₄H₂₈³⁵Cl₂NO₃: 568.1441 [M+H]⁺. Found 568.1440 [M+H]⁺; Analytical HPLC: 94.8% purity

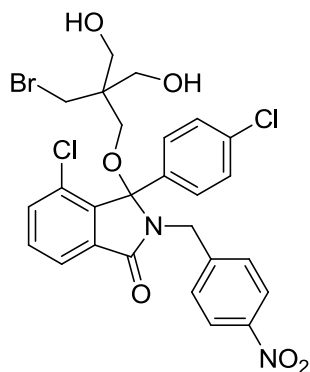
4-Chloro-3-(4-chlorophenyl)-3-hydroxy-2-(4-nitrobenzyl)isoindolin-2-one (**321**)

General procedure B: sodium 3-chloro-2-(4-chlorobenzoyl)benzoate (500 mg, 1.58 mmol) and 4-nitrobenzylamine hydrochloride (328 mg, 1.74 mmol). Chromatography (SP4, silica, 12-100% EtOAc, petrol) gave **321** as a white solid (187 mg, 28%). $R_f = 0.59$ (1:1 EtOAc:PE); mp. = 202.2-202.9 °C (lit. 202-203 °C)²⁴⁰; UV λ_{max} (EtOH): 272.0 nm; IR ν_{max} 1686 (C=O), 1589 (Amide C-N), 1515 cm^{-1} ; δ_H (500 MHz d_6 -DMSO): 4.41 (1H, d, $J = 16.2$ Hz, NCH₂), 4.54 (1H, d, $J = 16.2$ Hz, NCH₂), 7.28-7.33 (4H, m, Ar-H), 7.40 (2H, d, $J = 8.2$ Hz, Ar-H), 7.55 (1H, s, OH), 7.63-7.66 (2H, m, Ar-H), 7.72 (1H, d, $J = 5.5$ Hz, H^7), 8.04 (2H, d, $J = 8.2$ Hz, Ar-H); δ_C (125 MHz d_3 -MeCN): 41.3 (NCH₂), 89.9 (hemi-aminal), 121.4, 122.7, 127.8, 128.2, 128.7, 128.9, 131.6, 133.0, 135.5, 135.8, 143.5(CCCI), 145.4 (CH₂C), 146.5 (Ar-NO₂), 165.6 (carbonyl carbon); LCMS $R_t = 3.63$ min (1); MS (ESI+) m/z 429.07 [M+H]⁺

(3-Hydroxymethyloxetan-3-yl)-methanol (**318**)

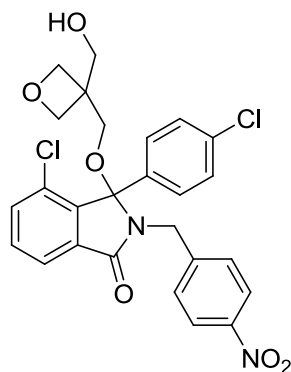
A mixture of 3-bromo-2,2-bis-hydroxymethylpropan-1-ol (100 mg, 0.50 mmol, 1 eq), ethanol (0.9 mL) and potassium hydroxide (32 mg, 0.60 mmol, 1.15 eq) was stirred for 2h at room temperature then reflux for 15 min, cooled to room temperature and filtered. The solid was washed with methanol (10 mL). The filtrate was evaporated *in vacuo* and residue purified by chromatography (silica, 10:90 MeOH:EtOAc) to give **318** as a colourless liquid (46 mg, 78%). $R_f = 0.3$ (1:9 MeOH:EtOAc); IR ν_{max} 3280 (OH), 2954, 2881 cm^{-1} ; δ_H (500 MHz CDCl₃): 2.20 (2H, s, OH), 3.95 (4H, s, CH₂OH), 4.41 (4H, s, CH₂O); δ_C (125 MHz CDCl₃): 44.6, (quaternary carbon), 66.7 (CH₂OH), 76.3 (CH₂O)

3-(2-Bromomethyl-3-hydroxy-2-hydroxymethyl-propoxy)-4-chloro-3-(4-chlorophenyl)-2-(4-nitrobenzyl)isoindolin-1-one (**322**)



General procedure C: 4-chloro-3-(4-chlorophenyl)-3-hydroxy-2-(4-nitrobenzyl)isoindolin-2-one (382 mg, 0.89 mmol, 1 eq) and 2-(bromomethyl)-2-(hydroxymethyl)propan-1,2-diol (354 mg, 1.78 mmol, 2 eq). Chromatography (SP4, silica, 17-100 % EtOAc, petrol) gave **322** as a white solid (227 mg, 42%). $R_f = 0.45$ (3:7 EtOAc:PE); mp = 185.7-185.4 °C; UV λ_{max} (EtOH): 262.0, 250.0 nm; IR ν_{max} 3376 (C=O), 2942, 2160 (Ethyne), 1695 (C=O), 1588 (Amide C-N), 757 (C-Cl), 655 cm^{-1} ; δ_H (500 MHz d_6): 2.86 (1H, d, $J = 8.5$ Hz, OCH₂), 3.24 (1H, d, $J = 8.5$ Hz OCH₂), 3.52-3.60 (4H, m, CH₂OH), 3.67 (1H, s, CH₂Br), 4.37 (1H, d, $J = 16.0$ Hz, NCH₂), 4.70 (1H, $J = 4.9$ Hz, OH), 4.76 (1H, t, $J = 4.8$ Hz, OH), 4.90 (1H, d, $J = 16.0$ Hz, NCH₂), 7.20-7.24 (6H, m, Ar-H), 7.76 (2H, d, $J = 4.1$ Hz, Ar-H), 7.94-7.98 (3H, m, Ar-H); δ_C (125 MHz d_6 DMSO): 36.7 (CBr), 41.1 (C(CH₂)₄), 44.6 (NCH₂), 60.4 (CH₂OH), 60.4 (CH₂OH), 62.0 (OCH₂), 93.0 (hemi-aminal carbon), 122.1, 122.8, 127.9, 128.4, 129.2, 129.2, 132.9, 133.2, 133.8, 134.1, 135.3, 139.8, 144.8, 146.0 (CNO₂), 165.8 (C=O); LCMS $R_t = 1.56$ min, (3); MS (ES-) m/z 655 [M+HCOO]⁻; HMRS: Calculated for C₂₆H₂₇⁷⁹Br³⁵Cl₂N₃O₆ 626.0455 [M+NH₄]⁺ Found 626.0437 [M+NH₄]⁺

4-Chloro-3-(4-chlorophenyl)-3-hydroxymethyloxetan-3-ylmethoxy)-2-(4-nitrobenzyl)isoindolin-2-one (**317**)



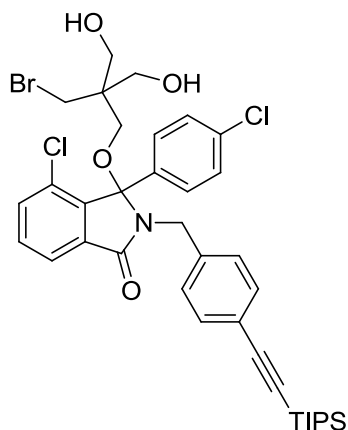
General procedure H: 3-(2-bromomethyl-3-hydroxy-2-hydroxymethyl-propoxy)-4-chloro-3-(4-chlorophenyl)-2-(4-nitrobenzyl)isoindolin-1-one (63 mg, 0.10 mmol). Chromatography (SP4, silica, 17-100% EtOAc, PE) gave the title compound as colourless oil (36 mg, 68%). $R_f = 0.27$ (3:7 EtOAc:PE); mp = 207.8-208.3 °C; UV λ_{max} (EtOH): 267.0 nm; IR ν_{max} 3408 (OH), 2875, 2163, 1687 (C=O), 1518 (Amide C-N), 1339 (NO₂) cm⁻¹; δ_H (500 MHz CDCl₃): 1.72 (1H, s, OH), 3.07 (1H, d, $J = 9.0$ Hz, OCH₂), 3.31 (1H, d, $J = 9.0$ Hz, OCH₂), 3.86 (2H, s, CH₂OH), 4.36-4.44 (4H, m, oxetane CH₂), 4.42 (1H, d, $J = 15.0$ Hz, NCH₂), 4.52 (1H, d, $J = 15.0$ Hz, NCH₂), 7.16-7.26 (6H, m, Ar-H), 7.50-7.51 (1H, m, H^5), 7.55-7.58 (1H, m, H^6), 7.90 (1H, dd, $J = 3.5$ and 7.5 Hz, H^7), 7.98 (2H, d, 8.5 Hz, CHCNO₂); δ_C (125 MHz CDCl₃): 42.2 (NCH₂), 44.0 (oxetane OCH₂C), 64.4 (OCH₂), 64.8 (CH₂OH), 75.6 (oxetane CH₂), 75.6 (oxetane CH₂), 94.4 (hemi-aminal), 122.6, 123.4, 128.8, 128.6, 129.6, 129.8, 132.3, 133.9, 134.3, 134.6, 135.1, 140.3, 144.1, 147.1 (C-NO₂), 166.8 (C=O); LCMS $R_t = 1.48$ min, (3); MS (ESI+) m/z 573 [M+HCOOH]⁺; HRMS m/z : Calc. for C₂₆H₂₆Cl₂N₃O₆ 546.1193 [M+NH₄]⁺. Found: 546.1190 [M+NH₄]⁺.; Analytical HPLC: 97.9% purity

Chiral Separation mobile phase hexane:ethanol 85:15:

326 Peak 1: (50 mg, 49%); Specific rotation $[\alpha] = -10.7^\circ$ (at 24.4 °C, wavelength = 589 nm, tube length = 0.1 dm, concentration = 0.560 g per 100 mL);

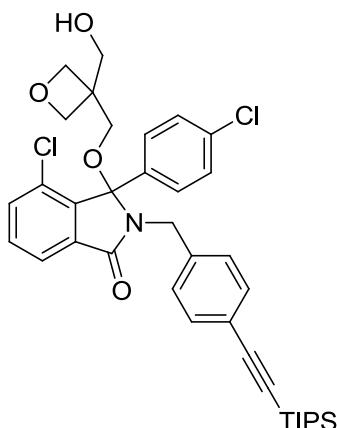
327 Peak 2: (50 mg, 49%); Specific rotation $[\alpha] = +30.3^\circ$ (at 24.5 °C, wavelength = 589 nm tube length = 0.1 dm, concentration = 0.462 g per 100 mL)

3-(2-Bromomethyl-3-hydroxy-2-hydroxymethyl-propoxy)-4-chloro-3-(4-chlorophenyl)-2-((4-triisopropylsilyl)ethynyl)benzyl)isoindolin-2-one (**323**)



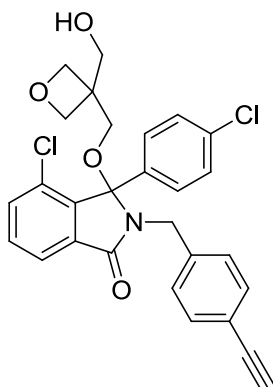
General procedure C: 3-Chloro-3-(4-chlorophenyl)-3-hydroxy-2-(4-((triisopropylsilyl)ethynyl)benzyl)isoindolin-1-one (334 mg, 0.59 mmol) and 2-(bromomethyl)-2-(hydroxymethyl)-1,3-propan-diol (236 mg, 1.19 mmol). Chromatography (SP4, silica, 10-80% EtOAc, PE) gave **323** as a colourless oil (135 mg, 31%). $R_f = 0.12$ (3:7 EtOAc:PE); UV λ_{max} (EtOH): 267.0, 255.0 nm; IR ν_{max} 3342 (OH), 2942, 2865, 2361, 2156 (Ethynyl), 1685 (C=O), 1589 (Amide C-N), 1041, 761 (C-Cl) cm^{-1} ; δ_H (500 MHz CDCl_3): 1.04 (18H, s, CH_3), 2.13 (1H, s, OH), 2.18 (1H, s, OH), 2.73 (1H, s, $J = 8.9$ Hz, CH_2Br), 3.10 (1H, d, $J = 8.9$ Hz, CH_2Br), 3.42 (1H, d, $J = 10.5$ Hz, OCH_2), 3.46 (1H, d, $J = 10.5$ Hz, OCH_2), 3.57-3.66 (4H, m, CH_2OH), 4.24 (1H, d, $J = 15.1$ Hz, NCH_2), 4.45 (1H, d, $J = 15.1$ Hz, NCH_2), 6.86 (2H, d, $J = 8.2$ Hz, benzyl Ar-H), 7.05-7.14 (6H, m, Ar-H), 7.40 (1H, dd, $J = 1.0$ and 8.0 Hz, H^5), 7.44-7.47 (1H, m, H^6), 7.79 (1H, dd, $J = 1.0$ and 7.4 Hz, H^7); δ_C (125 MHz CDCl_3): 11.3 (CH_3), 18.7 ($\text{CH}(\text{CH}_3)_2$), 34.7 (CH_2Br), 42.8 ($\text{C}(\text{CH}_2)_4$), 44.5 (NCH_2), 63.05 (OCH_2), 64.2 (CH_2OH), 64.5 (CH_2OH), 90.9 (ethynyl), 94.4 (ethynyl), 106.7 (hemi-aminal), 122.4, 122.5, 128.1, 128.4, 128.7, 129.7, 131.8, 132.2, 134.1, 134.2, 134.6, 134.9, 136.9, 140.2, 166.8 (C=O); LCMS $R_t = 2.26$ min, (4); HRMS m/z : Calc. for $\text{C}_{37}\text{H}_{48}^{79}\text{Br}^{35}\text{Cl}_2\text{NO}_4\text{Si}$: 761.1938 $[\text{M}+\text{NH}_4]^+$. Found 761.1934 $[\text{M}+\text{NH}_4]^+$.

4-Chloro-3-(4-chlorophenyl)-3-(3-hydroxymethyl-oxetan-3-ylmethoxy)-2-(((triisopropylsilyl)ethynyl)benzyl)isoindolin-1-one (**324**)



General procedure H: 3-(2-bromomethyl-3-hydroxy-2-hydroxymethyl-propoxy)-4-chloro-3-(4-chlorophenyl)-2-((4-triisopropylsilyl)ethynyl)benzyl)isoindolin-2-one (750 mg, 2.88 mmol). Chromatography (SP4, silica, 12-100% EtOAc, PE) gave **324** as a colourless oil (142 mg, 63%). $R_f = 0.18$ (1:1 EtOAc:PE); UV λ_{max} (EtOH): 262.0, 250.5 nm; IR ν_{max} 3362 (OH), 2842, 2865, 2156 (Ethynyl), 1694 (C=O), 1590 (Amide C-N), 815, 761 (C-Cl) cm^{-1} ; δ_H (500 MHz CDCl_3): 1.10 (18H, s, CH_3), 1.76 (1H, t, 4.5 Hz, OH), 2.99 (1H, d, $J = 9.0$ Hz, OCH_2), 3.17 (1H, d, $J = 9.0$ Hz, OCH_2), 3.71 (1H, dd, $J = 4.5$ and 10.8 Hz, CH_2OH), 3.79 (1H, dd, $J = 4.5$ and 10.8 Hz, CH_2OH), 4.20 (1H, d, $J = 15.0$ Hz, NCH_2), 4.29 (1H, d, $J = 6.25$ Hz, oxetane CH_2), 4.37-4.41 (3H, m, oxetane CH_2), 4.49 (1H, d, $J = 15.0$ Hz, NCH_2), 7.04 (2H, d, $J = 8.2$ Hz, benzyl Ar-H), 7.19-7.20 (4H, m, Ar-H), 7.25 (2H, d, $J = 8.2$ Hz, benzyl Ar-H), 7.46 (1H, dd, $J = 0.8$ and 8.0 Hz, H^5), 7.51-7.54 (1H, m, H^6), 7.87 (1H, dd, $J = 0.8$ and 7.4 Hz, H^7); δ_C (125 MHz CDCl_3): 11.3 (CH_3), 18.7 ($\text{CH}(\text{CH}_3)_2$), 42.8 (NCH_2), 43.9 (oxetane quat. C), 64.3 (OCH_2), 65.0 (CH_2OH), 75.4 (oxetane CH_2), 75.6 (oxetane CH_2), 91.1 (CC-Si), 94.7 (CC-Si), 106.6 (hemi-aminal), 122.5 (C-CC-Si), 122.7, 128.3, 128.6, 128.8, 129.6, 131.7, 132.1, 134.1, 134.1, 134.6, 134.9, 137.0, 140.0, 166.7 (C=O); LCMS $R_t = 2.20$ min, (5); MS (ESI+) m/z 664.5 $[\text{M}+\text{H}]^+$

4-Chloro-3-(4-chlorophenyl)-2-(4-ethynylbenzyl)-3-(3-hydroxymethyl-oxetan-3-ylmethoxy)isoindolin-1-one (**325**)

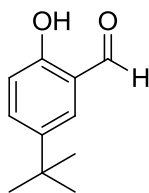


General procedure G: 4-chloro-3-(4-chlorophenyl)-3-(3-hydroxymethyl-oxetan-3-ylmethoxy)-2-(((triisopropylsilyl)ethynyl)benzyl)isoindolin-1-one (142 mg, 0.21 mmol). Chromatography (SP4, silica, 12-100% EtOAc, PE) gave **325** as a colourless oil (95 mg, 89%). $R_f = 0.18$ (1:1, EtOAc:PE); mp = 182.2-182.9 °C; UV λ_{max} (EtOH): 229.0 nm; IR ν_{max} 3447 (OH), 3296, 2924, 2872, 2360, 2162 (Ethynyl), 2026, 1709, 1683 (C=O), 1587 (Amide C-N), 762 (C-Cl) cm^{-1} ; δ_H (500 MHz CDCl_3): 1.58 (1H, t, $J = 5.3$ Hz, OH), 3.02 (1H, d, $J = 8.9$, OCH_2), 3.07 (1H, s, CCH), 3.21 (1H, d, $J = 8.9$ Hz, OCH_2), 3.74 (1H, dd, $J = 5.3$ and 10.9 Hz, CH_2OH), 3.80 (1H, dd, $J = 5.3$ and 10.9 Hz, CH_2OH), 4.17 (1H, d, $J = 15.1$ Hz, NCH_2), 4.31-4.40 (4H, m, oxetane CH_2), 4.58 (1H, d, $J = 15.1$ Hz, NCH_2), 7.13 (2H, d, $J = 8.2$ Hz, benzyl Ar-H), 7.24-7.43 (6H, m, Ar-H), 7.50 (1H, dd, $J = 0.9$ and 7.9 Hz, H^5), 7.55-7.59 (1H, m, H^6), 7.92 (1H, dd, $J = 0.9$ and 7.4 Hz, H^7); δ_C (125 MHz CDCl_3): 42.8 (NCH_2), 43.9 (oxetane OCH_2C), 64.4 (OCH_2), 65.0 (CH_2OH), 75.4 (oxetane CH_2), 75.6 (oxetane CH_2), 77.6 (CCH), 83.1 (CCH), 94.8 (hemi-aminal), 121.3, 122.5, 128.6, 128.9, 129.6, 132.1, 132.1, 134.1, 134.1, 134.6, 134.9, 137.7, 140.4, 166.8 (C=O); LCMS $R_t = 1.53$ min, (3); MS (ESI+) m/z 552 $[\text{M}+\text{HCOO}]^+$; HRMS m/z : Calc. for $\text{C}_{28}\text{H}_{23}^{35}\text{Cl}_2\text{NO}_4$ 508.1077 $[\text{M}+\text{H}]^+$. Found 508.1074 $[\text{M}+\text{H}]^+$; Analytical HPLC: 99.2% purity

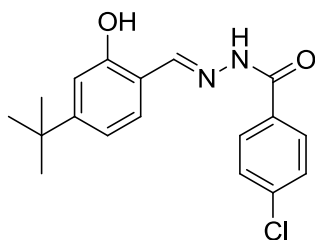
Chiral Separation mobile phase *tert* butyl methyl ether:isopropanol 95:5:

328 Peak 1: (38 mg, 42%); Specific rotation $[\alpha] = -7.74^\circ$ (at 25.6 °C, wavelength = 589 nm, tube length = 0.1 dm, concentration = 0.517 g per 100 mL);

329 Peak 2: (37 mg, 41%); Specific rotation $[\alpha] = +4.65^\circ$ (at 25.6 °C, wavelength = 589 nm tube length = 0.1 dm, concentration = 0.43 g per 100 mL)

5-*tert*-Butyl-2-hydroxybenzaldehyde (**340**)

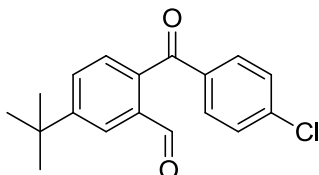
To a solution of 4-*tert*butylphenol (2.00 g, 13.3 mmol, 1 eq) in TFA (20 mL) was added hexamethylenetetramine (1.86 g, 13.3 mmol, 1 eq) and the reaction was heated to 120 °C for 30 min with microwave heating, cooled in an ice-bath, diluted with water (40 mL) and neutralised using K₂CO₃. The resulting aqueous solution was extracted with EtOAc (3 x 60 mL) and combined organic extracts dried over MgSO₄ and concentrated *in vacuo*. Chromatography (SP4, silica, 1-10% EtOAc, PE) gave **340** as a white oily solid (1.09 g, 46%). $R_f = 0.57$ (5:95 EtOAc:PE); UV λ_{\max} (EtOH): 335.0, 258.5, 220.0 nm; IR ν_{\max} 2963 (OH), 2160, 1652 (C=O), 1483 cm⁻¹; δ_H (500 MHz CDCl₃): 1.25 (9H, s, CH₃), 6.86 (1H, d, $J = 8.8$ Hz, H^3), 7.44 (1H, d, $J = 2.5$ Hz, H^6), 7.51 (1H, dd, $J = 2.5$ and 8.8 Hz, H^4), 9.81 (1H, s, OH), 10.80 (1H, s, CHO); δ_C (125 MHz CDCl₃): 31.4 (CH₃), 34.1 (C(CH₃)₃), 117.2 (C³), 120.0, 129.8, 134.8, 142.8 (CC(CH₃)₃), 157.8 (COH), 196.9 (C=O); LCMS $R_t = 1.52$ min, (3), MS (ESI+) m/z 179.2 [M+H]⁺

4-Chlorobenzoic acid (4-*tert*-butyl-2-hydroxy-benzylidene)hydrazine (**341**)

To a solution of **340** (1.06 g, 5.96 mmol, 1 eq) in AcOH (20 mL) was added 4-chlorobenzhydrazide (1.02 g, 5.96 mmol, 1 eq) and the reaction stirred at room temperature for 15 min, then added dropwise to ice-cold water (20 mL). The precipitate was collected by filtration, washed with ice-cold water (20 mL) and petrol, (10 mL) and dried over P₂O₅ to give **341** as a white solid (1.85 g, 94%). $R_f = 0.26$ (1:4 EtOAc:PE); mp = 225.2-228.0 °C; UV λ_{\max} (EtOH): 338.5, 290.5, 241.0 nm; IR ν_{\max} 2953 (OH), 2159 (C=N), 1642 (C=O), 826, 750 (C-Cl) cm⁻¹; δ_H (500 MHz *d*₆ DMSO): 1.29 (9H, s, CH₃), 6.89 (1H, dd, $J = 8.6$ Hz, H^6), 7.36 (1H, dd, $J = 2.2$ and 8.6 Hz, H^5), 7.53 (1H, d, $J = 2.2$ Hz, H^3), 7.64 (2H, d, $J = 8.1$ Hz, CHCl), 7.98 (2H,

d, $J = 8.1$ Hz, *CHCCO*), 8.66 (1H, s, CHN), 11.02 (1H, s, OH), 12.12 (1H, s, NH); δ_C (125 MHz d_6 DMSO): 31.2 (CH₃), 33.8 (C(CH₃)₃), 116.1 (C⁶), 17.9, 125.4 (C³), 128.6, 128.7, 129.6 (*CHCCI*), 131.6 (*CHCCO*), 136.7, 141.5, 148.8 (C=N), 155.3 (CO), 161.8 (C=O); LCMS $R_t = 1.60$ min, (3); MS (ESI+) m/z 331.2 [M+H]⁺; HRMS m/z : Calc. for C₁₈H₂₀³⁵ClN₂O₂: 331.1208 [M+H]⁺. Found 331.1207 [M+H]⁺.

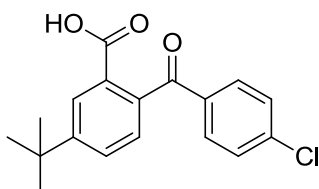
5-*tert*-Butyl-2-(4-chlorobenzoyl)benzaldehyde (**342**)



To **341** (500 mg, 1.51 mmol, 1 eq) in THF (11 mL) at 0 °C was added Pb(OAc)₄ (670 mg, 1.51 mmol, 1 eq) portionwise and stirred for 2 h at 0 °C, then concentrated *in vacuo*. The residue was dissolved in EtOAc (30 mL), filtered through Celite and washed with EtOAc (20 mL). The filtrate was washed with sat. NaHCO₃ solution (30 mL) and brine (30 mL), dried over Na₂SO₄ and concentrated *in vacuo*.

Chromatography (SP4, silica, 2-20% EtOAc, PE) gave **342** as a white solid (331 mg, 73%). $R_f = 0.51$ (1:9 EtOAc:PE); mp = 116.3-117.1 °C; UV λ_{max} (EtOH): 261.0 nm; IR ν_{max} 2963 (Aldehyde C-H), 2160, 1688 (Ketone C=O), 1657 (Aldehyde C=O), 1583 cm⁻¹; δ_H (500 MHz CDCl₃): 1.34 (9H, s, CH₃), 7.35-7.38 (3H, m, Ar-H), 7.64 (1H, dd, $J = 2.0$ and 8.0 Hz, H^5), 7.68 (2H, d, $J = 8.7$ Hz, Ar-H), 7.97 (1H, d, $J = 2.0$ Hz, H^7), 9.96 (1H, s, CHO); δ_C (125 MHz CDCl₃): 31.1 (CH₃), 35.2 (C(CH₃)₃), 127.4, 129.0, 129.0, 130.5, 131.3, 135.5, 135.7, 138.0, 140.0 (CCI), 154.7 (CC(CH₃)₃), 191.0 (CHO), 195.4 (CO); LCMS $R_t = 1.80$ min, (3); MS (ESI+) m/z 301.2 [M+H]⁺; HRMS m/z : Calc. for C₁₈H₁₈³⁵ClO₂: 301.0990 [M+H]⁺. Found 301.0997 [M+H]⁺.

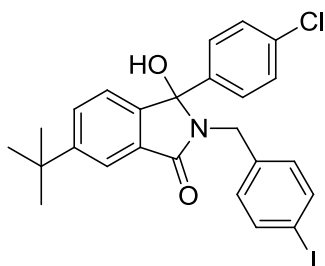
6-*tert*-Butyl-2-(4-chlorobenzoyl)benzoic acid (**343**)



To a solution of 5-*tert*-butyl-2-(4-chlorobenzoyl)-benzaldehyde (606 mg, 2.01 mmol, 1 eq) in MeCN (12 mL) was added sulfamic acid (364 mg, 2.62 mmol, 1.3 eq) in water (2 mL) and the reaction was stirred for 10 min before NaClO₂ (254 mg, 4.03

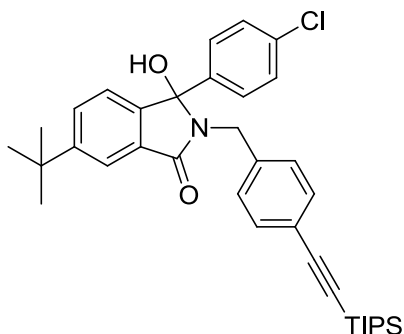
mmol, 2 eq) in water (2 mL) was added dropwise, and stirred 1.5 h, then concentrated *in vacuo*. The residue was suspended in water (30 mL) and extracted with EtOAc (3 x 40 mL). The combined organic layers were dried over Na₂SO₄ and evaporated *in vacuo*. Recrystallisation (EtOAc and petrol) gave **343** as a white fluffy solid (529 mg, 83%). *R*_f = 0.06 (3:7 EtOAc:PE); mp = 218.1-219.6 °C; UV λ_{max} (EtOH): 254.5 nm; IR ν_{max} (cm⁻¹) 2965 (OH), 2161, 2032, 1679 (Ketone C=O), 1584 (Acid C=O), 757 (C-Cl) cm⁻¹; δ_H (500 MHz *d*₆ DMSO): 1.36 (9H, s, CH₃), 7.39 (1H, d, *J* = 8.0 Hz, *H*³), 7.58 (2H, d, *J* = 8.5 Hz, CHCCl), 7.63 (2H, d, *J* = 8.5 Hz, CHCCO), 7.78 (1H, d, *J* = 8.0 Hz, *H*⁴), 7.98 (1H, s, *H*⁶), 13.2 (1H, s, OH); δ_C (125 MHz CDCl₃): 30.8 (CH₃), 34.6 (C(CH₃)₃), 126.2 (C⁶), 127.5 (C³), 128.8, 129.4 (CHCCl), 129.9 (C⁴), 130.5 (CHCCO), 135.9 (CCOOH), 137.9 (CCO), 138.2 (CCl), 152.7 (CC(CH₃)₃), 167.1 (COOH), 195.3 (CO); LCMS *R*_t = 1.58 min, (3); MS (ESI+) *m/z* 317.2 [M+H]⁺; HRMS *m/z*: Calc. for C₁₈H₁₈³⁵ClO₃: 317.0939 [M+H]⁺. Found 317.0942 [M+H]⁺.

6-*tert*-Butyl-3-(chlorophenyl)-3-hydroxy-2-(4-iodobenzyl)isoindolin-2-one (**334**)



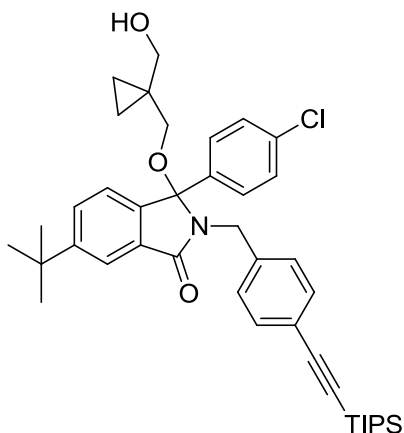
General procedure B: 6-*tert*-butyl-2-(4-chlorobenzoyl)-benzoic acid (500 mg, 1.58 mmol) and 4-iodobenzylamine hydrochloride (468 mg, 1.74 mmol). Chromatography (SP4, silica, 7-60 % EtOAc, PE) gave **334** as a white solid (724 mg, 86%). *R*_f = 0.68 (3:7 EtOAc:PE); mp = 223.6-226.1 °C; UV λ_{max} (EtOH): 228.5 nm; IR ν_{max} 3253 (OH), 2970, 2159, 1664 (C=O), 1623, 835, 695 (C-Cl) cm⁻¹; δ_H (500 MHz CDCl₃): 1.26 (9H, s, CH₃), 3.25 (1H, s, OH), 3.88 (1H, d, *J* = 15.1 Hz, NCH₂), 4.38 (1H, d, *J* = 15.1 Hz, NCH₂), 6.80 (2H, d, *J* = 8.3 Hz, benzyl Ar-H), 7.09-7.13 (5H, m, Ar-H), 7.37 (2H, d, *J* = 8.3 Hz, benzyl Ar-H), 7.47 (1H, dd, *J* = 1.8 and 8.1 Hz, *H*⁵), 7.81 (1H, d, *J* = 1.8 Hz, *H*⁷); δ_C (125 MHz CDCl₃): 31.4 (CH₃), 35.2 (C(CH₃)₃), 42.4 (NCH₂), 91.0 (Cl), 92.6 (hemi-aminal), 120.5, 122.3, 127.9, 128.6, 129.7, 130.5, 130.7, 134.5, 136.8, 137.3, 137.6, 145.7, 153.7 (CC(CH₃)₃), 168.1 (C=O); LCMS *R*_t = 1.87 min, (5); MS (ESI+) *m/z* 532.2 [M+H]⁺; HRMS *m/z*: Calc. for C₂₅H₂₃³⁵ClINO₂: 532.0535 [M+H]⁺. Found 532.0532 [M+H]⁺.

6-*tert*-Butyl-3-(4-chlorophenyl)-3-hydroxy-2-(4-((triisopropylsilyl)ethynyl)benzyl)isoindolin-1-one (**335**)



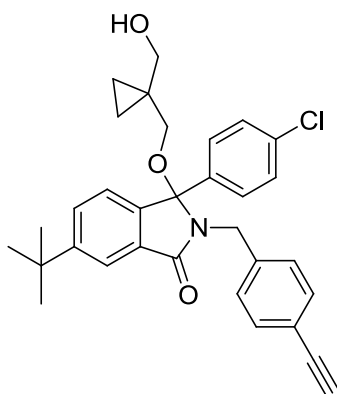
General procedure F: **334** (700 mg, 1.32 mmol, 1 eq) and triisopropylsilylacetylene (384 μ L, 1.71 mmol, 1.3 eq). Chromatography (SP4, silica, 3-30% EtOAc, PE) gave **335** as a white solid (708 mg, 91%). R_f = 0.34 (15:85 EtOAc:PE); mp = 165.8-167.7 $^{\circ}$ C; UV λ_{\max} (EtOH): 266.0, 254.5 nm; IR ν_{\max} 3285 (OH), 2945, 2866, 2153 (Ethyne), 1677 (C=O), 838 cm^{-1} ; δ_{H} (500 MHz CDCl_3): 1.01 (18H, s, $\text{Si}(\text{CH}(\text{CH}_3)_2)_3$), 1.23 (9H, s, $\text{C}(\text{CH}_3)_3$), 3.78 (1H, d, J = 15.1 Hz, NCH_2), 4.16 (1H, d, J = 15.1 Hz, NCH_2), 4.55 (1H, s, OH), 6.80 (2H, d, J = 8.2 Hz, benzyl Ar-H), 7.02-7.09 (6H, m, Ar-H), 7.42 (1H, dd, J = 1.6 and 8.1 Hz, H^5), 7.76 (1H, d, 1.6 Hz, H^7); δ_{C} (125 MHz CDCl_3): 11.3 ($\text{Si}(\text{CH}(\text{CH}_3)_2)_3$), 18.7 ($\text{Si}(\text{CH}(\text{CH}_3)_2)_3$), 31.4 ($\text{C}(\text{CH}_3)_3$), 35.1 ($\text{C}(\text{CH}_3)_3$), 42.6 (NCH_2), 90.4 (ethynyl), 90.9 (ethynyl), 107.0 (hemi-aminal), 120.4 (C-ethynyl), 122.1, 127.9, 128.4, 128.6, 129.8, 130.4, 131.7, 134.4, 137.1, 137.9, 146.1, 153.3 ($\text{CC}(\text{CH}_3)_3$), 168.5 (C=O); LCMS R_t = 2.50 min, (5); MS (ESI+) m/z 586.4 $[\text{M}+\text{H}]^+$; HRMS m/z : Calc. for $\text{C}_{36}\text{H}_{45}^{35}\text{ClNO}_2\text{Si}$: 586.2903 $[\text{M}+\text{H}]^+$. Found 586.2901 $[\text{M}+\text{H}]^+$.

6-*tert*-Butyl-3-(4-chlorophenyl)-3-(1-((hydroxymethyl)cyclopropane)methoxy)-2-(4-((triisopropylsilyl)ethynyl)benzyl)isoindolin-1-one (**336**)



General procedure C: 6-*tert*-butyl-3-(4-chlorophenyl)-3-hydroxy-2-(4-((triisopropylsilyl)ethynyl)benzyl)isoindolin-1-one (354 mg, 0.60 mmol, 1 eq) and bis(hydroxymethyl)cyclopropane (0.12 mL, 1.21 mmol). Chromatography (SP4, silica, 7-60 % EtOAc, PE) gave **336** as a colourless oil (200 mg, 50%). $R_f = 0.53$ (3:7 EtOAc:PE); UV λ_{max} (EtOH): 266.5, 254.5 nm; IR ν_{max} 2942, 2865, 2158 (Ethyne), 1685 (C=O) cm^{-1} ; δ_H (500 MHz CDCl_3): 0.11-0.15 (2H, m, cyclopropyl), 0.35-0.41 (2H, m, cyclopropyl), 1.09 (18H, s, $\text{Si}(\text{CH}(\text{CH}_3)_2)_3$), 1.33 (9H, s, $\text{C}(\text{CH}_3)_3$), 1.61 (1H, t, $J = 5.5$ Hz, OH), 2.63 (1H, d, $J = 9.5$ Hz, OCH_2), 2.82 (1H, d, $J = 9.5$ Hz, OCH_2), 3.34 (1H, dd, $J = 5.5$ and 11.3 Hz, CH_2OH), 3.46 (1H, dd, $J = 5.5$ and 11.3 Hz, CH_2OH), 4.16 (1H, d, $J = 15.0$ Hz, NCH_2), 4.55 (1H, d, $J = 15.0$ Hz, NCH_2), 7.03 (1H, d, $J = 8.0$ Hz, H^4), 7.11 (2H, d, $J = 8.2$ Hz, benzyl Ar-H), 7.15-7.19 (4H, m, Ar-H), 7.24 (2H, d, $J = 1.6$ Hz, Ar-H), 7.52 (1H, dd, $J = 1.8$ and 8.0 Hz, H^5), 7.90 (1H, d, $J = 1.8$ Hz, H^7); δ_C (125 MHz CDCl_3): 8.6 (cyclopropyl), 8.7 (cyclopropyl), 11.3 ($\text{Si}(\text{CH}(\text{CH}_3)_2)_3$), 18.7 ($\text{Si}(\text{CH}(\text{CH}_3)_2)_3$), 22.1 (cyclopropyl), 31.4 ($\text{C}(\text{CH}_3)_3$), 35.2 ($\text{C}(\text{CH}_3)_3$), 42.8 (NCH_2), 67.8 (CH_2OH), 68.1 (OCH_2), 90.7 (ethynyl), 94.7 (ethynyl), 106.8 (hemi-aminal), 120.6, 122.4, 122.5, 127.9, 128.6, 129.0, 130.3, 131.3, 131.8, 137.3, 137.7, 142.3, 153.8 ($\text{CC}(\text{CH}_3)_3$), 168.7 (C=O); LCMS $R_t = 2.66$ min, (5); MS (ESI+) m/z 670.5 $[\text{M}+\text{H}]^+$; HRMS m/z : Calc. for $\text{C}_{41}\text{H}_{53}^{35}\text{ClNO}_3\text{Si}$: 670.3478 $[\text{M}+\text{H}]^+$. Found 670.3477 $[\text{M}+\text{H}]^+$.

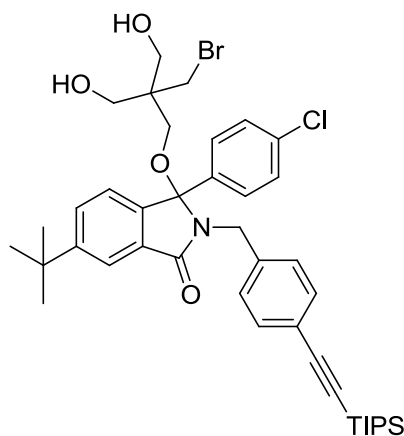
6-*tert*-Butyl-3-(4-chlorophenyl)-2-(4-ethynylbenzyl)-3-(1-((hydroxymethyl)cyclopropyl)methoxy)isoindolin-1-one (**330**)



General procedure G: 6-*tert*-butyl-3-(4-chlorophenyl)-3-(1-((hydroxymethyl)cyclopropane)methoxy)-2-(4-((triisopropylsilyl)ethynyl)benzyl)isoindolin-1-one (150 mg, 0.22 mmol). Chromatography (SP4, silica, 7-60% EtOAc, PE) gave **330** as a colourless oil (91 mg, 80%). $R_f = 0.36$ (3:7 EtOAc:PE); UV λ_{max} (EtOH): 230.0 nm;

IR ν_{\max} 3494 (OH), 3295, 2962, 2869, 2158 (Ethyne), 2030, 1686 (C=O), 1489 cm^{-1} ; δ_{H} (500 MHz CDCl_3): 0.08-0.11 (1H, m, cyclopropyl), 0.12-0.15 (1H, m, cyclopropyl), 0.36-0.42 (2H, m, cyclopropyl), 1.35 (9H, s, $\text{C}(\text{CH}_3)_3$), 1.67 (1H, s, OH), 2.63 (1H, d, $J = 9.5$ Hz, OCH_2), 2.84 (1H, d, $J = 9.5$ Hz, OCH_2), 3.04 (1H, s, CCH), 3.35 (1H, d, $J = 11.0$ Hz, CH_2OH), 3.47 (1H, d, $J = 11.0$ Hz, CH_2OH), 4.16 (1H, d, $J = 15.0$ Hz, NCH_2), 4.59 (1H, d, $J = 15.0$ Hz, NCH_2), 7.05 (1H, d, $J = 8.0$ Hz, H^4), 7.16-7.20 (6H, m, Ar-H), 7.30 (2H, d, $J = 8.2$ Hz, Ar-H), 7.54 (1H, dd, $J = 1.7$ and 8.0 Hz, H^5), 7.92 (1H, d, $J = 1.3$ Hz, H^7); δ_{C} (125 MHz CDCl_3): 8.6 (cyclopropyl), 8.6 (cyclopropyl), 22.1 (cyclopropyl), 31.4 ($\text{C}(\text{CH}_3)_3$), 35.2 ($\text{C}(\text{CH}_3)_3$), 42.8, (NCH_2), 67.8 (CH_2OH), 68.0 (OCH_2), 83.4 (ethyne), 94.8 (hemi-aminal) 120.6 (C-CCH), 121.0, 122.4, 127.9, 128.6, 129.1, 130.3, 131.3, 131.9, 134.5, 137.3, 138.4, 142.3, 153.8 ($\text{C}-t\text{Bu}$), 168.7 (C=O); LCMS $R_t = 2.66$ min, (5); HRMS m/z : Calc. for $\text{C}_{32}\text{H}_{32}^{35}\text{ClNO}_3$: 514.2143 $[\text{M}+\text{H}]^+$. Found: 514.2140 $[\text{M}+\text{H}]^+$; Analytical HPLC: 95.6% purity

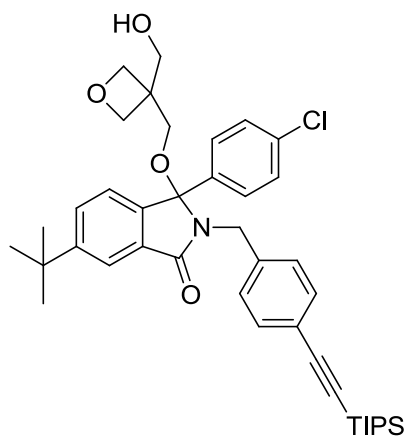
3-(2-Bromomethyl-2-hydroxymethyl-propoxy)-6-*tert*-butyl-3-(4-chlorophenyl)-2-(4-((triisopropylsilyl)ethynyl)benzyl)isoindolin-1-one (**349**)



General procedure D: **334** (266 mg, 0.45 mmol), 2-(bromomethyl)-2-(hydroxymethyl)propan-1,3-diol (902 mg, 4.34 mmol) in THF (5 mL). Reaction quenched after 3.5 h at 0 °C and 1 h at RT. Chromatography (SP4, silica, 7-60% EtOAc, PE) gave **349** as a colourless oil (300 mg, 87%). $R_f = 0.26$ (3:7 EtOAc:PE); UV λ_{\max} (EtOH): 267.0, 255.0 nm; IR ν_{\max} 3567 (OH), 2941, 2865, 2365, 2157 (Ethyne), 1685 (C=O), 839 cm^{-1} ; δ_{H} (500 MHz CDCl_3): 1.04 (18H, s, $\text{Si}(\text{CH}(\text{CH}_3)_2)_3$), 1.29 (9H, s, $\text{C}(\text{CH}_3)_3$), 1.96 (2H, s, OH), 2.74 (1H, d, $J = 9.1$ Hz, CH_2Br), 2.88 (1H, d, $J = 9.1$ Hz, CH_2Br), 3.40 (1H, d, $J = 10.4$ Hz, OCH_2), 3.44 (1H,

d, $J = 10.4$ Hz, OCH₂), 3.49-3.52 (4H, m, CH₂OH), 4.28 (1H, d, $J = 15.1$ Hz, NCH₂), 4.40 (1H, d, $J = 15.1$ Hz, NCH₂), 6.98-7.00 (3H, m, Ar-H), 7.02 (2H, d, $J = 8.6$ Hz, Ar-H), 7.09 (2H, d, $J = 8.9$ Hz, Ar-H), 7.17-7.19 (2H, m, Ar-H), 7.48 (1H, dd, $J = 1.8$ and 8.0 Hz, H^5), 7.82 (1H, d, $J = 1.8$ Hz, H^7); δ_C (125 MHz CDCl₃): 11.3 (Si(CH(CH₃)₂)₃), 18.7 (Si(CH(CH₃)₂)₃), 31.3 (C(CH₃)₃), 34.6 (CH₂Br), 35.2 (C(CH₃)₃), 42.9 (NCH₂), 44.4 (OCH₂C(CH₂)₃), 62.7 (OCH₂), 64.6 (CH₂OH), 64.7 (CH₂OH), 90.9 (ethynyl), 94.7 (ethynyl), 106.7 (hemi-aminal), 120.6 (C⁷), 122.6, 122.6, 127.8, 128.6, 128.8, 130.4, 131.3, 131.8, 134.6, 137.0, 137.5, 141.6, 154.1 (C(CH₃)₃), 168.8 (C=O); LCMS $R_t = 2.50$ min, (5); HRMS m/z : Calc. for C₄₁H₅₄⁷⁹Br³⁵ClNO₄Si: 766.2689 [M+H]⁺. Found 766.2690 [M+H]⁺.

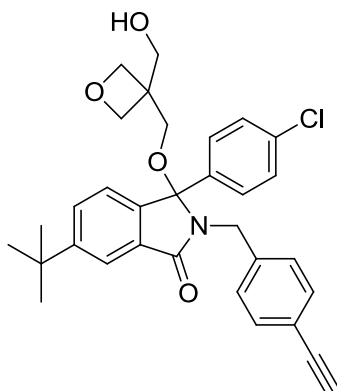
6-*tert*-Butyl-3-(4-chlorophenyl)-3-(3-hydroxymethyl-oxetan-3-ylmethoxy)-2-(4-((triisopropylsilyl)ethynyl)benzyl)isoindolin-1-one (**350**)



General procedure H: 349 (250 mg, 0.33 mmol). Chromatography (SP4, silica, 7-60% EtOAc, PE) gave **350** as a colourless oil (176 mg, 78%). $R_f = 0.13$ (3:7 EtOAc:PE); UV λ_{max} (EtOH): 266.5, 254.5 nm; IR ν_{max} 2944, 2866, 1689 (C=O), 728 C-Cl cm⁻¹; δ_H (500 MHz CDCl₃): 1.04 (18H, s, Si(CH(CH₃)₂)₃), 1.29 (9H, s, C(CH₃)₃), 1.62 (1H, s, OH), 2.94 (2H, s, OCH₂), 3.60 (1H, d, $J = 10.8$ Hz, CH₂OH), 4.13 (1H, d, $J = 15.0$ Hz, NCH₂), 4.22-4.30 (4H, m, oxetane CH₂), 4.50 (1H, d, $J = 15.0$ Hz), 6.94 (1H, d, $J = 8.0$ Hz, H⁴), 7.03 (2H, d, $J = 8.0$ Hz, benzyl Ar-H), 7.08 (2H, d, $J = 8.4$ Hz, Ar-H), 7.13 (2H, d, $J = 8.4$ Hz, Ar-H), 7.14 (2H, d, $J = 8.0$ benzyl Ar-H), 7.48 (1H, dd, $J = 1.3$ and 7.9 Hz, H^5), 7.89 (1H, d, $J = 1.3$ Hz, H^7); δ_C (125 MHz CDCl₃): 11.3 (Si(CH(CH₃)₂)₃), 18.7 (Si(CH(CH₃)₂)₃), 31.3 (C(CH₃)₃), 35.2 (C(CH₃)₃), 42.9 (NCH₂), 44.0 (oxetane quat. C), 64.1 (OCH₂), 65.0 (CH₂OH), 75.6 (oxetane CH₂), 75.6 (oxetane CH₂), 91.0 (ethynyl), 94.8 (ethynyl), 106.7 (hemi-

aminal), 120.8 (C-ethynyl), 122.3, 122.6, 127.8, 128.7, 128.9, 130.5, 131.3, 131.8, 134.6, 136.9, 137.5, 142.0, 154.0 (CC(CH₃)₃), 168.7 (C=O); LCMS R_t = 2.40 min, (5); MS (ESI+) m/z 686.6 [M+H]⁺; HRMS m/z: Calc. for C₄₁H₅₃³⁵ClNO₄Si: 686.3427 [M+H]⁺. Found 686.3427 [M+H]⁺.

6-*tert*-Butyl-3-(4-chlorophenyl)-2-(4-ethynylbenzyl)-3-(3-hydroxymethyloxetan-3-ylmethoxy)isoindolin-1-one (**351**)



General procedure G: 6-*tert*-butyl-3-(4-chlorophenyl)-3-(3-hydroxymethyl-oxetan-3-ylmethoxy)-2-(4-((triisopropylsilyl)ethynyl)benzyl)isoindolin-1-one (141 mg, 0.20 mmol). Chromatography (SP4, silica, 12-100 % EtOAc, PE) gave **351** as a colourless oil (62 mg, 59%). R_f = 0.28 (1:1 EtOAc:PE); UV λ_{max} (EtOH): 229.5 nm; IR ν_{max} 3300 (OH), 2963, 2874, 2160 (Ethynyl), 1687 (C=O), 1091, 907, 727 (C-Cl) cm⁻¹; δ_H (500 MHz CDCl₃): 1.30 (9H, s, ^tBu), 1.63 (1H, s, OH), 2.92 (2H, s, OCH₂), 2.97 (1H, s, ethynyl), 3.59 (1H, d, J = 11.0 Hz, CH₂OH), 3.62 (1H, d, J = 11.0 Hz, CH₂OH), 4.08 (1H, d, J = 15.0 Hz, NCH₂), 4.16 (1H, d, J = 6.2 Hz, oxetane CH₂), 4.23 (1H, d, J = 6.2 Hz, oxetane CH₂), 4.25 (1H, d, J = 6.2 Hz, oxetane CH₂), 4.28 (1H, d, 6.2 Hz, oxetane CH₂), 4.56 (1H, d, 15.0 Hz, NCH₂), 6.95 (1H, d, J = 8.0 Hz, H⁴), 7.08-7.10 (4H, m, Ar-H), 7.15 (2H, d, J = 8.9 Hz, Ar-H), 7.24 (2H, d, J = 8.2 Hz, Ar-H), 7.49 (1H, dd, J = 1.8 and 8.0 Hz, H⁵), 7.89 (1H, d, J = 1.8 Hz, H⁷); δ_C (125 MHz CDCl₃): 31.3 (C(CH₃)₃), 35.2 (C(CH₃)₃), 42.9 (NCH₂), 43.9 (oxetane OCH₂C), 64.1 (OCH₂), 64.9 (CH₂OH), 75.5 (oxetane CH₂), 75.6 (oxetane CH₂), 77.5 (CCH), 83.2 (CCH), 94.8 (hemi-aminal), 120.8, 121.2, 122.4, 127.8, 128.7, 129.0, 130.6, 131.3, 132.0, 134.7, 136.9, 138.2, 141.9, 154.1, 168.7 (C=O); LCMS R_t = 1.73 min, 2.(1); MS (ESI+) m/z 530.3 [M+H]⁺; HRMS m/z: Calc. for C₃₂H₃₃³⁵ClNO₄: 530.2093 [M+H]⁺. Found 530.2090 [M+H]⁺.; Analytical HPLC: 100.0% purity

8. Bibliography

1. http://info.cancerresearchuk.org/prod_consump/groups/cr_common/@nre/@sta/documents/generalcontent/018070.pdf (24.02.2011).
2. Pavet, V.; Portal, M. M.; Moulin, J. C.; Herbrecht, R.; Gronemeyer, H. Towards Novel Paradigms for Cancer Therapy. *Oncogene* **2011**, 30, 1-20.
3. Hanahan, D.; Weinberg, R. A. The Hallmarks of Cancer. *Cell* **2000**, 100, 57-70.
4. Hanahan, D.; Weinberg, R. A. Hallmarks of Cancer: The Next Generation. *Cell* **2011**, 144, 646-674.
5. Luo, J.; Solimini, N. L.; Elledge, S. J. Principles of Cancer Therapy: Oncogene and Non-oncogene Addiction. *Cell* **2009**, 136, 823-837.
6. Stryer, L. *Biochemistry*. 4th ed.; W.H. Freeman & Co. Ltd: 1995.
7. Noble, M. E. M.; Endicott, J. A.; Johnson, L. N. Protein Kinase Inhibitors: Insights into Drug Design from Structure. *Science* **2004**, 303, 1800-1805.
8. Janne, P. A.; Gray, N.; Settleman, J. Factors Underlying Sensitivity of Cancers to Small-Molecule Kinase Inhibitors. *Nat. Rev. Drug Disc.* **2009**, 8, 709-723.
9. van Montfort, R. L. M.; Workman, P. Structure-Based Design of Molecular Cancer Therapeutics. *Trends Biotechnol.* **2009**, 27, 315-328.
10. Zhang, J. M.; Yang, P. L.; Gray, N. S. Targeting Cancer with Small Molecule Kinase Inhibitors. *Nat. Rev. Cancer* **2009**, 9, 28-39.
11. Liu, Y.; Gray, N. S. Rational Design of Inhibitors that Bind to Inactive Kinase Conformations. *Nat. Chem. Biol.* **2006**, 2, 358-364.
12. Knight, Z. A.; Shokat, K. M. Features of Selective Kinase Inhibitors. *Chem. Biol.* **2005**, 12, 621-637.
13. Zuccotto, F.; Ardini, E.; Casale, E.; Angiolini, M. Through the "Gatekeeper Door": Exploiting the Active Kinase Conformation. *J. Med. Chem.* **2010**, 53, 2681-2694.
14. Vanhaesebroeck, B.; Waterfield, M. D. Signaling by Distinct Classes of Phosphoinositide 3-Kinases. *Exp. Cell Res.* **1999**, 253, 239-254.
15. Stein, R. C.; Waterfield, M. D. PI3-Kinase Inhibition: A Target for Drug Development? *Mol. Med. Today* **2000**, 6, 347-357.

16. Vanhaesebroeck, B.; Ali, K.; Bilancio, A.; Geering, B.; Foukas, L. C. Signalling by PI3K Isoforms: Insights from Gene-targeted Mice. *Trends Biochem. Sci.* **2005**, *30*, 194-204.
17. Smith, G. C. M.; Jackson, S. P. The PIKK Family of Protein Kinases. In *Handbook of Cell Signalling*, 1st ed.; Dennis, E. A., Ed. Academic Press: **2003**; Vol. 1, pp 557-561.
18. Lempiainen, H.; Halazonetis, T. D. Emerging Common Themes in Regulation of PIKKs and PI3Ks. *EMBO J.* **2009**, *28*, 3067-3073.
19. Abraham, R. T. PI 3-Kinase Related Kinases: 'Big' Players in Stress-Induced Signaling Pathways. *DNA Repair* **2004**, *3*, 883-887.
20. Perry, J.; Kleckner, N. The ATRs, ATMs, and TORs are Giant HEAT Repeat Proteins. *Cell* **2003**, *112*, 151-155.
21. Arias-Palomo, E.; Yamashita, A.; Fernandez, I. S.; Nunez-Ramirez, R.; Bamba, Y.; Izumi, N.; Ohno, S.; Llorca, O. The Nonsense-mediated mRNA Decay SMG-1 Kinase is Regulated by Large-scale Conformational Changes Controlled by SMG-8. *Genes Dev.* **2011**, *25*, 153-164.
22. Sibanda, B. L.; Chirgadze, D. Y.; Blundell, T. L. Crystal Structure of DNA-PKcs Reveals a Large Open-Ring Cradle Comprised of HEAT Repeats. *Nature* **2010**, *463*, 118-121.
23. Abraham, R. T.; Gibbons, J. J. The Mammalian Target of Rapamycin Signaling Pathway: Twists and Turns in the Road to Cancer Therapy. *Clin. Cancer Res.* **2007**, *13*, 3109-3114.
24. Efeyan, A.; Sabatini, D. M. mTOR and Cancer: Many Loops in One Pathway. *Curr. Opin. Cell Biol.* **2010**, *22*, 169-176.
25. Dunlop, E. A.; Tee, A. R. Mammalian Target of Rapamycin Complex 1: Signalling Inputs, Substrates and Feedback Mechanisms. *Cell. Signal.* **2009**, *21*, 827-835.
26. Inoki, K.; Ouyang, H.; Li, Y.; Guan, K. Signaling by Target of Rapamycin Proteins in Cell Growth Control. *Microbiol. Mol. Biol. Rev.* **2005**, *69*, 79-100.
27. Guertin, D. A.; Sabatini, D. M. Defining the Role of mTOR in Cancer. *Cancer Cell* **2007**, *12*, 9-22.
28. Chiang, G. C.; Abraham, R. T. Targeting the mTOR Signaling Network in Cancer. *Trends Mol. Med.* **2007**, *13*, 435-442.

29. Yap, T. A.; Garrett, M. D.; Walton, M. I.; Raynaud, F.; de Bono, J. S.; Workman, P. Targeting the PI3K-AKT-mTOR Pathway: Progress, Pitfalls, and Promises. *Curr. Opin. Pharmacol.* **2008**, *8*, 393-412.
30. Yip, C. K.; Murata, K.; Walz, T.; Sabatini, D. M.; Kang, S. A. Structural of the Human mTOR Complex 1 and Its Implication for Rapamycin Inhibition. *Mol. Cell* **2010**, *38*, 768-774.
31. Sabatini, D. M. mTOR and Cancer: Insights into a Complex Relationship. *Nat. Rev. Cancer* **2006**, *6*, 729-734.
32. Averous, J.; Proud, C. G. When Translation Meets Transformation: the mTOR Story. *Oncogene* **2006**, *25*, 6423-6435.
33. Guertin, D. A.; Stevens, D. M.; Saitoh, M.; Kinkel, S.; Crosby, K.; Sheen, J.; Mullholland, D. J.; Magnuson, M. A.; Wu, H.; Sabatini, D. M. mTOR Complex 2 Is Required for the Development of Prostate Cancer Induced by *Pten* Loss in Mice. *Cancer Cell* **2009**, *15*, 148-159.
34. Tsang, C. K.; Qi, H.; Liu, L. F.; Zheng, X. F. S. Targeting Mammalian Target of Rapamycin (mTOR) for Health and Diseases. *DDT* **2007**, *12*, 112-124.
35. Zoncu, R.; Efeyan, A.; Sabatini, D. M. mTOR: From Growth Signal Integration to Cancer, Diabetes and Ageing. *Nat. Rev. Mol. Cell Biol.* **2011**, *12*, 21-35.
36. Cybulski, N.; Hall, M. N. TOR Complex 2: a Signaling Pathway of its Own. *Trends Biochem. Sci.* **2009**, *34*, 620-627.
37. Sparks, C. A.; Guertin, D. A. Targeting mTOR: Prospects for mTOR Complex 2 Inhibitors in Cancer Therapy. *Oncogene* **2010**, *29*, 1-12.
38. Sarbassov, D. D.; Ali, S. M.; Sabatini, D. M. Growing roles for the mTOR pathway. *Curr. Opin. Cell Biol.* **2005**, *17*, 593-603.
39. Bai, X.; Ma, D.; Liu, A.; Shen, X.; Wang, Q. J.; Liu, Y.; Jiang, Y. Rheb Activates mTOR by Antagonizing Its Endogenous Inhibitor, FKBP38. *Science* **2007**, *318*, 977-980.
40. Wang, X.; Proud, C. G. The mTOR Pathway in the Control of Protein Synthesis. *Physiology* **2006**, *21*, 362-369.
41. Mamane, Y.; Petroulakis, E.; LeBacquer, O.; Sonenberg, N. mTOR, Translation Initiation and Cancer. *Oncogene* **2006**, *25*, 6416-6422.
42. Kim, J.; Guan, K. Amino Acid Signaling in TOR Activation. *Annu. Rev. Biochem.* **2011**, *80*, 1001-1032.

43. Vignot, S.; Faivre, S.; Aguirre, D.; Raymond, E. mTOR-targeted Therapy of Cancer with Rapamycin Derivatives. *Anal. Oncol.* **2005**, *16*, 525-537.
44. Graziani, E. I. Recent Advances in the Chemistry, Biosynthesis and Pharmacology of Rapamycin Analogs. *Nat. Prod. Rep.* **2009**, *26*, 602-609.
45. Hartford, C. M.; Ratain, M. J. Rapamycin: Something Old, Something New, Something Borrowed and Now Renewed. *Clin. Pharmacol. Ther.* **2007**, *82*, 381-388.
46. Burke, S. E.; Kuntz, R. E.; Schwartz, L. B. Zotarolimus (ABT-578) Eluting Stents. *Adv. Drug Deliv. Rev.* **2006**, *58*, 437-446.
47. Kwitkowski, V. E.; Prowell, T. M.; Ibrahim, A.; Farrell, A. T.; Justice, R.; Mitchell, S. S.; Sridhara, R.; Pazdur, R. FDA Approval Summary: Temsirolimus as Treatment for Advanced Renal Cell Carcinoma. *The Oncologist* **2010**, *15*, 428-435.
48. Mita, M.; Sankhala, K.; Abdel-Karim, I.; Mita, A.; Giles, F. Deferolimus (AP23573) a Novel mTOR Inhibitor in Clinical Development. *Expert Opin. Investig. Drugs* **2008**, *17*, 1947-1954.
49. Zhang, Y.; Duan, Y.; Zheng, X. F. S. Targeting the mTOR Kinase Domain: the Second Generation of mTOR Inhibitors. *DDT* **2011**, *16*, 325-331.
50. Peng, H.; Kim, D.-I.; Sarkiria, J. N.; Cho, Y.; Abraham, R. T.; Zalkow, L. H. Novel Pyrrolo-quinoline Derivatives as Potent Inhibitors for PI3-Kinase Related Kinases. *Bioorg. Med. Chem.* **2002**, *10*, 167-174.
51. Walker, E. H.; Pacold, M. E.; Perisic, O.; Stephens, L.; Hawkins, P. T.; Wymann, M. P.; Williams, R. L. Structural Determinants of Phosphoinositide 3-Kinase Inhibition by Wortmannin, Ly294002, Quercetin, Myricetin, and Staurosporine. *Mol. Cell.* **2000**, *6*, 909-919.
52. Norman, B. H.; Shih, C.; Toth, J. E.; Ray, J. E.; Dodge, J. A.; Johnson, D. W.; Rutherford, P. G.; Schultz, R. M.; Worzalla, J. F.; Vlahos, C. J. Studies on the Mechanism of Phosphatidylinositol 3-Kinase Inhibition by Wortmannin and Related Analogs. *J. Med. Chem.* **1996**, *39*, 1106-1111.
53. Han, E. K.-H.; Levenson, J. D.; McGonigal, T.; Shah, O. J.; Woods, K. W.; Hunter, T.; Giranda, V. L.; Luo, Y. Akt Inhibitor A-443654 Induces Rapid Akt Ser-473 Phosphorylation Independent of mTORC1 Inhibition. *Oncogene* **2007**, *26*, 5655-5661.
54. Hayakawa, M.; Kaizawa, H.; Moritomo, H.; Koizumi, T.; Ohishi, T.; Okada, M.; Ohta, M.; Tsukamoto, S.; Parker, P.; Workman, P.; Waterfield, M. Synthesis and

Biological Evaluation of 4-Morpholino-2-phenylquinazolines and Related Derivatives as Novel PI3 Kinase p110 α Inhibitors. *Bioorg. Med. Chem.* **2006**, 14, 6847-6858.

55. Hayakawa, M.; Kaizawa, H.; Moritomo, H.; Koizumi, T.; Ohishi, T.; Yamano, M.; Okada, M.; Ohta, M.; Tsukamoto, S.; Raynaud, F.; Workman, P.; Waterfield, M. D.; Parker, P. Synthesis and Biological Evaluation of Pyrido[3',2':4,5]furo[3,2-*d*]pyrimidine Derivatives as Novel PI3 Kinase p110 α Inhibitors. *Bioorg. Med. Chem. Lett.* **2007**, 17, 2438-2442.

56. Raynaud, F.; Eccles, S.; Clarke, P. A.; Hayes, A.; Nutley, B.; Alix, S.; Henley, A.; Di-Stefano, F.; Ahmad, Z.; Guillard, S.; Bjerke, L. M.; Kelland, L.; Valenti, M.; Patterson, L.; Gowan, S.; de Haven Brandon, A.; Hayakawa, M.; Kaizawa, H.; Koizumi, T.; Ohishi, T.; Patel, S.; Saghir, N.; Parker, P.; Waterfield, M.; Workman, P. Pharmacological Characterization of a Potent Inhibitor of Class I Phosphatidylinositide 3-Kinase. *Cancer Res.* **2007**, 67, 5840-5850.

57. Stauffer, F.; Maira, S.-M.; Furet, P.; Garcia-Echeverria, C. Imidazo[4,5-*c*]quinolines as Inhibitors of the PI3K/PKB-pathway. *Bioorg. Med. Chem. Lett.* **2008**, 18, 1027-1030.

58. Marone, R.; Erhart, D.; Mertz, A. C.; Bohnacker, T.; Schnell, C.; Cmijanovic, V.; Stauffer, F.; Garcia-Echeverria, C.; Giese, B.; Maira, S.-M.; Wymann, M. P. Targeting Melanoma with Dual Phosphoinositide 3-Kinase/Mammalian Target of Rapamycin Inhibitors. *Mol. Cancer Res.* **2009**, 7, 601-613.

59. Maira, S.-M.; Stauffer, F.; Brueggen, J.; Furet, P.; Schnell, C.; Fritsch, C.; Brachmann, S.; Chene, P.; De Pover, A.; Schoemaker, K.; Fabbro, D.; Gabriel, D.; Simonen, M.; Murphy, L.; Finan, P.; Sellers, W.; Garcia-Echeverria, C. Identification and Characterization of NVP-BEZ235, A New Orally Available Dual Phosphatidylinositol 3-Kinase/Mammalian Target of Rapamycin Inhibitor with Potent *In Vivo* Antitumour Activity. *Mol. Cancer Res.* **2008**, 7, 1851-1863.

60. Apsel, B.; Blair, J. A.; Gonzalez, B.; Nazif, T. M.; Feldman, M. E.; Aizenstein, B.; Hoffman, R.; Williams, R. L.; Shokat, K. M.; Knight, Z. A. Targeted Polypharmacology: Discovery of Dual Inhibitors of Tyrosine and Phosphoinositide Kinases. *Nat. Chem. Biol.* **2008**, 4, 691-699.

61. Feldman, M. E.; Apsel, B.; Uotila, A.; Loewith, R.; Knight, Z. A.; Ruggero, D. Active-Site Inhibitors of mTOR Target Rapamycin-Resistant Outputs of mTORC1 and mTORC2. *PLoS Biology* **2009**, 7, 371-383.

62. Liu, Q.; Chang, J. W.; Wang, J.; Kang, S. A.; Thoreen, C. C.; Markhard, A.; Hur, W.; Zhang, J.; Sim, T.; Sabatini, D. M.; Gray, N. Discovery of 1-(4-(4-Propionylpiperazin-1-yl)-3-(trifluoromethyl)phenyl)-9-(quinolin-3-yl)benzo[h][1,6]naphthyridin-2(1*H*)-one as a Highly Potent, Selective Mammalian Target of Rapamycin (mTOR) Inhibitor for the Treatment of Cancer. *J. Med. Chem.* **2010**, *53*, 7146-7155.
63. Liu, Q.; Wang, J.; Kang, S. A.; Thoreen, C. C.; Hur, W.; Ahmed, T.; Sabatini, D. M.; Gray, N. S. Discovery of 9-(6-Aminopyridin-3-yl)-1-(3-trifluoromethyl-phenyl)benzo[h][1,6]naphthyridin-2(1*H*)-one (Torin2) as a Potent, Selective, and Orally Available Mammalian Target of Rapamycin (mTOR) Inhibitor for Treatment of Cancer. *J. Med. Chem.* **2011**, *59*, 7146-7155.
64. Thoreen, C. C.; Kang, S. A.; Chang, J. W.; Liu, Q.; Zhang, J.; Gao, Y.; Reichling, L. J.; Sim, T.; Sabatini, D. M.; Gray, N. S. An ATP-competitive Mammalian Target of Rapamycin Inhibitor Reveals Rapamycin-resistant Functions of mTORC1. *J. Biol. Chem.* **2009**, *284*, 8023-8032.
65. Malagu, K.; Duggan, H.; Menear, K.; Hummersone, M.; Gomez, S.; Bailey, C.; Edwards, P.; Drzewiecki, J.; Leroux, F.; Jimenez Quesada, M.; Hermann, G.; Maine, S.; Molyneaux, C.-A.; Le Gall, A.; Pullen, J.; Hickson, I.; Smith, L.; Maguire, S.; Martin, N.; Smith, G. C. M.; Pass, M. The Discovery and Optimisation of Pyrido[2,3-*d*]pyrimidine-2,4-diamines as Potent and Selective Inhibitors of mTOR Kinase. *Bioorg. Med. Chem. Lett.* **2009**, *19*, 5950-5953.
66. Menear, K. A.; Gomez, S.; Malagu, K.; Bailey, C.; Blackburn, K.; Cockcroft, X.-L.; Ewen, S.; Fundo, A.; Le Gall, A.; Hermann, G.; Sebastian, L.; Sunose, M.; Presnot, T.; Torode, E.; Hickson, I.; Martin, N. M. B.; Smith, G. C. M.; Pike, K. G. Identification and Optimisation of Novel and Selective Small Molecular Weight Kinase Inhibitors of mTOR. *Bioorg. Med. Chem. Lett.* **2009**, *19*, 5898-5901.
67. Garcia-Martinez, J.; Moran, J.; Clarke, R. G.; Gray, A.; Cosulich, S. C.; Chresta, C. M.; Alessi, D. R. Ku-0063794 is a Specific Inhibitors of the Mammalian Target of Rapamycin (mTOR). *Biochem. J.* **2009**, *421*, 29-42.
68. Chresta, C. M.; Davies, B. R.; Hickson, I.; Harding, T.; Cosulich, S.; Critchlow, S. E.; Vincent, J. P.; Ellston, R.; Jones, D.; Sini, P.; James, D.; Howard, Z.; Dudley, P.; Hughes, G.; Smith, L.; Maguire, S.; MHummersone, M.; Malagu, K.; Menear, K.; Jenkins, R.; Jacobsen, M.; Smith, G. C. M.; Guichard, S.; Pass, M. AZD8055 is a Potent, Selective and Orally Bioavailable ATP-Competitive Mammalian Target of

- Rapamycin Kinase Inhibitor with *In vitro* and *In vivo* Antitumour Activity. *Cancer Res.* **2009**, 70, 288-298.
69. Curran, K.; Verheijen, J.; Kaplan, J.; Richard, D. J.; Toral-Braza, L.; Hollander, I.; Lucas, J.; Ayral-Kaloustian, S.; Yu, K.; Zask, A. Pyrazolopyrimidines as Highly Potent and Selective, ATP-competitive Inhibitors of the Mammalian Target of Rapamycin (mTOR): Optimization of the 1-substituent. *Bioorg. Med. Chem. Lett.* **2010**, 20, 1440-1444.
70. Yu, K.; Shi, C.; Toral-Braza, L.; Lucas, J.; Shor, B.; Kim, J. E.; Zhang, W. G.; Mahoney, R.; Gaydos, C.; Tardio, L.; Kim, S. K.; Conant, R.; Curran, K.; Kaplan, J.; Verheijen, J.; Ayral-Kaloustian, S.; Mansour, T. S.; Abraham, R. T.; Zask, A.; Gibbons, J. J. Beyond Rapalog Therapy: Preclinical Pharmacology and Antitumour Activity of WYE-125132, an ATP-competitive and Specific Inhibitor of mTORC1 and mTORC2. *Cancer Res.* **2010**, 70, 621-631.
71. Zask, A.; Verheijen, J. C.; Curran, K.; Richard, D. J.; Nowak, P.; Malwitz, D. J.; Brooijmans, N.; Bard, J.; Svenson, K.; Lucas, J.; Toral-Braza, L.; Zhang, W. G.; Hollander, I.; Gibbons, J. J.; Abraham, R. T.; Ayral-Kaloustian, S.; Mansour, T. S.; Yu, K. ATP-competitive Inhibitors of the Mammalian Target of Rapamycin: Design and Synthesis of Highly Potent and Selective Pyrazolopyrimidines. *J. Med. Chem.* **2009**, 52, 5013-5016.
72. Nowak, P.; Cole, D. C.; Brooijmans, N.; Bursavich, M. G.; Curran, K. J.; Ellingboe, J. W.; Gibbons, J. J.; Hollander, I.; Hu, Y.; Kaplan, J.; Malwitz, D. J.; Toral-Braza, L.; Verheijen, J. C.; Zask, A.; Zhang, W. G.; Yu, K. Discovery of Potent and Selective Inhibitors of the Mammalian Target of Rapamycin (mTOR) Kinase. *J. Med. Chem.* **2009**, 52, 7081-7089.
73. Richard, D. J.; Verheijen, J. C.; Curran, K.; Kaplan, J.; Toral-Braza, L.; Hollander, I.; Lucas, J.; Yu, K.; Zask, A. Incorporation of Water-solubilizing Groups in Pyrazolopyrimidine mTOR Inhibitors: Discovery of Highly Potent and Selective Analogs with Improved Human Microsomal Stability. *Bioorg. Med. Chem. Lett.* **2009**, 19, 6830-6835.
74. Verheijen, J.; Richard, D. J.; Curran, K.; Kaplan, J.; Lefever, M.; Nowak, P.; Malwitz, D. J.; Brooijmans, N.; Toral-Braza, L.; Zhang, W. G.; Lucas, J.; Hollander, I.; Ayral-Kaloustian, S.; Mansour, T. S.; Yu, K.; Zask, A. Discovery of 4-Morpholino-6-aryl-1H-pyrazolo[3,4-d]pyrimidines as Highly Potent and Selective

- ATP-competitive Inhibitors of the Mammalian Target of Rapamycin (mTOR): Optimization of the 6-Aryl Substituent. *J. Med. Chem.* **2009**, *52*, 8010-8024.
75. Kaplan, J.; Verheijen, J. C.; Brooijman, N.; Toral-Braza, L.; Hollander, I.; Yu, K.; Zask, A. Discovery of 3,6-Dihydro-2H-pyran as a Morpholine Replacement in 6-Aryl-1H-pyrazolo[3,4-d]pyrimidines and 2-Arylthieno[3,2-d]pyrimidines: ATP-competitive Inhibitors of the Mammalian Target of Rapamycin (mTOR). *Bioorg. Med. Chem. Lett.* **2010**, *20*, 640-643.
76. Zask, A.; Kaplan, J.; Verheijen, J. C.; Richard, D. J.; Curran, K.; Brooijmans, N.; Bennett, E. M.; Toral-Braza, L.; Hollander, I.; Ayril-Kaloustian, S.; Yu, K. Morpholine Derivatives Greatly Enhanced the Selectivity of Mammalian Target of Rapamycin (mTOR) Inhibitors. *J. Med. Chem.* **2009**, *52*, 7942-7945.
77. Verheijen, J. C.; Yu, K.; Toral-Braza, L.; Hollander, I.; Zask, A. Discovery of 2-Arylthieno[3,2-d]pyrimidines Containing 8-Oxa-3-azobicyclo[3.2.1]octane in the 4-position as Potent Inhibitors of mTOR with Selectivity Over PI3K. *Bioorg. Med. Chem. Lett.* **2010**, *20*, 375-379.
78. Zask, A.; Verheijen, J. C.; Richard, D. J.; Kaplan, J.; Curran, K.; Toral-Braza, L.; Lucas, J.; Hollander, I.; Yu, K. Discovery of 2-Ureidophenyltriazines Bearing Bridge Morpholines as Potent and Selective ATP-competitive mTOR Inhibitors. *Bioorg. Med. Chem. Lett.* **2010**, *20*, 2644-2647.
79. Verheijen, J. C.; Richard, D. J.; Curran, K.; Kaplan, J.; Yu, K.; Zask, A. 2-Arylureidophenyl-4-(3-oxa-8-azobicyclo[3.2.1]octan-8-yl)triazines as Highly Potent and Selective ATP Competitive mTOR Inhibitors: Optimization of Human Microsomal Stability. *Bioorg. Med. Chem. Lett.* **2010**, *20*, 2648-2653.
80. Richard, D. J.; Verheijen, J. C.; Yu, K.; Zask, A. Triazines Incorporating (*R*)-3-Methylmorpholine are Potent Inhibitors of the Mammalian Target of Rapamycin (mTOR) with Selectivity over PI3K α . *Bioorg. Med. Chem. Lett.* **2010**, *20*, 2654-2657.
81. Dehnhardt, C. M.; Venkatesan, A. M.; Delos Santos, E.; Chen, Z. C.; Santos, O.; Ayril-Kaloustian, S.; Brooijmans, N.; Mallon, R.; Hollander, I.; Feldberg, L.; Lucas, J.; Chaudhary, I.; Yu, K.; Gibbons, J.; Abraham, R.; Mansour, T. S. Lead Optimization of N-3-Substituted 7-Morpholinotriazolopyrimidines as Dual Phosphoinositide 3-Kinase/Mammalian Target of Rapamycin. *J. Med. Chem.* **2010**, *53*, 798-810.
82. Sutherlin, D. P.; Sampath, D.; Berry, M.; Castanedo, G.; Chang, Z.; Chuckowree, I.; Dotson, J.; Folkes, A.; Friedman, L.; Goldsmith, R.; Heffron, T.; Lee, L.; Lesnick,

- J.; Lewis, C.; Mathieu, S.; Nonomiya, J.; Olivero, A.; Pang, J.; Prior, W. W.; Salphati, L.; Sideris, S.; Tian, Q.; Tsui, V.; Wan, N. C.; Wang, S.; Wiesmann, C.; Wong, S.; Zhu, B. Y. Discovery of (Thienopyrimidin-2-yl)aminopyrimidines as Potent, Selective, and Orally Available Pan-PI3-Kinase and Dual Pan-PI3-Kinase/mTOR Inhibitors for the Treatment of Cancer. *J. Med. Chem.* **2010**, *53*, 1086-1097.
83. Knight, S. D.; Adams, N. D.; Burgess, J. L.; Chaudhari, A. M.; Darcy, M. G.; Donatelli, C. A.; Luenga, J. I.; Newlander, K. A.; Parrish, J. D.; Ridgers, L. H.; Sarpong, M. A.; Schmidt, S. J.; Van Aller, G. S.; Carson, J. D.; Diamond, M. A.; Elkins, P. A.; Gardiner, C. M.; Garver, E.; Gilbert, S. A.; Gontarek, R. R.; Jackson, J. R.; Kershner, K. L.; Luo, L.; Raha, K.; Sherk, C. S.; Sung, C.-M.; Sutton, D.; Tummino, P. J.; Wegrzyn, R. J.; Auger, K. R.; Dhanak, D. Discovery of GSK2126458, a Highly Potent Inhibitor of PI3K and the Mammalian Target of Rapamycin. *ACS Med. Chem. Lett.* **2010**, *1*, 39-43.
84. D'Angelo, N. D.; Kim, T.-S.; Andrews, K.; Booker, S. K.; Caenepeel, S.; Chen, K.; Freeman, D.; Jiang, J.; McCarter, J. D.; San Miguel, T.; Mullady, E. L.; Schrag, M.; Subramanian, R.; Tang, J.; Wahl, R. C.; Wang, L.; Whittington, D. A.; Wu, T.; Xi, N.; Xu, Y.; Yakowec, P.; Zalameda, L.; Zhang, N.; Hughes, P.; Norman, M. H. Discovery and Optimization of a Series of Benzothiazole Phosphoinositide 3-Kinase (PI3K)/ Mammalian Target of Rapamycin (mTOR) Dual Inhibitors. *J. Med. Chem.* **2011**, *54*, 1789-1811.
85. Nishimura, N.; Siegmund, A.; Liu, L.; Yang, K.; Bryan, M. C.; Andrews, K. L.; Bo, Y.; Booker, S. K.; Caenepeel, S.; Freeman, D.; Liao, H.; McCarter, J.; Mullady, E. L.; San Miguel, T.; Subramanian, R.; Tamayo, N.; Wang, L.; Whittington, D. A.; Zalameda, L.; Zhang, N.; Hughes, P. E.; Norman, M. H. Phosphoinositide 3-Kinase (PI3K)/Mammalian Target of Rapamycin (mTOR) Dual Inhibitors: Discovery and Structure-Activity Relationships of a Series of Quinoline and Quinoxaline Derivatives. *J. Med. Chem.* **2011**, *54*, 4735-4751.
86. Stec, M. M.; Andrews, K. L.; Booker, S. K.; Caenepeel, S.; Freeman, D. J.; Jiang, J.; Liao, H.; McCarter, J.; Mullady, E. L.; San Miguel, T.; Subramanian, R.; Tamayo, N.; Wang, L.; Yang, K.; Zalameda, L. P.; Zhang, N.; Hughes, P. E.; Norman, M. H. Structure-Activity Relationship of Phosphoinositide 3-Kinase (PI3K)/ Mammalian Target of Rapamycin (mTOR) Dual Inhibitors: Investigations of Various 6,5-Heterocycles to Improve Metabolic Stability. *J. Med. Chem.* **2011**, *54*, 5174-5184.

87. Crew, A. P.; Bhagwat, S. V.; Dong, H.; Bittner, M. A.; Chan, A.; Chen, X.; Coate, H.; Cooke, A.; Gokhale, P. C.; Honda, A.; Jin, M.; Kahler, J.; Mantis, C.; Mulvihill, M. J.; Tavares-Greco, P. A.; Volk, B.; Wang, J.; Werner, D. S.; Arnold, L. D.; Pachter, J. A.; Wild, R.; Gibson, N. W. Imidazo[1,5-*a*]pyrazines: Orally Efficacious Inhibitors of mTORC1 and mTORC2. *Bioorg. Med. Chem. Lett.* **2011**, 21, 2092-2097.
88. Rodrik-Outmezguine; Chandarlapaty, S.; Pagano, N. C.; Poulikakos, P. L.; Scaltriti, M.; Baselga, J.; Guichard, S.; Rosen, N. mTOR Kinase Inhibition Causes Feedback-Dependent Biphasic Regulation of AKT Signalling. *Cancer Disc.* **2011**, 1, 248-259.
89. Toogood, P. L. Inhibition of Protein-protein Association by Small Molecules: Approaches and Progress. *J. Med. Chem.* **2002**, 45, 1543-1558.
90. Cummings, C. G.; Hamilton, A. D. Disrupting Protein-protein Interactions with Non-peptidic, Small Molecule Alpha-helix Mimetics. *Curr. Opin. Chem. Biol.* **2010**, 14, 341-346.
91. Arkin, M. R.; Wells, J. A. Small-molecule Inhibitors of Protein-protein Interactions: Progressing Towards the Dream. *Nat. Rev. Drug Disc.* **2004**, 3, 301-317.
92. Clackson, T.; Wells, J. A. A Hot-Spot of Binding-Energy in a Hormone-Receptor Interface. *Science* **1995**, 267, 383-386.
93. Moreira, I. S.; Fernandes, P. A.; Ramos, M. J. Hot spots-A Review of the Protein-protein Interface Determinant Amino-acid Residues. *Proteins-Struct., Funct., Bioinf.* **2007**, 68, 803-812.
94. Arkin, M. Protein-protein Interactions and Cancer: Small Molecules Going in for the Kill. *Curr. Opin. Chem. Biol.* **2005**, 9, 317-324.
95. Wilson, A. J. Inhibition of Protein-protein Interactions Using Designed Molecules. *Chem. Soc. Rev.* **2009**, 38, 3289-3300.
96. Blundell, T. L.; Sibanda, B. L.; Wander Montalvao, R.; Brewster, S.; Chelliah, V.; Worth, C. L.; Harmer, N. J.; Davies, O.; Burke, D. Structural Biology and Bioinformatics in Drug Design: Opportunities and Challenges for Target Identification and Lead Discovery. *Phil. Trans. R. Soc. B* **2006**, 361, 413-423.
97. Singh, I. P.; Chauthe, S. K. Small Molecule HIV Entry Inhibitors: Part I. Chemokine Receptor Antagonists: 2004-2010. *Expert Opin. Ther. Patents* **2011**, 21, 227-269.
98. Dorr, P.; Westby, M.; Dobbs, S.; Griffin, P.; Irvine, B.; Macartney, M.; Mori, J.; Rickett, G.; Smith-Burchnell, C.; Napier, C.; Webster, R.; Armour, D.; Price, D.;

- Stammen, B.; Wood, A.; Perros, M. Maraviroc (UK-427, 857), a Potent, Orally Bioavailable, and Selective Small-Molecule Inhibitor of Chemokine Receptor CCR5 with Broad-Spectrum Anti-Human Immunodeficiency Virus Type 1 Activity. *Antimicrob. Agents Chemother.* **2005**, 49, 4721-4732.
99. Levine, A. J.; Oren, M. The First 30 Years of p53: Growing Ever More Complex. *Nat. Rev. Cancer* **2009**, 9, 749-758.
100. Moll, U. M.; Petrenko, O. The MDM2-p53 Interaction. *Mol. Cancer Res.* **2003**, 1, 1001-1003.
101. Wade, M.; Wang, Y. V.; Wahl, G. M. The p53 Orchestra: Mdm2 and Mdmx Set the Tone. *Trends Cell Biol.* **2010**, 20, 299-309.
102. Joerger, A. C.; Fersht, A. R. Structural Biology of the Tumour Suppressor p53. *Annu. Rev. Biochem.* **2008**, 77, 557-582.
103. Chene, P. The Role of Tetramerization in p53 Function. *Oncogene* **2001**, 20, 2611-2617.
104. Piette, J.; Neel, H.; Marechal, V. Mdm2: Keeping p53 Under Control. *Oncogene* **1997**, 15, 1001-1010.
105. Momand, J.; Wu, H.; Dasgupta, g. MDM2 - Master Regulator of the p53 Tumor Suppressor Protein. *Gene* **2000**, 242, 15-29.
106. Oliner, J. D.; Kinzler, K. W.; Meltzer, P. S.; George, D. L.; Vogelstein, B. Amplification of a Gene Encoding a p53-Associated Protein in Human Sarcomas. *Nature* **1992**, 358, 80-83.
107. Kruse, J. P.; Gu, W. Modes of p53 Regulation. *Cell* 2009, 137, 609-622.
108. Kussie, P. H.; Gorina, S.; Marechal, V.; Elenbaas, B.; Moreau, J.; Levine, A. J.; Pavletich, N. P. Structure of the MDM2 Oncoprotein Bound to the p53 Tumour Suppressor Transactivation Domain. *Science* **1996**, 274, 948-953.
109. Nie, L.; Sasaki, M.; Maki, C. G. Regulation of p53 Nuclear Export through Sequential Changes in Conformation and Ubiquitination. *J. Biol. Chem.* **2007**, 282, 14616-14625.
110. Macchiarulo, A.; Giacche, N.; Carotti, A.; Moretti, F.; Pellicciari, R. Expanding the Horizon of Chemotherapeutic Targets: From MDM2 to MDMX (MDM4). *Med. Chem. Comm.* **2011**, 2, 455-465.
111. Mancini, F.; Di Conza, G.; Monti, O.; Macchiarulo, A.; Pellicciari, R.; Pontecorvi, A.; Moretti, F. Puzzling Over MDM4-p53 Network. *Int. J. Biochem. Cell Biol.* **2010**, 42, 1080-1083.

112. Efeyan, A.; Serrano, M. p53: Guardian of the Genome and Policeman of the Oncogene. *Cell Cycle* **2007**, 6, 1006-1010.
113. Chene, P. Inhibiting the p53-MDM2 Interaction: An Important Target for Cancer Therapy. *Nat. Rev. Cancer* **2003**, 3, 102-109.
114. Toledo, F.; Wahl, G. M. Regulating the p53 Pathway: *In Vitro* Hypothesis, *In Vivo* Veritas. *Nat. Rev. Cancer* **2006**, 6, 909-923.
115. Maximov, G. K.; Maximov, K. G. The Role of p53 Tumour-Suppressor Protein in Apoptosis and Cancerogenesis. *Biotechnol. & Biotechnol. Eq.* **2008**, 22, 664-668.
116. Kastan, M. B.; Lim, D. S. The Many Substrates and Functions of ATM. *Nat. Rev. Mol. Cell Biol.* **2000**, 1, 179-186.
117. Antoni, L.; Sodha, N.; Collins, I.; Garrett, M. D. CHK2 Kinase: Cancer Susceptibility and Cancer Therapy - Two Sides of the Same Coin? *Nat. Rev. Cancer* **2007**, 7, 925-936.
118. Turenne, G. A.; Paul, P.; Laflair, L.; Price, B. D. Activation of p53 Transcriptional Activity Requires ATM's Kinase Domain and Multiple N-terminal Serine Residues of p53. *Oncogene* **2001**, 20, 5100-5110.
119. Sakaguchi, K.; Herrera, J. E.; Saito, S.; Miki, T.; Bustin, M.; Vassilev, A.; Anderson, C.; Appella, E. DNA Damage Activates p53 Through a Phosphorylation-acetylation Cascade. *Genes Dev.* **1998**, 12, 2831-2841.
120. Boehme, K. A.; Kulikov, R.; Blattner, C. p53 Stabilization in Response to DNA Damage Requires Akt/PKB and DNA-PK. *PNAS* **2008**, 105, 7785-7790.
121. Fuster, J. J.; Sanz-Gonzalez, S. M.; Moll, U. M.; Andres, V. Classic and Novel Roles of p53: Prospects for Anticancer Therapy. *Trends Mol. Med.* **2007**, 13, 192-199.
122. Taylor, W. R.; Stark, G. R. Regulation of the G2/M transition by p53. *Oncogene* **2001**, 20, 1803-1815.
123. Meek, D. W. Tumour Suppression by p53: a Role for the DNA Damage Response? *Nat. Rev. Cancer* **2009**, 9, 714-723.
124. Levine, A. J. p53, the Cellular Gatekeeper for Growth and Division. *Cell* **1997**, 88, 323-331.
125. Brown, C. J.; Lain, S.; Verma, C. S.; Fersht, A. R.; Lane, D. P. Awakening Guardian Angels: Drugging the p53 Pathway. *Nat. Rev. Cancer* **2009**, 9, 862-871.
126. Vousden, K. H.; Prives, C. Blinded by the Light: The Growing Complexity of p53. *Cell* **2009**, 137, 413-430.

127. Liebermann, D. A.; Hoffman, B. Gadd45 in Stress Signalling. *J. Mol. Signal.* **2008**, *3*.
128. Harris, S. L.; Levine, A. J. The p53 Pathway: Positive and Negative Feedback Loops. *Oncogene* **2005**, *24*, 2899-2908.
129. Cory, S.; Adams, J. M. The Bcl-2 Family: Regulators of the Cellular Life-or-Death Switch. *Nat. Rev. Cancer* **2002**, *2*, 647-656.
130. Chari, N. S.; Pinarire, N. L.; Thorpe, L.; Medeiros, L. J.; Routbort, M. J.; McDonnell, T. J. The p53 Tumour Suppressor Network in Cancer and the Therapeutic Modulation of Cell Death. *Apoptosis* **2009**, *14*, 336-347.
131. Vassilev, L. T.; Vu, B. T.; Graves, B.; Carvajal, D.; Podlaski, F.; Filipovic, Z.; Kong, N.; Kammlott, U.; Lukacs, C.; Klein, C.; Fotouhi, N.; Liu, E. A. *In Vivo* Activation of the p53 Pathway by Small-molecule Antagonists of MDM2. *Science* **2004**, *303*, 844-848.
132. Dickens, M. P.; Fitzgerald, R.; Fischer, P. M. Small-molecule Inhibitors of MDM2 as New Anticancer Therapeutics. *Semin. Cancer Biol.* **2010**, *20*, 10-18.
133. Bartkovitz, D. J.; Cai, J.; Chu, X.; Li, H.; Lovey, A. J.; Vu, B. T.; Zhao, C. Chiral Cis-imidazolines. WO/2009/047161, 2009.
134. Khoury, K.; Popowicz, G. M.; Holak, T. A.; Domling, A. The p53-MDM2/MDMX Axis - A Chemotype Perspective. *Med. Chem. Comm.* **2011**, *2*, 246-260.
135. Ding, K.; Lu, Y.; Nikolovska-Coleska, Z.; Qiu, S.; Ding, Y. S.; Gao, W.; Stuckey, J.; Krajewski, K.; Roller, P. P.; Tomita, Y.; Parrish, D. A.; Deschamps, J. R.; Wang, S. M. Structure-based design of potent non-peptide MDM2 inhibitors. *J. Am. Chem. Soc.* **2005**, *127*, 10130-10131.
136. Ding, K.; Lu, Y. P.; Nikolovska-Coleska, Z.; Wang, G. P.; Qiu, S.; Shangary, S.; Gao, W.; Qin, D. G.; Stuckey, J.; Krajewski, K.; Roller, P. P.; Wang, S. M. Structure-based Design of Spiro-oxindoles as Potent, Specific Small-molecule Inhibitors of the MDM2-p53 Interaction. *J. Med. Chem.* **2006**, *49*, 3432-3435.
137. Yu, S. H.; Qin, D. G.; Shangary, S.; Chen, J. Y.; Wang, G. P.; Ding, K.; McEachern, D.; Qiu, S.; Nikolovska-Coleska, Z.; Miller, R.; Kang, S. M.; Yang, D. J.; Wang, S. M. Potent and Orally Active Small-Molecule Inhibitors of the MDM2-p53 Interaction. *J. Med. Chem.* **2009**, *52*, 7970-7973.
138. Grasberger, B. L.; Lu, T. B.; Schubert, C.; Parks, D. J.; Carver, T. E.; Koblisch, H. K.; Cummings, M. D.; LaFrance, L. V.; Milkiewicz, K. L.; Calvo, R. R.; Maguire,

- D.; Lattanze, J.; Franks, C. F.; Zhao, S. Y.; Ramachandren, K.; Bylebyl, G. R.; Zhang, M.; Manthey, C. L.; Petrella, E. C.; Pantoliano, M. W.; Deckman, I. C.; Spurlino, J. C.; Maroney, A. C.; Tomczuk, B. E.; Molloy, C. J.; Bone, R. F. Discovery and Cocystal Structure of Benzodiazepinedione HDM2 Antagonists that Activate p53 in Cells. *J. Med. Chem.* **2005**, 48, 909-912.
139. Parks, D. J.; LaFrance, L. V.; Calvo, R. R.; Milkiewicz, K. L.; Gupta, V.; Lattanze, J.; Ramachandren, K.; Carver, T. E.; Petrella, E. C.; Cummings, M. D.; Maguire, D.; Grasberger, B. L.; Lu, T. B. 1,4-Benzodiazepine-2,5-diones as Small Molecule Antagonists of the HDM2-p53 Interaction: Discovery and SAR. *Bioorg. Med. Chem. Lett.* **2005**, 15, 765-770.
140. Marugan, J. J.; Leonard, K.; Raboisson, P.; Gushue, J. M.; Calvo, R.; Koblish, H. K.; Lattanze, J.; Zhao, S. Y.; Cummings, M. D.; Player, M. R.; Schubert, C.; Maroney, A. C.; Lu, T. B. Enantiomerically Pure 1,4-Benzodiazepine-2,5-diones as Hdm2 Antagonists. *Bioorg. Med. Chem. Lett.* **2006**, 16, 3115-3120.
141. Leonard, K.; Marugan, J. J.; Raboisson, P.; Calvo, R.; Gushue, J. M.; Koblish, H. K.; Lattanze, J.; Zhao, S. Y.; Cummings, M. D.; Player, M. R.; Maroney, A. C.; Lu, T. B. Novel 1,4-Benzodiazepine-2,5-diones as Hdm2 Antagonists With Improved Cellular Activity. *Bioorg. Med. Chem. Lett.* **2006**, 16, 3463-3468.
142. Cummings, M. D.; Schubert, C.; Parks, D. J.; Calvo, R. R.; LaFrance, L. V.; Lattanze, J.; Milkiewicz, K. L.; Lu, T. B. Substituted 1,4-Benzodiazepine-2,5-diones as Alpha-helix Mimetic Antagonists of the HDM2-p53 Protein-protein Interaction. *Chem. Biol. Drug Des.* **2006**, 67, 201-205.
143. Allen, J. G.; Bourbeau, M. P.; Wohlhieter, G. E.; Bartberger, M. D.; Michelsen, K.; Hungate, R.; Gadwood, R. C.; Gaston, R. D.; Evans, B.; Mann, L. W.; Matison, M. E.; Schneider, S.; Huang, X.; Yu, D.; Andrews, P. S.; Reichelt, A.; Long, A. M.; Yakowec, P.; Yang, E. Y.; Lee, T. A.; Oliner, J. D. Discovery and Optimization of Chromenotriazolopyrimidines as Potent Inhibitors of the Mouse Double Minute 2-Tumor Protein 53 Protein-Protein Interaction. *J. Med. Chem.* **2009**, 52, 7044-7053.
144. Beck, H. P.; DeGraffenreid, M.; Fox, B.; Allen, J. G.; Rew, Y.; Schneider, S.; Saiki, A. Y.; Yu, D.; Oliner, J. D.; Salyers, K.; Ye, Q.; Olson, S. Improvement of the Synthesis and Pharmacokinetic Properties of Chromenotriazolopyrimidine MDM2-p53 Protein-protein Inhibitors. *Bioorg. Med. Chem. Lett.* **2011**, 9, 2752-2755.
145. Popowicz, G. M.; Czarna, A.; Wolf, S.; Wang, K.; Wang, W.; Domling, A.; Holak, T. A. Structures of Low Molecular Weight Inhibitors Bound to MDMX and

- MDM2 Reveal New Approaches for p53-MDMX/MDM2 Antagonist Drug Discovery. *Cell Cycle* **2010**, 9, 1104-1111.
146. Popowicz, G. M.; Domling, A.; Holak, T. A. The Structure-Based Design of Mdm2/Mdmx-p53 Inhibitors Gets Serious. *Angew. Chem. Int. Ed.* **2011**, 50, 2680-2688.
147. Arris, C. E.; Boyle, F. T.; Calvert, A. H.; Curtin, N. J.; Endicott, J. A.; Garman, E. F.; Gibson, A. E.; Golding, B. T.; Grant, S.; Griffin, R. J.; Jewsbury, P.; Johnson, L. N.; Lawrie, A. M.; Newell, D. R.; Noble, M. E. M.; Sausville, E. A.; Schultz, R.; Yu, W. Identification of Novel Purine and Pyrimidine Cyclin-Dependent Kinase Inhibitors with Distinct Molecular Interactions and Tumor Cell Growth Inhibition Profiles. *J. Med. Chem.* **2000**, 43, 2797-2804.
148. Marchetti, F.; Cano, C.; Curtin, N. J.; Golding, B. T.; Griffin, R. J.; Haggerty, K.; Newell, D. R.; Parsons, R. J.; Payne, S. L.; Wang, L. Z.; Hardcastle, I. R. Synthesis and Biological Evaluation of 5-Substituted O4-Alkylpyrimidines as CDK2 Inhibitors. *Org. Biomol. Chem.* **2010**, 8, 2397-2407.
149. Marchetti, F.; Sayle, K. L.; Bentley, J.; Clegg, W.; Curtin, N. J.; Endicott, J. A.; Golding, B. T.; Griffin, R. J.; Haggerty, K.; Harrington, R. W.; Mesguiche, V.; Newell, D. R.; Noble, M. E. M.; Parsons, R. J.; Pratt, D. J.; Wang, L. Z.; Hardcastle, I. R. Structure-Based Design of 2-Arylamino-4-cyclohexylmethoxy-5-nitroso-6-aminopyrimidine Inhibitors of Cyclin-Dependent Kinase 2. *Org. Biomol. Chem.* **2007**, 5, 1577-1585.
150. Mesguiche, V.; Parsons, R. J.; Arris, C. E.; Bentley, J.; Boyle, F. T.; Curtin, N. J.; Davies, T. G.; Endicott, J. A.; Gibson, A. E.; Golding, B. T.; Griffin, R. J.; Jewsbury, P.; Johnson, L. N.; Newell, D. R.; Noble, M. E. M.; Wang, L. Z.; Hardcastle, I. R. 4-Alkoxy-2,6-Diaminopyrimidine Derivatives: Inhibitors of Cyclin Dependent Kinases 1 and 2. *Bioorg. Med. Chem. Lett.* **2003**, 13, 217-222.
151. Sayle, K. L.; Bentley, J.; Boyle, F. T.; Calvert, A. H.; Cheng, Y. Z.; Curtin, N. J.; Endicott, J. A.; Golding, B. T.; Hardcastle, I. R.; Jewsbury, P.; Mesguiche, V.; Newell, D. R.; Noble, M. E. M.; Parsons, R. J.; Pratt, D. J.; Wang, L. Z.; Griffin, R. J. Structure-Based Design of 2-Arylamino-4-Cyclohexylmethyl-5-Nitroso-6-Aminopyrimidine Inhibitors of Cyclin-Dependent Kinases 1 and 2. *Bioorg. Med. Chem. Lett.* **2003**, 13, 3079-3082.
152. Sayle, K. L. Design and Synthesis of Selective Kinase Inhibitors. Newcastle University, Newcastle upon Tyne, 2004.

153. Payne, S. L. In 2008.
154. Payne, S. L. Small-Molecule Inhibitors of mTOR and DNA-PK. Newcastle University, Newcastle-upon-Tyne, 2010.
155. Szczepankiewicz, B. G.; Kosogof, C.; Nelson, L. T. J.; Liu, G.; Liu, B.; Zhao, H.; Serby, M. D.; Xin, Z.; Liu, M.; Gum, R. J.; Haasch, D. L.; Wang, S.; Clampit, J. E.; Johnson, E. F.; Lubben, T. H.; Stashko, M. A.; Olejniczak, E. T.; Sun, C.; Dorwin, S. A.; Haskins, K.; Abad-Zapatero, C.; Fry, E. H.; Hutchins, C. W.; Sham, H. L.; Rondinone, C. M.; Trevillyan, J. M. Aminopyridine-Based c-Jun N-Terminal Kinase Inhibitors with Cellular Activity and Minimal Cross-Kinase Activity. *J. Med. Chem.* **2006**, 49, 3563-3580.
156. Feuer, H. *The Chemistry of the Nitro and Nitroso group*. Wiley Interscience: New York, **1969**.
157. Lukac, M.; Smolarikova, E.; Lacko, I.; Devinsky, F. The Methoxybenzyl Ethers as Useful Protecting Groups for Hydroxy Compounds: Methods of Deprotection. *Acta Facult. Pharm. Univ. Comenianae* **2005**, 52, 31-45.
158. Luo, G.; Chen, L.; Poindexter, G. S. Microwave-Assited Synthesis of Aminopyrimidines. *Tetrahedron Lett.* **2002**, 43, 5739-5742.
159. Marchetti, F. The Development of ATP-competitive Inhibitors of CDK2. Newcastle University, Newcastle Upon Tyne, 2008.
160. Marko, I. E.; Ates, A.; Augustyns, B.; Gautier, A.; Quesnel, Y.; Turet, L.; Wiaux, M. Remarkable Deprotection of THP and THF Ether Catalysed by Cerium Ammonium Nitrate (CAN) Under Neutral Conditions. *Tetrahedron Lett.* **1999**, 40, 5613-5616.
161. Furstner, A.; Radkowski, K.; Peters, H. Chasing a Phantom by Total Synthesis: The Butylcycloheptylprodigiosin Case. *Angew. Chem. Int. Ed.* **2005**, 44, 2777-2781.
162. Marchal, A.; Melguizo, M.; Nogueras, M.; Sanchez, A.; Low, J. N. Novel Procedure for Selective C-Nitrosation of Aminopyrimidine Derivatives Under Neutral Conditions. Scope and Synthetic Applications. *Synlett* **2002**, 255-258.
163. Rodriguez Aristegui, S.; Desage El-Murr, M.; Golding, B. T.; Griffin, R. J.; Hardcastle, I. R. Judicious Application of Allyl Protecting Groups for the Synthesis of 2-Morpholin-4-yl-4-oxo-4H-chromen-8-yl Triflate, a Key Precursor of DNA-Dependent Protein Kinase Inhibitors. *Org. Lett.* **2006**, 8, 5927-5929.
164. Ueda, H.; Satoh, H.; Matsumoto, K.; Sugimoto, K.; Fukuyama, T.; Tokuyama, H. Total Synthesis of (+)-Haplophytine. *Angew. Chem. Int. Ed.* **2009**, 48, 7600-7603.

165. Karpf, M.; Trussardi, R. New, Azide-Free Transformation of Epoxides into 1,2-Diamino Compounds: Synthesis of the Anti-Influenza Neuraminidase Inhibitor Oseltamivir Phosphate (Tamiflu). *J. Org. Chem.* **2001**, 66, 2044-2051.
166. Too, K.; Brown, D. M.; Bongard, E.; Yardley, V.; Vivas, L.; Loakes, D. Anti-Malarial Activity of N^6 -Modified Purine Analogues. *Bioorg. Med. Chem.* **2007**, 15, 551-5562.
167. Hockova, D.; Holy, A.; Masolidkova, M.; Andrei, G.; Snoeck, R.; De Clercq, E.; Balzarini, J. 5-Substituted-2,4-diamino-6-[2-(phosphonomethoxy)ethoxy]pyrimidines - Acyclic Nucleoside Phosphonate Analogues with Antiviral Activity. *J. Med. Chem.* **2003**, 46, 5064-5073.
168. Quiroga, J.; Trilleras, J.; Galvez, J.; Insuasty, B.; Abonia, R.; Nogueras, M.; Cobo, J.; Marchal, A. C- and N-Cyanoacetylation of 6-Aminopyrimidines with Cyanoacetic Acid and Acetic Anhydride. *Tetrahedron Lett.* **2008**, 49, 5672-5675.
169. Kirk, K. L. Fluorination in Medicinal Chemistry: Methods, Strategies and Recent Developments. *Org. Process Res. Dev.* **2008**, 12, 305-321.
170. Sankar Lal, G.; Pastore, W.; Pesaresi, R. A Convenient Synthesis of 5-Fluoropyrimidine Using 1-(Chloromethyl)-4-fluoro-1,4-diazabicyclo[2.2.2]octane Bis(tetrafluoroborate)-SELECTFLUOR Reagent. *J. Org. Chem.* **1995**, 60, 7340-7342.
171. Sankar Lal, G. Site-Selective Fluorination of Organic Compounds Using 1-Alkyl-4-fluoro-1,4-diazabicyclo[2.2.2]octane Salts (Selectfluor Reagents). *J. Org. Chem.* **1993**, 58, 2791-2796.
172. Furuya, T.; Ritter, T. Fluorination of Boronic Acids Mediated by Silver (I) Triflate. *Org. Lett.* **2009**, 11, 2860-2863.
173. Clapham, K. M. Synthesis and Reactions of New *N*-heteroaryl Boronic Acids. Durham University, Durham, 2008.
174. Manley, P. J.; Bilodeau, M. T. A Mild Method for the Formation and *In Situ* Reaction of Imidoyl Chlorides: Conversion of Pyridine-1-oxides to 2-Aminopyridine Amides. *Org. Lett.* **2002**, 4, 3127-3129.
175. Comins, D. L.; Jianhua, G. *N*- vs *O*- Alkylation in the Mitsunobu Reaction of 2-Pyridone. *Tetrahedron Lett.* **1994**, 35, 2819-2822.
176. Steenken, S.; O'Neill, P. Reaction of OH Radicals with 2- and 4-Pyridones in Aqueous Solution. An Electron Spin Resonance and Pulse Radiolysis Study. *J. Phys. Chem.* **1979**, 83, 2407-2412.

177. Schlegal, H. B.; Gund, P.; Fluder, E. M. Tautomerization of Formamide, 2-Pyridone, and 4-Pyridone - an Ab Initio Study. *J. Am. Chem. Soc.* **1982**, 104, 5347-5351.
178. Hollick, J. J. Pyran-4-one, Thiopyran-4-one and 4-Pyridone Inhibitors of the Phosphatidylinositol 3-Kinase-Related Kinase Family. University of Newcastle upon Tyne, 2004.
179. Hopkins, G. C.; Jonak, J. P.; Minnemeyer, H. J.; Tieckelmann, H. Alkylations of Heterocyclic Ambident Anions. II. Alkylation of 2-Pyridone Salts. *J. Am. Chem. Soc.* **1967**, 89, 4040-4044.
180. Braxmeier, T.; Demarcus, M.; T., F.; McAteer, S.; Kilburn, J. D. Identification of Sequence Selective Receptor for Peptides with a Carboxylic Acid Terminus. *Chem. Eur. J.* **2001**, 7, 1889-1898.
181. Prikhod'ko, S. A.; Oleinik, I. I.; Oleinik, I. V.; Ivanchev, S. S.; Tolstikov, G. A. Preparative Procedure for the Synthesis of 4-Allyloxypyridine-2,6-dicarboxylic Acid. *Rus. J. Org. Chem.* **2007**, 43, 156-157.
182. Kruizinga, W. H.; Strijtveen, B.; Kellogg, R. M. Cesium Carboxylates in Dimethyl formamide. Reagents for Introduction of Hydroxyl Groups by Nucleophilic Substitution and for Inversion of Configuration of Secondary Alcohols. *J. Org. Chem.* **1981**, 46, 4321-4323.
183. Maligres, P. E.; Waters, M. S.; Fleitz, F.; Askin, D. A Highly Catalytic Robust Palladium Catalyzed Cyanation of Aryl Bromides. *Tetrahedron Lett.* **1990**, 40, 8193-8195.
184. Carboni, R. A.; Coffman, D. D.; Howard, E. G. Cyanocarbon Chemistry. XI. Malononitrile Dimer. *J. Am. Chem. Soc.* **1958**, 80, 2838-2840.
185. Silver, J. L.; Al-Janabi, M. Y.; Johnson, R. M.; Burmeister, J. L. The Zinc(II)-Catalyzed Reaction of Malononitrile with Ethyl Alcohol *Inorg. Chem.* **1971**, 10, 994-997.
186. Junek, H.; Uray, G.; Kotzent, A. Isomere Diamino-alkoxy-pyridin-carbonitrile - ihre Trennung und Verwendung als Kupplungskomponenten. *Monatsh. Chem.* **1983**, 114, 973-982.
187. Joule, J. A.; Mills, K. *Heterocyclic Chemistry*. 4th ed.; Blackwell Publishing: Oxford, 2000.
188. http://evans.harvard.edu/pdf/evans.pKa_table.pdf (02.08.2011).

189. Parks, E. L.; Sandford, G.; Yufit, D. S.; Howard, J. A. K.; Christopher, J. A.; Miller, D. D. Trisubstituted Pyrimidine Derivatives from Tetrafluoropyrimidine. *Tetrahedron* **2010**, 66, 6195-6204.
190. Hardcastle, I. R.; Ahmed, S. U.; Atkins, H.; Farnie, G.; Golding, B. T.; Griffin, R. J.; Guyenne, S.; Hutton, C.; Kallbard, P.; Kemp, S.; Kitching, M. S.; Newell, D. R.; Norbedo, S.; Northen, J. S.; Reid, R. J.; Saravanan, K.; Willems, H. G. M.; Lunec, J. Small-Molecule Inhibitors of the MDM2-p53 Protein-Protein Interaction Based on an Isoindolinone Scaffold *J. Med. Chem.* **2006**, 49, 6209-6221.
191. Riedinger, C.; Endicott, J. A.; Kemp, S.; Smyth, L. A.; Watson, A.; Valeur, E.; Golding, B. T.; Griffin, R. J.; Hardcastle, I. R.; Noble, M. E.; McDonnell, J. M. Analysis of Chemical Shift Changes Reveals the Binding Modes of Isoindolinone Inhibitors of the MDM2-p53 Interaction. *J. Am. Chem. Soc.* **2008**, 130, 16038-16044.
192. Hardcastle, I. R.; Liu, J.; Valeur, E.; Watson, A.; Ahmed, S. U.; Blackburn, T. J.; Bennaceur, K.; Clegg, W.; Drummond, C.; Endicott, J. A.; Golding, B. T.; Griffin, R. J.; Gruber, J.; Haggerty, K.; Harrington, R. W.; Hutton, C.; Kemp, S.; Lu, X.; McDonnell, J. M.; Newell, D. R.; Noble, M. E. M.; Payne, S. L.; Reville, C. H.; Riedinger, C.; Xu, Q.; Lunec, J. Isoindolinone Inhibitors of the Murine Double Minute 2 (MDM2)-p53 Protein-Protein Interaction: Structure-Activity Studies Leading to improved Potency. *J. Med. Chem.* **2011**, 54, 1233-1243.
193. Riedinger, C.; Noble, M. E.; Wright, D. J.; Mulks, F.; Hardcastle, I. R.; Endicott, J. A.; McDonnell, J. M. Understanding Small-Molecule Binding to MDM2: Insights into Structural Effects of Isoindolinone Inhibitors from NMR Spectroscopy. *Chem. Biol. Drug Des.* **2011**, 77, 301-308.
194. Watson, A. .
195. Blackburn, T. J.
196. Clayden, J.; Greeves, N.; Warren, S.; Wothers, P. *Organic Chemistry*. Oxford University Press: 2001.
197. Newman, M. S.; Scheurer, P. G. The Behaviour of 3-Chlorophthalic Anhydride in Friedel-Crafts and Grignard Condensations. *J. Am. Chem. Soc.* **1956**, 78, 5004-5007.
198. Allahdad, A.; Knight, D. W. An Investigation of the Wittig Reaction between A Series of Monosubstituted Phthalic Anhydrides and Ethoxycarbonylmethylidetriphenylphosphorane. *J. Chem. Soc. Perkin Trans. 1* **1982**, 1855-1863.

199. Kitching, M. S. Development of Methodology for the Synthesis of Isoindolinone Libraries. University of Newcastle Newcastle, 1999.
200. Bhatt, M. V.; Kamath, K. M. Aspects of Tautomerism. Part I. Environmental and Substituent Effects on the Tautomerism of *o*-Benzoyl Benzoic Acids. *J. Chem. Soc. (B)* **1968**, 1036-1044.
201. Bhatt, M. V.; Kamath, K. M.; Ravindranathan, M. Aspects of Tautomerism. Part II. Reactions of the Pseudo-acid Chloride of *o*-Benzoylbenzoic Acid with Nucleophiles. *J. Chem. Soc. (C)* **1971**, 1772-1777.
202. Sloan, K. B.; Koch, S. A. M. Effect of Nucleophilicity and Leaving Group Ability on the S_N2 Reactions of Amines with (Acyloxy)alkyl alpha-Halides: A Product Distribution Study. *J. Org. Chem.* **1983**, 48, 635-640.
203. Lejkowski, M.; Banerjee, P.; Runsink, J.; H., G. Asymmetric Synthesis of Spiroketal, Spiroether, and Oxabicyclic Building Blocks via Stereoselective Spiro- and Bicycloannulation of 2-Hydroxy Dihydropyrans. *Org. Lett.* **2008**, 10, 2713-2716.
204. Carey, K. A.; Clegg, W.; M.R.J., E.; Golding, B. T.; Hill, M. N. S.; Maskill, H. Synthesis of Highly Hindered Oxepins and an Azepine from bis-Triptyl Carbenium Ions: Structural Characterisation by NMR and X-Ray Crystallography. *J. Chem. Soc. Perkin Trans. 1* **2002**, 2673-2679.
205. Wermuth, C. G. *The Practice of Medicinal Chemistry*. Academic Press: London, 1996.
206. Chinchilla, R.; Najera, C. The Sonogashira Reaction: A Booming Methodology in Synthetic Organic Chemistry. *Chem. Rev.* **2007**, 107, 874-922.
207. Park, C.; Bruncko, M.; Adickes, J.; Bauch, J.; Ding, H.; Kunzer, A.; Marsh, K. C.; Nimmer, P.; Shoemaker, A. R.; Song, X.; Tahir, S. K.; Tse, C.; Wang, X.; Wendt, M. D.; Yang, X.; Zhang, H.; Fesik, S. W.; Rosenberg, S. H.; Elmore, S. W. Discovery of an Orally Bioavailable Small Molecule Inhibitor of Prosurvival B-Cell Lymphoma 2 Proteins. *J. Med. Chem.* **2008**, 51, 6902-6915.
208. Tse, C.; Shoemaker, A. R.; Adickes, J.; Anderson, M. G.; Chen, J.; Jin, S.; Johnson, E. F.; Marsh, K. C.; Mitten, M. J.; Nimmer, P.; Roberts, L.; Tahir, S. K.; Xiao, Y.; Zhang, H.; Fesik, S.; Rosenberg, S. H.; Elmore, S. W. ABT-263: A Potent and Orally Bioavailable Bcl-2 Family Inhibitor. *Cancer Res.* **2008**, 68, 3421-3428.
209. Leach, C. A.; Liddle, J.; Zhang, J.; Terrell, L. R.; Smith, I. E. D.; Philip, J.; Peace, S. 1,6-Substituted (3R, 6R)-3-(2,3-Dihydro-1H-inden-2-yl)-2,5-

- piperazinedione Derivatives as Oxytocin Receptor Antagonists for the Treatment of Pre-term, Dysmenorrhea and Endometriosis. WO 2006.67462 A1, 29.06.2006, 2006.
210. Hansch, C.; Leo, A.; Taft, R. W. A Survey of Hammett Substituent Constants and Resonance and Field Parameters. *Chem. Rev.* **1991**, 91, 165-195.
211. Allen, J. R.; Amegadzie, A. K.; Gardinier, K. M.; Gregory, G. S.; Hitchcock, S. A.; Hoogestraat, P. J.; Jones Jr, W. D.; Smith, D. L. CB1 Modulator Compounds. WO 2005/066126, 2005.
212. Li, J. J. *Name Reactions*. 2nd ed.; Springer: 2003.
213. Yinglin, H.; Hongwen, H. A Convenient Synthesis of Primary Amines Using Sodium Diformylamide as a Modified Gabriel Reagent *Synthesis* **1990**, 122-124.
214. Yinglin, H.; Hongwen, H. A Convenient Synthesis of Aminomethyl Ketones (alpha-Amino Ketones). *Synthesis* **1990**, 615-618.
215. Suarez-Roriguez, D. *Tritylase Models for Coenzyme B₁₂-Dependent Mutases*. Newcastle University, Newcastle Upon Tyne, 2006.
216. Porter, J.; Lumb, S.; Lecomte, F.; Reuberson, J.; Foley, A.; Calmiano, M.; Le Riche, K.; Edwards, H.; Delgado, J.; Franklin, R. J.; Gascon-Simorte, J. M.; Maloney, A.; Meier, C.; Batchelor, M. Discovery of a Novel Series of Quinoxalines as Inhibitors of c-Met Kinase. *Bioorg. Med. Chem. Lett.* **2009**, 19, 397-400.
217. Hersberger, R.; Dawson, J.; Mueller, T. Synthesis of 4-(8-Benzo[1,2,5]oxadiazol-5-yl-[1,7]naphthyridine-6-yl)-benzoic Acid; a Potent and Selective Phosphodiesterase Type 4D Inhibitor. *Bioorg. Med. Chem. Lett.* **2002**, 12, 233.
218. Ohlmeyer, M. H. J.; Baldwin, J. J.; Dolle, R. E.; Paradkar, V.; Quintero, J. G.; Pan, G. Bradykinin B1 Receptor Antagonists. WO/2001/00578, 25.01.2001, 2001.
219. Mitsuya, H.; Weinhold, K. J.; Furman, P. A.; St. Clair, M. H.; S., N. L.; Gallo, R. C.; Bolognesi, D.; Barry, D. W.; Broder, S. 3'-Azido-3'-deoxythymidine (BW A509U): An Antiviral Agent that Inhibits the Infectivity and Cytopathic Effect of Human T-Lymphotropic Virus Type II/Lymphadenopathy-Associated Virus *In Vitro*. *PNAS* **1985**, 82, 7096-7100.
220. Parang, K.; Kohn, J. A.; Saldanha, S. A.; Cole, P. A. Development of Photo-Crosslinking Reagents for Protein Kinase-Substrate Interactions. *FEBS lett.* **2002**, 520, 156-160.
221. Zhu, W.; Ma, D. Synthesis of Aryl Azides and Vinyl Azides *via* Proline-Promoted CuI-Catalyzed Coupling Reactions. *Chem. Comm.* **2004**, 888-889.

222. Scriven, E. F. V. *Azides and Nitrenes*. Academic Press: London, 1984.
223. Ma, D.; Cai, Q. Copper/Amino Acid Catalyzed Cross-Couplings of Aryl and Vinyl Halides with Nucleophiles. *Acc. Chem. Res.* **2008**, 41, 1450-1460.
224. Griffin, R. J.; Evers, E.; Davison, R.; Gibson, A. E.; Layton, D.; Irwin, W. J. The 4-Azidobenzoyloxycarbonyl Function; Application as a Novel Protecting Group and Potential Prodrug Modification for Amines. *J. Chem. Soc. Perkin Trans. 1* **1996**, 1205-1211.
225. Takatori, K.; Nishihara, M.; Nishiyama, Y.; Kajiwara, M. A Asymmetric Synthesis of L-[3-¹³C]Phenylalanine and L-[3-¹³C]Tyrosine from [¹³C]Carbon Monoxide. *Tetrahedron* **1998**, 54, 15861-15869.
226. Bendall, J. G.; Payne, A. N.; Screen, T. E. O.; Holmes, A. B. Introduction of Bromine and Chlorine Substituents in Medium Ring Ethers and Lactones. *Chem. Comm.* **1997**, 1067-1068.
227. Oka, N.; Sanghvi, Y. S.; Theodorakis, E. A. 3,3'-Oxybis(dimethoxytrityl chloride) (O-DMTCl): Synthesis and Applications of a Novel Bifunctional Protecting Group. *Bioorg. Med. Chem.* **2004**, 14, 3241-3244.
228. Mathias, L. J. Esterification and Alkylation Reactions Employing Isoureas. *Synthesis* **1979**, 561-576.
229. Liu, Y. Isoureas: Versatile Alkylation Reagents in Organic Chemistry. *Synlett* **2009**, 1353-1354.
230. Wang, M. F.; Golding, B. T.; Potter, G. A. A Convenient Preparation of *p*-Methoxybenzyl Ester. *Synth. Commun.* **2000**, 30, 4197-4204.
231. Kaulen, J. Inversion of the Configuration of Secondary Alcohols *via* Isourea Ethers Prepared *in situ*. *Angew. Chem. Int. Ed. Engl.* **1987**, 26, 773-774.
232. Chinghine, A.; Crosignani, S.; Arnal, M.; Bradley, M.; Linclau, B. Microwave-Assisted Ester Formation Using *O*-Alkylisoureas: A Convenient Method for the Synthesis of Esters with Inversion of Configuration. *J. Org. Chem.* **2009**, 74, 4753-4762.
233. Wuitschik, G.; Carreira, E. M.; Wagner, B.; Fischer, H.; Parrilla, I.; Schuler, F.; Rogers-Evans, M.; Muller, K. Oxetanes in Drug Discovery: Structural and Synthetic Insights. *J. Med. Chem.* **2010**, 53, 3227-3246.
234. Burkhard, J. A.; Wuitschik, G.; Rogers-Evans, M.; Muller, K.; Carreira, E. M. Oxetanes as Versatile Elements in Drug Discovery and Synthesis. *Angew. Chem. Int. Ed.* **2010**, 49, 9052-9067.

235. Wuitschik, G.; Rogers-Evans, M.; Muller, K.; Fischer, H.; Wagner, B.; Schuler, F.; Polonchuk, L.; Carreira, E. M. Oxetanes as Promising Modules in Drug Discovery. *Angew. Chem. Int. Ed.* **2006**, *45*, 7736-7739.
236. Capraro, H.; Caravatti, G.; Furet, P.; Imbach, P.; J., L.; Pecchi, S.; Schoepfer, J. Substituted Imidazopyridazines and Pyrrolopyrimidines as Lipid Kinase Inhibitors. WO2008/138889, 2008.
237. Issidorides, C. H.; Matar, A. I. Pentaerythritol Derivatives. I. The Preparation of Pentaerythritol Monomethyl Ether. *J. Am. Chem. Soc.* **1955**, *77*, 6382-6383.
238. http://www.cyprotex.com/product_sheets/Cloe%20Screen%20Turbidimetric%20Solubility%20Product%20Sheet.pdf (07.08.2011).
239. Law, K. Synthesis and Properties of *tert*-Butyl-Substituted Vanadylphthalocyanine Dyes. *Inorg. Chem.* **1985**, *24*, 1778-1781.
240. Watson, A. Structure-Activity Studies for Inhibitors of two Cancer Targets: Tip60 Histone Acetyltransferase and MDM2-p53. Newcastle University, 2010.
241. Blackburn, T. J. In 2010.
242. Jacq, J.; Einhorn, C.; Einhorn, J. A Versatile and Regiospecific Synthesis of Functionalized 1,3-Diarylisobenzofurans. *Org. Lett.* **2008**, *10*, 3757-3760.
243. Lindoy, L. F.; Meehan, G. V.; Svenstrup, N. Mono- and Diformylation of 4-Substituted Phenols: A New Application of the Duff Reaction. *Synthesis* **1998**, 1029-1032.
244. Katritzky, A. R.; Harris, P. A.; Kotali, A. Mechanism of the Replacement of Phenolic Hydroxyl by Carbonyl on Lead Tetraacetate Treatment of *o*-Hydroxyaryl Ketone Acylhydrazones. *J. Org. Chem.* **1991**, *56*, 5049-5051.
245. Lampe, J. W.; Biggers, C. K.; Defauw, J. M.; Foglesong, R. J.; Hall, S. E.; Heerding, J. M.; Hollinshead, S. P.; Hu, H.; Hughes, P. F.; Jagdmann Jr, G. E.; Johnson, M. G.; Lai, Y.; Lowden, C. T.; Lynch, M. P.; Mendoza, J. S.; Murphy, M. M.; Wilson, J. W.; Ballas, L. M.; Carter, K.; Darges, J. W.; Davis, J. E.; Hubbard, F. R.; Stamper, M. L. Synthesis and Protein Kinase Inhibitory Activity of Balanol Analogues with Modified Benzophenone Subunits. *J. Med. Chem.* **2002**, *45*, 2624-2643.
246. Branden, C.; Tooze, J. *Introduction to Protein Structure*. 2nd ed.; Garland Science: 1998.

247. Sanders, D. A. R. Protein X-ray Crystallography. In *Handbook of Neurochemistry and Molecular Neurobiology: Practical Neurochemistry Methods*, 3rd ed.; Baker, G. B.; Dunn, S.; Holt, A., Eds. Springer: 2007.
248. <http://www.diamond.ac.uk/Home.html> (30.08.11).
249. Ericsson, U. B.; Hallberg, B. M.; Detitta, G. T.; Dekker, N.; Nordlund, P. Thermofluor-Based High-Throughput Stability Optimization of Proteins for Structural Studies. *Anal. Biochem.* **2006**, 357, 289-298.
250. <http://www.pti-nj.com/PlateReader/TechNotes/Fluorescence-basedThermalShiftAssay.pdf> (05.2011).
251. Pantoliano, M. W.; Petrella, E. C.; Kwasnoski, J. D.; Lobanov, V. S.; Myslik, J.; Graf, E.; Carver, T.; Asel, E.; Springer, B. A.; Lane, P.; Salemme, F. R. High-Density Miniaturized Thermal Shift Assays as a General Strategy for Drug Discovery. *J. Biomol. Screen.* **2001**, 6, 429-440.
252. Owicki, J. C. Fluorescence Polarization and Anisotropy in High Throughput Screening: Perspectives and primer. *J. Biomol. Screen.* **2000**, 5, 297-306.
253. Zhang, R.; Mayhood, T.; Lipari, P.; Wang, Y.; Durkin, J.; Syto, R.; Gesell, J.; McNemar, C.; Windsor, W. Fluorescence Polarization Assay and Inhibitor Design for MDM2/p53 Interaction. *Anal. Biochem.* **2004**, 331, 138-146.
254. Bissantz, C.; Kuhn, B.; Stahl, M. A Medicinal Chemist's Guide to Molecular Interactions. *J. Med. Chem.* **2010**, 53, 5061-5084.
255. Ibrahim, M. A. A. Molecular Mechanism Study of Halogen Bonding in Drug Discovery. *J. Comput. Chem.* **2011**, 32, 2564-2574.
256. Auffinger, P.; Hays, F. A.; Westhof, E.; Shing Ho, P. Halogen Bonds in Biological Molecules. *PNAS* **2004**, 101, 16789-16794.
257. Spath, E.; Koller, G. Die Synthese des Ricinins. *Chem. Ber.* **1923**, 56, 2454-2460.
258. Belley, M.; Colucci, J.; Girand, M.; Han, Y.; Lacombe, P. EP4 Receptor Agonist, Compositions and Methods thereof. WO2005/116010 A1, 08.12.2005, 2005.
259. Kohl, B.; Strum, E.; Senn-Bilfinger, J.; Simon, W. A.; Kruger, U.; Schaefer, H.; Rainer, G.; Figala, V.; Klemm, K.; Ife, R. J.; Leach, C. A. (H⁺, K⁺)-ATPase Inhibiting 2-[(2-Pyridylmethyl)sulfinyl]benzimidazoles. 4. A Novel Series of Dimethoxypyridyl-Substituted Inhibitors with Enhanced Selectivity. The Selection of Pantoprazole as a Clinical candidate. *J. Med. Chem.* **1992**, 35, 1049-1057.

260. Cully, S. Optimisation of Buchwald-type chemistry to synthesise 4-ethynyl substituted benzylamines. In 2011.
261. Gelman, D.; Buchwald, S. L. Efficient Palladium-Catalyzed Coupling of Aryl Chlorides and Tosylates with Terminal Alkynes: Use of a Copper Cocatalyst Inhibits the Reaction *Angew. Chem. Int. Ed.* **2003**, 42, 5993-5996.
262. Nelson, T. D.; Leblond, C. R.; Frantz, D. E.; Matty, L.; Mitten, M. V.; Weaver, D. G.; Moore, J. C.; Kim, J. M.; Boyd, R.; Kim, P.; Gbewanyo, K.; Brower, M.; Sturr, M.; McLaughlin, K.; McMasters, D. R.; Kress, M. H.; McNamara, J. M.; Dolling, U. H. Stereoselective Synthesis of a Potent Thrombin Inhibitor by a Novel P2-P3 Lactone Ring Opening. *J. Org. Chem.* **2004**, 69, 3620-3627.
263. Bottger, V.; Bottger, A.; Howard, S. F.; Picksley, S. M.; Chene, P.; Garcia-Echeverria, C.; Hochkeppel, H. K.; Lane, D. P. Identification of Novel MDM2 Binding Peptides by Phage Display. *Oncogene* **1996**, 13, 2141-2147.
264. Garcia-Echeverria, C.; Chene, P.; Blommers, M. J. J.; Furet, P. Discovery of Potent Antagonists of the Interaction between Human Double Minute 2 and Tumour Suppressor p53. *J. Med. Chem.* **2000**, 43, 3205-3208.
265. Zhao, Y. In 2011.
266. Zhang, F.; Throm, S. L.; Murley, L. L.; Miller, L. A.; Zatechka Jr, D. S.; Guy, R. K.; Kennedy, R.; Stewart, C. F. MDM2 Antagonist Nutlin-3a Reverses Mitoxantrone Resistance by Inhibiting Breast Cancer Resistance Protein Mediated Drug Transport. *Biochem. Pharmacol.* **2011**, 82, 24-34.
267. Bag, S.; N.R., T.; M.S, D.; Queener, S. F. Design, synthesis, biological evaluation and computational investigation of novel inhibitors of dihydrofolate reductase of opportunistic pathogens. *Bioorg. Med. Chem.* **2010**, 18, 3187-3197.
268. Read, M. L.; Braendvang, M.; Miranda, P. O.; Gundersen, L. Synthesis and biological evaluation of pyrimidine analogs of antimycobacterial purines. *Bioorg. Med. Chem.* **2010**, 18, 3885-3897.
269. Coperet, C.; Adolfsson, H.; Khuong, T. V.; Yudin, A.; Sharpless, K. B. A Simple and Efficient Method for the Preparation of Pyridine N-Oxides. *J. Org. Chem.* **1998**, 63, 1740-1741.
270. http://www.chemicalbook.com/ChemicalProductProperty_EN_CB2107965.htm (17.06.2011).

271. Cooper, C. G. F.; MacDonald, J. C.; Soto, E.; McGimpsey, W. G. Non-Covalent Assembly of a Photoswitchable Surface. *J. Am. Chem. Soc.* **2004**, 126, 1032-1033.

Appendix 1- Protein Crystallography

Methodology

MDM2 residues 17-109 or 17-125 expressed as a GST fusion. To a pellet equivalent to 1 L of culture was added DNAase (2 μ L) and lysozyme. After 20 min rotation at 4 °C, sample was lysated on ice for 3 min using sonication in 20 sec cycles with 40 sec rest. Sample centrifuged at 4 °C for 1 h at 20 000 rpm. Supernatant was loaded into gravity flow glutathione Sepharose column containing 2 mL of resin washed before use with PBS buffer. Column was washed with PBS buffer (20 mL) and protein eluded using 10 mL of glutathione buffer (PBS buffer with 20 mM glutathione). Cleavage was achieved using 1/20th (w/w) 3C protease (prepared in-house as a GST-fusion) overnight at 4 °C. Further purification achieved using size exclusion chromatography using highload 20/60 Superdex 200 column equilibrated with HEPES buffer.

Table 32 Conditions for crystallisation for each mutant

Mutant	Purchased trays	Custom Trays	Comments
K94A	Molecular Dimension 1+ 2, Wizard EDL, ST, Proplex	-	-
K94E95A	Insufficient protein	-	-
Wild type	AMD, Wizard EDL, ST, JCS6	PEG4000, PEG5000, PEG8000	-
E69K70A	-	PEG4000, 0.2 M (NH ₄) ₂ SO ₄ , 0.1 M NaOAc (pH adjusted to 4.6) and PEG4000, 0.2 M (NH ₄) ₂ SO ₄	Only with inhibitors NCL- 00018225 and NCL-00013774 Seeded
E69A (17-109)	1 st Morpheus, PEG/ION	PEG4000, 0.2 M (NH ₄) ₂ SO ₄ , 0.1 M NaOAc and PEG4000, 0.2 M (NH ₄) ₂ SO ₄	-

E69A (17-125)	-	PEG4000, 0.2 M (NH ₄) ₂ SO ₄ , 0.1 M NaOAc (adjusted to pH 4.6)	-
E69K70E9 4A	-	PEG5000, 0.5-2.0 M (NH ₄) ₂ SO ₄ and PEG8000, 0.2-0.35 M (NH ₄) ₂ SO ₄	-

Table 33 Conditions for crystallisation tray set-up

52% PEG5000, 0.05 M (NH ₄) ₂ SO ₄ , 215 µL water	54% PEG5000, 0.05 M (NH ₄) ₂ SO ₄ , 205 µL water	56% PEG5000, 0.05 M (NH ₄) ₂ SO ₄ , 195 µL water	58% PEG5000, 0.05 M (NH ₄) ₂ SO ₄ , 185 µL water	60% PEG5000, 0.05 M (NH ₄) ₂ SO ₄ , 175 µL water	62% PEG5000, 0.05 M (NH ₄) ₂ SO ₄ , 165 µL water
52% PEG5000, 0.1 M (NH ₄) ₂ SO ₄ , 190 µL water	54% PEG5000, 0.1 M (NH ₄) ₂ SO ₄ , 180 µL water	56% PEG5000, 0.1 M (NH ₄) ₂ SO ₄ , 170 µL water	58% PEG5000, 0.1 M (NH ₄) ₂ SO ₄ , 160 µL water	60% PEG5000, 0.1 M (NH ₄) ₂ SO ₄ , 150 µL water	62% PEG5000, 0.1 M (NH ₄) ₂ SO ₄ , 140 µL water
52% PEG5000, 0.15 M (NH ₄) ₂ SO ₄ , 165 µL water	54% PEG5000, 0.15 M (NH ₄) ₂ SO ₄ , 155 µL water	56% PEG5000, 0.15 M (NH ₄) ₂ SO ₄ , 145 µL water	58% PEG5000, 0.15 M (NH ₄) ₂ SO ₄ , 135 µL water	60% PEG5000, 0.15 M (NH ₄) ₂ SO ₄ , 125 µL water	62% PEG5000, 0.15 M (NH ₄) ₂ SO ₄ , 115 µL water
52% PEG5000, 0.2 M (NH ₄) ₂ SO ₄ , 140 µL water	54% PEG5000, 0.2 M (NH ₄) ₂ SO ₄ , 130 µL water	56% PEG5000, 0.2 M (NH ₄) ₂ SO ₄ , 120 µL water	58% PEG5000, 0.2 M (NH ₄) ₂ SO ₄ , 110 µL water	60% PEG5000, 0.2 M (NH ₄) ₂ SO ₄ , 100 µL water	62% PEG5000, 0.2 M (NH ₄) ₂ SO ₄ , 90 µL water

Table 34 Thermofluor plate set-up for identification of the optimal dye concentrations

7.5 μ L 5 x dye, 7.5 μ L 3 μ M protein	7.5 μ L 5 x dye, 7.5 μ L buffer	7.5 μ L 10 x dye, 7.5 μ L 3 μ M protein	7.5 μ L 15 x dye, 7.5 μ L 3 μ M protein	7.5 μ L 20 x dye, 7.5 μ L 3 μ M protein
7.5 μ L 5 x dye, 7.5 μ L 4 μ M protein	7.5 μ L 10 x dye, 7.5 μ L buffer	7.5 μ L 10 x dye, 7.5 μ L 4 μ M protein	7.5 μ L 15 x dye, 7.5 μ L 4 μ M protein	7.5 μ L 20 x dye, 7.5 μ L 4 μ M protein
7.5 μ L 5 x dye, 7.5 μ L 5 μ M protein	7.5 μ L 15 x dye, 7.5 μ L buffer	7.5 μ L 10 x dye, 7.5 μ L 5 μ M protein	7.5 μ L 15 x dye, 7.5 μ L 5 μ M protein	7.5 μ L 20 x dye, 7.5 μ L 5 μ M protein
7.5 μ L 5 x dye, 7.5 μ L 6 μ M protein	7.5 μ L 20 x dye, 7.5 μ L buffer	7.5 μ L 10 x dye, 7.5 μ L 6 μ M protein	7.5 μ L 15 x dye, 7.5 μ L 6 μ M protein	7.5 μ L 20 x dye, 7.5 μ L 6 μ M protein

Table 35 MDM2 and p53 concentrations to identify optimal conditions for fluorescence

[MDM2] (nM)	Fluorescently labelled p53 concentration (nM)											
5	1	4	7	10	13	16	19	22	25	28	31	34
10	2	8	14	20	26	32	38	44	50	56	62	68
15	4	16	28	40	52	64	76	88	100	112	124	136

Appendix 2 Crystallography of 127

Table 1. Crystal data and structure refinement for 127.

Identification code	127	
Chemical formula (moiety)	$C_{12}H_{17}NO$	
Chemical formula (total)	$C_{12}H_{17}NO$	
Formula weight	191.27	
Temperature	293(2) K	
Radiation, wavelength	MoK α , 0.71073 Å	
Crystal system, space group	monoclinic, P12 ₁ /c1	
Unit cell parameters	a = 9.4720(4) Å	$\alpha = 90^\circ$
	b = 10.8606(4) Å	$\beta = 102.654(4)^\circ$
	c = 10.5802(4) Å	$\gamma = 90^\circ$
Cell volume	1061.97(7) Å ³	
Z	4	
Calculated density	1.196 g/cm ³	
Absorption coefficient μ	0.076 mm ⁻¹	
F(000)	416	
Crystal colour and size	colourless, 0.50 × 0.40 × 0.40 mm ³	
Reflections for cell refinement	3781 (θ range 3.2 to 27.1°)	
Data collection method	Oxford Diffraction Gemini A Ultra	
diffractometer		
	thin-slice ω scans	
θ range for data collection	3.2 to 27.1°	
Index ranges	h -11 to 9, k -10 to 13, l -13 to 11	
Completeness to $\theta = 26.0^\circ$	87.8 %	
Reflections collected	6016	
Independent reflections	1880 ($R_{int} = 0.0172$)	
Reflections with $F^2 > 2\sigma$	1503	
Absorption correction	semi-empirical from equivalents	
Min. and max. transmission	0.9632 and 0.9704	
Structure solution	direct methods	
Refinement method	Full-matrix least-squares on F^2	
Weighting parameters a, b	0.0456, 0.0840	
Data / restraints / parameters	1880 / 0 / 128	
Final R indices [$F^2 > 2\sigma$]	R1 = 0.0310, wR2 = 0.0809	
R indices (all data)	R1 = 0.0422, wR2 = 0.0839	
Goodness-of-fit on F^2	1.087	
Extinction coefficient	0.022(5)	
Largest and mean shift/su	0.000 and 0.000	
Largest diff. peak and hole	0.16 and -0.14 e Å ⁻³	

Table 2. Atomic coordinates and equivalent isotropic displacement parameters (\AA^2) for **127**. U_{eq} is defined as one third of the trace of the orthogonalized U^{ij} tensor.

	x	y	z	U_{eq}
O(1)	0.28781(8)	0.03042(7)	0.06200(6)	0.0252(2)
N(1)	0.42847(10)	-0.18797(9)	0.38777(8)	0.0271(3)
C(1)	0.37117(11)	-0.07559(10)	0.39158(10)	0.0243(3)
C(2)	0.32505(11)	-0.00161(10)	0.28520(10)	0.0220(3)
C(3)	0.33582(11)	-0.04560(10)	0.16406(9)	0.0193(3)
C(4)	0.39456(11)	-0.16148(10)	0.15631(10)	0.0211(3)
C(5)	0.43863(11)	-0.22702(10)	0.27032(10)	0.0255(3)
C(6)	0.28700(12)	-0.01564(10)	-0.06602(9)	0.0219(3)
C(7)	0.21730(11)	0.08138(10)	-0.16215(9)	0.0207(3)
C(8)	0.05925(11)	0.10332(10)	-0.15656(10)	0.0236(3)
C(9)	-0.01086(12)	0.20023(10)	-0.25453(10)	0.0264(3)
C(10)	0.00011(12)	0.16367(11)	-0.39072(10)	0.0282(3)
C(11)	0.15706(12)	0.14177(11)	-0.39835(10)	0.0265(3)
C(12)	0.22849(12)	0.04559(10)	-0.29933(10)	0.0227(3)

Table 3. Bond lengths [\AA] and angles [$^\circ$] for **127**.

O(1)–C(3)	1.3561(12)	O(1)–C(6)	1.4423(12)
N(1)–C(1)	1.3399(15)	N(1)–C(5)	1.3362(14)
C(1)–H(1A)	0.930	C(1)–C(2)	1.3740(15)
C(2)–H(2A)	0.930	C(2)–C(3)	1.3924(14)
C(3)–C(4)	1.3857(15)	C(4)–H(4A)	0.930
C(4)–C(5)	1.3840(15)	C(5)–H(5A)	0.930
C(6)–H(6A)	0.970	C(6)–H(6B)	0.970
C(6)–C(7)	1.5121(14)	C(7)–H(7A)	0.980
C(7)–C(8)	1.5298(15)	C(7)–C(12)	1.5286(14)
C(8)–H(8A)	0.970	C(8)–H(8B)	0.970
C(8)–C(9)	1.5237(15)	C(9)–H(9A)	0.970
C(9)–H(9B)	0.970	C(9)–C(10)	1.5200(15)
C(10)–H(10A)	0.970	C(10)–H(10B)	0.970
C(10)–C(11)	1.5251(16)	C(11)–H(11A)	0.970
C(11)–H(11B)	0.970	C(11)–C(12)	1.5284(15)
C(12)–H(12A)	0.970	C(12)–H(12B)	0.970
C(3)–O(1)–C(6)	117.93(8)	C(1)–N(1)–C(5)	115.42(9)
N(1)–C(1)–H(1A)	117.8	N(1)–C(1)–C(2)	124.48(10)
H(1A)–C(1)–C(2)	117.8	C(1)–C(2)–H(2A)	120.7
C(1)–C(2)–C(3)	118.63(10)	H(2A)–C(2)–C(3)	120.7
O(1)–C(3)–C(2)	116.40(9)	O(1)–C(3)–C(4)	125.08(9)
C(2)–C(3)–C(4)	118.51(9)	C(3)–C(4)–H(4A)	121.2
C(3)–C(4)–C(5)	117.64(10)	H(4A)–C(4)–C(5)	121.2
N(1)–C(5)–C(4)	125.30(10)	N(1)–C(5)–H(5A)	117.4
C(4)–C(5)–H(5A)	117.4	O(1)–C(6)–H(6A)	110.2
O(1)–C(6)–H(6B)	110.2	O(1)–C(6)–C(7)	107.56(8)
H(6A)–C(6)–H(6B)	108.5	H(6A)–C(6)–C(7)	110.2
H(6B)–C(6)–C(7)	110.2	C(6)–C(7)–H(7A)	108.0
C(6)–C(7)–C(8)	111.68(9)	C(6)–C(7)–C(12)	110.52(8)
H(7A)–C(7)–C(8)	108.0	H(7A)–C(7)–C(12)	108.0
C(8)–C(7)–C(12)	110.39(8)	C(7)–C(8)–H(8A)	109.3

C(7)–C(8)–H(8B)	109.3	C(7)–C(8)–C(9)	111.45(9)
H(8A)–C(8)–H(8B)	108.0	H(8A)–C(8)–C(9)	109.3
H(8B)–C(8)–C(9)	109.3	C(8)–C(9)–H(9A)	109.5
C(8)–C(9)–H(9B)	109.5	C(8)–C(9)–C(10)	110.75(9)
H(9A)–C(9)–H(9B)	108.1	H(9A)–C(9)–C(10)	109.5
H(9B)–C(9)–C(10)	109.5	C(9)–C(10)–H(10A)	109.4
C(9)–C(10)–H(10B)	109.4	C(9)–C(10)–C(11)	111.15(9)
H(10A)–C(10)–H(10B)	108.0	H(10A)–C(10)–C(11)	109.4
H(10B)–C(10)–C(11)	109.4	C(10)–C(11)–H(11A)	109.4
C(10)–C(11)–H(11B)	109.4	C(10)–C(11)–C(12)	111.14(9)
H(11A)–C(11)–H(11B)	108.0	H(11A)–C(11)–C(12)	109.4
H(11B)–C(11)–C(12)	109.4	C(7)–C(12)–C(11)	111.39(9)
C(7)–C(12)–H(12A)	109.3	C(7)–C(12)–H(12B)	109.4
C(11)–C(12)–H(12A)	109.4	C(11)–C(12)–H(12B)	109.3
H(12A)–C(12)–H(12B)	108.0		

Table 4. Anisotropic displacement parameters (\AA^2) for **127**. The anisotropic displacement factor exponent takes the form: $-2\pi^2[h^2a^*2U^{11} + \dots + 2hka^*b^*U^{12}]$

	U^{11}	U^{22}	U^{33}	U^{23}	U^{13}	U^{12}
O(1)	0.0367(5) 0.0051(3)	0.0225(4)	0.0158(4)	0.0002(3)	0.0048(3)	
N(1)	0.0280(5) -0.0001(4)	0.0319(6)	0.0220(5)	0.0046(4)	0.0067(4)	
C(1)	0.0232(6) -0.0051(5)	0.0335(7)	0.0175(5)	-0.0027(5)	0.0070(4)	
C(2)	0.0218(6) -0.0010(5)	0.0226(6)	0.0220(6)	-0.0034(5)	0.0059(4)	
C(3)	0.0176(5) -0.0036(4)	0.0214(6)	0.0186(5)	0.0010(4)	0.0032(4)	
C(4)	0.0231(6) -0.0025(5)	0.0234(6)	0.0182(5)	-0.0023(4)	0.0074(4)	
C(5)	0.0266(6) 0.0012(5)	0.0236(6)	0.0275(6)	0.0026(5)	0.0084(5)	
C(6)	0.0260(6) 0.0005(5)	0.0235(6)	0.0164(5)	-0.0022(5)	0.0052(4)	
C(7)	0.0228(6) -0.0020(4)	0.0196(6)	0.0196(5)	-0.0002(4)	0.0044(4)	
C(8)	0.0257(6) -0.0008(5)	0.0255(6)	0.0208(5)	-0.0012(5)	0.0079(4)	
C(9)	0.0221(6) 0.0008(5)	0.0242(6)	0.0327(6)	0.0019(5)	0.0057(5)	
C(10)	0.0267(6) 0.0003(5)	0.0294(6)	0.0265(6)	0.0081(5)	0.0015(5)	
C(11)	0.0309(7) -0.0021(5)	0.0292(6)	0.0201(6)	0.0035(5)	0.0068(5)	
C(12)	0.0231(6) -0.0007(5)	0.0251(6)	0.0206(6)	0.0006(5)	0.0064(4)	

Table 5. Hydrogen coordinates and isotropic displacement parameters (\AA^2) for **127**.

	x	y	z	U
H(1A)	0.3620	-0.0456	0.4717	0.029
H(2A)	0.2874	0.0762	0.2939	0.026
H(4A)	0.4040	-0.1941	0.0773	0.025
H(5A)	0.4786	-0.3045	0.2647	0.031
H(6A)	0.2326	-0.0919	-0.0812	0.026
H(6B)	0.3851	-0.0316	-0.0750	0.026
H(7A)	0.2702	0.1587	-0.1397	0.025
H(8A)	0.0060	0.0267	-0.1742	0.028
H(8B)	0.0545	0.1301	-0.0701	0.028
H(9A)	-0.1118	0.2095	-0.2512	0.032
H(9B)	0.0368	0.2788	-0.2324	0.032
H(10A)	-0.0408	0.2284	-0.4509	0.034
H(10B)	-0.0555	0.0892	-0.4159	0.034
H(11A)	0.2103	0.2185	-0.3823	0.032
H(11B)	0.1604	0.1140	-0.4848	0.032
H(12A)	0.3296	0.0373	-0.3026	0.027
H(12B)	0.1821	-0.0335	-0.3214	0.027

Table 6. Torsion angles [$^\circ$] for **127**.

C(5)–N(1)–C(1)–C(2)	-0.33(16)	N(1)–C(1)–C(2)–C(3)	0.98(16)
C(6)–O(1)–C(3)–C(2)	-175.36(9)	C(6)–O(1)–C(3)–C(4)	5.05(15)
C(1)–C(2)–C(3)–O(1)	179.48(9)	C(1)–C(2)–C(3)–C(4)	-0.91(15)
O(1)–C(3)–C(4)–C(5)	179.85(9)	C(2)–C(3)–C(4)–C(5)	0.28(15)
C(1)–N(1)–C(5)–C(4)	-0.38(16)	C(3)–C(4)–C(5)–N(1)	0.40(16)
C(3)–O(1)–C(6)–C(7)	175.13(8)	O(1)–C(6)–C(7)–C(8)	-63.32(11)
O(1)–C(6)–C(7)–C(12)	173.38(8)	C(6)–C(7)–C(8)–C(9)	-179.44(8)
C(12)–C(7)–C(8)–C(9)	-56.06(12)	C(7)–C(8)–C(9)–C(10)	56.72(12)
C(8)–C(9)–C(10)–C(11)	-56.28(12)	C(9)–C(10)–C(11)–C(12)	55.76(12)
C(10)–C(11)–C(12)–C(7)	-55.44(12)	C(6)–C(7)–C(12)–C(11)	179.33(8)
C(8)–C(7)–C(12)–C(11)	55.29(12)		